TREFOIL 1

T/18P OFFSHORE BASS BASIN

WELL COMPLETION REPORT
INTERPRETIVE DATA

D.M. Brooks, M. Lonergan & J. Parvar
Origin Energy Resources Ltd
339 Coronation Drive
MILTON QLD 4064
Australia

SEPTEMBER 2005

Distribution List:

Chief Geologist

Chief Geophysicist

Exploration Manager, Offshore Australia

Contents

1. WELL INDEX SHEET 1
2. WELL SUMMARY 3
3. WELL RESULTS 5
3.1 Hydrocarbons Encountered 5
3.2 Stratigraphy 8
3.3 Reservoir Evaluation 16
3.3.1 Petrophysical Summary 16
3.3.2 Core Analysis Summary 18
3.3.3 Facies Interpretation 19
3.4 Hydrocarbon Source Evaluation 22
3.4.1 Maturation 22
3.4.2 Source Rock and Hydrocarbon Evaluation 23
3.5 MDT Pressure Data Interpretation 24
3.6 Drill Stem Testing Interpretation Results 24
4. GEOPHYSICAL DISCUSSION 26
4.1 Seismic Data 26
4.2 Structure 26
4.3 VSP and Well Tie 26
4.4 Actual versus Predicted Depths 27
4.5 Seismic Amplitudes 27
5. GEOLOGICAL DISCUSSION 35
5.1 Exploration History 35
5.2 Regional Geology 37
5.2.1 Structure 37
5.2.2 Stratigraphy 39
5.3 Contributions to Geological Concepts and Conclusions 41
6. REFERENCES 42

APPENDIX 1: PETROPHYSICS REPORT
APPENDIX 2: MDT INTERPRETATION REPORT
APPENDIX 3: DRILL STEM TESTING INTERPRETATION REPORTS
(A) Test Interpretation
(B) Sand Production
APPENDIX 4: GEOCHEMISTRY REPORT
APPENDIX 5: VITRINITE REFLECTANCE REPORT
APPENDIX 6: PALYNOLOGY REPORT
APPENDIX 7: PETROLOGY REPORT
APPENDIX 8: CORE INTERPRETATION
APPENDIX 9: SPECIAL CORE ANALYSIS
APPENDIX 10: FMI INTERPRETATION REPORT

APPENDIX 11: CASED HOLE DSI (SONIC) PROCESSING REPORT

ENCLOSURE 1: COMPOSITE LOG

1. WELL INDEX SHEET

Permit Interests:	Origin Energy Resources Ltd (41.4%) – OPERATOR AWE Petroleum Pty Ltd (22.6%) CalEnergy Gas (Australia) Ltd (23.5%) Wandoo Petroleum Pty Ltd (12.5%)
Rig on Location:	28/10/2004
Spud:	30/10/2004
Reached TD:	23/11/2004
Rig Released:	25/12/2004
Total Rig Days:	69.4
Rig Name:	ENSCO 102
Drilling Contractor:	ENSCO
Total Depth:	3545m mMDRT (D) 3505.1 mSS (D)
Well Status:	Cased & Suspended Gas Discovery

Well Name:	Trefoil 1
Basin:	Offshore Bass
Permit:	T/18P
Type:	Vertical Exploration Well
Water Depth:	68.9m (MSL to seabed)
Elevation:	39.9m (RT-sea level)
Latitude:	39° 51' 44.12"S
Longitude:	145° 22' 30.73"E
Easting:	361 026.14metres
Northing:	5 586 267.85metres
(GDA 94; UTM Zone 55S, Central Meridian 147° East).	
Seismic Reference:	Shelduck 2D Survey: Line ORS01-13, SP 1492
Actual Well Cost:	A$ 24,961,090

FORMATION TOPS

FORMATION / *SEISMIC MARKER*	**TOPS (m)**				**REMARKS/SHOWS**
	m MDRT	m TVDSS	THICK (m)	TWT (ms)	
Torquay Group	108.8	68.9	1040.3		No Returns 108.8 – 218.0 mMDRT. Bioclastic Limestone grading downhole to marl then calcareous claystone.
Extrusive Volcanics	*668.2*	*628.3*	*50.7*		*Crystalline volcanics (basalt?)*
Upper Angahook Fm	1149.1	1109.2	190.9		Calcareous Claystone
Angahook Volcanics equivalent	1340.0	1300.1	238.0		Calcareous claystone and siltstone
Oligocene Angahook Fm	1578.0	1538.1	282.1		Interbedded siltstone and minor claystone
Demons Bluff Formation	1860.1	1820.2	238.2		Siltstone with minor interbedded claystone and occasional dolomite
Eastern View Coal Measures	2098.3	2058.4	1446.7+		Interbedded Sandstone, siltstone, volcanics and minor claystone
TEV4	*2139.4*	*2099.5*	*44.5*		*Sandstone*
E1 unit	*2600.5*	*2560.6*	*81.9*		*Sandstone*
Eocene Unconformity	*2682.4*	*2642.5*			
P5 unit	*2689.0*	*2649.1*	*13.7*		*Sandstone*
P4 unit	*2733.3*	*2693.4*	*29.3*		*Sandstone*
P3 unit	*2820.6*	*2780.7*	*33.2*		*Sandstone*
P2 unit	*2859.2*	*2819.3*	*146.8*		*Gas-bearing sandstones*
P1 unit	*3006.0*	*2966.1*	*48.0*		*Gas-bearing sandstones*
Top Cretaceous	*3054.0*	*3014.1*	*491+*		*Gas-bearing sandstones*
Top T.lilliei	*3372.5*	*3332.6*	*172.5+*		
Cretaceous Volcanics	*3391.1*	*3351.2*			*Interbedded Volcanics, sandstone and siltstone*
TOTAL DEPTH	3545.0	3505.1			

FORMATION EVALUATION WHILE DRILLING

Hole Size (inches)	Interval (mMDRT)	MWD services	LWD services
16	215 - 666	DWD	none
12.25	666 – 2428	P4M-DIR-FE	DGR-EWR
8.5	2428 – 2735	P4M-DIR-FE-NUKE	DGR-EWR-CNP-SLD
8.5	2735 – 3442	P4M-DIR-FE-NUKE	DGR-EWR-CNP-SLD
8.5	3442 - 3545	P4M-DIR-FE-NUKE	DGR-EWR-CNP-SLD

WIRELINE LOGS

Suite #	Run #	Interval (mMDRT)	Logs Acquired
1	1	2420.1 - 3418.3 m	PEX-HRLA-CMR-SP-GR
1	2	319 – 3419 m	VSI-GR
1	3	2626 – 3390 m	MDT-GR (1)
			WIPER TRIP
1	4	2812 – 3046 m	MSCT (1)
1	5	2926 – 3524 m	MDT-GR (2)
1	6	2968.3 – 3018.2 m	MSCT (2)
1	7	3009 – 3414 m	MSCT (3)
1	8	2420.1 – 3527 m	FMI-DSI-HNGS

CORES

CONVENTIONAL

Core #	Interval (mMDRT)	Cut (m)	Rec (m)	Formation
1	2735.0 – 2742.25	8.2	7.3 (89%)	EVCM P5 sand

SIDEWALL

Suite#	Run#	Type	Interval (mMDRT)	Bullets	Mechanical Failure	Empty	Partial Recovery	Recovered
1	4	Rotary (MSCT)	3046.5 – 2812	35	9	16	0	10
1	6	Rotary (MSCT)	3018.2 – 2968.3	26	2	0	0	24
1	7	Rotary (MSCT)	3414 - 3009	12	0	4	3	5

PRESSURE TESTING AND FLUID SAMPLING

Suite#	Run#	Type	Interval (mMDRT)	Total Tests	Valid Tests	Supercharged	Tight Tests	Failed	Pump outs	Samples Collected
1	3	MDT	3390 – 2626	79	45	31	1	5	4	6
1	5	MDT	3528.7 - 2926	33	16	3	12	2	6	6

HOLE & CASING DETAILS

Hole Size	Interval (mMDRT)	Casing Size	Shoe Setting Depth (mMDRT)
26/36 "	108.8 - 218	20"	215
16 "	218 – 666.1	$13\ ^{3}/_{8}$ "	657
12 ¼ "	666.1 - 2428	$9\ ^{5}/_{8}$ "	2421
8 ½ "	2428 - 3545 (TD)	$6\ ^{5}/_{8}$ "	3458

2. WELL SUMMARY

Trefoil 1 was drilled as a vertical exploration well in the western part of the exploration permit T/18P in the offshore Bass Basin, Tasmania. The well is located 37 km west of the Yolla Gas Field, approximately 114km SW from the nearest point of the Victorian coast and 59km from the nearest landfall of the Tasmanian coast at Three Hummock Island (Figure 1). The well was drilled using the ENSCO 102 jack up drilling rig. Trefoil 1 was designed to target the sandstone reservoirs of the Eastern View Coal Measures (EVCM) which are proven to be hydrocarbon bearing in the nearby Yolla Field and White Ibis gas discovery.

Trefoil 1 spudded on the 30th October 2004. Primary objectives within the EVCM Palaeocene and Cretaceous, which were termed pre-drill as P1, P2, P3, P4, P5 and C1 sand units, were intersected close to prognosed depth. The Eocene objective (termed the E1 pre-drill) was intersected 56m low to prognosis. Multiple gas and condensate columns were discovered within the lower Palaeocene (pre-drill P1 and P2 zones) and Cretaceous sands (including the pre-drill C1 zone). Log analysis indicates the potential for 21 gas-bearing zones and MDT sampling and optical fluid analysis (OFA) confirmed at least 12 gas columns. MDT pressures show that the intra-EVCM in Trefoil 1 consists of several different over-pressurised and isolated layers. The well reached total depth of 3545mRT on 23rd November 2004. The sands within the lower Palaeocene and Cretaceous intervals were tested in 2 separate cased hole drill stem tests (CHDST) and flowed gas and condensate. CHDST#1 was conducted within the Cretaceous interval from 3141 to 3150 mRT and flowed gas at 14.4mmscf/d with CGR of 12.4stb/mmscf. CHDST#2 flowed gas at 9.5mmscf/d and associated CGR of 26.2stb/mmscf over the interval 3040.5 – 3046.5 mRT within the lower Palaeocene section. Following the drill stem testing, the rig was released to Esso on 25th December 2004.

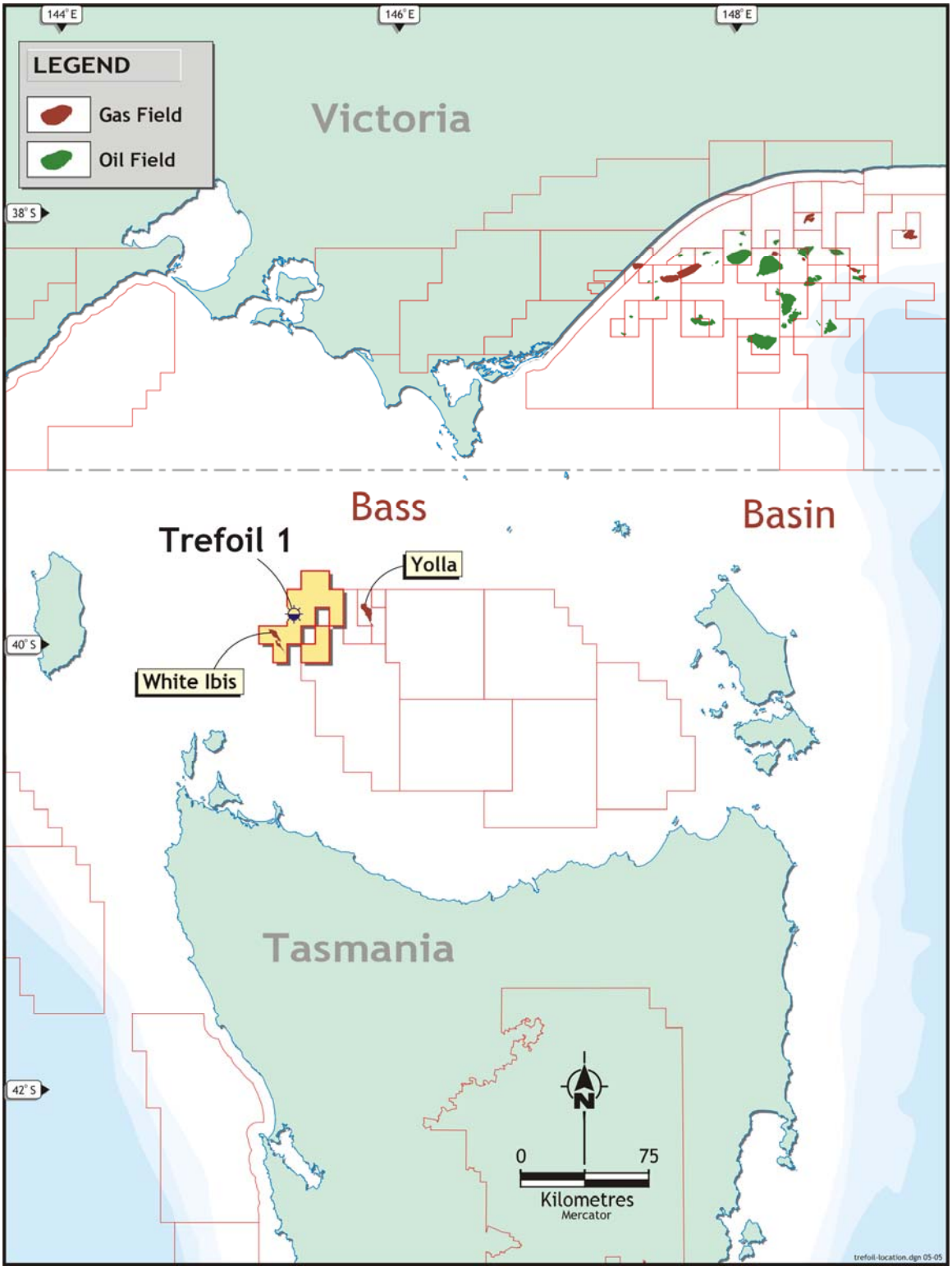


Figure 1: Trefoil 1 Location Map

3. WELL RESULTS

3.1 Hydrocarbons Encountered

Mudlog gas readings commenced from 666mRT. Gas levels were at or close to zero until 828mRT. The gas readings slowly increased from this depth to 884mRT at the top of the Lower Miocene Marl. Background total gas readings in Trefoil 1 remained fairly steady through the remainder of the Torquay Group, Angahook Formation, Demons Bluff Formation and the upper EVCM (total gas range 2 – 45 units). No significant gas peaks were recorded and no fluorescence was observed.

Immediately upon entering the P4 sand unit within the Eastern View Coal Measures gas readings climbed sharply from 2732mRT to a total gas peak of 140 units at 2740mRT. Gas wetness also increased to the highest levels seen in the whole well between 2732 – 2743mRT. 20 – 50% fluorescence was noted between 2735mRT and 2741mRT within core 1. The fluorescence is described as bright yellow, even fluorescence, moderately fast direct cut, trace dim white crush cut and thin dull yellow residue ring. Core and log analysis confirm that this zone is water wet.

Gas readings reduced to background levels averaging between 25 and 31 units between 2743mRT to 2819mRT within the siltstone separating the P4 and P3 sand units.

At the top of the P3 sand unit, at a depth of 2819mRT, total gas readings climbed again. Total gas ranged from 74 to 128 units from the top of the P3 to within the P2 unit at 2916mRT. Fluorescence was noted within the mud between 2835 – 2853mRT, 2859 – 2886mRT, 2892 – 2931mRT as well as within sandstone cuttings intermittently through this zone. The fluorescence in the mud is described as pale yellow/green, slow bleeding cut, with a thin residual ring. The sandstone cuttings fluorescence from 2853 – 2859mRT is 20% patchy dim white direct fluorescence, moderately fast cut, dull white crush cut, thin white residual ring. At 2907mRT sandstone fluorescence is 40% patchy dull yellow patchy direct fluorescence, blooming pale green crush cut, thin dim yellow residual ring. Between 2916 – 2919mRT and 2925 – 2931mRT, sandstone fluorescence is described as – 50% patchy moderately bright yellow, moderately fast cut, pale white blooming crush cut, thin dull green residual ring. MDT sampling and pretests have proven this zone to be water wet.

Below 2931mRT gas levels rose markedly. Over 25 gas peaks were encountered between 2931 – 3169mRT within the interbedded sands and siltstones of the lower Palaeocene and Cretaceous age (predrill termed the P2, P1 and C1) units of the EVCM. No fluorescence accompanied these gas shows. The average gas readings ranged from 95 to 1102 units. The largest total gas peak at 3145mRT was 1559 units. The sandstones between 3040.5 – 3046.5 and 3141 – 3150mRT were subsequently tested with cased hole drill stem tests and flowed maximum gas rates of 9.5MMscf/d and 16.2MMscf/d respectively. MDT samples and pretests taken from 2931 to 3169mRT are interpreted to show at least 11 separate gas columns are present and log analysis indicates the potential for 20 separate gas bearing zones (Table 1). Different water gradients interpreted from the MDT pre-tests reveal the interval to be a multi-system consisting of several over-pressurised layers. No actual gas-water contacts (GWC) were intersected however some water gradients can be interpreted from the MDT data and the GWC inferred in some cases. The range of possible GWC's and gas column heights shown in Table 1 are based on lowest known gas (LKG), interpreted water gradients and mapped lowest closing contours (LCC). Each gas zone has been named

according to the spore-pollen zone they occur within. Gas columns have been interpreted within the spore-pollen zones of the Palaeocene lower *L.balmei* and the Cretaceous upper *F.longus* and *T.lilliei.*

From 3169mRT to 3382mRT total gas levels remained at a high background level averaging 38 to 57 units. No fluorescence was encountered through the interval.

Sand interval m RT approx	Informal Zone Name*	Inferred GWC level				
		Shallowest			Deepest	
		Based on	mSS	Column (m)	Based on	mSS
2931 – 2934	TILb-10	LKG	2894.1	3.0	LCC	
2942 – 2952	TILb-20	LKG			LCC	
2957 – 2960	TILb-30	LKG	2920.1	3.0	LCC	
2967 – 2972	TILb-40	GWC	2954.1	27.0	GWC	2954.1
2979 – 2983	TILb-50	GWC	2961.1	22.0	GWC	2961.1
2991 – 3002	TILb-60	GWC	2963.1	12.0	GWC	2963.1
3018 – 3022	TILb-70	LKG	2982.1	4.0	3025	2985.1
3026 – 3029	TILb-80	LKG	2989.1	3.0	LCC	
3040 – 3047	TILb-90	LKG	3007.1	7.0	3069	3029.1
3054 – 3059	TuFl-10	LKG	3019.1	5.0	3060	3020.1
3066 – 3072	TuFl-20	LKG			LCC	
3094 – 3108	TuFl-30	LKG	3068.1	14.0	3128.4	3088.5
3109 – 3111	TuFl-40	LKG			LCC	
3121 - 3123	TuFl-50	LKG			LCC	
3126 - 3131	TuFl-60	LKG			LCC	
3132 - 3136	TuFl-70	LKG			LCC	
3141 - 3150	TuFl-80	LKG	3110.1	9.0	LCC	3110.1
3153 - 3158	TuFl-90	LKG			LCC	
3161 - 3163	TuFl-100	LKG			LCC	
3166 - 3169	TuFl-110	LKG	3129.1	3.0	LCC	
3385 - 3390	TTl-10	LKG	3347.1	2.0	HKW	3350.1

* T = Trefoil
lLb = lower *L.balmei*
uFl = upper *F.longus*
Tl = *T.lilliei*

Table 1: Trefoil 1 Gas Zones and Inferred Gas-Water Contacts in the Intra-EVCM

Between 3382 – 3388mRT (drillers depths) while drilling through a sandstone, streaming bright pale green to pale yellow fluorescence with instant cut was noted and an accompanying gas peak reached 1723 units. MDT and log interpretation confirm this interval to be gas-bearing. A water sample taken at 3388.7mRT (loggers depth) defines the highest known water (HKW) for this hydrocarbon zone (see Table 1).

Immediately below this gas-bearing sandstone Cretaceous extrusive basalt was intersected. Interbedded sandstone and siltstones were interspersed throughout the volcanic section from 3388mRT – TD at 3545mRT. Small gas peaks were noted at 3417mRT, 3432mRT, 3479mRT, 3481mRT, 3510mRT and 3519mRT. The highest of these was 302 units at 3432mRT. Background gas readings averaged from 8 to 31 units. Fluorescence was seen in the mud when drilling through sandstones between 3475 – 3490 and 3507 – 3527mRT. This fluorescence is bright pale green-white with instant cut and dull green yellow ring residue.

3.2 Stratigraphy

A generalised stratigraphy of the Bass Basin is illustrated in Figure 2. Figure 3 contains a comparison between the pre-drill prognosis and actual stratigraphy encountered at Trefoil 1. A report by Dr Roger Morgan (Morgan Palaeo Associates) on the age and palaeo-environment of 33 cuttings samples, 1 SWC and 1 core plug is included in Appendix 6. This report also contains maturity data derived from the spore colour index method.

Lithological descriptions from ditch cuttings, sidewall core and conventional core (see Appendices 1, 2 and 3, Trefoil 1 Well Completion Report Volume 1, Basic Data), together with the MWD and wireline log interpretation (Appendix 1, this volume), provide the basis for the stratigraphic breakdown as detailed below and shown in the Composite Well Log (Enclosure 1).

Torquay Group
(108.8 to 1149.1mRT, 68.9 to 1109.2mTVDSS)

The Torquay Group (not including the Angahook Formation) in Trefoil 1 is approximately 1037.2 m thick. The unit is interpreted to be deposited under shallow marine conditions and can be divided seismically into two upper units separated by a prominent seismic marker called the 'Lower Miocene Seismic event'. This event separates the Pliocene to Miocene mainly calcareous dominant lithology from the underlying Miocene age claystone. The third and lowermost unit of the group is the Angahook Formation, which itself can be divided into 3 sub-units and is discussed separately below.

Returns were established from 218mRT. The top portion of the Torquay Group consists of a bioclastic limestone. This upper limestone section comprises cream to off-white, white to light to medium grey and olive grey, and cream to light yellow-brown, translucent, coarse- to fine-grained friable to moderately hard, weakly cemented bioclastic calcarenite to calcirudite including skeletal debris consisting of pelecypods, bryozoans, foraminifera and gastropods. Between 666m and 718mRT a volcanic derived lithology was encountered. The crystalline volcanics are described as dark green to blue green to medium grey, mottled white with black specks which are moderately hard to hard and blocky with a trace of quartz. These volcanics were recognised on the pre-drill seismic data at the well location as very bright amplitudes with flow-shape morphology, implying extrusives would be present within the Torquay Group. Below the volcanics, the calcareous sediments become finer grained grading from calcarenite to dominantly calcisiltite with minor siltstone at the base at 884mRT. The siltstone is sideritic in part, red brown to medium brown and ochre brown to grey with black laminae, soft to moderately hard, blocky to fissile fracture, moderately strong siliceous cement and containing up to 30% calcareous clay size grains and trace coarse sand.

The lower portion of the Torquay Group, commencing from 884mRT, is described in Trefoil 1 as a marl grading downhole to calcareous claystone which is pale to light to medium grey, dark green-grey to olive grey, soft, sub-blocky, 20% to 50% calcareous, with trace amounts of: silt, fine sand, fossil fragments, bryozoans, shell fragments and carbonaceous matter. Minor dolomite is also described within this interval and is described as buff to brown-red-grey, hard to very hard, massive to blocky, silty with weak calcareous cement.

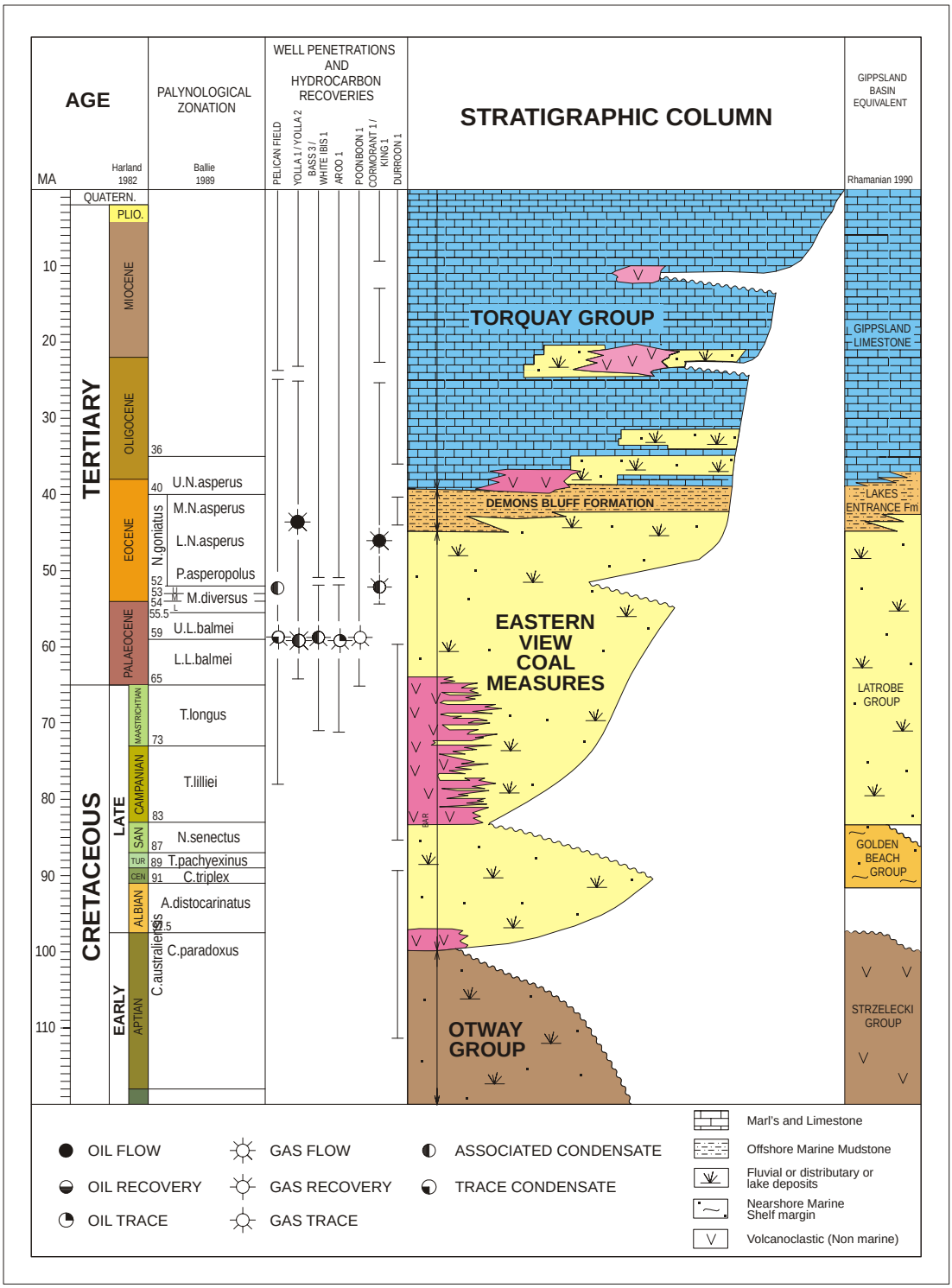


Figure 2: Generalised Stratigraphy of the Bass Basin

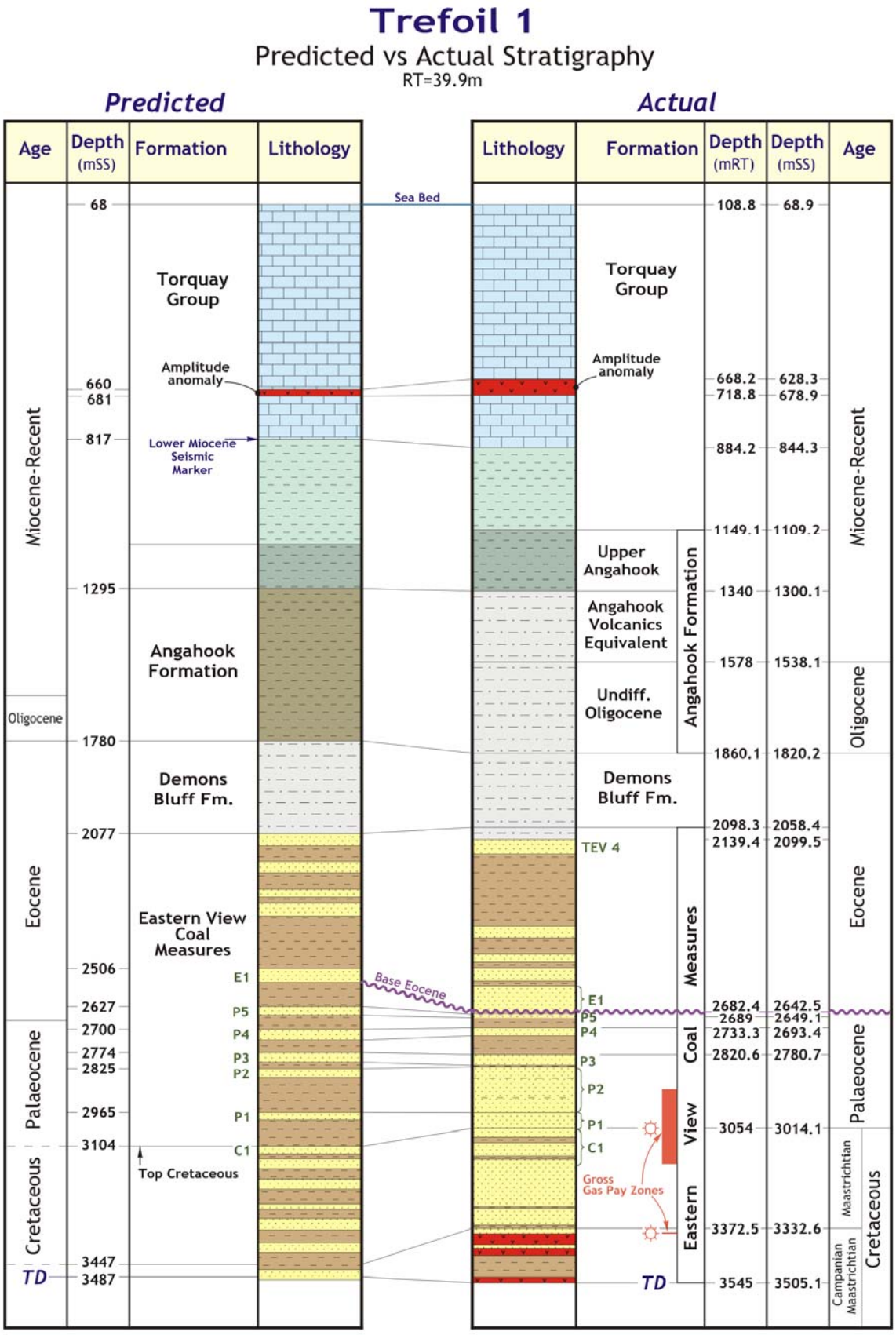


Figure 3: Trefoil 1 - Predicted versus Actual Stratigraphy

Angahook Formation
(1149.1 to 1860.1 mRT, 1109.2 to 1820.2 mTVDSS)

Overall the thickness of the Miocene to Oligocene Angahook Formation in Trefoil 1 is 713m. This unit is distinctive from the overlying upper units of the Torquay Group due to reworking and presence of volcanics and sediments proximal to centres of Miocene volcanism (*Lennon et al, 1999*).

Upper Angahook Formation
(1149.1 to 1340.0 mRT, 1109.2 to 1300.1 mTVDSS)

In Trefoil 1 the upper part of the Angahook Formation consists of calcareous claystone which is light green grey to medium grey, soft occasionally friable, sub-blocky to amorphous, calcareous and silty (grading to a silty claystone and siltstone in part), and contains common fossil/shell detritus and trace dolomite grains.

The log response through this interval is a fairly uniform GR and resistivity response with a slight decrease in GR from the top of the unit to the base suggesting a gradual fining upward trend in grainsize. The mudlog shows a minor but consistent increase in gas and wet gas from the top to the base.

Angahook Volcanics
(1340.0 to 1578.0 mRT, 1300.1 to 1538.1 mTVDSS)

The time equivalent to the volcanic-rich interval within the Angahook Formation in the Yolla Field is picked on the basis of log correlation using regional gamma ray and resistivity character. There is no volcanic lithology described in this interval in Trefoil 1.

This unit in Trefoil 1 is described as interbedded calcareous claystone and siltstone. The top of the unit shows a distinctive gamma-ray (GR) decrease which is probably in response to the increase in siltstone content compared to the overlying claystone dominated lithology. The GR steadily decreases from the top of the unit to the base showing a gradual increase in overall grain size corresponding to a further increase in the percentage of siltstone present.

The calcareous claystone is light green-grey to olive-grey, cream to light brown and light to medium brown-grey in colour, very soft to firm, sub-blocky to amorphous, and contains up to 20% calcareous grains, common clastic silt to very fine sand size grains (up to 20%), minor kaolinite and trace carbonaceous material and fossils. The siltstone is olive green to olive grey and light brown-grey to light green-grey, soft to friable, sub-blocky and contains 10 - 20% calcareous grains and clastic grains are 10 - 20% clay, 60 – 80% silt, 5 - 30% very fine sand and trace fine sand size grains, 3% glauconite and trace fossils. Dolomite is present in trace amounts and is described as orange-red-brown colour, hard and blocky.

Although not assessed in Trefoil 1, regional palynological data indicates that the Angahook Volcanics unit lies within the spore-pollen zone upper *P.tuberculatus* (lower Miocene). Elsewhere in the basin this unit is shown to be deposited in a marine environment with spore-pollen to dinoflagellate ratios suggesting a gradational deepening of water depth upwards in the stratigraphy.

Undifferentiated Oligocene
(1578.0 to 1860.1mRT, 1538.1 to 1820.2mTVDSS)

The remaining basal interval of the Angahook Formation is a clastic dominated marine unit of siltstone with minor interbedded claystone.

There is a gradual decrease in grain size down hole as shown by an increasing GR from top to the base of the interval. The overall GR and resistivity log responses (from the LWD tools) is fairly bland.

Siltstone is the dominant lithology in this interval and consists of light to medium brown to grey-brown to grey colour, friable to firm, sub-blocky to blocky fracture, minor to abundant calcareous cement, containing trace very fine sand size grains siliceous matrix, traces amounts of fossils, dolomite and pyrite, up to 3% glauconite grains. The claystone interbeds are light grey to light blue-grey and light to medium brown and light grey-brown coloured, mainly very soft but also moderately hard in part, amorphous to blocky, minor to very calcareous and contains trace quantities of very fine sand grains, shell fragments and pyrite, common kaolinite and minor dolomite.

Demons Bluff Formation
(1860.1 to 2098.3mRT, 1820.2 to 2058.4mTVDSS)

The Demons Bluff Formation lithology is dominated by siltstone within minor interbedded claystone and trace dolomite. This formation forms a thick regional seal over the EVCM.

The GR logs at the top of the unit show a distinct baseline shift indicating a reduction in overall grainsize compared to the Angahook Formation. The LWD GR and resistivity log responses throughout the interval are very uniform.

The siltstone is medium to light brown and light to dark grey-brown, soft to firm, sub-blocky to blocky, with 10-20% clay, 50-60% silt, trace-30% very fine sand, 10 – 15% fine sand size grains with trace dolomite and shell fragments and trace to 15% pyrite. The claystone interbeds are calcareous and silty, light grey to blue-grey and medium grey coloured, soft to firm, sub-blocky to blocky, 15 - 25% calcareous grains, 50 - 60% clastic clay grains, up to 30% silt, trace - 10% very fine sand, trace fossils and pyrite. The minor dolomite is described as yellow grey to medium to dark brown, silty, firm to very hard, blocky.

Eastern View Coal Measures
(2098.3 to 3545.0mRT (TD), 2058.4 to 3505.1mTVDSS)

The Eastern View Coal Measures (EVCM) is a very thick succession of non-marine fluvio-lacustrine and flood-plain deposits interspersed with extrusive volcanics at the base to nearshore and marginal marine sediments at the top of the formation. The formation ranges in age from Eocene to Campanian in Trefoil 1. Pre-drill EVCM objectives were predicted to be present at the base of the Eocene (E1), throughout the Palaeocene (P1, P2, P3, P4, P5) and at the top of the Cretaceous (C1).

Within Trefoil 1, the formation can be split into 4 broad units. The top unit is dated as Middle to Early Eocene, based on the presence of the *N.asperus* spore pollen zone near the top of the EVCM to lower *M.diversus* spore-pollen zone at the base of the interval. This top section is interpreted to be

deposited in a marginal marine to near-shore/shelfal marine environment. The second unit occurs below an interpreted unconformity or hiatus and is dated as Palaeocene as it includes the upper and lower *L.balmei* spore pollen zones. These sediments are interpreted to have been deposited in a marginal marine lagoonal to non-marine lakes and floodplain settings. The basal two intervals are Cretaceous. The uppermost zone is Maastrichtian and contains the *F.longus* spore-pollen zone and was deposited in a non-marine floodplain and swamp margin environment. The lowermost unit intersected in Trefoil 1 is interpreted as Maastrichtian to Campanian in age due to the occurrence of the *T.lilliei* spore pollen zone. The unit contains extrusive volcanics and the sediments are non-marine, probably of floodplain origin.

The topmost unit of the EVCM occurs between 2098.3 to 2693.8mRT in Trefoil 1. As soon as the top of the EVCM is penetrated the GR log shows reduced values indicating increasing grainsize accompanied by an increase in gas wetness readings. These both increase over the next 40 m, though the lithology is still dominantly siltstone with increasing fine sandstone appearing. The TEV4 unit (informal name) heralds the topmost sandstone of the EVCM in Trefoil 1. This interval is dominated by siltstone with increasing percentage of interbedded sandstone downhole, and minor claystone. No reservoired hydrocarbons are interpreted in the sands at the base of the Eocene (E1 objective) despite fluorescence being noted while drilling.

The siltstone is dark to light grey-brown to light grey and medium brown grading to cream and light brown near the base of the interval, firm to moderately hard, occasionally friable, sub-blocky to blocky, consisting of 20% clay, 70% silt and 10% very fine sand grains, with trace calcareous grains, and traces of fossils and coal/carbonaceous material, minor to 15% mica. The sandstone is off-white to light grey, light brown grey, clear to translucent and white, generally friable loose grains occasionally firm to hard, irregular fracture, composed of 0-10% clay, 0-10% silt, 0 – 80% very fine sand grains, 0 – 20% fine sand and 0 – 30% medium sand grains, 0 – 10% coarse sand grains, 0 – 80% very coarse and 0 – 10% granule sand grain size, which are poorly to well sorted, sub-rounded to sub-angular, sub spherical, weakly to moderately argillaceous and strong to nil silica cement, trace mica, pyrite and occasionally up to 3% siderite and up to 10% kaolinite, trace to 20% intergranular visual porosity. The minor claystone is described as off-white to light to pale grey colour, soft, amorphous to sub-blocky, trace calcareous and contains 15 – 30% silt, 10 – 15% very fine sand and trace fossils.

The base of the uppermost unit is interpreted to be an unconformity or depositional hiatus at the base of the Eocene based on evidence from regional log correlations which shows missing section at Trefoil 1 and Aroo 1 compared to the Yolla Field wells. This missing interval in Trefoil 1 is interpreted to occur within the top part of the upper *L.balmei* and the basal part of the lower *M.diversus* spore pollen zones.

The second informal division of the EVCM in Trefoil 1 occurs between 2693.8 to 3054.0mRT. This portion of the EVCM is Palaeocene and spans the upper and lower *L.balmei* spore pollen zones. Pre-drill targets in this zone were referred to as P1 to P5. A thin siltstone separates the top of the P5 from the overlying base Eocene event. The topmost target, the P5 sand, was present between 2693.8 and 2702.7mRT (8.9m thick) as a tight sandstone bed. From 2702.7 to 2820.5mRT the section is dominated by 2 thick siltstone beds which are separated by a thin sandy section between 2733.7 to 2762.1mRT. This thin sand unit corresponds to the pre-drill predicted P4 unit. Core 1 was taken from the top part of this sandstone

from 2735 – 2742.25mRT. Detailed descriptions of this core can be found in Appendix 8. This zone was found to be water wet despite promising gas shows while drilling and up to 50% fluorescence seen in sandstone chips described from the core (see section 3.1). Below the second thick siltstone the lithology changes to an interbedded sequence of sandstone and siltstone and these constitute the P3, P2 and P1 pre-drill objectives. The P3 unit (from 2820.6 – 2859.2mRT) is water wet in Trefoil 1 even though strong gas shows and fluorescence were noted while drilling this interval. The P2 and P1 units are difficult to distinguish compared to Aroo 1 and new terminology has been devised for the multiple gas zones which were discovered in these intervals in Trefoil 1.

The siltstones intersected are sandy in part, light to dark grey to medium brown and medium to dark grey-brown, mostly firm to very hard, occasionally friable, sub-blocky to blocky, composed of 10 – 30% clay, 60 – 80% silt, 0% – 30% very fine sand grains, nil - trace fine sand grains with traces of argillaceous matrix, pyrite and micro mica and up to 3% kaolinite and common carbonaceous laminae, grading to dark brown to black carbonaceous siltstone in part. The sandstones are described as kaolinitic in part, cream, white to clear to very pale to light to medium brown, some loose grains, friable to firm, occasionally moderately hard, and composed of 0 – 20% clay, 0 - 10% silt, 0 - 40% very fine sand, 0 – 70% fine sand, 20 – 80% medium sand, 0 - 40% coarse sand grains, 0 – 40% very coarse sand grained, 0 – 20% granular and 0 – 20% cobble size grains, very poorly to very well sorted, sub-rounded to angular, sub-spherical to spherical, and trace to weak argillaceous, trace to strong silica cement, trace coal and trace - 25% intergranular visual porosity.

Three MSCT samples from the Palaeocene were submitted for petrological studies (Appendix 7). Samples are texturally varied, with 2 being classified as very coarse grained arkoses and the third sample as a subarkose in which framework grains are mainly granite-derived quartz and K-feldspar and also include plagioclase, granitic rock fragments, metamorphic rock fragments, sedimentary rock fragments, mica and accessory heavy minerals. The sandstones are derived almost entirely from a nearby granitic provenance. The granitic-sourced sediment was diluted slightly by detritus derived from highly indurated quartzose sandstones and low-grade quartzose/micaceous/illitic metasedimentary rocks. Illite and kaolinite are the common clays present. Smectitic clays are absent. Diagenetic effects are quartz overgrowth and siderite cementation, authigenic clay formation, grain contact dissolution/microstylolitisation, physical compaction and labile grain dissolution. Quartz overgrowths do not exceed 3.5% and only partly occlude intergranular pores. Clay-/sandy matrix-rich sandstones (3000.2m, 3018.4m) contain less than 2.7% visible porosity, whereas clean sandstone (2996.8m) contains 12.8% visible porosity. Wide permeability variation reflects large textural differences, with very coarse grained sandstones that contain clay/fine sandy matrix (3000.2m, 3018.4m) having low to fair permeability (1.10mD, 10.8mD) and very coarse grained, clean sandstone (2996.8m) having high permeability (531mD).

The third informal division of the Trefoil1 EVCM from 3054.0m – 3372.5mRT is Maastrichtian age and contains the *F. longus* spore pollen zone. Sandstone is the dominant lithology with thin siltstone interbeds. The topmost sand of the Cretaceous was termed the C1 pre-drill and was considered one of the primary targets. The top sand-prone section (spanning the upper *F.longus* spore pollen zone) between 3056.5 – 3166.7mRT was found to contain multiple gas columns (see section 3.1 for details). The remainder of the Maastrichtian (interpreted to span the lower *F.longus* spore pollen zone) is water wet.

The sandstone is described as clear to opaque white grains in the upper *F.longus* zone and light grey to light brown in the lower *F.longus* zone, mainly loose, soft in part, consisting of 0 - 20% clay, 0 - 10% silt, 0 - 40% very fine sand and 0 - 70% fine sand, 0 – 30% medium sand, 10 – 40% coarse sand, 0 – 70% very coarse sand, 0 – 40% granule size grains and trace cobble size grains which are poorly to very poorly sorted, occasionally moderately to well sorted, angular to sub-angular, equant to spherical becoming sub-elongate with depth, trace to moderately cemented with silica and weak argillaceous matrix, 10 - 25% visual intergranular porosity. The siltstones are described as light grey to light brown and grey to brown, firm to moderately hard, blocky, composed of 10% clay, 60-90% silt, trace-30% very fine sand grains.

The basal informal interval of the EVCM in Trefoil 1 from 3372.5 to 3545mRT is dated as Maastrichtian to Campanian based on the interpreted presence of the *T.lilliei* spore pollen zone. This section consists of volcanic extrusive lithology interbedded with sandstone and siltstone. The top of the interval consists of a 12m thick siltstone overlying a 5.5m thick sandstone. The sandstone is interpreted from MDT data to contain a gas column (see section 3.1) with the GWC encountered at 3387.6mRT. The gas mudlog showed the highest liquids (high C4 and C5) potential for the well while drilling through the sand and streaming fluorescence in the mud led to an initial interpretation of an oil zone, but MDT samples confirmed the presence of gas with a CGR of 42.2bbls/mmscf and LPG ratio of 4.5 Tonnes/mmscf (see Appendix 2). This gas sand lies directly on volcanics which dominate the stratigraphy through to total depth (TD) of the well. No further hydrocarbon zones are interpreted in the well even though some gas peaks and fluorescence in the mud was observed while drilling this section.

The volcanics are generally fresh and occasionally altered. The altered volcanics consist of mottled white, green black with traces of tan to red coloured vein calcite, variously calcareous or siliceous, firm to very hard, recrystallised texture, irregular fracture containing up to 15% feldspar and 10% crystalline. The unaltered volcanic lithology is crystalline, black, green to white, light grey, dark grey, red to pink trace clear coloured, moderately hard to very hard, blocky to irregular fracture with 15% feldspar and trace calcareous. The sandstones are described as cream, light brown to grey, occasionally kaolinitc and off-white to white, mainly loose to friable, sub blocky in part, firm to moderately hard in part, very fine to very coarse grained, poorly to very well sorted, angular to sub-angular, sub-spherical to sub-equant, weakly argillaceous, siliceous cement, trace calcareous cement, trace to 20% visual intergranular porosity. The siltstone is dark grey to dark brown and medium brown, firm to moderately hard, occasionally friable to firm, blocky to brittle, composed of 10 - 30% clay, 90 - 70% silt and trace very fine sand grains and containing weak to moderately siliceous cement and moderately argillaceous.

3.3 Reservoir Evaluation

3.3.1 Petrophysical Summary

A comprehensive petrophysical review was conducted to assess the reservoir quality and hydrocarbon saturation of all zones within the lower part of the Eastern View Coal Measures (EVCM) which displayed good hydrocarbon shows while drilling (Appendix 1). The study entailed an analysis of all available lithological data, MSCT samples, core samples, MDT and drill stem test data. One full diameter core was acquired through the section known as the P4 sandstone and was analysed to determine RCA and SCAL properties which were then used to calibrate the log analysis. A summary of the log analysis is presented in Table 2. The results through the main gas reservoirs in the EVCM are summarized below:

Most of the reservoir zones are within the transition zone between irreducible gas saturation and the GWC. Hence, the calculated water saturations are quite high.

The well is interpreted to have 106.7mMD of net sand of which 49.0mMD constitutes net pay (Table 2) in the main reservoir intervals. This net pay is divided into numerous (possibly up to 20) discreet layers (Appendix 2).

Pre-drill, the reservoirs had been zoned into three basic units, P2, P1 and C1 and these sub-divisions are included here for reference only.

The top part of the lower *L.balmei* sands includes the section termed P2 pre-drill (2930 – 3018 mRT). This interval comprises the TILb-10 to TILb-60 gas zones and total 88mMD thick; contain 39mMD of net sand with an average porosity of 13.2% and permeability of 28mD. 19.3mMD is calculated to be net pay with an average porosity of 13.7%, permeability of 43mD and water saturation of 49%.

The interval previously termed P1 sandstones (3018 – 3121 mRT) now include part of the Cretaceous and therefore spans the lower *L.balmei* and upper *F.longus* spore-pollen zones. The gas zones in this interval are now termed TILb-70 to TuIB-90 and TuFl-10 to TuFl-40 and have a gross thickness of 103mMD; contain 25mMD of net sand with an average porosity of 12.3% and permeability of 14mD. 13.2mMD is calculated to be net pay with an average porosity of 12.7%, permeability of 22mD and water saturation of 51%.

The remainder of the Cretaceous has been subdivided into 3 zones for the purposes of the log analysis. The top unit within the upper *F.longus* spore-pollen zone spans 3121 – 3161mRT (40mMD gross thickness) and holds the gas zones TuFl-50 to TuFl-90 and contains 14mMD of net sand with an average porosity of 12.5% and permeability of 18mD. 10mMD is calculated to be net pay with an average porosity of 12.8%, permeability of 22mD and water saturation of 48%.

The middle Cretaceous interval (3161 – 3385 mRT) is interpreted to include the basal few metres of the upper *F.longus* (which contains 2 thin gas zones, TuFl-100 and TuFl-110), all of the lower *F.longus* and the top of the *T.lilliei* zones. It is predominantly non-net, but does contain 27mMD of net sand with an average porosity of 10.8% and permeability of 3.5mD. 5.3mMD is calculated to be net pay with an average porosity of 10.6%, permeability of 3.0mD and water saturation of 53%.

The lowest Cretaceous sandstone evaluated petrophysically (3385 – 3390 mRT) occurs within the *T.lilliei* spore-pollen zone and is 5mMD thick and contains 2.1mMD of net sand with an average porosity of 10.1% and permeability of 2mD. 1.5mMD is calculated to be net pay with an average porosity of 10.0%, permeability of 2.3mD and water saturation of 44%.

GROSS INTERVAL				NET PAY				
Reservoir Zone	Top mRT	Base mRT	Thickness mMD	Thickness mMD	Net / Gross [%]	Phi [%]	K [m]D	Sw [%]
Overburden	2420.0	2743.0	3232	0	0	0	0	0
Seal	2743.0	2844.0	101	0	0	0	0	0
Wet Sands	2844.0	2967.1	123.2	2.16	0.02	0.147	65.93	0.519
TlLb-10	2930	2941.9	11.9	1.2	0.10	0.144	53.1	0.463
TlLb-20	2941.9	2956.9	15.0	0.3	0.02	0.155	127.8	0.561
TlLb-30	2956.9	2966.9	10.0	1.1	0.11	0.142	47.7	0.543
TlLb-40	2966.9	2979.0	12.1	5.2	0.43	0.138	39.7	0.466
TlLb-50	2979.0	2989.9	10.9	5.9	0.54	0.141	40.2	0.482
TlLb-60	2989.9	3018.0	28.1	5.6	0.20	0.130	42.1	0.522
TlLb-70	3018.0	3025.9	7.9	2.4	0.30	0.113	7.8	0.475
TlLb-80	3025.9	3039.9	14.0	2.0	0.14	0.135	26.4	0.478
TlLb-90	3039.9	3053.9	14.0	4.4	0.31	0.125	12.8	0.491
TuFl-10	3053.9	3066.0	12.1	0.9	0.07	0.147	70.0	0.561
TuFl-20	3066.0	3093.9	27.9	0.0	0.00			
TuFl-30	3093.9	3109.9	15.1	2.4	0.16	0.122	10.6	0.545
TuFl-40	3109.9	3121.0	12.0	1.1	0.09	0.147	66.0	0.530
TuFl-50	3121.0	3125.9	4.9	1.4	0.28	0.148	74.5	0.383
TuFl-60	3125.9	3132.0	6.1	0.5	0.07	0.141	42.7	0.532
TuFl-70	3132.0	3140.4	8.4	0.9	0.11	0.117	7.3	0.529
TuFl-80	3140.4	3152.0	11.6	5.9	0.51	0.124	11.7	0.498
TuFl-90	3152.0	3155.9	3.9	0.0	0.00			
TuFl-100	3155.9	3160.9	5.0	1.1	0.21	0.128	16.8	0.473
TuFl-110	3160.9	3385.0	224.1	5.3	0.02	0.106	3.0	0.528
TTl-10	3385.0	3390.0	5.0	1.5	0.30	0.102	2.3	0.443

Cut-offs applied				
Zone	**shale volume**	**Porosity**	**permeability**	**Water saturation**
Above 2920mRt	< 40%	Not directly applied	> 1 mD	< 60%
Below 2920mRT	< 40%	Not directly applied	> 1 mD	< 60%

Table 2: Trefoil 1 Net Pay Summary

3.3.2 Core Analysis Summary

Routine Core Analysis (RCA) and Special Core Analysis (SCAL) were performed by ACS Laboratories Pty Ltd. The RCA report is contained in Appendix 4 of the Basic Well Completion Report. The Special Core Analysis (SCAL) report is included in Appendix 9 of this volume.

One 7.25m core was acquired in Trefoil 1 within the EVCM "P4" unit of the Palaeocene between 2735 – 2742.25mRT which occurs within the upper *L.balmei* spore pollen zone. In addition to the conventional core, 39 MSCT's were acquired between 2968.3 and 3027.9mRT from within some of the gas-bearing and one water-bearing Palaeocene sands within the lower *L.balmei* spore-pollen zone. One MSCT was also recovered from the basal Cretaceous (within the *T.lilliei* spore-pollen zone) interval at 3414mRT. A plot of the porosity versus permeability and porosity vs depth, both displayed by zone, are presented in Figures 4 and 5. The summary of the average porosity and permeability values for each of the reservoir intervals containing measured data is shown in Table 3 below.

There is a clear difference in the permeability/porosity trend between the P4 upper *L.balmei* sand core plug data and the P1 and P2 lower *L.balmei* MSCT data (Figure 4). This difference is interpreted to be due to different depositional facies. The quartz-rich upper *L.balmei* sandstone is interpreted as deposited in a shoreface environment with overall finer grain size (Appendix 8). The older and deeper lower *L.balmei* sands which are turbidite deposits are much coarser grain size, more poorly sorted, have high feldspar content and are mineralogically and texturally immature compared to the upper *L.balmei* sandstone. A large component of macro porosity in the high porosity lower *L.balmei* sands is due to the very coarse grain size in combination with late-stage secondary porosity resulting from partial to complete dissolution of feldspar and micaceous grains (Appendix 7).

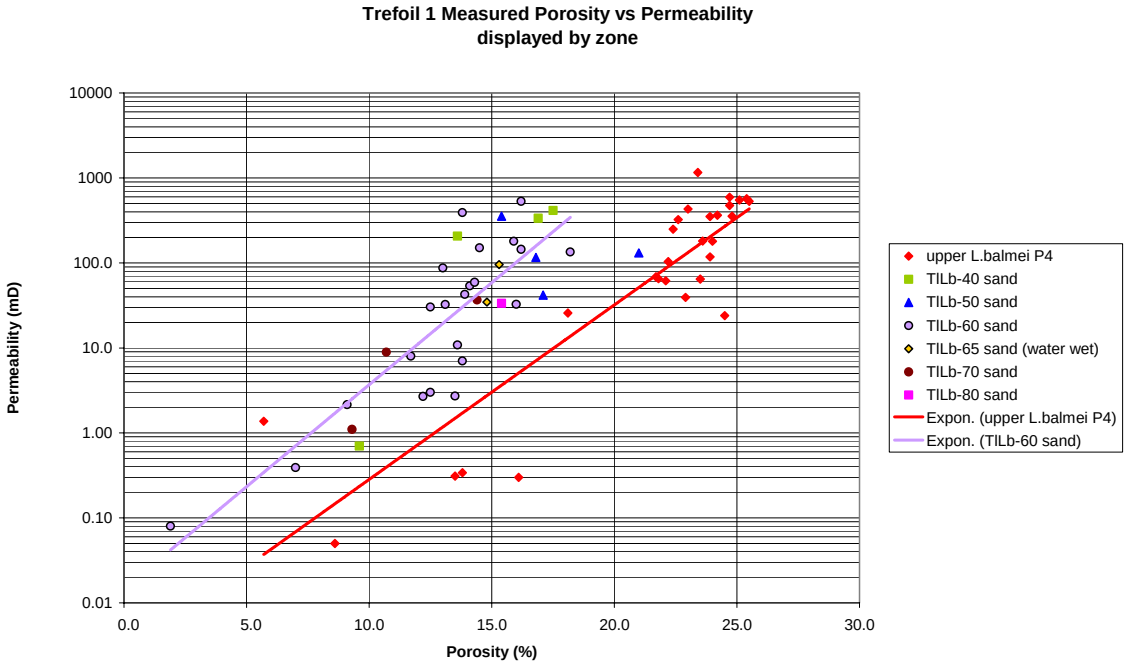


Figure 4: Trefoil 1: Measured Porosity versus Permeability

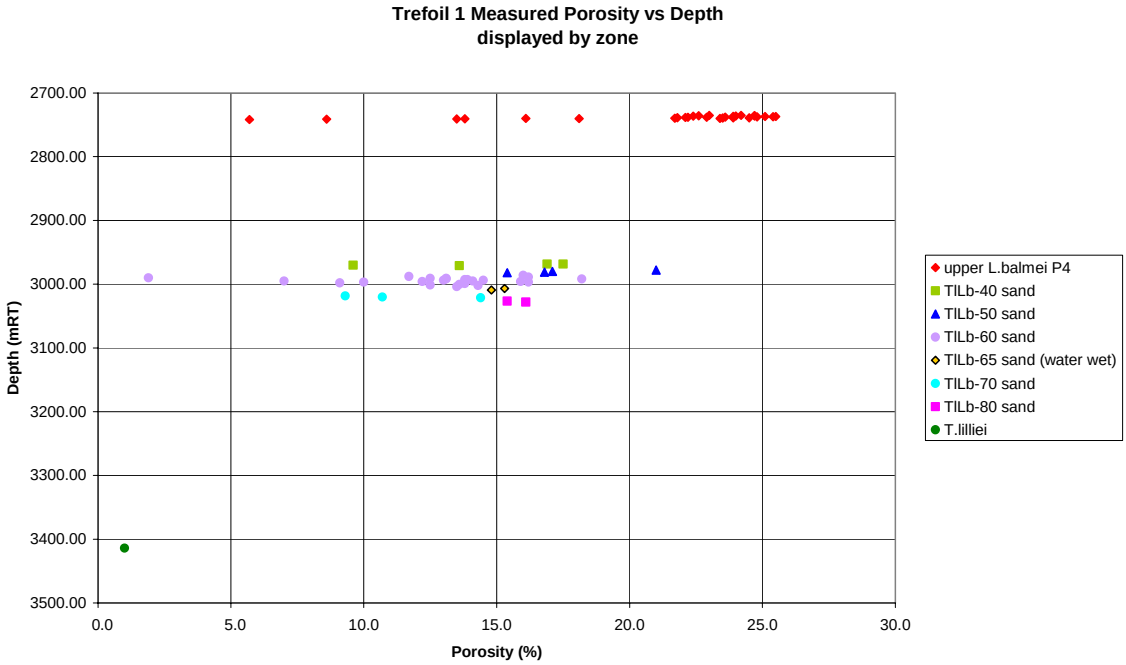


Figure 5: Trefoil 1: Measured Porosity versus Depth

Zone Name	Average Porosity	Average Permeability
Upper L.balmei (P4)	21.3%*	246.2mD*
TILb-40	14.4%	239.2mD
TILb-50	17.6%	161.2mD
TILb-60	12.9%	86.8mD
TILb-65 (water wet)	15.1%*	65.1mD*
TILb-70	11.5%	15.6mD
TILb-80	15.8%	33.4mD
T.lilliei	1%**	na**

* water zone
** only 1 MSCT's recovered

Table 3: Trefoil 1: Average Measured Porosity and Permeability Data

3.3.3 Facies Interpretation

A sedimentological study of Core 1 (2735 – 2743.2 m) from the upper *L.balmei* spore-pollen zone within the Eastern View Coal Measures in Trefoil 1 indicates that this interval was deposited in a progradational marginal marine/brackish water shoreface setting (Appendix 8). The well sorted, cross bedded and low angle laminated sandstone in the core indicates a moderate to high energy setting. The dominance of wave formed structures implies an open coast/strandplain setting. Interpreted depositional environments include shelf, lower offshore, proximal lower shoreface, middle and upper shoreface. The degree and diversity of bioturbation in the core indicate that the interval was subject to environmental stress, possibly reduced salinity. This is confirmed by a biostratigraphic sample from the shelf facies containing limited dinoflagellates and predominantly fresh water algae.

The succession is dominated by intervals in which there was an over supply of sediment relative to the rate of base level change, producing

progradational stacking. A sequence boundary (SB) separates the lower offshore from the proximal lower shoreface indicating a fall in relative base level. Reservoir quality is strongly influenced by facies, with the highest permeability occurring in the middle and upper shoreface facies. The degree of bioturbation does not control the reservoir quality in these facies as the majority of bioturbation comprises cryptobioturbation. The core description and facies study report including core photographs and graphical core log representations are included in Appendix 8.

FMI images within Trefoil 1 from the interval 2700 – 3400 m were interpreted and the detailed results are presented in Appendix 10. The studied succession within Trefoil 1 is of Cretaceous and Palaeocene age, and is characterised by variable structural dips, typically in the range 1-4º (see Table 4).

The section studied comprises a heterolithic succession of sandstones and mudstones with minor intervals of coal. The successions can be sub-divided into a number of discrete sub-units based upon log trends and stacking patterns of interpreted lithofacies. The intervals that alternate between sandstone and mudstone are consistent with a model of deposition in a sub-aqueous setting with periodic turbidity current deposition and suspension settling. The fining upward successions, with associated laminated mudstones and coal, are consistent with deposition in a fluvial setting. The upward coarsening parasequences described are consistent with a model of deposition in a marginal lacustrine environment, with upward coarsening profiles forming as a result of shoreface or delta front progradation.

Structural Zone	Depth Interval	Tectonic Tilt	Comments
2700 – 3400 m			
Zone I	2700 – 2734	1.4°/225°	Bounded by sandstone at base
Zone II	2734 – 2770	2.0°/113°	Bounded by maximum flooding surface
Zone III	2770 – 2826	1.2°/196°	Bounded by sandstone at base
Zone IV	2826 – 2918	2.8°/079°	Interbedded sandstone & mudstone, bounded by unconformity at 2918 m
Zone V	2918 - 3080	1.5°/252°	Bounded by maximum flooding surface
Zone VI	3080 – 3237	4.0°/286°	Bounded by flooding surface
Zone VII	3237 – 3374	4.2°/249°	Bounded by maximum flooding surface
Zone VIII	3374 – 3400	3.1°/032°	Bounded by volcanics

Table 4: Trefoil 1 - Lithofacies and structural dip from FMI interpretation 2700 – 3400mRT.

Lithofacies identified from FMI images have been calibrated with cuttings descriptions. Cuttings descriptions match well with lithofacies interpretations derived using wireline log response and FMI image fabrics, and indicate a succession comprising sandstone and mudstone with minor coal. Six lithofacies associations have been identified within the studied section. These are interpreted as having been deposited in fluvial, marginal lacustrine (shelf-shoreface?) and shelf settings. The lithofacies associations identified are summarised as follows:

I. Mudstones that either occur at the base of upward coarsening facies successions (interpreted as either prodeltaic muds, or shelf-shoreface deposits), or interbedded with sandstones that have sharp bases and tops (interpreted as suspension settling in a shelf

environment) or interbedded with sandstones and rare coal (interpreted as floodplain deposits).

II. Heterolithic intercalations of sandstone and mudstone, typically occurring within the lower-mid parts of upward coarsening facies successions (interpreted as shelf-shoreface deposits). When it is interbedded with Lithofacies Association IV, this implies a sub-aerial setting in a floodplain environment. This lithofacies association also occurs with Lithofacies Association V as possible thin bedded turbidite deposits.

III. Stratified sandstones with mottled image fabric and low angle (typically <5º) internal bedding surfaces, typically occurring towards the top of upward coarsening facies successions (shoreface deposits).

IV. Successions of thick bedded stratified sandstones and rare pebbly sandstones with dominant internal bedding fabrics inclined at angles <10°, rare intervals of up to 25°. These deposits represent fluvial channels.

V. Stratified sandstones with sharp bases and tops, interbedded with Lithofacies Association I, and characterised by low angle (typically <5º) internal bedding surfaces represent massive to parallel stratified sandstones deposited from turbidite flows.

VI. Coals (deposits of swampy coastal plain environments).

Palaeotransport analyses of sandstones from Lithofacies Association III reveals them to be characterised by internal stratification fabrics with very wide ranging sedimentary dip azimuth, suggesting they were originally deposited as "flat lying" strata. Few palaeotransport interpretations can be made for these sandstones. However, in some examples, a dominant sedimentary dip is present, and may represent the original palaeoslope, implying an E - W shoreline orientation.

The interpreted palaeotransport direction of Lithofacies Association IV is in an overall northerly direction. The relationship between intra-set lamination and coset boundaries suggest that sediment transport occurred normal to and at a high angle to the depositional dip, i.e. bedforms migrated laterally downcurrent.

The sandstones from Lithofacies Association V are almost exclusively dominated by low angle internal stratification fabrics with an overall easterly trend that may reflect the original palaeoslope.

In the absence of a detailed core calibration environmental interpretations are highly subjective. However, observed lithofacies stacking patterns do appear to be consistent with an interpretation of deposition of strata within fluvial, marginal lacustrine and shelf settings.

3.4 Hydrocarbon Source Evaluation

3.4.1 Maturation

Vitrinite Reflectance (Vr) studies were undertaken on a set of cuttings samples by Dr A. C. Cook of Keiraville Konsultants (Appendix 5). The results have been plotted against true vertical depth (Figure 6). The assumed source rocks for the Trefoil 1 gas accumulations are the Palaeocene to early Eocene coals within the EVCM (Boreham et al, 2003). All petroleum expulsion maturities quoted here are based on the coal maturity work as published by Boreham et al, 2003.

At the Trefoil 1 well location the maturity for the main oil expulsion window between Vr 0.75 and 0.95% occurs between 3500 – 4300mTVDSS (extrapolated) as shown in Figure 6. The main gas window at Vr > 1.2% commences well below TD of the well, at an extrapolated depth of 5200mTVDSS. The oil and gas expulsion maturities in Trefoil 1 occur approximately 1000m deeper than in the Yolla wells (Brooks et al 2005a). The Palaeocene to early Eocene interval is not mature for hydrocarbon generation at the Trefoil 1 well location where they are found between 2097 and 3056.5mRT. Lateral migration from the thicker and hotter depocentre of the Yolla Trough to the east of the well is the preferred model for the source of the hydrocarbons found in Trefoil 1.

The Vr results do not appear to be suppressed at all and can be used with high confidence. This assumption is corroborated by comparison of Vr with vitrinite-inertinte reflectance and fluorescence (VIRF) in other Bass Basin wells (Boreham et al 2003).

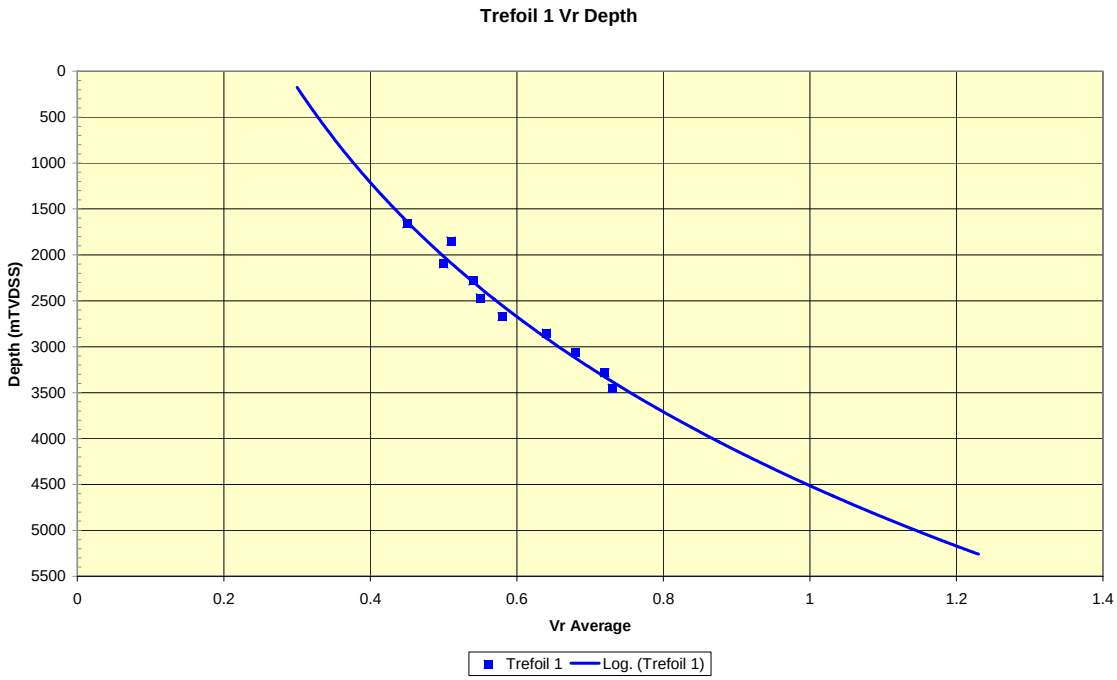


Figure 6: Vitrinite Reflectance profile with depth, Trefoil 1

3.4.2 Source Rock and Hydrocarbon Evaluation

Two condensate samples (one each from DST #1 and DST #2) and ten sediment samples (from 2901 – 3375mRT) from Trefoil 1 were sent for geochemical analyses (Appendix 4). The geochemical program was undertaken to evaluate the source rock potential, thermal maturity and depositional environment of the cuttings samples in the Palaeocene siltstone and silty claystones in a well that was essentially barren of coals, and to correlate these with accumulated hydrocarbons discovered in the well.

Previous published studies (eg. Boreham et al 2003) concluded that the coals within the EVCM were the source of gases and liquids discovered in the Bass Basin to date. The two Trefoil 1 condensate samples are believed to have been sourced from terrigenous organic matter, as indicated by sterane data and the presence of higher plant derived biomarkers. Steranes are however, observed in very low abundance in both condensate samples, resulting in calculated maturity parameters based on steranes being less reliable. The high pristane to phytane ratios characterise the depositional environment as having been highly oxic consistent with a coaly source. There is no indication of either biodegradation or water washing.

The ten cuttings samples from the depth range 2901m to 3375m are characterised as early mature and show potential for minor gas generation based on Rock Eval pyrolysis data. However the low total organic carbon (TOC) (between 0.51 – 1.11%) and hydrogen index (HI) (ranging between 129 to 169) values show that only very small quantities of gas would be generated and it is unlikely that sufficient hydrocarbons would be generated to reach a critical pore volume to initiate expulsion. All samples sent consisted of siltstone and silty claystone as very few coals are present in the well. GC-MS analysis of the extract from Trefoil 1 3375m indicates a moderate level of thermal maturity. Biomarker data also characterises the extract as having been sourced from terrestrial derived organic matter which was deposited under oxic conditions. There is no indication that either migration contamination or biodegradation has altered the composition of the free hydrocarbons.

The Trefoil 1 cuttings extract and the two fluid samples show comparable distributions of biomarker components indicating significant contribution from higher plant derived organic matter which, based on high pristane to phytane ratios, was deposited under oxic sedimentary conditions. Whilst thermal maturation data derived from Rock Eval data and both aromatic and branched/cyclic GC-MS analysis indicate the cuttings sample is not of high enough maturity to have directly sourced the condensate, the extract hydrocarbons and the condensates derive from very similar terrigenous coaly source facies.

The poor source potential and immaturity of the lower *L.balmei* siltstones and silty claystones evaluated lead to the conclusion that the reservoired hydrocarbons at Trefoil 1 were not sourced insitu and have migrated laterally from the east where the basin depocentre (the Yolla Trough shown in Figure 14) is interpreted to be thermally mature for hydrocarbon expulsion and to contain significant thickness of the coals which have been typed as the source of hydrocarbons elsewhere in the basin.

3.5 MDT Pressure Data Interpretation

The Trefoil 1 MDT programme was conducted over the interval 2626.0 – 3390.0mRT. The Schlumberger MDT tool with a pump-out module, resistivity tool, optical analyser, quartz and strain gauges was used to obtain pressure data and collect reservoir fluid samples. The tool was also fitted with 450cc and 250cc sample chambers. In total 112 pre-tests were performed. 61 pre-tests were valid, 34 were supercharged, 13 were tight tests and 7 failed. Seventeen samples were successfully recovered and 11 pumpout samples were analysed optically downhole. A summary of the pre-test data is included in Appendix 10 of the Trefoil 1 WCR Basic Data (Brooks et al, 2005b).

Interpretation of the MDT data indicates that at least 12 separate gas columns exist in Trefoil 1 and a further 9 zones can be identified from drill stem test results and log analysis (Appendix 2). Several overpressured systems are present in the well as evidenced by the necessity to interpret several different water gradients from the MDT pre-test, pumpout and sample data. Only 3 gas-water contacts can be verified in the well for the 3 gas sands at 2967mRT – 2972mRT, 2979mRT – 2983mRT and 2991mRT – 3002mRT. The water gradient defined for these gas columns places GWC's at 2953.7mRT, 2960.8mRT and 2964.0mRT respectively. A summary of the results is given in Table 1 in section 3.1.

3.6 Drill Stem Testing Interpretation Results

Two cased hole drill stem tests (CHDST) were conducted in Trefoil 1. Table 5 summarises the DST results and a detailed interpretation of the tests can be found in Appendix 3.

In CHDST #1 the depth interval 3141 – 3150mRT (informally referred to as the TuFl-80 zone) was perforated and a maximum flow rate of 16.3mmcfd accompanied by a condensate gas ratio (CGR) of 8.18stb/mmscf. During the sampling flow period the CGR increased to 12.7stb/mmscf.

The second CHDST saw the TlLb-90 zone tested in the depth range 3040.5 – 3046.5mRT. This interval achieved a maximum flow rate of 9.9mmcfd with an associated CGR of 26.0stb/mmscf.

Trefoil-1 CHDST Interpretation Summary

Test	Perfs Top m RT	Perfs Bot m RT	Flow Rate mmcfd	CGR stb/mmscf	FWHP psia	FWHT deg C	Choke /64"	SIWHP psia	Mid Perfs m SS	Gradient psi/m	FBHP psia@MPP	Pi (MDT) psia@MPP	k.h (est.) md.ft	Gas perm md	Total Skin	Comments
CHDST #1	3141.0	3150.0	16.3	8.18	1329	39	48	3493	3101.6	0.289	2613	4489	552	24	11.6	Two reservoir boundaries at 110 degrees at 42 and 46m from the well
CHDST #1 Sampling Flow			14.3	12.7	2004	38	36	3488	3101.6	0.289	3049				9.0	Skin decreased from main flow
CHDST #2	3040.5	3046.5	9.9	26.0	645	31	56	N/A	3003.6	0.334	1543	4305	870	49	64.6	Poor perforations, skin still decreasing. Possible pressure depletion but may be the effect of a leaking PCT valve.

Notes:

1 Reservoir boundaries seen in DST #1 may represent the GWC or possible stratigraphic or fault boundaries

2 Flowing bottomhole pressures, FWHP and FWHT were rising slowly during DST #2, indicating the zone was still cleaning up and stabilising

3 BHP interpretation results for CHDST #2 affected by a leaking PCT valve

4 Skin factors are based on the currently available test data and do not account for future completion practices, well cleanup and later condensate dropout effects

Table 5: Trefoil 1 CHDST Interpretation Summary

4. GEOPHYSICAL DISCUSSION

4.1 Seismic Data

The Trefoil 1 well location was chosen to target anomalous AVO amplitudes at prospective levels within the EVCM, namely the Top Palaeocene, P3, P1 and C1, whilst remaining as structurally crestal as possible at these levels (Figure 7). The well was drilled based on interpretation and mapping using 2002 reprocessing of the existing 2D seismic grid over Trefoil and incorporating line ORS01-13 from the 2001 Shelduck Seismic Survey. The 2002 reprocessing was undertaken to improve resolution within the EVCM section as well as to provide a uniformly processed seismic grid with 'true' amplitudes preserved from which previously recognized AVO anomalies at Trefoil could be assessed.

Further details of both the seismic reprocessing and the geophysical mapping and analysis can be found in the Trefoil Seismic Reprocessing 2002 Final Report, (Origin, 2003) and the 2002 Trefoil Prospect Evaluation, Geophysical Review (Lonergan and Pauli, 2002).

4.2 Structure

The Trefoil structure is a low-relief, four-way dip closed anticline located on the flanks of the Yolla trough. At the target Palaeocene/upper Cretaceous stratigraphic levels it is mapped as a largely fault-independent closure resulting from dip reversal on a northeast plunging structural nose situated on the northeastern side of the White Ibis High (Figure 8).

Trefoil is located in close proximity to Miocene-age volcanics which complicate the velocity field in the vicinity of Trefoil and indeed throughout the Bass Basin (Figure 8). Due to the complicated velocity field and the subtlety of the time closure at Trefoil (less than 20ms) as well as the prevalence of thin stacked gas sands of indeterminate lateral extent, the existing 2D seismic grid over Trefoil is considered to provide inadequate spatial and temporal sampling for sufficiently accurate determination of structural and reservoir configurations. 3D seismic coverage is necessary to better determine these.

Post drill maps to the top of the 3018 mRT and 3054 mRT sands at Trefoil are shown in Figure 9 and 10. These levels correspond to the TlLb-70 and TuFl-10 reservoir zones respectively, as discussed in Section 3.3. They were produced using horizon time picks and time to depth information derived from the VSP survey at Trefoil only (see next section) and do not account for possible subtle lateral variations in the velocity field.

4.3 VSP and Well Tie

A VSP was conducted in Trefoil 1 using Schlumberger's VSI-4 tool with the aim of providing an accurate seismic to well tie. This was especially important given the relatively poor seismic-to-well tie at Aroo 1 which is the only well in the vicinity of Trefoil to penetrate a large part of the Eocene and Palaeocene sections. Acquiring good VSP data at Trefoil 1 was therefore essential for establishing good well-to-seismic control for T/18P.

Processing of the VSP survey data yielded high quality checkshot and corridor stack data to enable confident seismic to well ties at the Trefoil 1 location. Synthetic seismogram and corridor stack trace ties are shown in Figures 11 and

12 respectively. An approximate +19ms bulkshift shift was applied to the checkshot synthetic and corridor stack trace to tie them to seismic line ORS01-13.

Further details of the VSP acquisition and processing may be found in the Trefoil 1 WCR, Basic Data Volume, Appendix 9 (Brooks et al, 2005b).

4.4 Actual versus Predicted Depths

Actual versus predicted formation tops are detailed in Figure 3. Errors in prognosis are due to either incorrect seismic markers being picked for a given horizon and/or the application of incorrect velocities in the pre-drill depth conversion.

The VSP tie to the seismic indicates that the pre-drill top EVCM seismic event was picked half a leg low and actually corresponds to the top TEV4 horizon in Trefoil 1. The top Palaeocene (=base Eocene Unconformity), top P3, top P1 seismic markers were all picked correctly pre-drill and correspond with well picks as demonstrated by the VSP tie (Figure 12). Also, the pre-drill top C1 (=top Cretaceous) marker is now shown to be an intra-Cretaceous seismic event with the actual top of the Cretaceous occurring a leg shallower (Figure 12).

4.5 Seismic Amplitudes

Preliminary analysis of the fluid factor amplitude anomalies associated with the base Eocene/top Palaeocene, P3, P1 and C1 markers indicates that all are valid indicators of in-situ gas. However, petrophysical analysis of the sands associated with anomalies for the base Eocene/top Palaeocene and P3 indicates that these levels contain residual or "fizz" gas only. The correlation between gas pay and AVO anomalies at the Trefoil 1 location is shown in Figure 13. Note that only a base gas sand anomaly (blue) is observed for the intra Cretaceous gas sands in the vicinity of Trefoil 1 on line ORS01-13.

Developing a clear post-drill understanding of the AVO anomalies at Trefoil is complicated by the thin, stacked nature of the gas sands which suggests that the observed anomalies are being generated by constructive and/or destructive interference from numerous contributing seismic interfaces. The planned 3D seismic programme over Trefoil will assist greatly with understanding the observed AVO anomalies whilst also providing a more quantitative means of interpreting them.

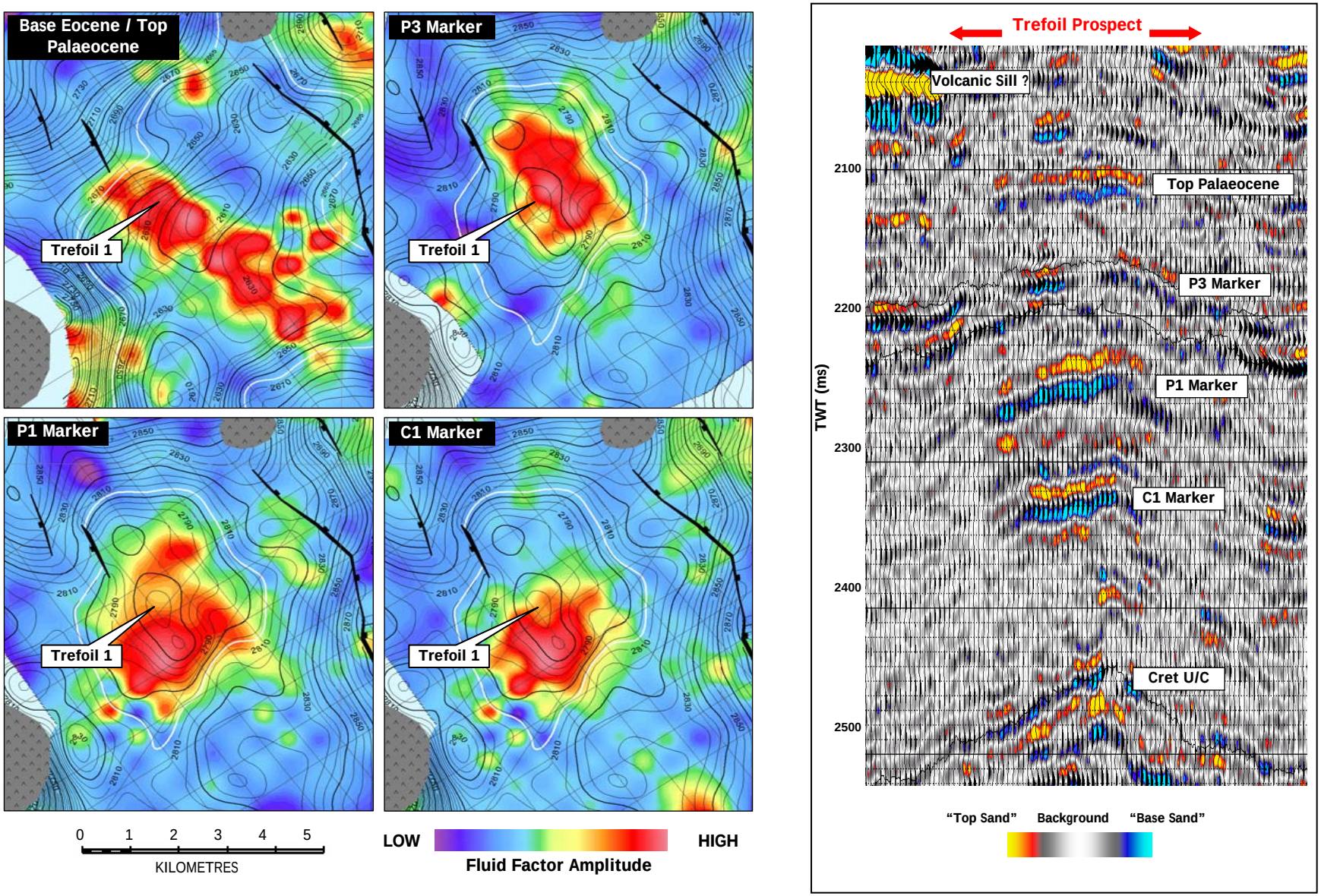


Figure 7: Summary of pre-drill "fluid factor" amplitude and structure mapping in the Trefoil area and example seismic line showing "fluid factor" anomalies

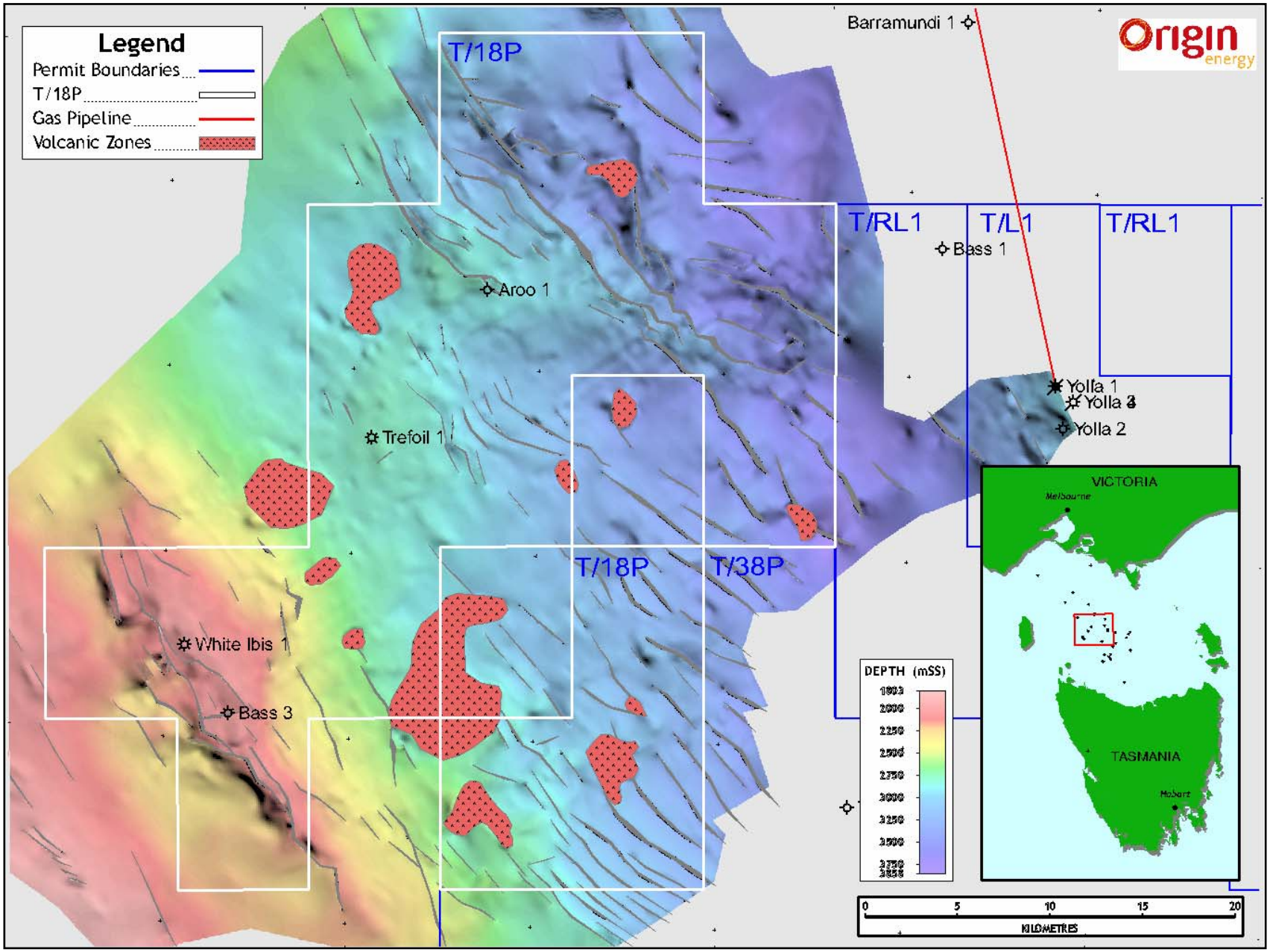


Figure 8: Regional Top P3 Marker Depth Structure Map showing structural configuration of Trefoil and distribution of Miocene-age volcanics

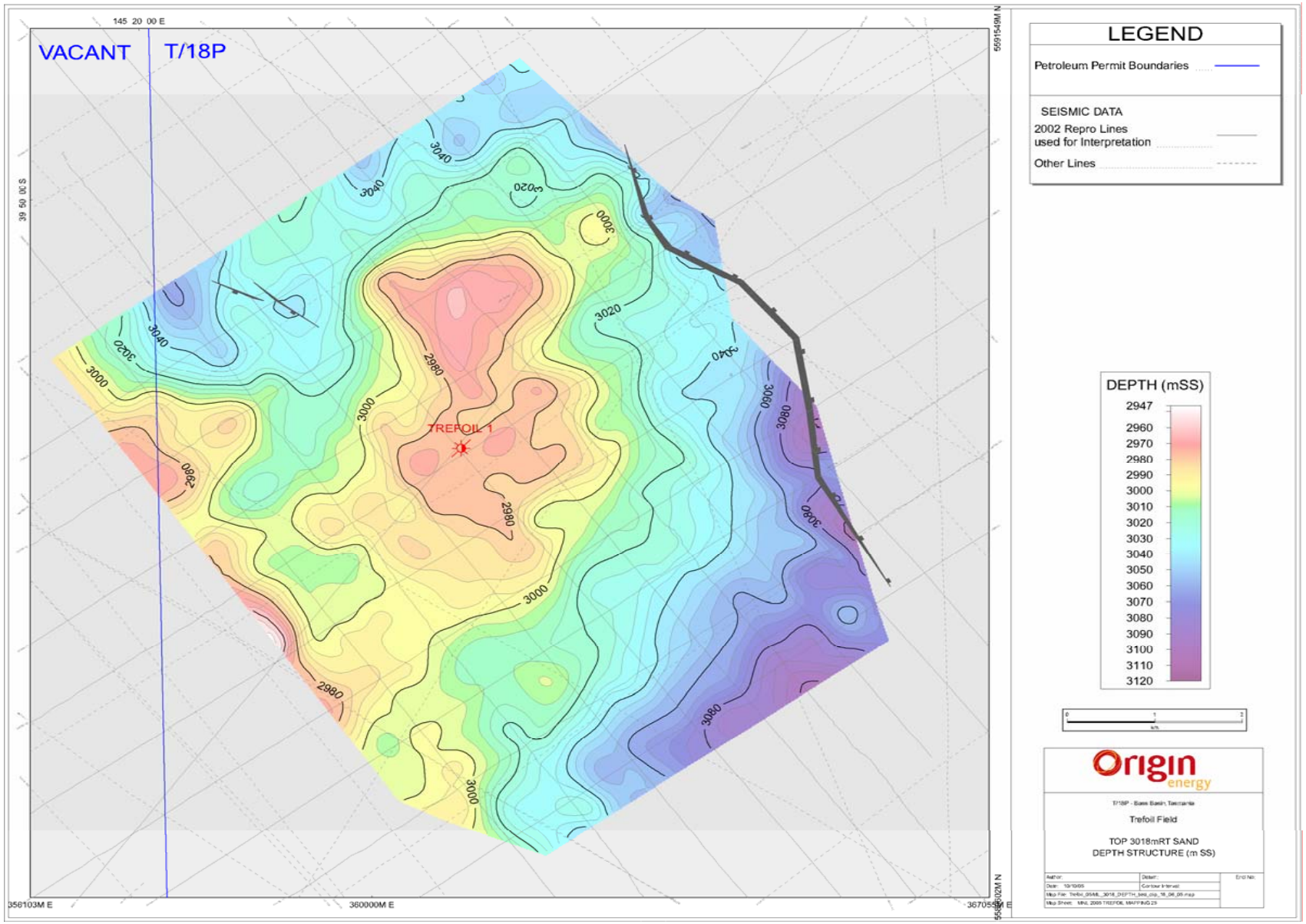


Figure 9: Depth Structure Map for 3018mRT Sand (=TlLb-70 reservoir zone)

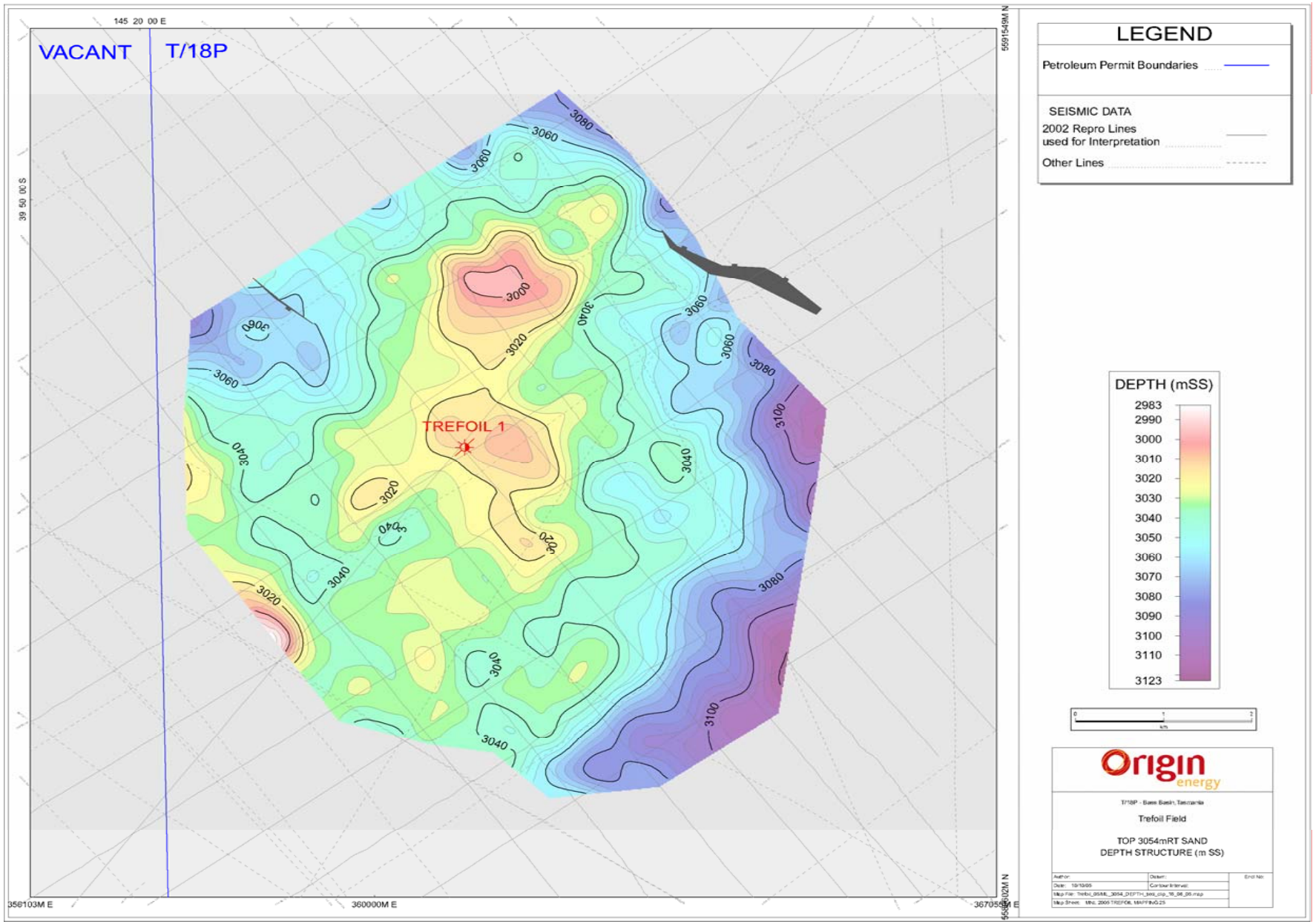


Figure 10: Depth Structure Map for 3018mRT Sand (=TuFl-10 reservoir zone)

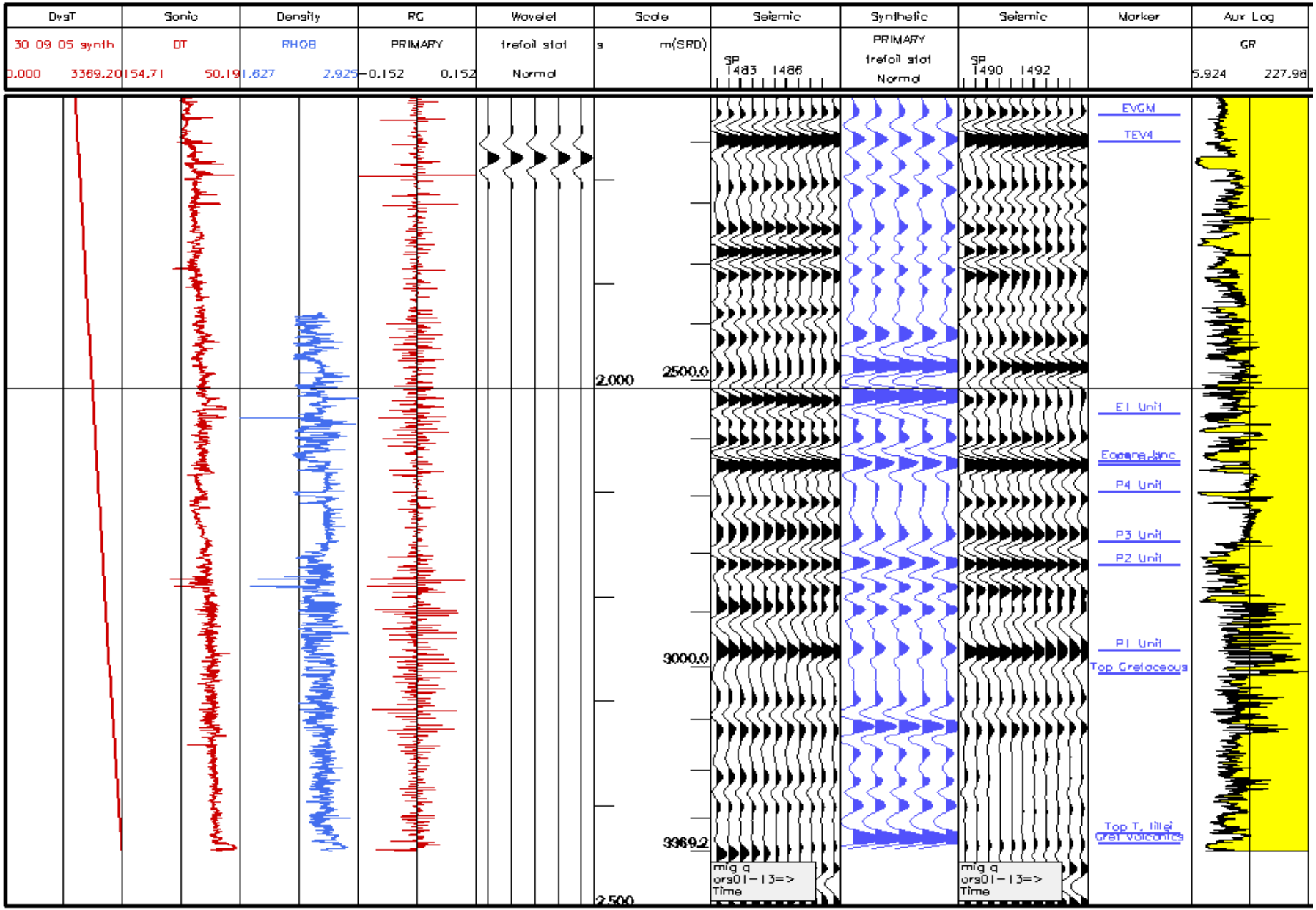


Figure 11: Synthetic seismogram (blue wiggle traces) tied to seismic line ORS01-13 (black wiggle traces) using Trefoil 1 checkshot data. A bulkshift of 19ms has been applied to the synthetic data to achieve the tie.

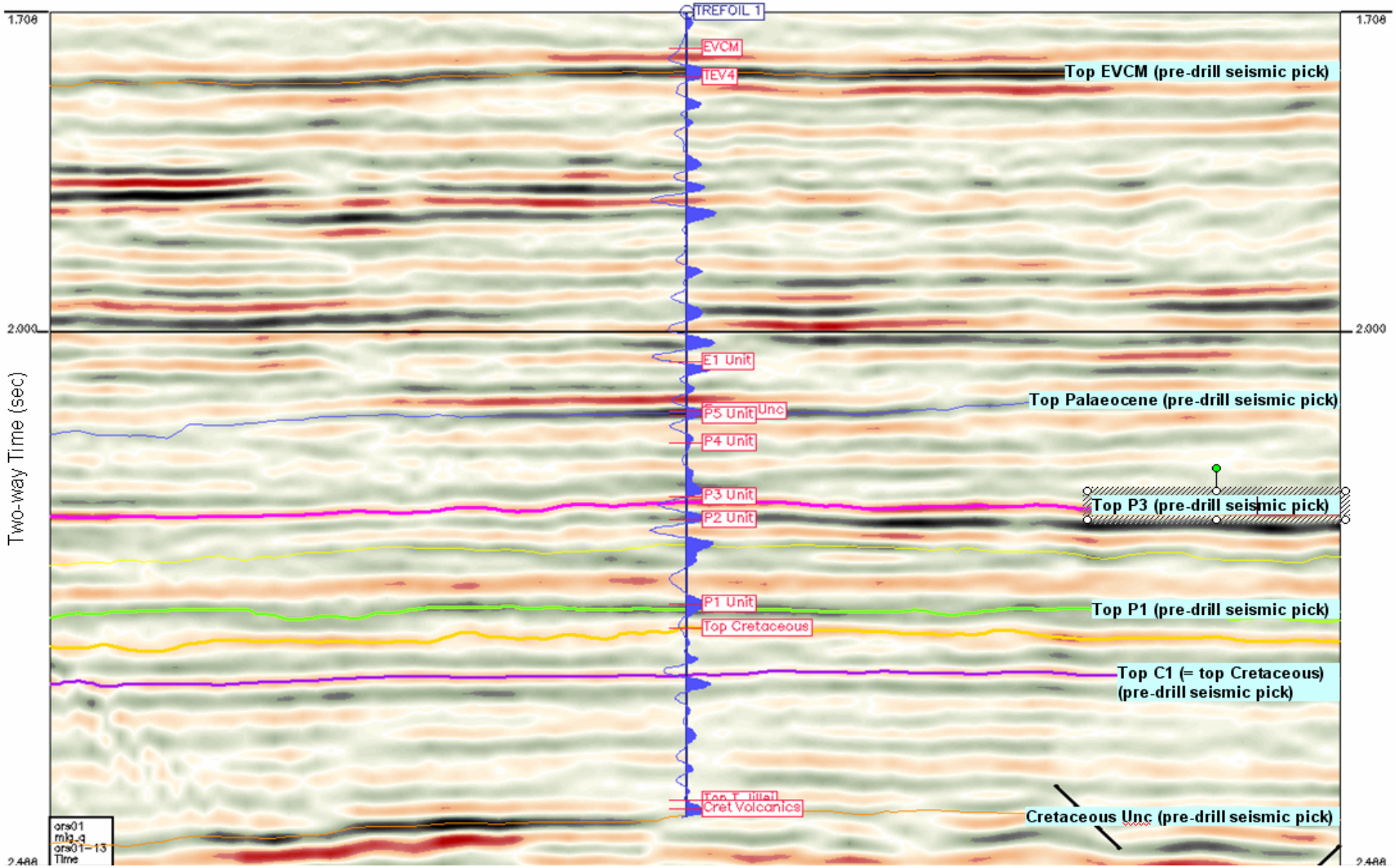


Figure 12: Corridor stack trace from Trefoil 1 VSP (blue wiggle trace) tied to seismic line ORS01-13. A bulkshift of 19ms has been applied to the corridor stack trace to achieve the tie. Pre-drill seismic picks are shown indicating top Palaeocene, P3 and P1 were picked correctly whilst top EVCM and top Cretaceous were picked low.

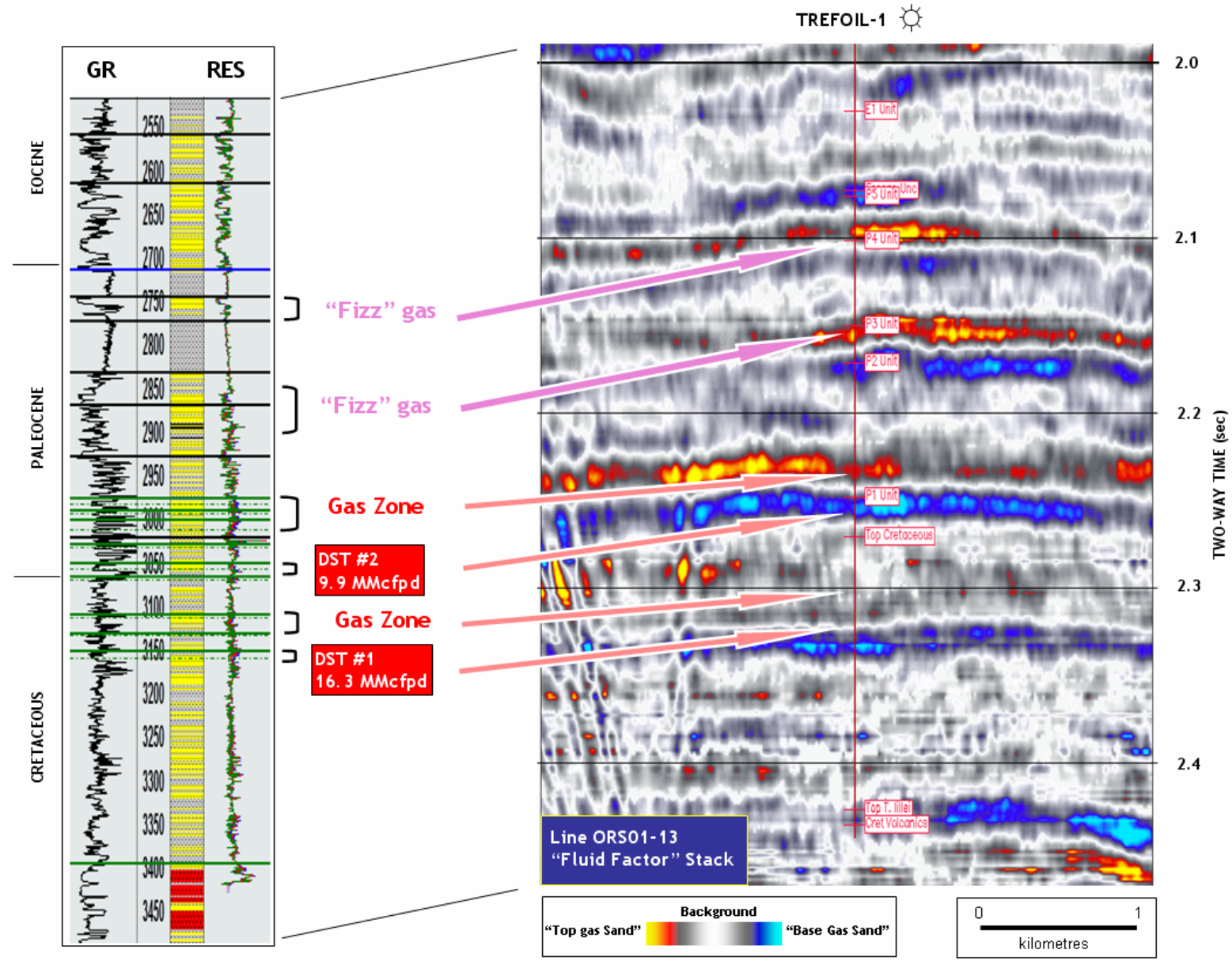


Figure 13: Correlation between gas zones consisting of thin, stacked gas sands and AVO anomalies at the Trefoil 1 location. Note base sand (blue) anomaly only for intra Cretaceous gas sands at this location.

5. GEOLOGICAL DISCUSSION

5.1 Exploration History

Exploration within the area of T/18P commenced in 1963 with the acquisition of regional 2D seismic data (Table 3). Many subsequent seismic surveys have been recorded within the permit with the latest in 2001, the Shelduck 2D survey, bringing the total 2D seismic acquisition in the permit to 6,946.80 km.

Year	Survey Name	No Kilometres
1963	B	146.3
	B63	263.8
1965	EB	62.0
	EK	80.2
1966	ES	29.5
1969	B69B	100.0
1971	B71A	230.5
1972	B72A	582.5
1973	HB73A	297.3
1975	HB75A	440.5
1977	HB77A	318.75
1981	BBS81	419.75
	BCSS81	14.75
1982	82BMR	178.0
	BB82A	34.5
1984	TNK4	660.5
1985	TP05	304.25
	TQH5	1135.25
1990	BS90B	201.5
1994	SB94A (Rocky Cape)	541.0
1996	Hummock	569
2001	Shelduck	376
	TOTAL	**6,946.80**

Table 3: Seismic Acquired within current T/18P permit boundaries

A total of 8 exploration wells have been drilled within the historical permit boundaries (Table 4). An uneconomic oil accumulation was discovered at Cormorant 1 in 1970. A two-metre oil column was identified from logs and a Formation Interval Test (FIT). Subsequent production testing was not performed. The King 1 well confirmed that the oil accumulation is uneconomic. White Ibis 1 discovered sub commercial quantities of gas. The nearest and most relevant wells to Trefoil 1 are Aroo 1, White Ibis 1 and Bass 3, which are all located within the Yolla Trough.

Year	Well Name	Operator	Well Type	Target	Total Depth (m)	Result	Flow Rate/ Recovery
1967	Bass 3	ESSO	Expl	EVCM	2432	P&A	Gas Shows
1970	Cormorant 1	ESSO	Expl	Mid EVCM	3001	P&A	FIT Oil Recovery
1972	Tarook 1	ESSO	Expl	Top EVCM	2774	P&A	-
1974	Toolka 1A	ESSO	Expl	EVCM	2715	P&A	Shows Gas & Condensate
1974	Aroo 1	Hematite	Expl	Mid EVCM	3692	P&A	Shows Gas & Condensate
1985	Koorkah 1	AMOCO	Expl	Basal EVCM	3147	P&A	-
1992	King 1	SAGASCO	Expl	Upper EVCM	2223	P&A	Oil & Gas Shows
1998	White Ibis 1	BORAL (Premier)	Expl	Upper EVCM	2220	P&S	Sub comm. Gas disc

Table 4: Wells Drilled within the historical bounds of T/18P

Aroo 1 was drilled in 1974 as an exploration well on a then interpreted four-way dip closure. The well encountered strong gas and oil shows in the Lower *L. balmei* with minor gas and water recovered on testing. The poor reservoir quality and minor hydrocarbon recovery resulted in the well being plugged and abandoned.

Remapping of the area indicates that no significant closure exists at Aroo 1 but the results of the well prove the migration of hydrocarbons into the area.

Bass 3 was drilled in 1967 as an exploration well on a fault-bounded closure on the southwestern margin of the Yolla Trough. Primary targets were sands in the intra-Eastern View Coal Measures (EVCM). A moderate gas peak in the upper Palaeocene was tested with a recovery of gas, condensate and water. A minor gas peak and fluorescence was also noted in the Late Cretaceous but not tested. The well was plugged and abandoned. The likely causes of failure are inadequate closure and/or fault seal breach.

White Ibis 1 was drilled in 1998 updip of Bass 3 in the adjacent fault block. Gas recoveries were made from sands in the Lower *L. balmei* and based on MDT and gas ratio data an oil leg is possible beneath the gas column. The well is currently suspended for possible future production.

5.2 Regional Geology

5.2.1 Structure

The Bass Basin is located offshore in south-eastern Australia between Victoria and Tasmania. It is one of a series of sedimentary basins that were formed in response to rifting during the Late Jurassic to Early Cretaceous between Australia and Antarctica (Williamson et al, 1987). The Bass Basin covers approximately 65,000 km^2 and water depths range from 30 to 90 m.

The Bass Basin is a failed intra-cratonic rift basin with structural features which highlight three separate phases of evolution: 1) initial northeast-southwest extension during the early Cretaceous, 2) Late Cretaceous to Pliocene thermal subsidence and 3) Miocene compression. The rifting created a series of northwest-southeast oriented graben offset by associated east-west wrench movement. The Pelican, Yolla and Cormorant Troughs comprise the major depocentres in the Bass Basin (Figure 14). The Trefoil structure is located on the flanks of the Yolla Trough. These depocentres are fault-bounded half-graben that progressively developed via growth faulting during the active rifting and thermal subsidence phases of basin evolution. The dominant structural trend in the basin is northwest-southeast, highlighted by the orientation of the major faults and troughs.

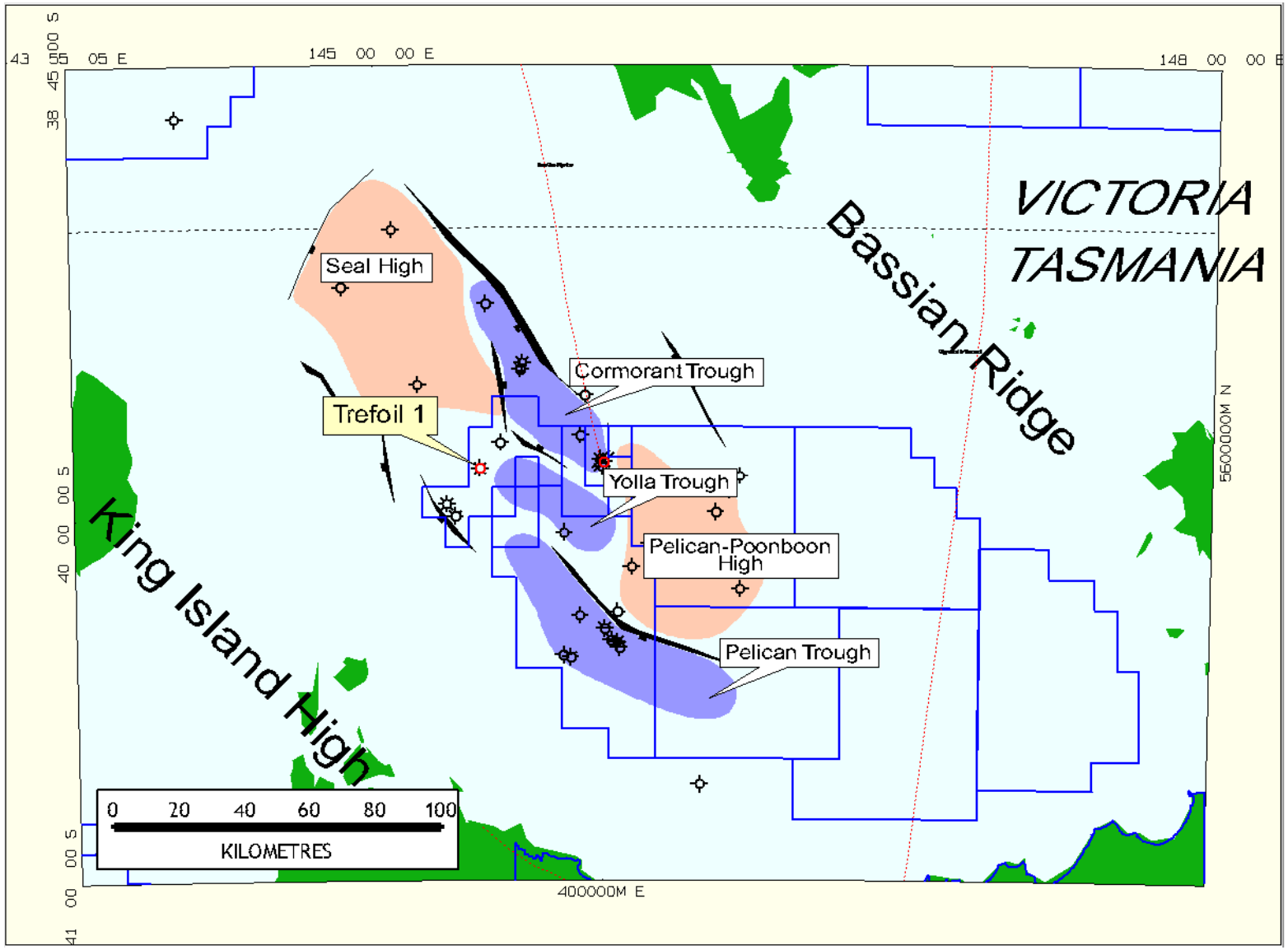


Figure 14: Bass Basin Structural Elements

5.2.2 Stratigraphy

The stratigraphic succession in the Bass Basin comprises sediments ranging in age from Early Cretaceous to Recent (Figure 2).

The Early Cretaceous Otway Group rests unconformably on pre-rift Palaeozoic black shales and quartzites and consists of clastic, volcaniclastic, fluvial and deltaic sediments ranging from coarse-grained sandstone to shale and coal. The Otway Group was deposited as a very thick sequence of sediments (*C. australiensis* to *C. paradoxus*) that have been intersected in the Bass Basin at only one locale, Durroon 1, in the extreme southeast.

Localised uplift and erosion then occurred on the basin margins as the initial rifting phase subsided (Middle Cretaceous). The Otway Drift phase then began along the southern margin of Australia, which was largely contemporaneous with the start of the Tasman Rifting event on the eastern edge of the southern margin. This recommenced rifting in the Bass Basin, which resulted in deposition of the prospective Early Cretaceous to Late Eocene Eastern View Coal Measures (EVCM) which comprise a thick succession of sandstone, siltstone, shale and coal, deposited primarily within fluvial, deltaic and lacustrine depositional environments. Seismic data suggests that the EVCM is over 4000m thick in the Troughs. The EVCM thins markedly towards the basin margins and exhibits both onlap onto basement and erosional truncation. In a broad sense, the EVCM can be divided into three sequences separated by erosional unconformities. The middle sequence was penetrated in Bass 1 and Yolla 1 and 2 and contains the major gas accumulations in the Yolla Field. This sequence is bounded at the base by the *N. senectus* unconformity and at the top by the upper *M. diversus* unconformity.

The Lower Eastern View Coal Measures (EVCM) depositional sequence was deposited from Cenomanian to Santonian times (*A. distocrinatus* to *N. senectus*). These units have only been intersected in Durroon 1 in the southeast of the Bass Basin and are equivalent to the Golden Beach Group in the Gippsland Basin.

An angular unconformity is identified over localised highs on the basin margins at the top of the *N. senectus* zone. The boundary is marked in places by significant extrusive volcanism, similar to that observed in the Gippsland Basin. This event signals the termination of Tasman rifting, which was followed by sea floor spreading in conjunction with the already active drift in the Otway region. During this time, thermal subsidence dominated throughout the basin and thick, ubiquitous deposition of the Late Cretaceous to Palaeocene Lower EVCM occurred (*T. lillei* to Lower *M. diversus/P. asperopolus*).

The Late Cretaceous sediments are restricted mainly to the basin depocentres (such as at Trefoil 1) and axial reaches where accommodation space was sufficient for deposition and subsequent preservation. The section is missing on the basin margins due to sediment bypass. The Palaeocene section is extensive throughout with the greatest thickness of sediments in the basin depocentres and significant thinning towards the basin flanks, as a result of both condensing of the section and basement onlap.

The Late Cretaceous/Palaeocene Lower EVCM has been intersected in numerous wells in the basin, identifying it as a continuos sequence of late low stand sediments grading through a transgressive systems tract and

finally capped by high stand sediments. Environments are gradational both laterally and temporally from alluvial through fluvio-deltaic and nearshore to deeper restricted lacustrine. Primary sediment input to the basin was from the southeast with minor localised input also deposited transversely from the flanks of the troughs. Extensive coal measures dominate the sedimentary sequence in the southeast of the basin (Pelican Trough) with increasingly thicker homogeneous shale units occurring through the Yolla and Cormorant Troughs.

The top of the Lower EVCM is identified by localised uplift and inversion of the pre-existing sedimentary sequence, caused by mild regional compression. The effects of this uplift are variable with the degree of erosion extending from the Mid *M. diversus* through to the *P. asperopolus* in places.

The Eocene upper EVCM (Mid *M. diversus*/*P. asperopolus* to Mid *N. asperus*) was then deposited under a regime of slower subsidence, resulting in more widespread, highly variable facies development. Fluctuating conditions of alluvial, fluvio-deltaic and shallow marine processes resulted with more extensive deposition of coal measure sediments. A regional marine transgression then occurred, resulting in the basin-wide deposition of the Demons Bluff, the base of which is marked by a locally very thick transgressive sand.

Conformably overlying the EVCM is the Late Eocene Demon's Bluff Formation. Lithologically this unit consists of a basal sequence of fine-grained carbonaceous shale and siltstone deposited in an open marine environment. The unit has an average thickness over the basin of approximately 120 m, but thins toward the basin margins. The Demon's Bluff Formation provides a regional top seal to hydrocarbons reservoired in the top-most sandstone units of the EVCM as demonstrated in Yolla 1.

The Demon's Bluff Formation is overlain by the Late Eocene to Pliocene age Torquay Group which broadly consists of a basal sequence of marls and calcareous shales which grade upwards into a succession of bioclastic limestones. The Torquay Group signifies continual deposition under pervasive marine conditions. The Torquay Group is punctuated in places by episodes of minor uplift and/or erosion accompanied by varying effects of volcanism. Large-scale extrusives (volcanoes) are observable on the seismic data (as seen near Trefoil 1) with extensive sill and dyke networks also resulting from these events (as intersected in the Yolla Field wells, Cormorant 1 and Aroo 1).

5.3 Contributions to Geological Concepts and Conclusions

Trefoil 1 has proven the presence of an active petroleum system within the Trefoil structure. Up to 21 separate gas columns have been discovered within Palaeocene and Cretaceous sandstones of the EVCM.

The large number of separate gas columns and several over-pressured zones show that the siltstones and claystones of the lower *L.balmei* and upper *F.longus* act as adequate intra-formational seals.

The Palaeocene and Cretaceous sandstones intersected are fluvial to lacustrine and proximal marginal marine shelf deposits which are mineralogically and texturally immature and were probably sourced from local granitic basement on the basin margin located in the vicinity of the White Ibis Gas discovery and/or from the NW basin margin.

Despite the lack of potential source rocks within Trefoil 1, the presence of gas and condensate proves that a lateral migration pathway exists to the Trefoil structure from the mature source rocks interpreted to be present within the Yolla Trough, to the east of Trefoil 1.

The Trefoil 1 VSP data enabled an excellent well-to-seismic tie for the stratigraphy of the prospective Eocene, Palaeocene and upper Cretaceous sections and will prove valuable in evaluating the Trefoil field as well as the prospectivity of T/18P as a whole. This was especially important given the poor seismic-to-well tie at Aroo 1 which was the only well in T/18P prior to Trefoil 1 to penetrate a large part of the Eocene and Palaeocene sections

AVO anomalies observed on seismic at Trefoil appear to correspond well with trapped gas however work needs to be carried out to understand the behaviour of thin, stacked gas sands and their influence on AVO effects.

3D seismic coverage over the Trefoil field is required to address the spatial sampling inadequacies of the existing 2D seismic grid. 3D seismic will also enable more detailed attribute mapping and provide greater velocity control for future depth conversion work which is necessary given the demonstrated subtlety of the Trefoil closure.

6. REFERENCES

Boreham, C.J., Blevin, J.E., Radlinski, A.P. and Trigg, K.R., 2003 – *Coal as a source of oil and gas: A case study from the Bass Basin, Australia*. APPEA Journal 43 (1) 117-148.

Brooks, D.M., Bierbrauer, K. and Parvar, J., 2005a – *Yolla 4 Well Completion Report Interpretive Volume*, unpublished, Origin Energy, pp 20-21.

Brooks, D.M., Parvar, J., and M. Nasarczyk 2005b – *Trefoil 1 Well Completion Report Basic Data Volume*, unpublished, Origin Energy.

Lennon, R.G., Suttill, R.J., Guthrie, D.A. and Waldron, A.R., 1999 - *The renewed search for oil and gas in the Bass Basin: Results of Yolla 2 and White Ibis 1*. APPEA Journal 39 (1) 248 – 262.

Lonergan, M., Pauli, A., 2002 – *2002 Trefoil Prospect Evaluation, Geophysical Review*, unpublished, Origin Energy.

Origin Energy, 2003 – *Trefoil Seismic Reprocessing 2002 Final Report*, unpublished, Origin Energy.

Williamson, P.E., Pigram, C.J., Colwell, J.B., Scherl, A.S., Lockwood, K.L. and Branson, J.C., 1987 – *Review of stratigraphy, structure and hydrocarbon potential of Bass Basin, Australia*. AAPG Bulletin V.71, No.3, 253-280.

APPENDIX 1: PETROPHYSICS REPORT

T/18P, BASS BASIN, TASMANIA

TREFOIL-1

PETROPHYSICAL INTERPRETATION

EASTERN VIEW COAL MEASURES

2420 – 3545 mRT

FINAL

Origin Energy Resources Limited
Second Floor, South Tower, John Oxley Centre
339 Coronation Drive
MILTON QLD 4064

Andy Hall, July 2005

EXECUTIVE SUMMARY

Trefoil-1 was drilled as an exploration well to determine the potential of an anticlinal structure on the western flank of the Bass basin. The well spudded on the 30th October 2004 and reached TD on the 23rd November 2004.

The petrophysical analysis was conducted using the wireline log data for porosity, permeability and shale volume calculation, but using the deep resistivity LWD log for calculating water saturation, since invasion appears to have affected even the deep resistivity wireline log.

One full diameter core was acquired in the interval above the gas bearing reservoirs and is not considered directly relevant to the reservoir sands. It was, however, used to calibrate the tool responses in the overlying interval and an excellent match was obtained between the core and log derived porosity and permeability.

Two production tests were conducted between 3040 – 3047 mRT (zone TlLb-90) and 3141 – 3150 mRT (zone TuFl-80). These resulted in gas flows of 9.9 mmscf/d and 16.3 mmscf/d respectively. The well has been plugged and suspended as a future producer.

Results

The results presented here follow the reservoir zonation presented by Origin in the Well Completion Report and used in the Petrel field model.

Most of the reservoir zones are within the transition zone between irreducible gas saturation and the GWC, hence the calculated water saturations are quite high.

The well is interpreted to have 106.7 mMD of net sand of which 49.0 mMD constitutes net pay (Table 1) in the main reservoir intervals. This net pay is divided into numerous (possibly up to 20) discreet layers (Reference 1).

The reservoir has been zoned into three basic units, P2, P1 and C1.

- The P2 sandstones (2930 – 3018 mRT) (zones TlLb-10 to TlLb-60) are 88 mMD thick and contain 39 mMD of net sand with an average porosity of 13.2% and permeability of 28 mD. 19.3 mMD is calculated to be net pay with an average porosity of 13.7%, permeability of 43 mD and water saturation of 49%.
- The P1 sandstones, which include some of the Cretaceous sands, (3018 – 3121 mRT) (zones PlLb-70 to TuFl-40) are 103 mMD thick and contain 25 mMD of net sand with an average porosity of 12.3% and permeability of 14 mD. 13.2 mMD is calculated to be net

pay with an average porosity of 12.7%, permeability of 22 mD and water saturation of 51%.

- The upper C1 sandstones (3121 – 3161 mRT) (zones TuFl-50 to TuFl-90) are 40 mMD thick and contain 14 mMD of net sand with an average porosity of 12.5% and permeability of 18 mD. 10 mMD is calculated to be net pay with an average porosity of 12.8%, permeability of 22 mD and water saturation of 48%.
- The mid-C1 interval (3161 – 3385 mRT) (zones TuFl-100 and TuFl-110) is predominantly non-net, but does contain 27 mMD of net sand with an average porosity of 10.8% and permeability of 3.5 mD. 5.3 mMD is calculated to be net pay with an average porosity of 10.6%, permeability of 3.0 mD and water saturation of 53%.
- The lower C1 sandstone (3385 – 3390 mRT) (zone TTl-10) is 5 mMD thick and contains 2.1 mMD of net sand with an average porosity of 10.1% and permeability of 2 mD. 1.5 mMD is calculated to be net pay with an average porosity of 10.0%, permeability of 2.3 mD and water saturation of 44%.

The results of the interpretation are presented in Table 1.

In three zones, TlLb-40, TlLb-50 and TlLb-60, the GWC are defined from the pressure data (Table 2). These zones have hydrocarbon column heights of 27, 22 and 13 mMD respectively. The GWC for all other zones was generated by comparing the log and capillary pressure derived water saturation. The column heights vary from less than 10 mMD to 20 mMD in zone TlLb-90.

Table 1: Net Sand and Net Pay Summary for Trefoil-1

Zone Name:	GROSS INTERVAL			NET SAND					NET PAY					
	TOP (mRT)	BASE (mRT)	THK (mMD)	THK (mMD)	NTG (Fraction)	Porosity (Fraction)	NPT (mMD)	Permeability (Geomean)	THK (mMD)	NTG (Fraction)	Porosity (Fraction)	NPT (mMD)	Permeability (Geomean)	Sw (Fraction)
Overburden	2420.0	2743.0	323.0	100.6	0.312	0.210	21.163	56.946	0.00	0.00	0.000	0.000	0.00	0.000
Seal	2743.0	2844.0	101.0	2.8	0.028	0.184	0.524	8.669	0.00	0.00	0.000	0.000	0.00	0.000
Wet Sands	2844.0	2967.1	123.2	49.9	0.405	0.168	8.401	12.17	2.16	0.02	0.147	0.316	65.93	0.519
P2	**2930.0**	**3018.0**	**88.0**	**39.1**	**0.444**	**0.132**	**5.157**	**28.0**	**19.3**	**0.219**	**0.137**	**2.654**	**43.2**	**0.492**
TlLb-10	2930.0	2941.9	11.9	3.4	0.286	0.145	0.493	57.1	1.2	0.10	0.144	0.174	53.1	0.463
TlLb-20	2941.9	2956.9	15.0	2.6	0.173	0.120	0.312	8.6	0.3	0.02	0.155	0.047	127.8	0.561
TlLb-30	2956.9	2966.9	10.0	3.5	0.350	0.132	0.462	21.9	1.1	0.11	0.142	0.156	47.7	0.543
TlLb-40	2966.9	2979.0	12.1	6.1	0.504	0.134	0.817	27.4	5.2	0.43	0.138	0.718	39.7	0.466
TlLb-50	2979.0	2989.9	10.9	7.3	0.670	0.139	1.015	35.2	5.9	0.54	0.141	0.832	40.2	0.482
TlLb-60	2989.9	3018.0	28.1	16.2	0.577	0.128	2.074	23.4	5.6	0.20	0.130	0.728	42.1	0.522
P1	**3018.0**	**3121.0**	**103.0**	**24.9**	**0.242**	**0.123**	**3.071**	**14.4**	**13.2**	**0.128**	**0.127**	**1.679**	**21.9**	**0.505**
TlLb-70	3018.0	3025.9	7.9	3.5	0.443	0.108	0.378	5.9	2.4	0.30	0.113	0.271	7.8	0.475
TlLb-80	3025.9	3039.9	14.0	2.6	0.186	0.132	0.343	21.1	2.0	0.14	0.135	0.271	26.4	0.478
TlLb-90	3039.9	3053.9	14.0	6.6	0.471	0.126	0.831	13.8	4.4	0.31	0.125	0.550	12.8	0.491
TuFl-10	3053.9	3066.0	12.1	2.1	0.174	0.135	0.284	27.6	0.9	0.07	0.147	0.133	70.0	0.561
TuFl-20	3066.0	3093.9	27.9	0.8	0.029	0.120	0.096	9.0	0.0	0.00		0.000		
TuFl-30	3093.9	3109.0	15.1	7.9	0.523	0.119	0.942	8.4	2.4	0.16	0.122	0.294	10.6	0.545
TuFl-40	3109.0	3121.0	12.0	1.4	0.117	0.141	0.197	42.8	1.1	0.09	0.147	0.161	66.0	0.530
C1	**3121.0**	**3160.9**	**39.9**	**14.1**	**0.353**	**0.125**	**1.762**	**24.4**	**9.7**	**0.244**	**0.128**	**1.244**	**22.1**	**0.481**
TuFl-50	3121.0	3125.9	4.9	1.4	0.286	0.148	0.207	74.5	1.4	0.29	0.148	0.203	74.5	0.383
TuFl-60	3125.9	3132.0	6.1	1.1	0.180	0.132	0.145	22.5	0.5	0.08	0.141	0.063	42.7	0.532
TuFl-70	3132.0	3140.4	8.4	1.2	0.143	0.120	0.144	8.5	0.9	0.11	0.117	0.106	7.3	0.529
TuFl-80	3140.4	3152.0	11.6	9.3	0.802	0.121	1.125	9.5	5.9	0.51	0.124	0.734	11.7	0.498
TuFl-90	3152.0	3155.9	3.9	0.0	0.000		0.000		0.0	0.00		0.000		
TuFl-100	3155.9	3160.9	5.0	1.1	0.220	0.128	0.141	16.8	1.1	0.22	0.128	0.137	16.8	0.473
TuFl-110	3160.9	3385.0	224.1	27.0	0.120	0.108	2.916	3.5	5.30	0.02	0.106	0.562	3.0	0.528
TTl-10	3385.0	3390.0	5.0	1.7	0.340	0.101	0.172	2.1	1.50	0.30	0.102	0.153	2.3	0.443

Table 2: Gas-Water Contacts Derived from the MDT and Log Interpretation

Zone	Top (mRT)	Base (mRT)	Thk (mMD)	Gas content verified by	MDT Interpretation			Log Analysis	
					Contact Type	Depth (mSS)	Depth (mRT)	Depth (mRT)	Column Height (mMD)
TlLb-10	2931	2934	3	MDT sample	LKG	2894.1	2934	2940	9
TlLb-20	2942	2952	10	No MDT or CHDST data				2947	5
TlLb-30	2957	2960	3	MDT pump-out	LKG	2920.4	2960.3	2961	4
TlLb-40	2967	2972	5	MDT sample	GWC	2953.7	2993.6	2993.6	26.6
TlLb-50	2979	2983	4	MDT sample	GWC	2960.8	3000.7	3000.7	21.7
TlLb-60	2991	3002	11	MDT sample	GWC	2964.0	3003.9	3003.9	12.9
TlLb-70	3018	3022	4	Not verified	LKG	2983.6	3023.5	3030	12
TlLb-80	3026	3029	3	MDT sample	LKG	2989.1	3029.0	3038	12
TlLb-90	3040	3047	7	CHDST	LKG	3007.1	3047.0	3060	20
TuFl-10	3054	3059	5	MDT sample	LKG	3019.1	3059.0	3059	5
TuFl-20	3066	3072	6	No MDT or CHDST data				Not evaluated	
TuFl-30	3094	3108	14	MDT pump-out	LKG	3068.0	3107.9	3108	14
TuFl-40	3109	3111	2	Not verified	LKG	3071.1	3111.0	3115	6
TuFl-50	3121	3123	2	Not verified	LKG	3082.6	3122.5	3135	14
TuFl-60	3126	3131	5	Not verified	LKG	3090.9	3130.8	3130	4
TuFl-70	3132	3136	4	No MDT or CHDST data				3150	18
TuFl-80	3141	3150	9	CHDST	LKG	3111.1	3151.0	3155	14
TuFl-90	3153	3158	5	MDT pump-out	LKG	3118.1	3158.0	3160	7
TuFl-100	3161	3163	2	No MDT or CHDST data				3170	9
TuFl-110	3166	3169	3	No MDT or CHDST data				3165	9
TTl-10	3385	3390	5	MDT sample	LKG	3347.7	3387.6	3395	10

TABLE OF CONTENTS

EXECUTIVE SUMMARY 2
Results 2

BOREHOLE DATA 8
Hole and Casing Size 8
Elevation and Deviation 8
Logging While Drilling (LWD) Data 8
Wireline Log Data 8
Mud Properties 9
Borehole Temperature 10
Core Data 10
Mud Log Data 12

LOG ANALYSIS METHODOLOGY 22
Shale Volume 22
Porosity 22
Permeability 23
Water Saturation 24
Formation Water Salinity 24
Calculation of Water Saturation 24
Gas-Water Contact 25
Net Pay Cut-offs 25

REFERENCES 27

Figures

Figure 1: Overburden vs Ambient Porosity / Permeability for the Full Diameter Core 14
Figure 2: Porosity Permeability Relationship for Trefoil-1 15
Figure 3: Determination of Cementation Exponent for the MSCT Plugs 16
Figure 4: Determination of Saturation Exponent for the MSCT Plugs 17
Figure 5: Residual Gas Saturation As a Function of Permeability 18
Figure 6: Capillary Pressure Curves (converted to 'J' Function vs Water Saturation) for the Trefoil MSCT Cores 19
Figure 7: Capillary Pressure Curves (converted to 'J' Function vs Water Saturation) for the Trefoil MSCT Cores Together with the Modelled Functions Used in the Petrophysics Interpretation 20
Figure 8: sand Quality Determination for the Core Plug Data 21
Figure 9: Horner Plot for Trefoil-1 13
Figure 10: Ionic Composition for the Trefoil-1 MDT Water Samples 26

Tables

Table 1: Net Sand and Net Pay Summary for Trefoil-1 4
Table 2: Gas-Water Contacts Derived from the MDT and Log Interpretation 5

Enclosures

1. Trefoil-1 EVCM (2450 – 3545 mRT) Petrophysical summary plot 1:500

BOREHOLE DATA

Hole and Casing Size

Borehole		Casing	
Diameter (inches)	Section TD (mRT)	Outer Diameter (inches)	Shoe Depth (mRT)
36	218	20	215
16	666	13 $^{3}/_{8}$	657
12 ¼	2428	9 $^{5}/_{8}$	2421
8 ½	3545	6 $^{5}/_{8}$	3458

Elevation and Deviation

The well datum, the rotary table elevation (RTE), was 39.9 metres above mean sea level. The water depth was 68.9 metres.

Maximum deviation was 0.73° at 3421 mRT. The correction between along hole and true vertical depth (RT) is 0.05 metres at TD.

Logging While Drilling (LWD) Data

LWD gamma and resistivity logs were acquired in the 12 ¼" hole section between 657 - 2428 mRT. The density and neutron logs were added to the LWD suite for the 8 ½" hole section (2421 – 3545 mRT).

A comparison of the LWD and wireline logs (acquired post-TD) was made. This showed that the LWD resistivity was read slightly higher than the true wireline resistivity and it is interpreted that even the deep wireline resistivity is affected by borehole fluid invasion. The LWD and wireline gamma and density curves were very similar. The LWD neutron log read significantly higher than the wireline equivalent in large portions of the hole.

All LWD logs were depth corrected to the wireline datum used in this well across the reservoir interval.

Wireline Log Data

Wireline runs #1, #2 and #3 / #3a would not pass below 3420 mRT due to a ledge or swelling clays in the hole. A wiper trip was conducted after Run #3 and logs were acquired to TD after this.

The MDT samples and pre-test pressures were acquired in two runs due to possible deteriorating hole condition and the possibility of getting stuck-in-hole (Reference 1).

- The first MDT run (#3), took 79 pre-test pressures and tested the moveable fluid using the pump-out facility. 12 samples were acquired.
- The second MDT run acquired 33 pre-test pressures and 6 samples. Further tests of the moveable fluid were made using the pump-out facility.

The MSCT cores were acquired in three runs. 10 plugs were acquired in the first tool run, 24 in the second and 9 in the third.

Run	Log	Top (mRT)	Base (mRT)	Maximum Temperature (°C)
#1	PEX-HRLA-CMR-SP-GR	2420.1	3418.3	117.0
#2	VSI-GR	319.0	3419.0	119.4
#3	MDT-GR (1)	2626.0	3390.0	
#4	MSCT (1)	2812.0	3046.5	115.0
#5	MDT-GR (2)	2926.0	3524.0	
#6	MSCT (2)	2968.3	3018.2	128.0
#7	MSCT (3)	3009.0	3414.0	128.0
#8	FMI-DSI-HNGS	2420.1	3527.0	133.0

The HRLA resistivity logs show significant drilling mud invasion in the potential reservoir intervals. A comparison between the calculated true resistivity (RT_HRLT) and the LWD deep resistivity (SEDP) suggests that the invasion is affecting even the deepest wireline log. Hence, depth corrected SEDP was used as the best measure of the true formation resistivity in the water saturation calculation.

Mud Properties

The following mud properties were taken from the Schlumberger log plot for Run #1 of the TD wireline logging suite.

Rm		Rmf		Rmc		Mud Weight
(Ω.m)	(°C)	(Ω.m)	(°C)	(Ω.m)	(°C)	(lb / gal)
0.206	25	0.174	25	0.280	25	9.4

Borehole Temperature

Bottom hole temperatures were recorded in 6 logging runs and for the MDT samples. After three logging runs, a wiper trip was performed. Since this will change the thermal field in the well, the logged temperatures after this time are used as a guide only and are not included in the Horner Plot.

The maximum temperature recorded in any logging run was 133°C at 3527 mRT (129°C at 3406.8 mRT) in the final logging run (FMI-DSI-HNGS), about 8 days after TD was reached, but after the wiper trip and associated recirculation.

Using the data from the borehole prior to the wiper trip, the bottom hole temperature is calculated to be 134.3°C at 3366.1 mTVDSS (3406.8 mRT), equivalent to a geothermal gradient of 38.3°Ckm^{-1} (Figure 1). Sea bed (108.8 mRT) temperature was assumed to be 8°C.

The temperature from Run 1 / 1 PEX-CMR-HRLA-GR (117°C at 3406.8 mRT) was used when applying corrections to the wireline logs. Water saturation was calculated using the LWD logs and so the true formation temperature calculated from the Horner Plot was used.

Core Data

Full diameter core was acquired between 2735 – 2742 mRT (drillers depth). Additionally, 39 rotary sidewall cores were acquired between 2968 – 3028 mRT and one at 3414 mRT in three runs of the MSCT.

Routine Core Analysis

Porosity, permeability and grain density were measured on 27 plugs from the full diameter core and attempted on all the MSCT plugs. Additionally, 8 overburden porosity and permeabilities were measured on the full diameter core data using an overburden pressure of 5000 psi. No overburden measurements were made on the MSCT plugs. A linear conversion was used for both the porosity and permeability conversion as given below (Figure 2) and applied to the full diameter and MSCT plug data:

$$\text{OB Porosity} = \text{Ambient Porosity} * 0.9505 \qquad \text{(Equation 1)}$$

$$\text{OB Permeability} = \text{Ambient Permeability} * 0.8558 \qquad \text{(Equation 2)}$$

A core gamma ray was recorded to enable the full diameter core to be depth matched with the wireline logs. Unfortunately, this is not very useful in this core as it is a featureless trend of increasing radioactivity towards the base with no good depth match features. Currently,

the two poor porosity plugs at the base of the core have been used to tie the depth to wireline (core 0.8 metres high of wireline datum). No depth correction is needed for the MSCT plugs.

The porosity – permeability relationship for the MSCT and full diameter cores (overburden corrected) is shown in Figure 3. There is an obvious difference between the porosity / permeability relationship for the full diameter core and MSCT samples that probably originates from the mineralogical composition of the sandstone and this is reflected in the gamma ray. The following relationships were used to derive the porosity related permeability (POPE):

Above 2920 mRT: $\text{OB Permeability (POPE)} = 0.00011 * e^{0.6321 * \text{OB Porosity}}$ (Equation 3)

Below 2920 mRT: $\text{OB Permeability (POPE)} = 0.00100 * e^{0.7574 * \text{OB Porosity}}$ (Equation 4)

The variation in porosity and permeability due to the thinly bedded lithology in the reservoir interval can be seen from two MSCT plugs, 1/7 and 2/14, acquired at the same depth (2993.8 mRT), within measurement error of the tool. The measured porosity varies from 10.8 to 12.4% and the permeability from 64 to 125 mD.

Special Core Analysis

The cementation exponent ('m') was measured on 1 plug from the full diameter core and 5 MSCT plugs. The measured value (1.86) for the full diameter core has been applied to all intervals above 2920 mRT. The Formation Resistivity Factor vs Porosity plot for the MSCT plugs (Figure 4) shows that 'm' is approximately 1.74. This value was applied below 2920 mRT.

The saturation exponent ('n') was also measured on one plug from the full diameter core and 5 MSCT plugs. The measured value (1.74) for the full diameter core has been applied to all intervals above 2920 mRT. These intervals were all water bearing. The saturation exponent data from the MSCT plugs was modelled without a variation against saturation (Figure 5) and was set to 1.61 for all intervals below 2920 mRT.

Residual gas saturation (assumed to be the lowest quoted saturation in the capillary pressure data) was plotted against core OB permeability (Figure 6). The residual gas saturation was calculated throughout the potential gas leg from the core derived permeability (POPE curve) using the function given on this chart.

Capillary pressure measurements have been made on three plugs from the full diameter core and 11 MSCT plugs. The plugs from the full diameter core are in a different facies to the gas - bearing sands and have not been included in this interpretation. The OB porosity and permeability data from each curve, along with the applied pressure and measured saturation, was used to calculate the 'J' function. The 'J' function was then plotted against water saturation (Figure 7). This shows a range between 15 – 30% for the residual water saturation in samples well above the GWC.

Three basic groups of capillary pressure curve were recognised - good sandstones, moderate sandstones and poor sandstones / siltstones (Figure 8).

Good Sandstones: $Sw_CP = 60.909 * J ^ -0.332$

Moderate Sandstones: $Sw_CP = 61.166 * J ^ -0.253$

Poor Sandstones: $Sw_CP = 67.951 * J ^ -0.218$

The core derived Reservoir Quality Index (RQI) (incorporating porosity and permeability) was plotted against porosity to differentiate between the plug quality (Figure 9). This was generally successful in discriminating between the capillary pressure categories given in Figure 8. The RQI was also calculated from log data and used to allocate capillary pressure curves for each data point.

The final input to calculate water saturation from capillary pressure curves is the depth of the Gas-Water-Contact (GWC). This was determined from the measured fluid gradients in zones where the GWC is clearly defined or by adjusting the GWC until it matched the calculated gas saturation in poorly defined zones. The definition of the GWC from the pressure data depended primarily upon the confidence that could be placed in the absolute value of the water gradient (Reference 1).

Mud Log Data

The well was logged throughout with the new Geoservices Reserval mud logging system. An informal report has been put together by Geoservices for this (Reference 2). This report used the mud gas ratios to determine properties of the hydrocarbons trapped.

Figure 1: Horner Plot for Trefoil-1

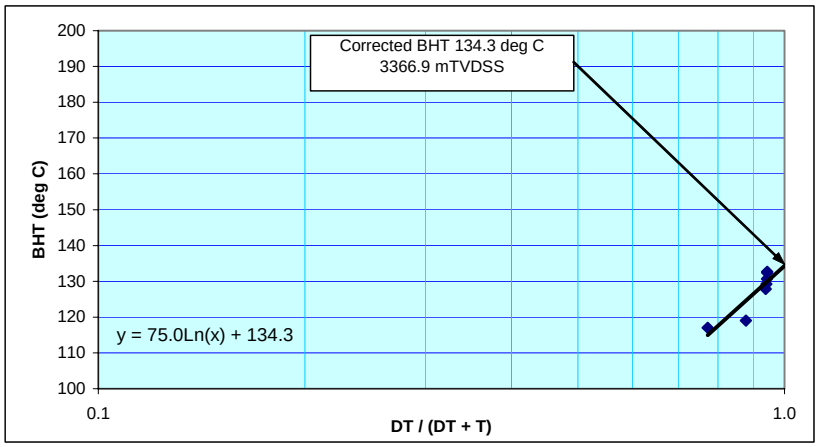
Trefoil-1
Suite 1
Horner Plot

TD reached	23/Nov/04 20:45	RTE (metres)	39.9
Time circulation stopped	24/Nov/04 00:45	Water Depth (metres)	68.9
Circulation time	4:00:00	Depth (mTVDSS)	3366.9
		Sea bed temperature (Deg C)	8

Log Run	Depth (mRT)	Depth (m TVDSS)	Measured BHT (oC)	Corrected BHT (oC)	Time Breakdown: On bottom	Time Breakdown: Since Circulation (Hrs)	DT / (T+DT)
SP_HRLA-PEX-CMR	3406.8	3366.9	117.0	117.0	24/Nov/04 14:20	13:35:00	0.773
VSI	3419.0	3379.1	119.4	119.0	25/Nov/04 05:45	29:00:00	0.879
MDT Run 1 S1.01	3264.0	3224.1	122.6	127.9	26/Nov/04 14:31	61:46:00	0.939
MDT Run 1 S1.02	3142.7	3102.8	119.4	129.2	26/Nov/04 16:28	63:43:00	0.941
MDT Run 1 S1.03	3057.2	3017.3	117.5	130.7	26/Nov/04 19:07	66:22:00	0.943
MDT Run 1 S1.04	3006.5	2966.6	117.1	132.4	26/Nov/04 19:21	66:36:00	0.943
MDT Run 1 S1.05	2968.7	2928.8	115.9	132.7	26/Nov/04 19:36	66:51:00	0.944

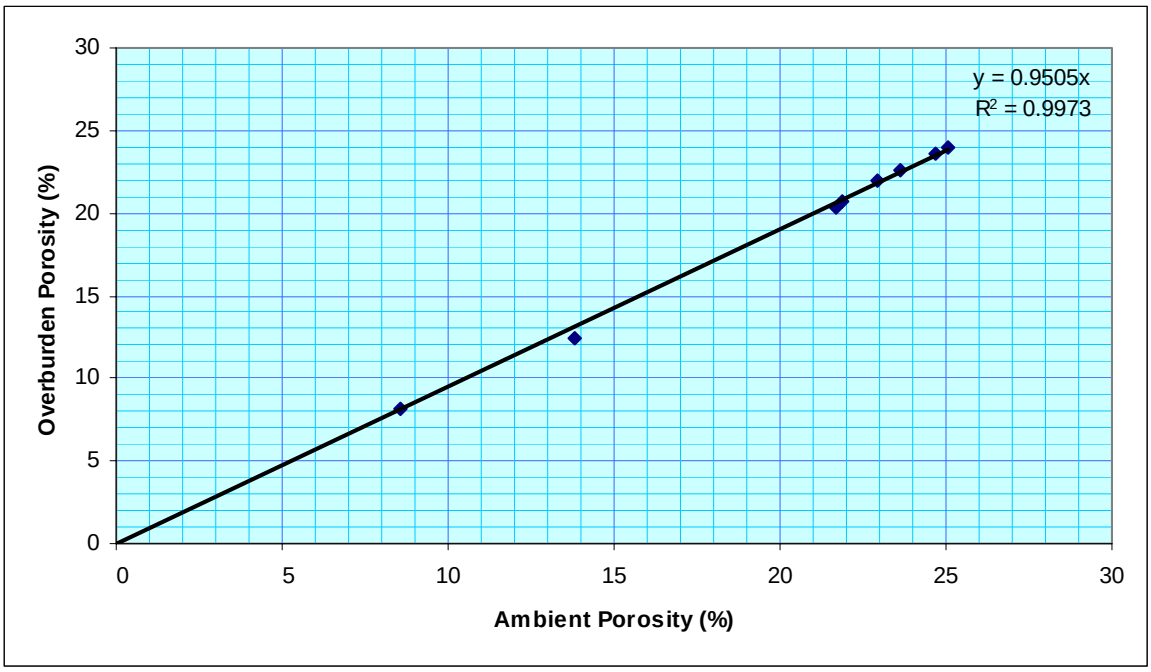
Wiper Trip

Log Run	Depth (mRT)	Depth (m TVDSS)	Measured BHT (oC)	Corrected BHT (oC)	Time Breakdown: On bottom	Time Breakdown: Since Circulation (Hrs)	DT / (T+DT)
MSCT Run 1	3046.5	3006.6	115	128.3	29/Nov/04 02:43		
MSCT Run 2	3018.2	2978.3	128	144.3	01/Dec/04 06:28		
MSCT Run 3	3414.0	3374.1	128	127.7	01/Dec/04 02:43		
FMI-DSI-HNGS	3527.0	3487.1	133	128.6	01/Dec/04 22:35		
MDT Run 2 S2.01	3388.7	3348.8	126.1	126.8	29/Nov/04 18:41		



Depth (m TVDSS)	3366.9
BHT	134.3
Sea bed temp (oC)	8
Water Depth	68.9
Geothermal Gradient (deg C per km)	38.3

Figure 2: Overburden vs Ambient Porosity / Permeability for the Full Diameter Core



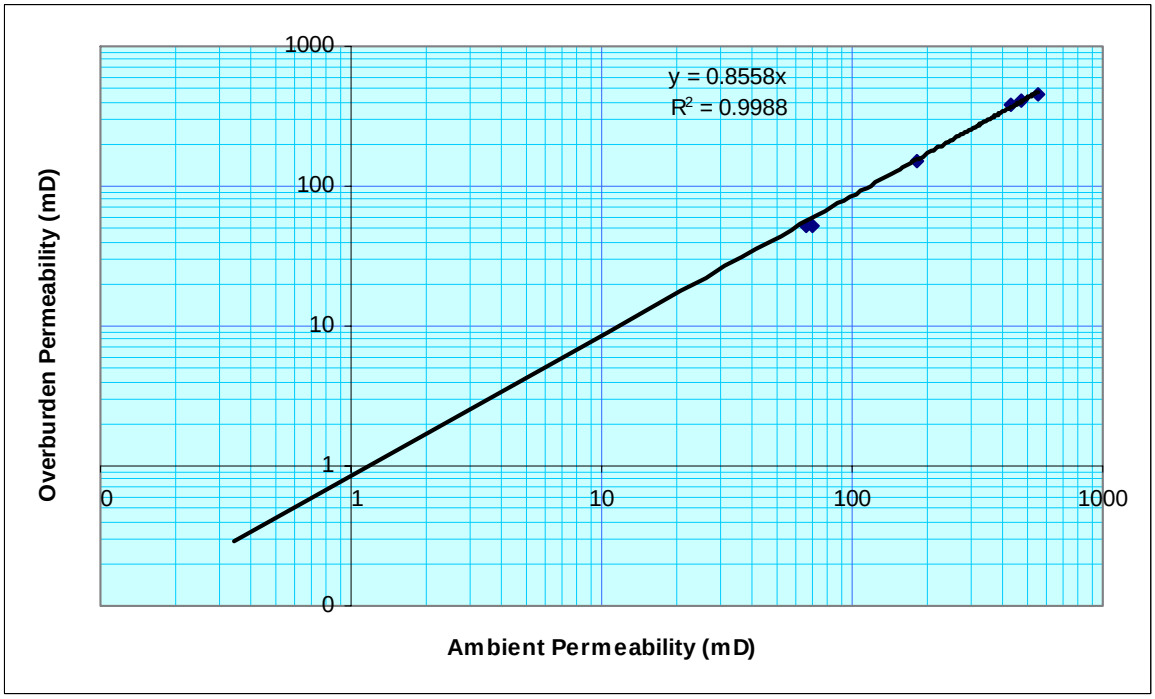


Figure 3: Porosity Permeability Relationship for Trefoil-1

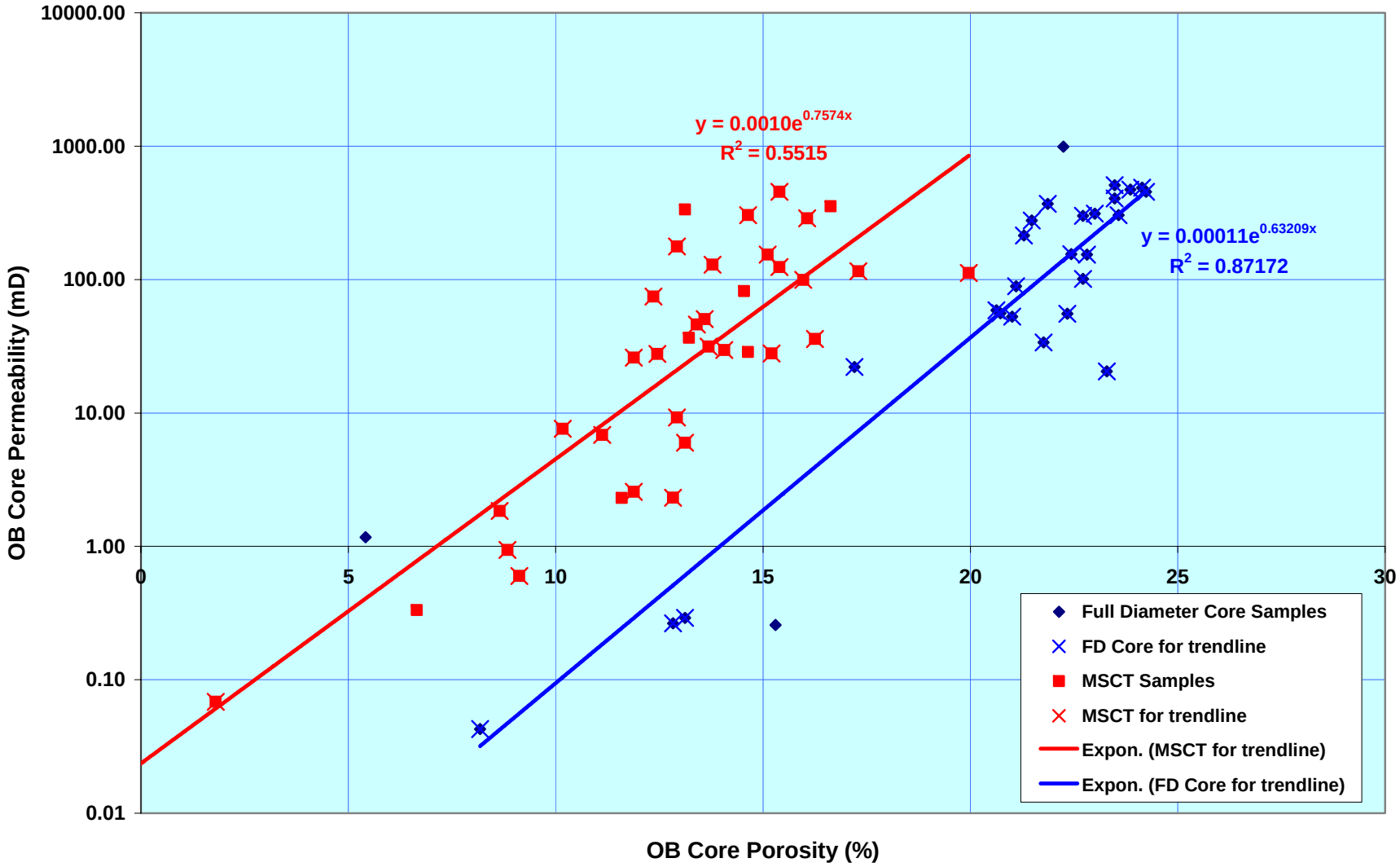


Figure 4: Determination of Cementation Exponent for the MSCT Plugs

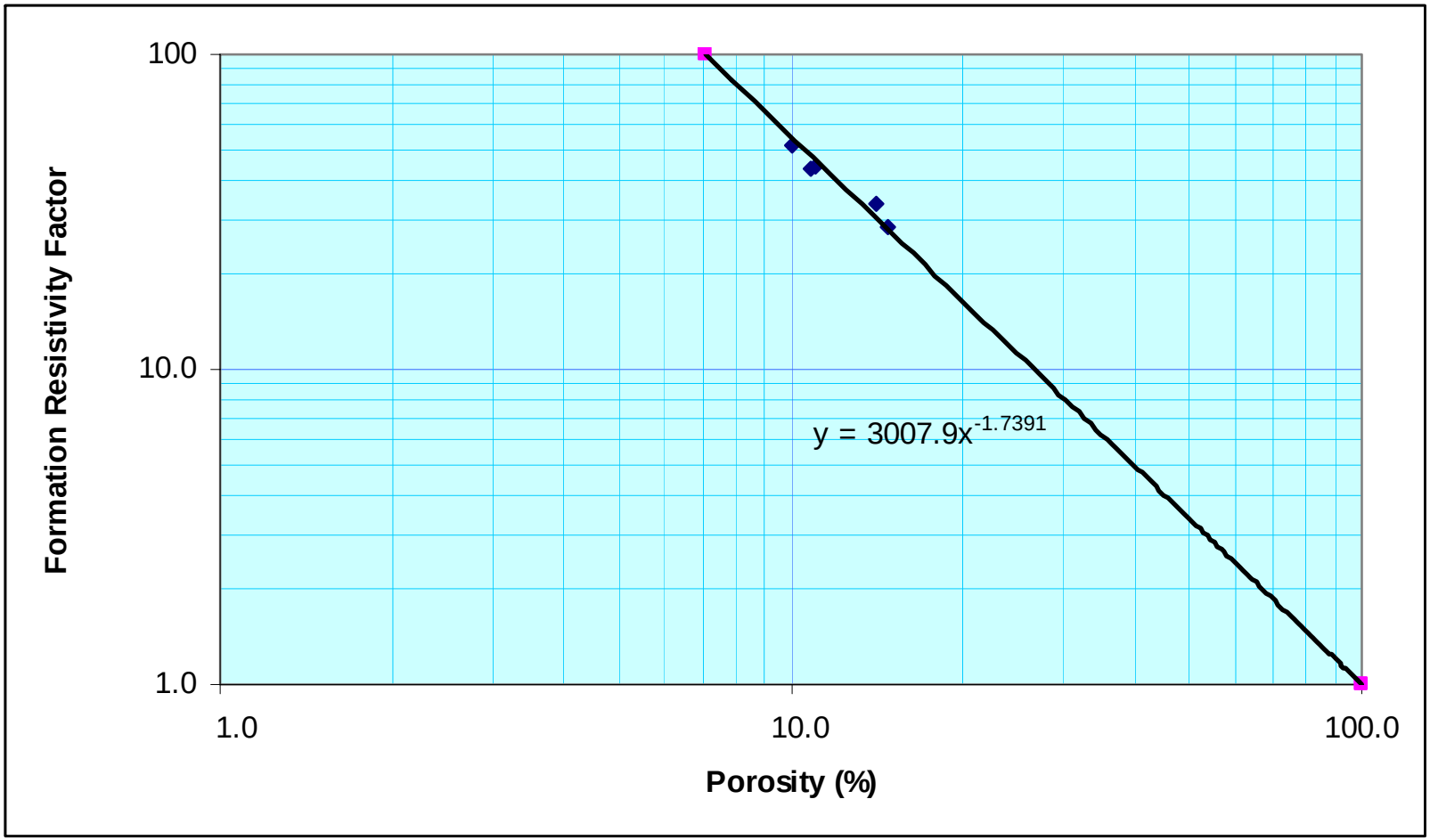


Figure 5: Determination of Saturation Exponent for the MSCT Plugs

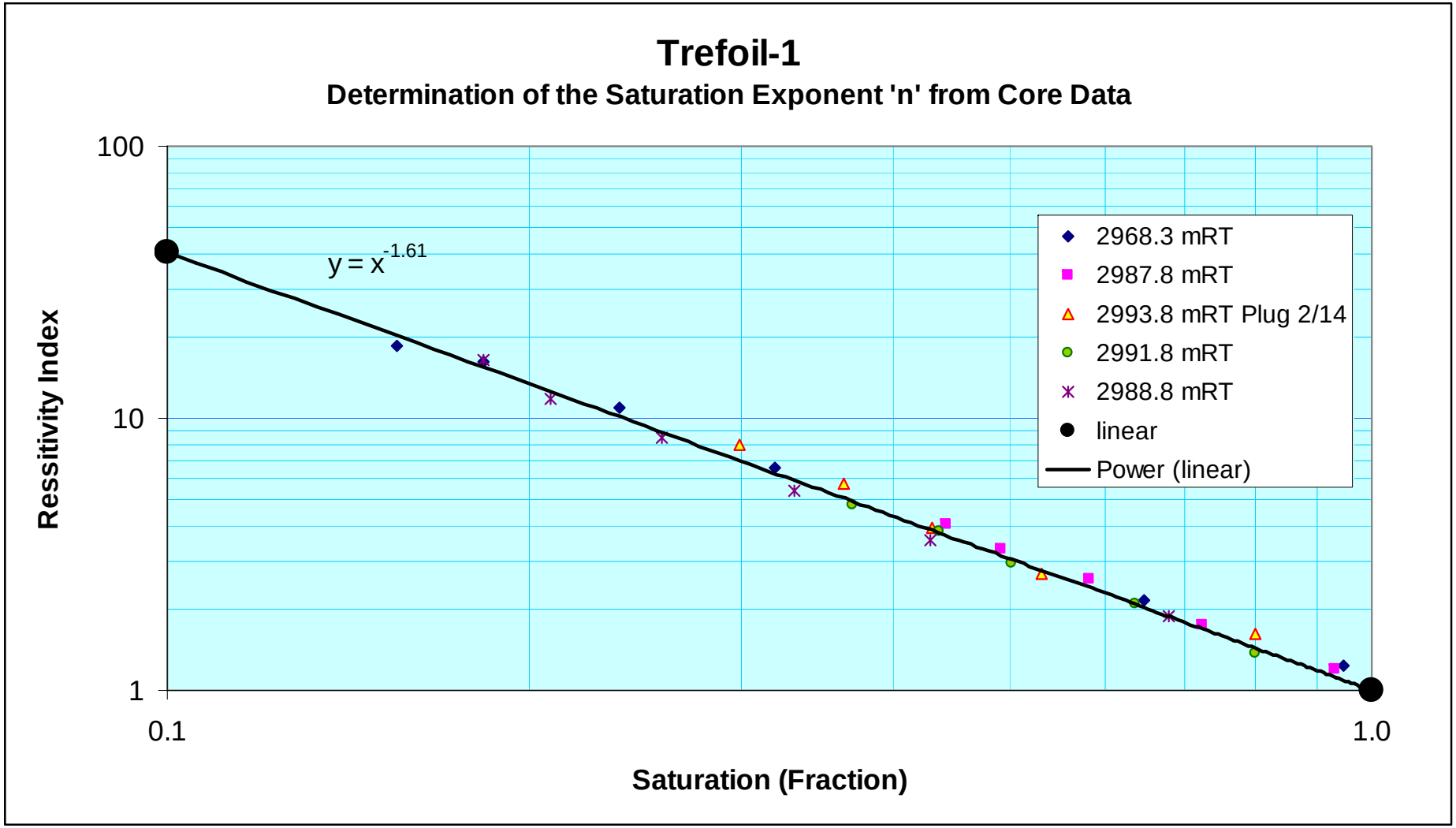


Figure 6: Residual Gas Saturation As a Function of Permeability

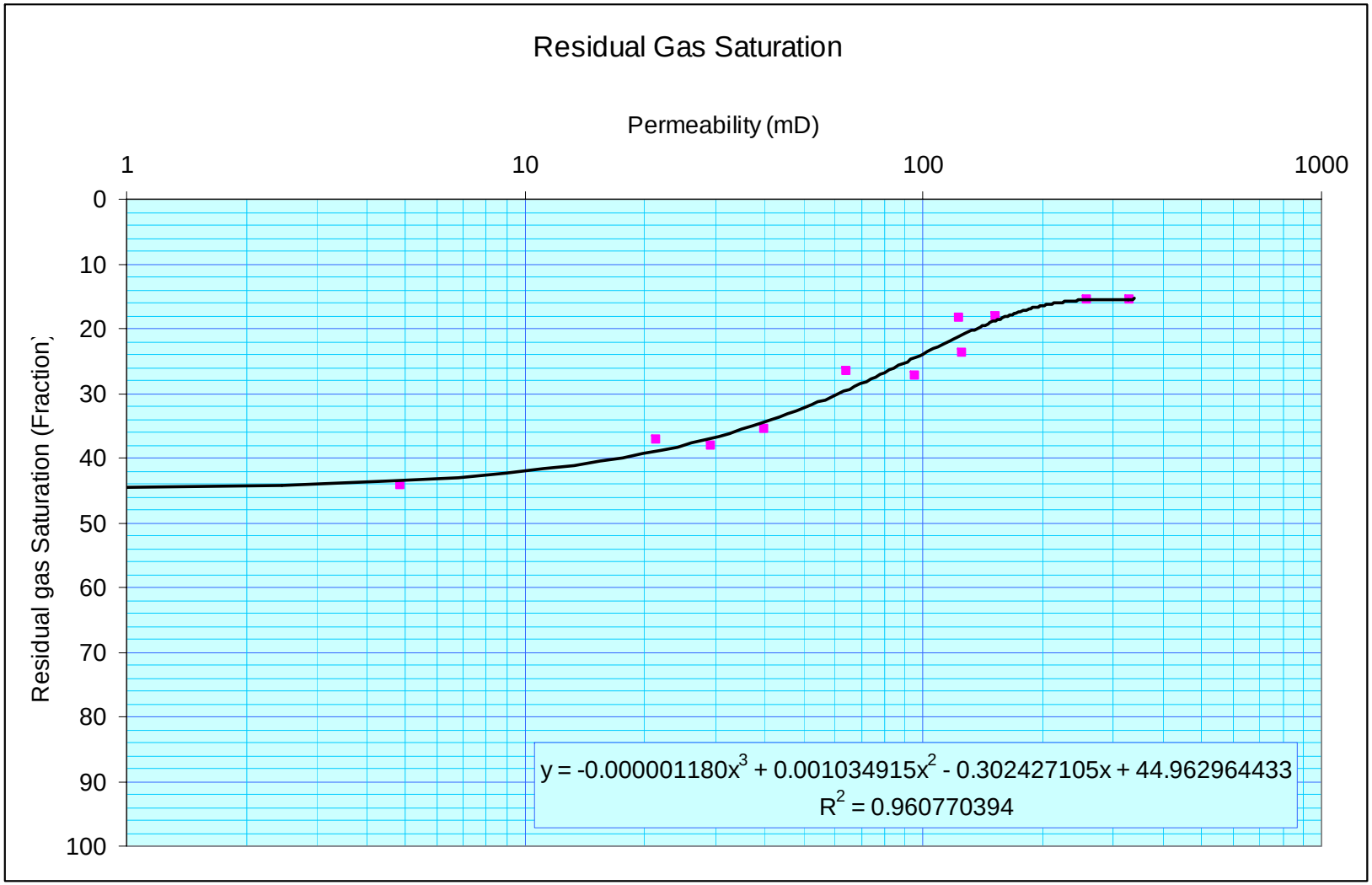


Figure 7: Capillary Pressure Curves (converted to 'J' Function vs Water Saturation) for the Trefoil MSCT Cores

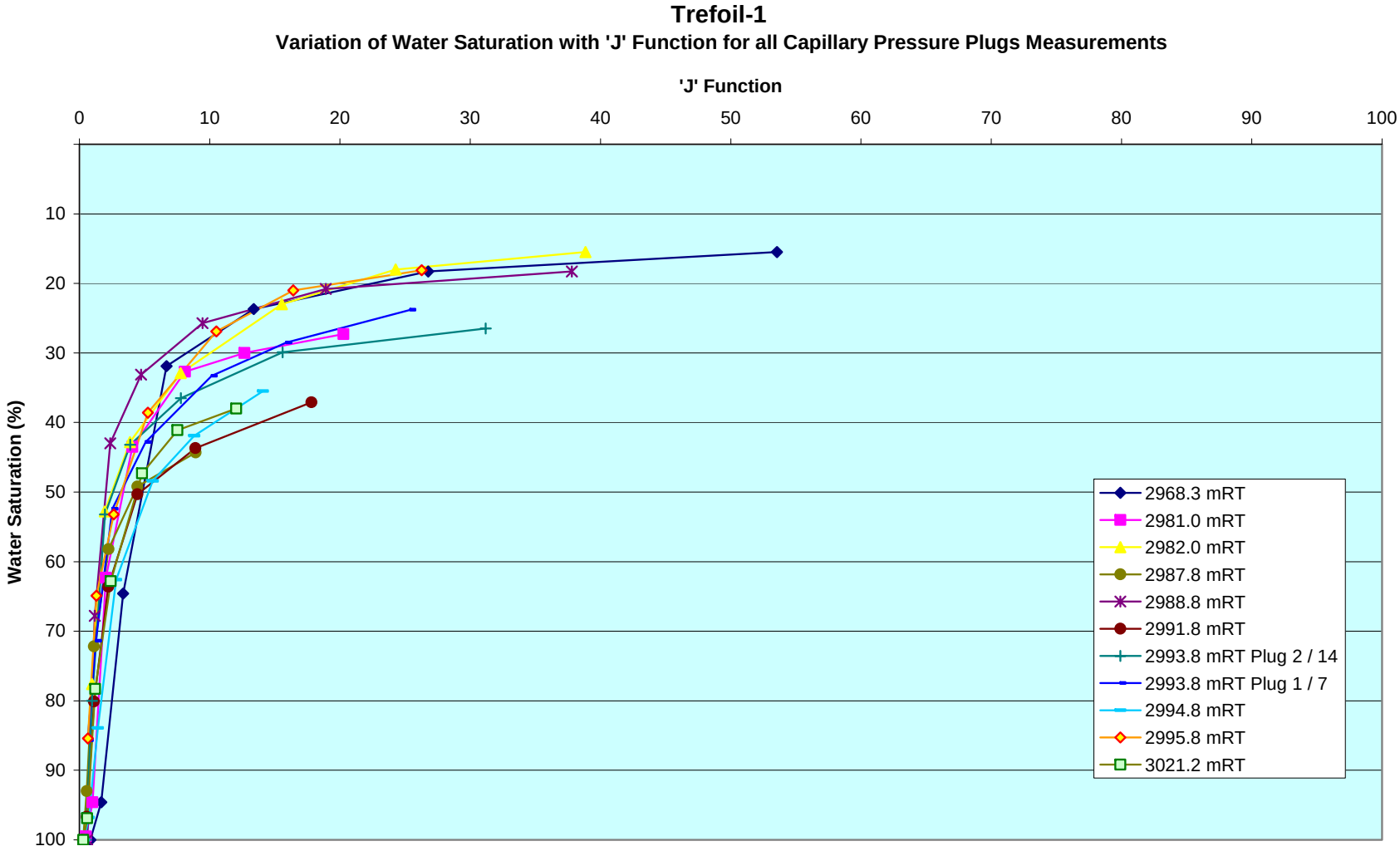


Figure 8: Capillary Pressure Curves (converted to 'J' Function vs Water Saturation) for the Trefoil MSCT Cores Together with the Modelled Functions Used in the Petrophysics Interpretation

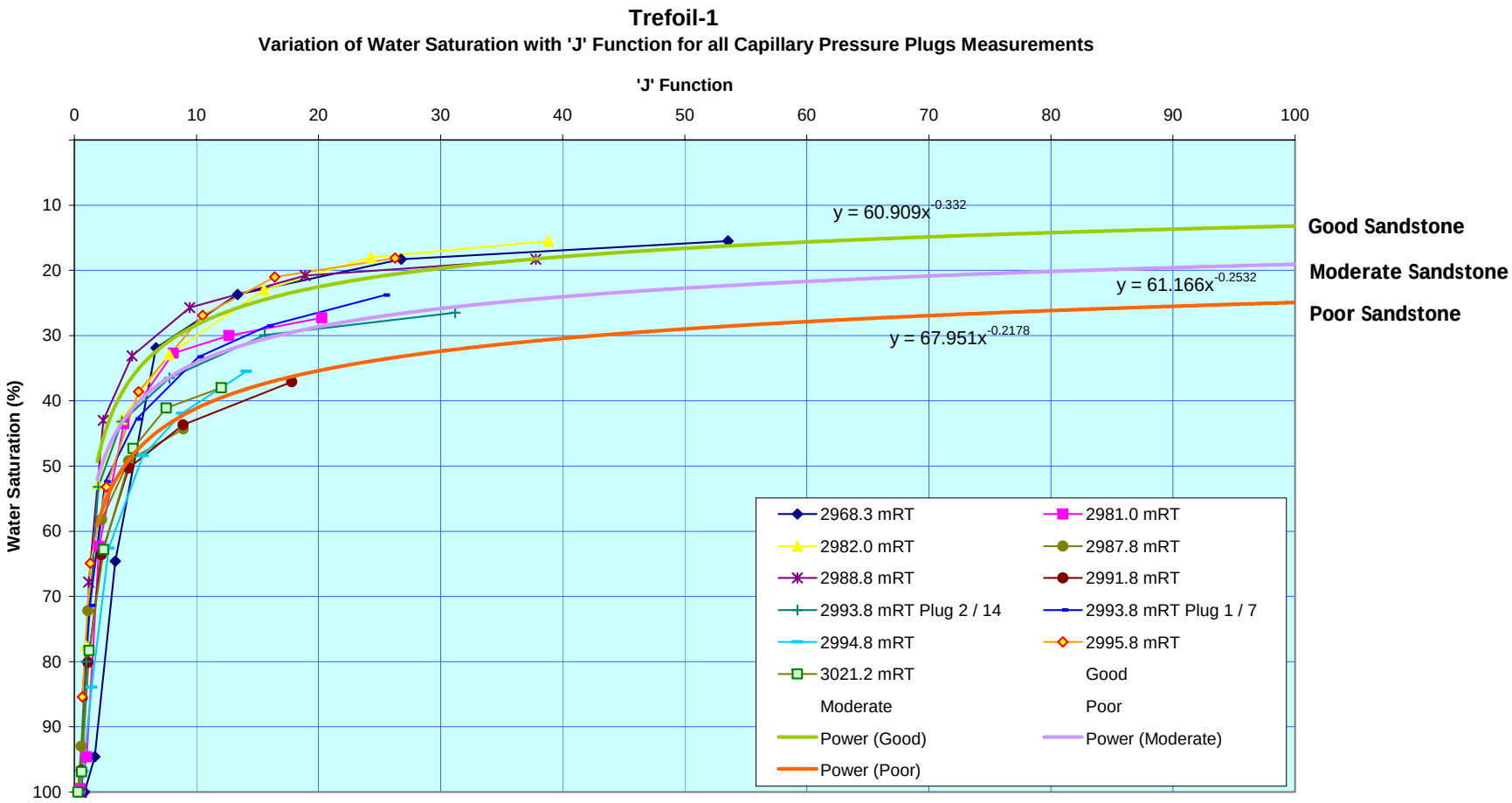
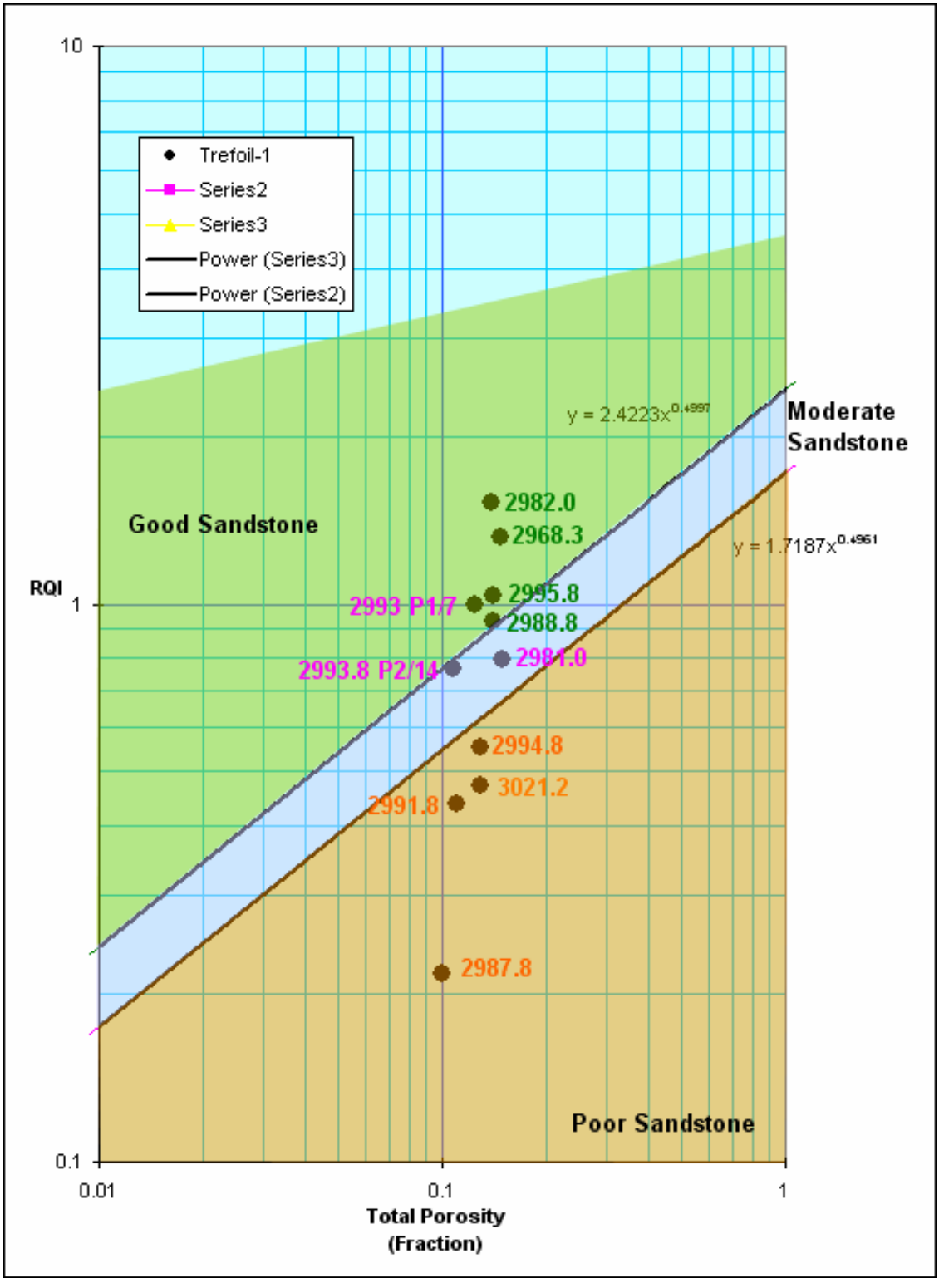


Figure 9: Sand Quality Determination for the Core Plug Data



*RQI = 0.0314 * SQRT (Core OB Permeability / Core OB Porosity)*

LOG ANALYSIS METHODOLOGY

Shale Volume

Shale volume was calculated from the minimum of the linear gamma ray determination and the neutron-density determination. The gamma ray clean line was shifted at 2920 mRT from 25 – 50 API to maintain a good correlation with the neutron-density plot through the entire hole.

Depth Interval	Clean GR	Shale GR
Above 2920 mRT:	25	136
2920 – 3168 mRT	50	175
Below 3168 mRT:	50	150

The minimum of the neutron-density and gamma ray derived shale volume was used in this interpretation.

Porosity

Total Porosity was derived from the CMR, density and neutron/density logs. The CMR log will under-read porosity in any gas zones due to the low proportion of hydrogen in gas. The CMR accurately measures bound fluid volume, since the bound fluid is always either oil or water (with a hydrogen index approximating to 1.0). The density will over-estimate porosity in the same zone (assuming a fluid density of water is used) due to the lower density of gas to formation water. The total porosity (Reference 1)in this interpretation was calculated from:

$$PHI_DMR = 0.60 * PHI_D + 0.04 * TCMR \quad \text{(Equation 5)}$$

Corrections were applied to PHI_DMR to honour the core data as closely as possible as follows:

Full Diameter Core		
< 2739.6 mRT	PHI_DMR = PHI_DMR * 0.923	(Equation 6a)
> 2739.6 mRT	PHI_DMR = PHI_DMR * 1.094	(Equation 6b)
MSCT Plugs	PHI_DMR = PHI_DMR * 0.781	(Equation 7)

Effective porosity was calculated by subtracting the CMR bound fluid volume (determined from logs TCMR minus CMFF) from PHI_DMR.

A comparison between the core OB and log derived porosity for the full diameter core interval shows that the log porosity (PHI_DMR) accurately represents the core derived porosity throughout this interval.

Determining a good relationship between core and log derived porosity was not straightforward as the log data is aliasing the core interpretation in the thin bed lithology. Hence, a procedure was followed, where the overburden corrected core porosity was interpolated in intervals where plugs were less than two metres apart. Interpolated intervals of significant variation from the log derived porosity, were nulled. This was then merged with the DMR (density / CMR combination) porosity, after calibration to the core data, to yield the porosity used in the interpretation.

Permeability

Permeability was derived from the full diameter and MSCT core derived porosity – permeability relationships using Equations 3 & 4. A non-linear correction was applied to the log permeability to tie the core data better above 2920 mRT as follows:

Above 2920 mRT:	POPE = POPE * 1.1104	(Equation 8)
Below 2920 mRT:	No correction applied	

A comparison between core OB permeability and log derived permeability (POPE) from the porosity-permeability cross-plot (Figure 3) indicates that the log derived permeability accurately represents the core permeability above 2920 mRT.

MDT permeabilities ranged from 786 mD/cp at 2697 mRT to tight measurements. These values approximate very well to the corrected POPE curve.

The preliminary well test interpretation suggests that DST#1 (3141 – 3150 mRT) had a permeability of 14 mD compared to a log derived geometric average (ga) permeability of 9 mD. The preliminary well test interpretation for DST#2 (3040.5 – 3046.5 mRT) suggests a permeability of 55 mD compared to a log derived ga permeability of 12 mD. No MSCT plugs were taken in this interval to calibrate the log response, but MDT mobilities ranged from 6.3 – 11.4 mD/cp.

As the core data could not be matched accurately from the core porosity / permeability trend or from the CMR derived permeabilities, the permeability used in the interpretation was

handled in a similar fashion to the porosity, with core data being used where possible and log data infilling gaps in the core distribution.

Water Saturation

Water saturation was calculated from the core-derived capillary pressure data using the GWC determined from the pressure analysis. In zones, such as TlLb-40, TlLb-50 & TlLb-60, where the GWC is known, the water saturation calculated from the wireline logs was adjusted to correspond to the capillary pressure derived saturation.

Residual water saturation was calculated from the core-derived residual water saturation vs permeability function (Figure 6). The difference between the two curves is the theoretical moveable gas saturation derived from the core measurements.

Formation Water Salinity

Seven formation fluid samples were taken as part of the MDT programme and have been analysed for their ionic composition along with a mud filtrate sample. The STIFF diagram for these samples (Figure 10) shows a significant amount of sulphate in the mud filtrate being replicated in the water samples. It is, therefore, likely that the samples are moderately to heavily contaminated with filtrate and the measured resistivity will not be representative of the formation. This corresponds with the very deep invasion profile seen on the wireline resistivity logs.

Formation water resistivity in the reservoirs was determined in the zones where the GWC is well defined and was determined by matching the water saturation calculated from the Indonesia equation to the capillary pressure derived water saturation. This yielded a water resistivity of 0.303 Ω.m at 25°C (19,060 ppm NaCl equiv) for this interval. Variation in this salinity could occur as the reservoirs are known to be compartmentalised. However, without any way of quantifying this, this salinity was applied between 2920 – 3400 mRT.

Salinities in other zones were determined from Pickett plots, as the zones were water bearing.

Calculation of Water Saturation

Water saturation in the blocky sandstones above 2920 mRT was calculated using the Archie and Indonesia equations. None of these sands had significant shows during drilling and the water saturation was calculated to be close to 1.0 across the interval.

The Indonesia equation was chosen as giving the best representation of the water saturation equation in the reservoir zone (2920 – 3400 mRT) as the formation water resistivity was calibrated using this equation. Use of a laminar resistivity equation might, at first, appear

best as the FMI suggests thin beds throughout the reservoir interval, but this was not applied as the water saturation would have needed to be recalibrated.

The LWD resistivity (SEDP) was used in preference to the wireline true formation resistivity (RT_HRLT) as the wireline log is considered to be affected by filtrate invasion.

Gas-Water Contact

In three zones, TlLb-40, TlLb-50 & TlLb-60, the Gas-Water-Contact (GWC) was accurately defined by pressure data. The water saturation from capillary pressure data from these zones was used to calibrate the formation water resistivity used in the log analysis. This water resistivity was then applied to all other reservoir zones and used to calibrate the hydrocarbon column height using the capillary pressure defined water saturation.

The GWC derived from this technique, together with the column height are given in Table 2.

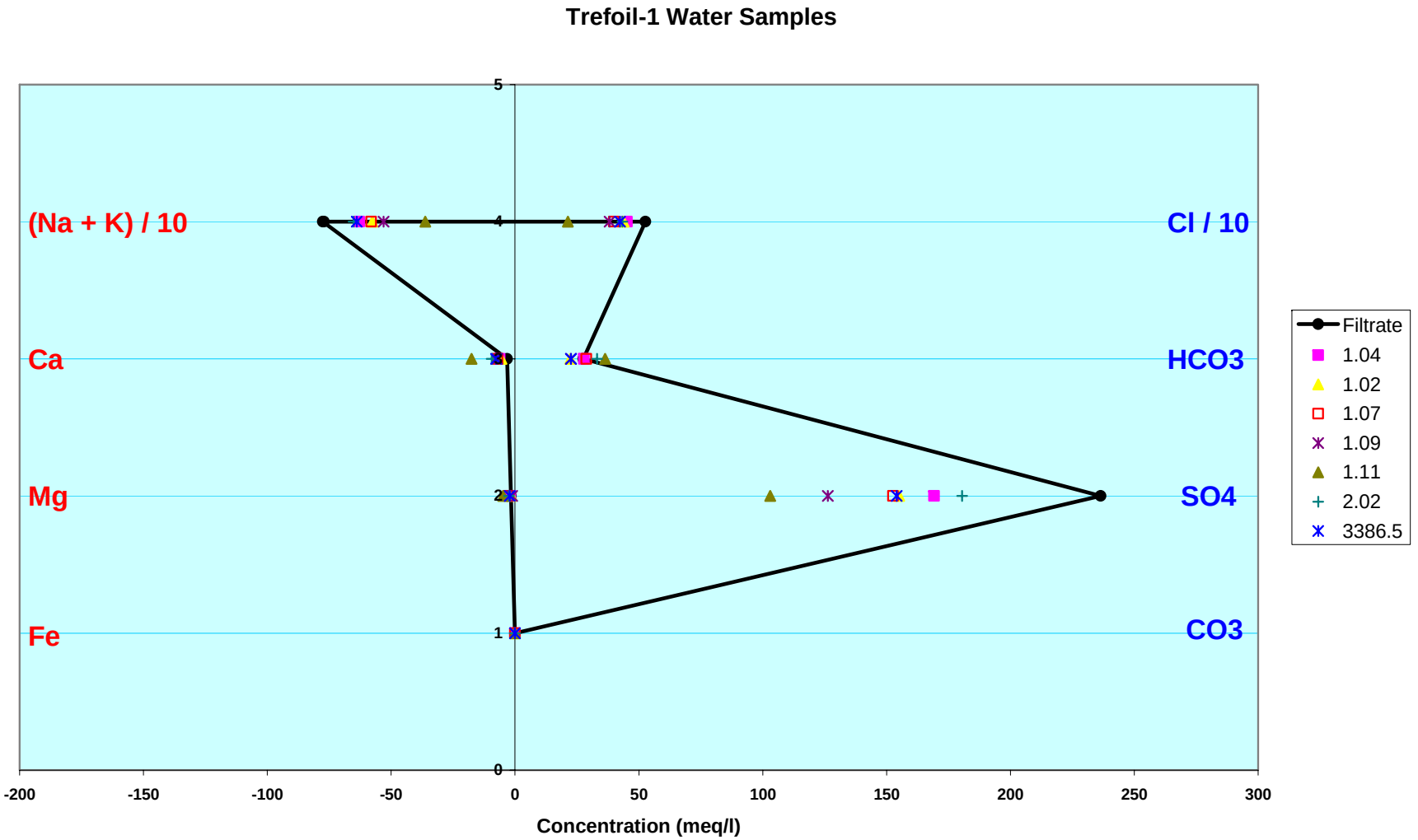
Net Pay Cut-offs

As above 2920 mRT the sandstones are water-bearing throughout, net sand has been defined to be where the VSH < 0.40 and permeability (POPE) > 1 mD (corresponding to a porosity of approximately 14%). The permeability cut-off was constrained to correspond with sands flowing water.

Below 2920 mRT, the sandstones are gas and water bearing. Net sand has been defined with the same VSH as above. Typically, gas will flow at permeabilities down to 0.1 mD, however, from the MSCT core porosity / permeability relationship, this would correspond with a porosity of approximately 3%. Since water is likely to flow with the gas in most of the sands (i.e. the sands are within the transition zone), then permeability (POPE) > 1.0 mD was also used to differentiate net sand. This corresponds with a porosity of approximately 7%.

Net pay was determined to be where net sand has a water saturation of less than 60%.

Figure 10: Ionic Composition for the Trefoil-1 MDT Water Samples



REFERENCES

1. Trefoil-1 – MDT Interpretation (June 2005), Origin Energy
2. INFACT Surface Gas Data Analysis – Trefoil-1 Well, Chauvin Hervé, Geoservices
3. Freedman R., Minh C.C., Gubelin G., Freeman J.J., McGinness T., Terry R. & Rawlence D. (1998) "Combining NMR and Density Logs for Petrophysical Analysis in Gas Bearing Formations", SPWLA

```
************************************************************************
* Mud properties RM (C7), RMF (C9), RMC (C5), MW (C25)
* Temperatures RM (C8), RMF (C10), RMC (C6)
*
* MW
        C25= 9.4
* Rm
        C7 = 0.206
        C8 = 25.0
* Rmf
        C9 = 0.174
        C10 = 25.0
* Rmc
        C5 = 0.280
        C6 = 24.9
PRINT Mud Properties entered
************************************************************************
*-----------------------------------------------------------------------
SET DEPTH INTERVAL 2700 3544
* Temperature Log
* SET BHT (C13) and Depth (C20), Surface Temp (C14) and Depth (C34)
        C13 = 117
        C20 = 3416
        C14 = 10
        C34 = 108.8
BEGIN
        VT= C14 + (C13 - C14) * (VDEPTH - C34) / (C20 - C34)
ENDBEGIN
PRINT Temperature Log Created
*-----------------------------------------------------------------------
*
************************************************************************
*
BEGIN
*********************************************
if (VDEPTH < 2921)
*       Matrix GR (C61), Density (C62), Neutron (C64)
                C61 = 20
                C62 = 2.648
                C63 = 55
                C64 = -0.05
*
*       Shale GR (C65), Density (C66), Neutron (C68), Resistivity (C19)
                C65 = 100
                C66 = 2.65
                C68 = 0.24
                C19 = 10
*
*       Fluid Density (C70), Neutron (C72), Resistivity (C11), Temperature (C12)
                C70 = 0.847
                C72 = 1.00
*       Archie Parameters
*       a (C16), m (C17), n(c18)
                C16 = 1.00
                C17 = 1.86
                C18 = 1.74
*
*       Water Resistivity
*       Set to 5,000 ppm NaCl from Pickett plot
                C11 = 0.5
                C12 = 95
endif
if (VDEPTH > 2921)
*       Matrix GR (C61), Density (C62), Neutron (C64)
                C61 = 20
                C62 = 2.648
```

```
                C63 = 55
                C64 = -0.05
*
*       Shale GR (C65), Density (C66), Neutron (C68), Resistivity (C19)
                C65 = 100
                C66 = 2.65
                C68 = 0.24
                C19 = 10
*
*       Fluid Density (C70), Neutron (C72), Resistivity (C11), Temperature (C12)
                C70 = 0.847
                C72 = 1.00
*       Archie Parameters
*       a (C16), m (C17), n(c18)
                C16 = 1.00
                C17 = 1.739
                C18 = 1.61
*
*       Water Resistivity
*       Set to 5,000 ppm NaCl from Pickett plot
                C11 = 0.5
                C12 = 95
endif
*******************************************************************************
*-------------------------------------------------
* Volcanics filter
*
                VVOLCANIC = 0
        if (VDEPTH > 3392.0 & VDEPTH < 3403.7)
                VVOLCANIC = 1
                GOTO ENDINTERP3
        endif
        if (VDEPTH > 3406.4 & VDEPTH < 3419.6)
                VVOLCANIC = 1
                GOTO ENDINTERP3
        endif
        if (VDEPTH > 3421.2 & VDEPTH < 3435.4)
                VVOLCANIC = 1
                GOTO ENDINTERP3
        endif
        if (VDEPTH > 3441.3 & VDEPTH < 3459.0)
                VVOLCANIC = 1
                GOTO ENDINTERP3
        endif
        if (VDEPTH > 3462.2 & VDEPTH < 3464.3)
                VVOLCANIC = 1
                GOTO ENDINTERP3
        endif
        if (VDEPTH > 3468.0 & VDEPTH < 3477.2)
                VVOLCANIC = 1
                GOTO ENDINTERP3
        endif
        if (VDEPTH > 3480.9 & VDEPTH < 3484.1)
                VVOLCANIC = 1
                GOTO ENDINTERP3
        endif
        if (VDEPTH > 3511 & VDEPTH < 3517.7)
                VVOLCANIC = 1
                GOTO ENDINTERP3
        endif
        if (VDEPTH > 3520.7 & VDEPTH < 3526.3)
                VVOLCANIC = 1
                GOTO ENDINTERP3
        endif
*-------------------------------------------------
* Coal Filter
```

```
*
        if (VWL_DENS < 2.20 & VWL_NPHI > 0.35)
                VCOAL = 1
                GOTO ENDINTERP3
        else
                VCOAL = 0
        endif
*-------------------------------------------------
* Shale volume
*
        if (VDEPTH > 2921 & VDEPTH < 3056)
*               Matrix GR (C61), Density (C62), Neutron (C64)
                        C61 = 60
                        C62 = 2.648
                        C63 = 55
                        C64 = -0.05
*
*               Shale GR (C65), Density (C66), Neutron (C68), Resistivity (C19)
                        C65 = 150
                        C66 = 2.65
                        C68 = 0.24
        endif
*
        VVSH_GRL = (VWL_GRMER-C61)/(C65 - C61)
        VVSH_PEF = (VWL_PEF - 1.8) / (3.42 - 1.8)
        VVSH_CMR = 1 - (VWIR_CMFF / VWIR_TCMR)
*
        VTEMPA = (C62 - C70) * (C72 - VWL_NPHI) - (VWL_DENS-C70) * (C72 - C64)
        VTEMPB = (C62 - C70) * (C72 - C68) - (C66 - C70) * (C72 - C64)
        VVSH_ND=VTEMPA / VTEMPB
*
        if (VVSH_GRL<=VVSH_ND)
                VVSH=VVSH_GRL
        else
                VVSH=VVSH_ND
        endif
*
        if (VDEPTH > 3033 & VDEPTH < 3037)
                VVSH = VVSH_ND
        endif
        if (VDEPTH > 3390 & VDEPTH < 3393)
                VVSH = VVSH_ND
        endif
        if (VVSH<0)
                VVSH=0
        endif
*-------------------------------------------------------------------------
* Porosity
*
        VPHI_D = (C62 - VWL_DENS) / (C62 - C70)
        VPHI_DW = (C62 - VWL_DENS) / (C62 - 1.00)
        VNPSC = VNPHI_SS - VVSH * 0.25
        VPHI_ND = @SQT((VPHI_D^2 + VNPSC^2) / 2)
        VPHI_DMR = VWIR_TCMR*0.4 + VPHI_DW*0.6
        VPHI_DMRC = VPHI_DMR
*
* Tie PHI_DMR to PHIT from core
* Full diameter core interval
        if (VDEPTH < 2739.6)
                VPHI_DMRC = 0.923 * VPHI_DMR
        endif
        if (VDEPTH > 2739.6 & VDEPTH < 2742)
                VPHI_DMRC = 1.094 * VPHI_DMR
        endif
*
* MSCT interval
```

```
*
        if (VDEPTH > 2920)
                VPHI_DMRC = 0.781 * VPHI_DMR
        endif
*
        VPHIT = VPHI_DMRC
        if (VCOREPORI > 0)
                VPHIT = VCOREPORI / 100
        endif
        VBFV=VWIR_TCMR-VWIR_CMFF
        if (VPHIT < VBFV)
                VPHIT = VBFV
        endif
        VPHIE = VPHIT-VBFV
*
        if (VDEPTH > 3390)
                VPHIT = VPHI_ND
                VPHIE = VPHIT - VVSH * 0.03
        endif
*
* ------------------------------------------------------------------
* Permeability
*
        if (VDEPTH < 2920)
                VPOPE = 0.00011 * @EXP(0.6321 * VPHIT *100)
*               VPOPE = VPOPE * 1.1104 + 0.01
                GOTO ENDPERM
        endif
                VPOPE = 0.00100 * @EXP (0.7574 * VPHIT * 100)
        if (VCOREPERI > 0)
                VPOPE = VCOREPERI
                GOTO ENDPERM
        endif
:ENDPERM
*
*
*------------------------------------------------------------------
* DMR SGXO
*
        if (VDEPTH < 3395)
*
                VL = (1.00 - 0.25) / (C62 - 1.00)
                VPG = 1 - @EXP(-1*(5/3))
                C58 = 0.4
                VSXO_DMR = 1 - (VPHI_DW - VWIR_TCMR)/((VPHI_DW*(1-C58*VPG))+(VL*VWIR_TCMR))
                if (VSXO_DMR > 1)
                        VSXO_DMR = 1
                endif
                if (VWL_DENS >2.8)
                        VSXO_DMR = 1
                endif
                if (VVSH > 0.6)
                        VSXO_DMR = 1
                endif
        endif
*
*------------------------------------------------------------------
* Reservoir quality indicators for allocation of SCAL plugs
*
        VRQI = 0.0314 * @SQT(VPOPE / VPHIT)
*
        VLINE1 = 1.7187 * VPHIT ^ 0.496
        VLINE2 = 2.4223 * VPHIT ^ 0.4997
*
*-----------------------------------------------------
* Capillary Pressure Data
```

```
* Setting contacts for multiple columns
* Zones where GWC defined by pressure data
*
        C35 = 0
* P2-40
        if (VDEPTH > 2966.6 & VDEPTH < 2972.6)
                C35 = 2993.6
                GOTO ENDGWC
        endif
*
* P2-50a
        if (VDEPTH > 2979.0 & VDEPTH < 2983.6)
                C35 = 3000.7
                GOTO ENDGWC
        endif
*
* P2-60
        if (VDEPTH > 2990.0 & VDEPTH < 3002.0)
                C35 = 3003.9
                GOTO ENDGWC
        endif
*
:ENDGWC
*
* Using SWT_IND to estimate contact depths
*
* -------
* Zone P2
*
* P2-10a
        if (VDEPTH > 2930 & VDEPTH < 2934.6)
                C35 = 2940
                GOTO ENDLKG
        endif
* P2-10b
        if (VDEPTH > 2934.6 & VDEPTH < 2940)
                C35 = 2938
                GOTO ENDLKG
        endif
* P2-20
        if (VDEPTH > 2942 & VDEPTH < 2957)
                C35 = 2947
                GOTO ENDLKG
        endif
* P2-30
        if (VDEPTH > 2957 & VDEPTH < 2964)
                C35 = 2961
                GOTO ENDLKG
        endif
* P2-50a
        if (VDEPTH > 2985 & VDEPTH < 2989)
                C35 = 3000.7
                GOTO ENDLKG
        endif
*--------
* Zone P1
*
* P1-10
        if (VDEPTH > 3018 & VDEPTH < 3026)
                C35 = 3030
                GOTO ENDLKG
        endif
* P1-20
        if (VDEPTH > 3026 & VDEPTH < 3030)
                C35 = 3038
                GOTO ENDLKG
```

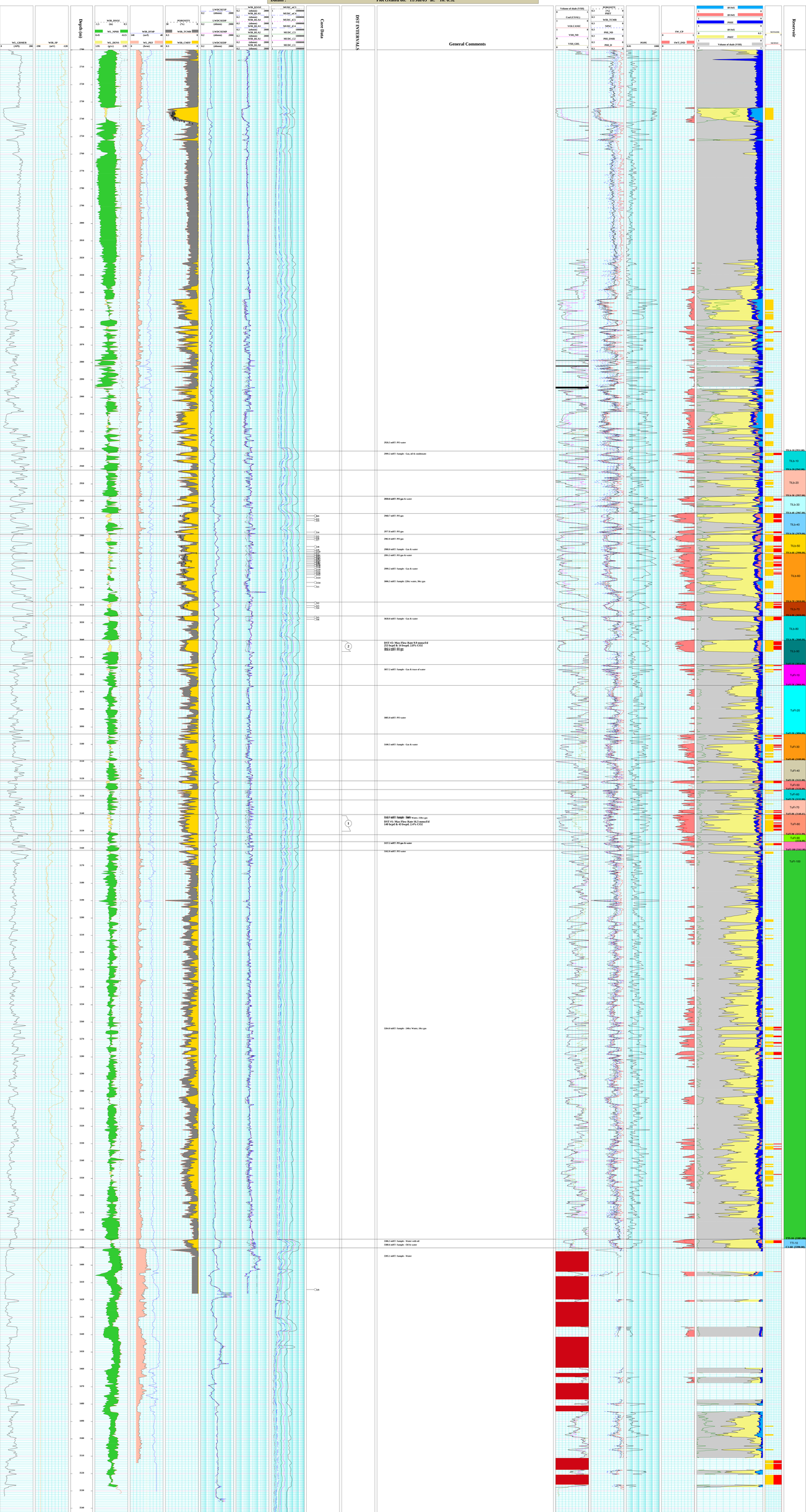
```
        endif
* P1-30
        if (VDEPTH > 3040 & VDEPTH < 3046.8)
                C35 = 3060
                GOTO ENDLKG
        endif
* P1-40
        if (VDEPTH > 3054 & VDEPTH < 3066)
                C35 = 3059
                GOTO ENDLKG
        endif
* P1-60
        if (VDEPTH > 3094 & VDEPTH < 3108)
                C35 = 3108
                GOTO ENDLKG
        endif
* P1-70
        if (VDEPTH > 3109 & VDEPTH < 3111)
                C35 = 3115
                GOTO ENDLKG
        endif
*--------
* Zone C1
*
* C1-10
        if (VDEPTH > 3121 & VDEPTH < 3126)
                C35 = 3135
                GOTO ENDLKG
        endif
* C1-20
        if (VDEPTH > 3126 & VDEPTH < 3132)
                C35 = 3130
                GOTO ENDLKG
        endif
* C1-25
        if (VDEPTH > 3137.7 & VDEPTH < 3139.4)
                C35 = 3150
                GOTO ENDLKG
        endif
* C1-30
        if (VDEPTH > 3140 & VDEPTH < 3152)
                C35 = 3155
                GOTO ENDLKG
        endif
* C1-40
        if (VDEPTH > 3152 & VDEPTH < 3156)
                C35 = 3160
                GOTO ENDLKG
        endif
* C1-47
        if (VDEPTH > 3156 & VDEPTH < 3161)
                C35 = 3165
                GOTO ENDLKG
        endif
* C1-45
        if (VDEPTH > 3161 & VDEPTH < 3163.4)
                C35 = 3170
                GOTO ENDLKG
        endif
* C1-50
        if (VDEPTH > 3385 & VDEPTH < 3387.8)
                C35 = 3395
                GOTO ENDLKG
        endif
:ENDLKG
* ------------------------------------------------------------------------
```

```
                VHEIGHT = C35 - VDEPTH
                if (VHEIGHT < 0)
                        VSW_CP = 1
                        GOTO ENDCP
                endif
*
        VLEV_J=((VHEIGHT * 0.33 * 3.28084) / 50) * (VPOPE / VPHIT)^0.5
*
* Set J to Sw_CP curve transition
*
        if (VDEPTH < 2931.5)
                GOTO ENDCP
        endif
*
* Poor Sandstone
        if (VRQI < VLINE1)
                C44 = 67.951
                C45 = -0.218
                VSW_CP = (C44 * VLEV_J^C45) / 100
                GOTO ENDCP
        endif
*
* Moderate Sandstone
        if (VRQI < VLINE2)
                C44 = 61.166
                C45 = -0.253
                VSW_CP = (C44 * VLEV_J^C45) / 100
                GOTO ENDCP
        endif
*
* Good Sandstone
* RQI > LINE 2
                C44 = 60.909
                C45 = -0.332
                VSW_CP = (C44 * VLEV_J^C45) / 100
:ENDCP
*
*-----------------------------------------------------
* Determination of formation water salinity
* using Archie equation assuming SW_CP correct
*
        VRWA = (VSW_CP^C18 * VPHIT ^ C17 * VLWDCSEDP) / C16
        VSALINITY = (300000 / (VRWA * ((VT *1.8 +32) + 6.77) - 1)) ^ 1.05
*-----------------------------------------------------
:RWSET1
        if (VDEPTH < 2720)
                C11 = 0.173
                C12 = 25
                GOTO RWSET
        endif
        if (VDEPTH < 2820)
                C11 = 0.225
                C12 = 25
                GOTO RWSET
        endif
        if (VDEPTH < 2920)
                C11 = 0.367
                C12 = 25
                GOTO RWSET
        endif
        if (VDEPTH > 2920 & VDEPTH < 3400)
* Rw determined from Archie equation using SW_CP as input
                C11 = 0.303
                C12 = 25
        endif
:RWSET
```

```
        VRW_T = C11 * (C12 + 21.5) / (VT + 21.5)
*-----------------------------------------------
*
* Archie
*
        VSW_ARCH = ((C16 / VPHIT^C17)*(VRW_T/VLWDCSEDP))^(1/C18)
*
* Indonesia
* Shale resistivity = C19
*
        C19 = 9
        C38 =  (VPHIE ** C17) / (C16 * VRW_T)
        C39 = VVSH^(2-VVSH)
        C37 = @SQT(((VPHIE^C17)*C39)/(C19*C16*VRW_T))
        VSWE_IND = 1/(VLWDCSEDP*(C38+(C39/C19)+(2*C37^0.5)))^(1/C18)
*
        if (VDEPTH > 3470)
                VSWE_IND = 1
                VSW_ARCH = 1
        endif
        if (VSWE_IND > 1)
                VSWE_IND = 1
        endif
        if (VSWE_IND > 1)
                VSWE_IND = 1
        endif
*
        VBVWE = VPHIE * VSWE_IND
*
        VSWT_IND = ((VPHIT - VPHIE) + VBVWE) / VPHIT
*
*-----------------------------------------------------
* Net Sand / Net Pay Flags
        C40 = 0.4
        C42 = 0.5
        C43 = 0.6
        if (VVSH < C40 & VPOPE > C42)
                VNETSAND = 1
        else
                VNETSAND = 0
        endif
        if (VNETSAND = 1 & VSWT_IND < C43)
                VNETPAY = 1
        else
                VNETPAY = 0
        endif
*
* ---------------------------------------------------------------------
* Residual Gas saturation from Core Data Analysis
*
        if (VDEPTH > 2931.5)
                VSG_RES=(-0.00000118*VPOPE^3+0.0010349*VPOPE^2-0.302427*VPOPE+44.963)/100
                C44 = 1 - VSG_RES
                if (C44 < VSW_CP)
                        VSG_RES = 1 - VSW_CP
                endif
        endif
*
:ENDINTERP3
ENDBEGIN
```

Trefoil-1

Permit: Trefoil	**RTE:** 39.9 m	**TD (logs):** 3545.0 m
Latitude : 39 51' 41.58"S	**Bit Size:** 8.5 in	**BHT:** 117.0 degC
Longtitude : 145 22' 30.87"E	**Rm:** 0.206 ohmm at: 25.0 degC	**Vertical Scale** 1:500 m
Easting :	**Rmf:** 0.174 ohmm at: 25.0 degC	**Interpreter :** Andy Hall
Northing :	**Rmc:** 0.280 ohmm at: 24.9 degC	
Datum :	**Plot created on:** 11/Jul/05 at: 16: 6:32	



APPENDIX 2: MDT INTERPRETATION REPORT

TREFOIL 1

MDT INTERPRETATION
By J. Parvar

JUNE 2005

DATE OF SURVEY:
25/11/2004 TO 30/11/2004

The MDT operation in Trefoil 1 consisted of two programs (logging run#3 and logging run#5). A Schlumberger MDT tool with pump out module, resistivity tool, optical analyser, quartz and strain gauges was used to obtain pressure data and collect reservoir fluid samples from Trefoil-1. The tool was also fitted with the following sample chambers.

MDT Program-1: 5x450cc MPSR & 8x250cc SPMC

The SPMC samples were analysed onsite and the MPSR samples were sent to PVT lab for detailed analysis (one MPSR sample failed).

MDT Program-2: 5x450cc MPSR & 1x250cc SPMC

All samples were sent to PVT lab for detailed analysis (one MPSR sample failed).

The first MDT program (logging run #3) had pre-tests taken from 2626mMD to 3109.9mMD. The MDT tool failed at the 3109.9mMD sample point (damaged O-ring seal in MDT tool). A rerun was made with the same assembly and additional pre-tests taken from 3109mMD to 3390mMD.

During the first MDT program a total of 79 pre-tests (including sampling points) were attempted of which 45 were successful, 2 were failed and 32 were tight or supercharged. MDT samples were also taken at 3386.5mMD, 3264mMD, 3142.7mMD, 3057.2mMD, 3006.5mMD and 2968.7mMD. Pumpouts were recorded at 3162mMD, 3045.2mMD, 2982.0mMD and 2977.8mMD.

The second MDT Program (logging run #5) was run to 2307mMD where the MDT tool failed at this point and the assembly was POOH and the fluid analyser component was changed out. Assembly #5 was rerun to 3528.7mMD where the tool stood up and pre-tests were taken from 2629mMD to 3524 mMD.

During the second MDT program a total of 33 pre-tests (including samples) were attempted of which 16 were successful, 2 were failed and 15 were tight or supercharged. MDT fluid samples were taken at 3388.7mMD, 3100.5mMD (not recovered), 3028.0mMD, 2999.2mMD, 2988.0mMD and 2933.0mMD. Pumpouts were recorded at 3157.2mMD, 3085.0mMD, 3046.0mMD, 2991.5mMD, 2959.0mMD and 2926.5mMD.

A summary of the pre-test data is included in Appendix 10 of the Trefoil 1 Well Completion Report Basic Data Volume.

One of the main objectives of the Trefoil 1 MDT programs was to collect several MDT fluid samples and to perform a number of pumpouts.

A total of 10 MPSR (450cc) and 9 SPMC (250cc) samples were attempted during the two MDT programs, with 17 samples successfully recovered (two MPSR samples failed). The sample details are included in Appendix 11 of the Trefoil 1 Well Completion Report Basic Data Volume while a summary is presented in the following table.

Summary Of Collected MDT Samples				
Depth (mMD)	MDT Program	MPSR (450cc)	SPMR (250cc)	Recovery
2933.0	2	1 (PVT Lab)	-	Mainly Gas
2968.7	1	1 (PVT Lab)	2(onsite)	Mainly Gas
2988.0	2	1 (PVT Lab)	-	Mainly Gas
2999.2	2	1 (PVT Lab)	-	Mainly Gas
3006.5	1	-	1(Lab)	Water
3028.0	2	1 (PVT Lab)	-	Mainly Gas
3057.2	1	1 (PVT Lab)	2(onsite)	Gas &Water
3142.7	1	1 (PVT Lab)	2(onsite)	Gas & Water
3264.0	1	-	1(Lab)	Water
3386.5	1	1 (PVT Lab)	-	Gas & Water
3388.7	2	-	1(Lab)	Water

A total of 8 MDT samples were sent to Petrolab for analysis. The fluid composition and analysis of these samples are included in Appendix 19 of the Trefoil WCR Basic Data and a summary is presented in the following table.

SUMMARY OF LAB ANALYSIS (PetroLab)						
Depth	**Sample**	**Volume**	**Content**	**CO2**	**Condensate Ratio**	**LPG Ratio**
mRT		CC		Mole%	bbls/mmscf	Tonnes/mmscf
2933.0	MDT	450	Gas	1.27	83.7	6.3
2968.7	MDT	450	Gas	2.54	65.2	3.5
2988.0	MDT	450	Gas	2.44	39.4	2.7
2999.2	MDT	450	Gas	2.11	43.5	2.7
3028.0	MDT	450	Gas	1.35	26.1	2.6
3057.2	MDT	450	Gas	3.87	27.4	2.7
3142.5	MDT	450	Gas	2.96	31.1	1.4
3386.5	MDT	450	GAS + Water	1.67	42.2	4.5
3040.5-3046.5	CHDST#2	Sep	Gas	3.99	39.4	3.5
3141.0-3150.0	CHDST#1	Sep	Gas	3.99	19.1	1.7

A number of onsite analyses including Mercury and H2S tests were also carried out by Oilphase. A complete report can be found in Appendix 19 of

the Trefoil 1 Well Completion Report Basic Data Volume and a summary is presented in the following table.

OILPHASE ONSITE ANALYSIS												
Depth	**Run**	**Volume**	**Sample#**	**Content**	**CO2**	**H2S**	**Mercury**	**Recovered Water**			**pump out volume**	**Min BHP**
		CC			Mole%	ppm	ppb	CC	ohm-m	deg C	lt	psia
2968.7	**1**	250cc	1.11	Gas	3.10	0.00	772.80	15	0.338	@ 26.3 °C	37.44	4161.000
		250cc	1..12					20	0.339	@ 26.1 °C	40.95	4161
3006.5	**1**	250cc	1.09	Water				220	0.234	@ 25.0 °C	28.60	4060
3057.0	**1**	250cc	1.07	Gas	3.00	0.00	501.80	105	0.211	@ 28.1 °C	46.80	4090
		250cc	1.08					105	0.222	@ 26.1 °C	49.00	4090
3142.5	**1**	250cc	1.04	Gas	3.00	0.00	473.80	100	0.205	@ 20.9 °C	25.16	4379
		250cc	1.05					100	0.200	@ 28.0 °C	26.91	4405
3264.0	**1**	250cc	1.02	Water				240	0.209	@ 24.8 °C	22.82	4266
3386.5	**1**	450cc	1.01	Gas/Water	No Onsite analysis				0.190	@ 25.8	50.00	3252
3388.7	**2**	250cc	2.01	Water	No Onsite analysis				0.180	@ 23.4 C	22.23	1396
3100.5	**2**	450cc	-	Water	No Onsite analysis (pressure lost)				0.190	@ 23.7 °C	43.65	2100

During the tests the pumpout sub with optical fluid analyser (OFA) was used to identify the reservoir fluid. The details can be found in the Appendix 11 of the Trefoil 1 Well Completion Report Basic Data Volume. A summary is presented in the following table.

Summary of Pumpouts			
Depth (mMD)	MDT Program	OFA*	Remarks
2926.0	2	Yes	Water
2959.0	2	Yes	Gas
2977.8	1	Yes	Gas
2982.0	1	Yes	Gas
2991.5	2	Yes	Gas & Water
3045.2	1	Yes	Gas
3046.0	2	Yes	Gas
3085.0	2	Yes	Water
3157.2	2	Yes	Gas+Water
3162.0	1	Yes	Water
3100.5	2	Yes	Sample taken at this point was lost but the OFA results indicate gas.
* Optical Fluid Analyser			

Water samples (and recoveries) collected during the MDT Program 1 & 2 were analysed by Amdel (Trefoil 1 Well Completion Report Basic Data

Volume Appendix 19). A summary of the analysis is presented in the following table.

		TREFOIL WATER SAMPLES									
Sample		**MDT**	**MDT**	**MDT**	**MDT**	**MDT**	**MDT**	**MDT**	**MDT**		
Zone		**3386.5 mRT**	**3264.0 mRT**	**3142.7 mRT**	**3057.2 mRT**	**3006.48 mRT**	**2968.7 mRT**	**3100.5 mRT**	**3388.7 mRT**		
Sampl#			**1.02**	**1.04**	**1.07**	**1.09**	**1.11**	**2.02**	**10007- MA**	**MUD FILTRATE**	
Fluid											
PROPERTIES: APHA 20th Ed											
pH at Measured Temp.		**6.8**	**7.5**	**7.7**	**7.6**	**7.2**	**7.8**	**7.8**	**7.4**	**8.2**	
Measured Temp.*	°C	**25.8**	**23.7**	**23.7**	**23.7**	**23.7**	**23.7**	**23.7**	**23.4**	**22.3**	
Electrical Conductivity @ 25°C*	µS/cm	**51800**	**50200**	**52600**	**48000**	**45000**	**30500**	**51600**	**55100**	**58100**	
Resistivity @ 25°C*	M.Ohm	**0.19**	**0.2**	**0.19**	**0.21**	**0.22**	**0.33**	**0.19**	**0.18**	**0.17**	
ANIONS mg/L APHA 20th ed											
Hydroxide as OH*	mg/L	**<1**	**<1**	**<1**	**<1**	**<1**	**<1**	**<1**	**<1**	**<1**	
Carbonate as CO3*	mg/L	**<1**	**<1**	**<1**	**<1**	**<1**	**<1**	**<1**	**<1**	**<1**	
Bicarbonate as HCO3*	mg/L	**1379**	**1359**	**1699**	**1759**	**1379**	**2219**	**2019**	**1415**	**1679**	
Chloride as Cl*	mg/L	**15025**	**15537**	**16001**	**14142**	**13534**	**7554**	**15363**	**18384**	**18673**	
Nitrate as NO3*	mg/L	**11**	**<0.1**	**<0.1**	**<0.1**	**<0.1**	**<0.1**	**<0.1**	**<0.1**	**<0.1**	
Sulphate as SO4*	mg/L	**7399**	**7451**	**8124**	**7332**	**6064**	**4947**	**8667**	**7924**	**11354**	
Total Anions*	mg/L	**23814**	**24347**	**25824**	**23233**	**20977**	**14720**	**26049**	**27723**	**31706**	
CATIONS mg/L APHA 20th ed											
Potassium as K*	mg/L	**1758**	**1557**	**1815**	**1641**	**1323**	**1090**	**1800**	**1734**	**2145**	
Sodium as Na*	mg/L	**13650**	**12330**	**13380**	**12390**	**11430**	**7700**	**13920**	**13410**	**16470**	
Barium as Ba*	mg/L										
Calcium as Ca*	mg/L	**154**	**111**	**124**	**141**	**143**	**352**	**188**	**119**	**65**	
Iron as Fe*	mg/L										
Magnesium as Mg*	mg/L	**26**	**17**	**22**	**33**	**14**	**59**	**30**	**18**	**20**	
Strontium as Sr*	mg/L										
Aluminium as Al*	mg/L										
Total Cations*	mg/L	**15588**	**14015**	**15341**	**14205**	**12910**	**9201**	**15938**	**15281**	**18700**	
DERIVED PARAMETERS APHA 20th ed											
Ion balance (Diff * 100/Sum)*	%	**3.88**	**2.67**	**0.88**	**0.92**	**0.86**	**4.48**	**1.3**	**5.29**	**0.88**	
Acceptance Criteria*	%	**5**	**5**	**5**	**5**	**5**	**5**	**5**	**5**	**5**	
Satisfactory		**Yes**	**Yes**	**Yes**	**Yes**	**Yes**	**Yes**	**Yes**	**No**	**Yes**	
Total Alkalinity (calc as CaCO3)*	mg/L	**1131**	**1114**	**1393**	**1442**	**1131**	**1819**	**1655**	**1160**	**1376**	
Total Cations + Anions*	mg/L	**39402**	**38362**	**41165**	**37438**	**33887**	**23921**	**41987**	**43004**	**50406**	
Hardness (calc as CaCO3)*	mg/L	**492**	**347**	**400**	**488**	**415**	**1122**	**593**	**371**	**245**	
Calculated Total Dissolved Solids	mg/L	**33152**	**32128**	**33664**	**30720**	**28800**	**19520**	**33024**	**35264**	**37184**	

Interpreted plots of the MDT data, recorded during Program 1 and 2, are shown in Figures 1 to 9. The outlines of these plots are as follows.

Figure 1: shows the initial mud hydrostatic pressures recorded by the quartz gauge during the MDT program 1 and 2.

Figure 2: illustrates the difference between the initial and final mud hydrostatic pressures recorded by the quartz gauge.

Figure 3: shows the pressure vs. depth plot for all the pre-test data. The plot indicates that all the sands above ~2930mMD (2890mSS) are water saturated while several gas and water bearing intervals are exist below this level.

Figure 4: shows the MDT profile for the data recorded below 2890mSS. This plot and the subsequent ones indicate that there are multiple water systems within this section of the Trefoil structure. It is not clearly understood why there are several water systems within this structure but as shown in the next two plots (Figures 5 and 6) multi-systems phenomena exits through out this basin although not to the extent seen in Trefoil.

Figure 5: demonstrates the pressure vs. depth profile for RFT data from Yolla 1, Yolla 2, Pelican 4, King 1, White Ibis 1 and Trefoil 1. As shown in this plot the deeper zones are comparatively over-pressurised and there is not a unique water system in this basin.

Figure 6: is the same pressure vs. depth profile seen in Figure 5 but it zooms out the deeper section which shows that multiple water systems widely exist within the lower EVCM.

Figure 7: shows the Trefoil MDT points recorded below 2890mSS. Those points which have the fluid content verified (gas or water) by sampling or pumpouts, have been highlighted in this plot. The C5+ ratio (which appears to decrease with depth) and water salinity of the recovered reservoir fluid samples are also marked in this figure. The locations of the CHDST1 and CHDST2 are also positioned.

As can be seen in this figure there are several potential gas columns and a number of water systems within this section of the Trefoil structure. This is fairly uncommon to have these many water systems (and also gas columns) within a relatively small section. With the exception of a small gas zone in the region of 3386.5mMD (3346.6mSS), the main area for potential gas columns is within the 2850 to 3150mSS interval which will be reviewed in the subsequent plots. An MDT sample taken from 3386.5mMD (3346.6mSS) recovered gas and water while a sample collected from 3388.7mMD (3348.8mSS) recovered only water. Based on these results the GWC was assumed to be at 3387.6mMD (3347.7mSS).

Figure 8: shows the Trefoil MDT points recorded between 2850 to 3150mSS. The open hole logs indicate the possibility of several gas intervals

within this section. These intervals, which have been marked by their measured depths and informal zone names are outlined below.

Log derived gas Potential columns

m RT approx.	Informal Zone Name
2931 - 2934	TlLb-10
2942 - 2952	TlLb-20*
2957 - 2960	TlLb-30
2967 - 2972	TlLb-40
2979 - 2983	TlLb-50
2991 - 3002	TlLb-60
3018 - 3022	TlLb-70
3026 - 3029	TlLb-80
3040 - 3047	TlLb-90
3054 - 3059	TuFl-10
3066 - 3072	TuFl-20 *
3094 - 3108	TuFl-30
3109 - 3111	TuFl-40
3121 - 3123	TuFl-50
3126 - 3131	TuFl-60
3132 - 3136	TuFl-70 *
3141 - 3150	TuFl-80
3153 - 3158	TuFl-90
3161 - 3163	TuFl-100 *
3156 - 3159	TuFl-110 *
3385 - 3390	TTl-10

* No MDT or CHDST information is available for this zone.

Of the above 21 log derived gas potential intervals 16 zones have been reviewed by taking into account the MDT pre-test data, MDT sampling results, MDT pumpout information and CHDST results. No MDT or CHDST information is available for TlLb-20, TuFl-20, TuFl-70, TuFl-100 and TuFl-110 intervals.

The MDT pre-tests, sampling, pumpouts and CHDST results confirm the presence of 12 gas bearing zones within this section (TlLb-10, TlLb-30, TlLb-40, TlLb-50, TlLb-60, TlLb-70, TlLb-90, TuFl-10, TuFl-30, TuFl-80, TuFl-90 and TTl-10). The fluid content of the P1-10, P1-70, C1-10 and C1-20 zones can not be verified by the MDT pre-test data (no MDT samples or pumpouts are available) although they are interpreted to be gas saturated by open-hole logs.

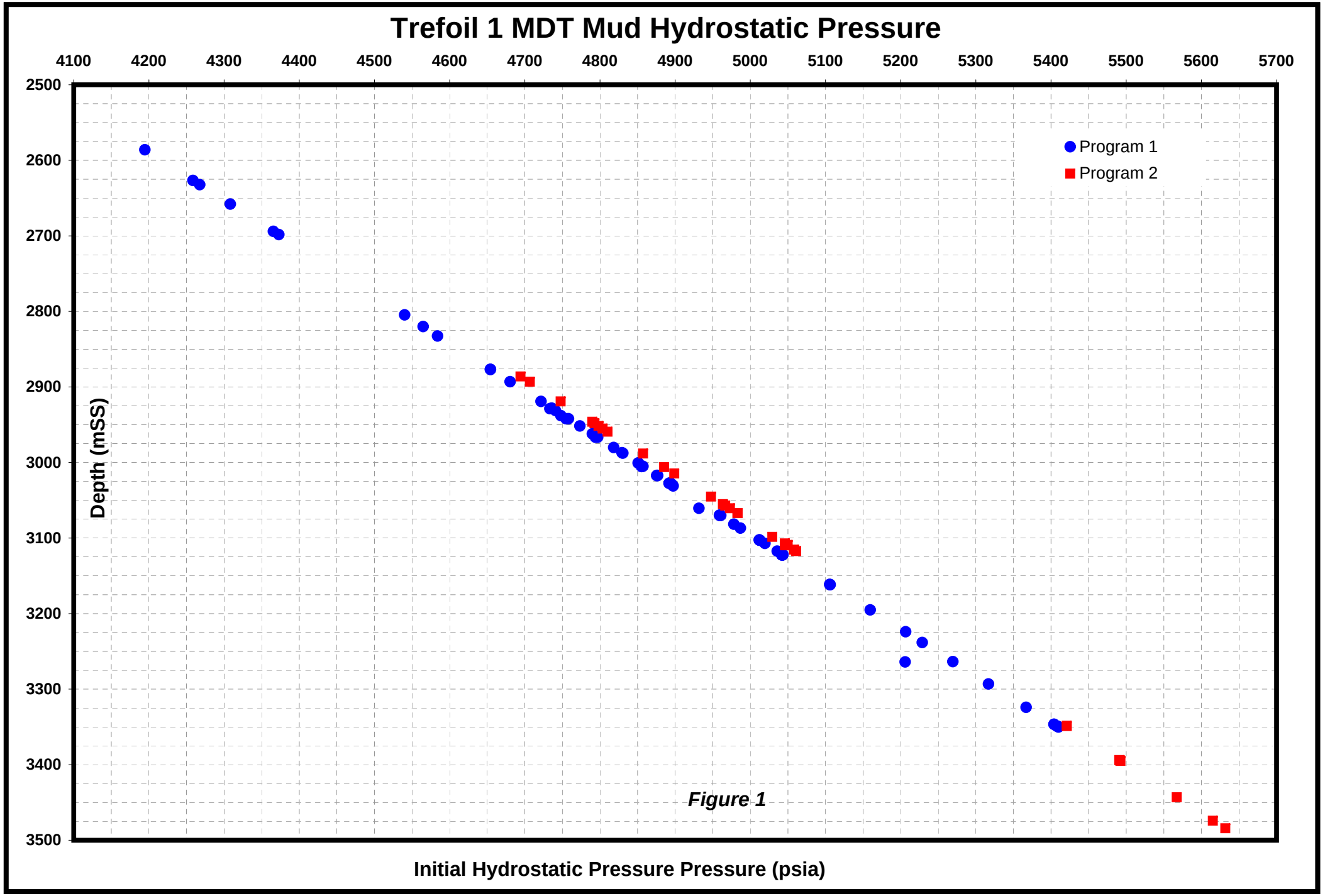
With the exception of TlLb-40, TlLb-50 and TlLb-60 (Figure 9) a GWC cannot be defined for most of these gas potential intervals due to the multi-systems characteristic of this formation. Consequently the LKG levels are recommended for the purpose of OGIP calculation for those zones. While no signs of field depletion were observed during the CHDST#1 (TuFl-80), the CHDST2 results indicate that the gas volume associated with the TlLb-90 zone is limited. This has been described by a dashed water line (drawn close to the bottom of CHDST2 perforation interval) on the MDT plot.

Figure 9: illustrates the MDT profile for TlLb-40, TlLb-50 and TlLb-60 assuming these zones are all part of one system characterised by a water line passing through a MDT point at 3006.5mMD (2966.6 mss). A fluid sample taken at this point (3006.5mMD) recovered only water (salinity=33887ppm, filtrate=50406ppm). A water gradient with 0.42 psi/ft, derived from the MDT data of the shallower section, was used to establish the above water line. Gas samples were collected from 2968.7mMD (TlLb-40), 2988.0mMD (TlLb-50) and 2999.2mMD (TlLb-60). Gas lines with gradients 0.107 psi/ft, 0.094 psi/ft and 0.095 psi/ft, consistent with measured densities of the recovered fluid samples characterising TlLb-40, TlLb-50 and TlLb-60 zones, were also established. These lines define GWC of 2953.7mSS, 2960.8mSS and 2964.0mSS for TlLb-40, TlLb-50 and TlLb-60 zones respectively.

A summary of the results are shown in the following table.

Trefoil-1 MDT Summary of Results

Sand Interval mMD approx	Informal Zone Name	Gas Content was verified by	GWC or LKG(log) mSS		Remarks
2931 – 2934	TlLb-10	MDT Sample	LKG	2894.1	LKG = Bottom of the zone. Sample taken at 2893.1mSS recovered reach gas.
2957 – 2960	TlLb-30	MDT Pumpout	LKG	2920.4	LKG= Bottom of the zone. Pumpout at 2919.1mSS indicates gas content.
2967 – 2972	TlLb-40	MDT Sample	GWC	2953.7	TlLb-40, TlLb-50 & TlLb-60 were assumed to be part of one system.
2979 – 2983	TlLb-50	MDT Sample	GWC	2960.8	TlLb-40, TlLb-50 & TlLb-60 were assumed to be part of one system.
2991 – 3002	TlLb-60	MDT Sample	GWC	2964.0	TlLb-40, TlLb-50 & TlLb-60 were assumed to be part of one system.
3018 – 3022	TlLb-70	Not verified	LKG	2982.6	LKG = Bottom of the Zone. Gas content was not verified by MDT.
3026 – 3029	TlLb-80	MDT Sample	LKG	2989.1	LKG = Bottom of the zone. Sample taken at 2988.1mSS recovered gas
3040 – 3047	TlLb-90	CHDST	LKG	3007.1	The CHDST#2 results indicate a limited gas column.
3054 - 3059	TuFl-10	MDT Sample	LKG	3019.1	LKG = Bottom of the zone. Sample taken at 3017.3mSS recovered gas
3094 - 3108	TuFl-30	MDT Pumpout	LKG	3068.0	LKG = Bottom of the zone. Pumpout at 3060.6mSS indicates gas content
3109 - 3111	TuFl-40	Not verified	LKG	3071.1	LKG = Bottom of the Zone. Gas content was not verified by MDT.
3121 - 3123	TuFl-50	Not verified	LKG	3082.6	LKG = Bottom of the Zone. Gas content was not verified by MDT.
3126 - 3131	TuFl-60	Not verified	LKG	3090.9	LKG = Bottom of the Zone. Gas content was not verified by MDT.
3141 - 3150	TuFl-80	CHDST	LKG	3111.1	No signs of field depletion were noticed during the CHDST#1.
3153 - 3158	TuFl-90	MDT Pumpout	LKG	3118.1	LKG = Bottom of the zone. Pumpout at 3117.3mSS indicates gas content
3385 - 3390	TTl-10	MDT Sample	GWC	3347.7	Estimated by MDT sampling.


Trefoil 1 MDT Mud Hydrostatic Pressure
4100
4200
4300
4400
4500
4600
4700
4800
4900
5000
5100
5200
5300
5400
5500
5600
5700
2500
2600
2700
2800
2900
3000
3100
3200
3300
3400
3500
Depth (mSS)
Program 1
Program 2
Figure 1
Initial Hydrostatic Pressure Pressure (psia)

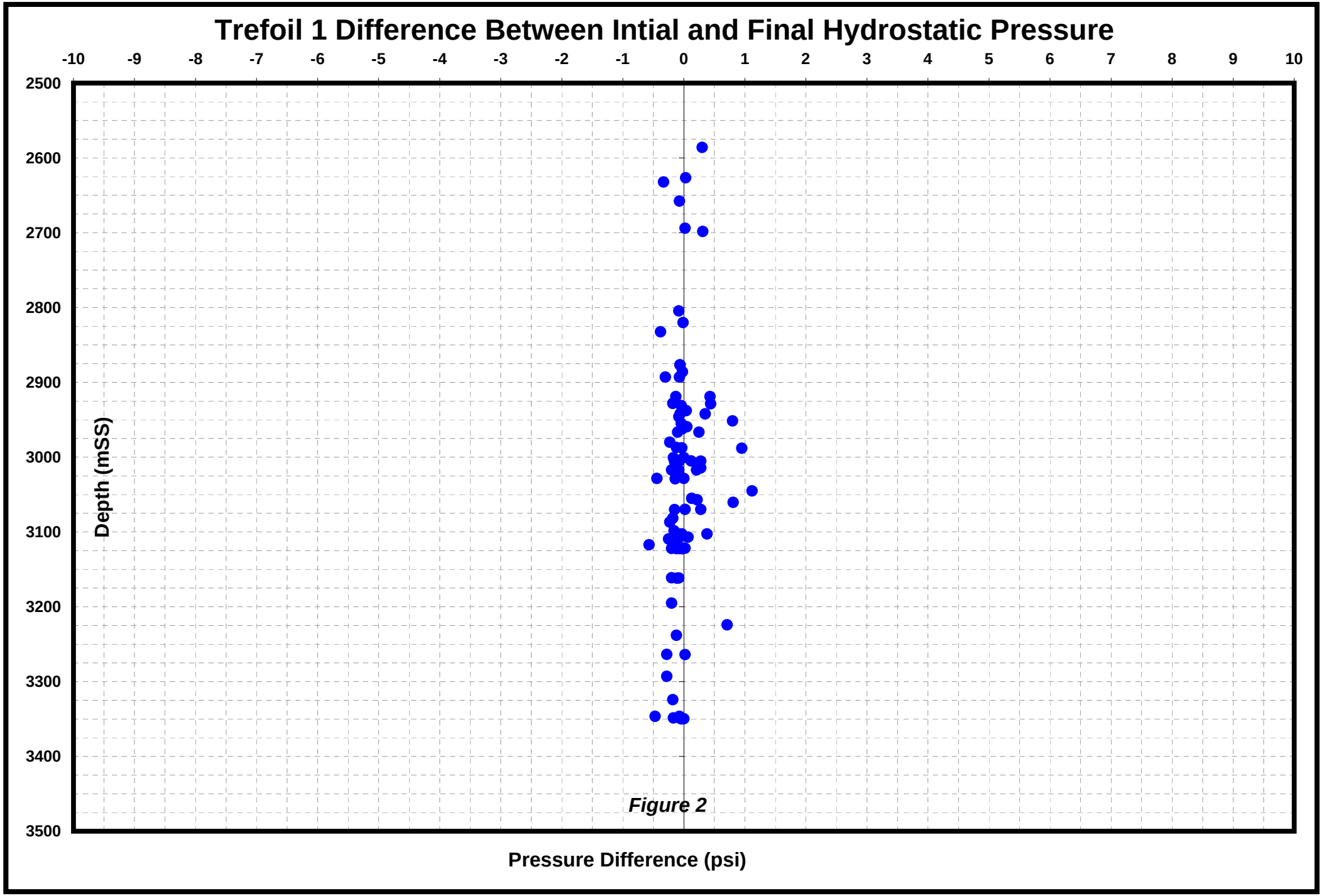

Trefoil 1 Difference Between Intial and Final Hydrostatic Pressure
-10
-9
-8
-7
-6
-5
-4
-3
-2
-1
0
1
2
3
4
5
6
7
8
9
10
2500
2600
2700
2800
2900
3000
3100
3200
3300
3400
3500
Depth (mSS)
Pressure Difference (psi)

Figure 2

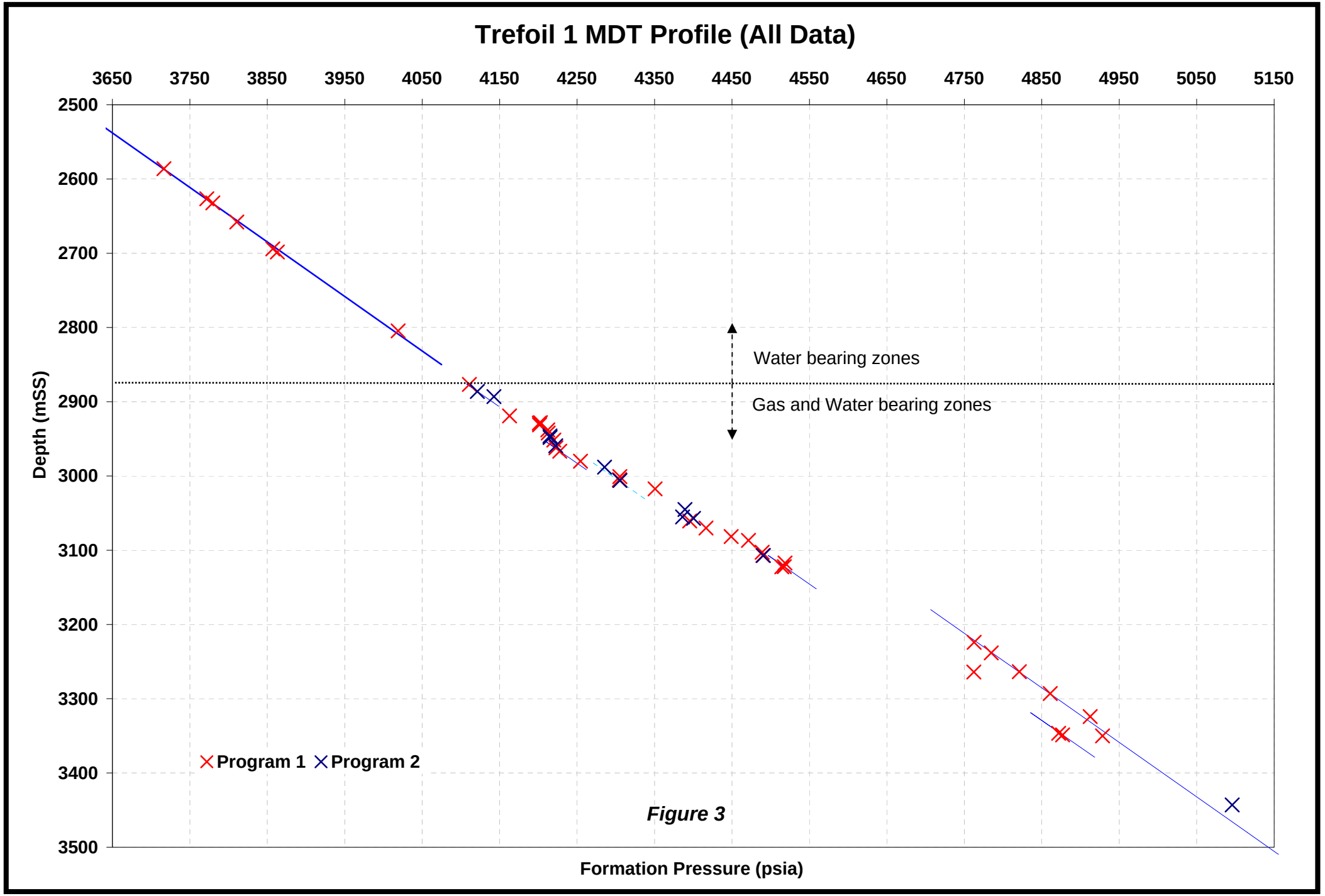

Trefoil 1 MDT Profile (All Data)
3650
3750
3850
3950
4050
4150
4250
4350
4450
4550
4650
4750
4850
4950
5050
5150
2500
2600
2700
2800
2900
3000
3100
3200
3300
3400
3500
Depth (mSS)
Water bearing zones
Gas and Water bearing zones
Program 1
Program 2
Formation Pressure (psia)

Figure 3

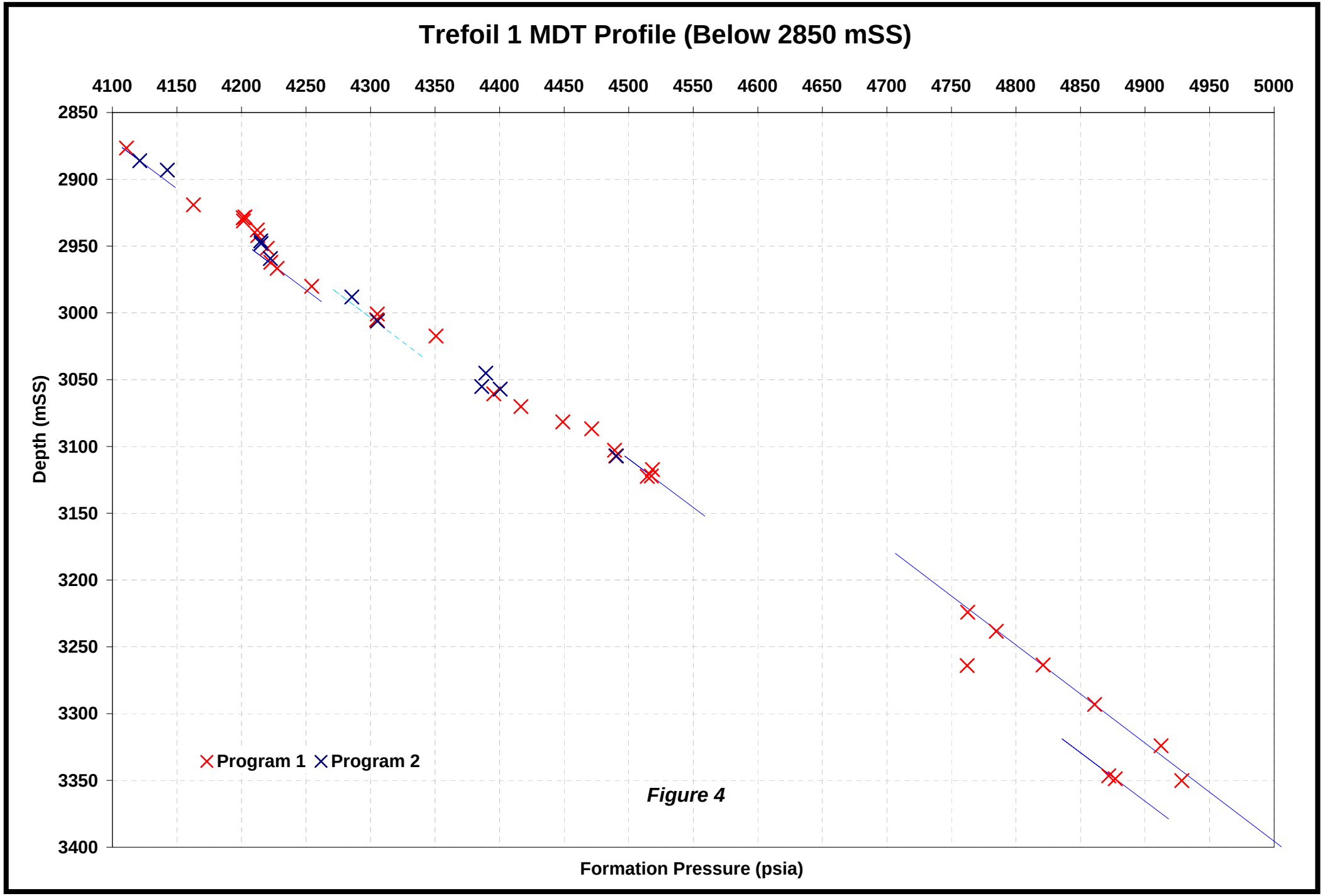

Trefoil 1 MDT Profile (Below 2850 mSS)
4100
4150
4200
4250
4300
4350
4400
4450
4500
4550
4600
4650
4700
4750
4800
4850
4900
4950
5000
2850
2900
2950
3000
3050
3100
3150
3200
3250
3300
3350
3400
Depth (mSS)
Program 1
Program 2
Formation Pressure (psia)

Figure 4

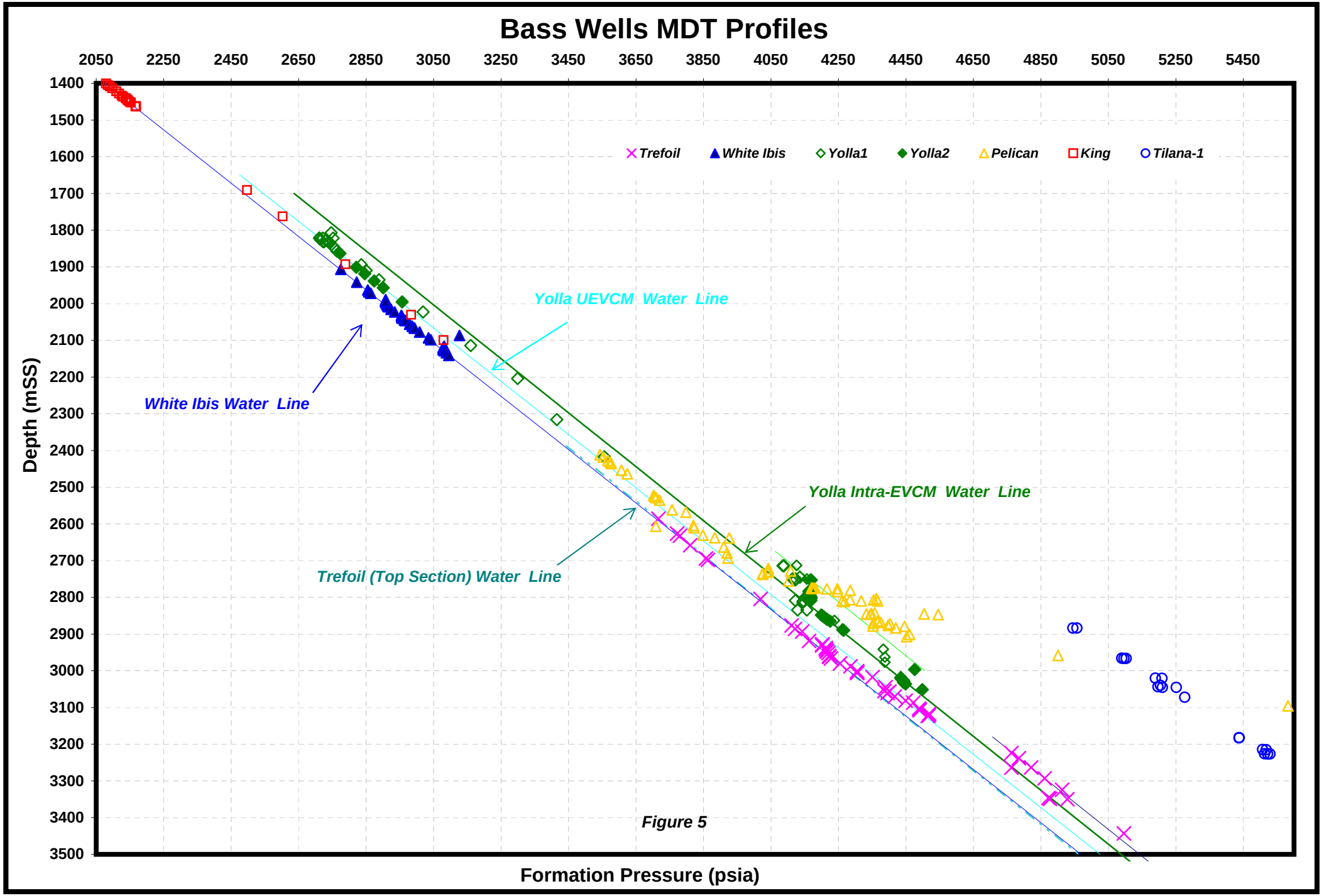

Bass Wells MDT Profiles
2050
2250
2450
2650
2850
3050
3250
3450
3650
3850
4050
4250
4450
4650
4850
5050
5250
5450
1400
1500
1600
1700
1800
1900
2000
2100
2200
2300
2400
2500
2600
2700
2800
2900
3000
3100
3200
3300
3400
3500
Depth (mSS)
Formation Pressure (psia)
Trefoil
White Ibis
Yolla1
Yolla2
Pelican
King
Tilana-1
Yolla UEVCM Water Line
White Ibis Water Line
Yolla Intra-EVCM Water Line
Trefoil (Top Section) Water Line

Figure 5

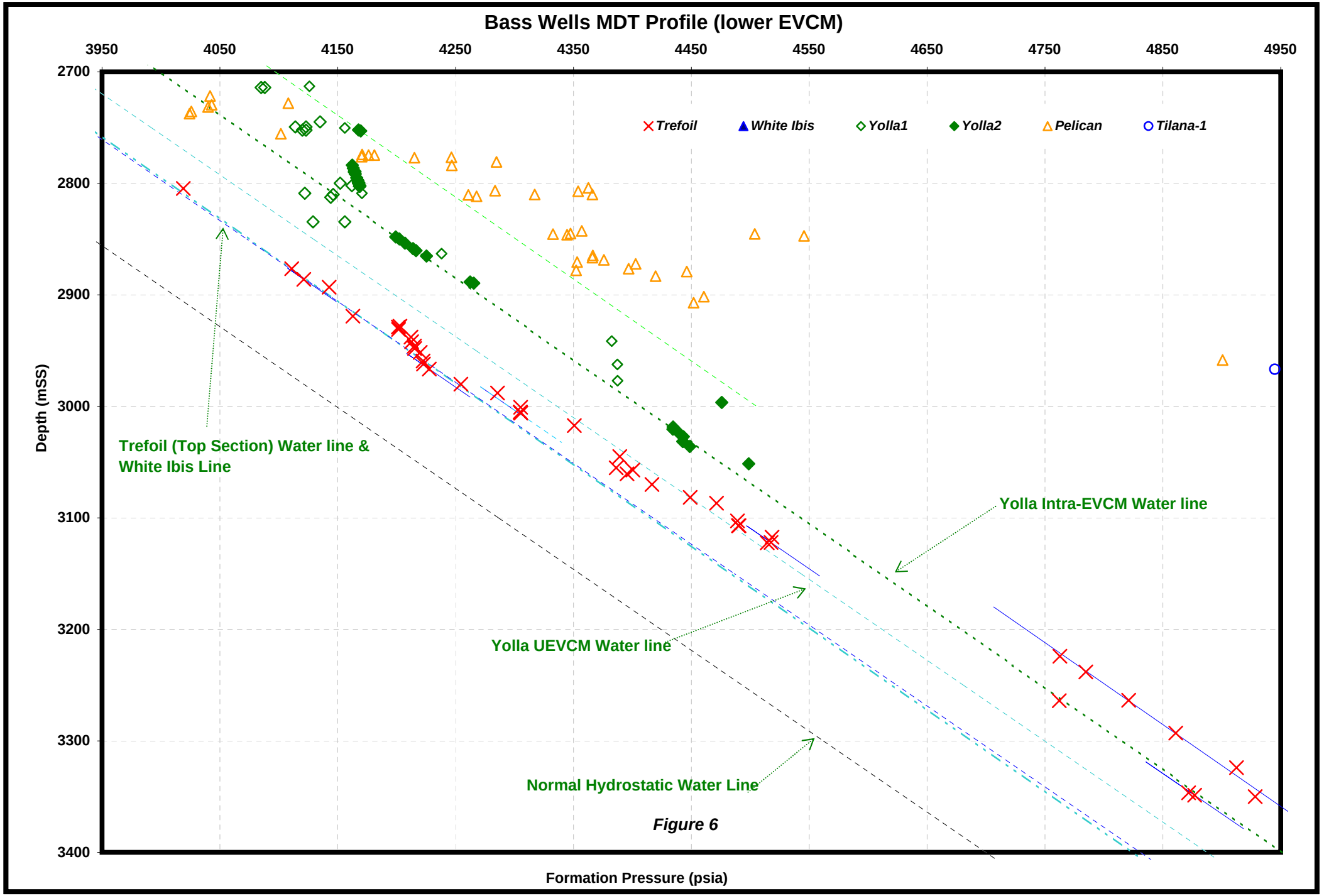

Bass Wells MDT Profile (lower EVCM)
3950
4050
4150
4250
4350
4450
4550
4650
4750
4850
4950
2700
2800
2900
3000
3100
3200
3300
3400
Depth (mSS)
Formation Pressure (psia)
Trefoil
White Ibis
Yolla1
Yolla2
Pelican
Tilana-1
Trefoil (Top Section) Water line &
White Ibis Line
Yolla Intra-EVCM Water line
Yolla UEVCM Water line
Normal Hydrostatic Water Line

Figure 6

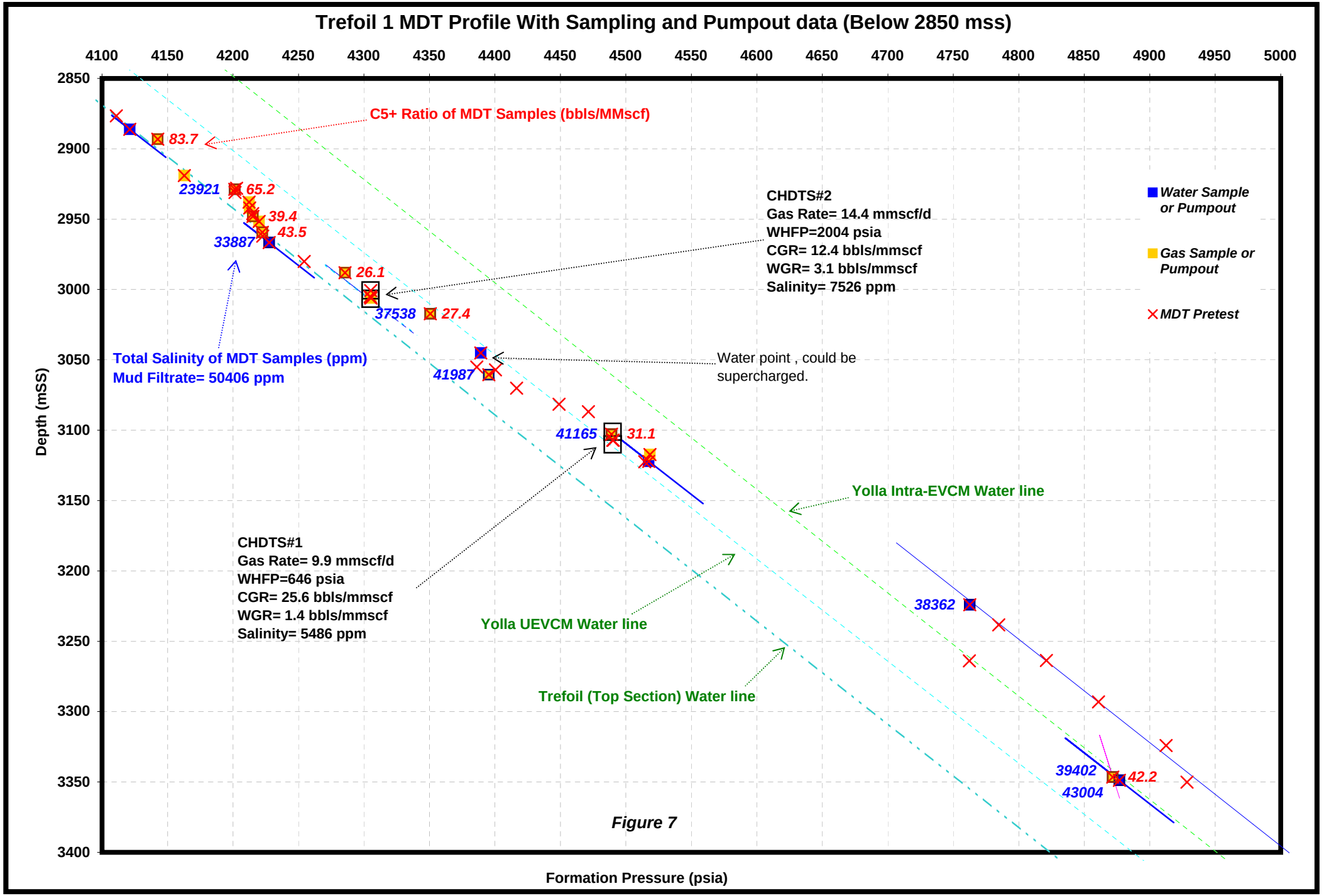

Trefoil 1 MDT Profile With Sampling and Pumpout data (Below 2850 mss)
4100
4150
4200
4250
4300
4350
4400
4450
4500
4550
4600
4650
4700
4750
4800
4850
4900
4950
5000
2850
2900
2950
3000
3050
3100
3150
3200
3250
3300
3350
3400
Depth (mSS)
Formation Pressure (psia)
C5+ Ratio of MDT Samples (bbls/MMscf)
83.7
23921
65.2
39.4
43.5
33887
26.1
37538
27.4
41987
41165
31.1
38362
39402
42.2
43004
CHDTS#2
Gas Rate= 14.4 mmscf/d
WHFP=2004 psia
CGR= 12.4 bbls/mmscf
WGR= 3.1 bbls/mmscf
Salinity= 7526 ppm
Water Sample or Pumpout
Gas Sample or Pumpout
MDT Pretest
Total Salinity of MDT Samples (ppm)
Mud Filtrate= 50406 ppm
Water point , could be supercharged.
Yolla Intra-EVCM Water line
CHDTS#1
Gas Rate= 9.9 mmscf/d
WHFP=646 psia
CGR= 25.6 bbls/mmscf
WGR= 1.4 bbls/mmscf
Salinity= 5486 ppm
Yolla UEVCM Water line
Trefoil (Top Section) Water line

Figure 7

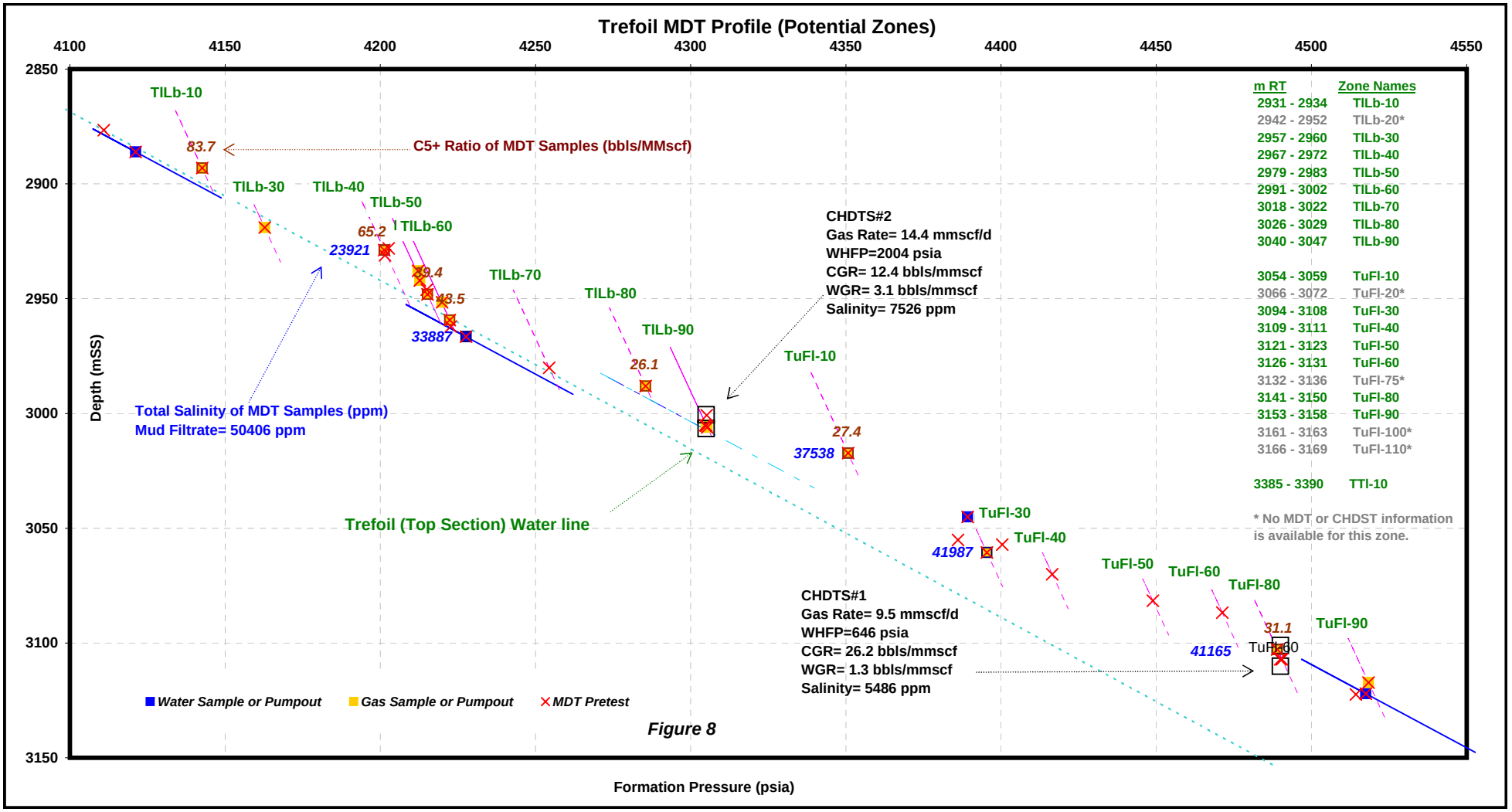

Trefoil MDT Profile (Potential Zones)
4100
4150
4200
4250
4300
4350
4400
4450
4500
4550
2850
2900
2950
3000
3050
3100
3150
Depth (mSS)
Formation Pressure (psia)
TILb-10
TILb-30
TILb-40
TILb-50
TILb-60
TILb-70
TILb-80
TILb-90
TuFl-10
TuFl-30
TuFl-40
TuFl-50
TuFl-60
TuFl-80
TuFl-90
TTI-10
83.7
65.2
23921
39.4
48.5
33887
26.1
27.4
37538
41987
31.1
41165
C5+ Ratio of MDT Samples (bbls/MMscf)
CHDTS#2
Gas Rate= 14.4 mmscf/d
WHFP=2004 psia
CGR= 12.4 bbls/mmscf
WGR= 3.1 bbls/mmscf
Salinity= 7526 ppm
Total Salinity of MDT Samples (ppm)
Mud Filtrate= 50406 ppm
Trefoil (Top Section) Water line
CHDTS#1
Gas Rate= 9.5 mmscf/d
WHFP=646 psia
CGR= 26.2 bbls/mmscf
WGR= 1.3 bbls/mmscf
Salinity= 5486 ppm
Water Sample or Pumpout
Gas Sample or Pumpout
MDT Pretest
m RT
Zone Names
2931 - 2934 TILb-10
2942 - 2952 TILb-20*
2957 - 2960 TILb-30
2967 - 2972 TILb-40
2979 - 2983 TILb-50
2991 - 3002 TILb-60
3018 - 3022 TILb-70
3026 - 3029 TILb-80
3040 - 3047 TILb-90
3054 - 3059 TuFl-10
3066 - 3072 TuFl-20*
3094 - 3108 TuFl-30
3109 - 3111 TuFl-40
3121 - 3123 TuFl-50
3126 - 3131 TuFl-60
3132 - 3136 TuFl-75*
3141 - 3150 TuFl-80
3153 - 3158 TuFl-90
3161 - 3163 TuFl-100*
3166 - 3169 TuFl-110*
3385 - 3390 TTI-10
* No MDT or CHDST information is available for this zone.

Figure 8

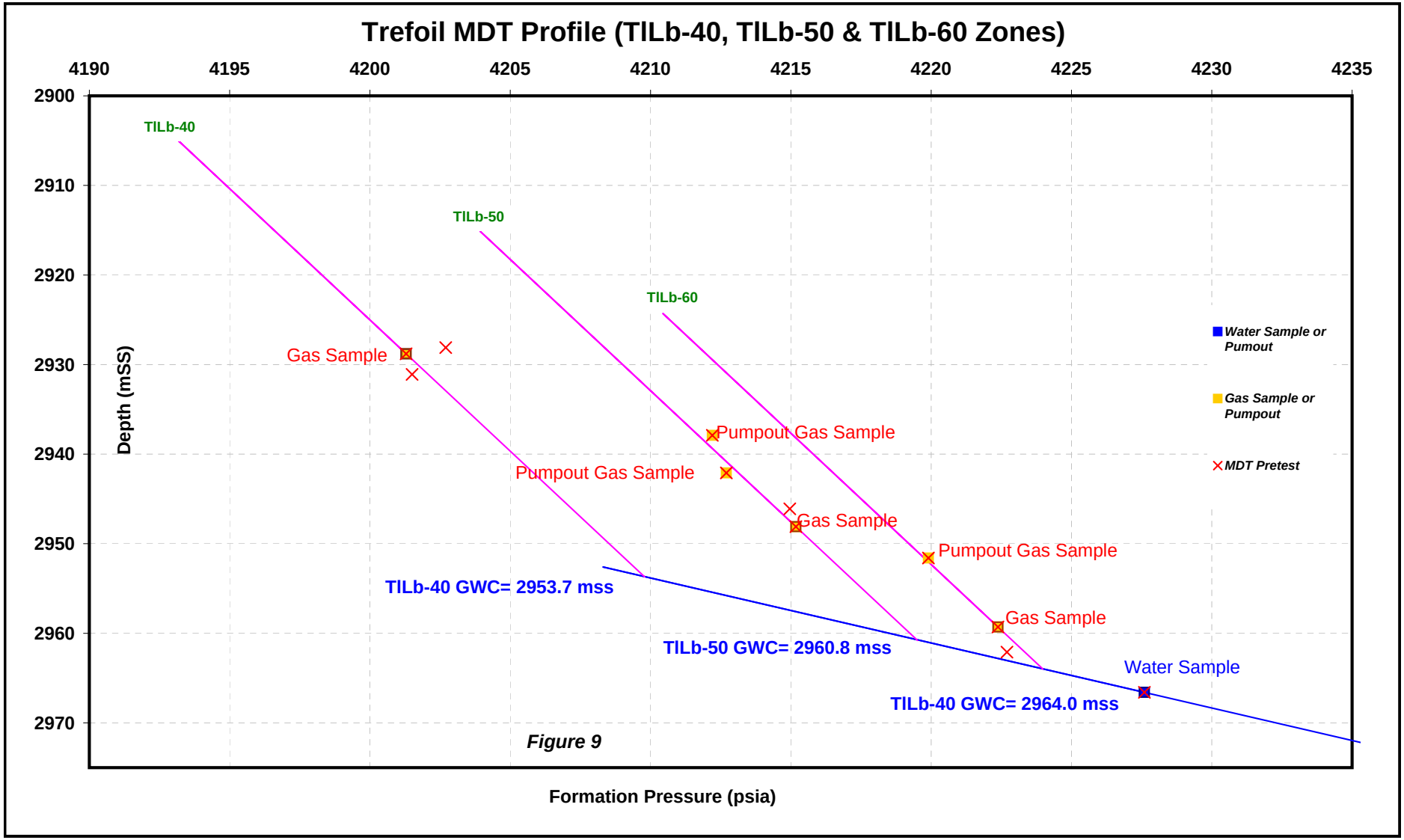

Trefoil MDT Profile (TILb-40, TILb-50 & TILb-60 Zones)
4190
4195
4200
4205
4210
4215
4220
4225
4230
4235
2900
2910
2920
2930
2940
2950
2960
2970
Depth (mSS)
TILb-40
TILb-50
TILb-60
Gas Sample
Pumpout Gas Sample
Pumpout Gas Sample
Gas Sample
Pumpout Gas Sample
Gas Sample
Water Sample
TILb-40 GWC= 2953.7 mss
TILb-50 GWC= 2960.8 mss
TILb-40 GWC= 2964.0 mss
Water Sample or Pumout
Gas Sample or Pumpout
MDT Pretest
Formation Pressure (psia)

Figure 9

APPENDIX 3: DRILL STEM TESTING INTERPRETATION REPORTS

(A) Test Interpretation

Trefoil-1 Cased Hole Drill Stem Test Interpretation

By Henry Irrgang

Table 1 provides a summary of the test results and Figure 1 shows an overview of the surface and bottomhole pressure and temperature data for the two tests.

Operations Summary – CHDST #1

(TuFl-80 Zone, 3141 – 3150m RT)

After running the DST string, circulating in a 64 bbl diesel cushion, and testing the surface equipment, the TCP guns were fired over the interval 3141 – 3150m RT at 17:35 on 11 December 2004, with THP rising rapidly to 716 psia against a closed choke manifold. The well was opened to flow at 17:37 on 16/64" choke and shut in at the PCT at 17:47 for the initial buildup (recovery was 3.7 bbls of diesel cushion). At 19:06 the well was opened on gradually increasing choke sizes up to 32/64" until gas and brine arrived at surface at 19:52. The well was beaned back and then beaned up again to 44/64" choke when flow was diverted to the separator. **Flow metering started at 21:50 on 48/64" choke and flow was stable at 16.3 mmcfd at a FTHP of 1329 psia and FTHT of 39 deg C, with an average condensate rate of 133 stb/d (CGR 8.18 stb/mmscf) and 2.3 bbls/mmscf of condensed water.** The well was shut-in at the PCT at 05:03 on 12 December for a 12 hour main buildup.

The PCT was re-opened for the sampling flow at 17:06 and SITHP climbed to 3493 psia. At 17:59 the well was opened for flow and gradually beaned up to 36/64" choke. Metering through the test separator commenced at 21:25 with a steady flow rate of 14.3 mmcfd at FTHP 2004 psia and FTHT 38 deg C with 182 stb/d of condensate (CGR 12.7 stb/mmscf) and 3.2 bbl/mmscf of condensed water. After taking duplicate surface samples, the well was shut-in at the choke manifold at 23:56 for about 5 hours of useable final buildup data.

Following the final shut-in, difficulty was experienced lowering wireline tools into the well and there were some brief flow periods to assist clearing possible hydrate blockages. A bridge plug was set above the DST 1 interval in preparation for DST 2.

Operations Summary – CHDST #2

(TILb-90 Zone, 3040.5 – 3046.5m RT)

After setting a wireline bridge plug at 3125.3m RT, and bleeding off tubing pressure to provide 1000 psi underbalance, the DST 2 interval, 3040.5 – 3046.5m RT, was perforated with 1 11/16" PJ Enerjet guns at 00:35 on 14 December. The well THP response was slow, building from 2524 psia to 3365 psia over 3.5 hours. After retrieving the guns, the well was opened at 4:52 and gradually beaned up to 32/64" choke. Metering through the separator started at 07:30 and the flow rate gradually rose from 6.7 mmcfd to 7.4 mmcfd over 5 hours. During this period, duplicate sets of surface samples were taken. The FTHP was about 1340 psia and FTHT was 31 deg C. In the last hour, the producing CGR fell from 20 stb/mmscf to 15 stb/mmscf and the condensed water rate also fell, suggesting the well was not effectively lifting liquids.

At 13:03 the choke was gradually increased to 56/64" and the flow rate gradually increased from 8.9 mmcfd to 9.9 mmcfd over 3 hours. **Final flowing conditions at 16:00 hours were 9.87 mmcfd with FTHP 645 psia, FTHT 31 deg C, CGR 26 stb/mmscf and water of**

condensation 1.4 bbls/mmscf. The sustained higher condensate yields during this flow confirmed the measured rates were too low during the sampling period.

The well was shut-in at the PCT at 16:02 for a 13.5 hour buildup, though the latter part of the buildup data was affected by wellbore and surface operations.

Bottomhole Pressure Interpretation

The bottomhole pressure data for the two tests were interpreted using the Saphir well test interpretation software. The program output reports, including comments on the data quality and interpretation results, are attached. CHDST #1 showed nearby reservoir boundaries which may be a combination of a GWC, stratigraphic boundaries or fault boundaries. CHDST #2 pressure buildup analysis indicated possible pressure depletion, but this conclusion is questionable in view of indications of a leaking downhole PCT valve with an uncertain leak rate. It should be noted that due to the high flowing drawdowns, the recombined CHDST surface samples may not be representative of the in-situ reservoir gas composition.

References

Further details of the testing are included in the appendices to the Trefoil-1 Well Completion Report – Basic Data volume. Appendix 20A is the Schlumberger Surface Data report, including an operational summary. Appendices 11 and 19 provide details of the MDT and DST sampling and analysis.

Table 1 **Trefoil-1 CHDST Interpretation Summary**

Test	Perfs Top m RT	Perfs Bot m RT	Flow Rate mmcfd	CGR stb/mmscf	FWHP psia	FWHT deg C	Choke /64"	SIWHP psia	Mid Perfs m SS	Gradient psi/m	FBHP psia@MPP	Pi (MDT) psia@MPP	k.h (est.) md.ft	Gas perm md	Total Skin	Comments
CHDST #1	3141.0	3150.0	16.3	8.18	1329	39	48	3493	3101.6	0.289	2613	4489	552	24	11.6	Two reservoir boundaries at 110 degrees at 42 and 46m from the well
CHDST #1 Sampling Flow			14.3	12.7	2004	38	36	3488	3101.6	0.289	3049				9.0	Skin decreased from main flow
CHDST #2	3040.5	3046.5	9.9	26.0	645	31	56	N/A	3003.6	0.334	1543	4305	870	49	64.6	Poor perforations, skin still decreasing. Possible pressure depletion but may be the effect of a leaking PCT valve.

Notes:

1 Reservoir boundaries seen in DST #1 may represent the GWC or possible stratigraphic or fault boundaries
2 Flowing bottomhole pressures, FWHP and FWHT were rising slowly during DST #2, indicating the zone was still cleaning up and stabilising
3 BHP interpretation results for CHDST #2 affected by a leaking PCT valve
4 Skin factors are based on the currently available test data and do not account for future completion practices, well cleanup and later condensate dropout effects

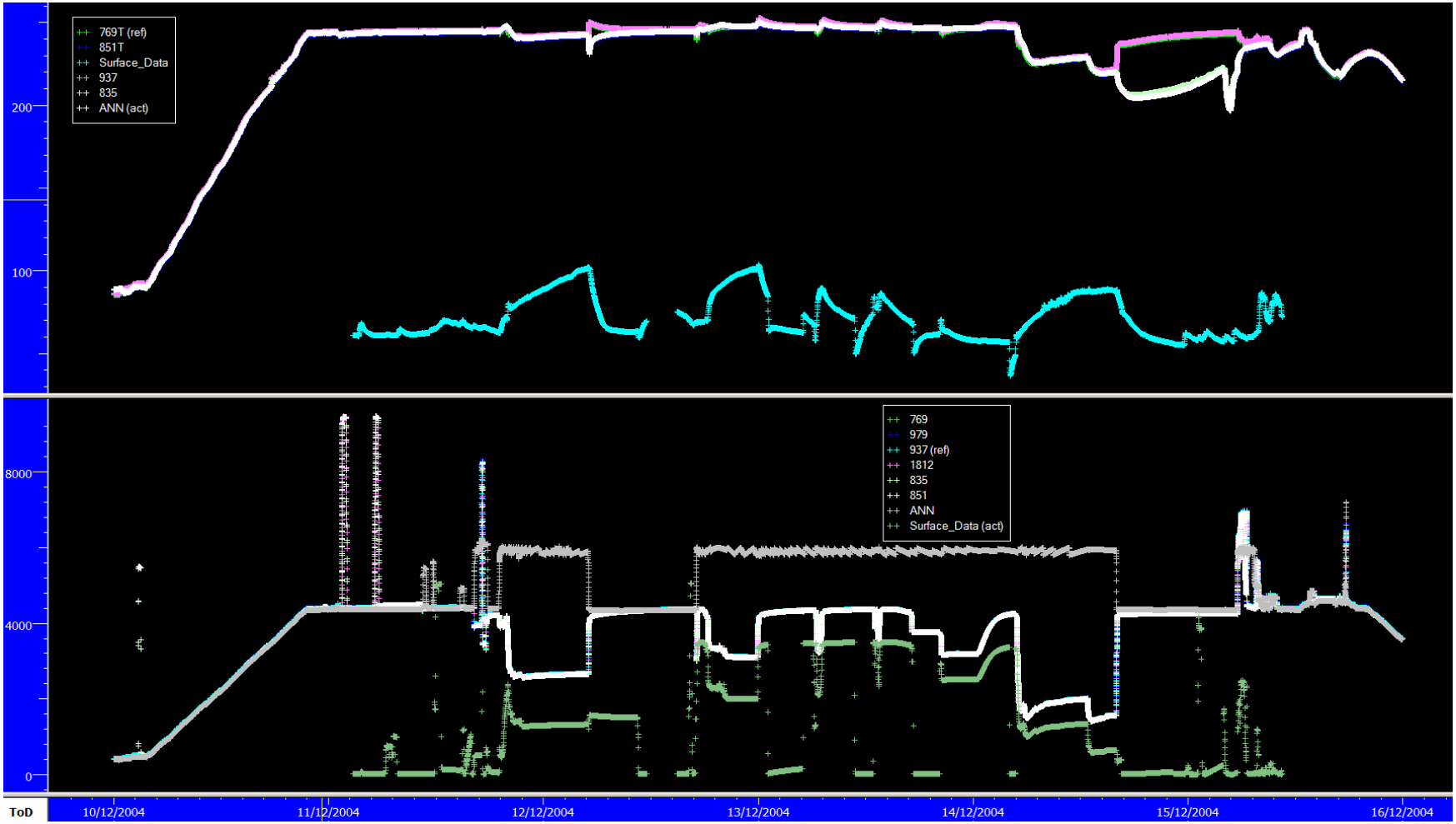


Figure 1 - Trefoil-1 Bottomhole and Surface Data Overview

Company Origin — Field Trefoil
Well Trefoil 1 — Test Name / # CHDST #1

Test date / time	10 December 2004
Formation interval	Lower EVCM
Perforated interval	3141 - 3150m RT
Gauge type / #	WTQR 937
Gauge depth	2943.58m RT (2903.68m SS)
TEST TYPE	Standard
Porosity Phi (%)	14.2
Well Radius rw	0.3542 ft
Pay Zone h	23 ft
Water Salt (ppm)	15000
Form. compr.	4E-6 psi-1
Reservoir T	255 °F
Reservoir P	4489 psia
FLUID TYPE	Gas

Gas

Gas Gravity	0.712711
Pseudo-Critical P	670.859 psia
Pseudo-Critical T	378.16 °R

Sour gas composition

Hydrogen sulphide	0
Carbon dioxide	0.0399
Nitrogen	0.0038

Water

Salinity, ppm	15000
Temperature	255 °F
Pressure	4489 psia
Properties	@ Reservoir T&P

Gas

Z	0.948804
Mug	0.0252052 cp
Bg	0.00427094 cf/scf
cg	1.66031E-4 psi-1
Rhog	0.204385 g/cc

Water

Rsw	23.4838 cf/bbl
Bw	1.04654 B/STB
cw	3.86633E-6 psi-1
Muw	0.234731 cp
Rhow	0.966554 g/cc
Total Compr. ct	9.54355E-5 psi-1
Connate Water (%)	46

Selected Model

Model Option	Standard Model
Well	Storage + Skin
Reservoir	Homogeneous
Boundary	Intersecting Faults (angle)

Results

TMatch	1080 [hr]**-1
PMatch	3.33E-8 [psi2/cp]**-1
C	0.006 bbl/psi
Skin	11.6
Delta P Skin	956.337 psi
Pi	4446.18 psia
k.h	552 md.ft
k	24 md
L1 - No Flow	150 ft
L2 - No Flow	170 ft
Angle	110 °

The pressure gauge data quality was high and the gauges were consistent. Gauge 937 in the bottom gauge carrier was used for analysis with pressures reported at the gauge depth of 2943.6m RT. The PCT leaked slightly for the first 6 minutes of the shut-in after the main flow, but this did not adversely affect the interpretation. Otherwise, the test was mechanically successful. Fluid properties used are from correlations using the measured gas properties, and petrophysical properties are from the analysis by A. Hall (email of 7 April 2005). The maximum temperature reached at the gauges was 252 deg F, which would be less than the reservoir temperature.

A reasonable match to the middle and late time pressure buildup was obtained with a homogeneous reservoir model with 2 no-flow boundaries at 110 degrees to each other, being about 46m and 42m from the well. The afterflow period was not well matched due to varying wellbore storage resulting from the large pressure drawdown, but this does not affect the later buildup interpretation.

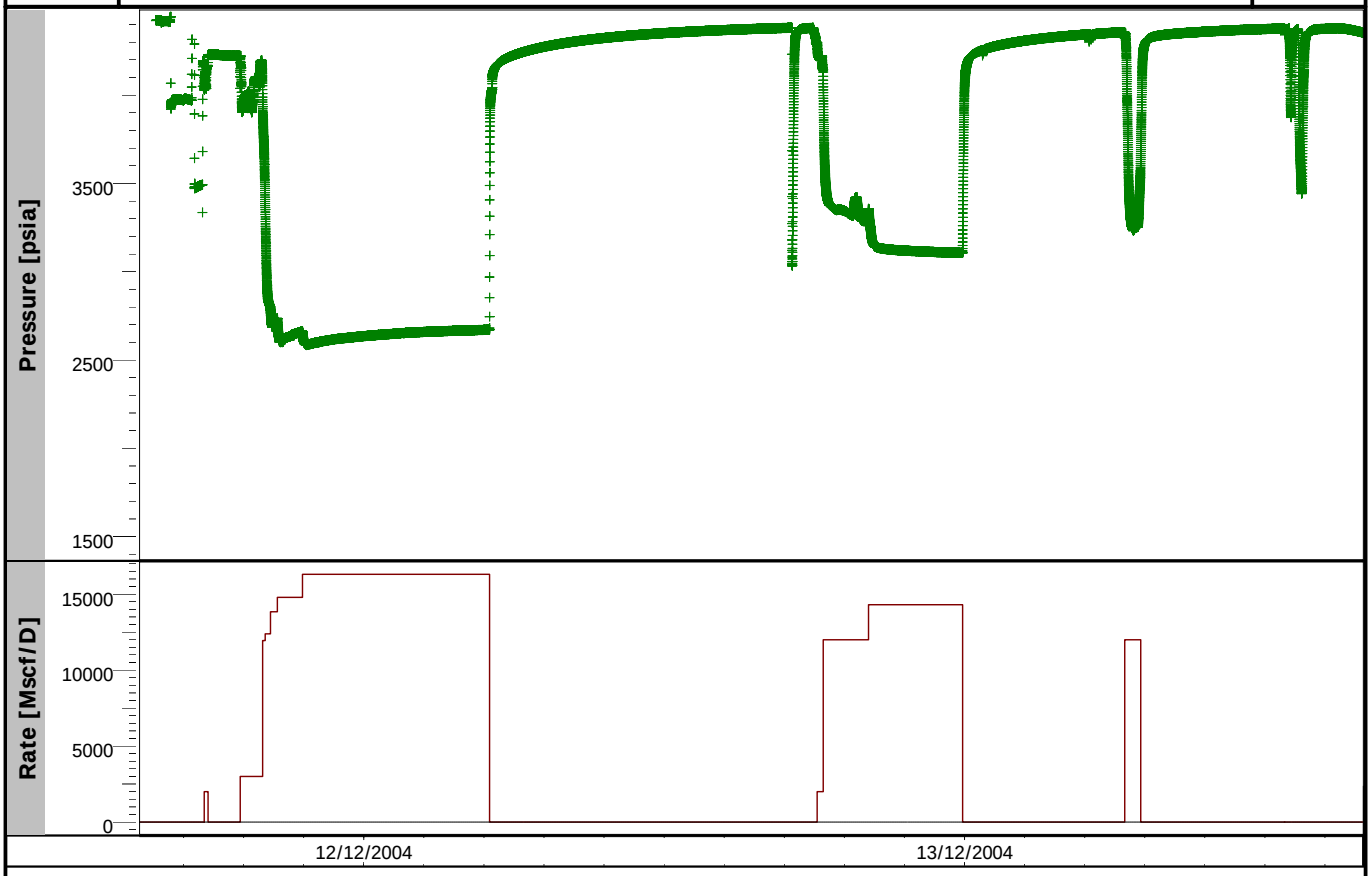
The MDT pressure was 4489 psia at 3142.7m RT, equivalent to 4431 psia at the DST gauge depth of 2943.6m RT (using a gas gradient 0.289 psi/m). The initial flow did not remove completion brine from below PCT - therefore the measured initial buildup pressure is lower than expected if there were a gas gradient below the gauges, being affected by an uncertain amount of brine below the gauges. Therefore, the initial buildup cannot be used to confirm the MDT data as there is an uncertain correction from gauge to perforation depth. The implied initial pressure, from the above model match to the main buildup data, is about 15 psi higher than the MDT, suggesting that the reservoir boundaries have less late time impact than modeled (as also suggested by the flattening of the derivative at the very end of the buildup).

There was no significant indication of pressure depletion or closed boundaries within the distance investigated (about 220m). It should be noted that the apparent reservoir boundaries referenced above may be the effect of a nearby GWC. The absence of pressure depletion and additional reservoir boundaries suggests that the well may be on the flank of the accumulation at this level (as suggested by the seismic attribute analysis).

The flowing bottomhole pressure was not well matched as the well was continuing to clean up throughout the test (i.e. decreasing skin). The reported skin of 11.6 is at the end of the main flow, and dropped further to about 9 for the sampling flow. For this reason, it is not possible to estimate the non-Darcy flow coefficient.

Date	ToD	FP #	Gas rate Mscf/D	Duration hr
10/12/2004	00:00:00	1	0	41.6253
11/12/2004	17:37:31	2	2000	0.153778
11/12/2004	17:46:45	3	0	1.28372
11/12/2004	19:03:46	4	3000	0.898611
11/12/2004	19:57:41	5	11940	0.0986111
11/12/2004	20:03:36	6	12381	0.213889
11/12/2004	20:16:26	7	13838	0.277778
11/12/2004	20:33:06	8	14784	1.00278
11/12/2004	21:33:16	9	16300	7.47469
12/12/2004	05:01:45	10	0	12.0698
12/12/2004	17:05:56	11	1	1.01667
12/12/2004	18:06:56	12	2000	0.241667
12/12/2004	18:21:26	13	12000	1.80833
12/12/2004	20:09:56	14	14300	3.76217
12/12/2004	23:55:40	15	0	6.47116
13/12/2004	06:23:56	16	12000	0.638889
13/12/2004	07:02:16	17	0	5.74861
13/12/2004	12:47:11	18	1	59.2125

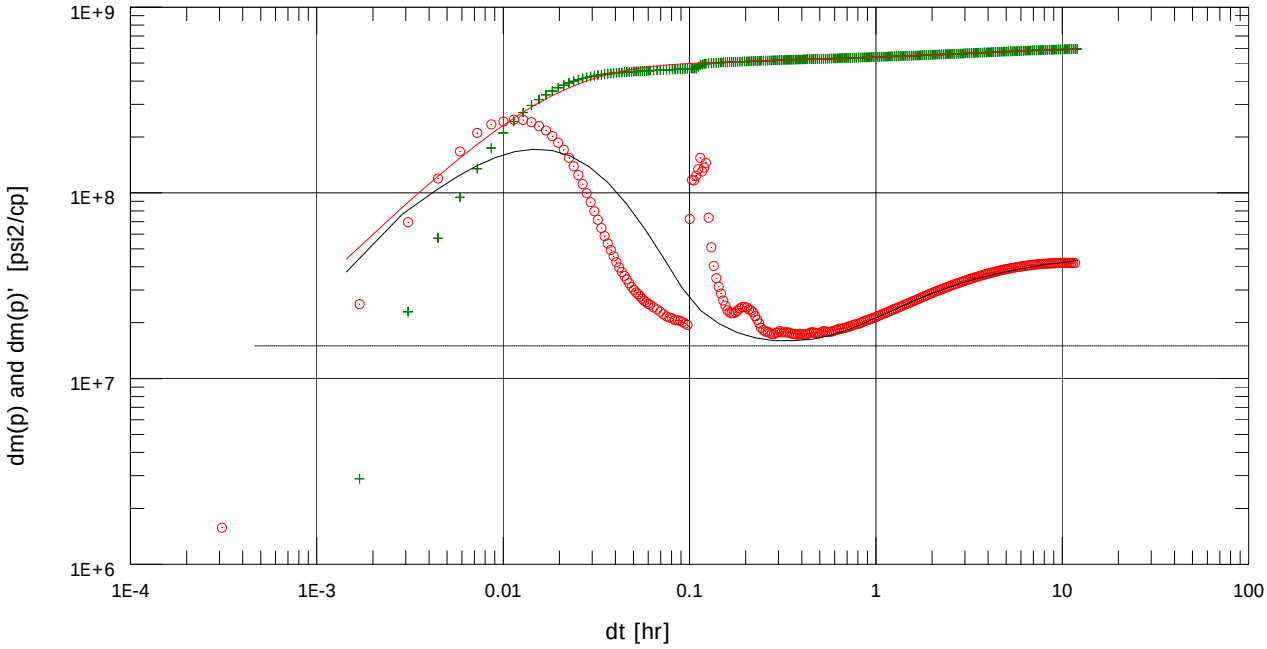
QA / QC	Analysis 1
Company Origin	Field Trefoil
Well Trefoil 1	Test Name / # CHDST #1



Pressure [psia], Gas Rate [Mscf/D] vs Time [ToD]

Pressure
++ 937 bottom carrier (act & ref)

Log-Log plot	Analysis 1
Company Origin	Field Trefoil
Well Trefoil 1	Test Name / # CHDST #1



937 bottom carrier build-up #2

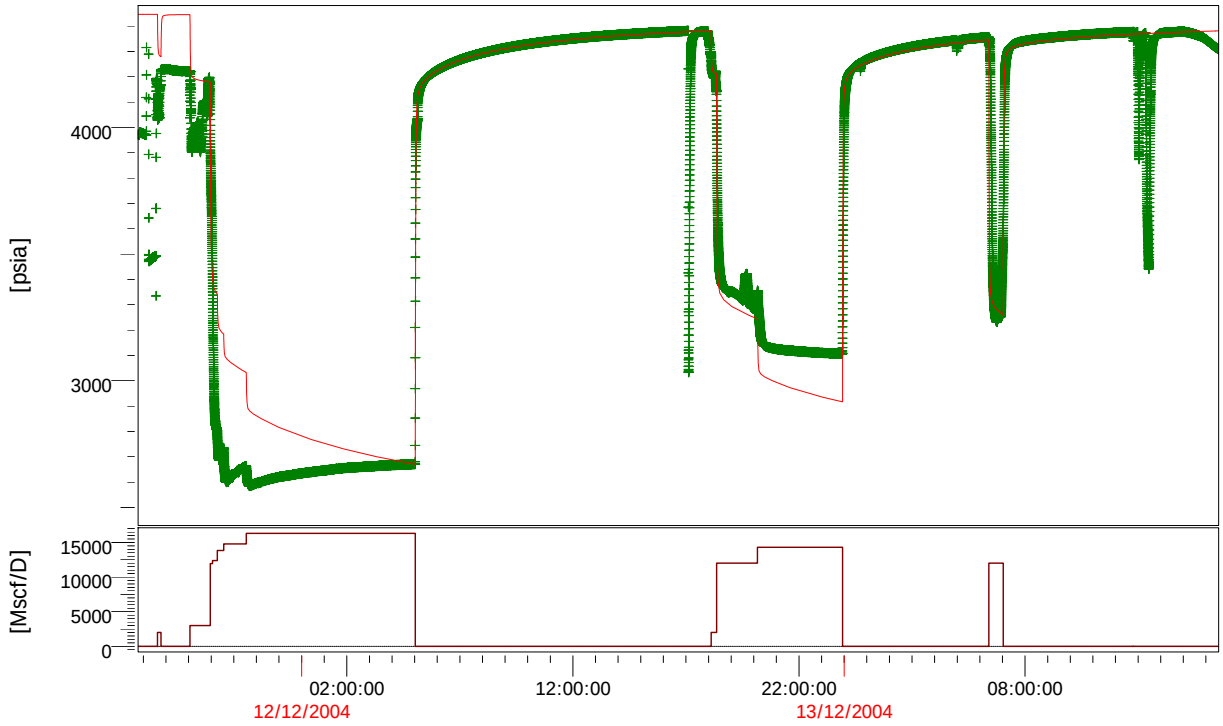
Rate	0 Mscf/D
Rate change	16300 Mscf/D
P@dt=0	2670.32 psia
Pi	4446.18 psia
Smoothing	0.1

Selected Model

Model Option	Standard Model
Well	Storage + Skin
Reservoir	Homogeneous
Boundary	Intersecting Faults (angle)

Results

TMatch	1080 [hr]**-1
PMatch	3.33E-8 [psi2/cp]**-1
C	0.006 bbl/psi
Skin	11.6
Delta P Skin	956.337 psi
Pi	4446.18 psia
k.h	552 md.ft
k	24 md
L1 - No Flow	150 ft
L2 - No Flow	170 ft
Angle	110 °



Pressure [psia], Gas Rate [Mscf/D] vs Time [ToD]

— Gas rate

937 bottom carrier build-up #2

Rate	0 Mscf/D
Rate change	16300 Mscf/D
P@dt=0	2670.32 psia
Pi	4446.18 psia
Smoothing	0.1

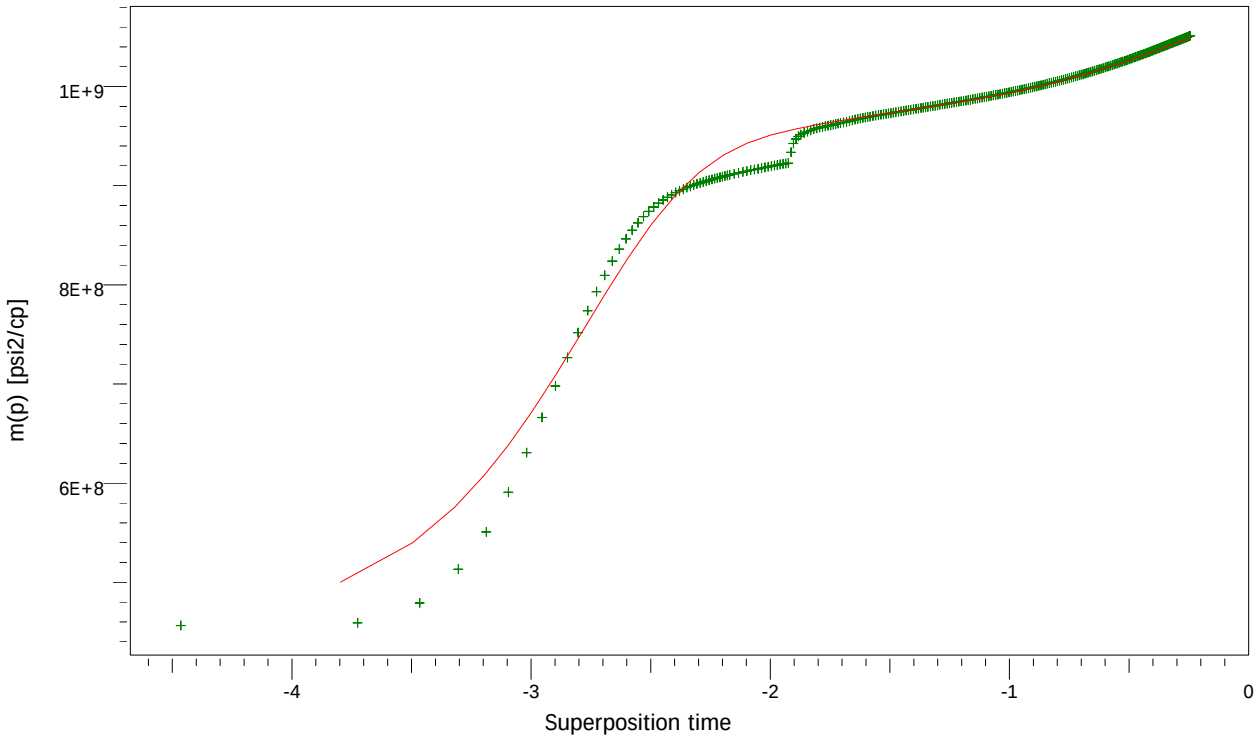
Selected Model

Model Option	Standard Model
Well	Storage + Skin
Reservoir	Homogeneous
Boundary	Intersecting Faults (angle)

Results

TMatch	1080 [hr]**-1
PMatch	3.33E-8 [psi2/cp]**-1
C	0.006 bbl/psi
Skin	11.6
Delta P Skin	956.337 psi
Pi	4446.18 psia
k.h	552 md.ft
k	24 md
L1 - No Flow	150 ft
L2 - No Flow	170 ft
Angle	110 °

Semi-Log plot	Analysis 1
Company Origin	Field Trefoil
Well Trefoil 1	Test Name / # CHDST #1



937 bottom carrier build-up #2

Rate	0 Mscf/D
Rate change	16300 Mscf/D
P@dt=0	2670.32 psia
Pi	4446.18 psia
Smoothing	0.1

Selected Model

Model Option	Standard Model
Well	Storage + Skin
Reservoir	Homogeneous
Boundary	Intersecting Faults (angle)

Results

TMatch	1080 [hr]**-1
PMatch	3.33E-8 [psi2/cp]**-1
C	0.006 bbl/psi
Skin	11.6
Delta P Skin	956.337 psi
Pi	4446.18 psia
k.h	552 md.ft
k	24 md
L1 - No Flow	150 ft
L2 - No Flow	170 ft
Angle	110 °

Test date / time	14 December 2004
Formation interval	Lower EVCM
Perforated interval	3040.5 - 3046.5m RT
Gauge type / #	WTQR 937
Gauge depth	2943.58m RT (2903.68m SS)
TEST TYPE	Standard
Porosity Phi (%)	14.9
Well Radius rw	0.3542 ft
Pay Zone h	17.7 ft
Water Salt (ppm)	15000
Form. compr.	4E-6 psi-1
Reservoir T	248 °F
Reservoir P	4267 psia
FLUID TYPE	Gas

Gas

Gas Gravity	0.812
Pseudo-Critical P	658.087 psia
Pseudo-Critical T	395.636 °R

Sour gas composition

Hydrogen sulphide	0
Carbon dioxide	0.04
Nitrogen	0.0085

Water

Salinity, ppm	15000
Temperature	248 °F
Pressure	4267 psia
Properties	@ Reservoir T&P

Gas

Z	0.909818
Mug	0.0273735 cp
Bg	0.00426634 cf/scf
cg	1.7071E-4 psi-1
Rhog	0.23311 g/cc

Water

Rsw	22.0338 cf/bbl
Bw	1.04381 B/STB
cw	3.7832E-6 psi-1
Muw	0.242792 cp
Rhow	0.96908 g/cc
Total Compr. ct	8.79082E-5 psi-1
Connate Water (%)	52

Selected Model

Model Option	Standard Model
Well	Storage + Skin
Reservoir	Radial Composite
Boundary	Circle

Results

TMatch	6700 [hr]**-1
PMatch	8.75E-8 [psi2/cp]**-1
C	0.0014 bbl/psi
Skin	64.6
Delta P Skin	2351.3 psi
Pi	4266.75 psia
Pbar	4263.13 psia
k.h	870 md.ft
k	49.2 md
Ri	110 ft
M	0.5
D	0.5
Re - No Flow	1850 ft
Test. Vol.	5.05051E+6 Barrels

The pressure gauge data quality was good, with the gauges in good agreement with each other. Gauge 937 in the bottom gauge carrier was used for this analysis, with pressure data reported at the gauge depth of 2943.6m RT. The later part of the final buildup was marred by wellbore effects related to operation of the surface valves in preparation for killing the well, which resulted in some pressure irregularities in the downhole gauges. The rise in SITHP, between when the master valve was shut (395 psia after 30 minutes shut-in) and when it was re-opened (1614 psia after about 7 hours SI), provided evidence of a small leak in the downhole PCT valve (the flow rate, estimated from the rate of tubing pressure buildup, was about 0.1 mmcfd), and this may explain why the surface operations affected the bottomhole pressure buildup. The bottomhole pressure started falling after about 5.75 hours of buildup, making this data unusable, however it is not clear whether the earlier buildup data was also affected (see discussion below). The maximum BH temperature reached was 244 deg Fat the gauges and still rising, so the reservoir temperature would be higher than that.

PVT properties were obtained from correlations using the measured reservoir gas composition and were in reasonable agreement with the laboratory measured z factor. Petrophysical properties were provided by A. Hall by email on 7 April 2005.

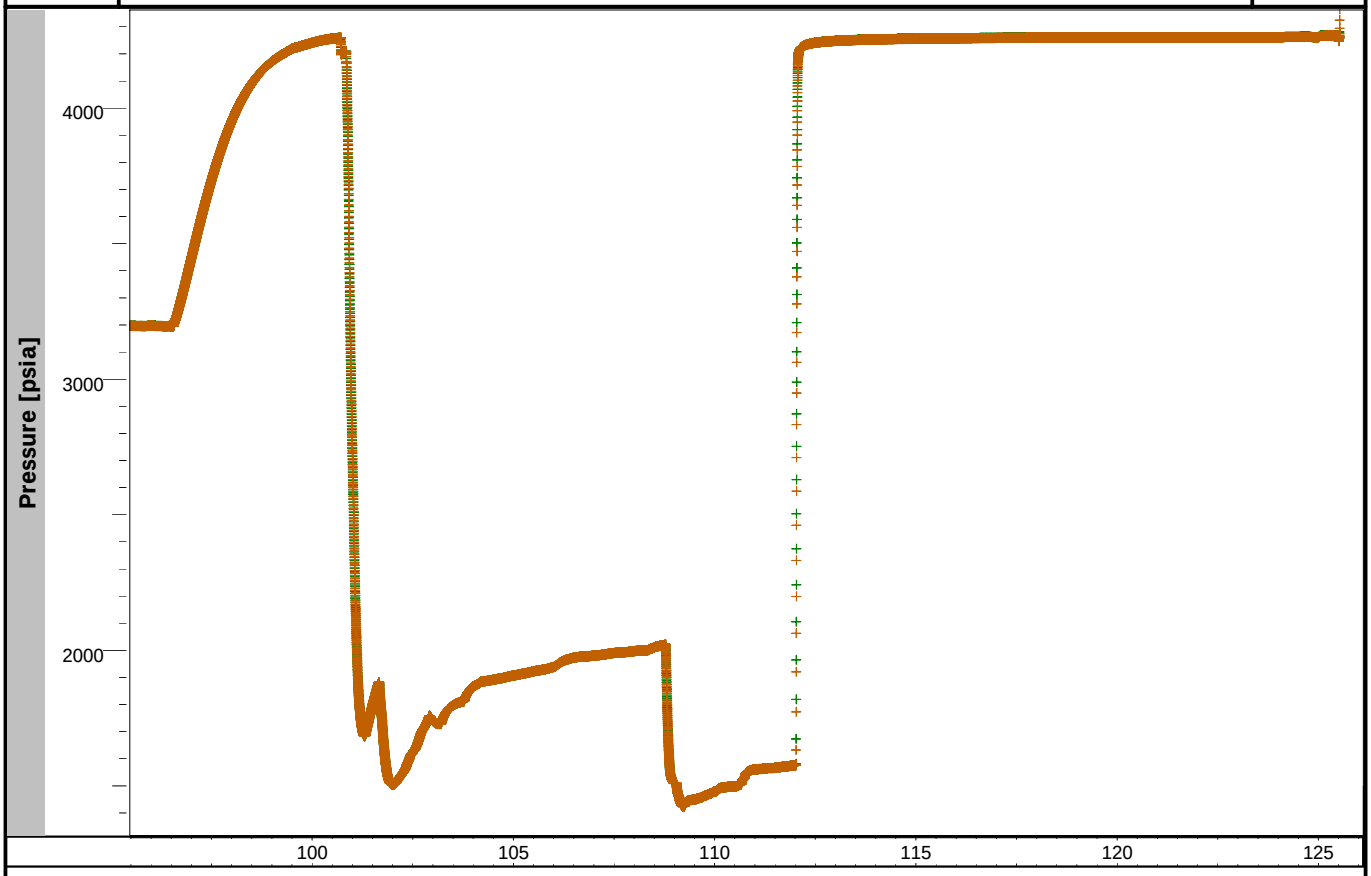
Review of the initial pressure buildup data (immediately after perforating) showed a long period of afterflow (the well was shut-in at the surface, not down hole) and it was not possible to accurately determine the initial reservoir pressure from this data. The MDT pressure in this zone was 4305 psia at 3045.2m RT, equivalent to 4271 psia at gauge depth 2943.6m RT using a gas gradient of 0.334 psi/m. This initial pressure estimate is consistent with the interpretation model for the main buildup described below.

A good match to the middle time data for the final buildup was obtained with a radial composite model with 870 md.ft near the well and a doubling of permeability about 34m from the well. The well had a very high skin factor at the time of shut-in but was still cleaning up right to the end of the flow period. The high skin factor indicates the 1 11/16" Enerjet guns did not provide adequate perforations.

The late pressure derivative after about 3.8 hours of buildup started falling, suggesting a reservoir depletion effect, and this could be reasonably well matched with a circular bounded reservoir model with a radius of 1850' (564m). It is not clear whether the late falling derivative represents pressure depletion of the gas zone or is a wellbore artifact. The falling pressure late in the buildup (beyond the data analysed) is a clear indication of wellbore effects affecting the well bottomhole pressure at that time, however a review of the operational records did not indicate a reason for the falling pressure or when these wellbore effects may have started. There were no pressure irregularities in the earlier part of the buildup which might have resulted from intermittent leaking of the PCT. Attempts were made to explain the falling late pressure derivative (apparent pressure depletion effect) by assuming that the PCT was leaking steadily. However, this assumption was not quantitatively consistent with the late falling derivative observed. The bounded reservoir model could represent a GWC at about 1850' radius - this model would contain about 3.2 BCF OGIP.

Date	ToD	FP #	Gas rate Mscf/D	Duration hr
10/12/2004	00:00:00	1	0	100.85
14/12/2004	04:51:01	2	5000	0.829167
14/12/2004	05:40:46	3	7300	7.10833
14/12/2004	12:47:16	4	9870	3.23678
14/12/2004	16:01:28	5	0	8.74513
15/12/2004	00:46:11	6	1	23.2292

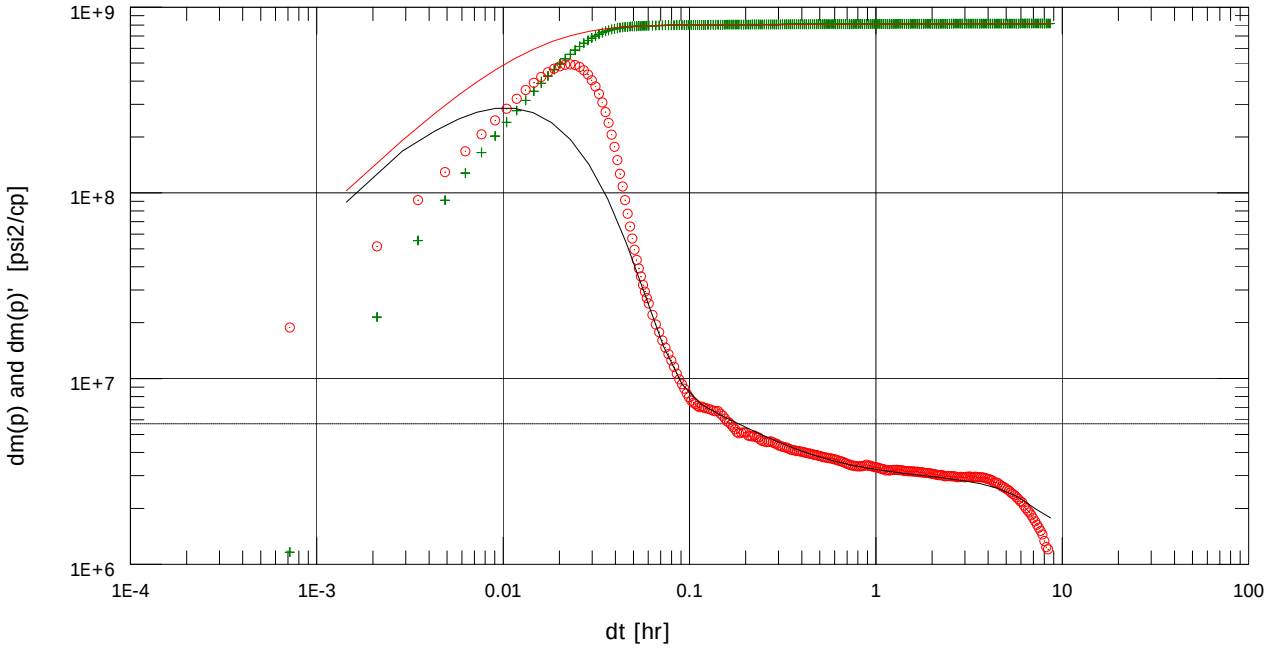
KAPPA	QA / QC	RadComp(Bnded)
	Company Origin	Field Trefoil
	Well Trefoil 1	Test Name / # CHDST #2



Pressure [psia] vs Time [hr]

Pressure
++ 937 (ref)
++ 769 (act)

Log-Log plot	RadComp(Bnded)
Company Origin	Field Trefoil
Well Trefoil 1	Test Name / # CHDST #2



937 build-up #1

Rate	0 Mscf/D
Rate change	9870 Mscf/D
P@dt=0	1575.34 psia
Pi	4266.75 psia
Smoothing	0.1

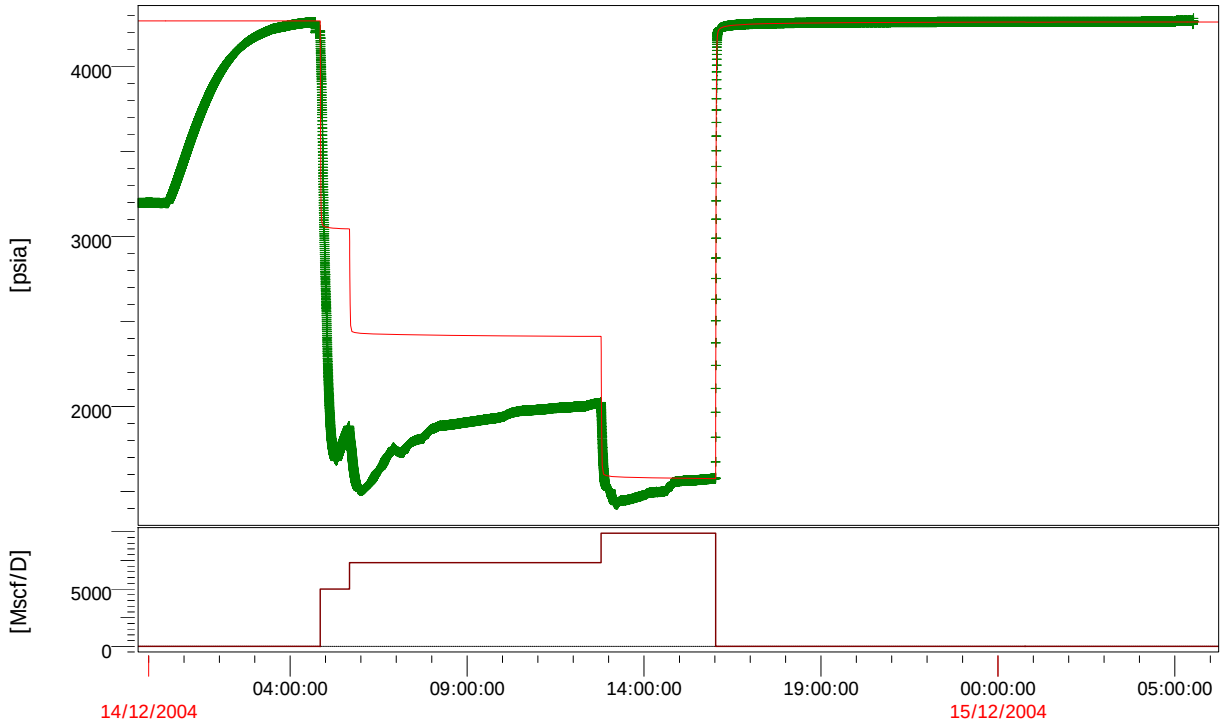
Selected Model

Model Option	Standard Model
Well	Storage + Skin
Reservoir	Radial Composite
Boundary	Circle

Results

TMatch	6700 [hr]**-1
PMatch	8.75E-8 [psi2/cp]**-1
C	0.0014 bbl/psi
Skin	64.6
Delta P Skin	2351.3 psi
Pi	4266.75 psia
Pbar	4263.13 psia
k.h	870 md.ft
k	49.2 md
Ri	110 ft
M	0.5
D	0.5
Re - No Flow	1850 ft
Test. Vol.	5.05051E+6 Barrels

History plot	RadComp(Bnded)
Company Origin	Field Trefoil
Well Trefoil 1	Test Name / # CHDST #2



Pressure [psia], Gas Rate [Mscf/D] vs Time [ToD]

— Gas rate

937 build-up #1

Rate	0 Mscf/D
Rate change	9870 Mscf/D
P@dt=0	1575.34 psia
Pi	4266.75 psia
Smoothing	0.1

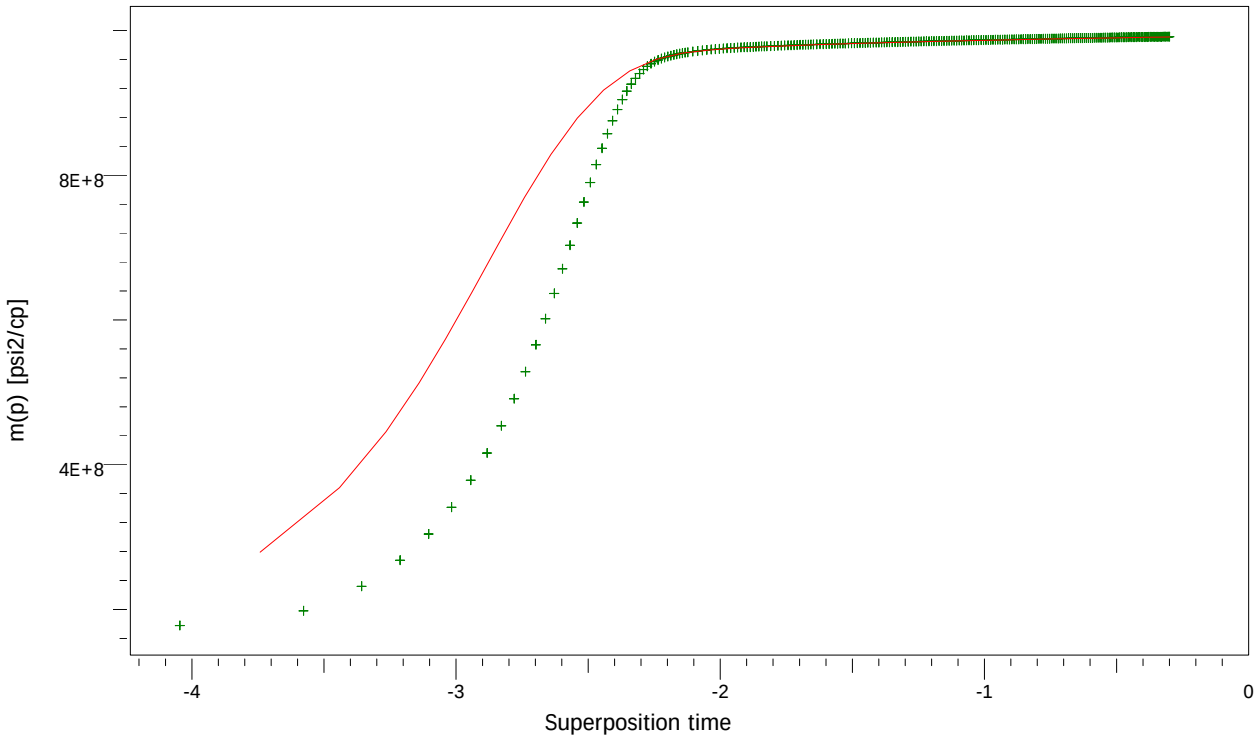
Selected Model

Model Option	Standard Model
Well	Storage + Skin
Reservoir	Radial Composite
Boundary	Circle

Results

TMatch	6700 [hr]**-1
PMatch	8.75E-8 [psi2/cp]**-1
C	0.0014 bbl/psi
Skin	64.6
Delta P Skin	2351.3 psi
Pi	4266.75 psia
Pbar	4263.13 psia
k.h	870 md.ft
k	49.2 md
Ri	110 ft
M	0.5
D	0.5
Re - No Flow	1850 ft
Test. Vol.	5.05051E+6 Barrels

Semi-Log plot	RadComp(Bnded)
Company Origin	Field Trefoil
Well Trefoil 1	Test Name / # CHDST #2



937 build-up #1

Rate	0 Mscf/D
Rate change	9870 Mscf/D
P@dt=0	1575.34 psia
Pi	4266.75 psia
Smoothing	0.1

Selected Model

Model Option	Standard Model
Well	Storage + Skin
Reservoir	Radial Composite
Boundary	Circle

Results

TMatch	6700 [hr]**-1
PMatch	8.75E-8 [psi2/cp]**-1
C	0.0014 bbl/psi
Skin	64.6
Delta P Skin	2351.3 psi
Pi	4266.75 psia
Pbar	4263.13 psia
k.h	870 md.ft
k	49.2 md
Ri	110 ft
M	0.5
D	0.5
Re - No Flow	1850 ft
Test. Vol.	5.05051E+6 Barrels

(B) Sand Production

CLAMPON
ULTRASONIC SAND DETECTION

WELL TEST REPORT

ORIGIN ENERGY - TREFOIL

Customer : Origin Energy
Performed by : Aquip Systems
Test Engineer : Simon Mason
Test Date : 11/12/04 to 14/12/04

Report Overview:

This report provides a summary of sand production during testing of the Trefoil reservoir on board the Ensco 102.

1. Trefoil – Lower Zone (3141 –3150)

Clean up and Main Flow:

The well clean up flow commenced at 19:04 (11/12/04). Flow was diverted to the separator at 20:41. Moderate particle production was recorded up to 22:41 after which the captured data indicated successful well clean up had been achieved. No further sand production was recorded for the remainder of the main flow period until the well was shut in at 05:04 (12/12/04).
Total sand production for this flow period = 10.66kg
(See fig 1.)

Sampling Flow:

Sand production during the sampling flow period was minimal.
Total mass recorded = 3.8kg
(See fig 2.)

2. Trefoil – Upper Zone (3040.5 – 3046.5)

Clean up / Main and Sampling Flow:

This combined flow period demonstrated negligible solids production. Correlation with Schlumberger acquired well test data indicates the recorded mass is most likely due to ice breaking away from hydrates formed upstream of the installed location of the ClampOn sand particle detector.
Total mass = 0.05kg
(See Fig 3.)

Fig 1. (3141 –3150)

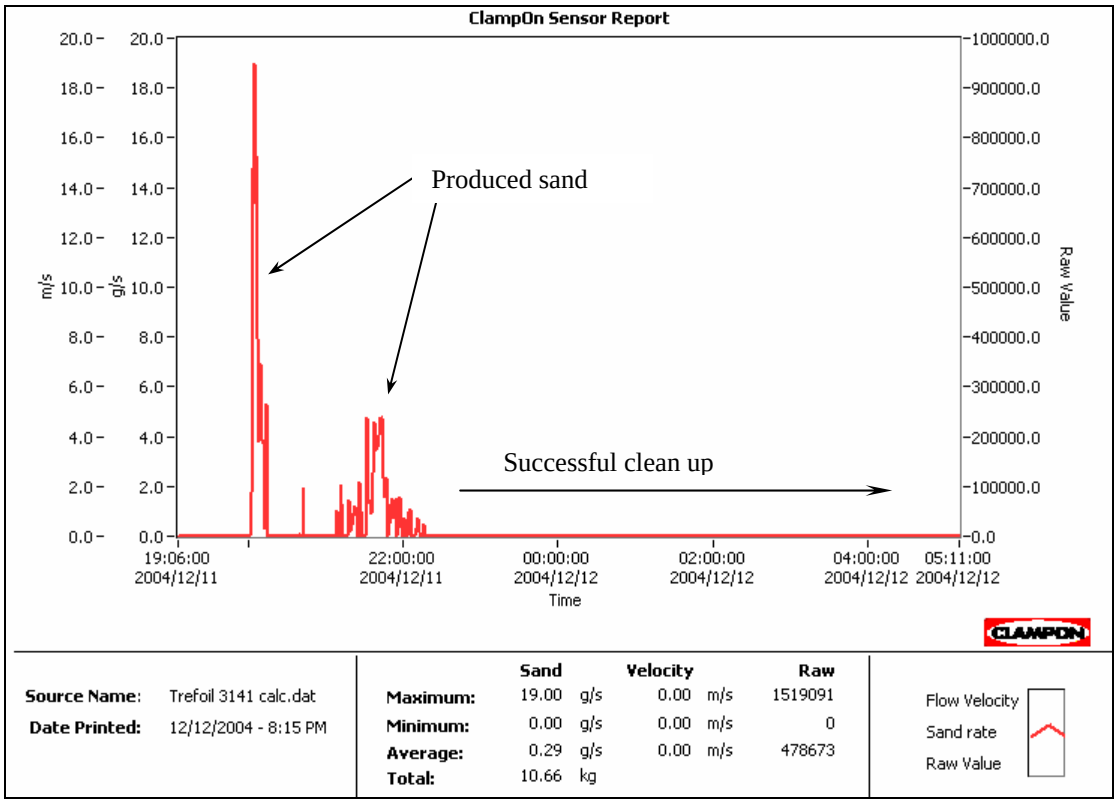


Fig 2. (3141 –3150)

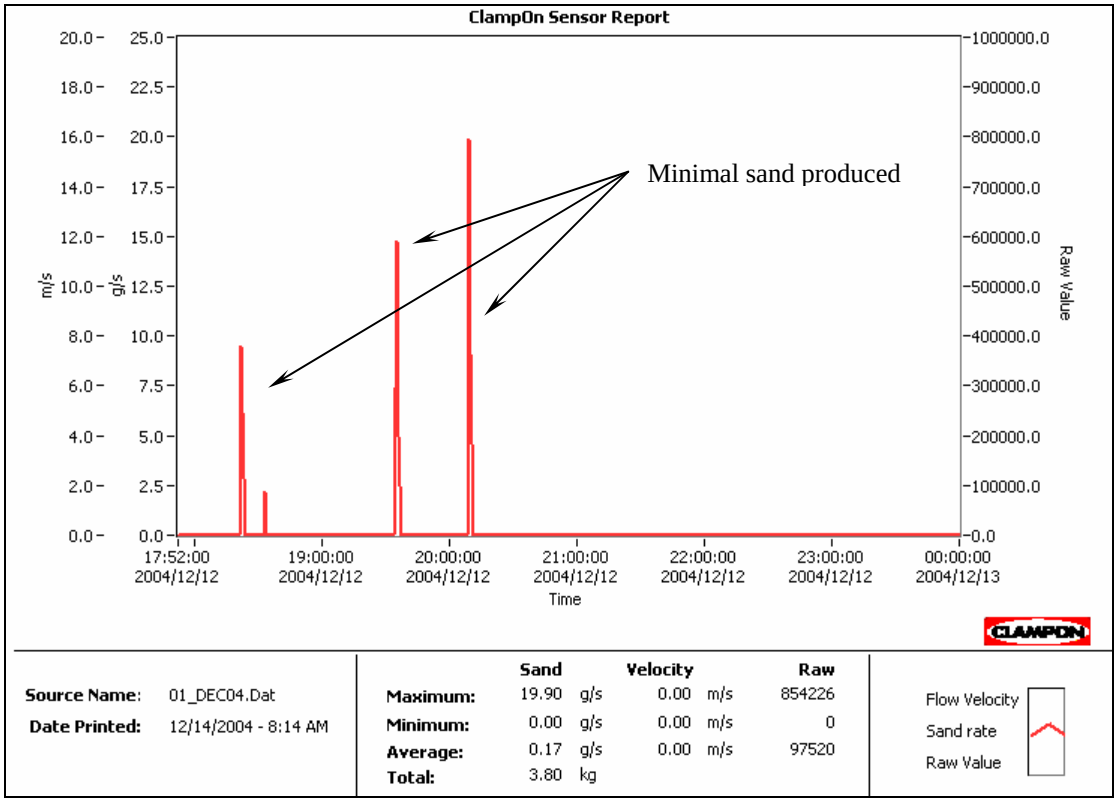
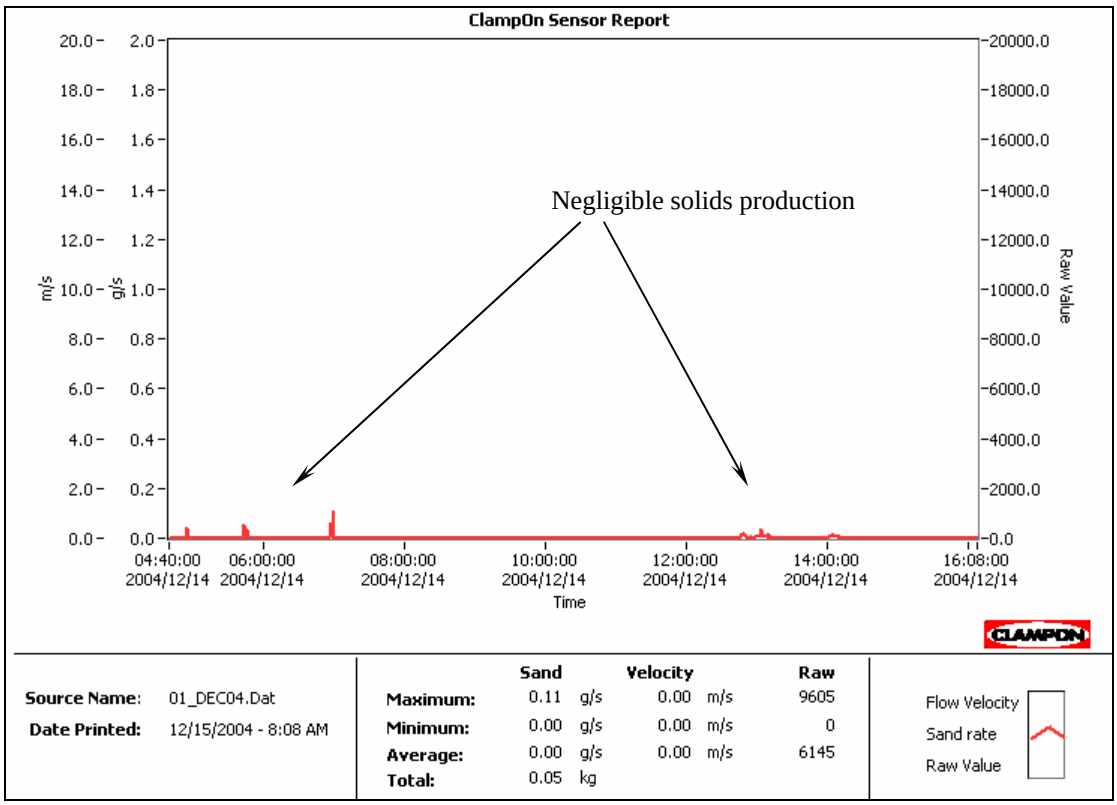


Fig 3. (3040.5 – 3046.5)



APPENDIX 4: GEOCHEMISTRY REPORT

HYDROCARBON CHARACTERISATION STUDY

TREFOIL-1

PROFESSIONAL OPINION

Prepared by:
Cindy Barber

Prepared for:
Origin Energy

September 2005

GEOTECH
GEOTECHNICAL SERVICES PTY LTD
41- 45 Furnace Road, Welshpool, Western Australia. 6106
Locked Bag 27, Cannington, Western Australia. 6987
Email: geotech@geotechnical-services.com.au
Telephone: (08) 9458 8877 (24 Hours)
Facsimile: (08) 9458 8857
ACN 050 543 194
Quality Endorsed Company
ABN 58 050 543 194

EXECUTIVE SUMMARY

A sample suite from Trefoil-1, drilled by Origin Energy, was submitted for geochemical analysis. The sample suite comprised the following samples:

- Ten cuttings samples from the depth range 2901m-3375m
- Two condensate samples from 3040.5-3046.5m and 3141-3150m

The geochemical program was undertaken to evaluate the source rock potential, thermal maturity and depositional environment of the cuttings samples and to correlate these with fluids recovered from the Trefoil-1 well.

This report provides a compilation of geochemical data obtained from analysis of the hydrocarbons extracted from the sediments and the condensate samples together with an interpretation of these data.

Trefoil-1 Cuttings

The ten cuttings samples from the depth range 2901m to 3375m are characterised as early mature and show potential for gas generation based on Rock Eval pyrolysis data. GC-MS analysis of the extract from Trefoil-1 3375m indicates a moderate level of thermal maturity. Biomarker data also characterises the extract as having been sourced from terrestrial derived organic matter which was deposited under oxic conditions. There is no indication that either migration contamination or biodegradation has altered the composition of the free hydrocarbons.

Trefoil-1 Condensates

The two Trefoil-1 condensate samples are believed to have been sourced from terrigenous organic matter, as indicated by sterane data and the presence of higher plant derived biomarkers. Steranes are however, observed in very low abundance in both condensate samples, resulting in calculated maturity parameters based on steranes less reliable. The high pristane to phytane ratios characterise the depositional environment as having been highly oxic. There is no indication of either biodegradation or water washing.

Correlation

The Trefoil-1 cuttings extract and the two fluid samples show comparable distributions of biomarker components indicating significant contribution from higher plant derived organic matter which, based on high pristane to phytane ratios, was deposited under oxic sedimentary conditions. Whilst thermal maturation data derived from Rock Eval data and both aromatic and branched/cyclic GC-MS analysis indicate the cuttings sample is not of high

enough maturity to have directly sourced the condensate, the extract hydrocarbons and the condensates derive from very similar coaly source facies.

HYDROCARBON CHARACTERISATION STUDY

TREFOIL-1

TABLE OF CONTENTS

		Page Number
1	INTRODUCTION	5
2	ANALYTICAL PROCEDURES	6
	2.1 SEDIMENTS	6
	2.2 CONDENSATES	6
3	RESULTS AND INTERPRETATION	8
	3.1 SEDIMENTS	8
	3.2 CONDENSATES	15
	3.3 CORRELATION	21
4	CONCLUSION	23
5	REFERENCES	24

APPENDIX A: DATA AND TABLES

APPENDIX B: THEORY AND METHODS

1 INTRODUCTION

A sample suite from Trefoil-1, drilled by Origin Energy, was submitted for geochemical analyses. The sample suite comprised the following samples:

- Ten cuttings samples from the depth range 2901m to 3375m
- Two condensate samples taken from 3040.5m - 3046.5m (DST-2) and 3141m - 3150m (DST-1)

This report provides a compilation of geochemical data obtained from analysis of the hydrocarbons extracted from the sediments and the condensate samples, together with an interpretation of these data.

One hardcopy and one electronic copy of this report have been sent to Deidre Brooks at Origin Energy. Any queries related to it may be directed to Cindy Barber or Dr Birgitta Hartung-Kagi at Geotechnical Services Pty Ltd.

All data and information are proprietary to Origin Energy and regarded as highly confidential by all Geotech personnel.

Geotechnical Services has endeavoured to use techniques and equipment to achieve results and information as accurately as it possibly can. However, such equipment and techniques are not necessarily perfect. Therefore, Geotechnical Services shall not be held responsible or liable for the results of any actions taken on the basis of the information contained in this document. Moreover, this report should not be the sole reference when considering issues that may have commercial implications.

2 ANALYTICAL PROCEDURES

2.1 SEDIMENTS

Ten cuttings samples from the depth range 2901m to 3375m were analysed for total organic carbon (TOC) content. On the basis of these data, 4 samples (2901m, 3264m, 3324m, 3375m) were selected by staff at Origin Energy for Rock-Eval pyrolysis.

Three samples (2901m, 3093m, 3375m) were selected by staff at Origin Energy for solvent extraction and characterisation of the extracted hydrocarbons. The whole extracts were initially analysed by gas chromatography-mass spectrometry (GC-MS) and subsequently subjected to liquid chromatographic separation in order to isolate the saturate, aromatic and polar fractions. The saturate fractions from all 3 extracts were analysed by GC-MS. One sample (3375m) was chosen for detailed molecular characterisation involving GC-MS analysis of the aromatic and the branched/cyclic fractions. The branched/cyclic components were isolated from the saturate fraction by treatment with ZSM5 molecular sieves and these components were then analysed by GC-MS.

2.2 CONDENSATES

Two condensate samples were initially analysed according to Geotech's whole oil GC-MS protocol. The two samples were subsequently submitted for liquid chromatography. The saturate, aromatic and branched/cyclic fractions were analysed by GC-MS.

The geochemical program for Trefoil-1 is summarised in Table 1.

Table 1. Trefoil-1 geochemical program

SAMPLE	SAMPLE PREP.	TOC	ROCK EVAL	SOLVENT EXTRACTION	WHOLE EXTRACT (GC-MS)	LIQUID CHROMATOGRAPHY	SATURATE (GC-MS)	AROMATIC (GC-MS)	BRANCHED/CYCLIC (GC-MS)	WHOLE OIL (GC-MS)
Cuttings										
2901m	X	X	X	X	X	X	X			
2925m	X	X								
2973m	X	X								
2997m	X	X								
3042m	X	X								
3093m	X	X		X	X	X	X			
3156m	X	X								
3264m	X	X	X							
3324m	X	X	X							
3375m	X	X	X	X	X	X	X	X	X	
Condensates										
3040.5m-3046.5m						X	X	X	X	X
3141m-3150m						X	X	X	X	X

3 RESULTS AND INTERPRETATION

3.1. SEDIMENTS

3.1.1. TOC and Rock Eval

Ten cuttings samples from the depth range 2901m to 3375m yielded TOC values ranging from 0.51% to 1.11% and characterising the samples as having moderate organic richness. Cuttings samples from 2901m, 3264m, 3324m and 3375m which yielded TOC values in excess of 0.9% were submitted for Rock-Eval pyrolysis. Tmax values for 2901m, 3264m and 3324m range from 429º to 433ºC, characterising the sediments as being early mature. Sample 3375m is slightly more mature, producing a Tmax value of 440ºC. S2 values are relatively low (1.16 to 1.72mg/g) as are hydrogen indicies (129 to 169) suggesting the sediments are primarily gas-prone with little potential for oil generation. No indication of contamination was apparent from the Rock Eval data.

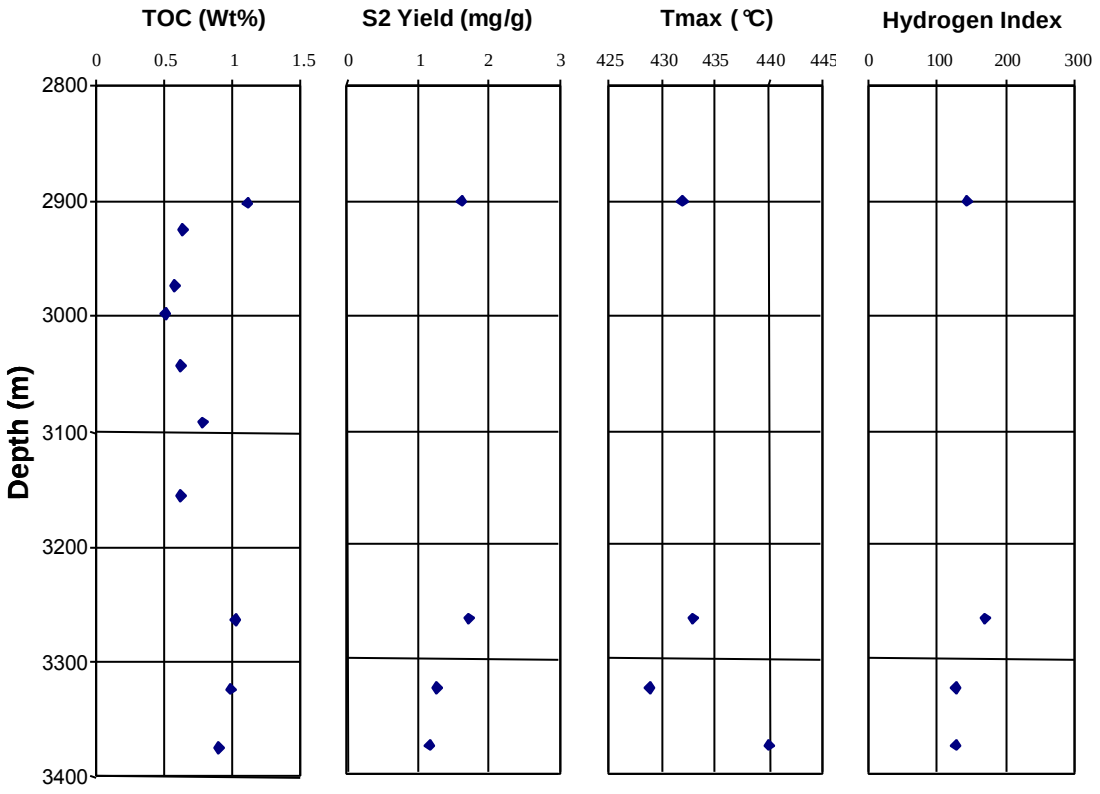


Figure 1. Source Rock Summary for Trefoil-1

3.1.2. Whole Extract

Three cuttings samples (2901m, 3093m and 3375m) were submitted for solvent extraction in order to characterise the free hydrocarbons, whether indigenous, migrated and/or contaminants. Figure 2 shows the mass chromatograms obtained from whole extract GC-MS

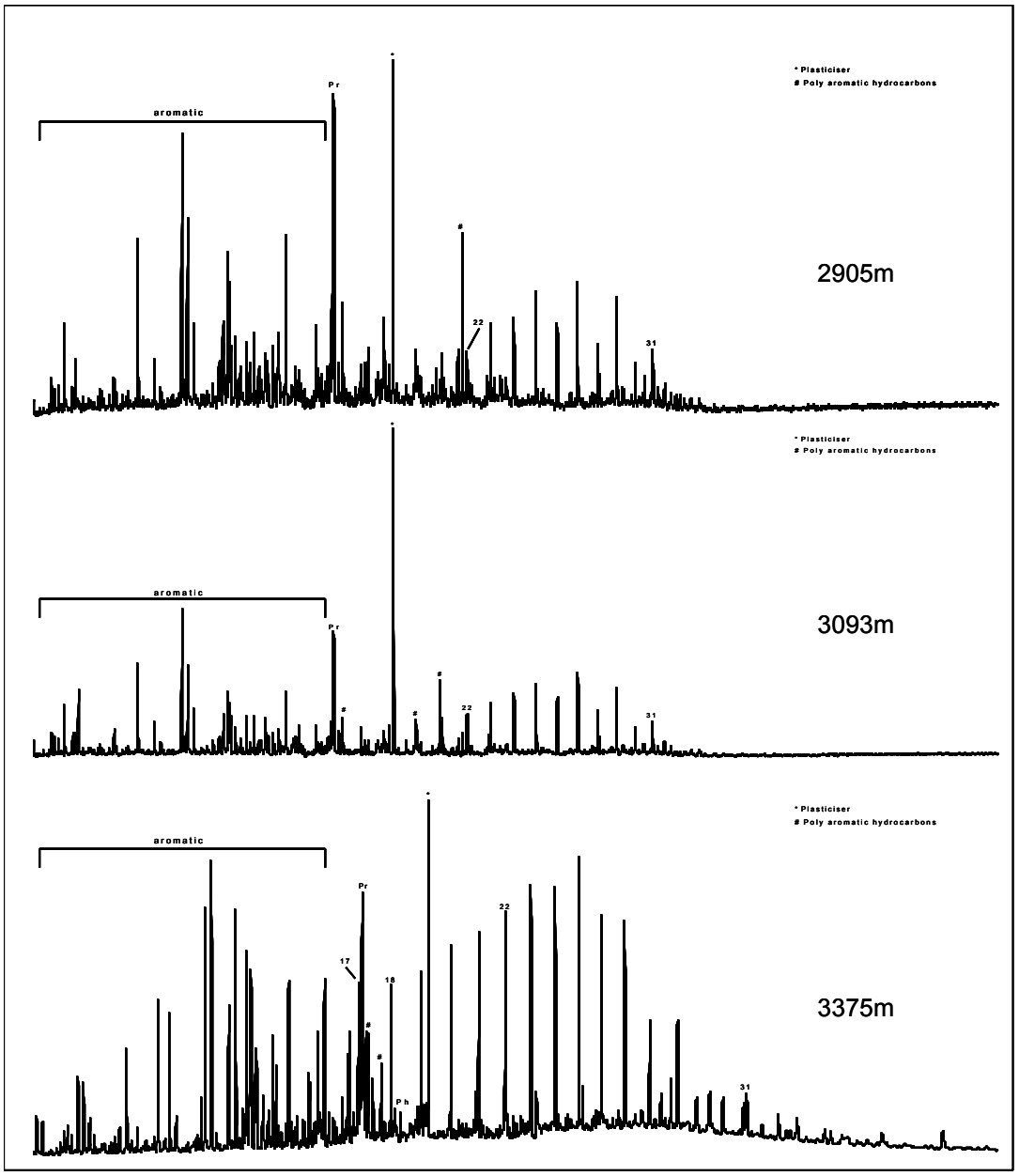


Figure 2. Mass chromatograms obtained from whole extract GC-MS analysis of Trefoil-1 cuttings

analysis. Total extract yields were low to moderate, ranging from 300 to 474ppm. Whilst all 3 extracts show the presence of plasticiser components eluting around *n*-C19, there is no indication of any significant contamination from drilling mud additives. The paraffin distributions for all 3 samples are biased towards the waxy higher molecular weight components and have a distinct odd-over-even predominance consistent with the sediments

being of low thermal maturity and deriving from a coaly/terrigenous source facies. A high abundance of low molecular weight aromatic components, relative to the *n*-alkanes, is a distinct feature of all 3 extracts which, although unusual for hydrocarbon extracts in general, is not uncommon in samples from the Bass Basin.

3.1.3. Saturate SCAN

Liquid chromatography was performed on each of the 3 Trefoil-1 extracts (2901m, 3093m and 3375m) to afford the saturate hydrocarbon fraction which was subsequently analysed via GC-MS. Figure 3 shows the saturate chromatogram obtained from each of the three extracts. Whilst tetradecene (a compound present in synthetic based muds) is present as a prominent component of two of the samples (2905m and 3375m), the extracts do not appear to have been contaminated with other drilling mud additives to any significant extent.

The three extract samples yielded saturate chromatograms with common molecular features. All 3 show bimodal *n*-alkane distributions, with a high relative abundance of high molecular weight components maximising around C_{25}. The samples also show a distinct odd-over-even predominance in the high molecular weight range. Collectively, these features indicate significant terrestrial organic matter input whilst the odd over even predominance also attests to the samples being of low thermal maturity. Pristane/*n*-C_{17} ratios greater than one are similarly suggestive of low thermal maturity which supports the Rock Eval pyrolysis data which characterise the samples as being early mature. The lower pristane/*n*-C_{17} ratio and higher relative abundance of lower molecular weight components for Trefoil-1 3375m reflect the slightly higher maturity of the sample, as indicated by Rock Eval pyrolysis data (Tmax of 440°C).

All 3 extract samples show particularly high pristane to phytane ratios (8.2-9.4) suggesting strongly oxic conditions generally existed at the time of deposition.

3.1.4. Aromatic SIM

One extract sample (Trefoil-1 3375m) was submitted for GC-MS analysis of the aromatic and branched/cyclic components in order to fully characterise the hydrocarbon content of the extract.

Figure 4 shows the distributions of tri-, tetra- and pentamethylnaphthalene components in the Trefoil-1 cuttings sample; distributions which reflect the moderate level of thermal maturity of the sample. A methylphenanthrene index (MPI) value of 0.46 and dimethylnaphthalene ratio (DNR-1) of 4.42 is similarly consistent with a moderate level of maturity.

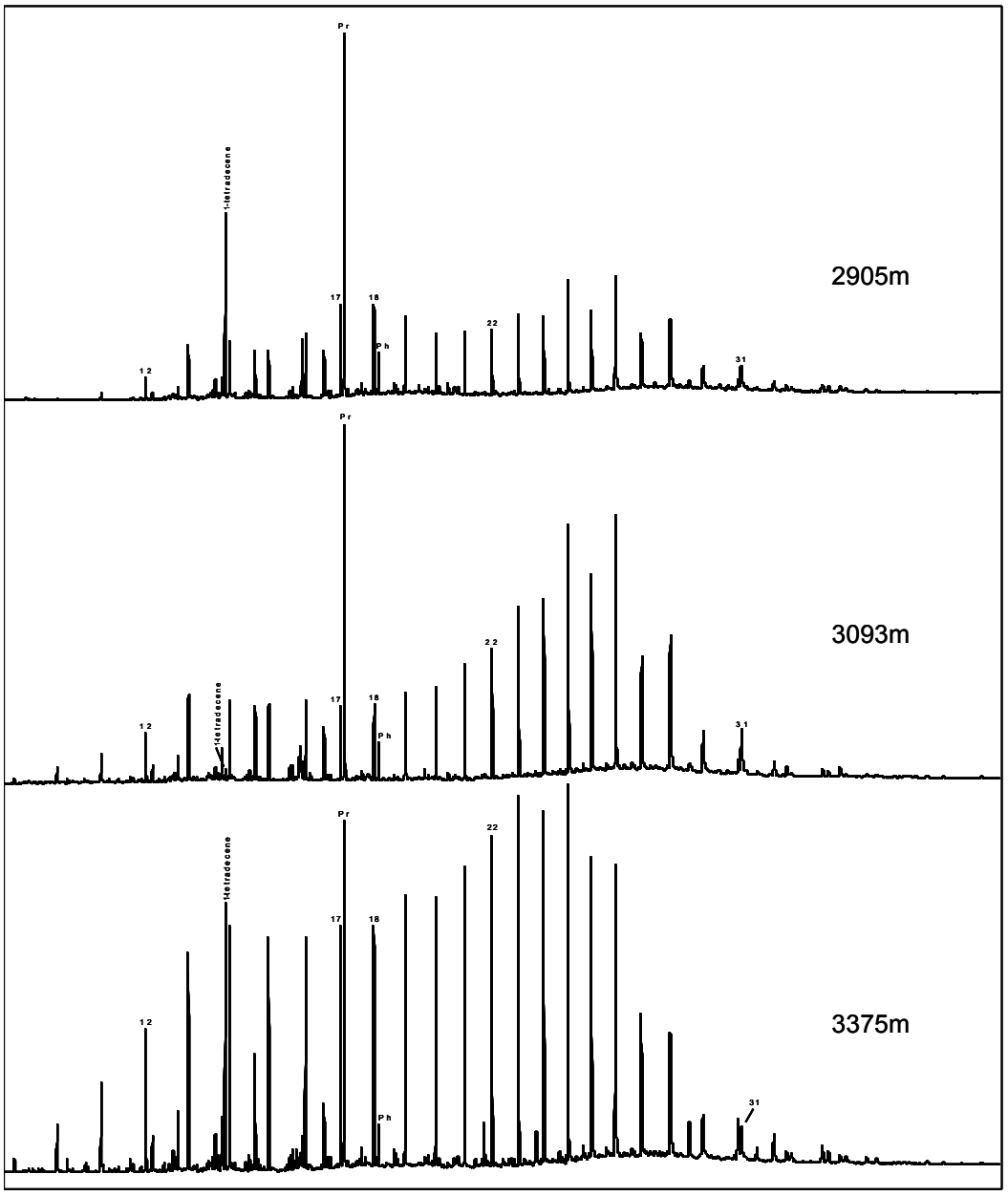


Figure 3. Mass chromatograms obtained from saturate GC-MS analysis of Trefoil-1 cuttings

Retene, cadalene and i-HMN-IV are all present in the aromatic fraction of the sample, together producing a higher plant index (HPI) value of 1.52. Since these components enter the geosphere through incorporation of plant detrital matter into sediments, the presence of these higher plant biomarkers is indicative of significant terrigenous organic matter input. A terrestrial source of organic matter into the Trefoil-1 sediment is further supported by the very low abundance of sulfur containing compounds such as dibenzothiophene (Figure 4).

3.1.5. Branched/Cyclic SIM

Figure 5 presents the partial *m/z* 217 mass chromatogram from Trefoil-1 3375m showing the distribution of steranes. The low C27/C29 diasterane and sterane ratios (0.33 and 0.37, respectively) support a significant terrestrial organic matter input to the sediments.

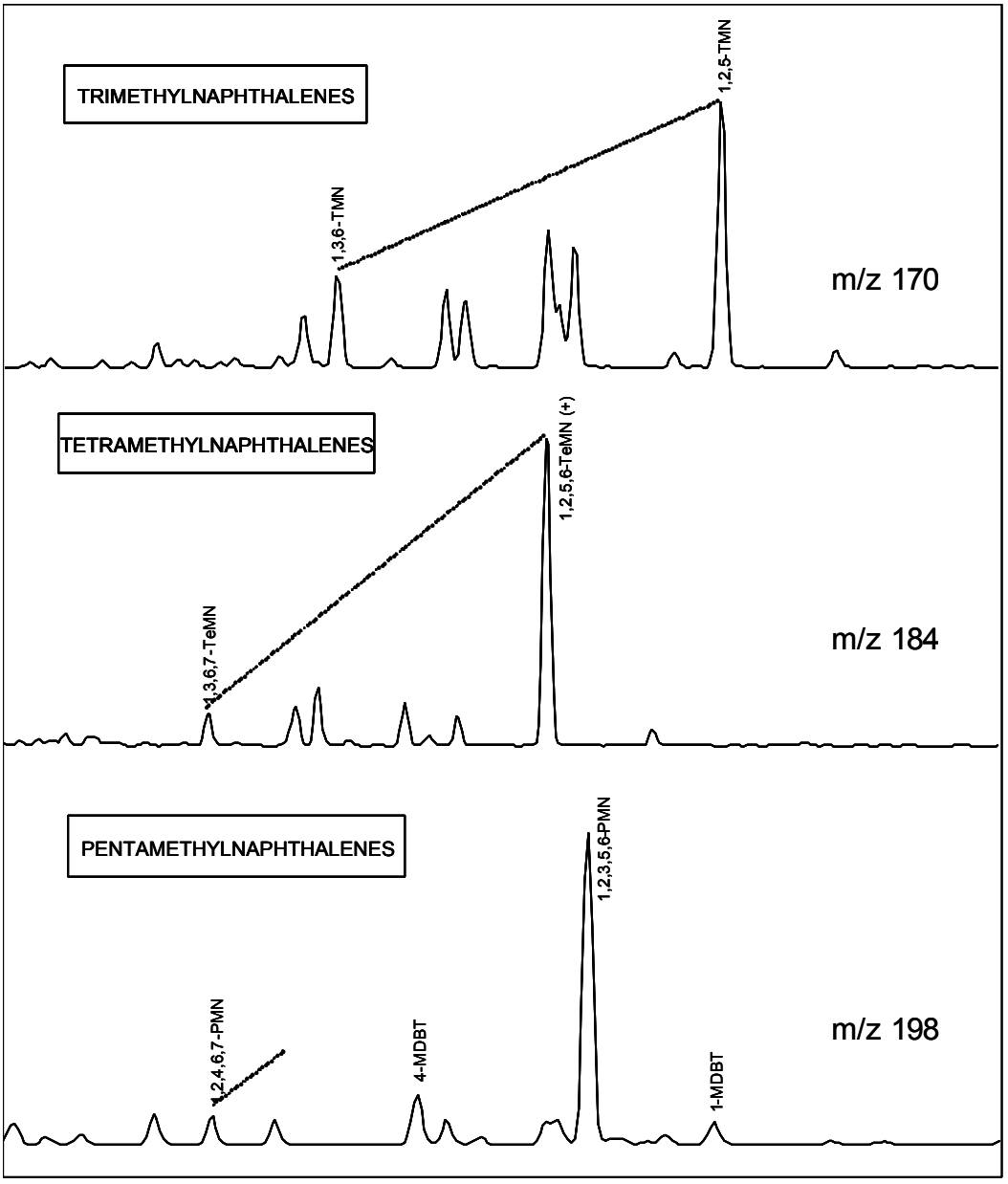


Figure 4. Partial *m/z* 170, 184 and 198 mass chromatograms showing the distribution of naphthalene components in Trefoil-1 3375m

Figure 6 presents the partial *m/z* 191 mass chromatogram from Trefoil-1 3375m showing the distribution of hopanes. Although the sediment is relatively immature, it is characterised by a particularly low Ts/Tm ratio of only 0.07 possibly indicative of a coaly source facies. The sample is also characterised by a high abundance of C_{29} hopane relative to C_{30} hopane.

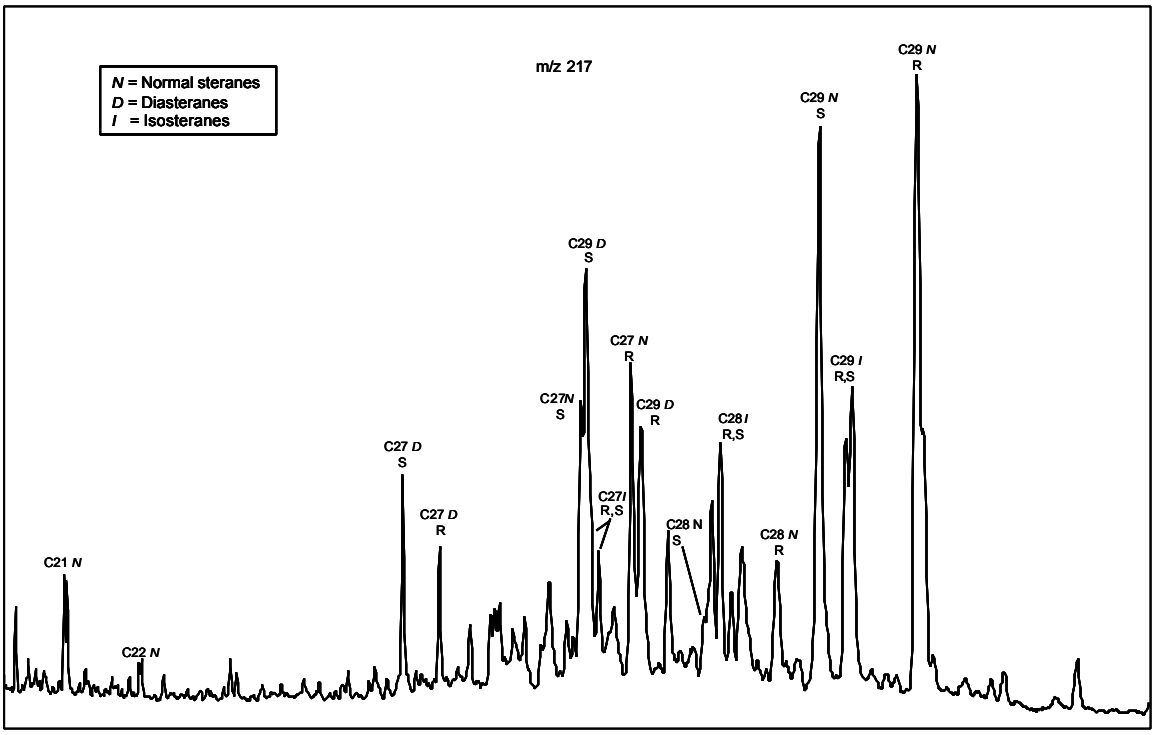


Figure 5. Partial *m/z* 217 mass chromatogram showing the distribution of steranes in Trefoil-1 3375m

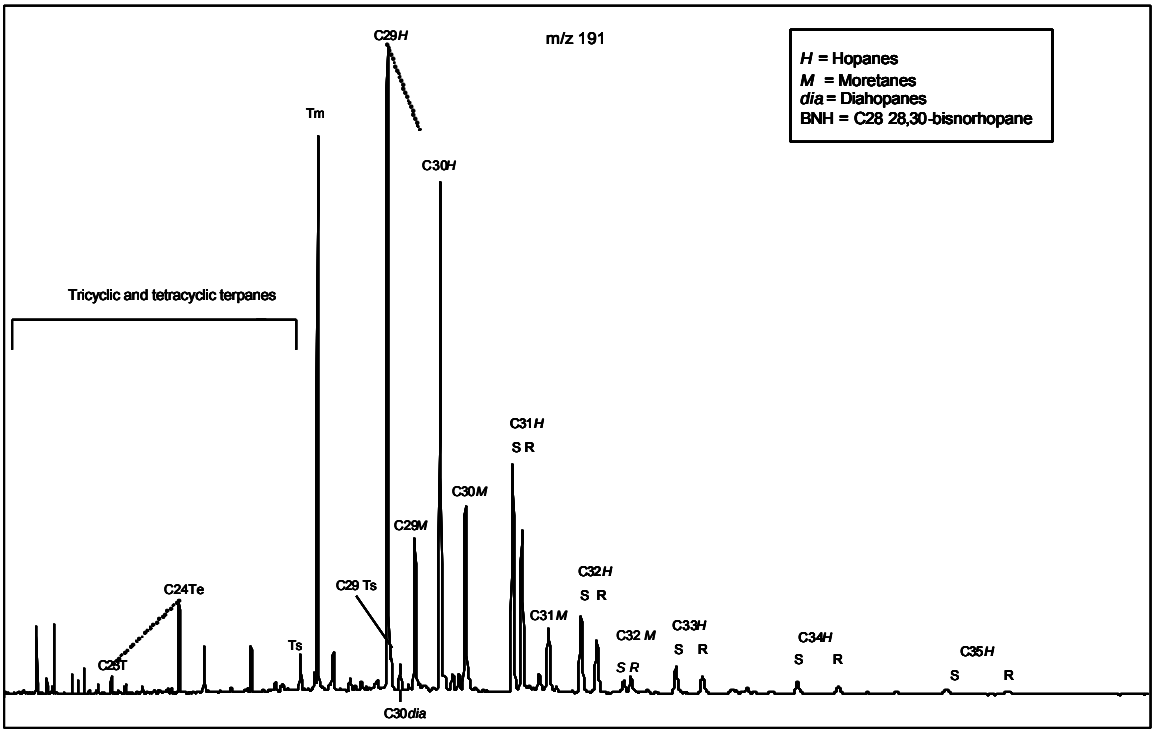


Figure 6. Partial m/z 191 mass chromatogram showing the distribution of hopanes in Trefoil-1 3375m

Whilst an enhancement of the C_{29} component is a general characteristic of evaporite-carbonate rocks, high C_{29}/C_{30} hopane ratios are often observed from Australian samples which contain abundant terrestrial organic matter. In such cases, particularly in the absence of geological evidence for the presence of carbonates, high C_{29}/C_{30} hopane ratios are often inferred as being indicative of hydrocarbon derivation from coaly/terrigenous source facies. A high abundance of the C_{24} tetracyclic terpane relative to the C_{23} tricyclic terpane, as observed in the Trefoil-1 extract, further supports this interpretation.

Overall, the hopanes are in high abundance relative to the steranes, producing a ratio of C_{30} (hopane + moretane)/ C_{29} (sterane + diasterane) of 4.52. Such high values are typically observed from samples containing abundant terrestrially derived organic matter although high values may also be indicative of microbially reworked organic matter (cf. Peters and Moldowan, 1993).

Tri- and tetracyclic diterpanes including phyllocladane and beyerane have also been identified in low relative abundance in the branched/cyclic fraction of the extract (Figure 7). These components are reported to derive from higher plant resin and thus suggest the extract as being terrestrially derived, the organic matter having been deposited under highly oxic conditions.

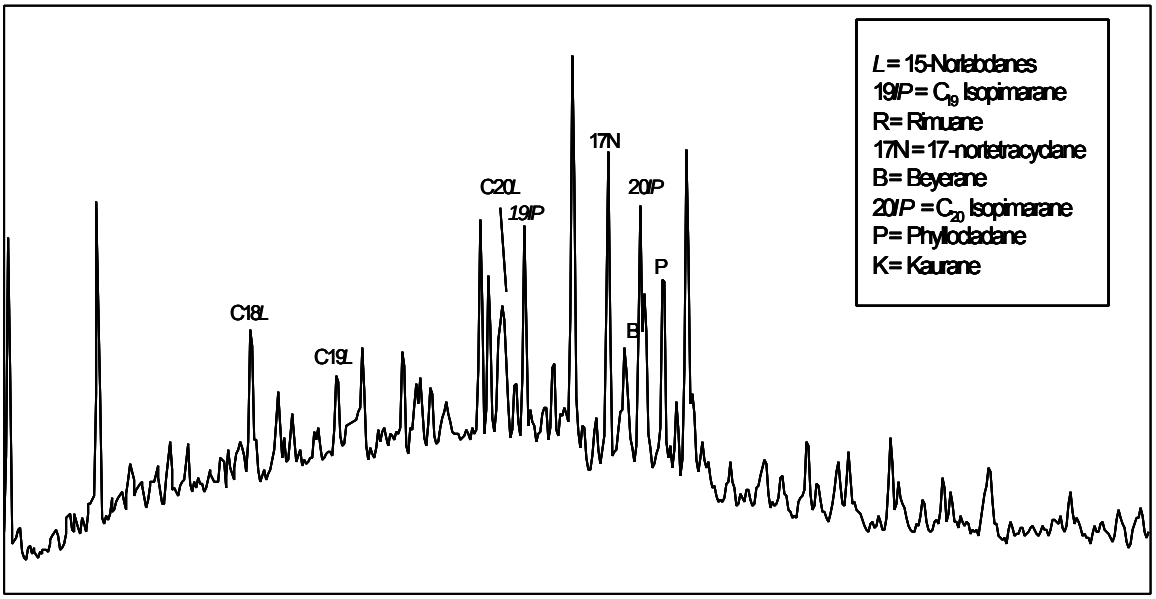


Figure 7. Patial m/z 123 mass chromatogram showing the distribution of higher plant derived terpanes in Trefoil-1 3375m

3.2. CONDENSATES

3.2.1. Whole Oil

Whole oil GC-MS allows for analysis of the gasoline range hydrocarbons as well as providing an overall profile of components up to approximately C_{30}. The distribution and relative abundance of the gasoline range hydrocarbons are readily altered by the physical processes of biodegradation and water washing.

Two condensate samples were provided for whole oil GC-MS analysis (DST-2, 3040.5-3046.5m and DST-1, 3141-3150m). Figure 8 shows the whole oil chromatograms of the 2 samples, both of which are characterised by bimodal *n*-alkane distributions with maxima at approximately C_{10} and C_{20}. The high relative abundance of C_{23+} n-alkanes suggests a significant contribution from higher plant derived organic matter to both samples.

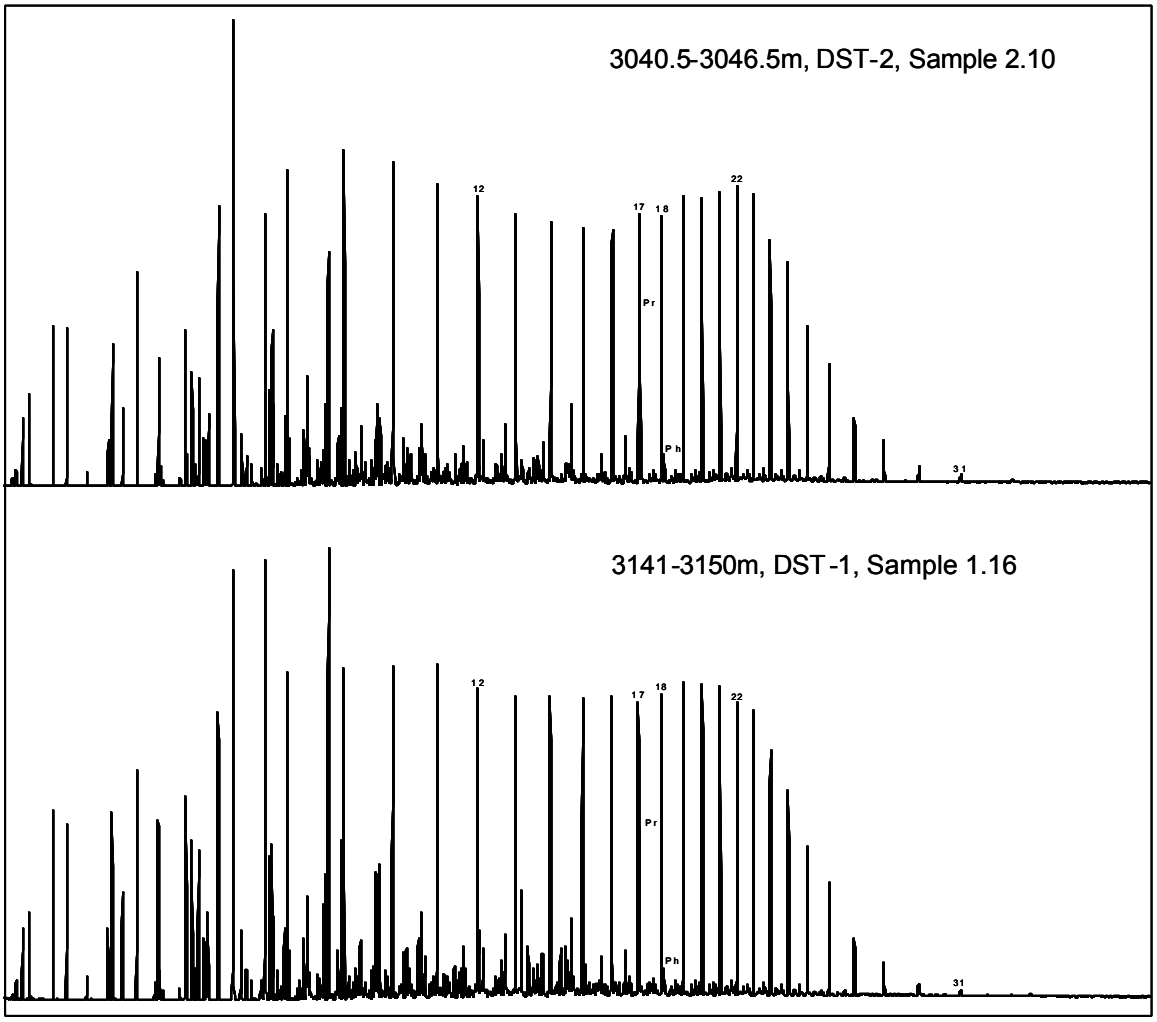


Figure 8. Mass chromatograms obtained from whole oil GC-MS analysis of Trefoil-1 condensates

The distribution of gasoline range hydrocarbons from both DST-1 and DST-2 (Figure 9) show no indication of biodegradation, both samples producing low I/J (0.5 and 0.4, respectively) and V/U (1.2 and 1.3, respectively) biodegradation ratios. This is further supported by the absence of a baseline 'hump' in the whole oil mass chromatograms. Low I/M and V/X water washing ratios also suggest the composition of neither sample has been altered by water washing. Both condensate samples show a high abundance of low molecular weight aromatic components relative to the *n*-alkanes.

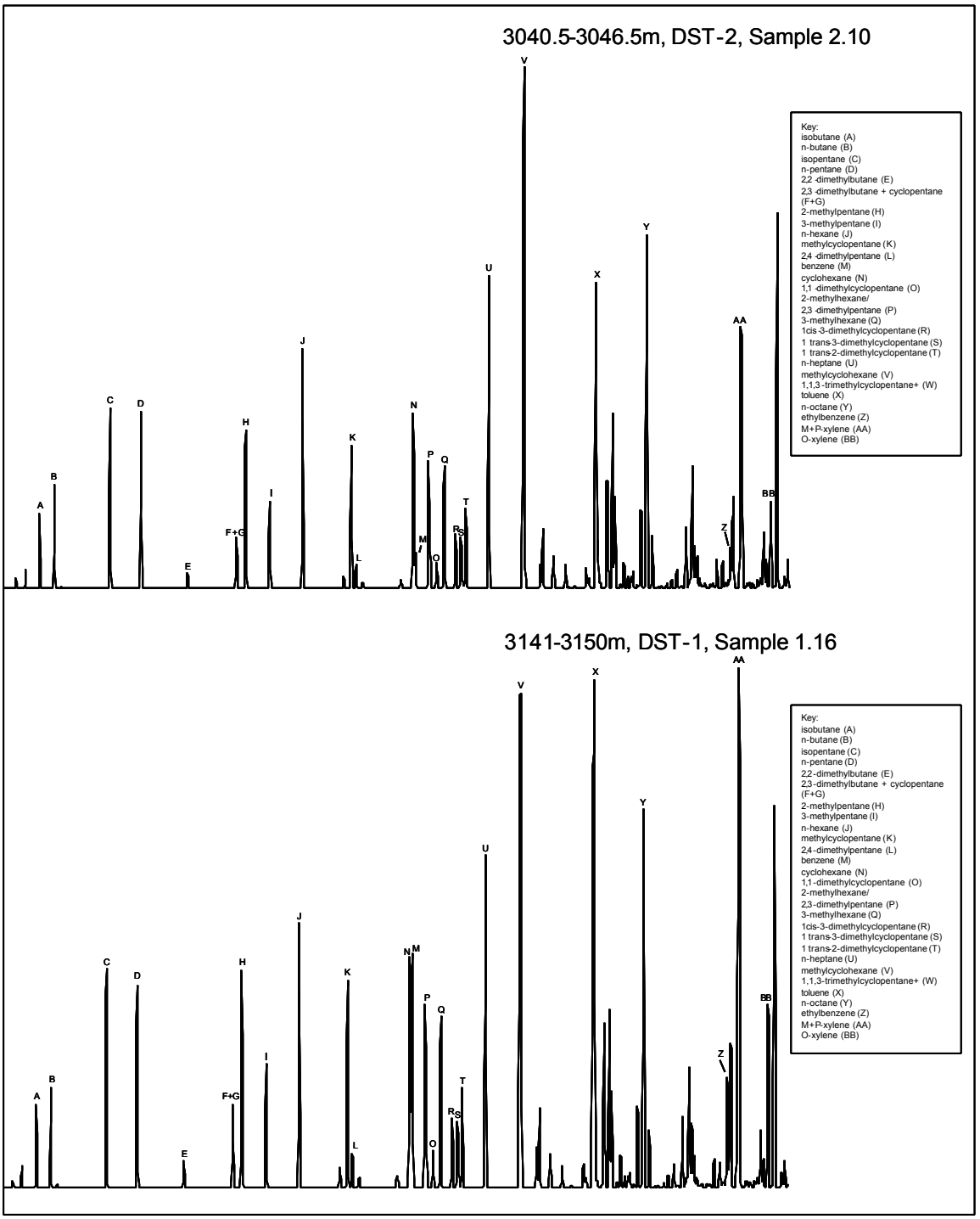


Figure 9. Distributions of gasoline range hydrocarbons in Trefoil-1 condensates

3.2.2. Saturate GC-MS

The two Trefoil-1 condensates were submitted for liquid chromatographic separation, each yielding almost 90% saturates. Figure 10 shows mass chromatograms of the saturate fractions obtained from the Trefoil-1 condensate samples. Both samples show bimodal *n*-alkane distributions, a high relative abundance of high molecular weight components which maximise at C_{22} and extend out to C_{31}. These features collectively suggest derivation of organic matter from a terrigenous source facies.

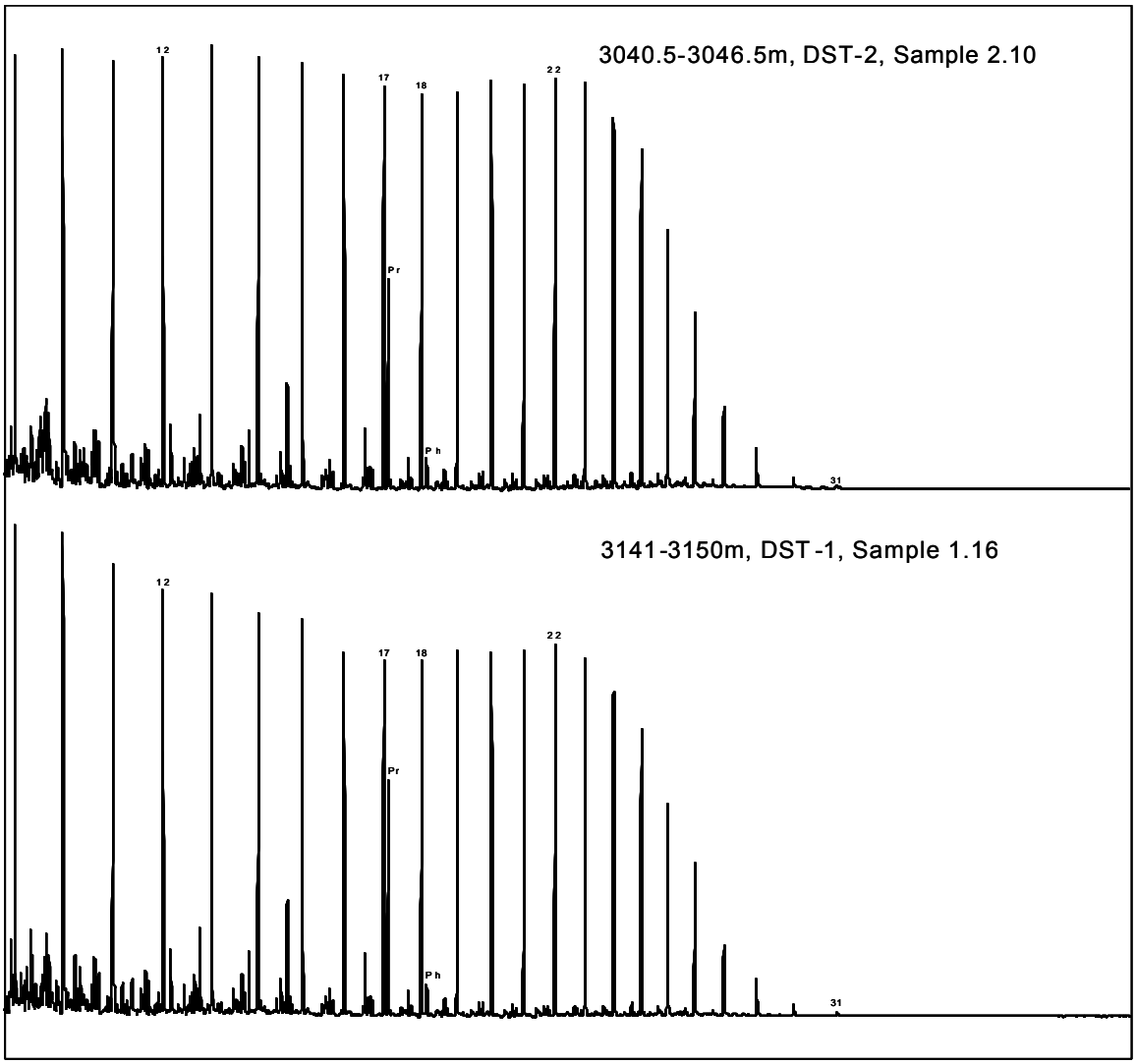


Figure 10. Mass chromatograms obtained from saturate GC-MS analysis of Trefoil-1 condensates

Both Trefoil condensates produce Carbon Preference Index values of approximately 1, consistent with a high level of thermal maturity. Pristane/*n*-C_{17} values similarly suggest high maturity and further support derivation of organic matter from a terrestrial source.

Pristane/phytane ratios approaching 7 suggest deposition of organic matter under strongly oxic environmental conditions.

3.2.3. Aromatic SIM

Figure 11 shows the total ion chromatograms (TIC) of the aromatic fraction from the 2 Trefoil-1 condensate samples. The samples contain a high relative abundance of lower molecular weight components, consistent with a moderate to high level of thermal maturity. Aromatic maturity parameters based on naphthalenes and phenanthrenes similarly indicate moderate to full maturity for both samples.

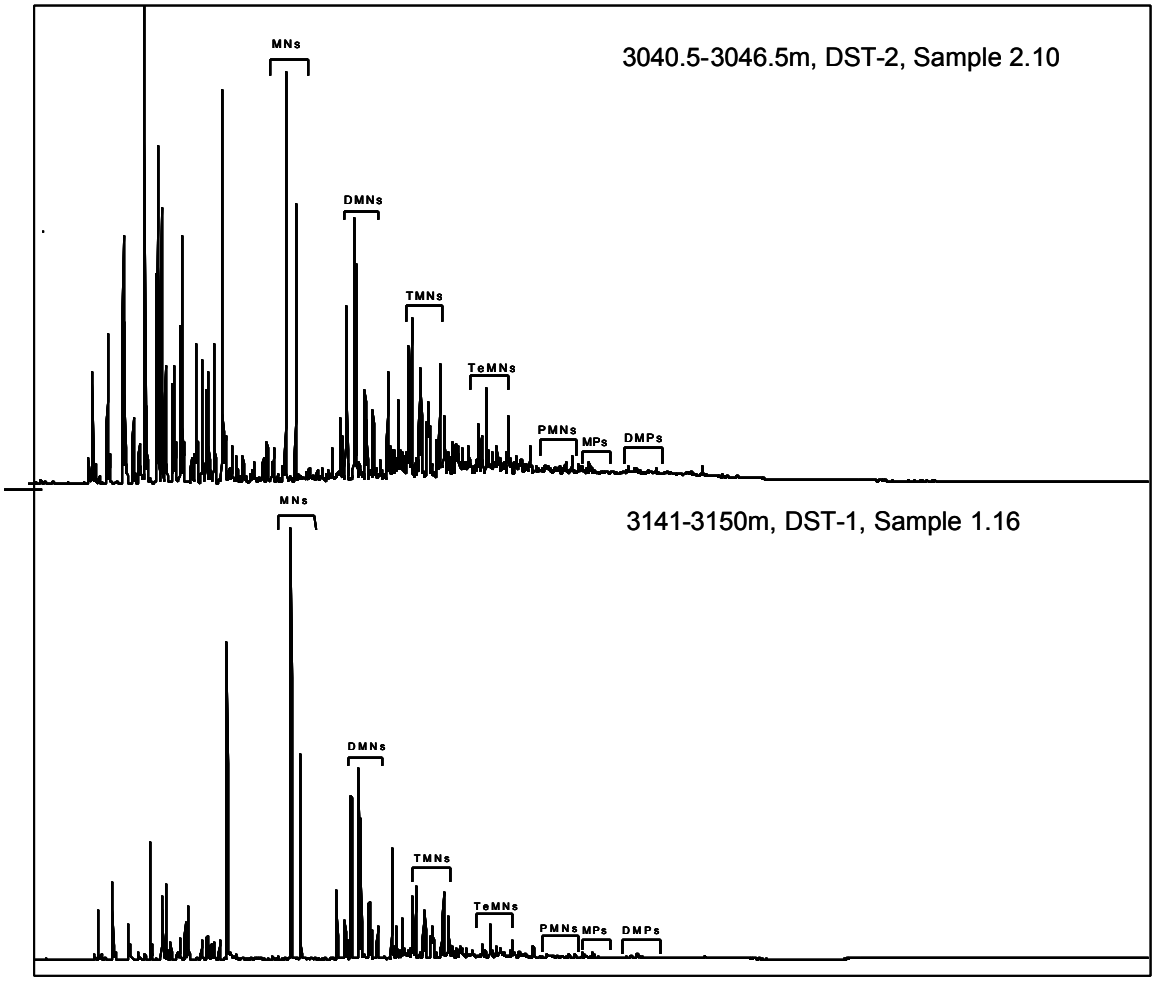


Figure 11. Total ion chromatograms of the aromatic fractions of Trefoil-1 condensates

The relative distributions of individual tri-, tetra- and pentamethylnaphthalenes in the Trefoil-1 DST-1 condensate (Figure 12 and 13) suggest the sample consists of a single mature phase which has not been altered by biodegradation. Comparable naphthalene distributions are also observed from Trefoil-1 DST-2, similarly indicating the sample has not been altered by either multiple charging or biodegradation. This assessment supports the whole oil GC-MS data.

Higher plant derived biomarkers including retene and cadalene are observed in the aromatic fraction of both DST-1 and DST-2, producing higher plant index values of 0.85 and 0.37, respectively.

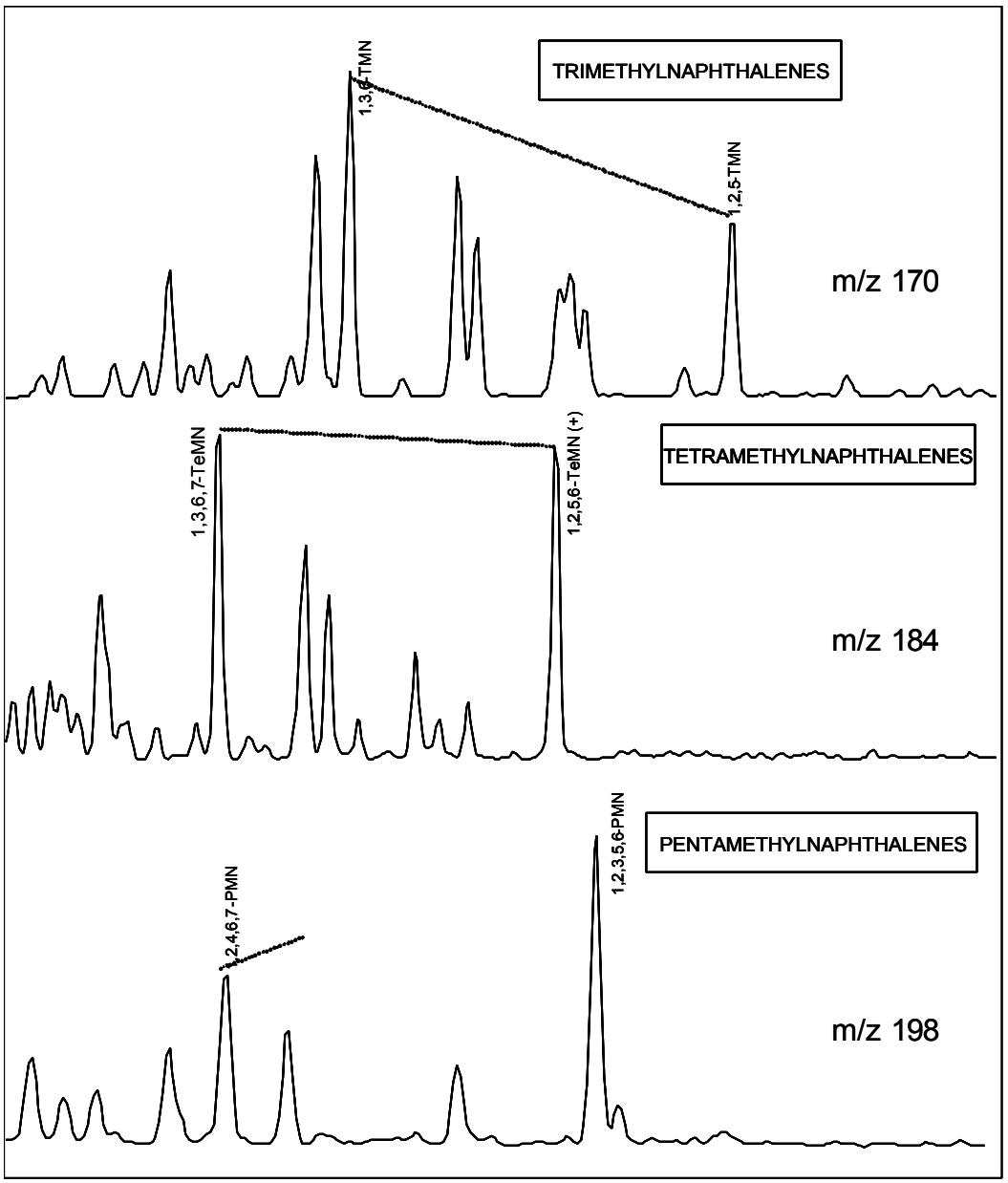


Figure 12. Partial *m/z* 170, 184 and 198 mass chromatograms showing the distribution of naphthalene components in Trefoil-1 3040.5-3046.5m condensate

3.2.4. Branched/Cyclic SIM

Analysis of the 2 Trefoil-1 samples show biomarker components to be in low relative abundance, making 'topping' of the condensates necessary. ('Topping' is a procedure whereby the low molecular weight hydrocarbons are removed via a nitrogen stream in order

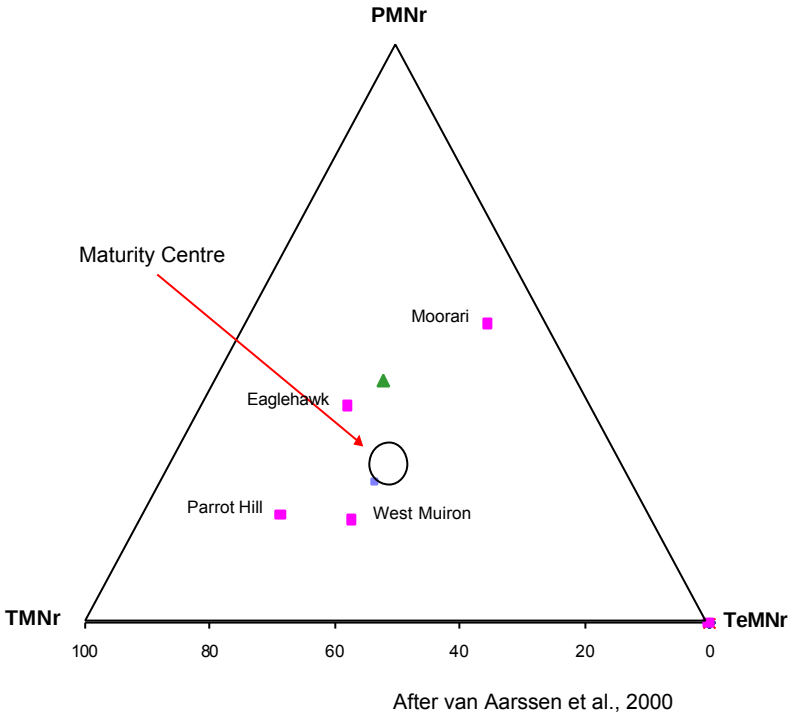


Figure 13. Ternary diagram showing the relative abundance of naphthalenes in Trefoil-1 condensates

to increase the concentration of higher molecular weight biomarker components). Even following 'topping', the relative abundance of branched/cyclic components remained low, resulting in poor peak resolution which in turn makes the calculated biomarker parameters less reliable.

Despite the low biomarker content of both samples, branched/cyclic GC-MS analysis characterises both samples as having been sourced from terrestrial organic matter. A low C_{27}/C_{29} diasterane ratio of 0.21 in DST-2 and high hopane/sterane ratios from both DST-1 and DST-2 (1.67 and 1.89, respectively) are consistent with this assessment. (No C_{27}/C_{29} diasterane ratio is reported for DST-1 due to levels of these components). Higher plant derived diterpenes, including phyllocladane have also been identified in both condensates, albeit in low relative abundance.

Figure 14 shows partial m/z 191 mass chromatograms of the 2 Trefoil-1 condensates. Both samples show particularly low Ts/Tm values (approximately 0.4) consistent with a predominantly terrestrial source of organic matter. Whilst Ts/Tm is often used to infer maturity level, the ratio is also effected by the source of organic matter, particularly in terrestrial derived samples where the ratio is generally found to be very low. A high abundance of the

C_{29} hopane relative the C_{30} component (approaching 1) is also consistent with a predominantly terrestrial source of organic matter.

Sterane maturity parameters were only reported for DST-2 due to the low relative abundance of the relevant components. The $C_{29}S/C_{29}R$ sterane ratio of 0.84 characterises this sample as mature which is in agreement with the aromatic GC-MS assessment.

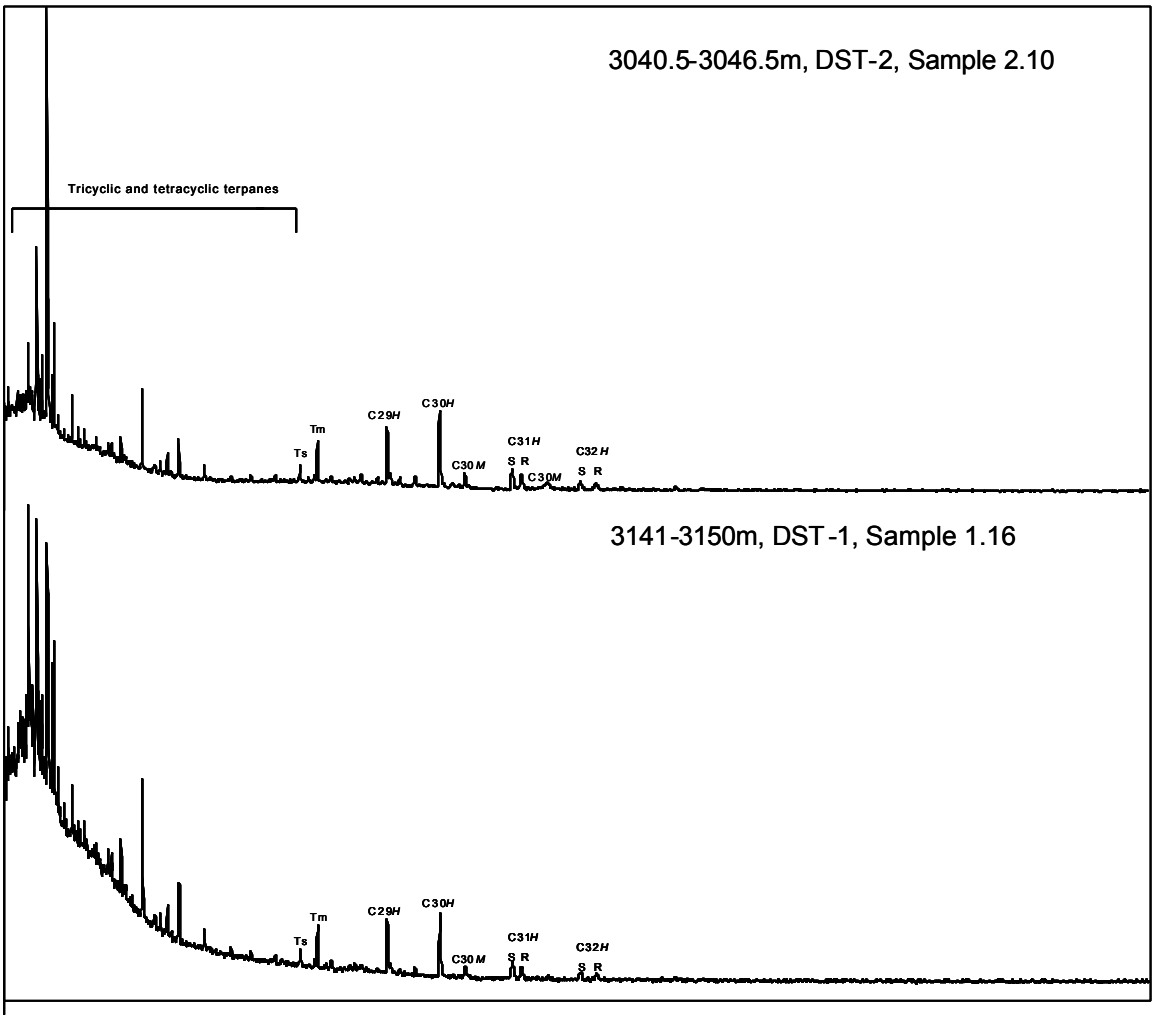


Figure 14. Partial m/z 191 mass chromatograms showing the distribution of hopanes in Trefoil-1 condensates

3.3. CORRELATION

The high sample maturity together with the very low biomarker content of the Trefoil-1 condensates limits correlation with the extract from Trefoil-1 3375m. Chromatograms obtained from saturate GC-MS analysis of the Trefoil-1 3375m extract and the two Trefoil-1 condensates however, show common features including bimodal n-alkane profiles and high pristane/ phytane ratios (>6), although the cuttings extract shows a higher abundance of high

molecular weight (>C20) relative to low molecular weight components. The sediment extract and the condensates all show high diasterane/sterane ratios, high hopane/sterane ratios, and low C27/C29 sterane ratios. Furthermore all samples show the presence of higher plant biomarkers including retene and cadalene.

Many differences are observed between the biomarker profiles of the sediment and the condensates, differences which are likely to reflect maturity rather than differences in source or depositional environment. For example, the condensate samples are more abundant in diasteranes relative to normal steranes whereas the opposite is observed from the cuttings sample. In addition, rearranged drimanes are in higher abundance relative to normal drimanes in the condensates whilst the cuttings show higher relative abundance of normal drimanes. The Trefoil-1 condensates also produce lower HPI values (0.37-0.85) whilst that of the extract is 1.52.

The generally consistent saturate and branched/cyclic hydrocarbon profiles are believed to be indicative of deposition of both the extract and condensate samples from similar terrestrial/coaly source facies under oxic environmental conditions. Overall however, the sediments analysed from Trefoil-1 are believed to be too immature to have directly sourced the Trefoil-1 fluids.

4 CONCLUSIONS

Trefoil-1 Cuttings

Total organic carbon contents and Rock Eval pyrolysis data obtained from the Trefoil-1 cuttings suggest the interval has moderate hydrocarbon generation potential although it appears to be primarily gas prone. Furthermore, the organic matter is only of moderate maturity based on Tmax values and is therefore not of sufficient thermal maturity to have sourced hydrocarbons.

The hydrocarbon content of the extract from Trefoil-1 3375m is believed to be indigenous; there is no evidence of either mud contamination or migrated hydrocarbons. The saturate profile in addition to branched/cyclic and aromatic biomarker distributions are characteristic of low maturity organic matter, derived primarily from terrigenous material. The depositional environment is inferred, primarily from the high pristane/phytane ratio, to have been oxic.

Trefoil-1 Condensates

The 2 fluid samples from Trefoil-1 do not show molecular evidence for drilling mud contamination. Both samples show consistent saturate, branched/cyclic and aromatic biomarker profiles the distributions of which suggest derivation of organic matter primarily from terrestrial material. Like the Trefoil-1 3375m extract, pristane/phytane ratios are consistent with oxic environmental conditions of deposition.

Oil-Source Rock Correlation

The Trefoil-1 cuttings extract and the two fluid samples show comparable distributions of biomarker components indicating significant contribution from higher plant derived organic matter which, based on high pristane to phytane ratios, was deposited under oxic sedimentary conditions. Whilst thermal maturation data derived from Rock Eval data and both aromatic and branched/cyclic GC-MS analysis indicate the cuttings sample is not of high enough maturity to have directly sourced the condensate, the extract hydrocarbons and the condensates derive from very similar coaly source facies.

5 REFERENCES

van Aarssen, B.G.K., Alexander, R. and Kagi, R.I. (2000) Reconstructing the geological history of Australian crude oils using aromatic hydrocarbons. *The APPEA Journal*, 283-292.

Alexander, R., Kagi, R.I., Rowland, S.J., Sheppard, P.N. and Chirila, T.V. (1985) The effects of thermal maturity on distributions of dimethylnaphthalenes and trimethylnaphthalenes in some Ancient sediments and petroleums. *Geochimica et Cosmochimica Acta* **49**, 385-395.

Huang, W.-Y. and Meinschein, W.G. (1979) Sterols as ecological indicators. *Geochimica et Cosmochimica Acta* **43**, 739-745.

Hunt, J.M. (1979) *Petroleum Geochemistry and Geology*. San Francisco: W.H. Freeman.

Peters, K.E. and Moldowan, J.M., 1993 –The Biomarker Guide - Interpreting molecular fossils in petroleum and ancient sediments. Prentice Hall, Englewood Cliffs, New Jersey 07632.

Radke, M. and Welte, D.H., 1983 – The methylphenanthrene index (MPI). A maturity parameter based on aromatic hydrocarbons. Advances in Org. Geochem., 1981. J. Wiley and Sons, New York, 504-512.

Thompson, K.F.M., 1983 – Classification and thermal history of petroleum based on light hydrocarbons. Geochim. Cosmochim. Acta. **47**, 303-316.

Tissot, B.P. and Welte, D.H., 1984 – Petroleum formation and Occurrence. Springer-Verlag, Berlin.

van Aarssen, B.G.K., Bastow, T.P., Alexander, R and Kagi, R.I., 1999 – Distributions of methylated naphthalenes in crude oils: indicators of maturity, biodegradation and mixing. Org. Geochem. **30**, 1213-1227.

Volkman, J.K., Alexander, R., Kagi, R.I., Rowland, S.J. and Sheppard, P.N., 1984 – Biodegradation of aromatic hydrocarbons in crude oils from the Barrow Sub-basin of Western Australia. Org. Geochem. **6**, 619-632.

APPENDIX A

DATA AND TABLES

DATA AND TABLES

WELLNAME

TABLE OF CONTENTS

Analysis	Table	Figure
Total Organic Carbon / Rock-Eval Pyrolysis	1	-
Solvent Extraction (Sediments)	2	-
Whole Extract GC-MS	-	1
Liquid Chromatography / Saturate GC-MS (Sediments)	3 & 4	2
Whole Oil GC-MS	5	3
Liquid Chromatography / Saturate GC-MS (Oils)	6 & 7-	4
Aromatic GC-MS	8	5
Branched/Cyclic GC-MS	9	6

TABLE 1

ANALYSIS OF ORGANIC MATTER BY ROCK-EVAL PYROLYSIS

TREFOIL-1

GEOTECH

Depth (m)		*Tmax*	*S1*	*S2*	*S3*	*S1+S2*	*S2/S3*	*PI*	*TOC*	*HI*	OI
2901.0	Ctgs	432	0.16	1.61	3.75	1.77	0.43	0.09	1.11	145	338
2925.0	Ctgs	nd	nd	nd	nd	nd	nd	nd	0.64	nd	nd
2973.0	Ctgs	nd	nd	nd	nd	nd	nd	nd	0.58	nd	nd
2997.0	Ctgs	nd	nd	nd	nd	nd	nd	nd	0.51	nd	nd
3042.0	Ctgs	nd	nd	nd	nd	nd	nd	nd	0.63	nd	nd
3093.0	Ctgs	nd	nd	nd	nd	nd	nd	nd	0.79	nd	nd
3156.0	Ctgs	nd	nd	nd	nd	nd	nd	nd	0.62	nd	nd
3264.0	Ctgs	433	0.20	1.72	2.53	1.92	0.68	0.10	1.02	169	248
3324.0	Ctgs	429	0.15	1.26	2.95	1.41	0.43	0.11	0.99	127	298
3375.0	Ctgs	440	0.14	1.16	1.73	1.30	0.67	0.11	0.90	129	192

A TMAX value is not reported if the S2 is <0.2mg/g

TMAX = Max. temperature S2 (^{o}C)
S1 = Volatile hydrocarbons (HC) (mg/g rock)
S2 = HC generating potential (mg/g rock)
S1+S2 = Potential yield (mg/g rock)
S3 = Organic carbon dioxide (mg/g rock)
PI = Production index
OI = Oxygen Index
TOC = Total organic carbon (wt % of rock)
HI = Hydrogen index
nd = no data

GEOTECHNICAL SERVICES PTY LTD

TABLE 2

SOLVENT EXTRACTION DATA

TREFOIL-1

DEPTH	Sample Type	Weight of Material Extd. (g)	Total Extract (mg)	Total Extract (ppm)
2901.0m	Cuttings	18.2	8.6	474
3093.0m	Cuttings	19.0	6.4	337
3375.0m	Cuttings	17.0	5.1	300

nd = no data

FIGURE 1-1

Sample : **TREFOIL-1, 2901.0m, Cuttings**
File ID : **346501X**

GEOTECH

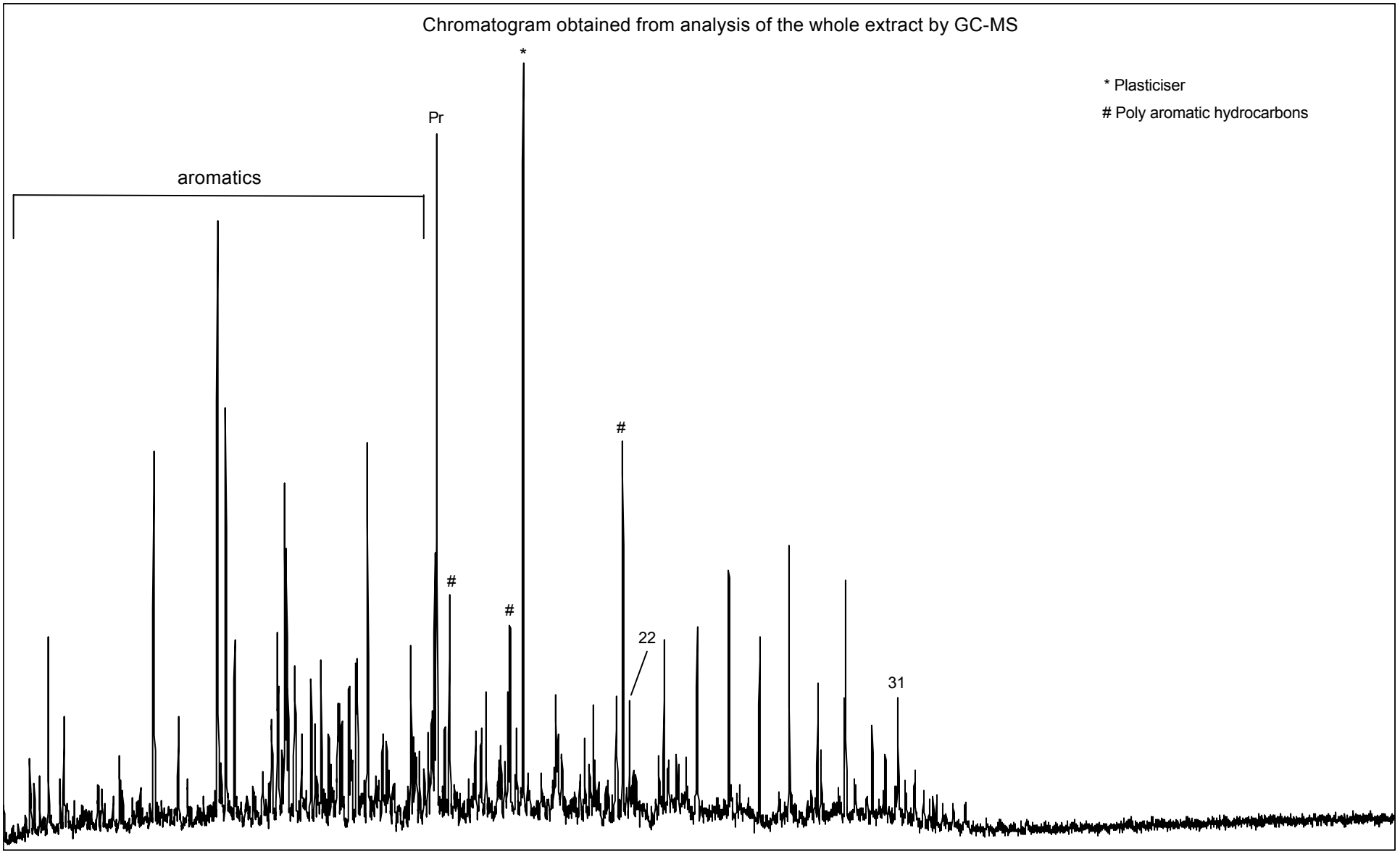


FIGURE 1-2

Sample : **TREFOIL-1, 3093.0m, Cuttings**
File ID : **346506X**

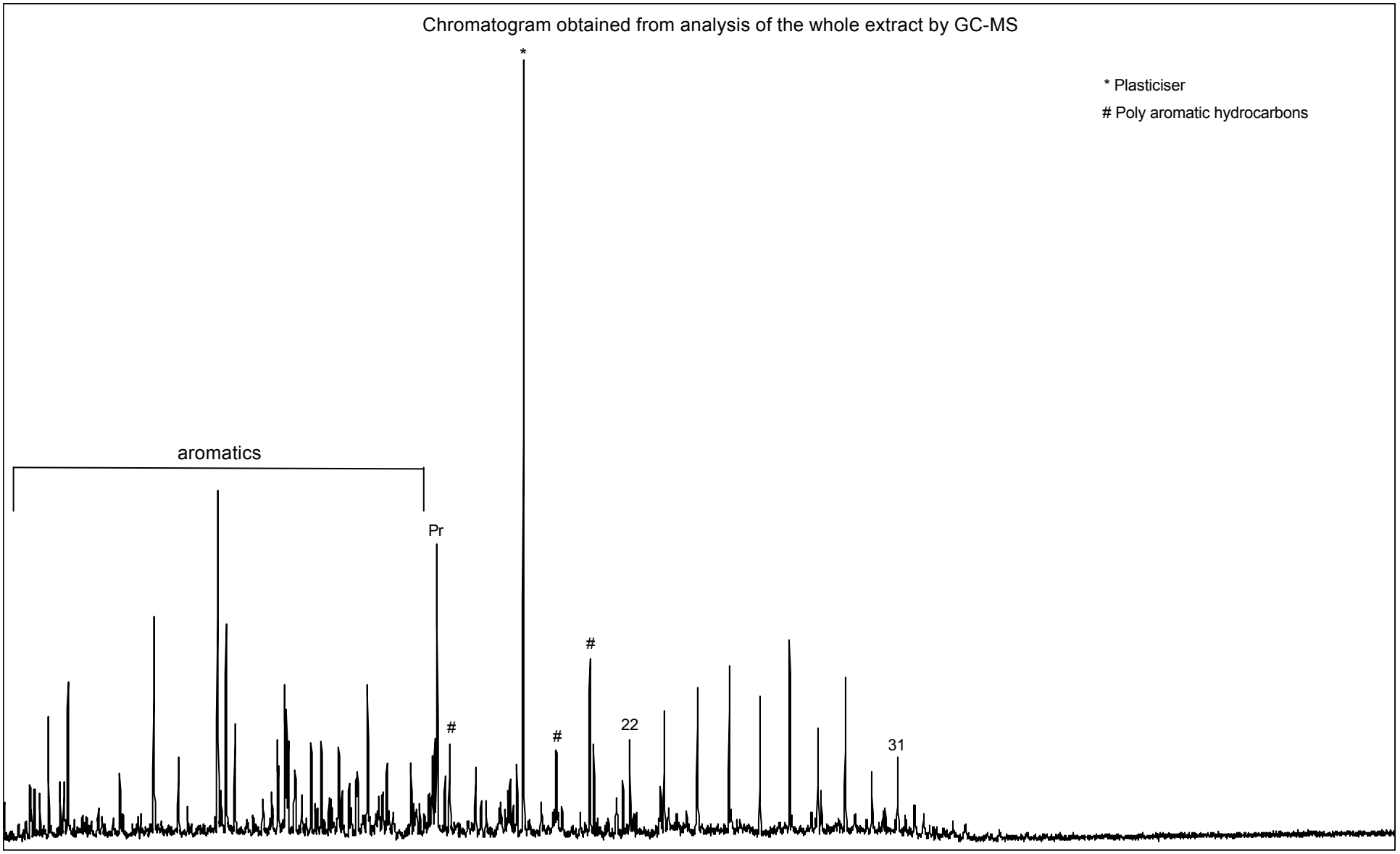


FIGURE 1-3

Sample : **TREFOIL-1, 3375.0m, Cuttings**
File ID : **346510X**

GEOTECH

Chromatogram obtained from analysis of the whole extract by GC-MS

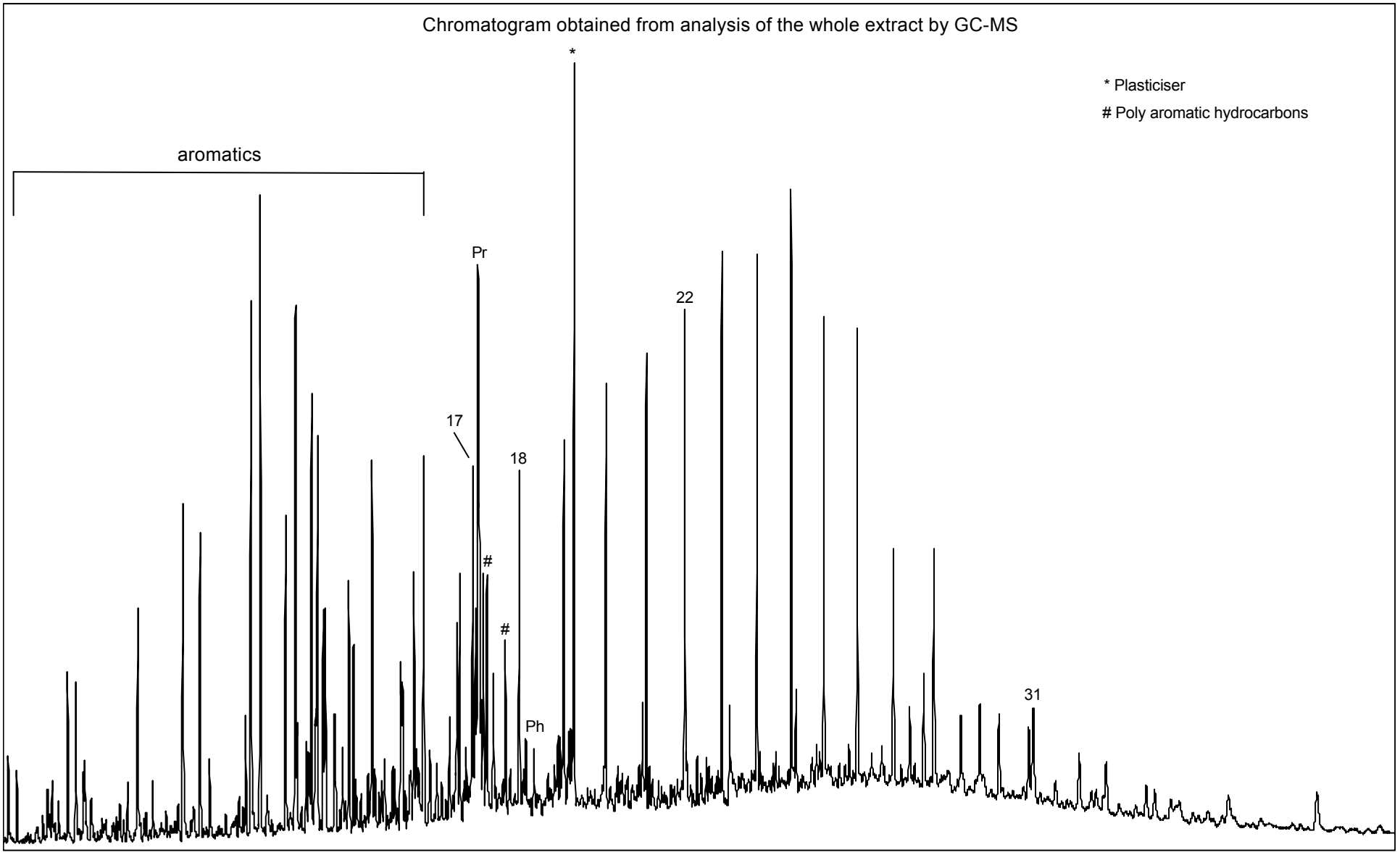


TABLE 3

LIQUID CHROMATOGRAPHY DATA

EXTRACT

TREFOIL-1

A. Yields (ppm)

DEPTH	Sample Type	-------Hydrocarbons------- Sats	Aros	HC's	------Non-hydrocarbons------ NSOs	Asph.	Non HC's	Loss on column
2901.0m	Cuttings	nd	nd	nd	nd	nd	nd	nd
3093.0m	Cuttings	nd	nd	nd	nd	nd	nd	nd
3375.0m	Cuttings	nd	nd	nd	nd	nd	nd	nd

TREFOIL-1

B. Yields (%) and Selected Ratios

DEPTH	Sample Type	------Hydrocarbons------ Sats	Aros	HC's	------Non-hydrocarbons------ NSOs	Asph.	Non HC's	Sats / Aros	Asph. / NSO	HC / Non HC
2901.0m	Cuttings	nd	nd	nd	nd	nd	nd	nd	nd	nd
3093.0m	Cuttings	nd	nd	nd	nd	nd	nd	nd	nd	nd
3375.0m	Cuttings	nd	nd	nd	nd	nd	nd	nd	nd	nd

5/09/2005

nd = no data

TABLE 4

ANALYSIS OF SATURATED HYDROCARBONS BY GC-MS

EXTRACT

TREFOIL-1

A. Selected Ratios

DEPTH	Sample Type	Prist./Phyt.	Prist./n-C17	Phyt./n-C18	CPI(1)	CPI(2)	(C21+C22)/(C28+C29)
2901.0m	Cuttings	8.23	4.96	0.57	1.47	1.38	0.64
3093.0m	Cuttings	9.40	5.79	0.59	1.46	1.37	0.66
3375.0m	Cuttings	8.22	1.70	0.20	1.20	1.15	1.53

TREFOIL-1

B. n-Alkane Distributions

DEPTH	nC12	nC13	nC14	nC15	nC16	nC17	Pr	nC18	Ph	nC19	nC20	nC21	nC22	nC23	nC24	nC25	nC26	nC27	nC28	nC29	nC30	nC31
2901.0m	1.2	2.8	3.2	2.4	3.2	4.2	20.9	4.4	2.5	4.1	3.1	3.2	3.3	4.3	4.2	6.1	4.8	7.3	4.3	5.7	2.0	2.7
3093.0m	1.8	3.0	2.6	2.4	2.7	2.4	13.6	2.5	1.4	3.0	3.1	3.6	4.2	5.5	5.8	8.4	6.7	9.8	5.2	6.7	2.3	3.4
3375.0m	2.7	4.1	4.5	4.2	4.2	4.2	7.2	4.3	0.9	4.8	4.9	5.4	5.9	6.7	6.4	7.2	5.9	6.2	3.8	3.6	1.3	1.3

$$CPI(1) = \frac{(C23+C25+C27+C29)+(C25+C27+C29+C31)}{2x(C24+C26+C28+C30)}$$

$$CPI(2) = \frac{(C23+C25+C27)+(C25+C27+C29)}{2x(C24+C26+C28)}$$

5/09/2005

nd = no data

FIGURE 2-1

Sample : **TREFOIL-1, 3375.0m, Cuttings**
File ID : 346510SB

GEOTECH

Chromatogram obtained from the analysis of saturated hydrocarbons by GC-MS

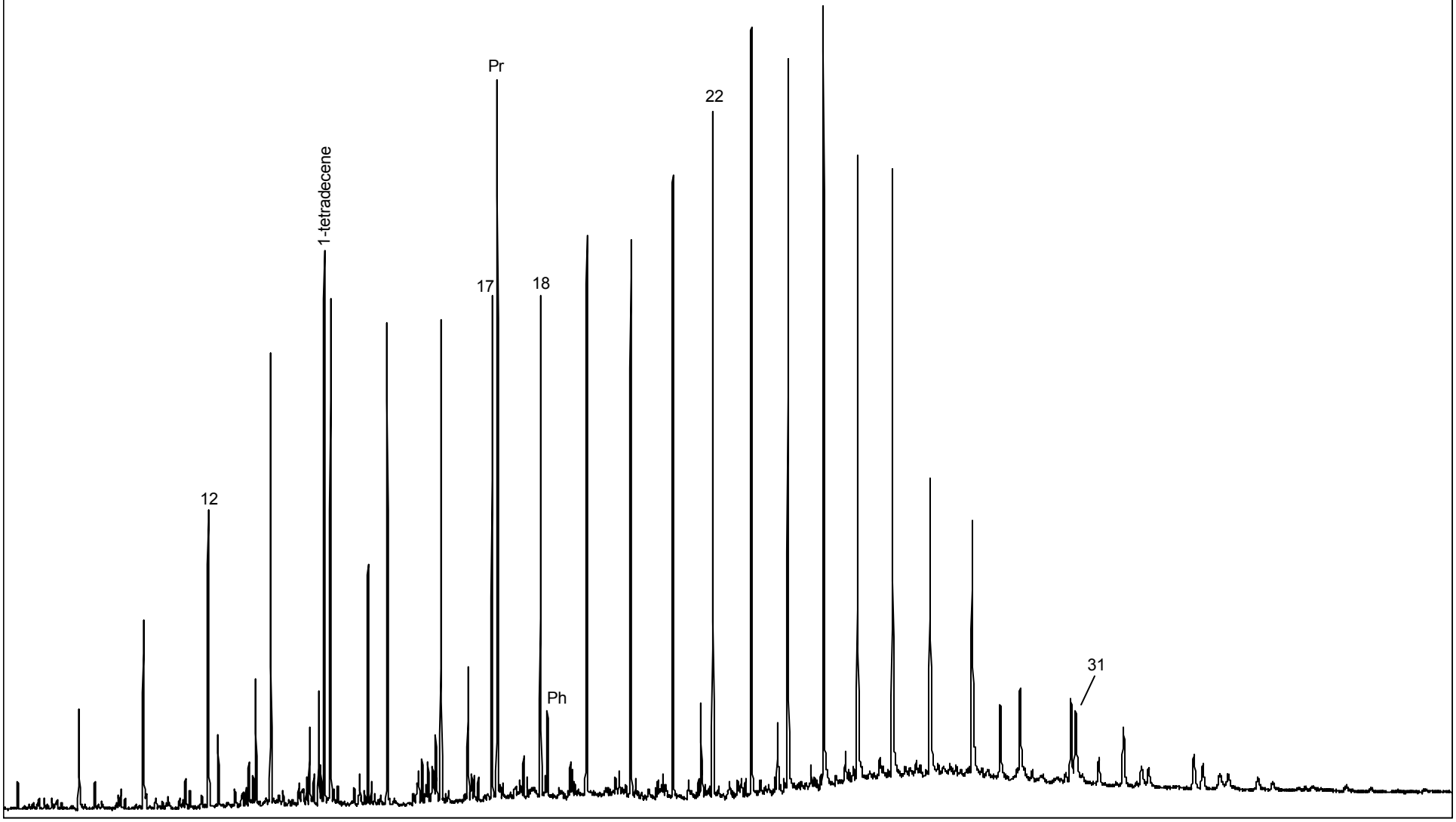


FIGURE 2-2

Sample : **TREFOIL-1, 2901.0m, Cuttings**
File ID : 346501SB

GEOTECH

Chromatogram obtained from the analysis of saturated hydrocarbons by GC-MS

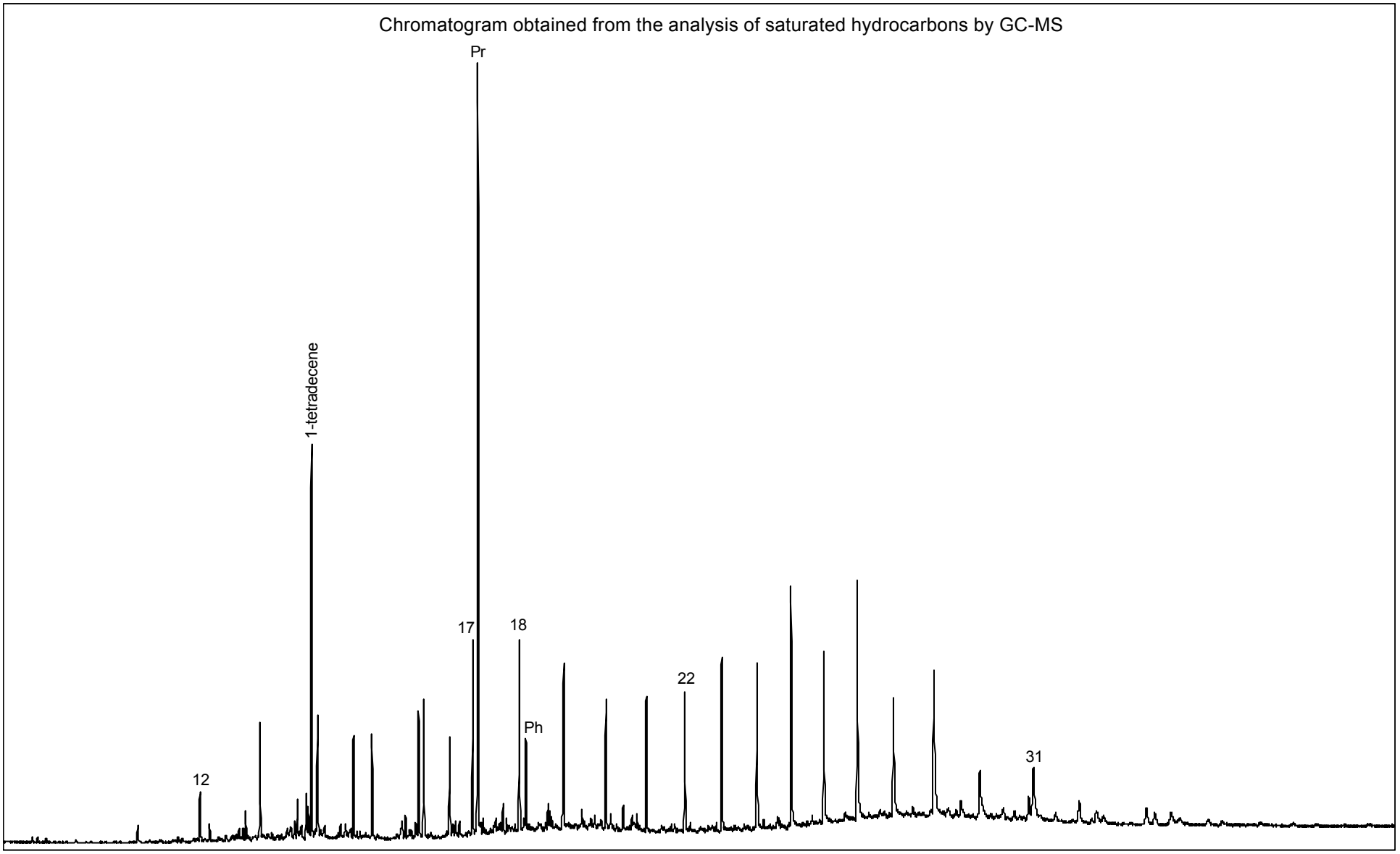


FIGURE 2-3

Sample : **TREFOIL-1, 3093.0m, Cuttings**
File ID : 346506SB

GEOTECH

Chromatogram obtained from the analysis of saturated hydrocarbons by GC-MS

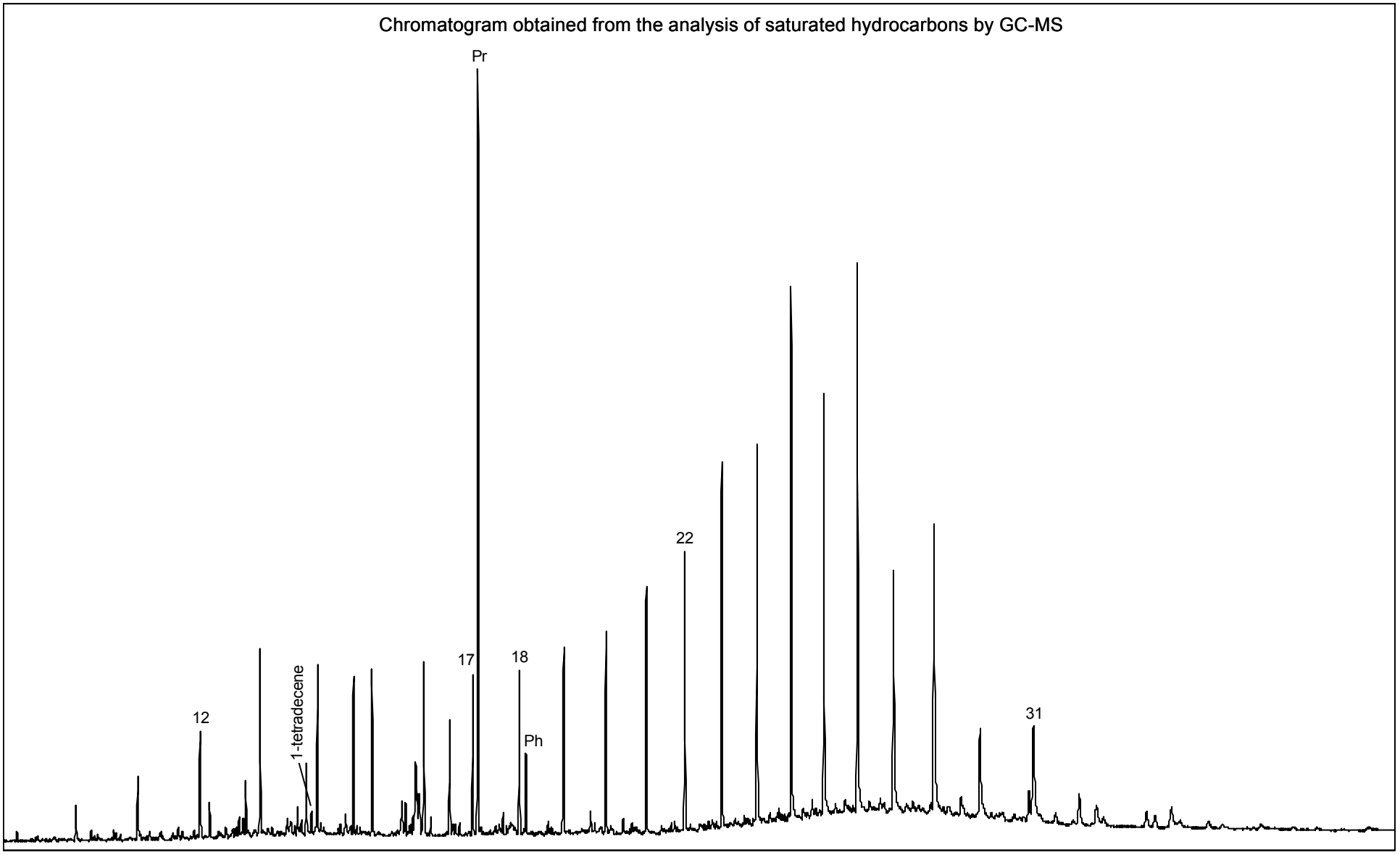


TABLE 5-1

ANALYSIS OF CRUDE OIL BY GC-MS

TREFOIL-1, DST-2, 3040.5-3046.5m, Sample# 2.10, Condensate

GEOTECH

Composition of C4 to C8 Fraction

Compound	*Rel.Wt%*	*Compound*	*Rel.Wt%*
isobutane (A)	1.1	1,1-dimethylcyclopentane (O)	0.7
n-butane (B)	1.7	2-methylhexane/2,3-dimethylpentane (P)	4.9
isopentane (C)	3.8	3-methylhexane (Q)	3.9
n-pentane (D)	3.9	1 cis-3-dimethylcyclopentane (R)	1.3
2,2-dimethylbutane (E)	0.3	1 trans-3-dimethylcyclopentane (S)	1.3
(cyclopentane		1 trans-2-dimethylcyclopentane (T)	2.0
2,3-dimethylbutane (F+G))	1.6	n-heptane (U)	11.0
2-methylpentane (H)	4.3	methylcyclohexane (V)	14.3
3-methylpentane (I)	2.0	1 cis-2-dimethylcyclopentane (W) +	-
n-hexane (J)	5.0	toluene (X)	4.7
methylcyclopentane (K)	3.3	n-octane (Y)	13.2
2,4-dimethylpentane (L)	0.7	ethylbenzene (Z)	1.0
benzene (M)	0.8	M+P-xylene (AA)	7.8
cyclohexane (N)	3.4	O-xylene (BB)	2.0

Calculated Data from the C4 to C8 Fraction

Paraffin Index I	1.9	I/M (Water washing)	2.5
Paraffin Index II	25.8	V/X (Water washing)	3.0
J/K (Maturity)	1.5	I/J (Biodegradation)	0.4
		V/U (Biodegradation)	1.3

- = Below detection limit or not determined
5/09/2005

Paraffin Index I = (P+Q)/(R+S+T)
Paraffin Index II = %U in N to V

FIGURE 3A-1

Sample : **TREFOIL-1, 3040.5-3046.5m, DST-2, Sample 2.10, Condensate**
File ID : **346511WB**

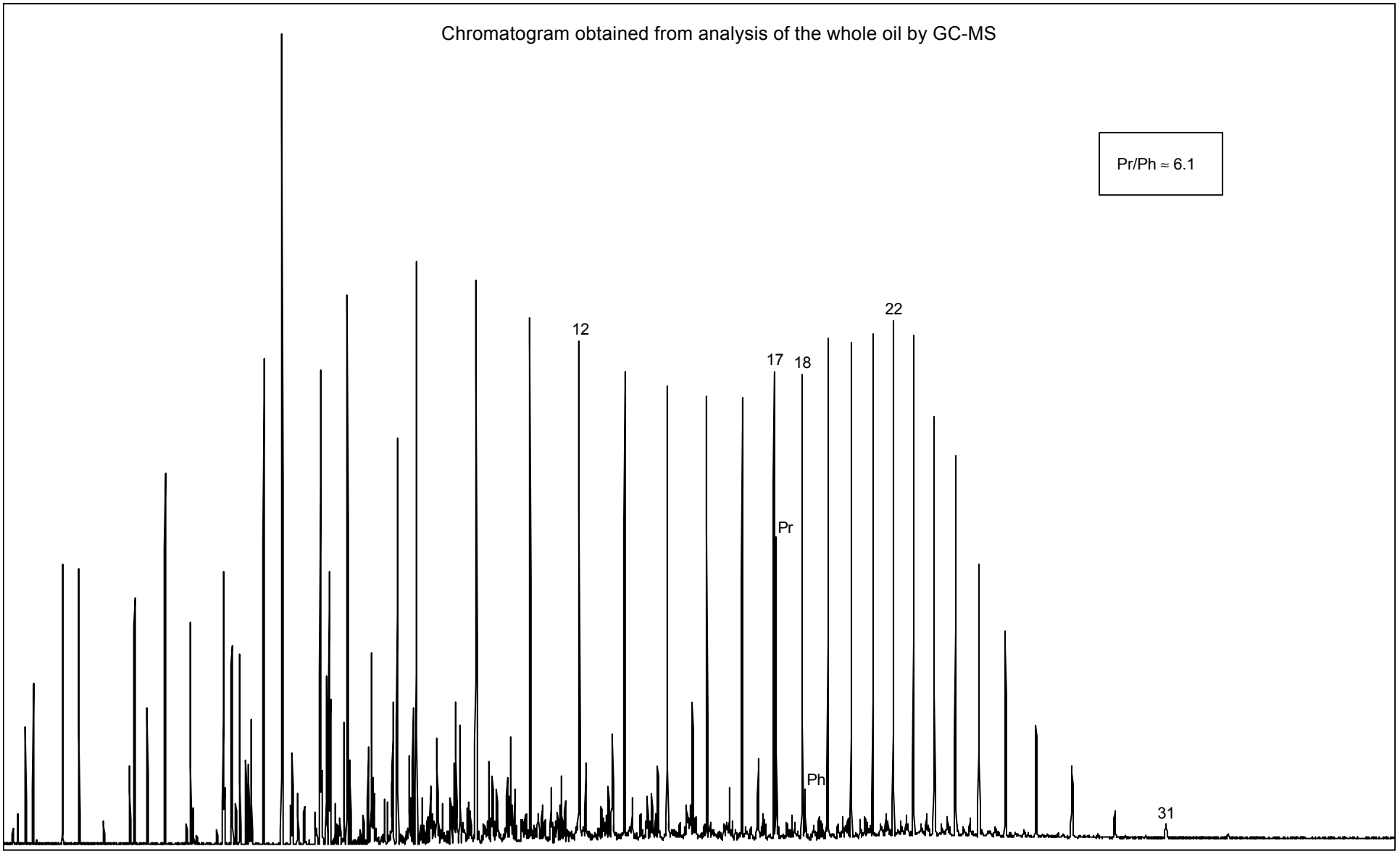
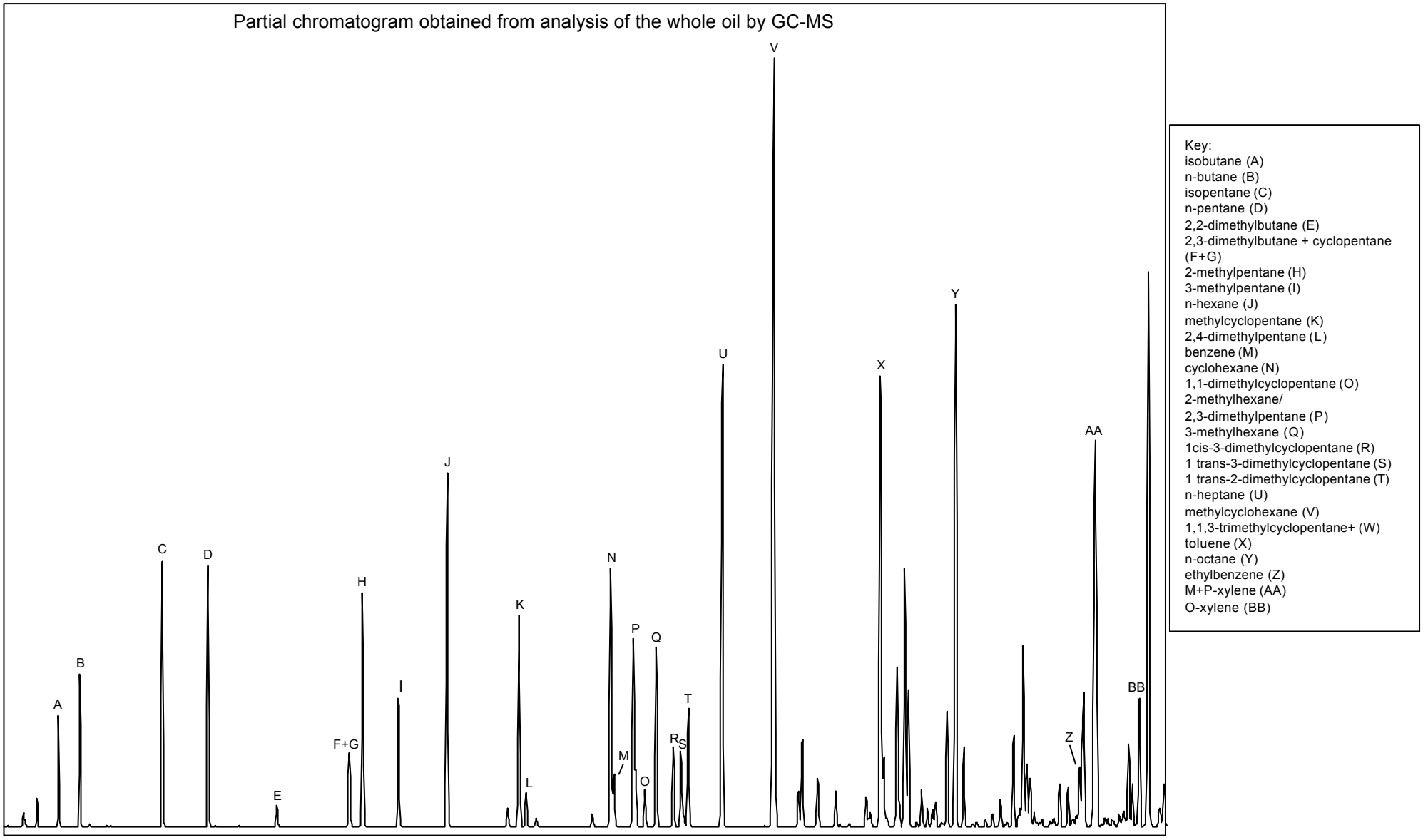


FIGURE 3B-1

Sample : **TREFOIL-1, 3040.5-3046.5m, DST-2, Sample 2.10, Condensate**
File ID : **346511WB**



GEOTECHNICAL SERVICES PTY LTD

ANALYSIS OF CRUDE OIL BY GC-MS

TREFOIL-1, DST-1, 3141-3158m, Sample# 1.16, Condensate

GEOTECH

Composition of C4 to C8 Fraction

Compound	*Rel.Wt%*	*Compound*	*Rel.Wt%*
isobutane (A)	1.0	1,1-dimethylcyclopentane (O)	0.6
n-butane (B)	1.5	2-methylhexane/2,3-dimethylpentane (P)	4.7
isopentane (C)	3.6	3-methylhexane (Q)	3.7
n-pentane (D)	3.1	1 cis-3-dimethylcyclopentane (R)	1.1
2,2-dimethylbutane (E)	0.4	1 trans-3-dimethylcyclopentane (S)	1.2
(cyclopentane		1 trans-2-dimethylcyclopentane (T)	1.6
2,3-dimethylbutane (F+G))	1.7	n-heptane (U)	8.4
2-methylpentane (H)	3.9	methylcyclohexane (V)	10.2
3-methylpentane (I)	1.9	1 cis-2-dimethylcyclopentane (W) +	-
n-hexane (J)	3.9	toluene (X)	10.0
methylcyclopentane (K)	3.4	n-octane (Y)	9.8
2,4-dimethylpentane (L)	0.6	ethylbenzene (Z)	1.8
benzene (M)	3.7	M+P-xylene (AA)	12.0
cyclohexane (N)	3.1	O-xylene (BB)	2.9

Calculated Data from the C4 to C8 Fraction

Paraffin Index I	2.1	I/M (Water washing)	0.5
Paraffin Index II	24.2	V/X (Water washing)	1.0
J/K (Maturity)	1.2	I/J (Biodegradation)	0.5
		V/U (Biodegradation)	1.2

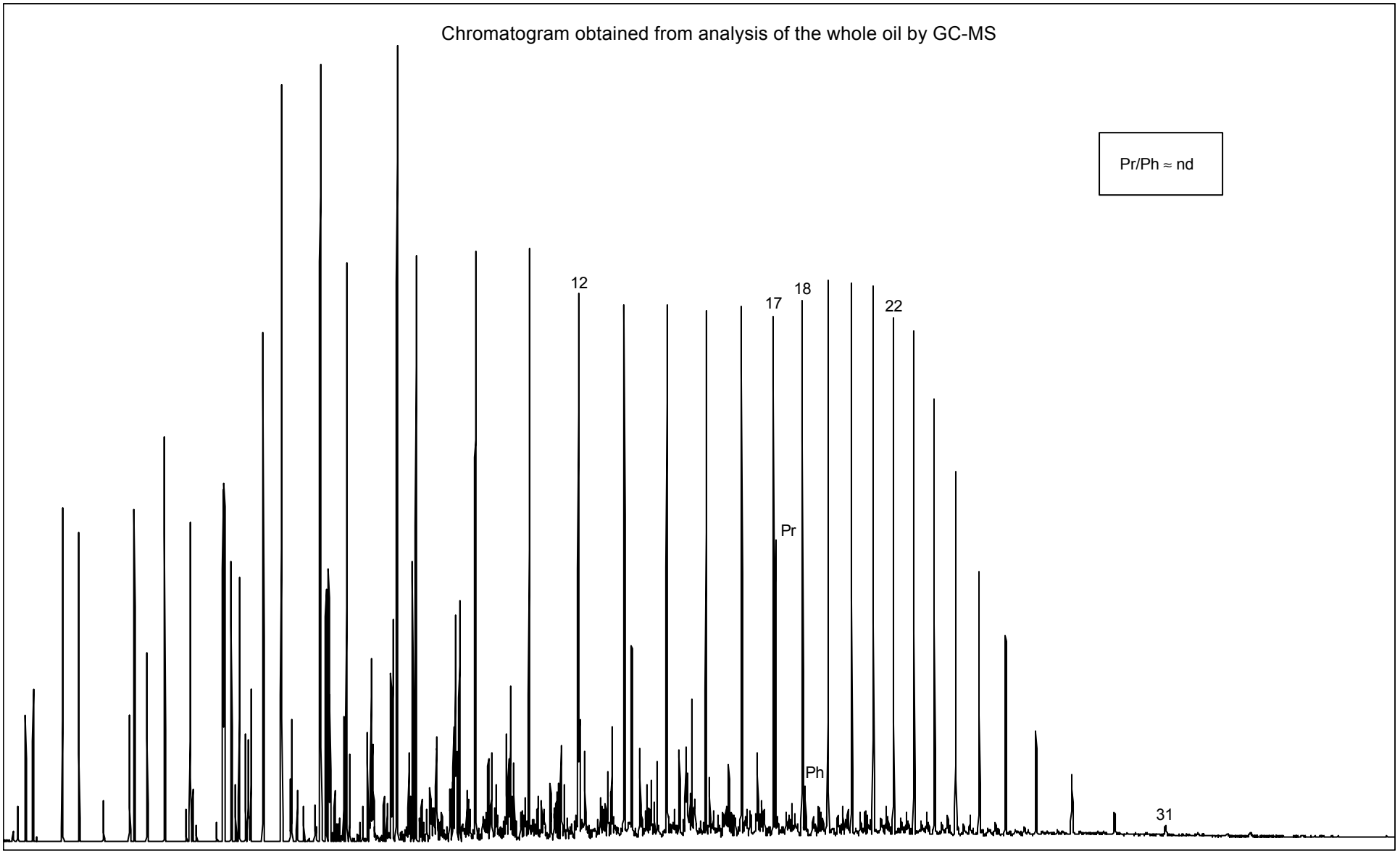
- = Below detection limit or not determined
5/09/2005

Paraffin Index I = (P+Q)/(R+S+T)
Paraffin Index II = %U in N to V

FIGURE 3A-2

Sample : **TREFOIL-1, 3141-3150m, DST-1, Sample 1.16, Condensate**
File ID : **346512WB**

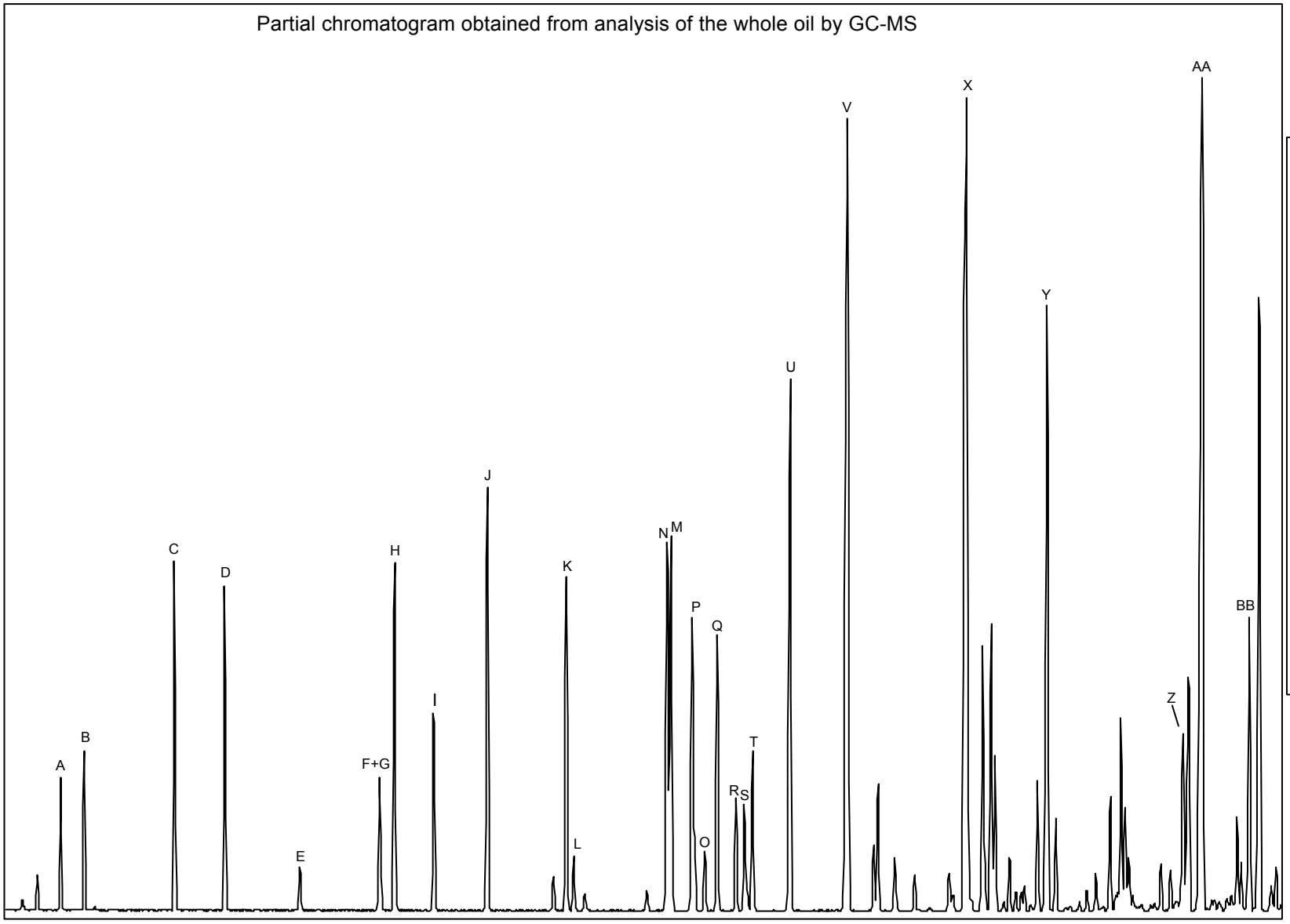
GEOTECH



GEOTECHNICAL SERVICES PTY LTD

FIGURE 3B-2

Sample : **TREFOIL, 3141-3150m, DST-1, Sample 1.16, Condensate**
File ID : **346512WB**



Key:
isobutane (A)
n-butane (B)
isopentane (C)
n-pentane (D)
2,2-dimethylbutane (E)
2,3-dimethylbutane + cyclopentane (F+G)
2-methylpentane (H)
3-methylpentane (I)
n-hexane (J)
methylcyclopentane (K)
2,4-dimethylpentane (L)
benzene (M)
cyclohexane (N)
1,1-dimethylcyclopentane (O)
2-methylhexane/
2,3-dimethylpentane (P)
3-methylhexane (Q)
1cis-3-dimethylcyclopentane (R)
1 trans-3-dimethylcyclopentane (S)
1 trans-2-dimethylcyclopentane (T)
n-heptane (U)
methylcyclohexane (V)
1,1,3-trimethylcyclopentane+ (W)
toluene (X)
n-octane (Y)
ethylbenzene (Z)
M+P-xylene (AA)
O-xylene (BB)

TABLE 6

LIQUID CHROMATOGRAPHY DATA

OIL

TREFOIL-1

Yields (%) and Selected Ratios

		------Hydrocarbons------			------Non-hydrocarbons------			Sats / Aros	Asph. / NSO	HC / Non HC
DEPTH	Sample Type	Sats	Aros	HC's	NSOs	Asph.	Non HC's			
3040.5-3046.5m	Condensate	89.5	10.3	99.8	0.2	nd	0.2	8.7	nd	562.0
3141-3150m	Condensate	86.3	13.1	99.5	0.5	nd	0.5	6.6	nd	184.3

5/09/2005
nd = no data

TABLE 7

ANALYSIS OF SATURATED HYDROCARBONS BY GC-MS

OIL

TREFOIL-1

A. Selected Ratios

DEPTH	Sample Type	Prist./Phyt.	Prist./n-C17	Phyt./n-C18	CPI(1)	CPI(2)	(C21+C22)/(C28+C29)
3040.5m-3046.5m	Condensate	6.76	0.62	0.09	1.06	1.04	4.96
3141.0m-3150.0m	Condensate	6.97	0.75	0.11	1.08	1.07	4.79

TREFOIL-1

B. n-Alkane Distributions

DEPTH	nC12	nC13	nC14	nC15	nC16	nC17	Pr	nC18	Ph	nC19	nC20	nC21	nC22	nC23	nC24	nC25	nC26	nC27	nC28	nC29	nC30	nC31
3040.5m-3046.5m	7.5	7.0	6.5	6.4	6.1	6.0	3.7	6.0	0.5	6.2	6.1	6.0	6.1	5.9	5.4	4.9	3.8	3.0	1.6	0.9	0.3	0.1
3141.0m-3150.0m	7.6	7.2	6.7	6.5	6.0	6.0	4.5	5.9	0.6	6.0	5.9	6.0	6.0	5.8	5.3	4.7	3.5	2.8	1.5	1.0	0.4	0.2

$$CPI(1) = \frac{(C23+C25+C27+C29)+(C25+C27+C29+C31)}{2x(C24+C26+C28+C30)}$$

$$CPI(2) = \frac{(C23+C25+C27)+(C25+C27+C29)}{2x(C24+C26+C28)}$$

5/09/2005

nd = no data

FIGURE 4-1

Sample : **TREFOIL-1, 3040.5-3046.5m, DST-2, Sample 2.10, Condensate**
File ID : 346511S

GEOTECH

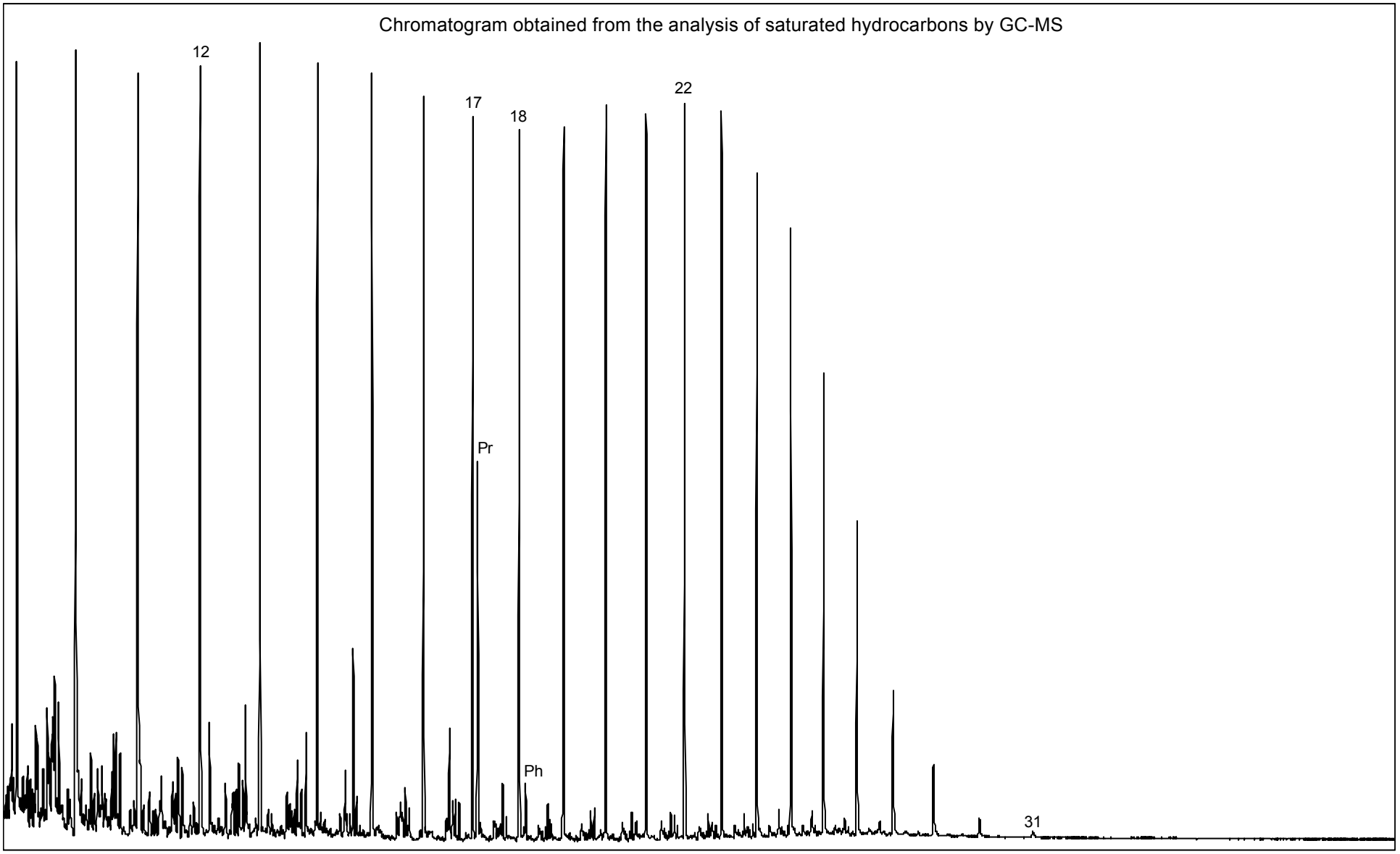


FIGURE 4-2

Sample : **TREFOIL-1, 3141-3150m, DST-1, Sample 1.16, Condensate**
File ID : 346512S

GEOTECH

Chromatogram obtained from the analysis of saturated hydrocarbons by GC-MS

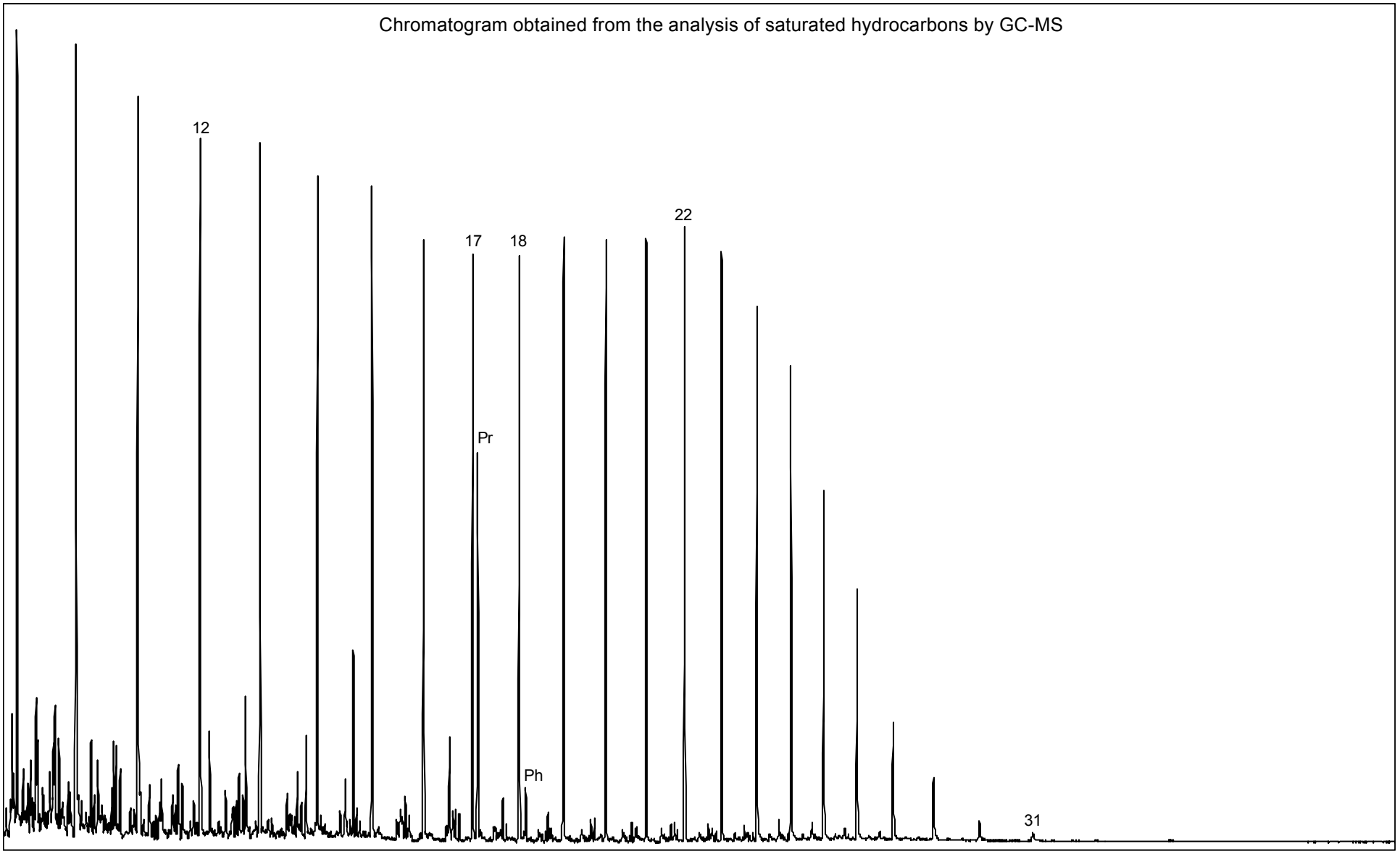


TABLE 8

ANALYSIS OF AROMATIC HYDROCARBONS BY GC-MS

TREFOIL-1

DEPTH	TYPE	DNR-1	DNR-5	DNR-6	TNR-1	TNR-5	TNR-6	MPR-1	MPI-1	MPI-2	Rc(a)	Rc(b)
3040.5-3046.5m	Condensate	6.37	nd	2.77	0.69	0.57	0.42	2.28	0.58	0.54	0.75	1.95
3141-3150.0m	Condensate	11.25	nd	4.07	1.07	0.46	0.37	3.72	0.80	0.70	0.88	1.82
3375m	Cuttings	4.42	nd	1.80	0.92	2.86	2.88	1.66	0.46	0.48	0.68	2.02

response factors have not been applied to these ratios

TREFOIL-1

DEPTH	TYPE	1,7-DMP/X (m/z 206)	RETENE/9-MP (m/z 219,192)	1MP/9MP	HPI
3040.5-3046.5m	Condensate	0.30	0.49	0.64	0.85
3141-3150.0m	Condensate	0.29	0.34	0.58	0.37
3375-	Cuttings	0.64	0.13	0.77	1.52

HPI = Higher Plant Index (i.e (retene + cadalene + iHMN-IV)/1,3,6,7-TeMN))

FIGURE 5A-1

Sample: **TREFOIL-1, 3040.5-3046.5m, DST-2, Sample 2.10, Condensate**

File ID: **346511A**

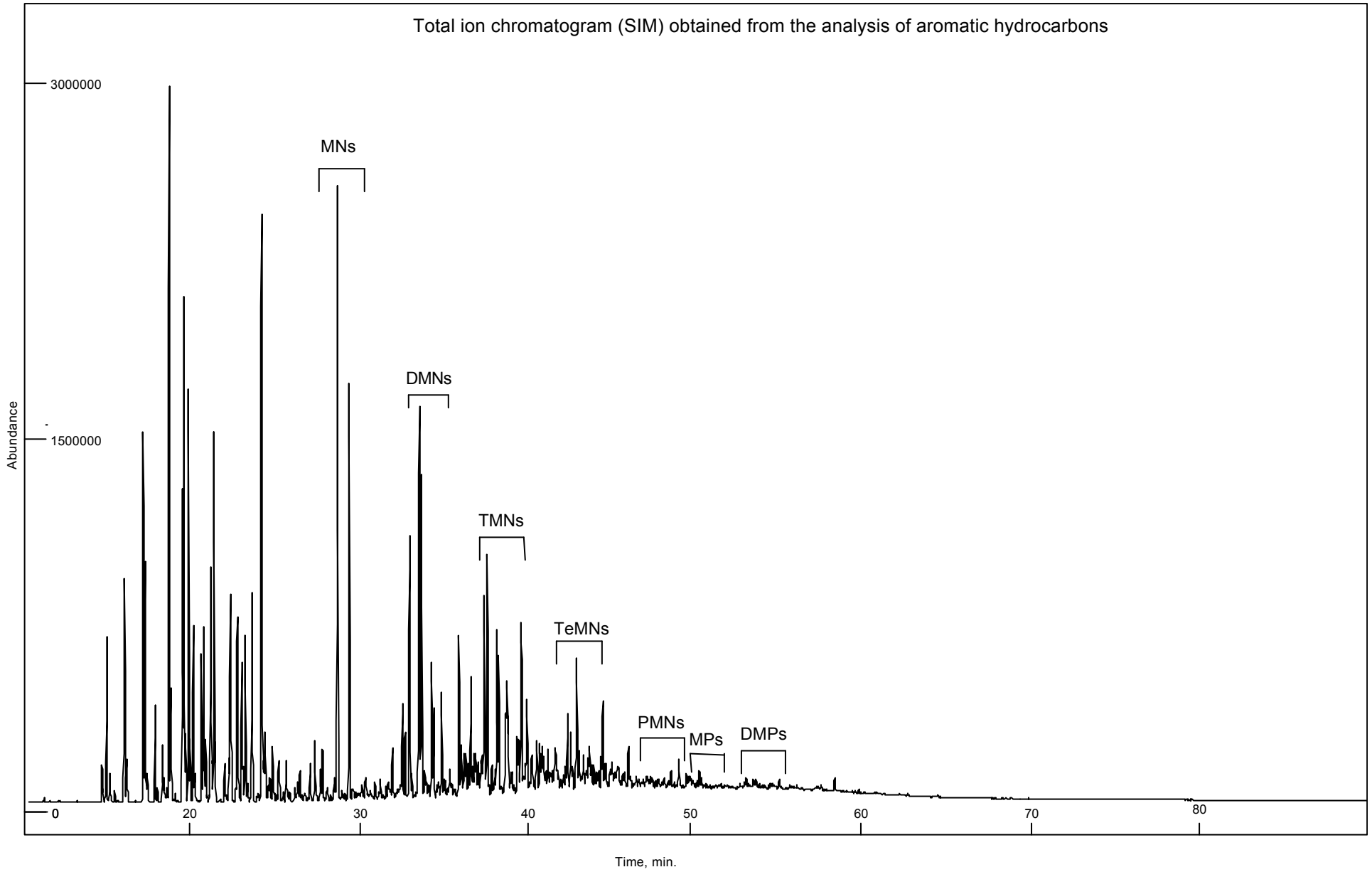


FIGURE 5B-1

Sample: **TREFOIL-1, 3040.5-3046.5m, DST-2, Sample 2.10, Condensate**

File ID: **346511A**

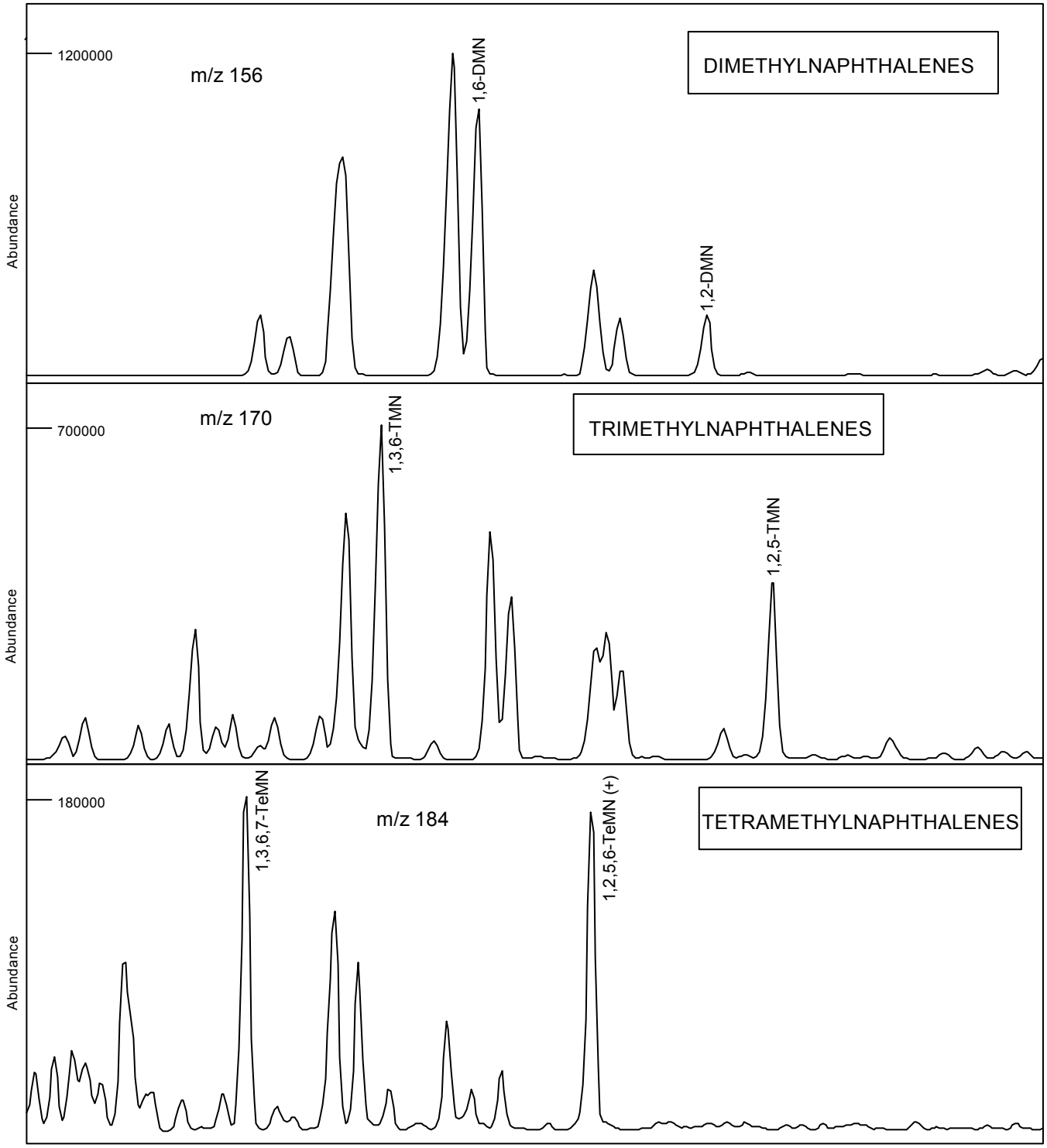


FIGURE 5C-1

Sample: **TREFOIL-1, 3040.5-3046.5m, DST-2, Sample 2.10, Condensate**

File ID: **346511A**

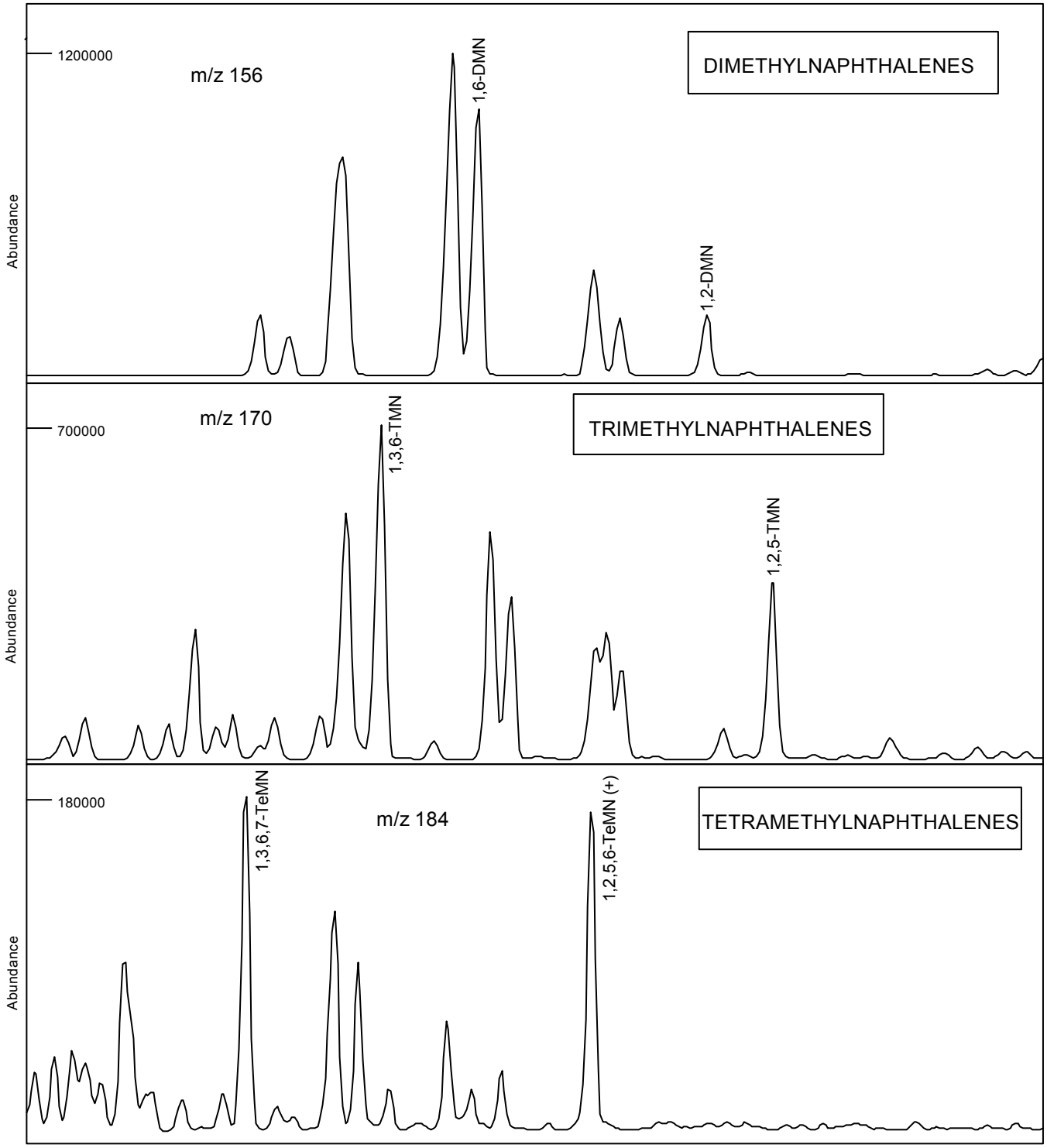


FIGURE 5D-1

Sample: **TREFOIL-1, 3040.5-3046.5m, DST-2, Sample 2.10, Condensate**

File ID: **346511A**

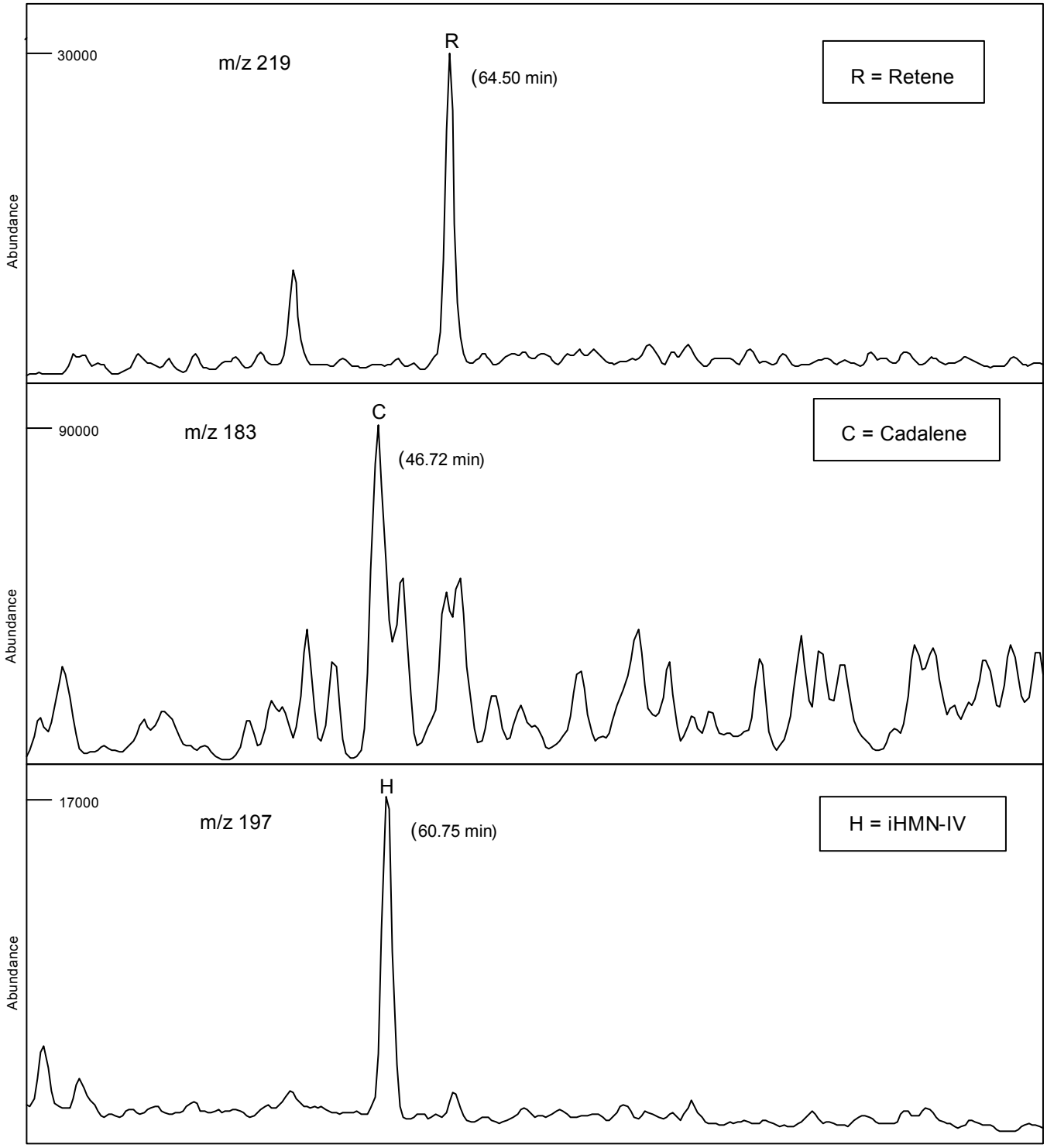


FIGURE 5E-1

Sample: **TREFOIL-1, 3040.5-3046.5m, DST-2, Sample 2.10, Condensate**

File ID: **346511A**

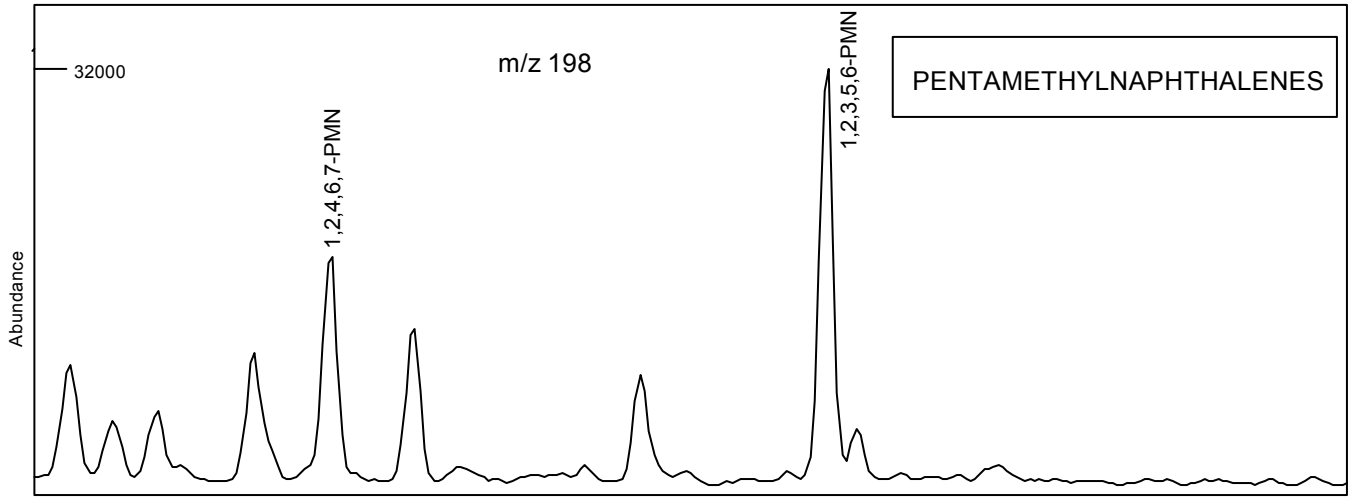


FIGURE 5A-2

Sample: **TREFOIL-1, 3141-3150m, DST-1, Sample 1.16, Condensate**

File ID: **346512AB**

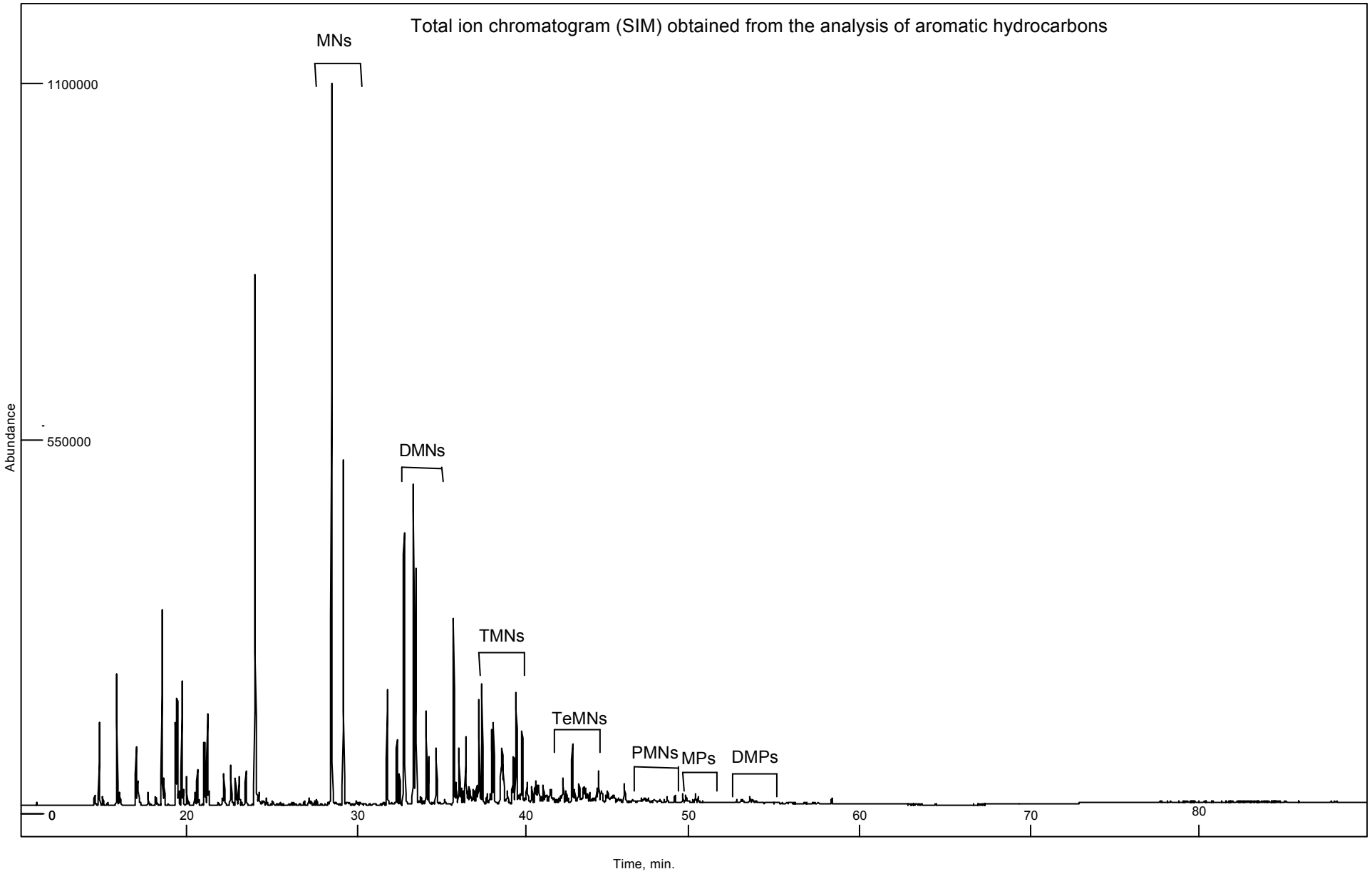


FIGURE 5B-2

Sample: **TREFOIL-1, 3141-3150m, DST-1, Sample 1.16, Condensate**

File ID: **346512AB**

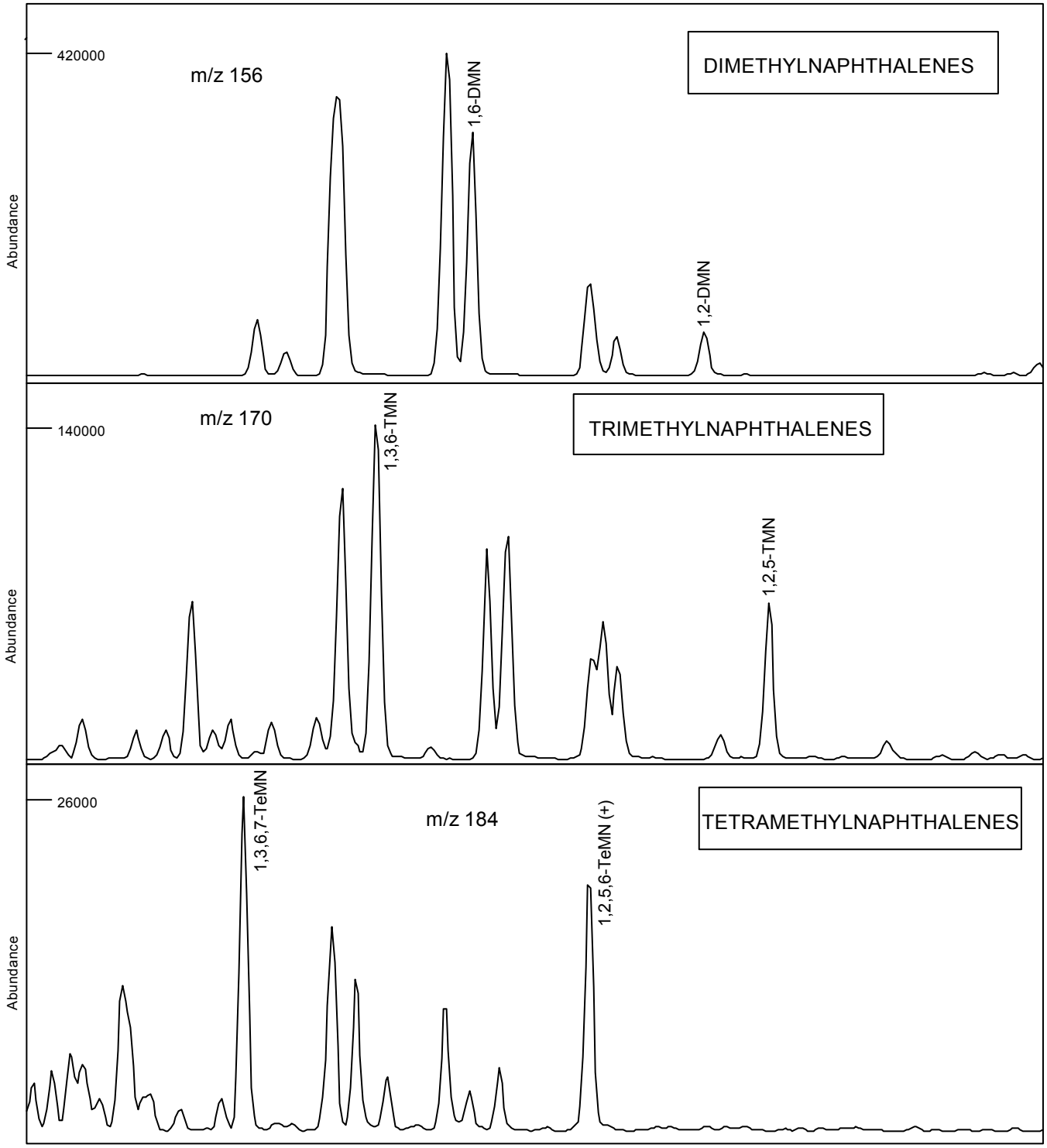


FIGURE 5C-2

Sample: **TREFOIL-1, 3141-3150m, DST-1, Sample 1.16, Condensate**

File ID: **346512AB**

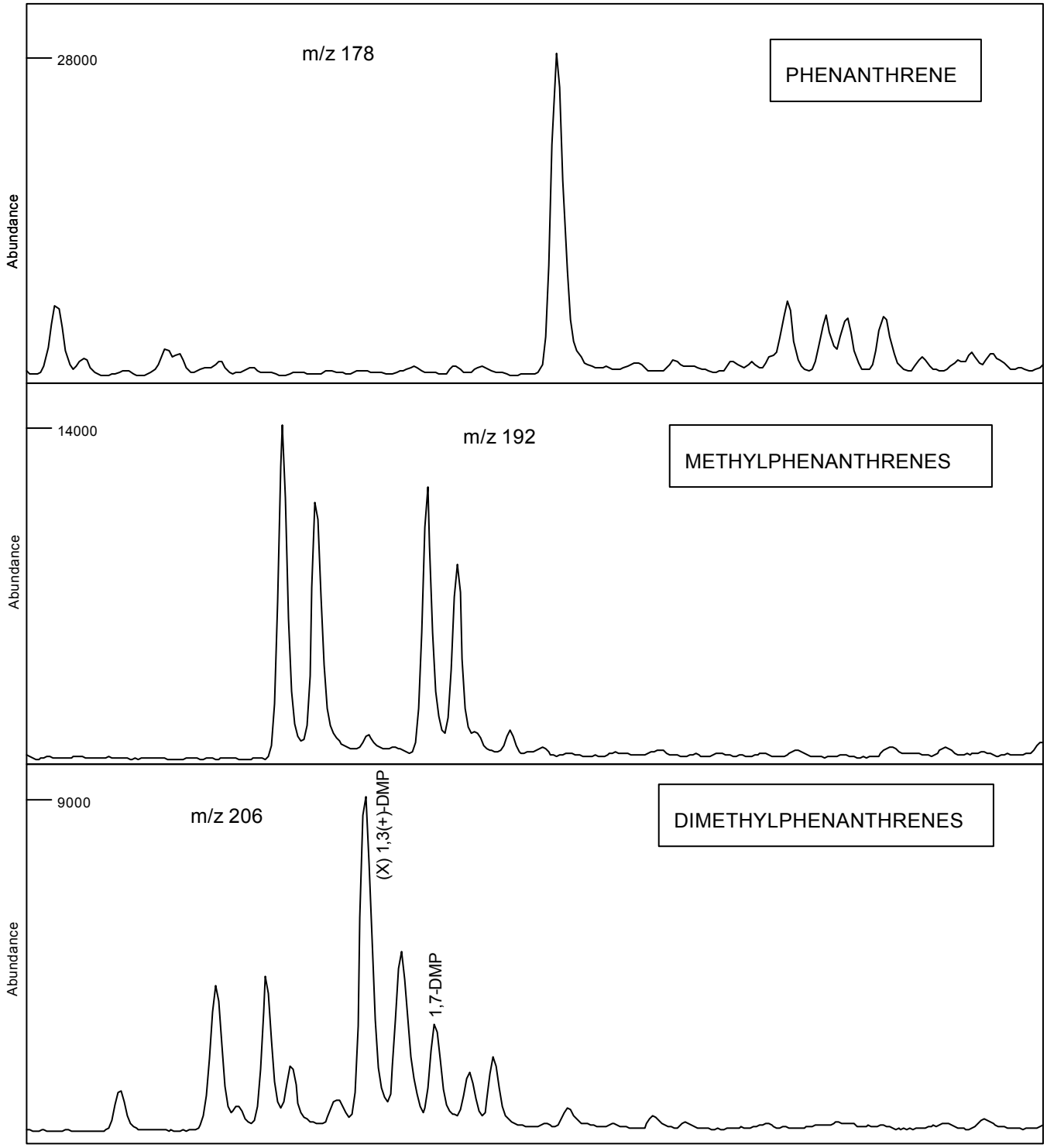


FIGURE 5D-2

Sample: **TREFOIL-1, 3141-3150m, DST-1, Sample 1.16, Condensate**

File ID: **346512AB**

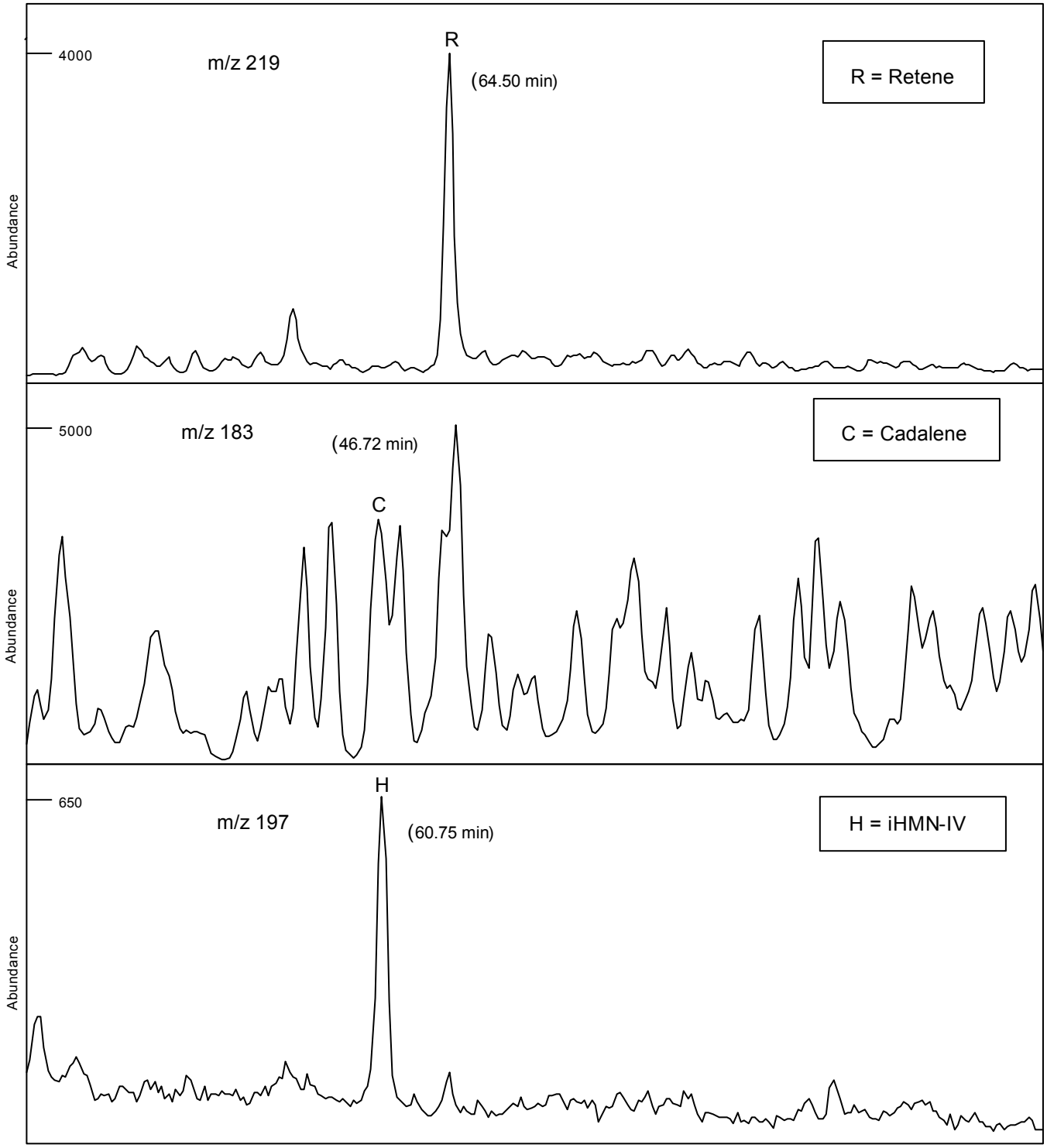


FIGURE 5E-2

Sample: **TREFOIL-1, 3141-3150m, DST-1, Sample 1.16, Condensate**

File ID: **346512AB**

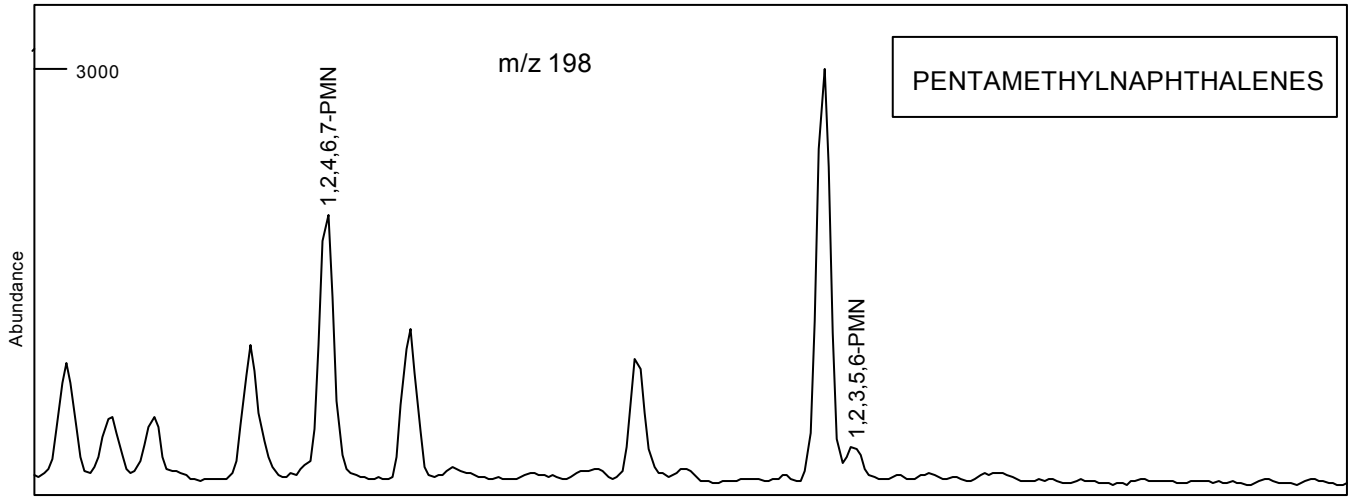
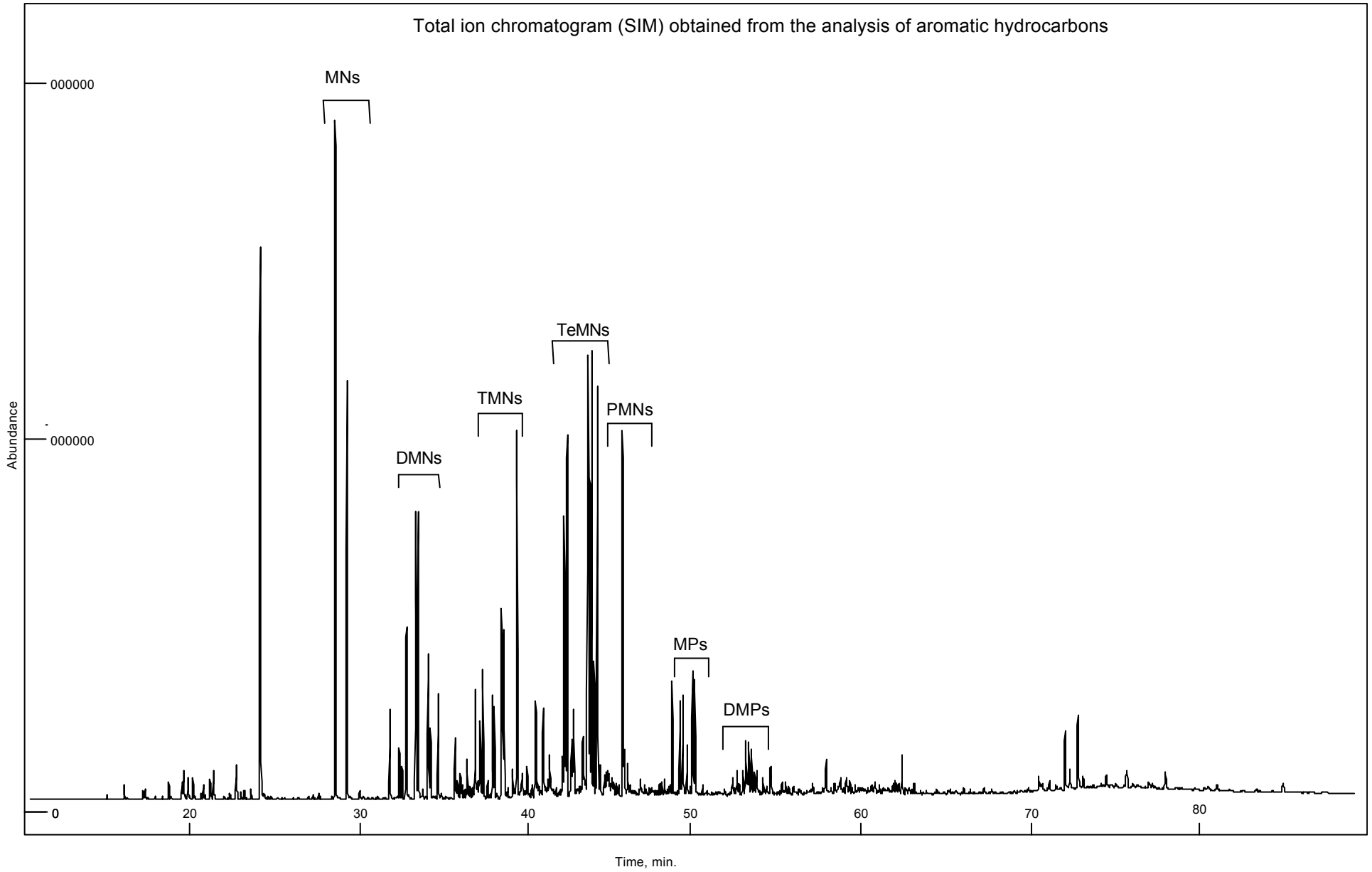


FIGURE 5A-3

Sample: TREFOIL-1**, 3375m, Cuttings**

File ID: **346510A**



GEOTECHNICAL SERVICES PTY LTD

FIGURE 5B-3

Sample: **TREFOIL-1, 3375M, Cuttings**

File ID: **346510A**

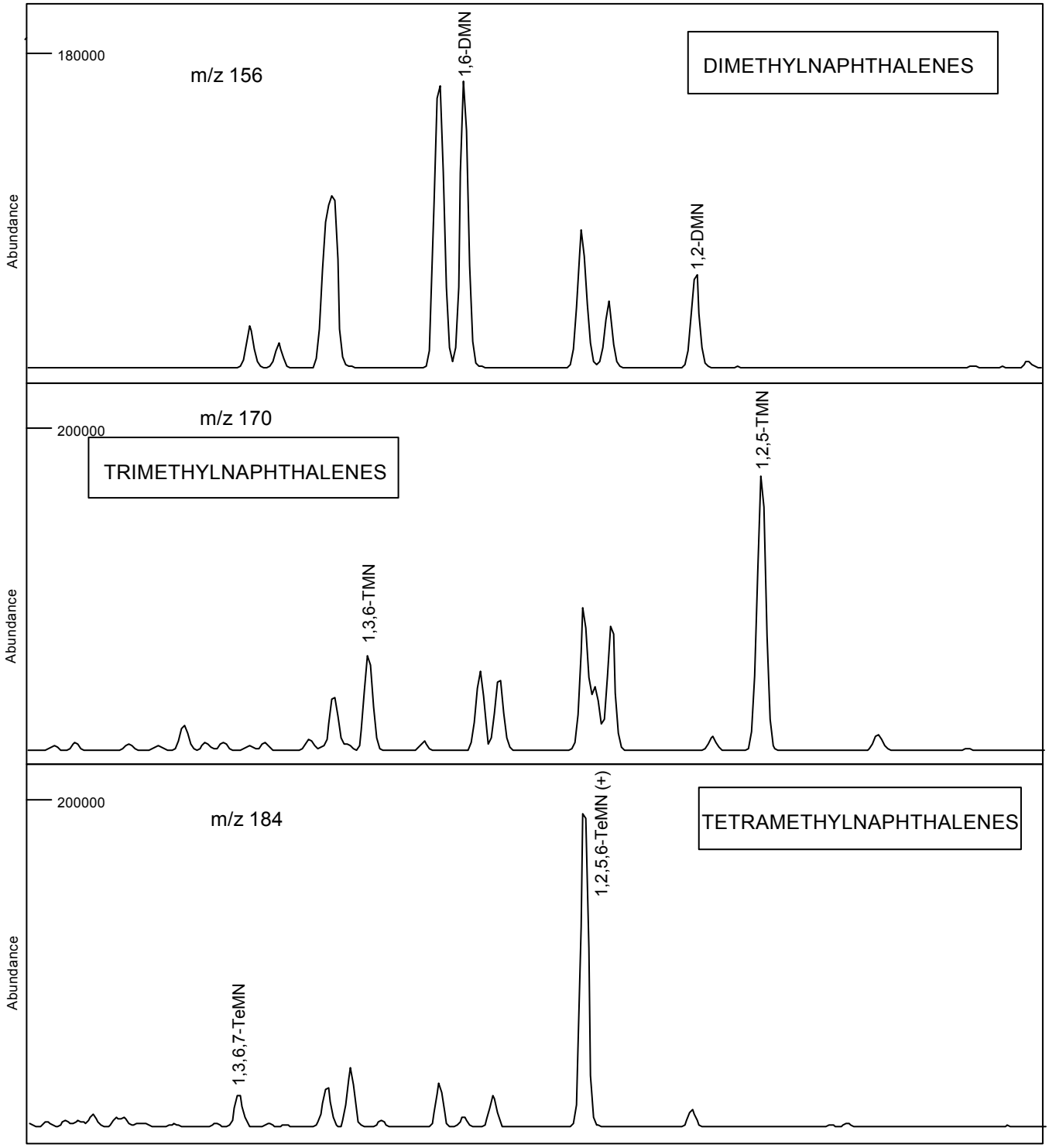


FIGURE 5C-3

Sample: **TREFOIL-1, 3375M, Cuttings**

File ID: **346510A**

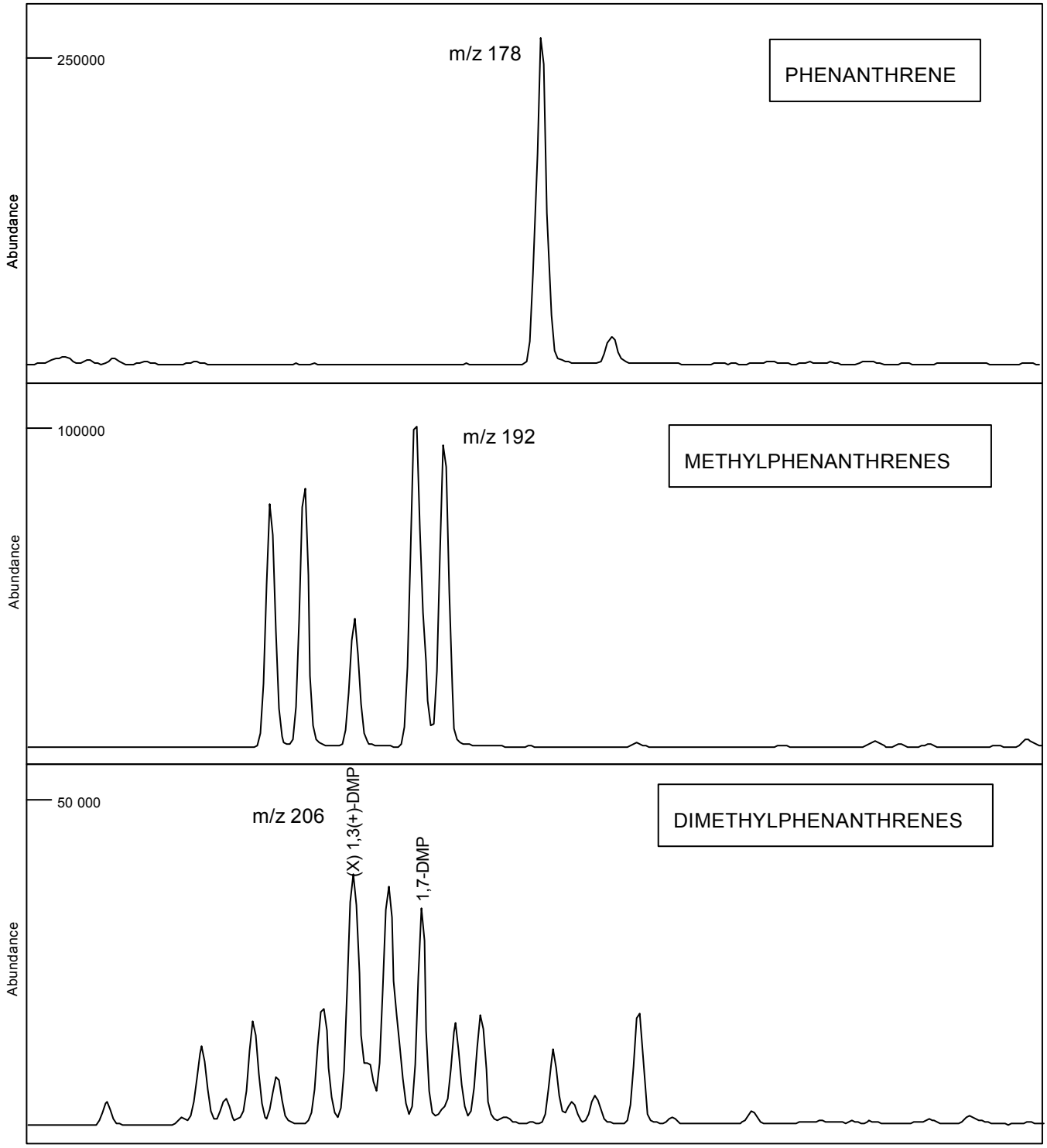


FIGURE 5D-3

Sample: **TREFOIL-1, 3375M, Cuttings**

File ID: **346510A**

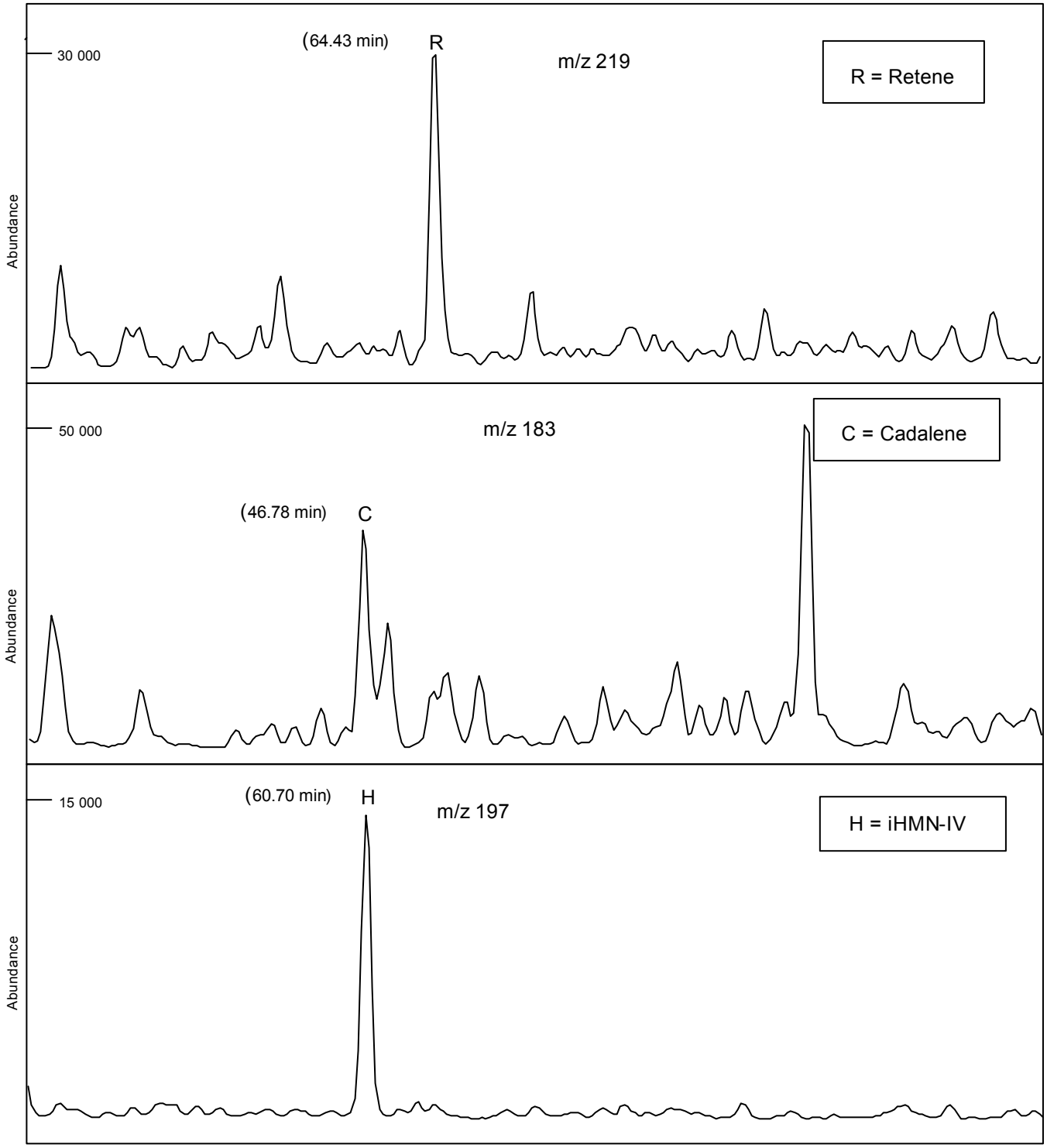


FIGURE 5E-3

Sample: **TREFOIL-1, 3375M, Cuttings**

File ID: **346510A**

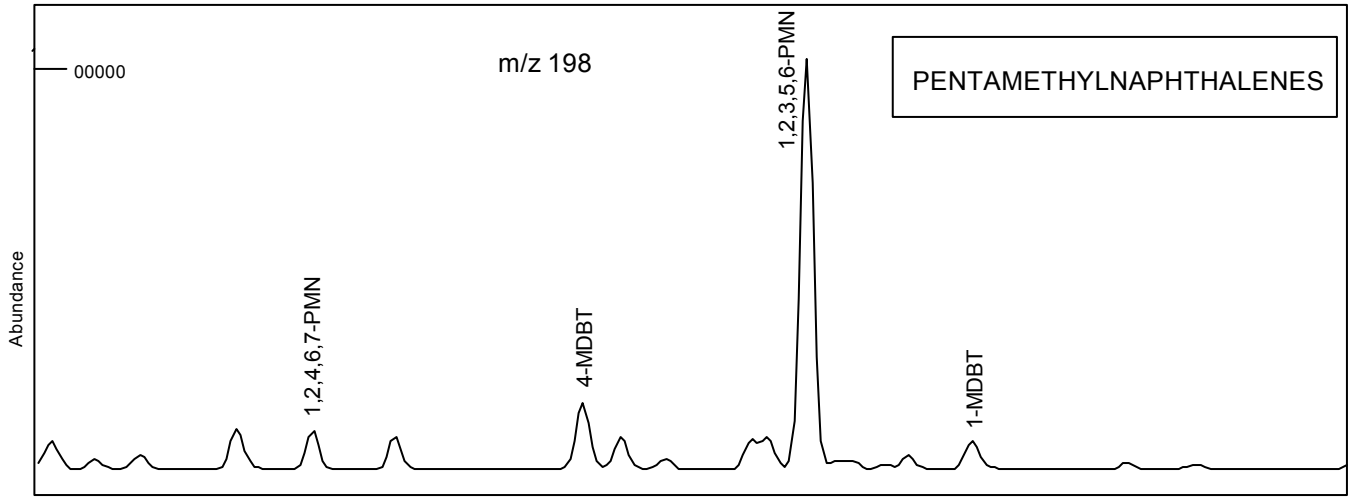


TABLE 9-1

ANALYSIS OF BRANCHED AND CYCLIC SATURATED HYDROCARBONS BY GC-MS

TREFOIL-1, 3375m, Cuttings

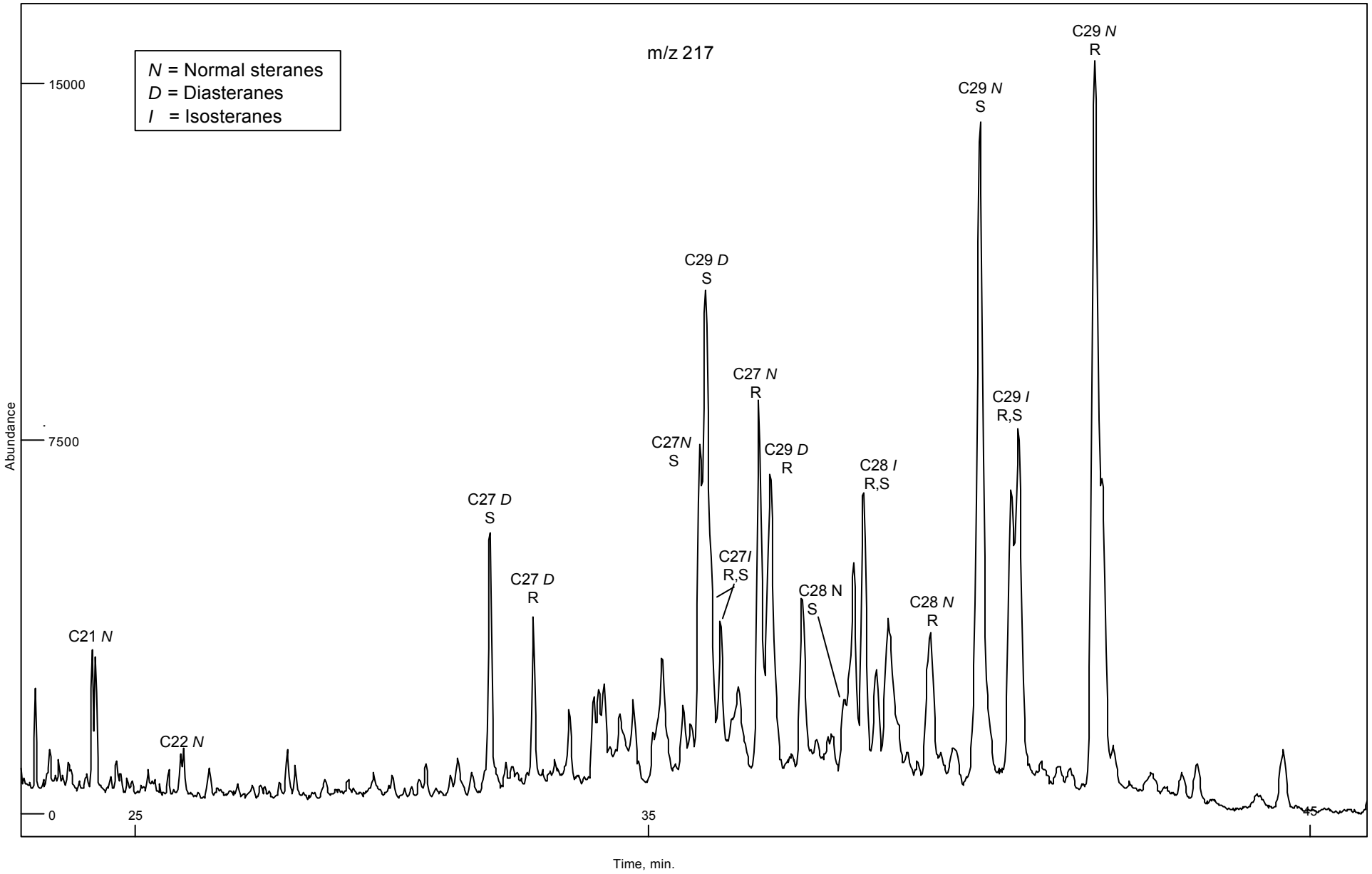
	Selected Parameters	*Ion(s)*	*Value*
1.	18α(H)-hopane/17α(H)-hopane (Ts/Tm)	191	0.07
2.	C30 hopane/C30 moretane	191	2.55
3.	C31 22S hopane/C31 22R hopane	191	1.38
4.	C32 22S hopane/C32 22R hopane	191	1.29
5.	C29 20S ααα sterane/C29 20R ααα sterane	217	0.92
6.	C29 ααα steranes (20S / 20S+20R)	217	0.48
7.	$\frac{\text{C29 } \alpha\beta\beta \text{ steranes}}{\text{C29 } \alpha\alpha\alpha \text{ steranes + C29 } \alpha\beta\beta \text{ steranes}}$	217	0.29
8.	C27/C29 diasteranes	259	0.33
9.	C27/C29 steranes	217	0.37
10.	18α(H)-oleanane/C30 hopane	191	nd
11.	$\frac{\text{C29 diasteranes}}{\text{C29 } \alpha\alpha\alpha \text{ steranes + C29 } \alpha\beta\beta \text{ steranes}}$	217	0.33
12.	$\frac{\text{C30 (hopane + moretane)}}{\text{C29 (steranes + diasteranes)}}$	191/217	4.52
13.	C15 drimane/C16 homodrimane	123	0.21
14.	Rearranged drimanes/normal drimanes	123	0.14

nd = no data

FIGURE 6A-1

Sample : **TREFOIL-1, 3375m, Cuttings**

File ID : 346510B

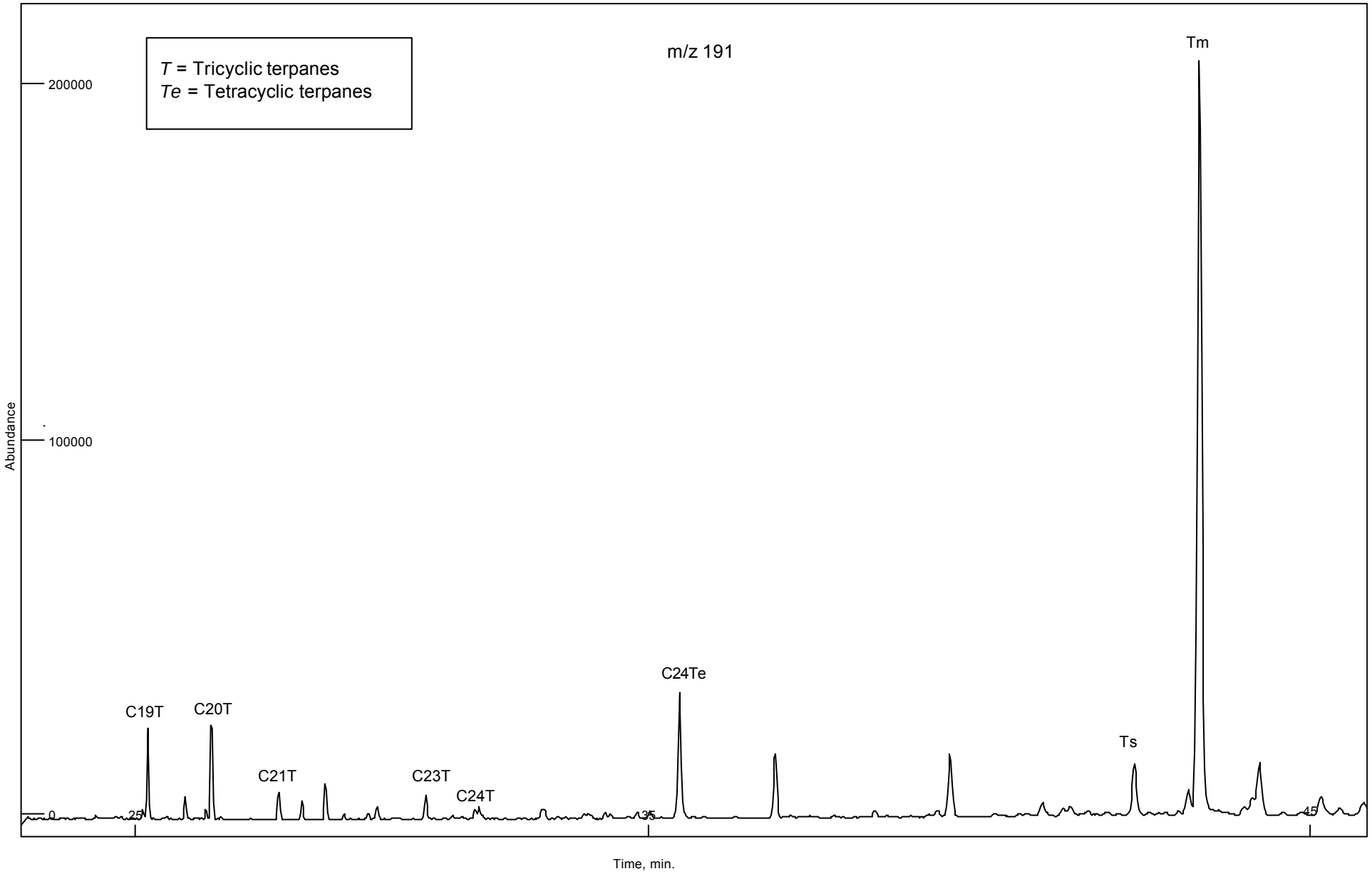


GEOTECHNICAL SERVICES PTY LTD

FIGURE 6B-1

Sample : **TREFOIL-1, 3375m, Cuttings**

File ID : 346510B

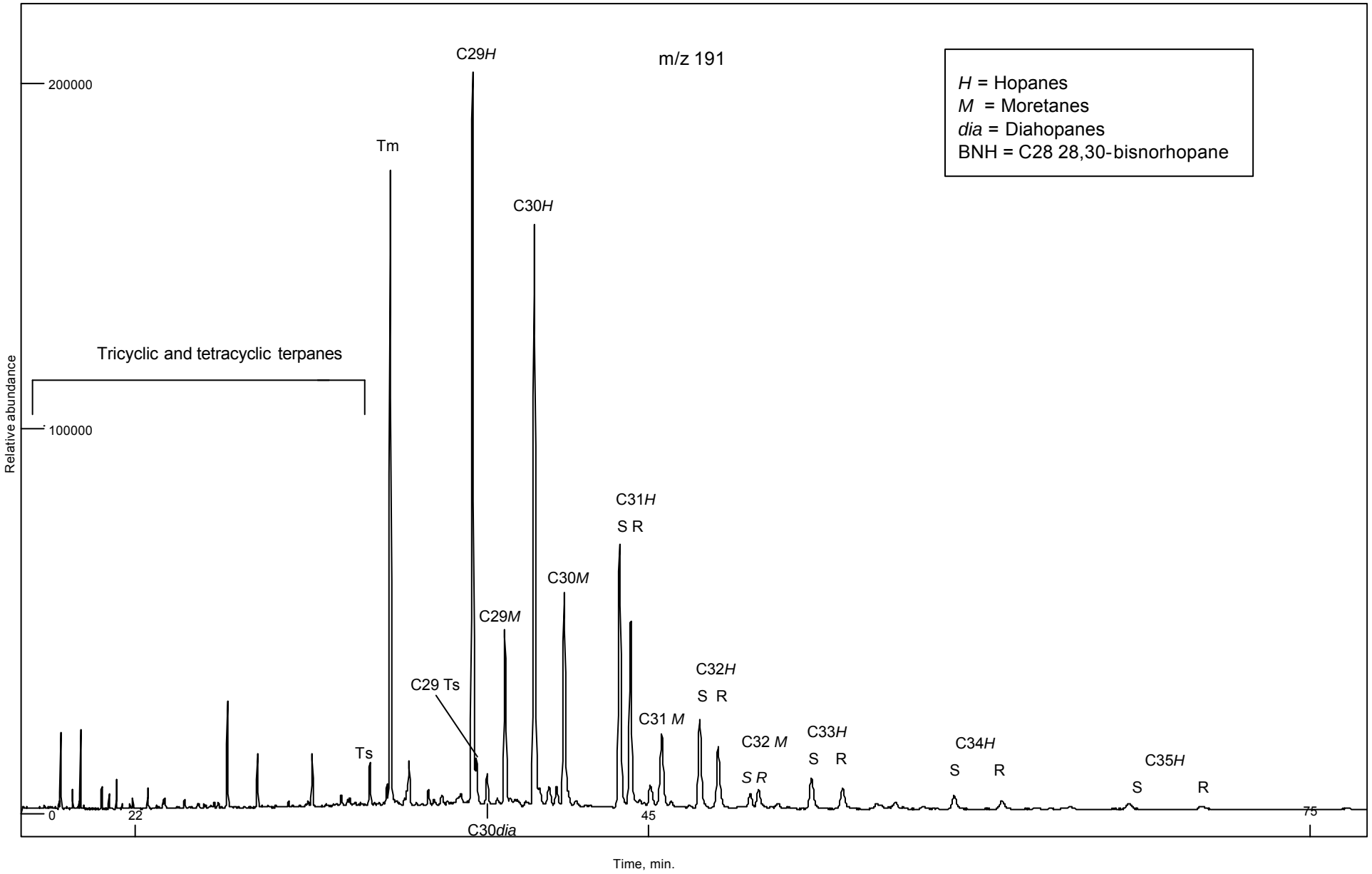


GEOTECHNICAL SERVICES PTY LTD

FIGURE 6C-1

Sample : **TREFOIL-1, 3375m, Cuttings**

File ID : 346510B



GEOTECHNICAL SERVICES PTY LTD

FIGURE 6D-1

Sample : **TREFOIL-1, 3375m, Cuttings**

File ID : 346510B

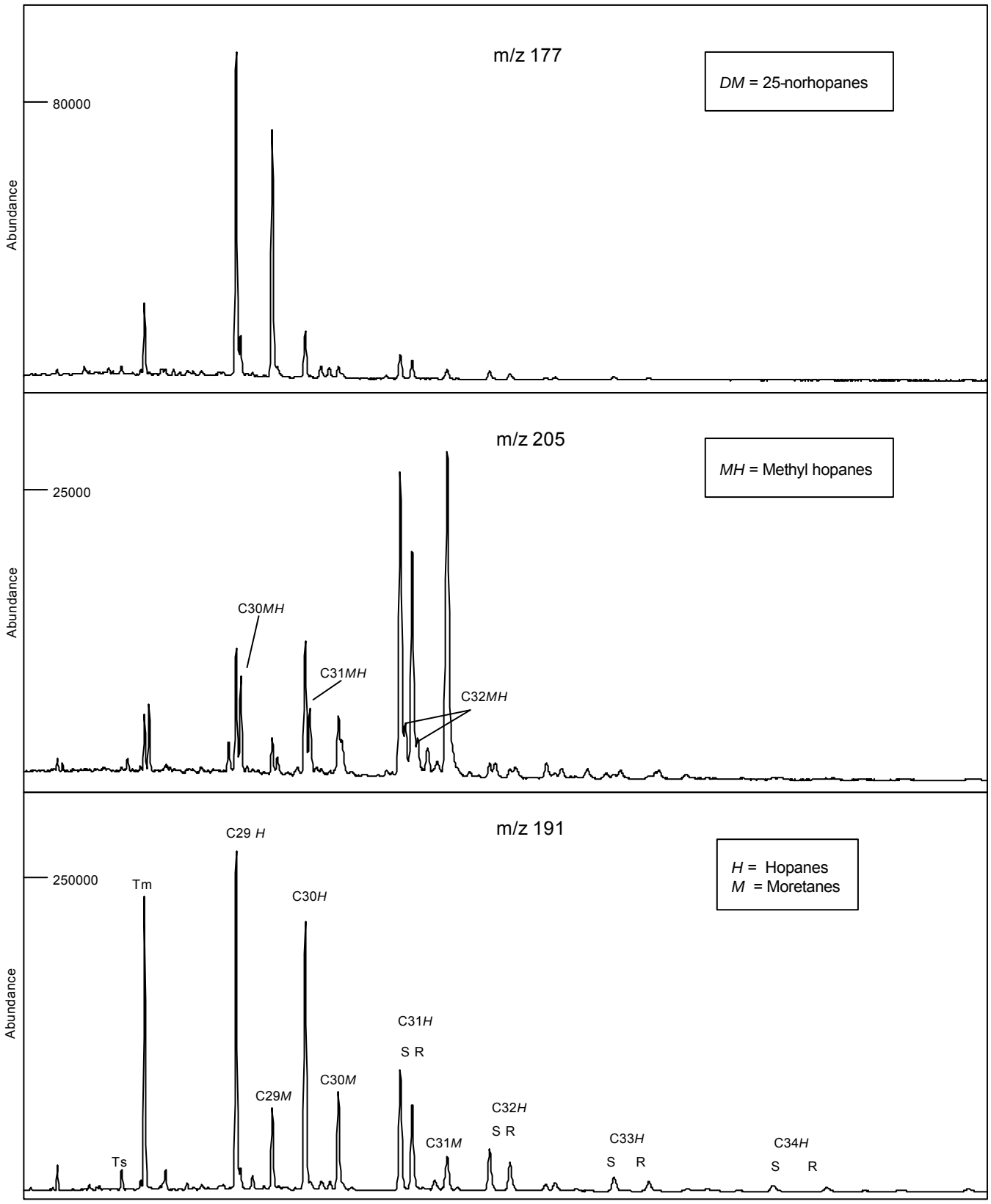
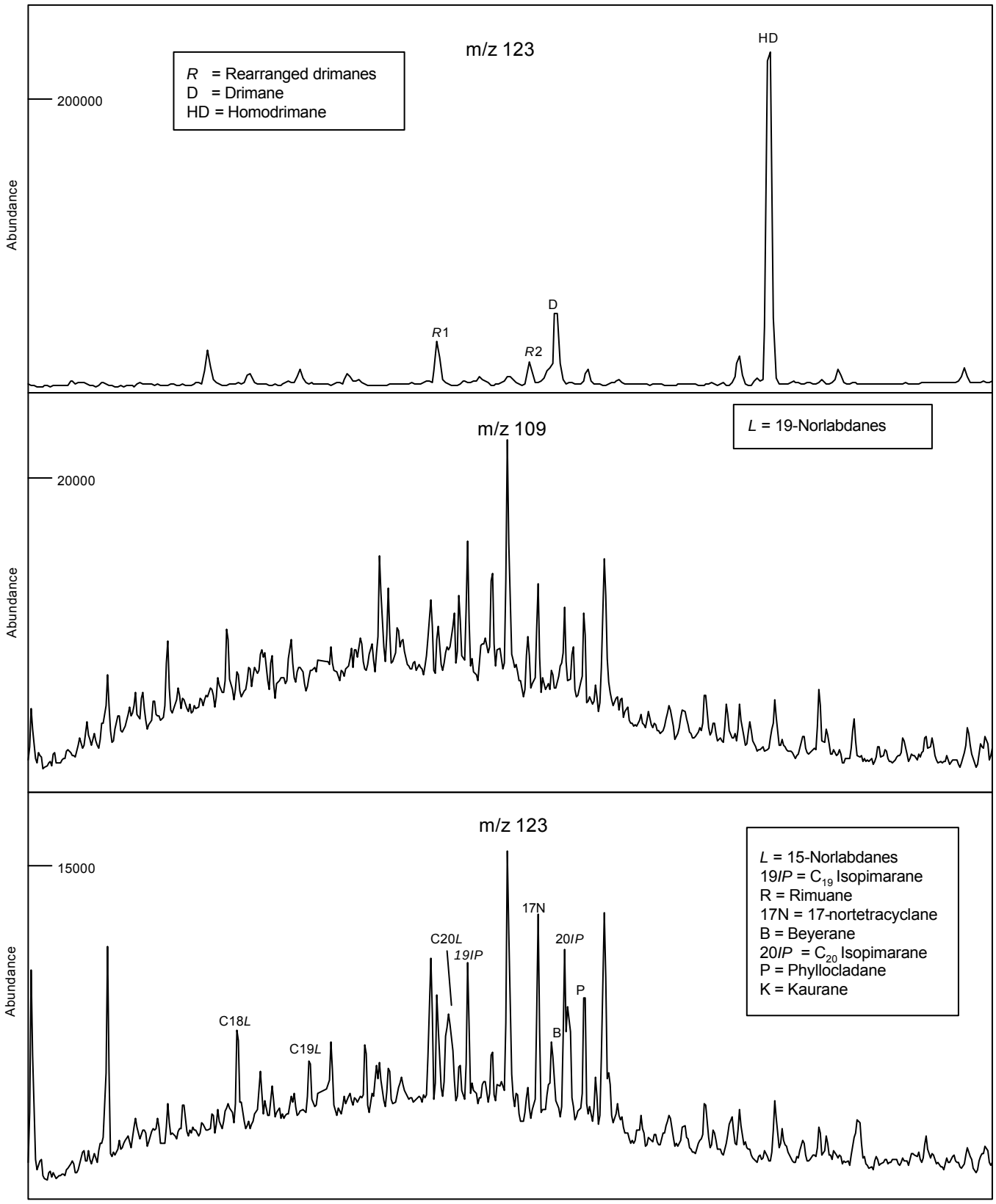


FIGURE 6E-1

Sample : **TREFOIL-1, 3375m, Cuttings**

File ID : 346510B



GEOTECHNICAL SERVICES PTY LTD

FIGURE 6F-1

Sample : **TREFOIL-1, 3375m, Cuttings**

File ID : 346510B

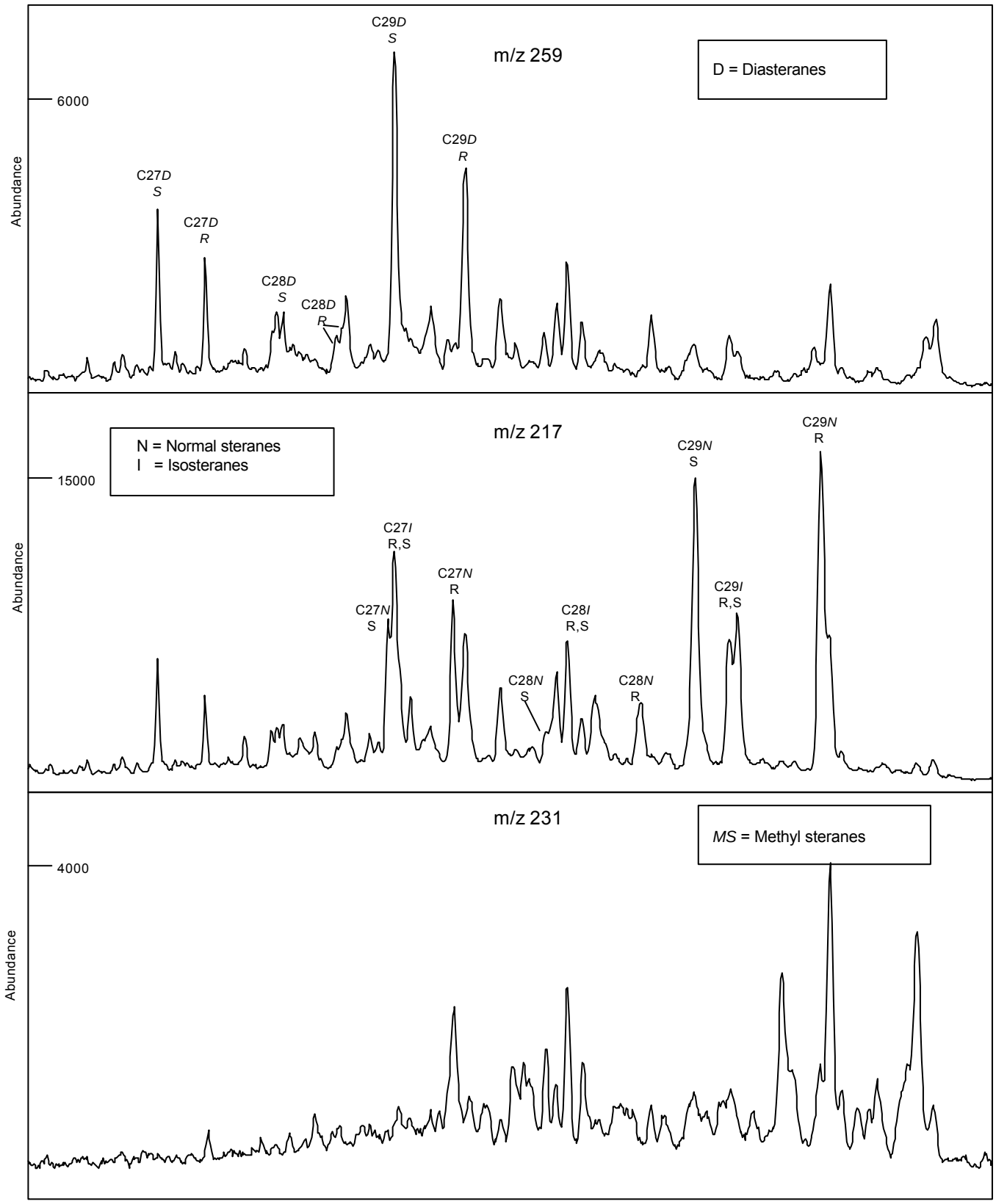


TABLE 9-2

ANALYSIS OF BRANCHED AND CYCLIC SATURATED HYDROCARBONS BY GC-MS

TREFOIL-1, 3040.5-3046.5m, DST-2, Sample 2.10, Condensate, Topped

	Selected Parameters	*Ion(s)*	*Value*
1.	18α(H)-hopane/17α(H)-hopane (Ts/Tm)	191	0.39
2.	C30 hopane/C30 moretane	191	4.86
3.	C31 22S hopane/C31 22R hopane	191	1.39
4.	C32 22S hopane/C32 22R hopane	191	1.52
5.	C29 20S ααα sterane/C29 20R ααα sterane	217	0.84
6.	C29 ααα steranes (20S / 20S+20R)	217	0.46
7.	$\frac{\text{C29 } \alpha\beta\beta \text{ steranes}}{\text{C29 } \alpha\alpha\alpha \text{ steranes + C29 } \alpha\beta\beta \text{ steranes}}$	217	0.47
8.	C27/C29 diasteranes	259	0.21
9.	C27/C29 steranes	217	nd
10.	18α(H)-oleanane/C30 hopane	191	nd
11.	$\frac{\text{C29 diasteranes}}{\text{C29 } \alpha\alpha\alpha \text{ steranes + C29 } \alpha\beta\beta \text{ steranes}}$	217	1.35
12.	$\frac{\text{C30 (hopane + moretane)}}{\text{C29 (steranes + diasteranes)}}$	191/217	1.67
13.	C15 drimane/C16 homodrimane	123	1.07*
14.	Rearranged drimanes/normal drimanes	123	1.07*

* Parameters generated from Untopped Sample

nd = no data

FIGURE 6A-2

Sample : **TREFOIL-1, 3040.5-3046.5m, DST-2, Sample 2.10, Condensate**

File ID : 346511K (Topped)

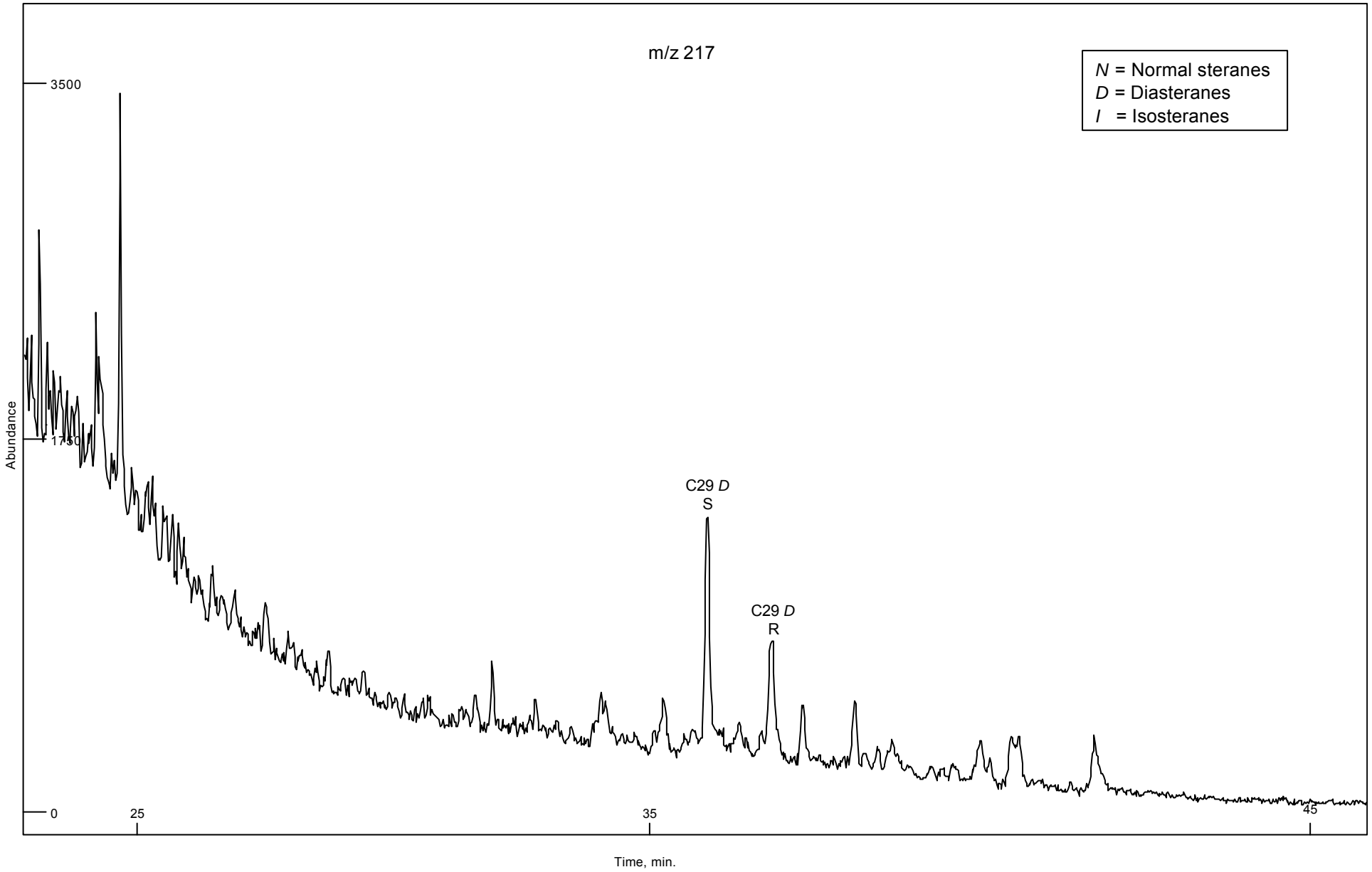


FIGURE 6B-2

Sample : **TREFOIL-1, 3040.5-3046.5m, DST-2, Sample 2.10, Condensate**

File ID : 346511K (Topped)

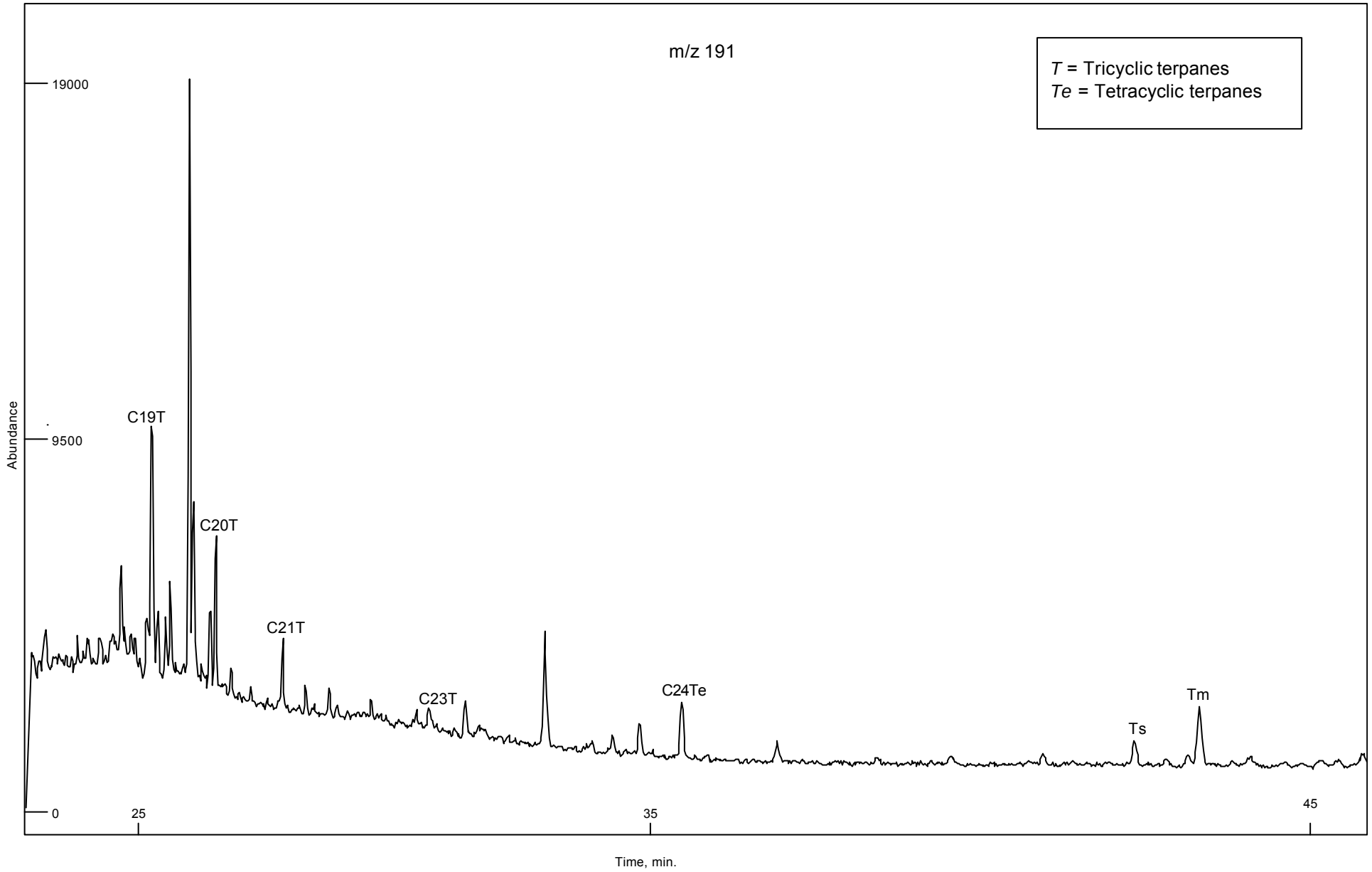
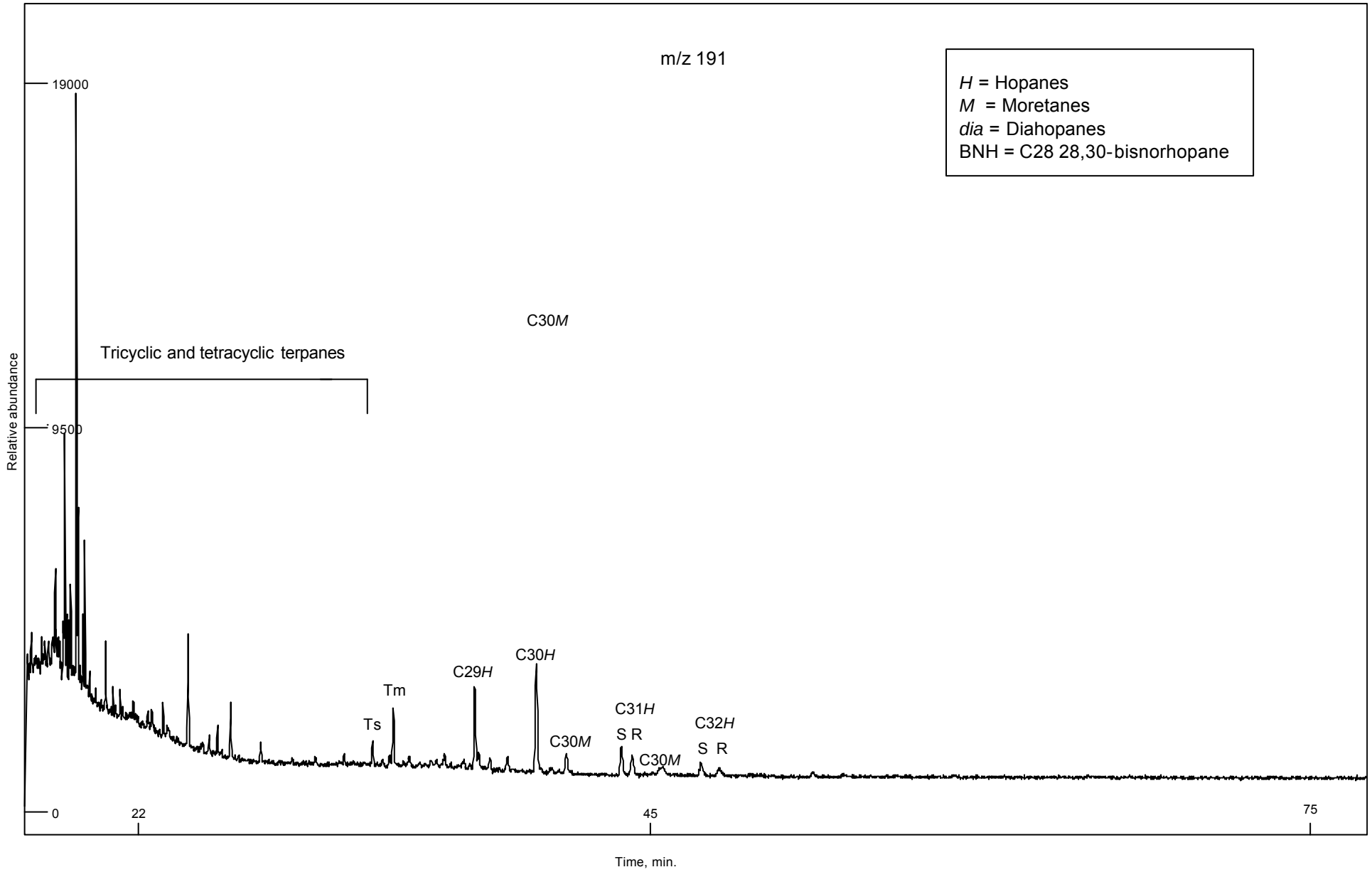


FIGURE 6C-2

Sample : **TREFOIL-1, 3040.5-3046.5m, DST-2, Sample 2.10, Condensate**

File ID : 346511K (Topped)



GEOTECHNICAL SERVICES PTY LTD

FIGURE 6D-2

Sample : **TREFOIL-1, 3040.5-3046.5m, DST-2, Sample 2.10, Condensate**

File ID : 346511K (Topped)

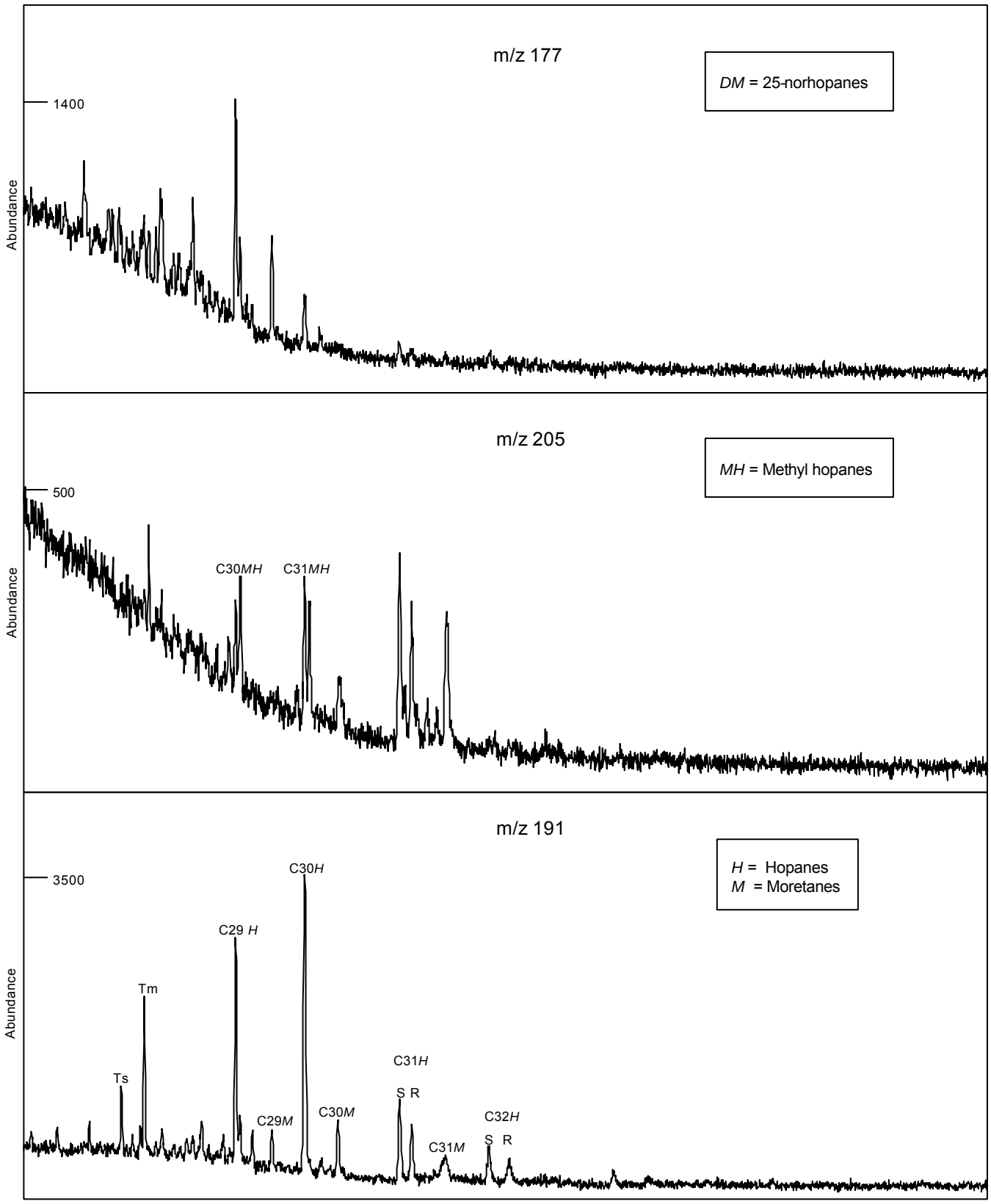


FIGURE 6E-2

Sample : **TREFOIL-1, 3040.5-3046.5m, DST-2, Sample 2.10, Condensate**

File ID : 346511B (Untopped)

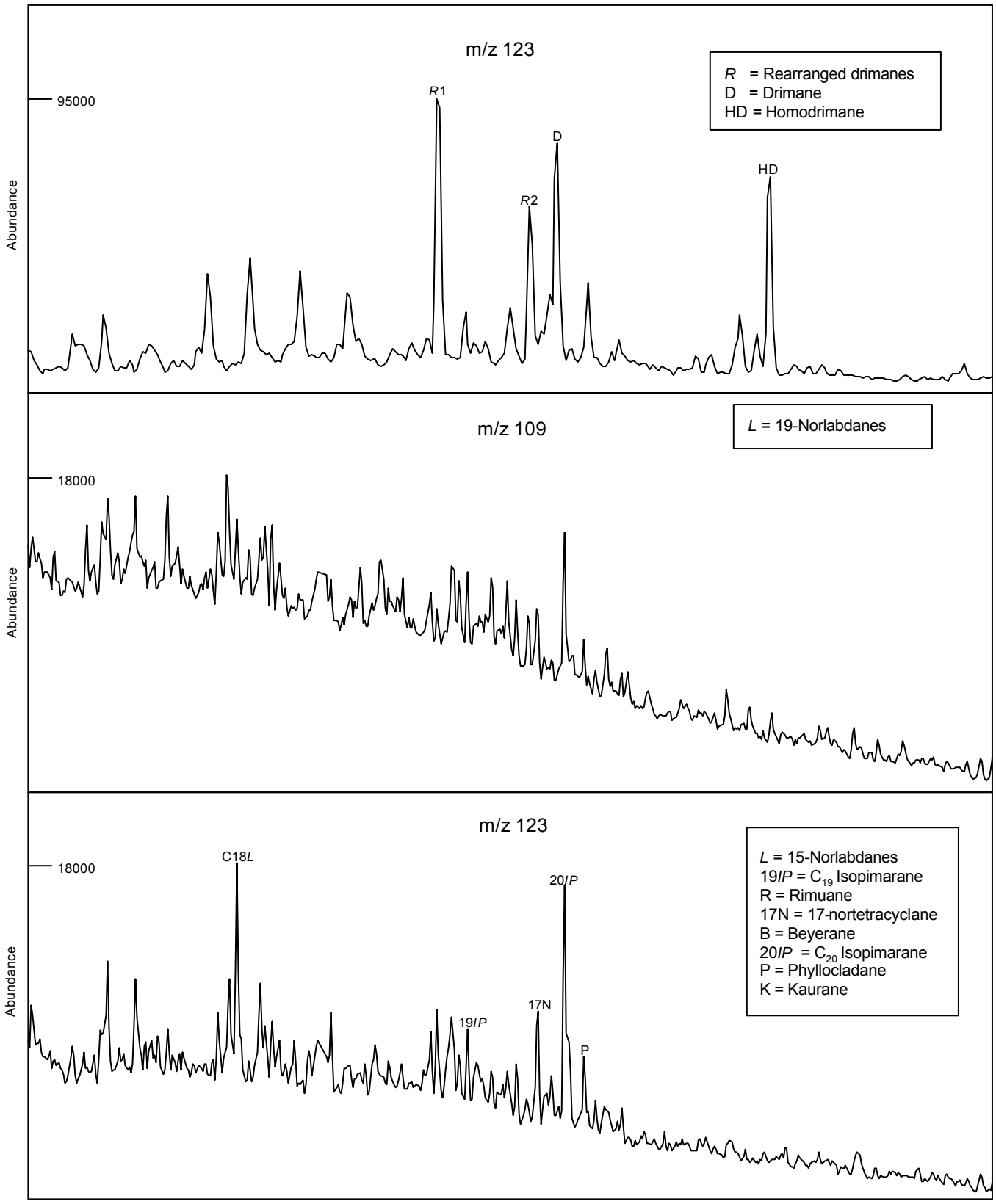


FIGURE 6F-2

Sample : **TREFOIL-1, 3040.5-3046.5m, DST-2, Sample 2.10, Condensate**

File ID : 346511K (Topped)

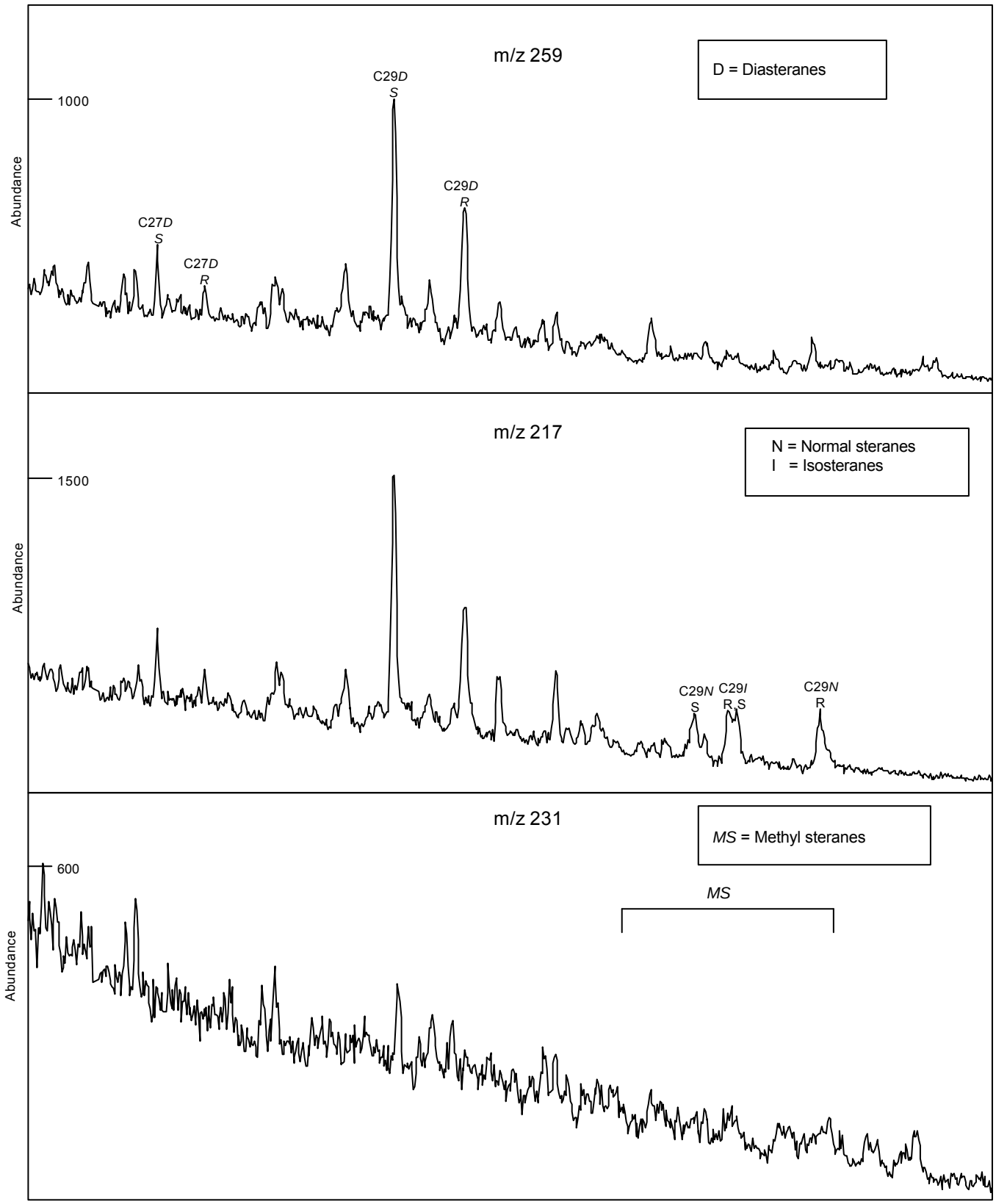


TABLE 9-3

ANALYSIS OF BRANCHED AND CYCLIC SATURATED HYDROCARBONS BY GC-MS

TREFOIL-1, 3141-3150m, DST-1, Sample 1.16, Condensate, Topped

	Selected Parameters	*Ion(s)*	*Value*
1.	18α(H)-hopane/17α(H)-hopane (Ts/Tm)	191	0.38
2.	C30 hopane/C30 moretane	191	4.24
3.	C31 22S hopane/C31 22R hopane	191	1.18
4.	C32 22S hopane/C32 22R hopane	191	nd
5.	C29 20S ααα sterane/C29 20R ααα sterane	217	nd
6.	C29 ααα steranes (20S / 20S+20R)	217	nd
7.	$\frac{\text{C29 }\alpha\beta\beta\text{ steranes}}{\text{C29 }\alpha\alpha\alpha\text{ steranes + C29 }\alpha\beta\beta\text{ steranes}}$	217	nd
8.	C27/C29 diasteranes	259	nd
9.	C27/C29 steranes	217	nd
10.	18α(H)-oleanane/C30 hopane	191	nd
11.	$\frac{\text{C29 diasteranes}}{\text{C29 }\alpha\alpha\alpha\text{ steranes + C29 }\alpha\beta\beta\text{ steranes}}$	217	nd
12.	$\frac{\text{C30 (hopane + moretane)}}{\text{C29 (steranes + diasteranes)}}$	191/217	1.89
13.	C15 drimane/C16 homodrimane	123	0.78*
14.	Rearranged drimanes/normal drimanes	123	2.52*

* Parameters generated from Untopped Sample

nd = no data

FIGURE 6A-3

Sample : **TREFOIL-1, 3041-3150m, DST-1, Sample 1.16, Condensate**
File ID : 346512K (Topped)

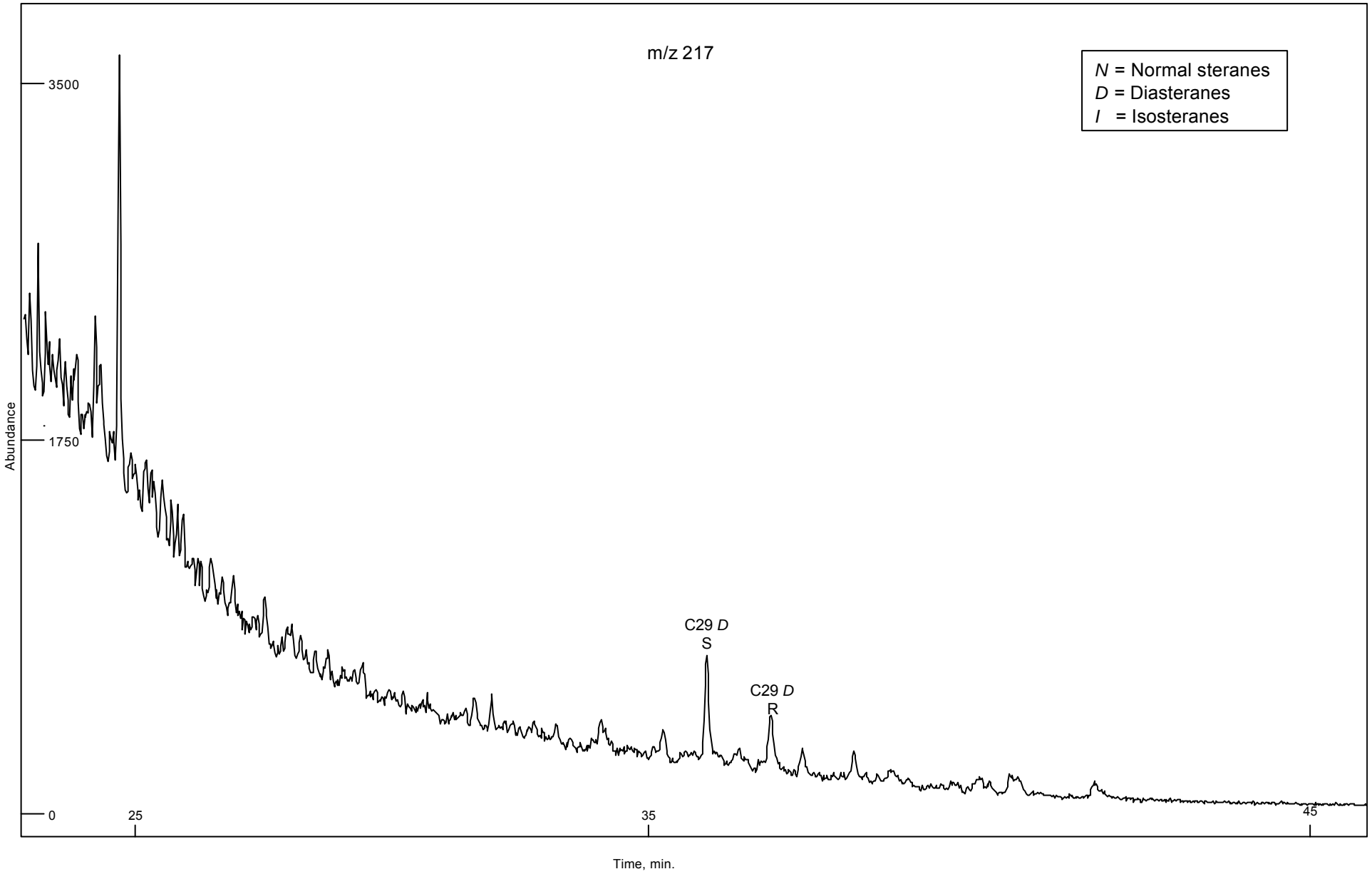


FIGURE 6B-3

Sample : **TREFOIL-1, 3041-3150m, DST-1, Sample 1.16, Condensate**
File ID : 346512K (Topped)

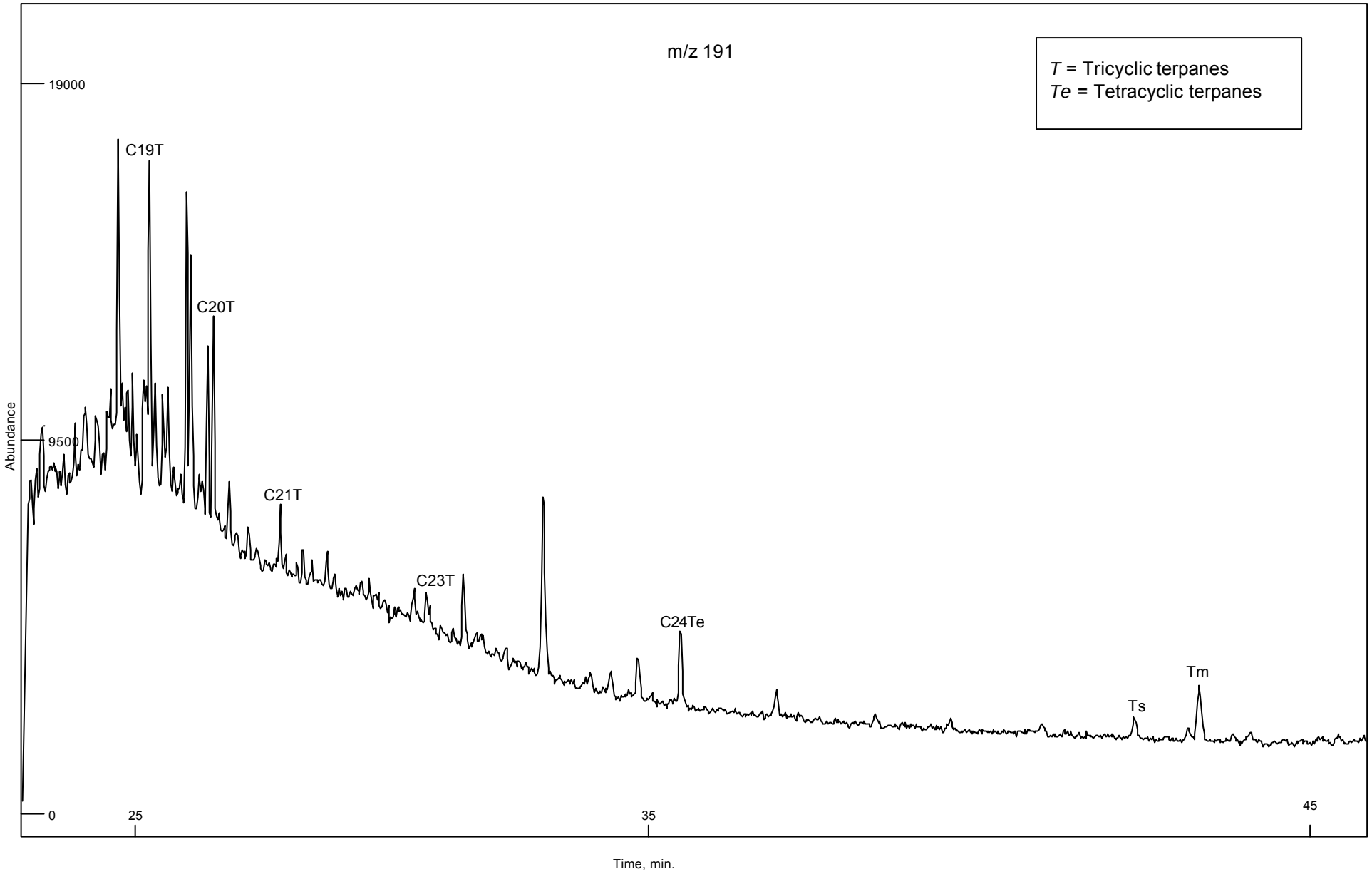


FIGURE 6C-3

Sample : **TREFOIL-1, 3041-3150m, DST-1, Sample 1.16, Condensate**
File ID : 346512K (Topped)

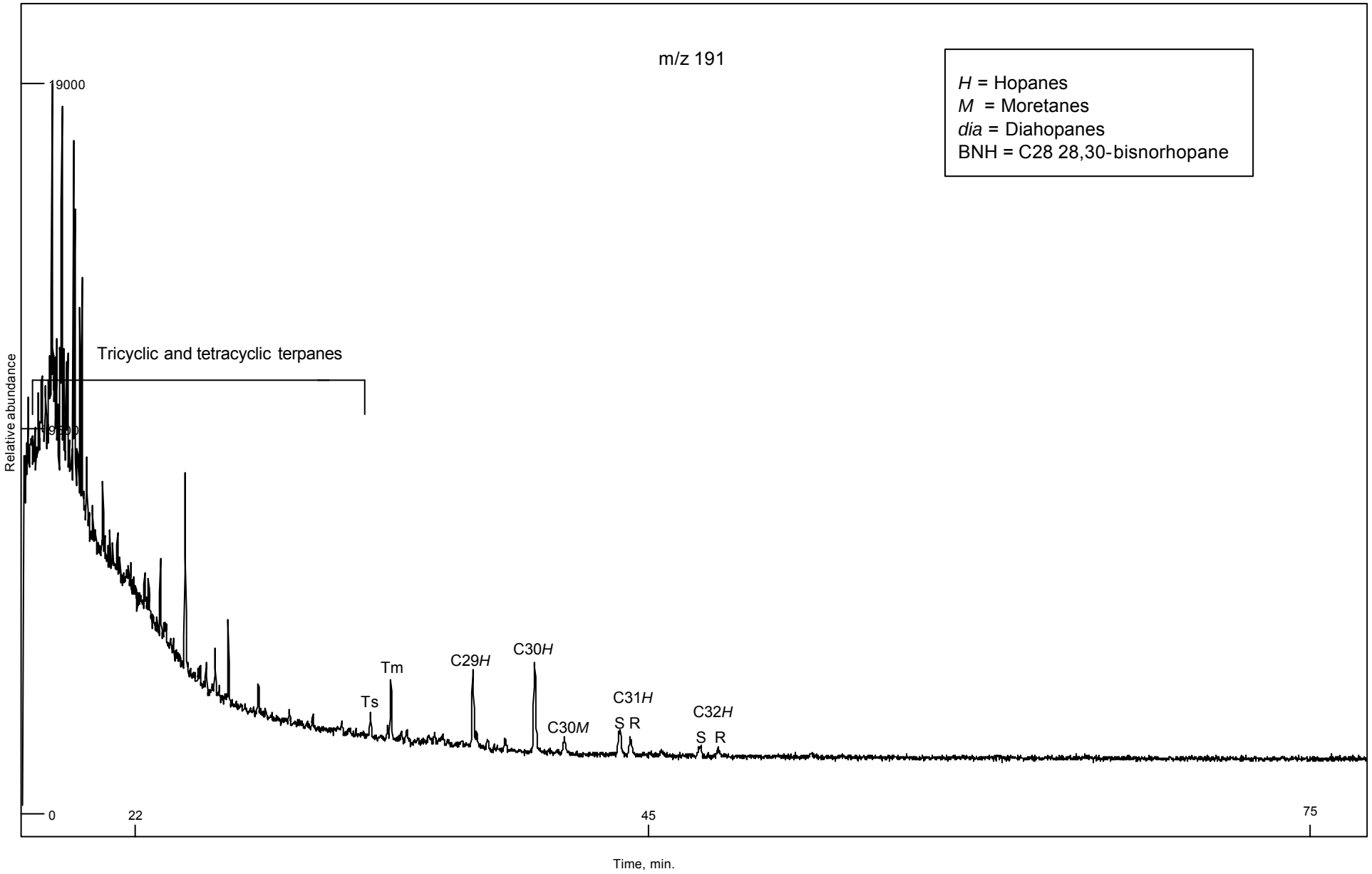


FIGURE 6D-3

Sample : **TREFOIL-1, 3041-3150m, DST-1, Sample 1.16, Condensate**

File ID : 346512K (Topped)

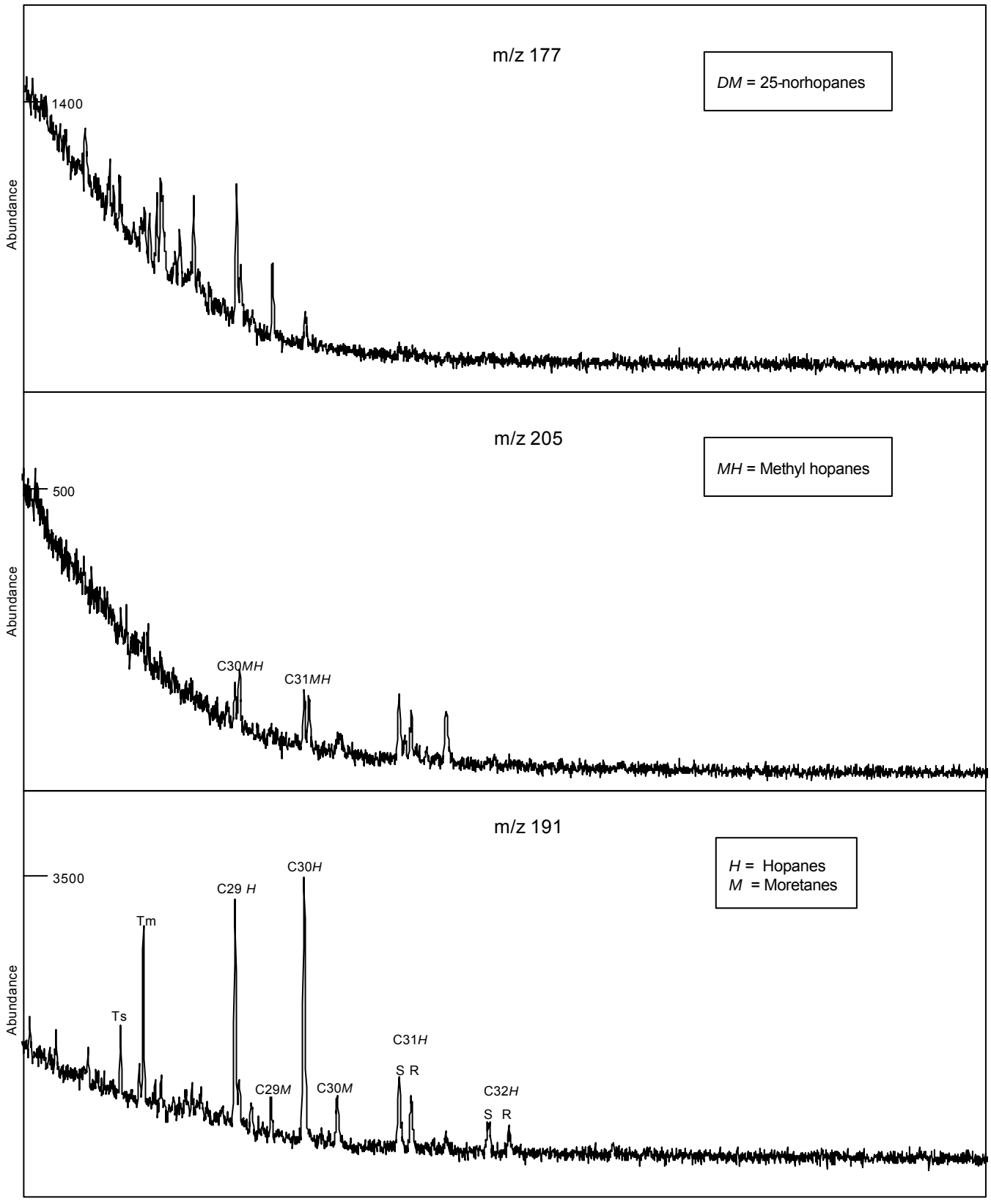
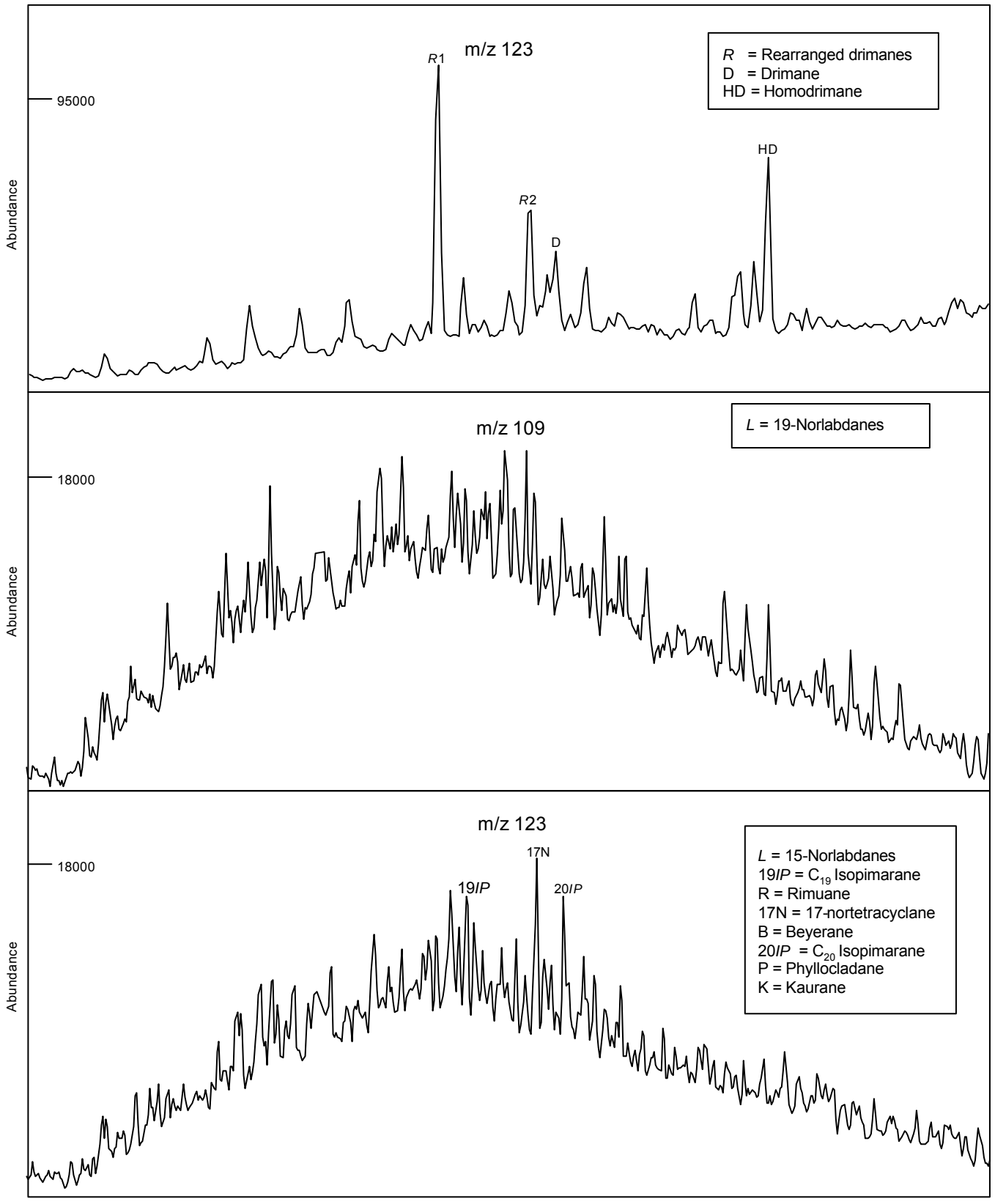


FIGURE 6E-3

Sample : **TREFOIL-1, 3041-3150m, DST-1, Sample 1.16, Condensate**

File ID : 346512K (untopped)

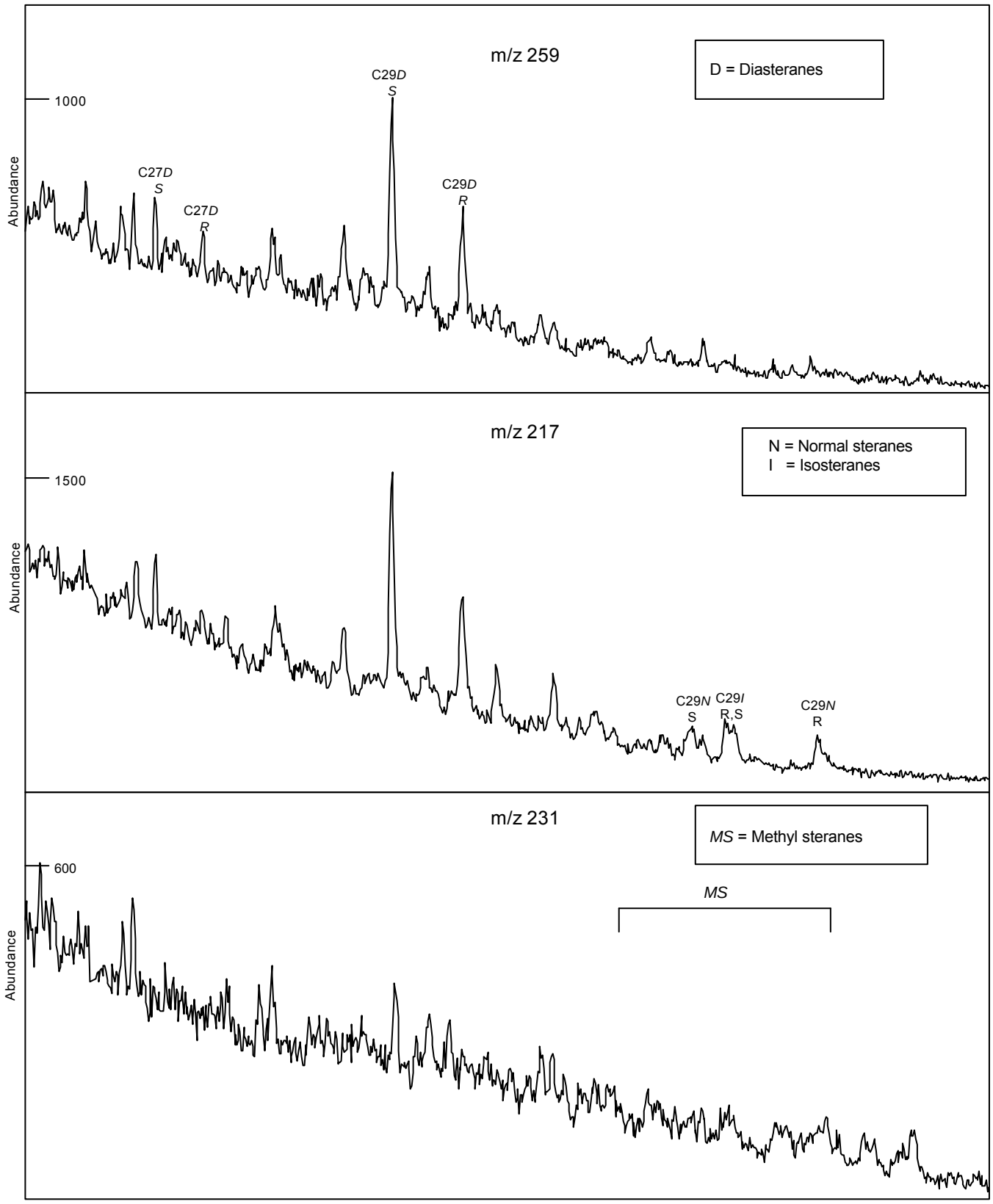


GEOTECHNICAL SERVICES PTY LTD

FIGURE 6F-3

Sample : **TREFOIL-1, 3041-3150m, DST-1, Sample 1.16, Condensate**

File ID : 346512K (Topped)



APPENDIX B

THEORY AND METHODS

PETROLEUM GEOCHEMISTRY

1.0 INTRODUCTION

Petroleum geochemistry is primarily concerned with the application of organic chemistry to samples of geological interest in hydrocarbon exploration.

Analyses can be carried out on cuttings, sidewall cores, conventional cores, relatively unweathered outcrop samples and fluid hydrocarbons (oil, condensate, gas).

Source rock evaluation is best performed on sidewall cores, since cuttings are more susceptible to contamination from both cavings and organic additives in the mud system. In petroleum geochemical studies it is vitally important for the geochemist/geologist to be aware of the type of mud additives used and the stage at which they are used during the drilling program. Any anomalous results must be carefully considered in conjunction with mud system records.

Petroleum geochemistry in exploration is applied for three major purposes:

1. Identification of richness, maturity and type of kerogen in (a large number of) whole rock samples by screening analyses.

2. Semi-detailed characterisation of kerogen in sediments from selected source intervals, to determine maturity, source type and genetic potential.

3. Detailed characterisation of petroleum fluids (extracts, oils and condensates) by assessment of thermal maturity, source type and depositional environment to enable oil-to-oil and oil-to-source rock correlation studies.

2.0 THEORY & METHODS

Samples are analysed according to the scheme illustrated in Figure 1 which shows the order and type of analysis for both screening and detailed tests.

2.1 Screening Analyses of Whole Rock Samples

2.1.1 Headspace/Cuttings Gas Analysis

The headspace sample is usually provided in a sealed tin can which holds both cuttings and water to approximately three quarters capacity. This allows the volatile hydrocarbons to diffuse easily into an appreciable headspace.

The gas is taken into a syringe through a silicone seal on the lid of the container and analysed by packed column gas chromatography using the following conditions:

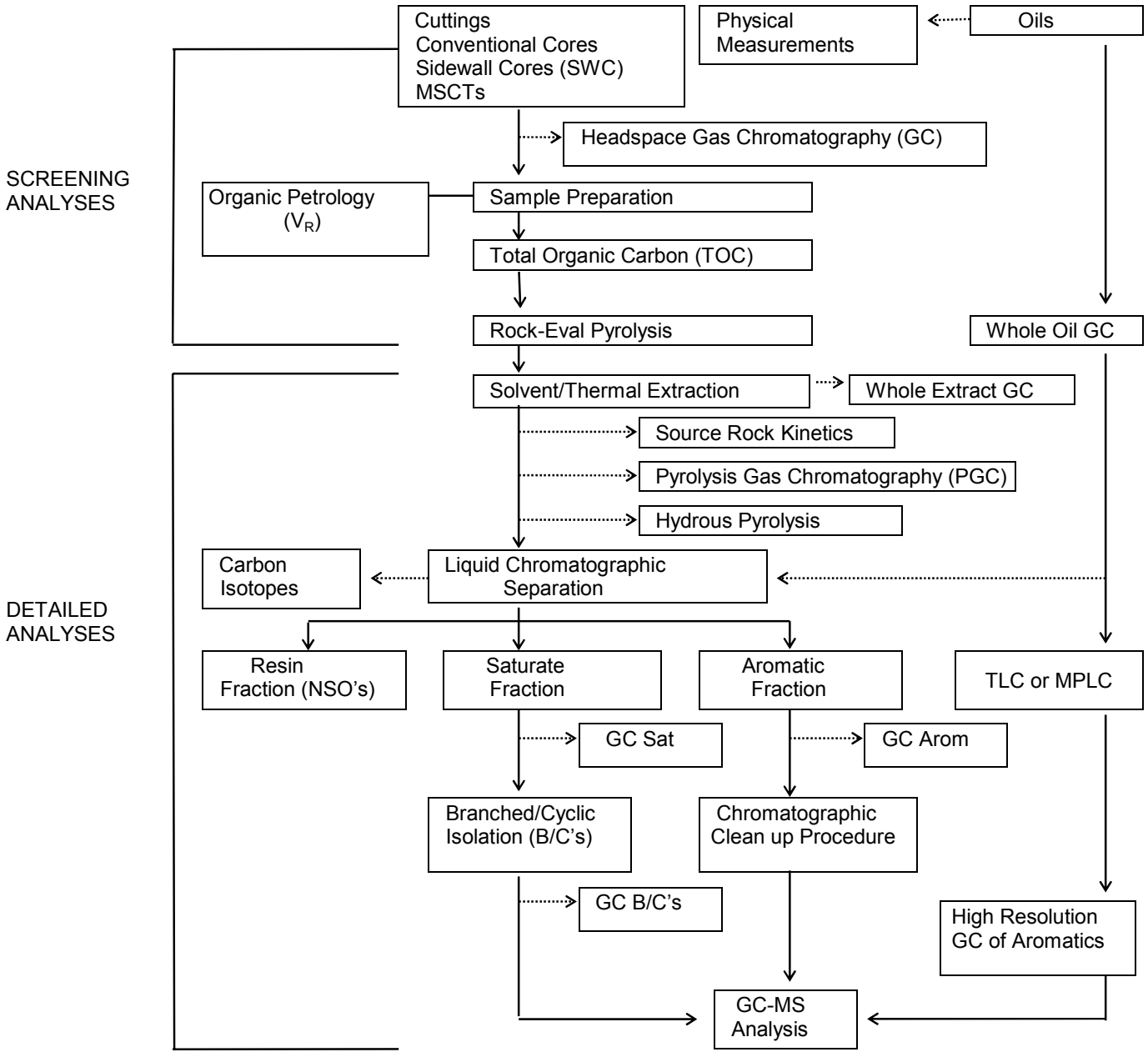
Instrument:	Shimadzu GC-8APF
Column:	6'x 1/8" Chromosorb 102
Injector/Detector Temperature:	120^{o}C
Column Temperature:	110^{o}C
Carrier Gas:	Nitrogen

Cuttings gas analysis is performed in the same manner but on samples which do not liberate volatile gases readily. These sediments are subjected to very vigorous agitation prior to sampling.

Values are given as volume of gas per million volumes of sediment (ppm) for each hydrocarbon (methane, ethane, propane, iso- and n-butane), as composite values including C_5-C_7, and as ratios.

FIGURE 1

FLOW DIAGRAM FOR PETROLEUM GEOCHEMICAL ANALYSES



Headspace/cuttings gas analyses are used as a screening technique to identify zones of significant gas generation and out-of-place gas (Letran et al, 1974). The classification for gas content is listed below:

Total gas content (C_1;C_2-C_4; or C_5-C_7)	Description
10 -100ppm	very lean - lean
100-1,000	lean - moderate
1,000-10,000	moderate - rich
10,000-100,000	rich - very rich

The abundance of C_2-C_4 components (wet gas) is used to locate the zone of oil generation, since wet gas is commonly associated with petroleum (Fuex, 1977).

It is important to ensure that the gases analysed are not of a biogenic origin, so an anti-bacterial agent must be added to the cuttings when they are stored in water.

2.1.2 Sample Preparation

Depending on drilling mud content, cuttings samples may be water washed before they are air dried, picked free of contaminants and cavings, and then crushed to 0.1mm using a ring pulveriser.

Sidewall cores are freed of mud cake and other visible contaminants, sampled according to homogeneity, air dried and hand crushed to 0.1mm grain size.

Conventional core and outcrop samples are inspected for visible contaminants and crushed to 1/8" chips using a jaw crusher. After air drying, the chips are crushed with a ring pulveriser to small particle size (0.1mm).

Petroleum aqueous mixtures are separated into oil and water/mud fractions by decanting off the oil layer and producing a clean separation by gently centrifuging the oil. If separation by this method is not effective, the petroleum is solvent extracted.

2.1.3 Total Organic Carbon(TOC)

The TOC value is determined on crushed sediment. The minimum sample requirement is one gram, however, results may be obtained from as little as 0.2mg in very rich samples. Carbonate minerals are first removed by acid digest (HCl) and the remaining sample heated to 1700^{o}C (Leco Induction Furnace) in an atmosphere of pure oxygen. The CO_2 produced is measured with an infra-red detector, and values calculated according to standard calibration.

TOC is expressed as % of rock and is used as a screening procedure to classify source rock richness:

Classification	Clastics	Carbonates
Poor	0.00 - 0.50	0.00 - 0.25
Fair	0.50 - 1.00	0.25 - 0.50
Good	1.00 - 2.00	0.50 - 1.00
Very Good	2.00 - 4.00	1.00 - 2.00
Excellent	> 4.00	> 2.00

2.1.4 Rock-Eval Pyrolysis

Although a preliminary source rock classification is made using TOC data, a more accurate assessment of organic source type and maturity is possible by Rock-Eval pyrolysis. Two types of Rock-Eval analyses are offered: "one run" which involves pyrolysis of the crushed but otherwise untreated sediment and "two run" which involves pyrolysis of both the crushed, untreated sediment and the decarbonated sediment. The "two run" method provides more accurate S_3 values that the "one run" method. S_1 and S_2 values are of the same accuracy in both methods.

The method requires 0.4g of sample material, although reliable results can often be obtained from smaller amounts.

The crushed sediment is heated in an inert atmosphere of helium over a programmed temperature range.

Hydrocarbons present in the free or adsorbed state (S_1) are thermally distilled at 300^{o}C and measured by a flame ionisation detector (FID). Hydrocarbons are then cracked from the kerogen (S_2) during a temperature ramp from 300^{o} to 550^{o}C and also measured by FID. CO_2 released during the kerogen cracking process (S_3) is trapped and subsequently measured by a thermal conductivity detector.

The amount of free hydrocarbons in the sediment (S_1) represents milligrams of hydrocarbons distilled from one gram of rock and is a measure of both in situ and out-of-place petroleum.

Free hydrocarbon richness is described by the following:

S_1 (mg/g)	**Characterisation**
0.20 - 0.40	fair
0.40 - 0.80	good
0.80 - 1.60	very good
> 1.60	excellent

The total amount of hydrocarbons present in the free state and as kerogen is a measure of the potential yield (genetic potential) of the sample ($S_1 + S_2$) and is expressed as mg/g of rock.

Source rocks are classified accordingly:

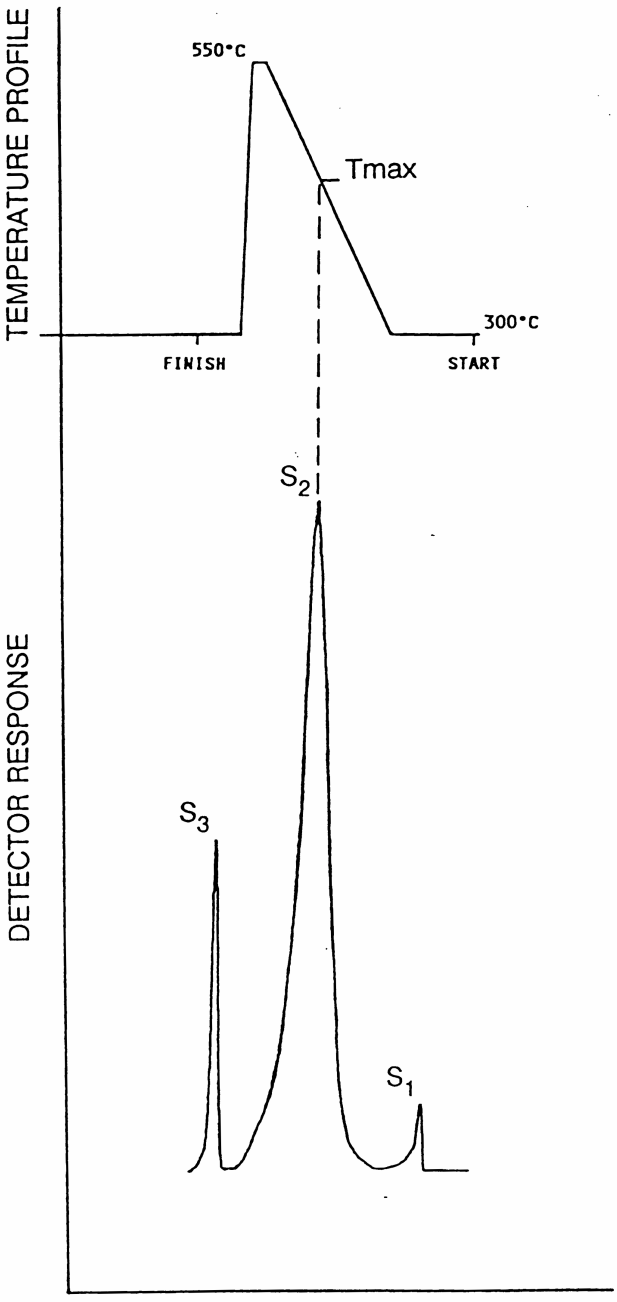
$S_1 + S_2$ (mg/g)	**Source Rock Quality**
0.00 - 1.00	poor
1.00 - 2.00	marginal
2.00 - 6.00	moderate
6.00 - 10.00	good
10.00 - 20.00	very good
> 20.00	excellent

The Production Index (PI) represents the amount of petroleum generated relative to the total amount of hydrocarbons present ($S_1/S_1 + S_2$). It is a measure of the level of maturity of the sample. For oil prone sediments PI ranges from 0.1 at the onset of oil generation to 0.4 at peak oil generation. For gas prone sediments, PI shows only a small change with increasing maturity.

The temperature at which the maximum amount of S_2 hydrocarbons is generated is called T_{MAX}. This temperature increases with the increasing maturity of sediments.

FIGURE 2

SCHEMATIC PYROGRAM OF ROCK-EVAL PYROLYSIS



The variation of T_{MAX} is summarised as

< 430°C	immature
430/435° – 460°C	mature (oil window)
> 460°C	overmature

Hydrogen Index (HI = S_2 x 100/TOC) and Oxygen Index (OI = S_3 x 100/TOC), when plotted against one another, provide information about the type of kerogen and the maturity of the sample. Both parameters decrease in value with increasing maturity. Samples with high HI and low OI are dominantly oil prone and samples with low HI and high OI are gas prone.

2.2 Analysis of Kerogen

2.2.1 Organic Petrology - Vitrinite Reflectance

Vitrinite is a coal maceral which responds to increasing levels of thermal maturity. This response is measured microscopically by the percent of light reflected off the polished surface of a vitrinite particle immersed in oil.

Measurement of vitrinite reflectance can be carried out on uncrushed, washed and dried cuttings (10-50gms of sample material required), sidewall cores (2-10gms), conventional cores (2-10 gms) or outcrop samples (2-10gms).

The values given are for standard lower size limits. In special cases, however, useful data may be obtained from as little as 0.1gm.

For each sample a minimum of 25 fields is measured in order to establish a range and mean for reflectance values.

Maturity classifications according to vitrinite reflectance values are:

% V_R (approx)	**Maturity**
0.2 - 0.55	immature
0.55 - 1.2	mature
1.2 - 1.8	overmature
> 1.8	severely altered

Following vitrinite reflectance measurements, microscopic examination in fluorescence mode allows the description of liptinite macerals and an estimate of their abundances. The amount of dispersed organic matter is reported and its composition described.

Vitrinite reflectance results and maceral descriptions are best obtained from coals or rocks deposited in environments which received large influxes of terrestrially derived organic matter. Vitrinite reflectance cannot be measured in rocks older than Devonian age, since land plants had not evolved prior to this time.

2.2.2 Pyrolysis Gas Chromatography

Pyrolysis gas chromatography (PGC) is performed on solvent extracted source rocks or isolated kerogens. The sample is pyrolysed by an SGE pyrojector which is coupled directly to a Hewlett Packard 5890 gas chromatograph. The operating conditions are:

Pyrolysis temperature:	600^{o}C
Column:	25m x 0.22mm ID BP-1 (SGE)
Carrier gas:	helium
Oven conditions:	-20^{o} to 280^{o}C @ 4^{o}/min

Data are collected and recovered using DAPA scientific software.

Pyrolysis GC allows the examination of kerogen on the molecular level and thereby a better classification of source rocks with regard to source type and generative capacity than conventional bulk pyrolysis (ie. Rock-Eval). The analytical procedure is semi quantitative (with yield related to S_2 of Rock-Eval).

Samples are characterised according to the amounts of aliphatic, aromatic and phenolic components in the kerogen. The aliphatic carbon content of a kerogen is the critical factor in determining catagenic hydrocarbon yields in the earth's crust, while the gas/oil ratio is dictated by the distribution of the various structural elements in the kerogen (Larter, 1985). Using pyrogram fingerprint data, it is possible to distinguish substantial variations between kerogens, even those of the same bulk chemical type.

A major strength of pyrolysis methods is that, while quantitative yields of kerogens are maturity related, the qualitative pyrogram fingerprints obtained are relatively rank independent over much of the oil window (Espitatlie et al, 1977; Van Graas et al, 1980; Larter, 1985). At high maturities (>1.2% V_R) characteristics for all kerogen types tend to converge (Horstfield, 1984).

Data are presented by percentage and mg/g of individual substances as well as groups of compounds.

Significant parameters are:

$(C_1 – C_5)/C_6$ + abundance	gas/oil ratio
$C_9 – C_{31}$ (alkenes + alkanes)	oil yield
Type Index R:	aromaticity

(Larter & Douglas 1979, Larter and Senftle, 1985).

2.3 Detailed Analyses of Petroleum Fluids

2.3.1 Solvent Extraction of Sediment

The finely crushed sample (up to 100g) is extracted with dichloromethane (300mL) using sonic vibration. After Buchner flask filtration, the filtrate is re-vibrated with activated copper powder (1g) to remove elemental sulphur. The extractable organic matter (EOM) is afforded by further filtration and fractional distillation of the solvent.

Source rock richness based upon EOM is classified accordingly:

Yield	**ppm**
Poor	< 500
Fair/Good	500 - 2000
Very Good	2000 - 4000
Excellent	>4000

2.3.2 Liquid Chromatographic Separation

Sediment extracts, crude oil and condensate samples are separated into fractions corresponding to three structural types:

saturated hydrocarbons	(SAT)
aromatic hydrocarbons	(AROM)
resins plus ashphaltenes	(NSO)

This separation is achieved by liquid column chromatography using activated silicic acid adsorbent and eluting solvents of varying polarity. Saturated, aromatic and NSO concentrates are recovered by fractional distillation/evaporation of the solvent and quantitative transfer to a small vial.

The amount of hydrocarbons (SAT plus AROM) can be used to classify source rock richness and the amount of saturates to classify oil source potential, according to the following criteria:

Classification	**ppm HC**	**ppm SAT**
Poor	0 - 300	0 - 200
Fair	300 - 600	200 - 400
Good	600 - 1200	400 - 800
Very Good	1200 - 2400	800 - 1600
Excellent	>2400	>1600

The composition of the extracts can also provide information about their levels of maturity and/or source type (LeTran et. al., 1974; Philippi, 1974). Generally, marine extracts have relatively low concentrations of saturated and NSO compounds at low levels of maturity, but these concentrations increase with increasing maturation. Terrestrially derived organic matter often has a low level of saturates and large amount of aromatic and NSO compounds, irrespective of the level of maturity.

Specific ratios are measured from solvent extraction and liquid chromatography data which give an indication of source type and maturity. EOM (mg)/TOC(g) can be used as a maturation indicator when plotted against depth for a given sedimentary sequence. Generally an EOM/TOC value of >100 indicates high maturity. If such a sample has a SAT (mg)/TOC(g) ratio <20, it is likely that the organic matter is gas prone. A value for SAT (mg)/TOC (g) >40 suggests an oil prone source type.

2.3.3 Capillary Gas Chromatography (GC)

C_{12+} gas chromatography is most commonly carried out on saturate fractions, but in certain instances it is used to examine whole extracts/oils, aromatic or branched/cyclic fractions. It is also used as a tool to identify contamination. The analyses are performed under the following conditions:

Instruments:	Hewlett Packard 5890 Gas Chromatography
Injector:	SGE 0CI-3 on column
Column:	25m x 0.2mm ID BP-1
Injector Temp:	280°C
Detector Temp:	320°C
Column Temp:	45°C to 280°C at 4°/min
Carrier Gas:	Hydrogen

Data are collected using an IBM compatible PC and DAPA scientific software.

2.3.3.1 C_{12+} Saturate Gas Chromatography

Saturate GC results provide information pertaining to source type, maturity and depositional environment.

The n-alkane distribution from n-C_{12} to n-C_{31} is determined from the area under the peaks representing each of these n-alkanes. The profile can yield information about maturity and source type and is quantified in the C_{21} + C_{22}/C_{28} + C_{29} ratio and Carbon Preference Indices (CPI 1 and 2).

$$CPI\,(1) = \frac{(C_{23} + C_{25} + C_{27} + C_{29})\ wt\% + (C_{25} + C_{27} + C_{29} + C_{31})\ wt\%}{2\ x\ (C_{24} + C_{26} + C_{28} + C_{30})\ wt\%}$$

$$CPI\,(2) = \frac{(C_{23} + C_{25} + C_{27})\ wt\% + (C_{25} + C_{27} + C_{29})\ wt\%}{2\ x\ (C_{24} + C_{26} + C_{28})\ wt\%}$$

Carbon preference indices:

- are approximately 1 for marine samples, regardless of maturity
- decrease from 20--> 1 for terrestrial samples as maturity increases

The C_{21} + C_{22}/C_{28} + C_{29} ratio is generally >1.5 for aquatic source material and <1.2 for terrestrial organic matter, however, the values increase with maturity.

Pristane/phytane (Pr/Ph) ratios can indicate depositional environments:

.	<3.0	- relatively reducing depositional environments;
.	3.0-4.5	- mixed (reducing/oxidising) environments;
.	>4.5	- relatively oxidising depositional environments.

2.3.3.2 $C_1 – C_{31}$ Whole Oil Gas Chromatography

This analytical method is applied to oil and condensate samples. It provides a picture of the whole oil up to n-C_{31} and allows quantitation of components with more than 4 carbon atoms. Several parameters are measured which illustrate changes in the degree of biodegradation and water washing in the reservoir. Because these measurements are performed on very volatile components in the oil, care should be taken during sampling, transportation and storage of the fluid to minimise evaporation.

Whole oil analytical conditions are listed below:

Instrument:	Shimadzu GC-9A
Column:	25m x 0.2mm ID BP-1
Injector/Detector Temperature:	290^{o}C
Column Temperature:	-20^{o}C to 280^{o}C at 4^{o}/min
Carrier Gas:	hydrogen

2.3.4 Carbon Isotope Analysis

This measurement is normally carried out on one or more of the following mixtures: topped oil, saturate fraction, aromatic fraction, NSO fraction. The organic matter is combusted in oxygen to produce carbon dioxide which is purified and transferred to an isotope mass spectrometer. The carbon isotope ratio ($\delta C_{13}/\delta C_{12}$) is measured and compared to an international standard (the Peedee Belemnite Limestone - PDB).

Carbon isotope analysis is most commonly used to identify the source of methane according to the following criteria (Fuex 1977):

$\delta^{13}C$ $^{o}/_{oo}$ PDB	Source
-75 to -55	Biogenic methane
-58 to -40	Methane associated with oil
-40 to -25	Thermal methane

Source rock-crude oil correlations have been attempted by observing the change in $\delta^{13}C$ values of components of oils and rocks (Stahl 1977). Source rock extracts are usually isotopically heavier than the corresponding crude oil but are lighter than the asphaltenes of the oil and the kerogen of the rock (Hunt 1979). It has also been observed that marine organic carbon is generally isotopically heavier than contemporaneous terrestrial organic carbon (Tissot & Welte 1978). However, it should be noted that increasing maturity and biodegradation produce a shift toward heavier isotope values.

2.3.5 Gas Chromatography - Mass Spectrometry (GC/MS)

GC/MS analysis is normally performed on the branched and cyclic alkane fraction and/or the aromatic fraction of oils, condensates and sediment extracts. The specific fraction is first isolated and then injected into a gas chromatograph which is linked in series with a mass spectrometer. As compounds are eluted from the chromatography column they are bombarded with high energy electrons. This causes them to fragment into a number of ions each with a molecular weight less than that of the parent molecule. Individual compounds give a characteristic fragmentation pattern (mass spectrum), the major ions of which are presented in a series of mass fragmentograms [ie. plots of ion concentration against GC retention time].

GC/MS analysis can be carried out using one of the following modes of operation:

(i) Acquire mode - in which all ions (within a broad range) in each mass spectrum are memorised by the data system.

(ii) Selective Ion Monitoring (SIM) mode - in which only selected ions of interest are memorised by the data system.

2.3.5.1 GC/MS Analysis of Branched/Cyclic Alkanes

The group of compounds to be analysed is first isolated from the saturate fraction by refluxing the sample with activated 5Ä molecular sieves in cyclohexane for 24 hours. Branched/ cyclic alkanes, including alkylcyclohexanes, are recovered from the solvent by fractional distillation.

For condensates, and samples where information about alkylcyclochexanes is not required, the saturate fraction is passed through a small column packed with silicalite adsorbent. The branched/cyclic alkanes are recovered from the eluting solvent by fractional distillation.

Analysis is carried out in the SIM mode with a total of 33 ions being recorded over different time spans.

Operating conditions are:

Instrument:	5987HP GC mass spec data system
Column:	60m x 0.25mm ID cross linked methyl-silicone DB-1 (J&W) column of 0.25 micron film thickness connected directly to the ion source
Injector:	OCI-3(SGE)
Carrier gas:	hydrogen
Oven Conditions:	50^{o} to 274^{o}C at 8^{o} /min
	274^{o} to 280^{o}C at 1^{o} /min
EM Voltage:	2,000 - 2,300V
Electron Energy:	70eV
Source temperature:	250^{o}C

GC/MS mass fragmentograms are examined for particular 'biomarker' compounds which can be related to biological precursors. These allow the characterisation of petroleum with regard to thermal maturity, source, depositional environment and biodegradation.

The significance of selected parameters from branched/cyclic GC/MS analysis is outlined over the page.

1. 18α (H)-hopane/17α (H)-hopane (Ts/Tm)

Maturity indicator. The ratio of 18α (H) trisnorhopane to 17α (H) trisnorhopane increases exponentially with increasing maturity from approximately 0.2 at the onset to approximately 1.0 at the peak of oil generation, ie. Tm decreases with maturity. This parameter is not reliable in very immature samples.

2. C_{30} hopane/C_{30} moretane

Maturity indicator. The conversion of C_{30} 17β, 21β hopane to 17β, 21α moretane is maturity dependent. Values increase from approximately 2.5 at the onset of oil generation to approximately 10. Once the hopane/moretane ratio has reached 10, no further changes occur. A value of 10 is believed to represent a maturity stage just after the onset of oil generation and hopane/moretane ratios are therefore useful mainly as indicators of immaturity in a qualitative sense.

3&4. C_{31} and C_{32} 22S/22R hopanes

Maturity indicator. An equilibrium between the biological R- and the geological S-configuration occurs on mild thermal maturation. A ratio of S:R = 60:40, ie, a value of 1.5, characterises this equilibrium which occurs before the onset of oil generation. The C_{32} hopane pair is often more reliable for this purpose since co-elution sometimes affects the C_{31} ratio.

5. C_{29}20S ααα/C_{29}20Rααα steranes

Maturity indicator. Upon maturation, the biologically produced 20R sterioisomer is diminished relative to the 20S form and a stabilisation is reached at approximately 55% 20R and 45% 20S compounds. V_R equivalents are approximately 0.45% for a 20S/20R value of 0.2 and 0.8% for a 20S/20R value of 0.75. This parameter is most useful between maturity ranges equivalent to 0.4% to 1.0 V_R.

6. C_{29}20S αααα /C_{29}20R ααα+ C_{29}20S ααα steranes

Maturity indicator. This ratio is a different way of expressing the relative abundance of the biological 20R to the geological 20S normal sterane (see parameter 5). Expressed as a percentage, a value of about 25% indicates the onset of oil generation, and of about 50% the peak of oil generation.

7. C_{29} αββ /C_{29} ααα + C_{29} αββ steranes

Maturity indicator. The αα form is produced biologically. Its abundance diminishes upon maturation until a mixture of 65% ββ(iso) steranes and 35% αα (normal) steranes is reached, which is equivalent to approximately 0.9% V_R.

8&9. C_{27}/C_{29} diasteranes and steranes

Source indicator. It has been suggested that marine phytoplankton is characterised by a dominance of C_{27} steranes and diasteranes whereas a preponderance of C_{29} compounds indicates strong terrestrial contributions. Values smaller than 0.85 for C_{27}/C_{29} diasterane and sterane ratios are believed to be indicative for terrestrial organic matter, values between 0.85 and 1.43 for mixed organic material, and values greater than 1.43 for an input of predominantly marine organic matter.

It has been suggested, however, that marine sediments can also contain a predominance of C_{29} steranes, so the above rules have to be applied with caution. Any simplistic interpretation of C_{27}/C_{29} steranes and diasteranes can be dangerous and the interpretation of these data should be consistent with other geological evidence.

10. 18α (H) - oleanane/C_{30} hopane

Source indicator. Oleanane is a triterpenoid compound which has often been reported from deltaic sediments of Late Cretaceous to Tertiary age. It is thought to be derived from certain angiosperms which developed in the late Cretaceous. If the 18α (H) - oleanane/C_{30} hopane ratio is below 10, no significant proportions of oleanane are present. At higher values, it can be used as indicator for a reducing environment during deposition of land plant-derived organic matter.

11. C_{29} diasteranes/C_{29} ααα steranes + C_{29} αβ steranes

Source indicator. This parameter is used to characterise the oxidity of depositional environments. High values (up to 10) indicate oxic conditions, low values (down to 0.1) indicate reducing environments.

12. C_{30} (hopanes + moretanes)/C_{29} (steranes + diasteranes)

Source indicator. Triterpanes are believed to be of prokariotic (bacterial) origin, whereas steranes are derived from eukariotic organisms. This ratio reflects the preservation of primary organic matter derived from eukariots, relative to growth and preservation of bacteria in the sediment after deposition.

13. C_{15} drimane/C_{16} homodrimane

Drimanes and homodrimanes are ubiquitous compounds most likely derived from microbial activity in sediments. The C_{15} drimane/C_{16} homodrimane ratio is a useful parameter for correlation purposes in the low molecular weight region, especially for condensates which lack most conventional biomarkers. Drimanes are also useful to assess the degree of biodegradation as the removal of C_{15} to C_{16} bicyclics characterises an extensive level of biodegradation.

14. Rearranged/normal drimanes

Like parameter 13, this ratio can be used for correlation purposes in samples without conventional biomarkers, and to assess levels of biodegradation.

2.3.5.2 GC/MS Analysis of Aromatics

The aromatic fraction or the oil to be analysed is first subjected to thin layer chromatography (TLC) or medium pressure liquid chromatography (MPLC), depending upon the analytical requirements.

1. Di- and tri- nuclear aromatic compounds are isolated by TLC. To effect this separation, the sample is applied to an alumina coated glass plate (0.6mm thickness). The plate is developed with hexane and the required band located using short wavelength UV light. The fraction is recovered by extraction and fractional distillation.

   This aromatic fraction may be analysed by GC-FID, but GC/MS is recommended because of possible co-elution problems during GC.

   Samples are analysed by GC/MS in the acquire mode scanning from 50 to 450 atomic mass units (amu).

Analytical conditions are:

Instrument:	HP5970 MSD
Column:	60m x 0.25mm ID, 0.25 micron film thickness, 5% phenylmethyl silicone column DB-5 (J&W) connected directly to the ion source
Injector:	automatic on-column
Carrier Gas:	helium
Oven Conditions:	70°C for 1 min
	70°C --> 300°C at 3°/min
Data collection commences at 10 mins	
Mass spectrometry	
Em Voltage	1500 - 1800V
Electron Energy	70eV

Mass fragmentograms are presented for alkylbiphenyls, alkylnaphthalenes, alkylfluorenes and alkylphenanthrenes from a comprehensive data base. Aromatic compounds provide valuable information concerning thermal maturity since they can be applied outside the dynamic range

of saturate biomarker indicators and are particularly useful when conventional biomarkers are present in low amounts (Radke & Welte, 1983; Alexander et al, 1985). Maturity ratios are tabled below over the page.

Aromatic Maturity Indicators

Abbrev.	Definition	oil onset	Range Wet gas
DNR 1	(2,6DMN, + 2,7DMN)/1,5DMN	1.5	10
DNR 2	2,7DMN/1,8DMN	50	2500
DNR 5	1,6DMN/1,8DMN	50	>3000
DNR 6	(2,6DMN + 2,7DMN)/(1,4DMN + 2,3 DMN)	0.8	2
TNR 1	2,3,6TMN/(1,4,6TMN + 1,3,5TMN)	0.5	4
MPR 1	(2MP + 3MP)/1MP	1.5	3
MPI 1	1.5 x (2MP + 3MP)/(PH + 1MP + 9MP)	0.3	1
MPI 2	(3 x 2MP)/(PH + 1MP + 9MP)	0.3	2
Rc(a)	0.6(MPI-1) + 0.4 (for % Rm <1.35)		
Rc(b)	-0.6(MPI-1) + 2.3 (for % Rm ·1.35)		

(from Radke et al, 1982; Radke & Welte, 1983; Alexander et al, 1985)

Some aromatic marker compounds have specific natural product precursors and can be used as signatures for sediments of a particular source, depositional environment or geological age:

TNR 5	1,2,5TMN/1,3,6TMN	
TNR 6	1,2,7TMN/1,3,7TMN	(Strachen et al, 1988)
1,7/X	1,7DMP/(1,3 + 3,9 + 2,10 + 3,10 DMP)	
Retene/9MP		
1MP/9MP		(Alexander et al, 1988)

2. Mono- and triaromatic steranes are analysed by GC/MS under the same analytical conditions as used for di- and tri-nuclear aromatics. However, isolation of this fraction is performed by MPLC. To achieve this, the saturate plus aromatic mixture is injected onto a Merck Si60 column. The separation is monitored with a refractive index detector for saturates and a UV absorbance detector for aromatics.

   As aromatic steranes are generally present in low abundances, especially in oils, samples are analysed in the SIM mode and 16 ions are recorded.

   The conversion of monoaromatic steranes to triaromatic steranes and the dimethylation of triaromatic steranes in sediments are considered to be maturity dependent (Mackenzie et al, 1981; Mackenzie, 1984). The triaromatic sterane maturity indicator should, however, not be applied to crude oils because migration effects appear to selectively deplete the triaromatic steranes.

APPENDIX 5: VITRINITE REFLECTANCE REPORT

TREFOIL-1, p1

KK # / Ref #.	Depth (m)	$R_v$max Mean	$R_v$max Range	$R_v$max SD	$R_v$max N	Sample description including liptinite fluorescence maceral abundances, mineral fluorescence
L0201	1700	0.45	0.42-0.47	0.025	2	Rare lamalginite and liptodetrinite yellow to orange. (Argillaceous siltstone>claystone. Dom rare, L>V>I. All three maceral groups rare. Mineral fluorescence weak orange to none. Iron oxides rare. Pyrite sparse.)
Ctgs	$\overline{R}_I$max	1.76	-	-	1	
L0202	1890	0.51	0.45-0.54	0.042	3	Fluorescing liptinite absent. (Argillaceous siltstone>sandstone. Dom rare, V>I. Vitrinite and inertinite rare, liptinite absent. Rare foraminiferal tests. Mineral fluorescence weak to moderate orange. Iron oxides rare. Pyrite sparse.)
Ctgs	$\overline{R}_I$max	0.98	-	-	1	
L0203	2136	0.50	0.38-0.59	0.063	8	Rare sporinite and liptodetrinite orange. (Argillaceous siltstone> claystone>sandstone. Dom rare, V>L>I. All three maceral groups rare. Rare foraminiferal tests. Mineral fluorescence weak to moderate orange. Iron oxides common. Pyrite sparse.)
Ctgs	$\overline{R}_I$max	-	-	-	-	
L0204	2322	0.54	0.42-0.66	0.049	18	Rare sporinite and liptodetrinite yellow to orange, rare cutinite yellow. (Sandstone>argillaceous siltstone>claystone. Dom sparse, V>L>I. Vitrinite sparse, liptinite rare to sparse, inertinite rare. Mineral fluorescence moderate orange to none. Iron oxides sparse. Pyrite sparse.)
Ctgs	$\overline{R}_I$max	1.33	1.02-1.64	0..310	2	
L0205	2508	0.55	0.44-0.65	0.049	25	Common sporinite and sparse liptodetrinite yellow to orange, sparse cutinite orange. (Argillaceous siltstone>sandstone> claystone>carbonate. Dom abundant, V>L>I. Vitrinite and liptinite common, inertinite rare. Mineral fluorescence moderate orange to none. Iron oxides sparse. Pyrite sparse.)
Ctgs	$\overline{R}_I$max	1.54	1.20-1.84	0..263	3	
L0206	2712	0.58	0.45-0.70	0.048	25	Common sporinite and sparse liptodetrinite yellow to dull orange, rare cutinite dull orange, rare resinite greenish yellow. (Calcareous claystone>argillaceous siltstone>carbonate. Dom common, L>I>V. Liptinite common, inertinite sparse to common, vitrinite sparse. Yellow fluorescing oil droplets in siltstone. Mineral fluorescence patchy moderate orange. Iron oxides rare. Pyrite common.)
Ctgs	$\overline{R}_I$max	1.39	1.06-1.80	0..252	10	
L0207	2892	0.64	0.53-0.75	0.057	25	Common sporinite and sparse liptodetrinite orange to dull orange, rare cutinite dull orange, rare resinite greenish yellow. (Calcareous claystone>argillaceous siltstone>coal>sandstone>shaly coal. Coal abundant V, vitrite. Coal comprise about 3% of the sample and consists exclusively of vitrinite. Shaly coal sparse, V>L, clarite. Dom common, L>V>I. Liptinite and vitrinite common, inertinite sparse. Most of the coal grains are weakly “frypanned”, ,measurements were taken away from the rims. Mineral fluorescence weak to moderate orange. Iron oxides rare. Pyrite sparse.)
Ctgs	$\overline{R}_I$max	1.55	1.26-1.90	0..230	5	
L0208	3105	0.68	0.57-0.80	0.050	18	Rare sporinite and liptodetrinite dull orange. (Sandstone> argillaceous siltstone>>coal. Coal rare, V, vitrinite. Dom sparse, I>V>L. Inertinite sparse, vitrinite rare to sparse, liptinite rare. Mineral fluorescence mostly none, weak to moderate orange in fine grained sediments. Iron oxides rare. Pyrite rare.)
Ctgs	$\overline{R}_I$max	1.45	1.00-2.16	0..361	10	

TREFOIL-1

KK # / Ref #.	Depth (m)	$R_v$max Mean	$R_v$max Range	SD	N	Sample description including liptinite fluorescence maceral abundances, mineral fluorescence
L0209	3324	0.72	0.62-0.88	0.067	27	Rare sporinite and liptodetrinite orange to dull orange. (Sandstone>
Ctgs	$\overline{R}_I$max	1.80	1.14-2.48	0.354	20	argillaceous siltstone>claystone>carbonate>coal. Coal rare, V, vitrinite. Dom sparse, I>V>L. Inertinite sparse, vitrinite rare to sparse, liptinite rare. Mineral fluorescence mostly none, moderate orange in fine grained sediments. Iron oxides sparse. Pyrite rare.)
L0210	3492	0.73	0.64-0.90	0.065	25	Rare sporinite and liptodetrinite dull orange, rare cutinite orange.
Ctgs	$\overline{R}_I$max	1.61	1.06-2.42	0..418	10	(Sandstone>argillaceous siltstone>carbonate. Dom sparse to common, V>I>L. Vitrinite and inertinite sparse, liptinite rare. Mineral fluorescence mostly none, weak to moderate orange in fine grained sediments. Iron oxides sparse. Pyrite rare.)

The section is immature down to about 2100m, mid-mature at about 2900m and mid- to late-mature at 3492m. Most of the organic matter is either coal or dom that is related to coals. No evidence was found of the effects of igneous rocks.

The source potential ranges from fair to moderate, but humic maceral groups are much more abundant compared with liptinite.

ACC 29 December 2004

R	No Read	Pop Range	R	No Read	Pop Range	R	No Read	Pop Range	R	No Read	Pop Range	R	No Read	Pop Range	R	No Read	Pop Range	R	No Read	Pop Range	R	No Read	Pop Range	R	No Read	Pop Range
0.10			0.40			0.70			1.00			1.30			1.60			1.90			2.20			2.50		
0.11			0.41			0.71			1.01			1.31			1.61			1.91			2.21			2.51		
0.12			0.42	1	↑	0.72			1.02			1.32			1.62			1.92			2.22			2.52		
0.13			0.43		FGV	0.73			1.03			1.33			1.63			1.93			2.23			2.53		
0.14			0.44		|	0.74			1.04			1.34			1.64			1.94			2.24			2.54		
0.15			0.45		|	0.75			1.05			1.35			1.65			1.95			2.25			2.55		
0.16			0.46		FGV	0.76			1.06			1.36			1.66			1.96			2.26			2.56		
0.17			0.47	1	↓	0.77			1.07			1.37			1.67			1.97			2.27			2.57		
0.18			0.48			0.78			1.08			1.38			1.68			1.98			2.28			2.58		
0.19			0.49			0.79			1.09			1.39			1.69			1.99			2.29			2.59		
0.20			0.50			0.80			1.10			1.40			1.70			2.00			2.30			2.60		
0.21			0.51			0.81			1.11			1.41			1.71			2.01			2.31			2.61		
0.22			0.52			0.82			1.12			1.42			1.72			2.02			2.32			2.62		
0.23			0.53			0.83			1.13			1.43			1.73			2.03			2.33			2.63		
0.24			0.54			0.84			1.14			1.44			1.74			2.04			2.34			2.64		
0.25			0.55			0.85			1.15			1.45			1.75			2.05			2.35			2.65		
0.26			0.56			0.86			1.16			1.46			1.76	1	Inert	2.06			2.36			2.66		
0.27			0.57			0.87			1.17			1.47			1.77			2.07			2.37			2.67		
0.28			0.58			0.88			1.18			1.48			1.78			2.08			2.38			2.68		
0.29			0.59			0.89			1.19			1.49			1.79			2.09			2.39			2.69		
0.30			0.60			0.90			1.20			1.50			1.80			2.10			2.40			2.70		
0.31			0.61			0.91			1.21			1.51			1.81			2.11			2.41			2.71		
0.32			0.62			0.92			1.22			1.52			1.82			2.12			2.42			2.72		
0.33			0.63			0.93			1.23			1.53			1.83			2.13			2.43			2.73		
0.34			0.64			0.94			1.24			1.54			1.84			2.14			2.44			2.74		
0.35			0.65			0.95			1.25			1.55			1.85			2.15			2.45			2.75		
0.36			0.66			0.96			1.26			1.56			1.86			2.16			2.46			2.76		
0.37			0.67			0.97			1.27			1.57			1.87			2.17			2.47			2.77		
0.38			0.68			0.98			1.28			1.58			1.88			2.18			2.48			2.78		
0.39			0.69			0.99			1.29			1.59			1.89			2.19			2.49			2.79		

VITRINITE <0.1%		INERTINITE <0.1%						LIPTINITE <0.1%								OIL DROPS	BITUMEN
TV	DV	Sfus	Scler	Fus	Macr	ID	Micr	Spor	Cut	Sub	Res	Ld <0.1	Bituminite	Telalginite	Lamalginite <0.1	Oil cut	

Sample Number..L0201.....Well Name..TREFOIL-1 .....ORIGIN..... Depth...1700m..... ..... SampleType....Ctgs...
Date. ..28/12/2004.. Op..SPR..... FGV - First Generation Vitrinite, RV - Reworked Vitrinite, BTT - Bituminite, B - Bitumen, Inert - Inertinite, Cav - Cavings, DA - Drilling Mud Additives Copyright Keiraville Konsultants MICR D:\RWORK.ms6\misc04vr.doc

R	No Read	Pop Range	R	No Read	Pop Range	R	No Read	Pop Range	R	No Read	Pop Range	R	No Read	Pop Range	R	No Read	Pop Range	R	No Read	Pop Range	R	No Read	Pop Range	R	No Read	Pop Range
0.10			0.40			0.70			1.00			1.30			1.60			1.90			2.20			2.50		
0.11			0.41			0.71			1.01			1.31			1.61			1.91			2.21			2.51		
0.12			0.42			0.72			1.02			1.32			1.62			1.92			2.22			2.52		
0.13			0.43			0.73			1.03			1.33			1.63			1.93			2.23			2.53		
0.14			0.44			0.74			1.04			1.34			1.64			1.94			2.24			2.54		
0.15			0.45	1	↑	0.75			1.05			1.35			1.65			1.95			2.25			2.55		
0.16			0.46		FGV	0.76			1.06			1.36			1.66			1.96			2.26			2.56		
0.17			0.47			0.77			1.07			1.37			1.67			1.97			2.27			2.57		
0.18			0.48			0.78			1.08			1.38			1.68			1.98			2.28			2.58		
0.19			0.49			0.79			1.09			1.39			1.69			1.99			2.29			2.59		
0.20			0.50			0.80			1.10			1.40			1.70			2.00			2.30			2.60		
0.21			0.51			0.81			1.11			1.41			1.71			2.01			2.31			2.61		
0.22			0.52			0.82			1.12			1.42			1.72			2.02			2.32			2.62		
0.23			0.53		FGV	0.83			1.13			1.43			1.73			2.03			2.33			2.63		
0.24			0.54	2	↓	0.84			1.14			1.44			1.74			2.04			2.34			2.64		
0.25			0.55			0.85			1.15			1.45			1.75			2.05			2.35			2.65		
0.26			0.56			0.86			1.16			1.46			1.76			2.06			2.36			2.66		
0.27			0.57			0.87			1.17			1.47			1.77			2.07			2.37			2.67		
0.28			0.58			0.88			1.18			1.48			1.78			2.08			2.38			2.68		
0.29			0.59			0.89			1.19			1.49			1.79			2.09			2.39			2.69		
0.30			0.60			0.90			1.20			1.50			1.80			2.10			2.40			2.70		
0.31			0.61			0.91			1.21			1.51			1.81			2.11			2.41			2.71		
0.32			0.62			0.92			1.22			1.52			1.82			2.12			2.42			2.72		
0.33			0.63			0.93			1.23			1.53			1.83			2.13			2.43			2.73		
0.34			0.64			0.94			1.24			1.54			1.84			2.14			2.44			2.74		
0.35			0.65			0.95			1.25			1.55			1.85			2.15			2.45			2.75		
0.36			0.66			0.96			1.26			1.56			1.86			2.16			2.46			2.76		
0.37			0.67			0.97			1.27			1.57			1.87			2.17			2.47			2.77		
0.38			0.68			0.98	1	Inert	1.28			1.58			1.88			2.18			2.48			2.78		
0.39			0.69			0.99			1.29			1.59			1.89			2.19			2.49			2.79		

VITRINITE <0.1%		INERTINITE <0.1%						LIPTINITE -%								OIL DROPS	BITUMEN
TV	DV	Sfus	Scler	Fus	Macr	ID	Micr	Spor	Cut	Sub	Res	Ld	Bituminite	Telalginite	Lamalginite	Oil	cut

Sample Number..L0202.....Well Name..TREFOIL-1 .....ORIGIN..... Depth...1890m..... ..... SampleType....Ctgs...

Date. ..28/12/2004.. Op..SPR..... FGV - First Generation Vitrinite, RV - Reworked Vitrinite, BTT - Bituminite, B - Bitumen, Inert - Inertinite, Cav - Cavings, DA - Drilling Mud Additives Copyright Keiraville Konsultants MICR D:\RWORK.ms6\misc04vr.doc

R	No Read	Pop Range	R	No Read	Pop Range	R	No Read	Pop Range	R	No Read	Pop Range	R	No Read	Pop Range	R	No Read	Pop Range	R	No Read	Pop Range	R	No Read	Pop Range	R	No Read	Pop Range
0.10			0.40			0.70			1.00			1.30			1.60			1.90			2.20			2.50		
0.11			0.41			0.71			1.01			1.31			1.61			1.91			2.21			2.51		
0.12			0.42			0.72			1.02			1.32			1.62			1.92			2.22			2.52		
0.13			0.43			0.73			1.03			1.33			1.63			1.93			2.23			2.53		
0.14			0.44	1		0.74			1.04			1.34			1.64			1.94			2.24			2.54		
0.15			0.45			0.75			1.05			1.35			1.65			1.95			2.25			2.55		
0.16			0.46			0.76			1.06			1.36			1.66			1.96			2.26			2.56		
0.17			0.47			0.77			1.07			1.37			1.67			1.97			2.27			2.57		
0.18			0.48	1		0.78			1.08			1.38			1.68			1.98			2.28			2.58		
0.19			0.49			0.79			1.09			1.39			1.69			1.99			2.29			2.59		
0.20			0.50			0.80			1.10			1.40			1.70			2.00			2.30			2.60		
0.21			0.51	1		0.81			1.11			1.41			1.71			2.01			2.31			2.61		
0.22			0.52	1		0.82			1.12			1.42			1.72			2.02			2.32			2.62		
0.23			0.53			0.83			1.13			1.43			1.73			2.03			2.33			2.63		
0.24			0.54			0.84			1.14			1.44			1.74			2.04			2.34			2.64		
0.25			0.55	2		0.85			1.15			1.45			1.75			2.05			2.35			2.65		
0.26			0.56			0.86			1.16			1.46			1.76			2.06			2.36			2.66		
0.27			0.57			0.87			1.17			1.47			1.77			2.07			2.37			2.67		
0.28			0.58		FGV	0.88			1.18			1.48			1.78			2.08			2.38			2.68		
0.29			0.59	1	↓	0.89			1.19			1.49			1.79			2.09			2.39			2.69		
0.30			0.60			0.90			1.20			1.50			1.80			2.10			2.40			2.70		
0.31			0.61			0.91			1.21			1.51			1.81			2.11			2.41			2.71		
0.32			0.62			0.92			1.22			1.52			1.82			2.12			2.42			2.72		
0.33			0.63			0.93			1.23			1.53			1.83			2.13			2.43			2.73		
0.34			0.64			0.94			1.24			1.54			1.84			2.14			2.44			2.74		
0.35			0.65			0.95			1.25			1.55			1.85			2.15			2.45			2.75		
0.36			0.66			0.96			1.26			1.56			1.86			2.16			2.46			2.76		
0.37			0.67			0.97			1.27			1.57			1.87			2.17			2.47			2.77		
0.38	1	↑	0.68			0.98			1.28			1.58			1.88			2.18			2.48			2.78		
0.39		FGV	0.69			0.99			1.29			1.59			1.89			2.19			2.49			2.79		

VITRINITE <0.1%		INERTINITE <0.1%						LIPTINITE <0.1%								OIL DROPS	BITUMEN
TV	DV	Sfus	Scler	Fus	Macr	ID	Micr	Spor <0.1	Cut	Sub	Res	Ld <0.1	Bituminite	Telalginite	Lamalginite	Oil cut	

Sample Number..L0203.....Well Name..TREFOIL-1 .....ORIGIN..... Depth...2136m..... ..... SampleType....Ctgs...

Date. ..29/12/2004.. Op..SPR..... FGV - First Generation Vitrinite, RV - Reworked Vitrinite, BTT - Bituminite, B - Bitumen, Inert - Inertinite, Cav - Cavings, DA - Drilling Mud Additives Copyright Keiraville Konsultants MICR D:\RWORK.ms6\misc04vr.doc

R	No Read	Pop Range	R	No Read	Pop Range	R	No Read	Pop Range	R	No Read	Pop Range	R	No Read	Pop Range	R	No Read	Pop Range	R	No Read	Pop Range	R	No Read	Pop Range	R	No Read	Pop Range
0.10			0.40			0.70			1.00			1.30			1.60			1.90			2.20			2.50		
0.11			0.41			0.71			1.01			1.31			1.61			1.91			2.21			2.51		
0.12			0.42	1	↑	0.72			1.02	1	↑	1.32			1.62			1.92			2.22			2.52		
0.13			0.43		FGV	0.73			1.03		Inert	1.33			1.63		Inert	1.93			2.23			2.53		
0.14			0.44			0.74			1.04			1.34			1.64	1	↓	1.94			2.24			2.54		
0.15			0.45			0.75			1.05			1.35			1.65			1.95			2.25			2.55		
0.16			0.46			0.76			1.06			1.36			1.66			1.96			2.26			2.56		
0.17			0.47			0.77			1.07			1.37			1.67			1.97			2.27			2.57		
0.18			0.48			0.78			1.08			1.38			1.68			1.98			2.28			2.58		
0.19			0.49	2		0.79			1.09			1.39			1.69			1.99			2.29			2.59		
0.20			0.50	1		0.80			1.10			1.40			1.70			2.00			2.30			2.60		
0.21			0.51			0.81			1.11			1.41			1.71			2.01			2.31			2.61		
0.22			0.52	1		0.82			1.12			1.42			1.72			2.02			2.32			2.62		
0.23			0.53	2		0.83			1.13			1.43			1.73			2.03			2.33			2.63		
0.24			0.54	4		0.84			1.14			1.44			1.74			2.04			2.34			2.64		
0.25			0.55	1		0.85			1.15			1.45			1.75			2.05			2.35			2.65		
0.26			0.56	2		0.86			1.16			1.46			1.76			2.06			2.36			2.66		
0.27			0.57			0.87			1.17			1.47			1.77			2.07			2.37			2.67		
0.28			0.58	2		0.88			1.18			1.48			1.78			2.08			2.38			2.68		
0.29			0.59			0.89			1.19			1.49			1.79			2.09			2.39			2.69		
0.30			0.60	1		0.90			1.20			1.50			1.80			2.10			2.40			2.70		
0.31			0.61			0.91			1.21			1.51			1.81			2.11			2.41			2.71		
0.32			0.62			0.92			1.22			1.52			1.82			2.12			2.42			2.72		
0.33			0.63			0.93			1.23			1.53			1.83			2.13			2.43			2.73		
0.34			0.64			0.94			1.24			1.54			1.84			2.14			2.44			2.74		
0.35			0.65		FGV	0.95			1.25			1.55			1.85			2.15			2.45			2.75		
0.36			0.66	1	↓	0.96			1.26			1.56			1.86			2.16			2.46			2.76		
0.37			0.67			0.97			1.27			1.57			1.87			2.17			2.47			2.77		
0.38			0.68			0.98			1.28			1.58			1.88			2.18			2.48			2.78		
0.39			0.69			0.99			1.29			1.59			1.89			2.19			2.49			2.79		

VITRINITE 0.2%		INERTINITE <0.1%						LIPTINITE 0.1%								OIL DROPS	BITUMEN
TV	DV	Sfus	Scler	Fus	Macr	ID	Micr	Spor <0.1	Cut <0.1	Sub	Res	Ld <0.1	Bituminite	Telalginite	Lamalginite	Oil cut	

Sample Number..L0204.....Well Name..TREFOIL-1 .....ORIGIN..... Depth...2322m..... ..... SampleType....Ctgs...
Date. ..29/12/2004.. Op..SPR..... FGV - First Generation Vitrinite, RV - Reworked Vitrinite, BTT - Bituminite, B - Bitumen, Inert - Inertinite, Cav - Cavings, DA - Drilling Mud Additives Copyright Keiraville Konsultants MICR D:\RWORK.ms6\misc04vr.doc

R	No Read	Pop Range	R	No Read	Pop Range	R	No Read	Pop Range	R	No Read	Pop Range	R	No Read	Pop Range	R	No Read	Pop Range	R	No Read	Pop Range	R	No Read	Pop Range	R	No Read	Pop Range
0.10			0.40			0.70			1.00			1.30			1.60			1.90			2.20			2.50		
0.11			0.41			0.71			1.01			1.31			1.61			1.91			2.21			2.51		
0.12			0.42			0.72			1.02			1.32			1.62			1.92			2.22			2.52		
0.13			0.43			0.73			1.03			1.33			1.63			1.93			2.23			2.53		
0.14			0.44	1	↑	0.74			1.04			1.34			1.64			1.94			2.24			2.54		
0.15			0.45		FGV	0.75			1.05			1.35			1.65			1.95			2.25			2.55		
0.16			0.46			0.76			1.06			1.36			1.66			1.96			2.26			2.56		
0.17			0.47	1		0.77			1.07			1.37			1.67			1.97			2.27			2.57		
0.18			0.48			0.78			1.08			1.38			1.68			1.98			2.28			2.58		
0.19			0.49			0.79			1.09			1.39			1.69			1.99			2.29			2.59		
0.20			0.50	2		0.80			1.10			1.40			1.70			2.00			2.30			2.60		
0.21			0.51	2		0.81			1.11			1.41			1.71			2.01			2.31			2.61		
0.22			0.52			0.82			1.12			1.42			1.72			2.02			2.32			2.62		
0.23			0.53	4		0.83			1.13			1.43			1.73			2.03			2.33			2.63		
0.24			0.54			0.84			1.14			1.44			1.74			2.04			2.34			2.64		
0.25			0.55	4		0.85			1.15			1.45			1.75			2.05			2.35			2.65		
0.26			0.56	3		0.86			1.16			1.46			1.76			2.06			2.36			2.66		
0.27			0.57	3		0.87			1.17			1.47			1.77			2.07			2.37			2.67		
0.28			0.58	1		0.88			1.18			1.48			1.78			2.08			2.38			2.68		
0.29			0.59			0.89			1.19			1.49			1.79			2.09			2.39			2.69		
0.30			0.60			0.90			1.20	1	↑	1.50			1.80			2.10			2.40			2.70		
0.31			0.61	1		0.91			1.21		Inert	1.51			1.81			2.11			2.41			2.71		
0.32			0.62			0.92			1.22			1.52			1.82			2.12			2.42			2.72		
0.33			0.63			0.93			1.23			1.53			1.83		Inert	2.13			2.43			2.73		
0.34			0.64	2	FGV	0.94			1.24			1.54			1.84	1	↓	2.14			2.44			2.74		
0.35			0.65	1	↓	0.95			1.25			1.55			1.85			2.15			2.45			2.75		
0.36			0.66			0.96			1.26			1.56			1.86			2.16			2.46			2.76		
0.37			0.67			0.97			1.27			1.57			1.87			2.17			2.47			2.77		
0.38			0.68			0.98			1.28			1.58	1		1.88			2.18			2.48			2.78		
0.39			0.69			0.99			1.29			1.59			1.89			2.19			2.49			2.79		

VITRINITE 1.4%		INERTINITE <0.1%						LIPTINITE 0.9%							OIL DROPS	BITUMEN
TV	DV	Sfus	Scler	Fus	Macr	ID	Micr	Spor 0.6	Cut 0.2	Sub	Res	Ld 0.1	Bituminite	Telalginite	Lamalginite	Oil cut

Sample Number..L0205.....Well Name..TREFOIL-1 .....ORIGIN..... Depth...2508m..... ..... SampleType....Ctgs...
Date. ..29/12/2004.. Op..SPR..... FGV - First Generation Vitrinite, RV - Reworked Vitrinite, BTT - Bituminite, B - Bitumen, Inert - Inertinite, Cav - Cavings, DA - Drilling Mud Additives Copyright Keiraville Konsultants MICR D:\RWORK.ms6\misc04vr.doc

R	No Read	Pop Range	R	No Read	Pop Range	R	No Read	Pop Range	R	No Read	Pop Range	R	No Read	Pop Range	R	No Read	Pop Range	R	No Read	Pop Range	R	No Read	Pop Range	R	No Read	Pop Range
0.10			0.40			0.70	1	↓	1.00			1.30			1.60			1.90			2.20			2.50		
0.11			0.41			0.71			1.01			1.31			1.61			1.91			2.21			2.51		
0.12			0.42			0.72			1.02			1.32			1.62			1.92			2.22			2.52		
0.13			0.43			0.73			1.03			1.33			1.63			1.93			2.23			2.53		
0.14			0.44			0.74			1.04			1.34			1.64			1.94			2.24			2.54		
0.15			0.45	1	↑	0.75			1.05			1.35			1.65			1.95			2.25			2.55		
0.16			0.46		FGV	0.76			1.06	1	↑	1.36			1.66			1.96			2.26			2.56		
0.17			0.47			0.77			1.07		Inert	1.37			1.67			1.97			2.27			2.57		
0.18			0.48			0.78			1.08			1.38			1.68			1.98			2.28			2.58		
0.19			0.49			0.79			1.09			1.39			1.69			1.99			2.29			2.59		
0.20			0.50			0.80			1.10			1.40			1.70			2.00			2.30			2.60		
0.21			0.51			0.81			1.11			1.41			1.71			2.01			2.31			2.61		
0.22			0.52	1		0.82			1.12			1.42			1.72	1		2.02			2.32			2.62		
0.23			0.53	1		0.83			1.13			1.43			1.73			2.03			2.33			2.63		
0.24			0.54	2		0.84			1.14	1		1.44			1.74			2.04			2.34			2.64		
0.25			0.55	1		0.85			1.15			1.45			1.75			2.05			2.35			2.65		
0.26			0.56	3		0.86			1.16			1.46			1.76			2.06			2.36			2.66		
0.27			0.57	1		0.87			1.17			1.47			1.77			2.07			2.37			2.67		
0.28			0.58	2		0.88			1.18	1		1.48			1.78			2.08			2.38			2.68		
0.29			0.59	6		0.89			1.19			1.49			1.79		Inert	2.09			2.39			2.69		
0.30			0.60	1		0.90			1.20	2		1.50			1.80	1	↓	2.10			2.40			2.70		
0.31			0.61	1		0.91			1.21			1.51			1.81			2.11			2.41			2.71		
0.32			0.62	2		0.92			1.22			1.52	1		1.82			2.12			2.42			2.72		
0.33			0.63	1		0.93			1.23			1.53			1.83			2.13			2.43			2.73		
0.34			0.64			0.94			1.24			1.54	1		1.84			2.14			2.44			2.74		
0.35			0.65			0.95			1.25			1.55			1.85			2.15			2.45			2.75		
0.36			0.66			0.96			1.26			1.56	1		1.86			2.16			2.46			2.76		
0.37			0.67	1		0.97			1.27			1.57			1.87			2.17			2.47			2.77		
0.38			0.68			0.98			1.28			1.58			1.88			2.18			2.48			2.78		
0.39			0.69			0.99			1.29			1.59			1.89			2.19			2.49			2.79		

VITRINITE 0.3%		INERTINITE 0.5%						LIPTINITE 0.7%							OIL DROPS	BITUMEN
TV	DV	Sfus	Scler	Fus	Macr	ID	Micr	Spor 0.6	Cut <0.1	Sub	Res <0.1	Ld 0.1	Bituminite	Telalginite	Lamalginite	Oil cut

Sample Number..L0206.....Well Name..TREFOIL-1 .....ORIGIN..... Depth...2712m..... ..... SampleType....Ctgs...

Date. ..29/12/2004.. Op..SPR..... FGV - First Generation Vitrinite, RV - Reworked Vitrinite, BTT - Bituminite, B - Bitumen, Inert - Inertinite, Cav - Cavings, DA - Drilling Mud Additives Copyright Keiraville Konsultants MICR D:\RWORK.ms6\misc04vr.doc

R	No Read	Pop Range	R	No Read	Pop Range	R	No Read	Pop Range	R	No Read	Pop Range	R	No Read	Pop Range	R	No Read	Pop Range	R	No Read	Pop Range	R	No Read	Pop Range	R	No Read	Pop Range
0.10			0.40			0.70			1.00			1.30			1.60	1		1.90	1	↓	2.20			2.50		
0.11			0.41			0.71			1.01			1.31			1.61			1.91			2.21			2.51		
0.12			0.42			0.72	2		1.02			1.32			1.62			1.92			2.22			2.52		
0.13			0.43			0.73			1.03			1.33			1.63			1.93			2.23			2.53		
0.14			0.44			0.74	1	FGV	1.04			1.34	1		1.64			1.94			2.24			2.54		
0.15			0.45			0.75	1	↓	1.05			1.35			1.65			1.95			2.25			2.55		
0.16			0.46			0.76			1.06			1.36			1.66	1		1.96			2.26			2.56		
0.17			0.47			0.77			1.07			1.37			1.67			1.97			2.27			2.57		
0.18			0.48			0.78			1.08			1.38			1.68			1.98			2.28			2.58		
0.19			0.49			0.79			1.09			1.39			1.69			1.99			2.29			2.59		
0.20			0.50			0.80			1.10			1.40			1.70			2.00			2.30			2.60		
0.21			0.51			0.81			1.11			1.41			1.71			2.01			2.31			2.61		
0.22			0.52			0.82			1.12			1.42			1.72			2.02			2.32			2.62		
0.23			0.53	1	↑	0.83			1.13			1.43			1.73			2.03			2.33			2.63		
0.24			0.54		FGV	0.84			1.14			1.44			1.74			2.04			2.34			2.64		
0.25			0.55			0.85			1.15			1.45			1.75			2.05			2.35			2.65		
0.26			0.56	1		0.86			1.16			1.46			1.76			2.06			2.36			2.66		
0.27			0.57			0.87			1.17			1.47			1.77			2.07			2.37			2.67		
0.28			0.58	3		0.88			1.18			1.48			1.78			2.08			2.38			2.68		
0.29			0.59	2		0.89			1.19			1.49			1.79			2.09			2.39			2.69		
0.30			0.60	1		0.90			1.20			1.50			1.80			2.10			2.40			2.70		
0.31			0.61			0.91			1.21			1.51			1.81			2.11			2.41			2.71		
0.32			0.62	4		0.92			1.22			1.52			1.82			2.12			2.42			2.72		
0.33			0.63			0.93			1.23			1.53			1.83			2.13			2.43			2.73		
0.34			0.64			0.94			1.24			1.54			1.84			2.14			2.44			2.74		
0.35			0.65	1		0.95			1.25			1.55			1.85			2.15			2.45			2.75		
0.36			0.66	2		0.96			1.26	1	↑	1.56			1.86			2.16			2.46			2.76		
0.37			0.67	3		0.97			1.27		Inert	1.57			1.87			2.17			2.47			2.77		
0.38			0.68	1		0.98			1.28			1.58			1.88			2.18			2.48			2.78		
0.39			0.69	2		0.99			1.29			1.59			1.89		Inert	2.19			2.49			2.79		

VITRINITE 3.6%		INERTINITE 0.3%						LIPTINITE 1.4%							OIL DROPS	BITUMEN
TV	DV	Sfus	Scler	Fus	Macr	ID	Micr	Spor 1.2	Cut <0.1	Sub	Res <0.1	Ld 0.2	Bituminite	Telalginite	Lamalginite	Oil cut

Sample Number..L0207.....Well Name..TREFOIL-1 .....ORIGIN..... Depth...2892m..... ..... SampleType....Ctgs...
Date. ..29/12/2004.. Op..SPR..... FGV - First Generation Vitrinite, RV - Reworked Vitrinite, BTT - Bituminite, B - Bitumen, Inert - Inertinite, Cav - Cavings, DA - Drilling Mud Additives Copyright Keiraville Konsultants MICR D:\RWORK.ms6\misc04vr.doc

R	No Read	Pop Range	R	No Read	Pop Range	R	No Read	Pop Range	R	No Read	Pop Range	R	No Read	Pop Range	R	No Read	Pop Range	R	No Read	Pop Range	R	No Read	Pop Range	R	No Read	Pop Range
0.10			0.40			0.70	1		1.00	1	↑	1.30			1.60			1.90			2.20			2.50		
0.11			0.41			0.71			1.01		Inert	1.31			1.61			1.91			2.21			2.51		
0.12			0.42			0.72	1		1.02			1.32	1		1.62			1.92			2.22			2.52		
0.13			0.43			0.73			1.03			1.33			1.63			1.93			2.23			2.53		
0.14			0.44			0.74	1		1.04			1.34			1.64			1.94			2.24			2.54		
0.15			0.45			0.75	1		1.05			1.35			1.65			1.95			2.25			2.55		
0.16			0.46			0.76			1.06			1.36			1.66	1		1.96			2.26			2.56		
0.17			0.47			0.77			1.07			1.37			1.67			1.97			2.27			2.57		
0.18			0.48			0.78			1.08			1.38			1.68			1.98			2.28			2.58		
0.19			0.49			0.79		FGV	1.09			1.39			1.69			1.99			2.29			2.59		
0.20			0.50			0.80	1	↓	1.10			1.40			1.70			2.00			2.30			2.60		
0.21			0.51			0.81			1.11			1.41			1.71			2.01			2.31			2.61		
0.22			0.52			0.82			1.12			1.42	1		1.72			2.02	1		2.32			2.62		
0.23			0.53			0.83			1.13			1.43			1.73			2.03			2.33			2.63		
0.24			0.54			0.84			1.14			1.44			1.74			2.04			2.34			2.64		
0.25			0.55			0.85			1.15			1.45			1.75			2.05			2.35			2.65		
0.26			0.56			0.86			1.16			1.46			1.76			2.06			2.36			2.66		
0.27			0.57	1	↑	0.87			1.17			1.47			1.77			2.07			2.37			2.67		
0.28			0.58		FGV	0.88			1.18			1.48			1.78			2.08			2.38			2.68		
0.29			0.59			0.89			1.19			1.49			1.79			2.09			2.39			2.69		
0.30			0.60			0.90			1.20	1		1.50			1.80			2.10			2.40			2.70		
0.31			0.61			0.91			1.21			1.51			1.81			2.11			2.41			2.71		
0.32			0.62	1		0.92			1.22	2		1.52			1.82			2.12			2.42			2.72		
0.33			0.63			0.93			1.23			1.53			1.83			2.13			2.43			2.73		
0.34			0.64	2		0.94			1.24	1		1.54			1.84			2.14			2.44			2.74		
0.35			0.65	1		0.95			1.25			1.55			1.85			2.15		Inert	2.45			2.75		
0.36			0.66	1		0.96			1.26			1.56			1.86			2.16	1	↓	2.46			2.76		
0.37			0.67	2		0.97			1.27			1.57			1.87			2.17			2.47			2.77		
0.38			0.68	3		0.98			1.28			1.58			1.88			2.18			2.48			2.78		
0.39			0.69	2		0.99			1.29			1.59			1.89			2.19			2.49			2.79		

VITRINITE 0.1 %		INERTINITE 0.2%						LIPTINITE <0.1%								OIL DROPS	BITUMEN
TV	DV	Sfus	Scler	Fus	Macr	ID	Micr	Spor <0.1	Cut	Sub	Res	Ld <0.1	Bituminite	Telalginite	Lamalginite	Oil cut	

Sample Number..L0208.....Well Name..TREFOIL-1 .....ORIGIN..... Depth...3105m..... ..... SampleType....Ctgs...

Date. ..29/12/2004.. Op..SPR..... FGV - First Generation Vitrinite, RV - Reworked Vitrinite, BTT - Bituminite, B - Bitumen, Inert - Inertinite, Cav - Cavings, DA - Drilling Mud Additives Copyright Keiraville Konsultants MICR D:\RWORK.ms6\misc04vr.doc

R	No Read	Pop Range	R	No Read	Pop Range	R	No Read	Pop Range	R	No Read	Pop Range	R	No Read	Pop Range	R	No Read	Pop Range	R	No Read	Pop Range	R	No Read	Pop Range	R	No Read	Pop Range
0.10			0.40			0.70	4		1.00			1.30			1.60			1.90			2.20			2.50		
0.11			0.41			0.71			1.01			1.31			1.61			1.91			2.21			2.51		
0.12			0.42			0.72	1		1.02			1.32			1.62			1.92	1		2.22			2.52		
0.13			0.43			0.73	1		1.03			1.33			1.63			1.93			2.23			2.53		
0.14			0.44			0.74	1		1.04			1.34			1.64	3		1.94			2.24			2.54		
0.15			0.45			0.75			1.05			1.35			1.65			1.95			2.25			2.55		
0.16			0.46			0.76	1		1.06			1.36	1		1.66			1.96	1		2.26			2.56		
0.17			0.47			0.77	2		1.07			1.37			1.67			1.97			2.27			2.57		
0.18			0.48			0.78	1		1.08			1.38			1.68			1.98			2.28	1		2.58		
0.19			0.49			0.79			1.09			1.39			1.69			1.99			2.29			2.59		
0.20			0.50			0.80	1		1.10			1.40			1.70	1		2.00			2.30			2.60		
0.21			0.51			0.81	1		1.11			1.41			1.71			2.01			2.31			2.61		
0.22			0.52			0.82			1.12			1.42			1.72			2.02			2.32			2.62		
0.23			0.53			0.83	2		1.13			1.43			1.73			2.03			2.33			2.63		
0.24			0.54			0.84			1.14	1	↑	1.44			1.74			2.04			2.34			2.64		
0.25			0.55			0.85			1.15		Inert	1.45			1.75			2.05			2.35			2.65		
0.26			0.56			0.86			1.16			1.46			1.76			2.06	1		2.36			2.66		
0.27			0.57			0.87		FGV	1.17			1.47			1.77			2.07			2.37			2.67		
0.28			0.58			0.88	1	↓	1.18			1.48	1		1.78	1		2.08			2.38			2.68		
0.29			0.59			0.89			1.19			1.49			1.79			2.09			2.39			2.69		
0.30			0.60			0.90			1.20			1.50			1.80	2		2.10			2.40			2.70		
0.31			0.61			0.91			1.21			1.51			1.81			2.11			2.41			2.71		
0.32			0.62	2	↑	0.92			1.22			1.52			1.82			2.12			2.42			2.72		
0.33			0.63		FGV	0.93			1.23			1.53			1.83			2.13			2.43			2.73		
0.34			0.64	1		0.94			1.24			1.54	1		1.84	1		2.14			2.44	1		2.74		
0.35			0.65	1		0.95			1.25			1.55			1.85			2.15			2.45			2.75		
0.36			0.66	1		0.96			1.26			1.56			1.86			2.16			2.46			2.76		
0.37			0.67	1		0.97			1.27			1.57			1.87			2.17			2.47		Inert	2.77		
0.38			0.68	3		0.98			1.28	1		1.58			1.88			2.18	1		2.48	1	↓	2.78		
0.39			0.69	2		0.99			1.29			1.59			1.89			2.19			2.49			2.79		

VITRINITE 0.1 %		INERTINITE 0.2%						LIPTINITE <0.1%							OIL DROPS	BITUMEN
TV	DV	Sfus	Scler	Fus	Macr	ID	Micr	Spor <0.1	Cut	Sub	Res	Ld <0.1	Bituminite	Telalginite	Lamalginite	Oil cut

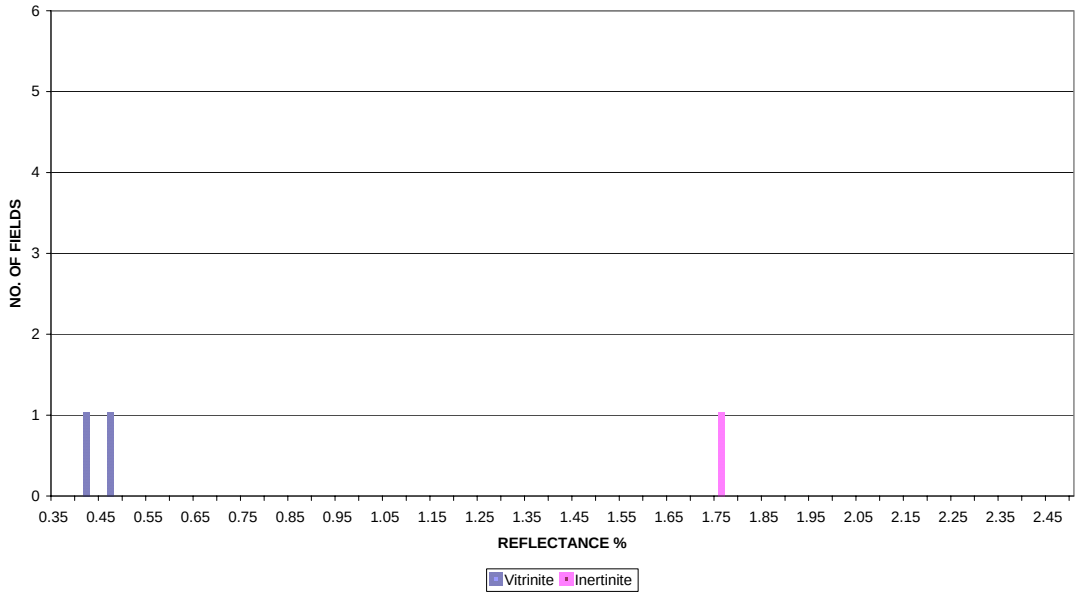
Sample Number..L0209.....Well Name..TREFOIL-1 .....ORIGIN..... Depth...3324m..... ..... SampleType....Ctgs...
Date. ..29/12/2004.. Op..SPR..... FGV - First Generation Vitrinite, RV - Reworked Vitrinite, BTT - Bituminite, B - Bitumen, Inert - Inertinite, Cav - Cavings, DA - Drilling Mud Additives Copyright Keiraville Konsultants MICR D:\RWORK.ms6\misc04vr.doc

R	No Read	Pop Range	R	No Read	Pop Range	R	No Read	Pop Range	R	No Read	Pop Range	R	No Read	Pop Range	R	No Read	Pop Range	R	No Read	Pop Range	R	No Read	Pop Range	R	No Read	Pop Range
0.10			0.40			0.70	1		1.00			1.30			1.60			1.90			2.20			2.50		
0.11			0.41			0.71	2		1.01			1.31			1.61			1.91			2.21			2.51		
0.12			0.42			0.72	1		1.02			1.32			1.62	1		1.92			2.22			2.52		
0.13			0.43			0.73	3		1.03			1.33			1.63			1.93			2.23			2.53		
0.14			0.44			0.74	2		1.04			1.34			1.64			1.94			2.24			2.54		
0.15			0.45			0.75	3		1.05			1.35			1.65			1.95			2.25			2.55		
0.16			0.46			0.76			1.06	1	↑	1.36			1.66			1.96			2.26			2.56		
0.17			0.47			0.77			1.07		Inert	1.37			1.67			1.97			2.27			2.57		
0.18			0.48			0.78	1		1.08			1.38			1.68			1.98			2.28			2.58		
0.19			0.49			0.79			1.09			1.39			1.69			1.99			2.29			2.59		
0.20			0.50			0.80	1		1.10			1.40			1.70			2.00			2.30			2.60		
0.21			0.51			0.81			1.11			1.41			1.71			2.01			2.31			2.61		
0.22			0.52			0.82	1		1.12			1.42			1.72			2.02			2.32			2.62		
0.23			0.53			0.83			1.13			1.43			1.73			2.03			2.33			2.63		
0.24			0.54			0.84			1.14	1		1.44			1.74			2.04			2.34			2.64		
0.25			0.55			0.85			1.15			1.45			1.75			2.05			2.35			2.65		
0.26			0.56			0.86	1		1.16			1.46			1.76			2.06			2.36			2.66		
0.27			0.57			0.87			1.17			1.47			1.77			2.07			2.37			2.67		
0.28			0.58			0.88			1.18			1.48			1.78			2.08			2.38			2.68		
0.29			0.59			0.89		FGV	1.19			1.49			1.79			2.09			2.39			2.69		
0.30			0.60			0.90	1	↓	1.20	1		1.50	1		1.80			2.10			2.40			2.70		
0.31			0.61			0.91			1.21			1.51			1.81			2.11			2.41		Inert	2.71		
0.32			0.62			0.92			1.22			1.52	1		1.82			2.12			2.42	1	↓	2.72		
0.33			0.63			0.93			1.23			1.53			1.83			2.13			2.43			2.73		
0.34			0.64	1	↑	0.94			1.24			1.54			1.84			2.14			2.44			2.74		
0.35			0.65	2	FGV	0.95			1.25			1.55			1.85			2.15			2.45			2.75		
0.36			0.66	3		0.96			1.26			1.56	1		1.86			2.16	1		2.46			2.76		
0.37			0.67	1		0.97			1.27			1.57			1.87			2.17			2.47			2.77		
0.38			0.68			0.98			1.28			1.58			1.88	1		2.18			2.48			2.78		
0.39			0.69	1		0.99			1.29			1.59			1.89			2.19			2.49			2.79		

VITRINITE 0.3%		INERTINITE 0.2%						LIPTINITE <0.1%							OIL DROPS	BITUMEN
TV	DV	Sfus	Scler	Fus	Macr	ID	Micr	Spor <0.1	Cut <0.1	Sub	Res	Ld <0.1	Bituminite	Telalginite	Lamalginite	Oil cut

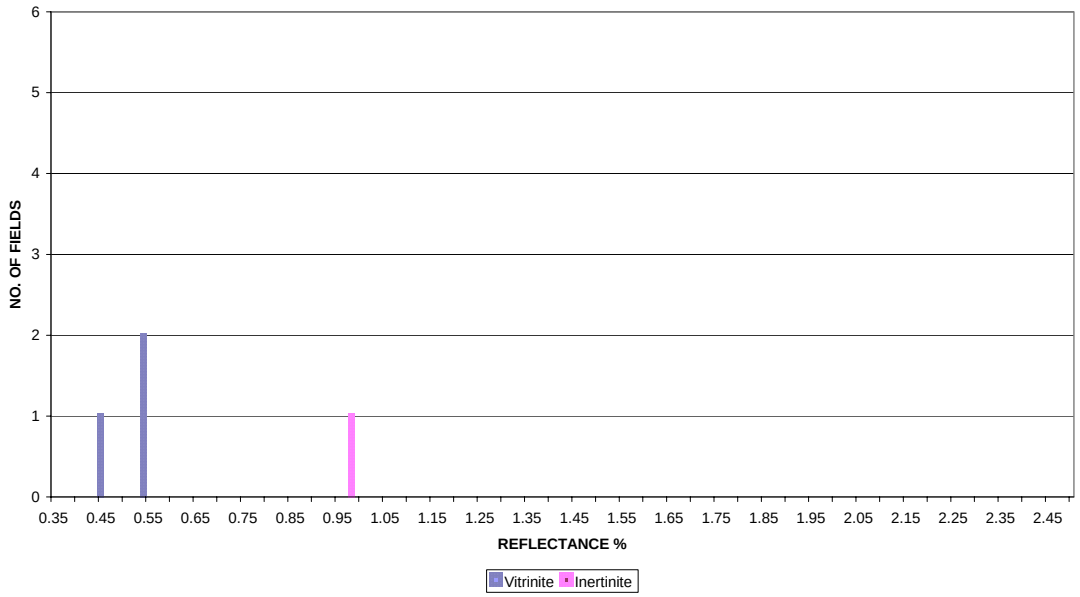
Sample Number..L0210.....Well Name..TREFOIL-1 .....ORIGIN..... Depth...3492m..... ..... SampleType....Ctgs...
Date. ..29/12/2004.. Op..SPR..... FGV - First Generation Vitrinite, RV - Reworked Vitrinite, BTT - Bituminite, B - Bitumen, Inert - Inertinite, Cav - Cavings, DA - Drilling Mud Additives Copyright Keiraville Konsultants MICR D:\RWORK.ms6\misc04vr.doc

Trefoil 1 1700m, Ctgs



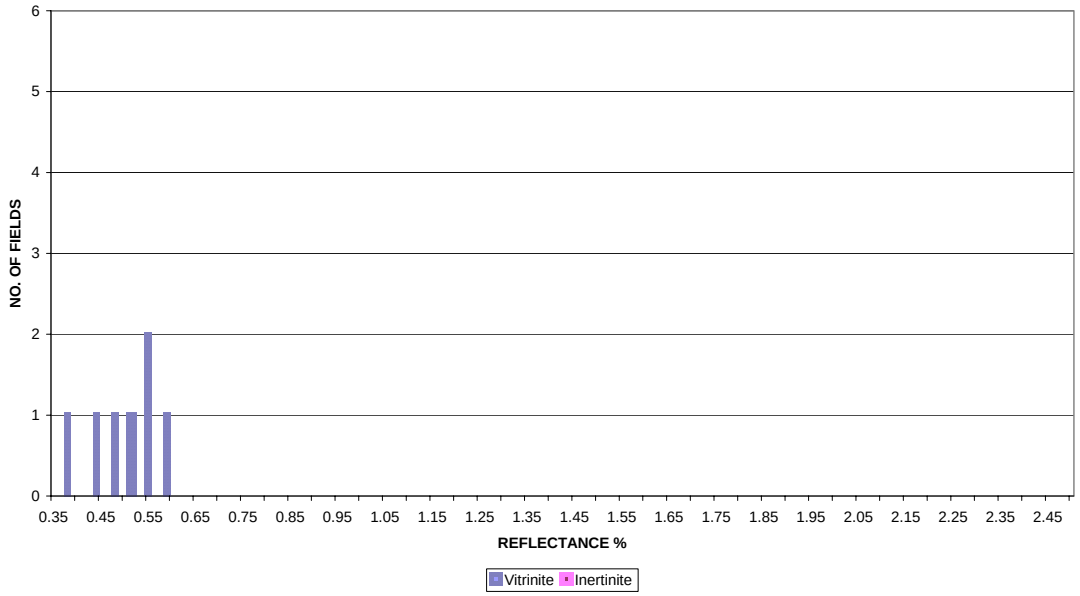
Maceral	No. of Readings	Mean	Standard Deviation
Vitrinite	2	0.45	0.025
Inertinite	1	1.76	

Trefoil 1 1890m, Ctgs



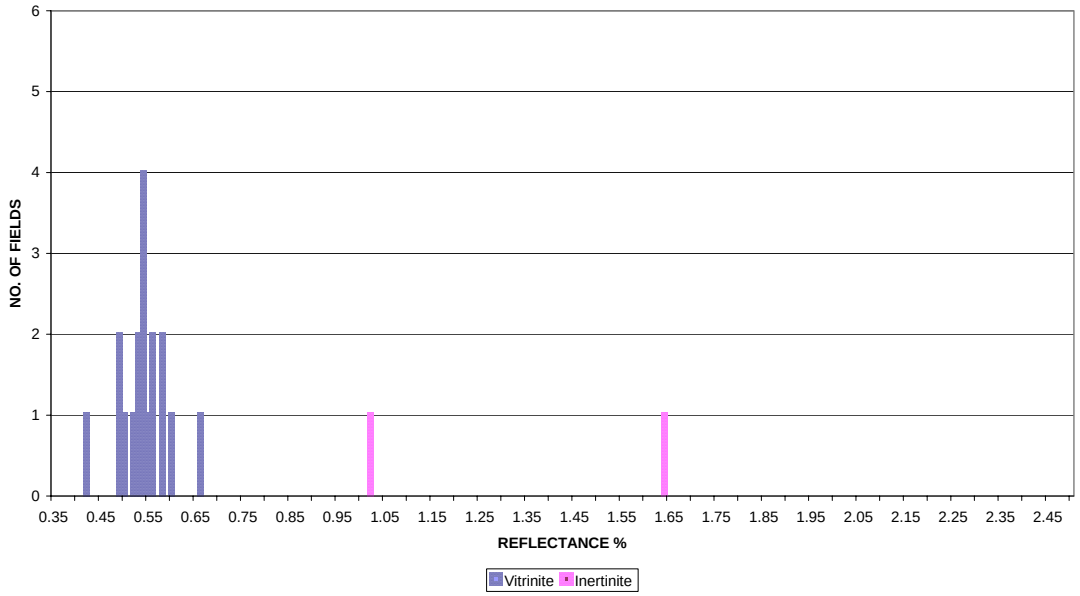
Maceral	No. of Readings	Mean	Standard Deviation
Vitrinite	3	0.51	0.042
Inertinite	1	0.98	

Trefoil 1 2136m, Ctgs



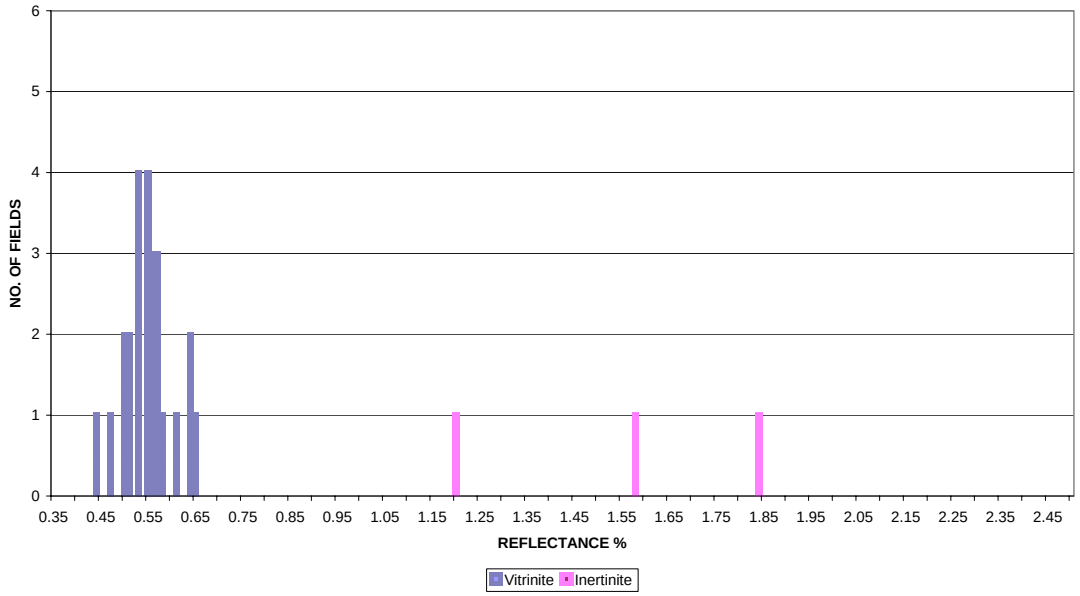
Maceral	No. of Readings	Mean	Standard Deviation
Vitrinite	8	0.50	0.063
Inertinite	0		

Trefoil 1 2322m, Ctgs



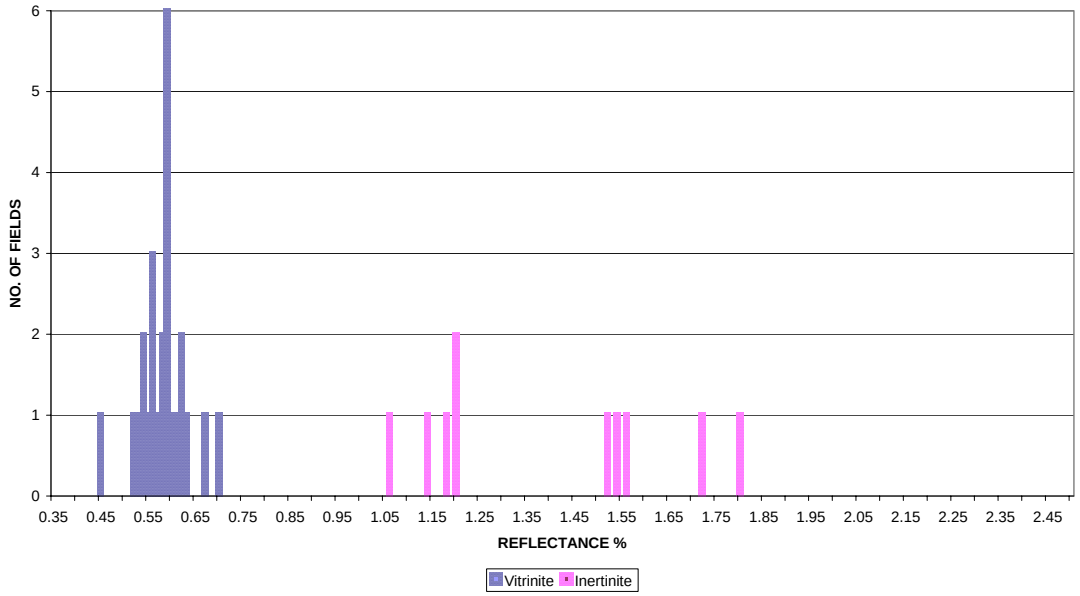
Maceral	No. of Readings	Mean	Standard Deviation
Vitrinite	18	0.54	0.049
Inertinite	2	1.33	0.310

Trefoil 1 2508m, Ctgs



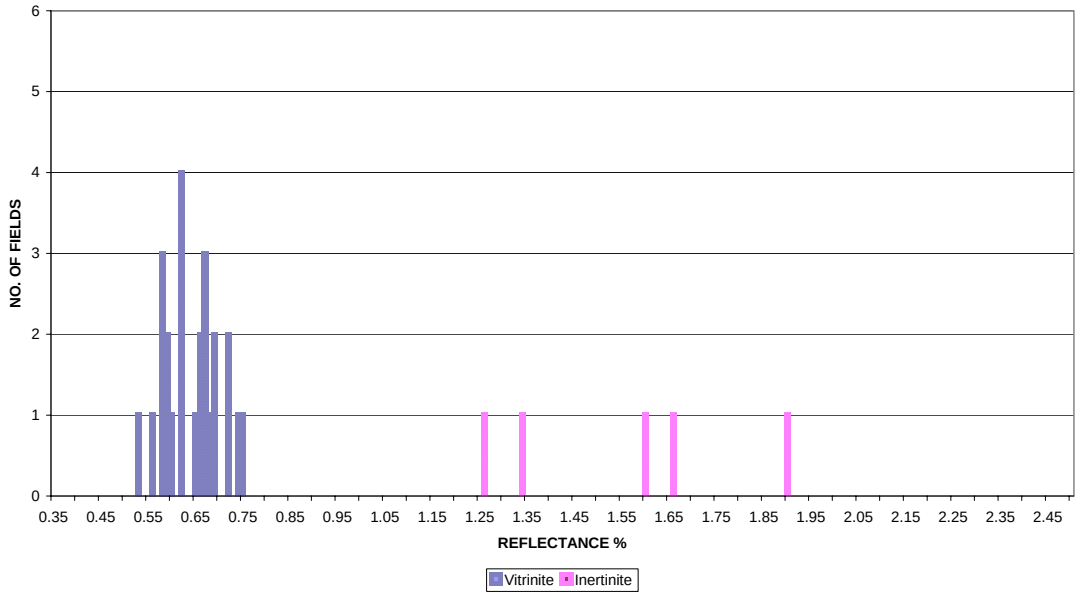
Maceral	No. of Readings	Mean	Standard Deviation
Vitrinite	25	0.55	0.049
Inertinite	3	1.54	0.263

Trefoil 1 2712m, Ctgs



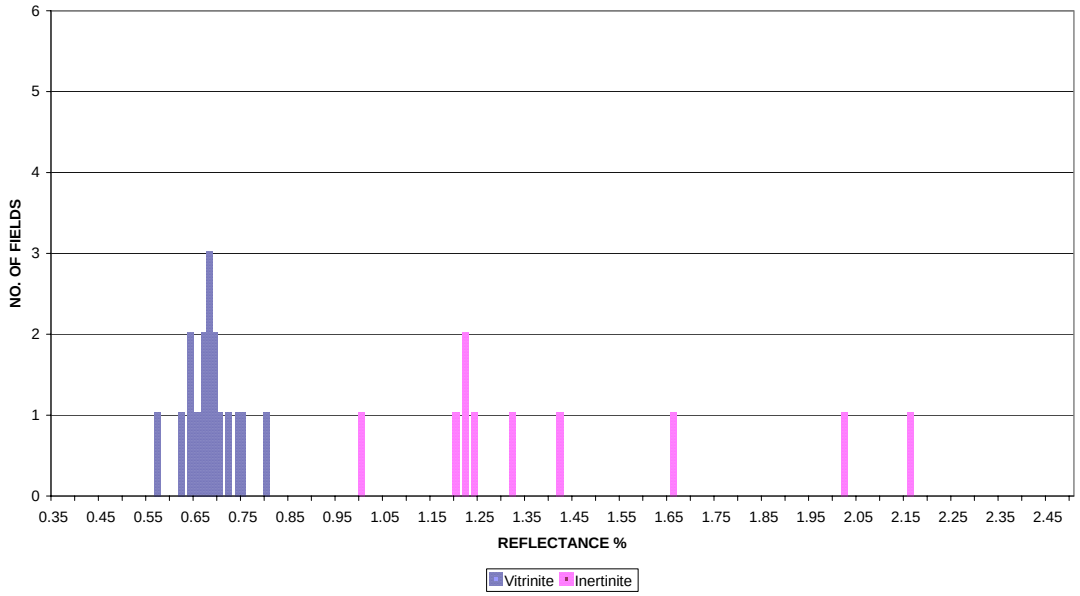
Maceral	No. of Readings	Mean	Standard Deviation
Vitrinite	25	0.58	0.048
Inertinite	10	1.39	0.252

Trefoil 1 2892m, Ctgs



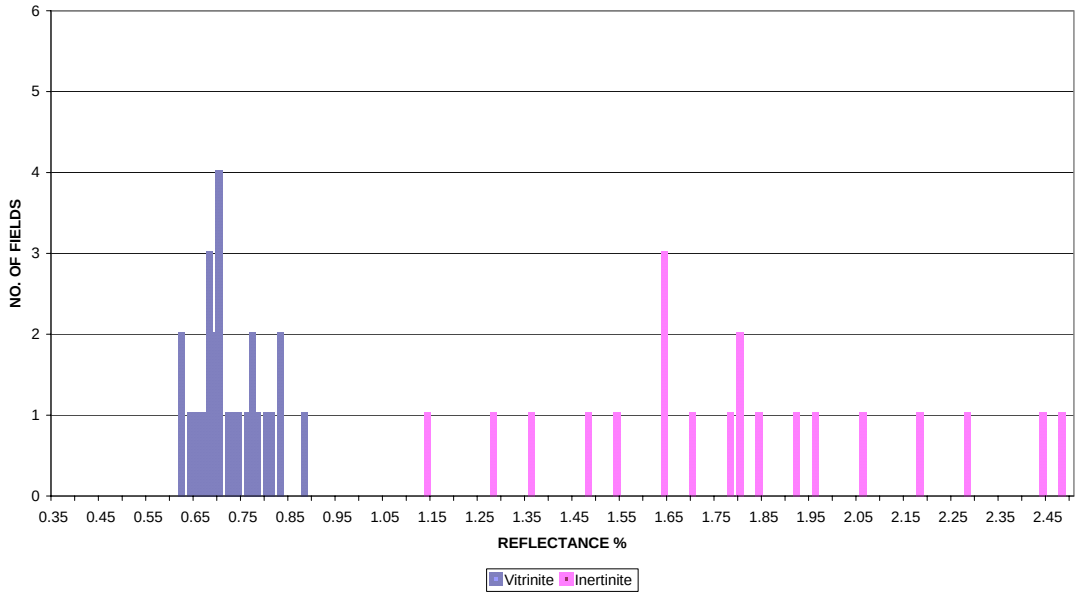
Maceral	No. of Readings	Mean	Standard Deviation
Vitrinite	25	0.64	0.057
Inertinite	5	1.55	0.230

Trefoil 1 3105m, Ctgs



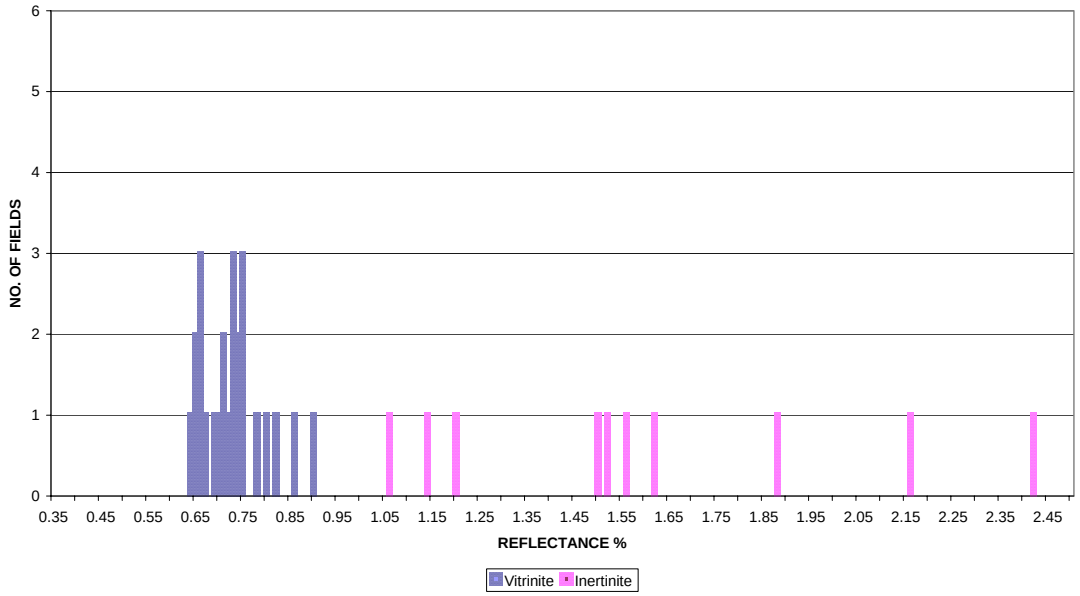
Maceral	No. of Readings	Mean	Standard Deviation
Vitrinite	18	0.68	0.050
Inertinite	10	1.45	0.361

Trefoil 1 3324m, Ctgs



Maceral	No. of Readings	Mean	Standard Deviation
Vitrinite	27	0.72	0.067
Inertinite	20	1.80	0.354

Trefoil 1 3492m, Ctgs



Maceral	No. of Readings	Mean	Standard Deviation
Vitrinite	25	0.73	0.065
Inertinite	10	1.61	0.418

APPENDIX 6: PALYNOLOGY REPORT

PALYNOLOGY OF

TREFOIL-1

BASS BASIN, AUSTRALIA

by

ROGER MORGAN

Prepared for
ORIGIN ENERGY

April 2005

REF: BAS.TREFOIL-1 REPORT

PALYNOLOGY OF

TREFOIL-1

BASS BASIN, AUSTRALIA

CONTENTS **PAGE**

1	SUMMARY	3
2	INTRODUCTION	4
3	PALYNOSTRATIGRAPHY	8
4	REFERENCES	14

Table 1 Individual Sample Summary, Trefoil-1

Figure 1 Tertiary Zonation Scheme (Partridge 1976)
Figure 2 Maturity Profile, Trefoil-1

Enclosure 1 Species distribution chart

1 SUMMARY

2322 m (cutts) : ?*N. asperus* Zone : Middle Eocene : marginal marine lagoon : marginal mature

2433 m (cutts) *: P. asperopolus* Zone : Middle Eocene : ?marginal marine lagoon : marginal mature

2508 m (cutts) : *M. diversus* Zone, upper subone : Early Eocene : marginal marine lagoon : marginal mature

2559 m (cutts) : *M. diversus* Zone, middle subzone : Early Eocene : marginal marine : marginal mature

2616 m (cutts) – 2685 m (cutts) : *M. diversus* Zone, lower subzone : Early Eocene : nearshore to shelfal marine : marginal mature

2694 m (cutts) – 2775 m (cutts) : *L. balmei* Zone, upper subzone : Paleocene : mostly marginal marine lagoon : early mature for oil, early marginal mature for gas/condensate

2868 m (cutts) – 3048 m (cutts) : *L. balmei* Zone, lower subzone : Paleocene : mostly non-marine lakes and floodplain : early mature for oil, early marginal mature for gas/condensate

3060 m (cutts) – 3162 m (cutts) : *F. longus* Zone, upper subzone : Maastrichtian : ?non-marine floodplain : early mature for oil, early marginal mature for gas/condensate

3219 m (cutts) – 3360 m (cutts) : *F. longus* Zone, lower subzone : Maastrichtian : non-marine floodplain and swamp margin : mature for oil, early mature for gas/condensate

3375 m (cutts) – 3513 m (cuttts) : *T. lilliei* Zone : Maastrichtian-Campanian : non-marine floodplain : mature for oil, early mature for gas/condensate

2 INTRODUCTION

Six cuttings samples were studied in two batches as “hot samples” in Sale, Victoria, during drilling. Twenty-nine followup samples (27 cutts, 1 swc, 1 conventional core) have been studied since to provide routine correlation. This report incorpates all samples.

The Tertiary zonation framework is shown in Figure 1, from Partridge (1973) modified for the Bass Basin. The zonation was subsequently published as Partridge (1976) and privately circulated against the Haq time scale. Comparisons are made in the text with the earlier reports for Yolla-1 by Morgan (1985) and Yolla-4 by Morgan (2004).

Palaeoenvironmental assessments are based on specimen counts of 100 specimens, also providing a percentage content of all species. Criterea for the palaeo-environmental subdivisions are given on Table 1. Backup data (listing % content of major plant groups) is given as Table 2. In running text, rare = <1-3%, frequent = 4-10%, common = 11-30%, abundant = 31-50% and superabundant = 51-100%.

Maturity data was generated in the form of Spore Colour Index, and are plotted on Figure 2 Maturity Profile, Trefoil-1. The oil and gas windows follow the general consensus of geochemical literature. The oil window corresponds to spore colours of light-mid brown (Staplin Spore Colour Inex of 2.7) to dark brown (3.6) equal to vitrinite reflectanus of 0.6% to 1.3%.

.

TABLE 1

SUMMARY OF PALYNOLOGICAL DATA : TREFOIL-1

LOG DEPTH (m)	SAMPLE TYPE	MICROFOSSIL YIELD	PERCENTAGE				DIVERSITY *1		SPORE-POLLEN SUBZONE	DINOFLAGELLATE ZONE/ACME	ENVIRONMENT*2
			MICROPLANKTON			SPORE-POLLEN-	SALINE MICROPLANKTON	SPORE-POLLEN			
			SALINE DINOFLAG	SPINY AC.	FRESH ALGAE						
2322	CUTTS	VERY LOW	<1	0	40	60	EX LOW	HIGH	?N. ASPERUS		?MARGINAL MARINE LAGOON
2433	CUTTS	LOW	(2)	0	20	78	EX LOW	HIGH	P. ASPEROPOLUS		?MARGINAL MARINE LAGOON
2508	CUTTS	LOW	<1	0	13	87	EX LOW	HIGH	M. DIVERSUS, UPPER		?MARGINAL MARINE LAGOON
2559	CUTTS	LOW	2	0	5	93	LOW	HIGH	M. DIVERSUS, MIDDLE		MARGINAL MARINE
2616	CUTTS	MODERATE	35	2	24	39	MODERATE	MODERATE	M. DIVERSUS, LOWER		SHELFAL MARINE
2685	CUTTS	MODERATE	24	0	5	71	MODERATE	HIGH	M. DIVERSUS, LOWER		NEARSHORE MARINE
2694	CUTTS	LOW	7	0	1	92	MODERATE	HIGH	L. BALMEI, UPPER		VERY NEARSHORE MARINE
2712	CUTTS	LOW	<1	0	48	52	EX LOW	HIGH	L. BALMEI, UPPER		MARGINAL MARINE LAGOON
2741.72	CORE	LOW	3	0	32	65	LOW	HIGH	L. BALMEI, UPPER		MARGINAL MARINE LAGOON
2775	CUTTS	LOW	0	0	16	84	NIL	HIGH	L. BALMEI, UPPER		FRESHWATER LAKE
2868	CUTTS	LOW	0	0	0	100	NIL	HIGH	L. BALMEI, LOWER		NON-MARINE, FLOODPLAIN
2901	CUTTS	LOW	0	0	1	99	NIL	HIGH	L. BALMEI, LOWER		NON-MARINE, FLOODPLAIN
2925	CUTTS	LOW	0	0	3	97	NIL	HIGH	L. BALMEI, LOWER		NON-MARINE, FLOODPLAIN
2994.8	SWC	NEAR BARREN	-	-	-	-	-	-	-		-
3015	CUTTS	LOW	0	0	9	91	NIL	HIGH	L. BALMEI, LOWER		NON-MARINE, FLOODPLAIN
3021	CUTTS	LOW	3	0	22	75	EX LOW	HIGH	L. BALMEI, LOWER		MARGINAL MARINE LAGOON
3042	CUTTS	LOW	0	0	21	79	NIL	HIGH	L. BALMEI, LOWER		NON-MARINE, LAKE
3105	CUTTS	LOW	0	0	6	94	NIL	HIGH	F. LONGUS, UPPER		NON-MARINE, FLOODPLAIN
3048	CUTTS	LOW	0	0	2	98	NIL	HIGH	L. BLAMEI, LOWER		NON-MARINE, FLOODPLAIN
3060	CUTTS	LOW	(1)	0	12	87	EX LOW	HIGH	F. LONGUS, UPPER		NON-MARINE, FLOODPLAIN
3078	CUTTS	LOW	0	0	6	94	NIL	HIGH	F. LONGUS, UPPER		NON-MARINE, FLOODPLAIN
3093	CUTTS	LOW	0	0	5	95	NIL	HIGH	F. LONGUS, UPPER		NON-MARINE, FLOODPLAIN
3132	CUTTS	LOW	(1)	0	2	98	(EX LOW)	HIGH	F. LONGUS, UPPER		?NON-MARINE, FLOODPLAIN
3156	CUTTS	LOW	0	0	(<1)	100	(EX LOW)	HIGH	F. LONGUS, UPPER		?NON-MARINE, FLOODPLAIN
3162	CUTTS	LOW	(2)	0	9	89	(EX LOW)	HIGH	F. LONGUS, UPPER		?NON-MARINE, FLOODPLAIN
3219	CUTTS	LOW	0	0	8	92	NIL	HIGH	F. LONGUS, LOWER		NON-MARINE, SWAMP MARGIN
3255	CUTTS	LOW	0	0	3	97	NIL	HIGH	F. LONGUS, LOWER		NON-MAINE, SWAMP
3264	CUTTS	LOW	0	0	8	92	NIL	HIGH	F. LONGUS, LOWER		NON-MARINE, SWAMP MARGIN
3324	CUTTS	EX LOW	0	0	0	100	NIL	MODERATE	INDETERMINATE		NON-MARINE, FLOODPLAIN
3360	CUTTS	LOW	0	0	0	100	NIL	HIGH	F. LONGUS, LOWER		NON-MARINE, FLOODPLAIN
3375	CUTTS	LOW	0	0	5	95	NIL	HIGH	T. LILLIEI		NON-MARINE, FLOODPLAIN
3390	CUTTS	EX LOW	0	0	1	99	NIL	HIGH	INDETERMINATE		NON-MARINE, FLOODPLAIN
3492	CUTTS	LOW	0	0	0	100	NIL	HIGH	T. LILLIEI		NON-MARINE, FLOODPLAIN
3513	CUTTS	LOW	0	0	1	99	NIL	HIGH	T. LILLIEI		NON-MARINE, FLOODPLAIN

*1 DIVERSITY	
V HIGH	30+ SPECIES
HIGH	20-29 SPECIES
MOD	10-19 SPECIES
LOW	5-9 SPECIES
EX LOW	1-4 SPECIES

*2 ENVIRONMENTS	DINOFLAGELLATE CONTENT%	DINOFLAGELLATE DIVERSITY	FRESHWATER ALGAE CONTENT %
OFFSHORE MARINE	67 to 100	VERY HIGH	LOW
SHELFAL MARINE	34 to 66	HIGH	"
NEARSHORE MARINE	11 to 33	MODERATE	"
VERY NEARSHORE MARINE	5 to 10	MODERATE-LOW	"
MARGINAL MARINE	<1 to 4	LOW-VERY LOW	"
BRACKISH	0, SPINY ACRITARCHS ONLY	EXTREMELY LOW	"
NON-MARINE (UNDIFF)	0, NO SPINY ACRITARCHS	NIL	LOW
NON-MARINE (LACUSTRINE)	0, NO SPINY ACRITARCHS	NIL	MODERATE 10%+

BRACKETS ( ) IN CUTTINGS INDICATES LIKELY CAVING

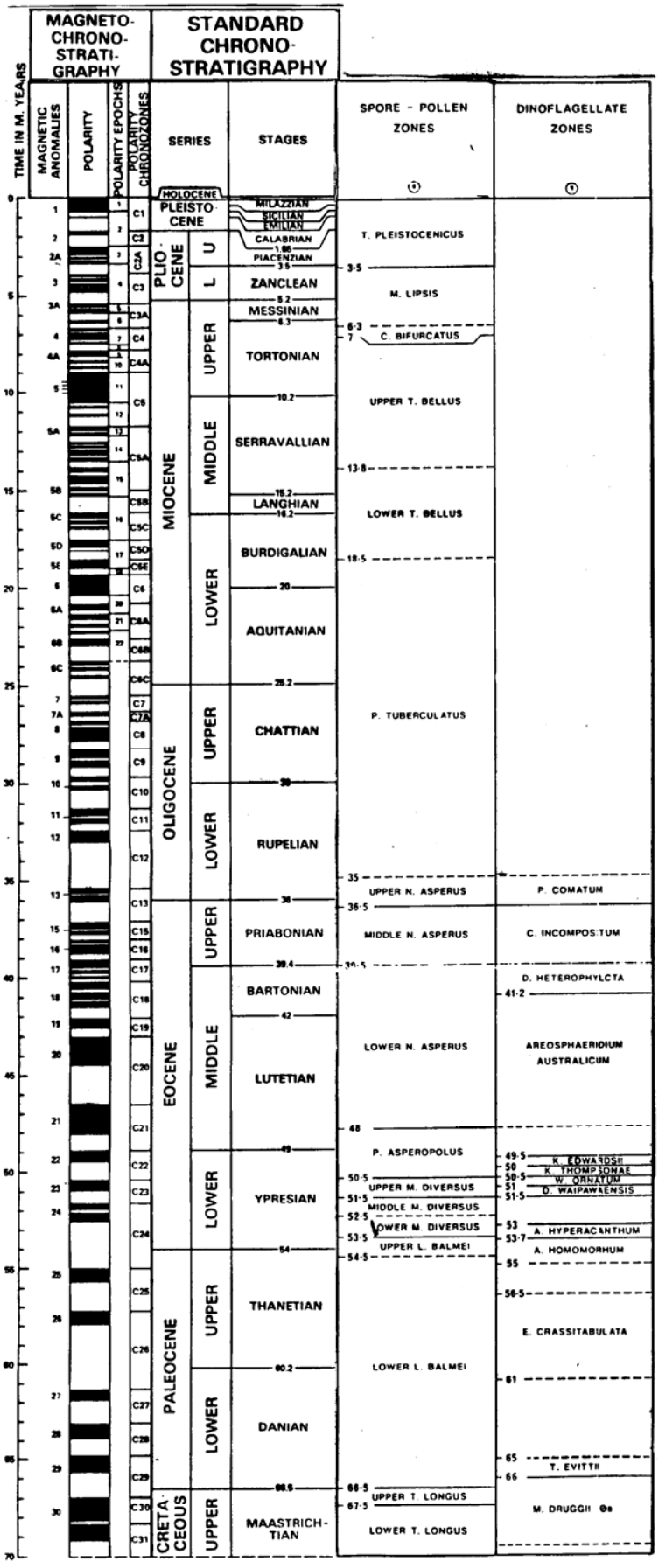
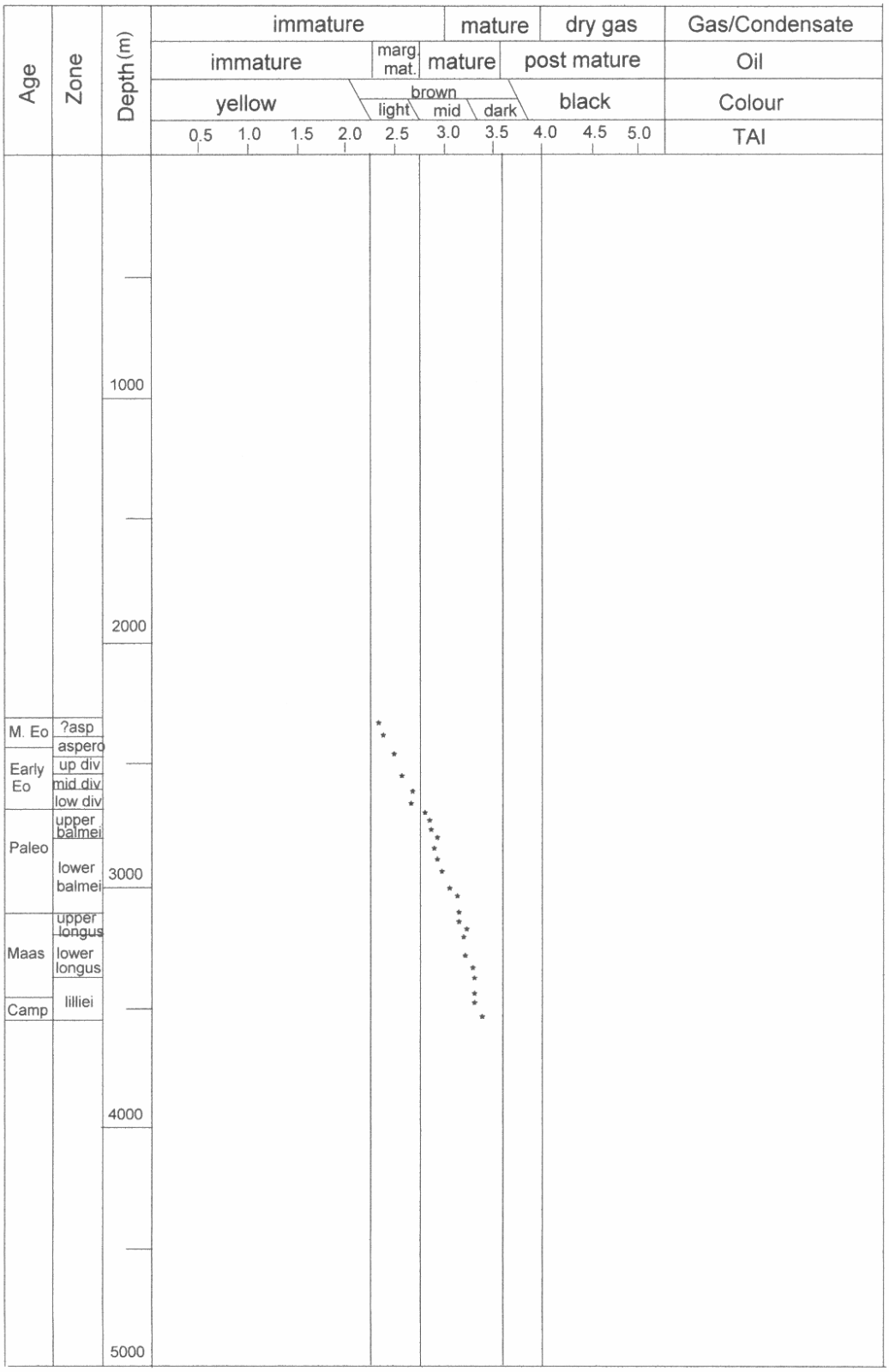


FIGURE 1 **TERTIARY ZONATION SCHEME (Partridge 1976 and pers. comm. using time scale of Haq et al)**

FIGURE 2 MATURITY PROFILE : TREFOIL-1



3 PALYNOSTRATIGRAPHY

3.1 2322 m (cutts) : ?*N. asperus* Zone

This lean and low diversity assemblage is not confidently assigned but the presence of common *Nothofagidites* spp. without older markers suggest the assignment. Common are *Falcisporites similis, Nothofagidites* (especially *N. flemingii*) and *Vitreisporites pallidus*. Other elements are rare and long-ranging include *Phyllocladidites mawsonii* and *Verrucosisporites kopukensis.*

Microplankton are common but are almost entirely the freshwater alga *Botryococcus* suggesting a significant large lake. However, rare saline dinoflagellates include *Spiniferites ramosus* and *Operculodinium centrocarpum*. These might be caved as this sample is ditch cuttings, but if in place indicate marginal marine lagoonal environments.

Light brown spore colours suggest marginal maturity for oil, but immaturity for gas/condensate.

3.2 2433 m (cutts) : *P. asperopolus* Zone

Zonal assignment is suggested by the downhole influx of *Haloragacidites harrisii* (the "*harrisii* reversal" of Stover and Partridge) and youngest *Intratriporopollenites notabilis, Proteacidites grandis, Proteacidites tuberculiformis* and *Proteacidites ornatus*. Common are *F. similis, H. harrisii* and *Nothofagidites emarcidus* with frequent *Cyathidites minor, N. flemingii, Proteacidites* spp. and *V. pallidus*. Rare elements not mentioned above include *Cicatricosisporites australiensis* and *Proteacidites kopiensis*.

Microplankton are common but comprise mostly the freshwater alga *Botryococcus* suggesting a significant lake However, rare saline dinoflagellates (*Diphes colligerum, Phthanoperidinium comatum* and *S. ramosus*) suggest marginal marine conditions, but these could be caved. If any of these are in place, marginal marine lagoonal environments are likely.

Light brown spore colours suggest marginal maturity for oil but immaturity for gas/condensate.

3.3 2508 m (cutts) : *M. diversus* Zone, upper subzone

Assignment is indicated by oldest *Proteacidites pachypolus* considered to be in place, although this could conceivably be caved slightly. Common are *F. similis* and *H. harrisii* with frequent *Araucariacites australis, C. minor, Microcachryidites antarcticus, N. emarcidus* and *Proteacidites* spp. Rare elements include *I. notabilis, Malvacipollis subtilis, P. grandis, P. ornatus, P. pachypolus, Sapotaceodaepollenites rotundus* and *Spinozonocolpites prominatus.*

Microplankton include common freshwater *Botryococcus* suggesting a large lake. However, rare marine dinoflagellates (*S. ramosus*) and the possibly freshwater dinoflagellate *Morkallacysta* sp. suggest marginal marine environments. If the marine dinoflagellates are in place and not caved, a marginal marine lagoon seems likely.

Light brown spore colours suggest marginal maturity for oil but immaturity for gas/condensate.

3.4 2559 m (cutts) : *M. diversus* Zone, middle subzone

Assignment is indicated by oldest *P. tuberculiformis* without younger markers. Other oldest occurrences usually indicating the base of the lower subzone include *I. notabilis* and *S. prominatus*. Common are *H. harrisii* and *N. flemingii* with frequent *A. australis, Cyathidites australis, C. minor, F. similis, M. subtilis, M. antarcticus, Proteacidites* spp. and *P. grandis*. Rare elements include *I. notabilis, P. ornatus, P. tuberculiformis* and *S. prominatus*.

Microplankton are minor but include freshwater types (*Botryococcus, Morkallacysta, Cyclopsiella vieta* and minor saline dinoflagellates (*Apectodinium homomorphum, Oligosphaeridium, Spiniferites*) and suggest marginal marine environments if they are in place.

Light brown spore colours suggest marginal maturity for oil but immaturity for gas/condensate.

3.5 2616 m (cutts) – 2685 m (cutts) : *M. diversus* Zone, lower subzone

Assignment is indicated by the absence of younger markers considered in place, and the lack of older markers, and confirmed by the dinoflagellates. Considered caved are single specimens of *P. ornatus* at 2616 m and *P. pachypolus* at 2685 m. At 2616 m, frequent are *C. minor* and *F. similis* with rare elements including *P. ornatus* and *P. grandis*. Dinoflagellates are abundant. At 2685 m, common are *A. australis, C. minor* and *F. similis* with frequent *Proteacidites* spp. and *V. pallidus*. Rare elements include *Malvacipollis diversus, P. grandis* and the single caved *P. pachypolus.* Dinoflagellates are common.

Microplankton are abundant to common and comprise mostly dinoflagellates.

At 2616 m, common are *Apectodinium homomorphum, Morkallacysta* sp. and *S. ramosus*, with frequent *Cordosphaeridium fibrospinosum*. Rare elements include *Adnatosphaeridium* sp., *Muratodinium fimbriatum, Thalassiphora pelagica* and *Wetzeliella articulata*. Top common *Morkallacysta* sp. ocurs in Yolla-1 at 2711 m and Yolla-4 at 2859 m in the lower *M. diversus* subzone.

At 2685 m, frequent are *A. homomorphum, C. multispinosum* and *S. ramosus* with rare elements including *Adnatosphaeridium* sp. *M. fimbriatum* and *W. articulata*. Frequent *Apectodinium* below common *Morkallacysta* sp. occurs in Yolla-1 at 2783 m and Yolla-4 at 2925 m in the lower *M. diversus* subzone.

Nearshore (2685 m) to shelfal (2616 m) marine environments are indicated by the common and diverse dinoflagellates even assuming that the flood of *Morkallacysta* sp. is sourced from nearby fresh water. Spores and pollen are still common and diverse.

Light brown spore colours suggest marginal maturity for oil but immaturity for gas/condensate.

3.6 2694 m (cutts) – 2775 m (cutts) : *L. balmei* Zone, upper subzone

Assignment is indicated at the top by youngest *Gambierina rudata* and *Lygistepollenites balmei* and at the base by oldest *P. grandis* (possibly partly caved) confirmed by oldest *Proteacidites incurvatus* and *Cyathidites gigantis* at 2712 m. Common are *C. minor, Dilwynites granulatus, F. similis* with frequent *M. antarcticus, P. mawsonii* and *V. pallidus*. Intermittently frequent are *Australopollis*

obscurus (2694 m) and *Stereisporites antiquasporites* (2775 m). Rare elements include *C. gigantis, G. rudata, L. balmei, P. grandis, P. incurvatus* and *Peninsulapollis gillii*.

Microplankton are minor at 2694 m, but common below where *Morkallacysta* sp. occurs in flood proportions, as it does in the upper *L. balmei* subzone in Yolla-1. *Saeptodinium* spp. are also frequent and may also be freshwater. Also present in minor porportions (but absent at 2775 m) are saline dinoflagellates with the most persistent being *Cordosphaeridium, Hystrichodinium tubiferum* and *S. ramosus.* These indicate marginal marine environments if in place. Marginal marine lagoon conditions seem most likely at 2712 m and 2741.72 m. Frequent saline dinoflagellates suggest very nearshore marine at 2695 m and absent saline dinoflagellates suggest non-marine lake at 2775 m.

Mid brown spore colours indicate early maturity for oil and early marginal maturity for gas/condensate.

3.7 2868 m (cutts) – 3040 m (cutts) : *L. balmei* Zone, lower subzone

Assignment is indicated at the top by the absence of younger markers and confirmed by youngest *Tetracolporites verrucosus* at 2901 m, and at the base by the absence of older markers. Abundant is *F. similis* with common *M. antarcticus* and *P. mawsonii* and frequent *C. australis, C. minor, D. granulatus* and *V. pallidus*. Rare elements include *G. rudata, L. balmei, P. gillii* and *T. verrucosus*.

Microplankton are mostly minor and mostly freshwater (*Botryococcus, Morkallacysta* sp., *Saeptodinium* suggesting non-marine floodplain) with the only saline dinoflagellates being *Escharisphaeridia* at 3021 m suggesting marginal marine lagoon. Freshwater algal maxima occur near the base of the interval (3015 m, 3021 m, 3042 m) suggesting large lake or lagoon developments.

Mid brown spore colours indicate early maturity for oil and early marginal maturity for gas/condensate.

3.8 3060 m (cutts) – 3162 m (cutts) : *F. longus* Zone, upper subzone

Assignment is indicated at the top by youngest *Forcipites longus* (3105 m)and *Grapnelispora evansii* (3060 m), coincident with a downhole decrease in *L. balmei* and increase in *G. rudata*. The base is marked by a downhole decrease in *G. rudata* above a downhole increase of *N. endurus* with oldest *Stereisporites punctatus* considered in place a short distance above (at 3156 m). Within the interval, common is *F. similis* with frequent *A. australis, C. minor, D. granulatus, M. antarcticus, P. mawsonii, Proteacidites* and *V. pallidus*. Rare elements include *A. obscurus, Camarazonosporites ohaiensis, F. longus, G. evansii, P. gillii, Tricolpites confessus* and *Tricolpites waiparaensis.*

Microplankton are rare and are mostly freshwater (*Botryococcus, Morkallacysta, Saeptodinium*) but may be largely caved. Very rare saline dinoflagellates are considered all caved from the rich Eocene assemblages above. Saccate pollen dominance suggests floodplain conditions.

Mid brown spore colours indicate early maturity for oil and early marginal maturity for gas/condensate.

3.9 3219 m (cutts) – 3360 m (cutts) : *F. longus* Zone, lower subzone

Assignment is indicated at the top by the downhole influx of *N. endurus* and at the base by oldest consistent *F. longus* above youngest *Forcipites sabulosus*. Youngest *Tubuliforidites lilliei* occurs at 3219 m and oldest *T. verrucosus* occurs at 3264 m. Oldest consistent *F. longus* occurs at 3375 m with *Triporopollenites "megasectilis"* (an unpublished species mainly seen near the base of the *F. longus* Zone). It is possible that the base of the zone is picked slightly too high but in cuttings it is not possible to be more definitive. Common to abundant is *F. similis* with common *C. australis, C. minor* and *N. endurus*, and frequent *G. rudata, P. gillii, P. mawsonii* and *V. pallidus*. Rare elements include *F. longus, G. evansii* (down to 3264 m), *Tricolpites confessus, T. verrucosus* and *T. lilliei*. A single *S. punctatus* at 3264 m and *L. balmei* at 3255 m are considered caved.

Microplankton are minor and all freshwater (*Botryococcus* and probably partly caved *Saeptodinium* sp.). Common saccate pollen suggest dry floodplain, while co-dominant spores and saccate pollen suggest swamp margin.

Mid to dark brown spore colours indicate maturity for oil and maturity for gas/condensate.

3.10 3375 m (cutts) – 3513 m (cutts) : *T. lilliei* Zone

Assignment is indicated at the top by youngest *Forcipites sabulosus* and the same sample sample contains oldest consistent *F. longus* and *T. "megasectilis"*. These events normally mark the base of the *F. longus* Zone and so are considered here to be caved slightly. The base is assigned on oldest *Battenipollis sectilis*. Abundant is *F. similis* with common *C. minor* and *M. antarcticus*, and frequent *D. granulatus, P. mawsonii* and *Proteacidites* spp. Rare elements include *G. rudata, P. gillii, B. sectilis* and *T. lilliei*.

Microplankton are extremely rare and comprise freshwater taxa (*Botryococcus* and probably partly caved *Saeptodinium* spp.) Non-marine elements are therefore indicated and with common saccate pollen and rare freshwater algae, dry floodplain conditions seem likely.

Mid to dark brown spore colours indicate maturity for oil and maturity for gas/condensate.

4 REFERENCES

Morgan, R.P., (1985) Palynology of Amoco Yolla-1, Bass Basin, Australia unpubl rept for Amoco Australia

Morgan, R.P., (2004) Palynology of Yolla-4, Bass Basin, Australia unpubl. rept. for Origin

Partridge, A D (1973) Revision of the spore-pollen zonation in the Bass Basin, Esso unpubl. palaeo. rept. 1973/4

Partridge, A D (1976) The geological expression of eustacy in the Early Tertiary of the Gippsland Basin Aust. Pet. Explor. Assoc., J, 16:73-79

Well Name : TREFOIL-1

Operator : ORIGIN ENERGY
Interval : 2302m - 3533m
Scale : 1:5000
Chart date: 26 August 2005

Palynological Data Chart : BASIC DATA
% Abundance histogram : Highest occurrence
Roger Morgan

TREFOIL-1

Morgan Palaeo Associates
Maitland, South Australia

Enclosure 1

Sampling
Cutting
Core
Sidewall core

Text Keys
*1 % within discipline (40mm=100%)
*2 In-Situ occurrences

Depth | **Samples** (Samples in Discipline(s): Paly)

Dinoflagellate Cysts — % within discipline (40mm=100%); In-Situ occurrences

Operculodinium centrocarpum
Spiniferites ramosus
Diphyes colligerum
Phthanoperidinium comatum
Morkallacysta spp.
Apectodinium homomorphum
Cribroperidinium sp.
Cyclopsiella vieta
Oligosphaeridium complex
Achomosphaera alcicornu
Adnatosphaeridium sp.
Apectodinium homomorphum (long spines)
Apectodinium pentagonum
Apectodinium sumissima
Cordosphaeridium fibrospinosum
Homotryblium tasmaniense
Muratodinium fimbriatum
Systematophora placacantha
Thalassiphora pelagica
Wetzeliella articulata
Areoligera spp.
Cleistosphaeridium spp.
Cordosphaeridium multispinosum
Gotnisiella borussica
Glaphyrocysta sp.
Hystrichosphaeridium tubiferum
Septodinium spp.
Cordosphaeridium inodes
Eocharlesphaeridia spp.
Kokerisporites polypes
Microforams.

FT — *1 *2

AL — *1 *2
Circulosporites sp.
Rimosicysta kupperii

ALBO — *1 *2
Botryococcus spp.

MP — *1 *2
Reworking - Permian
Reworking - Triassic

Spores And Pollen — % within discipline (40mm=100%); In-Situ occurrences

Araucariacites australis
Cyathidites australis
Cyathidites minor
Cyathidites splendens
Dictyophyllidites spp.
Dilwynites granulatus
Dilwynites tuberculatus
Ericipites scabratus
Falcisporites similis
Laevigatosporites ovatus
Microcachryidites antarcticus
Nothofagidites brachyspirulosus
Nothofagidites emarcidus
Nothofagidites flemingii
Osmundacidites wellmanii
Phyllocladidites mawsonii
Podosporites microsaccatus
Proteacidites grandis
Proteacidites spp.
Verrucosisporites kopukuensis
Vitreisporites pallidus
Australopollis obscurus
Cicatricosisporites australiensis
Cycadopites follicularis
Dilwynites "pusillum"
Gleicheniidites spp.
Haloragacidites harrisii
Intratriporopollenites notabilis
Lygistepollenites florinii
Proteacidites kopiensis
Proteacidites ornatus
Proteacidites pseudomoides
Proteacidites tuberculiformis
Retitriletes austroclavatidites
Stereisporites antiquasporites
Malvacipollis subtilis
Nothofagidites deminutus
Proteacidites pachypolus
Sapotaceoidaepollenites rotundus
Spinozonocolpites prominatus
Stereisporites punctatus
Falcisporites grandis
Periporopollenites polyoratus
Tricolpites phillipsii
Clavifera triplex
Proteacidites incurvatus
Proteacidites reticuloscabratus
Malvacipollis diversus
Gambierina rudata
Lygistepollenites balmei
Peninsulapollis gillii
Phyllocladidites verrucatus
Cameronzonosporites ohaiensis
Cyathidites gigantis
Gambierina edwardsii
Proteacidites palisadus
Annulisporites folliculosa
Ceratosporites equalis
Cingutriletes clavus
Nothofagidites endurus
Tetracolporites verrucosus
Triporoletes reticulatus
Perotriletes jubatus/morganii
Callialasporites dampieri
Callialasporites turbatus
Contignisporites cooksoniae
Corollina torosa
Grapnelispora evansii
Forcipites longus
Batten ipollis sectilis
Perinopollenites elatoides
Tricolpites confessus
Tricolpites waiparaensis
Aequitriradites spinulosus
Tubulifloridites lilliei
Forcipites sabulosus
Forcipites stipulatus
Triporoletes simplex
Triporopollenites "megasectilis"
Stereisporites regium
Cicatricosisporites ludbrookiae
Tubulifloridites cf. lilliei
Fungae .

FU — *1 *2

Samples (Samples in Discipline(s): Paly)

Depth	Samples	Total Count	% Category
2350m	2322.00m CU	95	
2400m	2433.00m CU	100	
2450m			
2500m	2508.00m CU	93	
2550m	2559.00m CU	100	
2600m	2616.00m CU	94	
2650m			
2700m	2685.00m CU	89	
	2694.00m CU	100	
	2712.00m CU	106	
2750m	2741.72m CO	100	
	2775.00m CU	100	
2800m			
2850m			
	2868.00m CU	100	
2900m	2901.00m CU	100	
	2925.00m CU	100	
2950m			
3000m	2994.80m SC	14	
	3015.00m CU	100	
	3021.00m CU	100	
	3042.00m CU	100	
3050m	3048.00m CU	100	
	3060.00m CU	100	
	3078.00m CU	100	
3100m	3093.00m CU	100	
	3105.00m CU	100	
	3132.00m CU	100	
3150m	3156.00m CU	100	
	3162.00m CU	100	
3200m			
	3219.00m CU	100	
3250m	3255.00m CU	100	
	3264.00m CU	100	
3300m			
	3324.00m CU	52	
3350m	3360.00m CU	79	
	3375.00m CU	93	
3400m	3390.00m CU	116	
3450m			
	3492.00m CU	70	
3500m	3513.00m CU	74	

Total Count — In-Situ occurrences; Total count: Total Count

% Category — In-Situ occurrences; Category %: % Category

FU
MP
AL
FT
DC
ALBO
SP

Well Name : TREFOIL-1

Operator : ORIGIN ENERGY

Interval : 2302m - 3533m — **Palynological Data Chart : INTERPRETIVE DATA**

Scale : 1:5000 — **% Abundance histogram : Highest occurrence**

Chart date: 26 August 2005 — **Roger Morgan**

TREFOIL-1

Morgan Palaeo Associates
Maitland, South Australia

Enclosure 1

Sampling
Cutting
Core
Sidewall core

Text Keys
*1 % within discipline (40mm=100%)
*2 In-Situ occurrences

Depth | **Samples** (Samples in Discipline(s) : Paly) | **Chronostratigraphy** Age | **Miospore Zones** Zone

Dinoflagellate Cysts — % within discipline (40mm=100%); In-Situ occurrences (*2)

Operculodinium centrocarpum
Spiniferites ramosus
Diphyes colligerum
Phthanoperidinium comatum
Monkallacysta spp.
Apectodinium homomorphum
Cribroperidinium sp.
Cyclopsiella vieta
Oligosphaeridium complex
Achomosphaera alcicornu
Adnatosphaeridium sp.
Apectodinium homomorphum (long spines)
Apectodinium pentagonum
Apectodinium sumissima
Homotryblium tasmaniense
Homotryblium vallense
Muratodinium fimbriatum
Systematophora placacantha
Thalassiphora pelagica
Wetzeliella articulata
Apteodinium spp.
Cleistosphaeridium spp.
Cordosphaeridium multispinosum
Rottnestia borussica
Glaphyrocysta sp.
Hystrichosphaeridium tubiferum
Saeptodinium spp.
Cordosphaeridium inodes
Escharisphaeridia spp.
Kokaniasum polypes
Microdinums

FT (*1 *2)

AL — *Circulosporites sp.* (*1 *2); *Rimosocysta klaszii*

ALBO — *Botryococcus spp.* (*1 *2)

MP (*1 *2)

Reworking - Permian
Reworking - Triassic
Araucariacites australis
Cyathidites australis
Cyathidites minor
Cyathidites splendens
Dictyophyllidites spp.
Dilwynites granulatus
Dilwynites tuberculatus
Ericipites scabratus
Falcisporites similis

Spores And Pollen — % within discipline (40mm=100%); In-Situ occurrences (*2)

Laevigatosporites ovatus
Microcachryidites antarcticus
Nothofagidites brachyspinulosus
Nothofagidites emarcidus
Nothofagidites flemingii
Osmundacidites wellmanii
Phyllocladidites mawsonii
Podosporites microsaccatus
Proteacidites grandis
Proteacidites spp.
Verrucosisporites kopukuensis
Vitreisporites pallidus
Australopollis obscurus
Cicatricosisporites australiensis
Cycadopites follicularis
Dilwynites "pusillum"
Gleicheniidites spp.
Haloragacidites harrisii
Intratriporopollenites notabilis
Lygistepollenites florinii
Proteacidites kopiensis
Proteacidites ornatus
Proteacidites pseudomoides
Proteacidites tuberculiformis
Retitrilites austroclavatidites
Stereisporites antiquasporites
Malvacipollis subtilis
Nothofagidites deminutus
Proteacidites pachypolus
Sapotaceoidaepollenites rotundus
Spinozonocolpites prominatus
Stereisporites punctatus
Falcisporites grandis
Periporopollenites polyoratus
Tricolpites phillipsii
Clavifera triplex
Proteacidites incurvatus
Proteacidites reticulocabratus
Malvacipollis diversus
Gambierina rudata
Lygistepollenites balmei
Peninsulapollis gillii
Phyllocladidites verrucatus
Cameronzonosporites ohaiensis
Cyathidites giganteus
Gambierina edwardsii
Proteacidites palisadus
Annulisporites folliculosa
Ceratosporites equalis
Cingutriletes clavus
Nothofagidites endurus
Tetracolporites verrucosus
Triporoletes reticulatus
Periretilites jubatusmorganii
Cellulosisporites pseudolevis
Callialasporites turbatus
Corollina torosa
Grapnelispora evansii
Forcipites longus
Battenipollis sectilis
Perinopollenites elatoides
Tricolpites confessus
Tricolpites waiparaensis
Aequitriradites spinulosus
Tubulifloridites lilliei
Forcipites sabulosus
Forcipites stipulatus
Triporoletes simplex
Triporopollenites "megasectilis"
Stereisporites regium
Cicatricosporites ludbrookiae
Tubulifloridites cf. lilliei
Fungae

FU (*1 *2)

Samples (Samples in Discipline(s) : Paly)

Total Count — In-Situ occurrences — Total count: Total Count (100)

% Category — In-Situ occurrences — Category %: % Category

FU
MP
AL
FT
DC
ALBO
SP

Depth	Age	Zone	Samples	Total Count
2322.00m CU	Middle Eocene	?N. asperus	2322.00m CU	95
2433.00m CU		P. asperopolus	2433.00m CU	100
2508.00m CU	Early Eocene	M. diversus, upper	2508.00m CU	93
2559.00m CU		M. diversus, middle	2559.00m CU	100
2616.00m CU		M. diversus, lower	2616.00m CU	94
2685.00m CU	Paleocene	L. balmei, upper	2685.00m CU	89
2694.00m CU			2694.00m CU	100
2712.00m CU			2712.00m CU	106
2741.72m CO			2741.72m CO	100
2775.00m CU			2775.00m CU	100
2868.00m CU		L. balmei, lower	2868.00m CU	100
2901.00m CU			2901.00m CU	100
2925.00m CU			2925.00m CU	100
2994.80m SC			2994.80m SC	14
3015.00m CU			3015.00m CU	100
3021.00m CU			3021.00m CU	100
3042.00m CU			3042.00m CU	100
3048.00m CU		F. longus, upper	3048.00m CU	100
3060.00m CU	Maastrichtian		3060.00m CU	100
3078.00m CU			3078.00m CU	100
3093.00m CU			3093.00m CU	100
3105.00m CU			3105.00m CU	100
3132.00m CU			3132.00m CU	100
3156.00m CU			3156.00m CU	100
3162.00m CU		F. longus, lower	3162.00m CU	100
3219.00m CU			3219.00m CU	100
3255.00m CU			3255.00m CU	100
3264.00m CU			3264.00m CU	100
3324.00m CU			3324.00m CU	52
3360.00m CU		T. lilliei	3360.00m CU	78
3375.00m CU	Maastrichtian - Campanian		3375.00m CU	93
3390.00m CU			3390.00m CU	116
3492.00m CU			3492.00m CU	70
3513.00m CU			3513.00m CU	74

APPENDIX 7: PETROLOGY REPORT

RESERVOIR SOLUTIONS PTY LTD
LEVEL 2, 2 PARK RD, MILTON, 4064, QLD
PO BOX 2098, MILTON, 4064, QLD
ABN 27 088 995 073

PETROLOGY, DIAGENESIS AND RESERVOIR QUALITY OF MSCT SAMPLES FROM TREFOIL-1

Julian C. Baker PhD

A report to:

Origin Energy Resources Ltd
339 Coronation Drive
Milton QLD 4064

29 March, 2005

C O N T E N T S

Page

EXECUTIVE SUMMARY **1**

1. INTRODUCTION **2**

2. ANALYTICAL PROGRAM

2.1 THIN-SECTION ANALYSIS 2

2.2 X-RAY DIFFRACTION ANALYSIS 2

2.3 SCANNING ELECTRON MICROSCOPY 2

3. TEXTURE **3**

4. THIN-SECTION COMPOSITION

4.1 FRAMEWORK GRAINS 3

4.2 CLAYS 6

4.3 CEMENTS 6

4.4 VISIBLE POROSITY 7

5. X-RAY DIFFRACTION ANALYSES **7**

6. DIAGENESIS **9**

7. RESERVOIR QUALITY **10**

8. SUMMARY AND CONCLUSIONS **12**

C O N T E N T S cont.

Page

FIGURES

FIGURE 1. QFR COMPOSITION 5

FIGURE 2. POROSITY/PERMEABILITY CROSS-PLOT..... 11

TABLES

TABLE 1. THIN-SECTION AND CORE ANALYSES 4

TABLE 2. BULK-ROCK XRD ANALYSES 8

TABLE 3. FINE-FRACTION CLAY MINERALOGY 8

APPENDICES

APPENDIX 1. X-RAY DIFFRACTOGRAMS

APPENDIX 2. PHOTOMICROGRAPHS

EXECUTIVE SUMMARY

A petrological study was carried out on three msct samples from 2996.8-3018.4m in Trefoil-1. Analytical techniques used were thin-section analysis, bulk-rock/fine-fraction X-ray diffraction analysis and scanning electron microscopy.

Samples are texturally varied, very coarse grained arkoses and a subarkose in which framework grains are mainly granite-derived quartz and K-feldspar and also include plagioclase, granitic rock fragments, metamorphic rock fragments, sedimentary rock fragments, mica and accessory heavy minerals.

Illitic detrital clay forms pervasive matrix at 3000.2m and is thinly dispersed throughout much of the fine sandy matrix that supports common, very coarse sand- to pebble-sized grains at 3018.4m. Sandstone at 2996.8m is essentially clean. Authigenic clay is mainly kaolinite that forms scattered patches where labile grains have altered and where detrital clay matrix has recrystallised. At 3018.4m, detrital clay matrix has recrystallised to illitic clay. Smectitic clays are absent.

Diagenetic effects are quartz overgrowth and siderite cementation, authigenic clay formation, grain contact dissolution/microstylolitisation, physical compaction and labile grain dissolution. Quartz overgrowths do not exceed 3.5% and only partly occlude intergranular pores.

Clay-/sandy matrix-rich sandstones (3000.2m, 3018.4m) contain less than 2.7% visible porosity, whereas clean sandstone (2996.8m) contains 12.8% visible porosity. Visible porosity is accounted for mainly by primary intergranular pores and subordinate secondary pores that result from labile grain dissolution.

Almost complete intergranular porosity obliteration in clay-/fine sandy matrix-rich sandstones (3000.2m, 3018.4m) results from clay pore filling, grain contact dissolution/microstylolitisation, siderite cementation and, at 3018.4m, localised quartz overgrowth cementation. Significant porosity reduction in clean sandstone (2996.8m) results from quartz overgrowth cementation, grain contact dissolution, authigenic kaolinite formation and physical compaction.

Wide permeability variation reflects large textural differences, with very coarse grained sandstones that contain clay/fine sandy matrix (3000.2m, 3018.4m) having low to fair permeability (1.10mD, 10.8mD) and very coarse grained, clean sandstone (2996.8m) having high permeability (531mD).

High grain density reflects elevated siderite content.

1. INTRODUCTION

A petrological study was carried out on three msct samples from 2996.8-3018.4m in Trefoil-1 in order to provide information on mineralogy, diagenetic effects and controls on reservoir quality. Sample depths and core analyses performed by ACS Laboratories Pty Ltd are given in Table 1.

2. ANALYTICAL PROGRAM

2.1 THIN-SECTION ANALYSIS

Thin-sections were cut in kerosene, impregnated with blue-dyed epoxy resin to aid porosity recognition, and stained with sodium cobaltinitrite to aid feldspar identification. Mineral composition and visible porosity were determined by a count of 400 points, and mean grain size and sorting were estimated in thin-section with the aid of an eyepiece graticule. Photomicrographs were taken of each thin-section to illustrate texture, composition, clay distribution, diagenetic effects and porosity.

2.2 X-RAY DIFFRACTION ANALYSIS

Bulk-rock X-ray diffraction (XRD) analysis was carried out on each sample in order to quantify mineral abundance. The XRD analysis used a finely ground whole rock powder sample and the SIROQUANT processing technique was used to calculate mineral abundance.

XRD analysis was carried out on the fine fraction of each sample in order to precisely determine clay mineralogy. The fine fraction was separated from each sample by disaggregation and settling in distilled water and was air dried on glass discs to produce oriented specimens for XRD analysis. Samples were analysed in air dried condition and also following treatment with ethylene glycol.

2.3 SCANNING ELECTRON MICROSCOPY

Scanning electron microscopy (SEM) was carried out on each sample in order to provide information on clay distribution, diagenetic effects and porosity characteristics. Analyses were done on freshly exposed surfaces that had been thoroughly washed in shellite to remove any volatile hydrocarbons.

3. TEXTURE

Thin-section texture is given in Table 1. Samples are well-compacted, texturally varied, very coarse grained sandstones with a mean grain size between 1.04mm and 1.84mm.

MSCT #2/17 (2996.8m) is clean, massive, grain supported and moderately sorted. MSCT #2/21 (3000.2m) is argillaceous, grain supported and moderately sorted and contains pervasive, sandy, partly kaolinitised/sideritised detrital clay matrix. MSCT #3/2 (3018.4m) is very poorly sorted, being a pebbly sandstone in which scattered coarse sand- to pebble-sized grains up to 7mm long are supported by fine sandy/slightly argillaceous matrix.

Framework grains have long, embayed and, particularly in #2/21 (3000.2m), sutured (including microstylolitic) grain contacts.

Most fine to coarse sand-sized quartz grains are angular to subrounded, whereas most coarse sand- to pebble-sized quartz grains are subrounded to rounded.

4. THIN-SECTION COMPOSITION

Thin-section composition is given in Table 1, QFR composition is plotted in Figure 1, and annotated photomicrographs are presented in Appendix 2.

4.1 FRAMEWORK GRAINS

Samples are arkoses (#2/17, 2996.8m; #3/2, 3018.4m) and a subarkose (#2/21, 3000.2m) ($Q_{72}F_{23}R_5$ mean) in which framework grains are mainly quartz and K-feldspar and also include plagioclase, granitic rock fragments, metamorphic rock fragments, sedimentary rock fragments, mica and accessory heavy minerals.

Detrital quartz content ranges from 51.6% to 62.9% and averages 56.8%. Fine to coarse sand-sized quartz grains are mainly monocrystalline, whereas very coarse sand- to pebble-sized quartz grains include a significant component of granitic polycrystalline quartz. K-feldspar, brown tourmaline and biotite intergrowths are included in some quartz grains. Where interstitial areas are not filled by clay, quartz grains are commonly enveloped by euhedral quartz overgrowths.

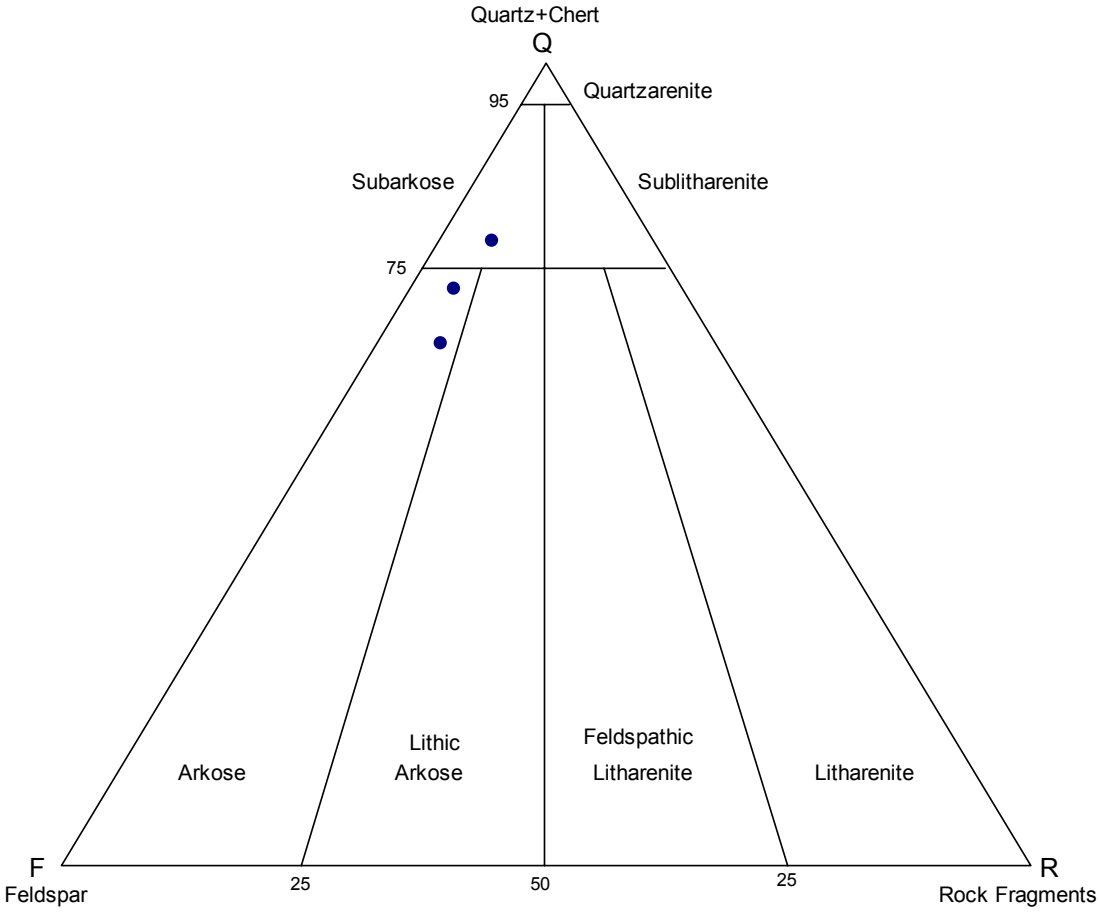
Total feldspar content ranges from 13.0% to 22.6%. Feldspar is overwhelmingly dominated by K-feldspar (12.5-19.4%), although plagioclase (0.5-3.2%) is a major constituent of many granitic rock fragments and also occurs as a constituent of common perthite/microperthite grains. K-feldspar is granitic, fresh to moderately altered (clear-turbid) orthoclase, perthite, microperthite and microcline that rarely include brown tourmaline intergrowths. Plagioclase is granitic, fresh to moderately sericitised albite and oligoclase. Feldspar grains are commonly etched/partly dissolved in #2/17 (2996.8m) and are commonly compactionally fractured/crushed in #2/17 (2996.8m) and #2/21 (3000.2m).

Lithic grains do not exceed 4.8% and consist of granitic rock fragments (coarsely intergrown quartz, K-feldspar, plagioclase, mica) (1.5-3.8%) and subordinate low-grade metasedimentary rock fragments (quartzose/mica-bearing metasandstone with slight foliation; illitic meta-argillite; phyllite) (0.5-1.1%) and sedimentary rock fragments (tightly

TABLE 1. THIN-SECTION AND CORE ANALYSES

MSCT #	2/17	2/21	3/2
Depth (mRT)	2996.8	3000.2	3018.4
Detrital quartz	55.8	62.9	51.6
Quartz overgrowths	3.5	-	1.4
K-feldspar	18.0	12.5	19.4
Plagioclase	0.9	0.5	3.2
Granitic rock fragments	1.5	2.0	3.8
Metamorphic rock fragments	1.1	0.5	1.0
Sedimentary rock fragments	0.7	1.5	-
Mica	1.5	0.8	2.5
Heavy minerals	0.9	0.3	1.5
Bitumen	-	-	0.3
Siderite	0.3	5.8	4.4
Authigenic kaolinite	2.2	4.0	4.0
Authigenic illitic clay	-	-	2.0
Detrital clay	0.8	8.2	2.3
Primary porosity	7.3	0.3	1.8
Secondary porosity	5.5	0.7	0.8
Q (quartz + chert)	72.8	78.7	65.9
F (feldspar)	23.2	16.3	28.1
R (rock fragments)	4.0	5.0	6.0
Mean grain size (mm)	1.04	1.84	1.10
Grain size class	v crs	v crs	v crs
Sorting class	mod	mod	v poor
He-injection porosity (%)	16.2	13.6	9.3
Permeability (air) (mD)	531	10.8	1.10
Grain density (g/cm^3)	2.63	2.68	2.67

FIGURE 1. QFR COMPOSITION



quartz overgrowth-cemented quartzarenite; illitic quartzarenite) (<0.3-1.5%). There is gradation between highly indurated quartzose sandstone rock fragments and quartzite (metasedimentary) rock fragments.

Granules and pebbles consist of granitic quartz and K-feldspar and, less commonly, granitic rock fragments.

Mica ranges up to 2.5% and consists of muscovite and subordinate biotite. Some muscovite is probably biotite that has been leached of iron.

Accessory heavy minerals are relatively common, ranging up to 1.5%, and consist almost entirely of brown tourmaline (dravite). Other heavy minerals include zircon, monazite, sphene and opaques (Fe-Ti oxides). Radiogenically-immobilised bitumen encases monazite grains in #3/2 (3018.4m).

Sandstones are derived almost entirely from a nearby granitic provenance. Granitic sediment was diluted slightly by detritus derived from highly indurated quartzose sandstones and low-grade quartzose/micaceous/illitic metasedimentary rocks.

4.2 Clays

MSCT #2/17 (2996.8m) is essentially a clean sandstone, whereas #2/21 (3000.2m) and #3/2 (3018.4m) are an argillaceous sandstone and slightly argillaceous sandstone, respectively.

Illitic detrital clay is common (8.2%) in #2/21 (3000.2m), where, together with fine sand, it pervasively fills intergranular spaces between well compacted coarse sand- to pebble-sized grains. Minor (2.3%) detrital clay is thinly dispersed throughout much of the fine sandy matrix that supports coarse sand- to pebble-sized grains in #3/2 (3018.4m). In #2/17 (2998.8m), very minor (0.8%) illitic detrital clay partly occupies a few intergranular pores.

Authigenic clay ranges up to 6.0% and is mainly patchy kaolinite that is a product of micaceous grain and feldspar alteration and detrital clay recrystallisation. Mica and feldspar grains are locally partly altered to kaolinite. In #3/2 (3018.4m), thinly dispersed authigenic illitic clay is a product of detrital clay matrix recrystallisation and micaceous grain alteration.

4.3 Cements

Sandstones are cemented by siderite and quartz overgrowths. MSCTs #2/21 (3000.2m) and #3/2 (3018.4m) contain 5.8% and 4.4% siderite, respectively, that forms scattered microconcretions, anhedral/subhedral rhombic crystals and finely/medium-crystalline patches that replace clay matrix and altered biotite grains and, in #3/2, fill intergranular pores. In #2/17 (2996.8m), very minor (0.3%) microcrystalline siderite locally replaces altered biotite grains.

Quartz overgrowths range up to 3.5% in #2/17 (2996.8m), where they commonly partly occlude intergranular spaces. Minor (1.4%) quartz overgrowth cement that occurs in #3/2 (3018.4m) is restricted to localised areas that contain little or no dispersed clay matrix. In #2/21 (3000.2m), quartz overgrowth cementation was prevented by the presence of pervasive clay matrix.

4.4 VISIBLE POROSITY

MSCT #2/17 (2996.8m) contains 12.8% visible porosity, whereas #2/21 (3000.2m) and #3/2 (3018.4m) contain 1.0% and 2.6% visible porosity, respectively.

In #2/17 (2996.8m), visible porosity is accounted for mainly by large primary intergranular pores and subordinate secondary pores that result from feldspar and micaceous grain dissolution. Some secondary pores in #2/17 are partly filled by loosely packed authigenic kaolinite that is the altered remnant of pore-precursor grains. Significant porosity reduction in #2/17 results from quartz overgrowth cementation, grain contact dissolution, authigenic kaolinite formation and physical compaction (brittle grain deformation).

In #3/2 (3018.4m), minor primary intergranular porosity is preserved in localised areas where there is little or no dispersed clay matrix. Severe intergranular porosity reduction in #3/2 results from grain contact dissolution/microstylolitisation, localised quartz overgrowth cementation and pore filling by clay, siderite and compacted micaceous grains.

Little intergranular porosity is preserved in #2/21 (3000.2m) due mainly to pore filling by pervasive detrital clay matrix and associated authigenic kaolinite and siderite. Porosity reduction in #2/21 also results from advanced grain contact dissolution/microstylolitisation between coarse framework grains.

5. X-RAY DIFFRACTION ANALYSES

Quantitative bulk-rock and fine-fraction XRD analyses were carried out on each sample. Quantitative XRD analyses are given in Table 2, clay mineralogy is given in Table 3, and annotated XRD traces are presented in Appendix 1.

Quantitative XRD analyses complement the thin-section analyses but cannot be compared directly. This is because thin-section clay includes microporosity, and therefore total thin-section clay is elevated relative to other components. In addition, XRD analyses do not include visible porosity. Therefore, in the case of the moderately macroporous sandstone (#2/17, 2996.8m), component amounts as determined by XRD analysis will be higher than those determined by thin-section analysis. Finally, the thin-section detrital clay and rock fragment component includes quartz, feldspar, kaolinite and illite/mica that are recorded as these phases by XRD.

Quantitative XRD analyses show that sandstones consist mainly of quartz (64.0-75.8%) and K-feldspar (14.1-22.1%) and also include plagioclase (3.3-5.2%), kaolinite (1.1-2.1%), illite/mica (1.7-1.9%) and siderite (0.5-8.3%).

Fine-fraction XRD analyses (Table 3) show that kaolinite dominates over illite/mica and mixed-layer illite/smectite in all samples and that trace chlorite occurs in #2/21 (3000.2m) and #3/2 (3018.4m). Mixed-layer illite/smectite, which, like chlorite, is insufficiently abundant for detection by bulk-rock XRD analysis, contains about 65-70% illite interlayers. Smectitic clays are absent.

Detected kaolinite has an authigenic origin and would also occur as a constituent of detrital clay. Detected illite is present as a constituent of detrital clay and as fine detrital mica and, like detected mixed-layer illite/smectite, is also a product of diagenesis.

TABLE 2. BULK-ROCK XRD ANALYSES

MSCT #	2/17	2/21	3/2
Depth (mRT)	2996.8	3000.2	3018.4
Quartz	75.8	71.3	64.0
K-feldspar	17.5	14.1	22.1
Plagioclase	3.3	3.3	5.2
Kaolinite	1.1	1.1	2.1
Illite/mica	1.8	1.9	1.7
Siderite	0.5	8.3	4.9

TABLE 3. FINE-FRACTION CLAY MINERALOGY

MSCT #	2/17	2/21	3/2
Depth (mRT)	2996.8	3000.2	3018.4
Kaolinite	M	M	M
Illite/mica	m	m	m
Illite/smectite	m	m	m
Smectite	-	-	-
Chlorite	-	T	T
Illite/smectite illite %	65-70	65-70	65-70

A = abundant; M = major; m = minor; T = trace

6. DIAGENESIS

The main diagenetic effects are quartz overgrowth and siderite cementation, authigenic clay formation, grain contact dissolution, physical compaction and labile grain dissolution.

Quartz overgrowths, which appear to be one of the latest diagenetic effects, are most common in the clean sandstone (#2/17, 2996.8m), where they partly occlude some intergranular pores (Plates 2, 3). In #3/2 (3018.4m), quartz overgrowths partly fill intergranular pores in localised areas that are largely free of thinly dispersed illitic clay matrix (Plate 10; Plate 11, Fig. 2; Plate 12, Fig. 1). MSCT #2/21 (3000.2m) lacks quartz overgrowth cement on account of containing pervasive clay matrix.

Siderite cement is common in #2/21 (3000.2m) and #3/2 (3018.4m), where it forms scattered microconcretions, anhedral/subhedral rhombic crystals and finely/medium-crystalline patches that replace clay matrix and altered biotite grains and, in #3/2, fill intergranular pores (Plates 4, 5; Plate 6, Fig. 2; Plates 9, 10). In #2/17 (2996.8m), microcrystalline siderite locally replaces altered biotite grains. Siderite occurs along microstylolitic contacts, probably indicating that siderite formed prior to grain contact dissolution/microstylolitisation. Paragenetic relationships between siderite and other diagenetic effects are unclear.

Authigenic kaolinite forms scattered, highly microporous patches where mica and feldspar grains have altered (Plates 1, 3, 10) and where detrital clay matrix has recrystallised (Plates 4, 5; Plate 6, Fig. 2; Plate 7, Fig. 2; Plate 12, Fig. 2). Mica and feldspar grains are locally partly altered to kaolinite. In #3/2 (3018.4m), thinly dispersed detrital clay matrix has recrystallised to illitic clay.

Framework grain packing density has been increased significantly by grain contact dissolution to form long, embayed and sutured (including microstylolitic) grain contacts (Plates 1, 4, 9, 10). Microstylolitic grain contacts between coarse framework grains are particularly common in #2/21 (3000.2m), where grain contact dissolution/microstylolitisation was promoted by the presence of thin illitic clay films (finely dispersed detrital clay matrix) between grains (Plate 5; Plate 7, Fig. 1). Thinly dispersed illitic clay has also promoted grain contact dissolution/microstylolitisation in parts of #3/2 (3018.4m).

Framework grain packing density has also been increased by physical compaction effects, particularly brittle deformation of feldspar grains in #2/17 (2996.8m) and #2/21 (3000.2m) (Plate 1) and ductile deformation of micaceous grains in #3/2 (3018.4m). Feldspar grains in #2/17 and #2/21 are commonly severely fractured and crushed due to compaction.

A large component of macroporosity in #2/17 (2996.8m) is late-stage (post grain contact dissolution) secondary porosity that results from partial to complete dissolution of feldspar and micaceous grains (Plate 1). In the other two samples, very minor secondary porosity results from partial to complete dissolution of plagioclase grains (Plate 10; Plate 11, Fig. 2; Plate 12, Fig. 1).

7. RESERVOIR QUALITY

Samples have variable reservoir quality, with He-injection porosity and permeability ranging from 9.3% to 16.2% and 1.10mD to 531mD (Table 1, Fig. 2). Figure 2, which includes all available core analyses for Trefoil-1 (2968.3-3026.7m), shows that the three petrology samples cover most of the permeability range within the section, with #2/17 (2996.8m) accounting for the highest measured permeability value. Porosity and permeability variation between the three sandstones reflects large textural differences, with the sandstones being clean, matrix-rich and very poorly to moderately sorted. Sandstones are described individually in order of increasing reservoir quality.

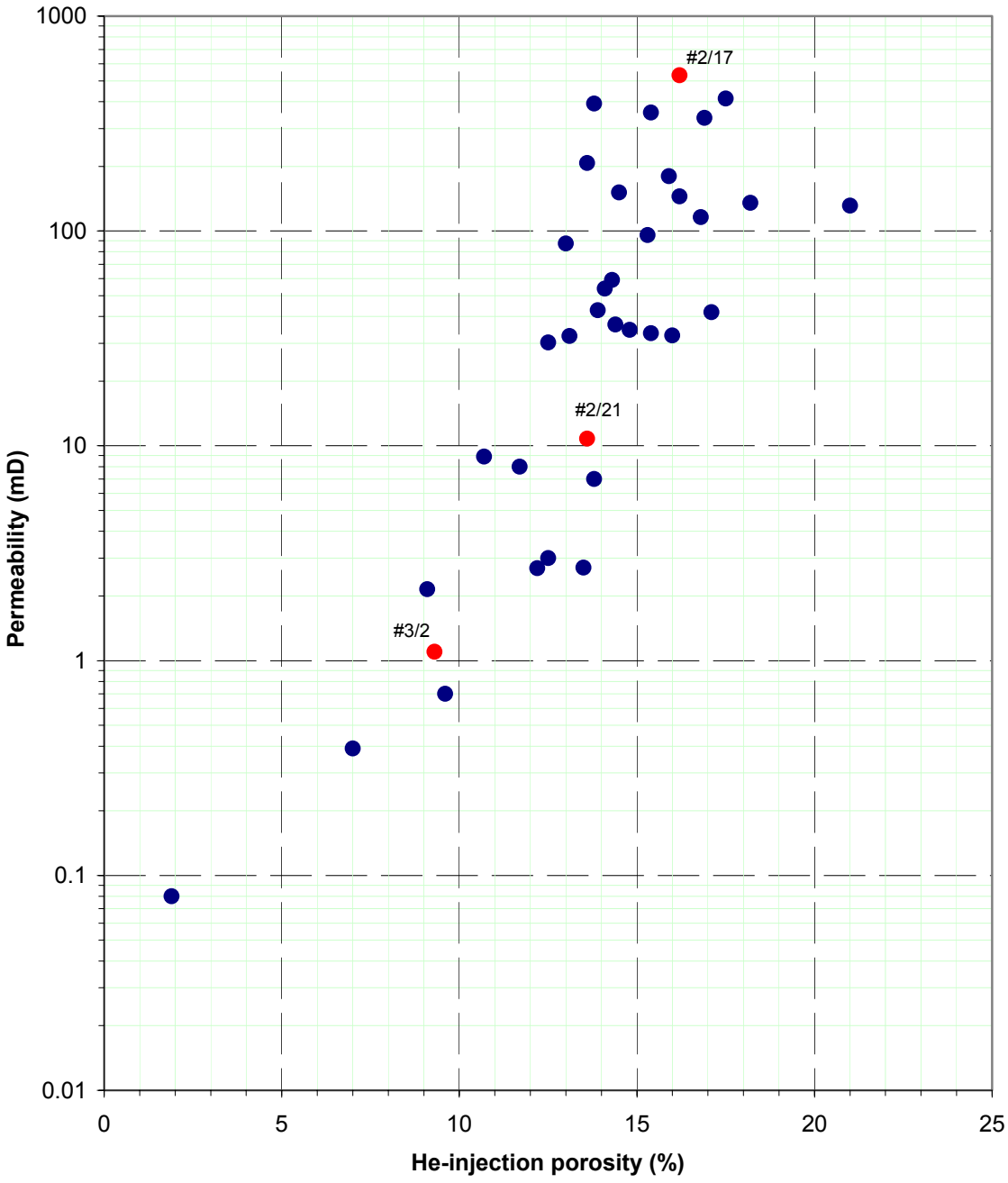
MSCT #3/2 (3018.4m): This pebbly sandstone has low permeability (1.10mD) largely on account of being very poorly sorted, slightly argillaceous and, despite being classed as a very coarse grained sandstone, composed mainly of fine grained sandy matrix that was very susceptible to the deleterious effects of diagenesis. Within the fine grained sandy matrix, which supports common very coarse sand- to pebble-sized grains, intergranular porosity has been almost completely eliminated by grain contact dissolution (including microstylolitisation), micaceous grain deformation, authigenic kaolinite formation, siderite cementation and pore filling by recrystallised, thinly-dispersed, illitic detrital clay matrix, the presence of which promoted grain contact dissolution/microstylolitisation. Localised areas that are largely free of illitic clay matrix are cemented by quartz overgrowths that only partly occlude intergranular spaces. However, with most fine sandy matrix being tight and with the sandstone being very poorly sorted, intergranular pores that are preserved within these cleaner areas have little interconnectivity on a thin-section scale.

MSCT #2/21 (3000.2m): This sandstone has only fair permeability (10.8mD), despite being very coarse grained, on account of most interstices between coarse grains being completely filled by sandy, microporous, illitic detrital clay matrix, much of which has recrystallised to kaolinite and is replaced by siderite. The presence of illitic clay matrix prevented quartz overgrowth cementation but, where thinly dispersed, has promoted grain contact dissolution/microstylolitisation, which, between some coarse grains, has advanced sufficiently to produce triple point grain contacts. Very minor macroporosity occurs where sideritic clay incompletely fills intergranular areas and where feldspar is dissolved and compactionally fractured/crushed, but the macroporosity is erratically distributed and thus is poorly interconnected throughout the sandstone.

MSCT #2/17 (2996.8m): In contrast to the previous two sandstones, this moderately sorted, very coarse grained sandstone is essentially clean and consequently contains good primary intergranular porosity, despite significant porosity reduction by the combined effect of quartz overgrowth cementation, grain contact dissolution (including minor microstylolitisation), patchy authigenic kaolinite formation and physical compaction (feldspar brittle deformation). Quartz overgrowths are common, but invariably only partly occlude intergranular pores. Primary pores provide connection for scattered secondary pores that occur where feldspar and micaceous grains have dissolved. High permeability (531mD) reflects the presence of good primary and secondary intergranular macroporosity together with very coarse grain size.

High grain density within the sampled section would reflect elevated siderite content, with the two siderite-cemented samples (#2/21, 3000.2m; #3/2, 3018.4m) having a much higher grain density than the non-siderite-cemented sample (#2/17, 2996.8m) (Table 1).

FIGURE 2. MEASURED POROSITY/PERMEABILITY CROSS-PLOT



8. SUMMARY AND CONCLUSIONS

- Three msct samples from 2996.8-3018.4m in Trefoil-1 are texturally varied, very coarse grained arkoses and a subarkose in which framework grains are mainly quartz and K-feldspar and also include plagioclase, granitic rock fragments, metamorphic rock fragments, sedimentary rock fragments, mica and accessory heavy minerals.

- Sandstones are derived almost entirely from a nearby granitic provenance.

- Illitic detrital clay forms pervasive matrix at 3000.2m and is thinly dispersed throughout much of the fine sandy matrix that supports common, very coarse sand- to pebble-sized grains at 3018.4m. Sandstone at 2996.8m is essentially clean.

- Authigenic clay is mainly kaolinite that forms scattered patches where labile grains have altered and where detrital clay matrix has recrystallised. At 3018.4m, detrital clay matrix has recrystallised to illitic clay.

- XRD analyses indicate that the clay mineral suite is dominated by kaolinite and illitic clays. Mixed-layer illite/smectite contains 65-70% illite interlayers. Smectitic clays are absent.

- Diagenetic effects are quartz overgrowth and siderite cementation, authigenic clay formation, grain contact dissolution/microstylolitisation, physical compaction and labile grain dissolution. Quartz overgrowths do not exceed 3.5% and only partly occlude intergranular pores.

- Clay-/sandy matrix-rich sandstones (3000.2m, 3018.4m) contain less than 2.7% visible porosity, whereas clean sandstone (2996.8m) contains 12.8% visible porosity. Visible porosity is accounted for mainly by primary intergranular pores and subordinate secondary pores that result from labile grain dissolution.

- Almost complete intergranular porosity obliteration in clay-/fine sandy matrix-rich sandstones (3000.2m, 3018.4m) results from clay pore filling, grain contact dissolution/microstylolitisation, siderite cementation and, at 3018.4m, localised quartz overgrowth cementation. Significant porosity reduction in clean sandstone (2996.8m) results from quartz overgrowth cementation, grain contact dissolution, authigenic kaolinite formation and physical compaction.

- Wide permeability variation reflects large textural differences, with very coarse grained sandstones that contain clay/fine sandy matrix (3000.2m, 3018.4m) having low to fair permeability (1.10mD, 10.8mD) and very coarse grained, clean sandstone (2996.8m) having high permeability (531mD).

- High grain density reflects elevated siderite content.

APPENDIX 1.

X-RAY DIFFRACTOGRAMS

Key to abbreviations:

C = chlorite

I = illite/mica

I/S = mixed-layer illite/smectite

Ha = contaminant halite

K = kaolinite

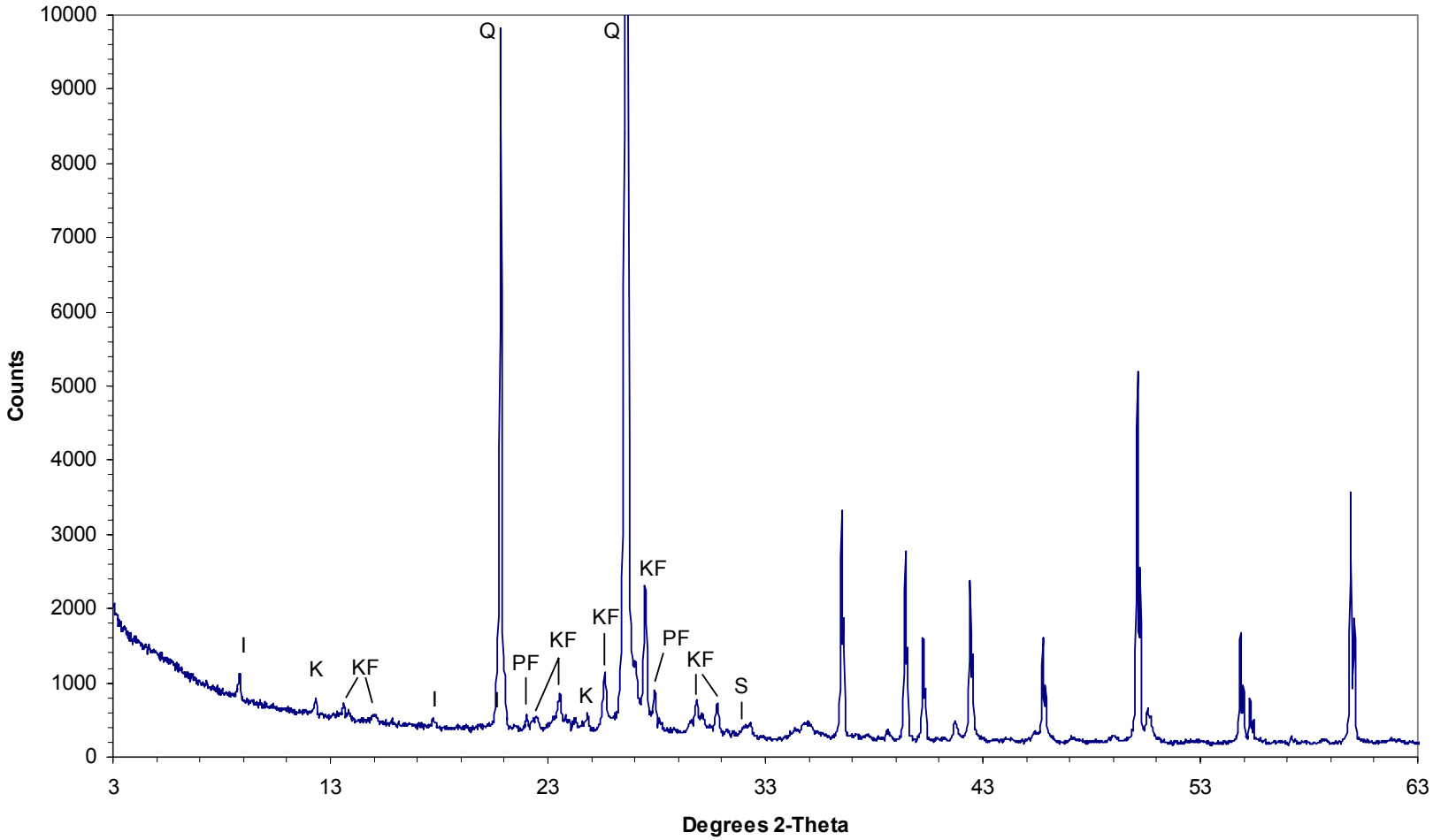
KF = K-feldspar

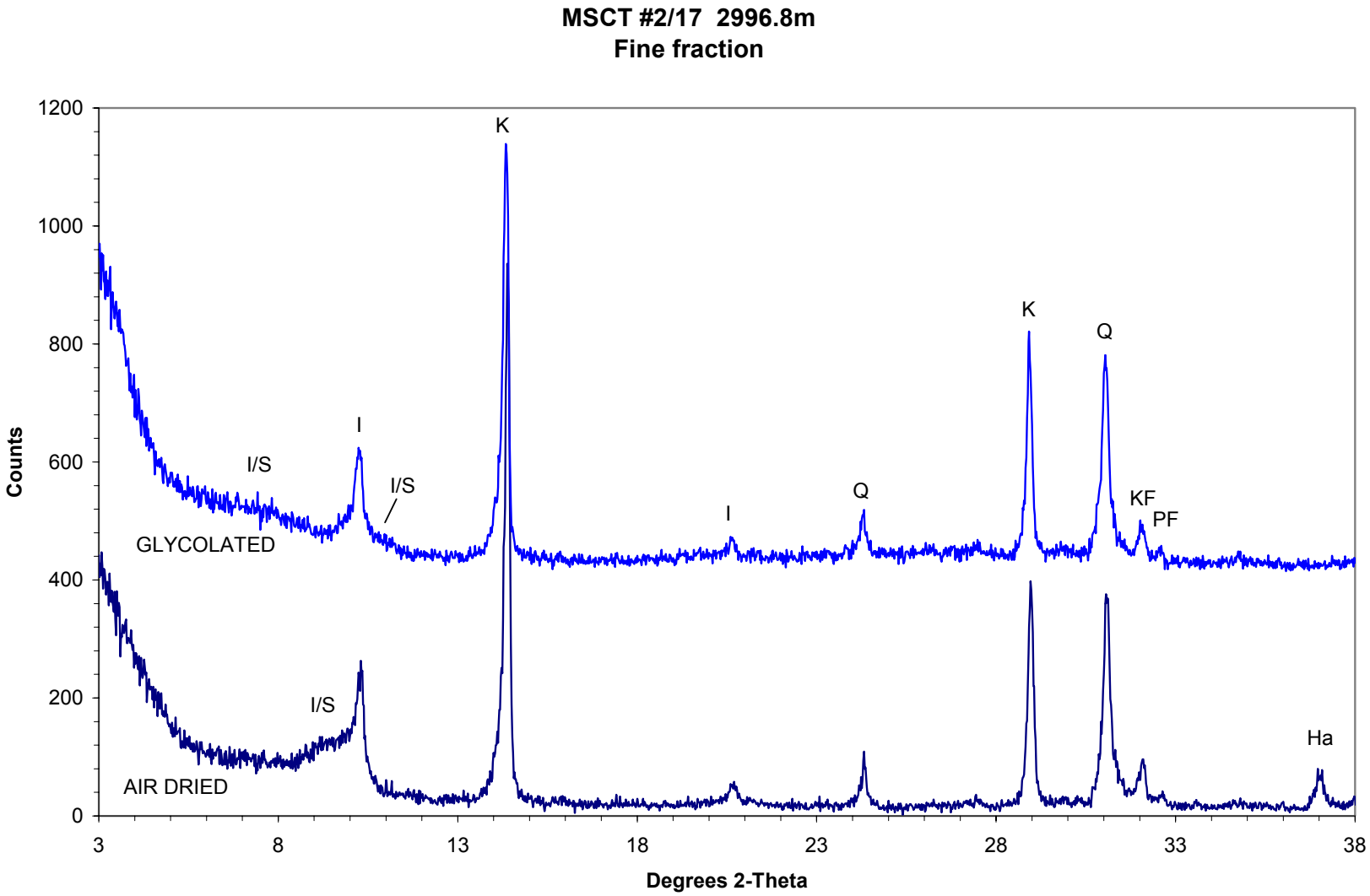
PF = plagioclase

Q = quartz

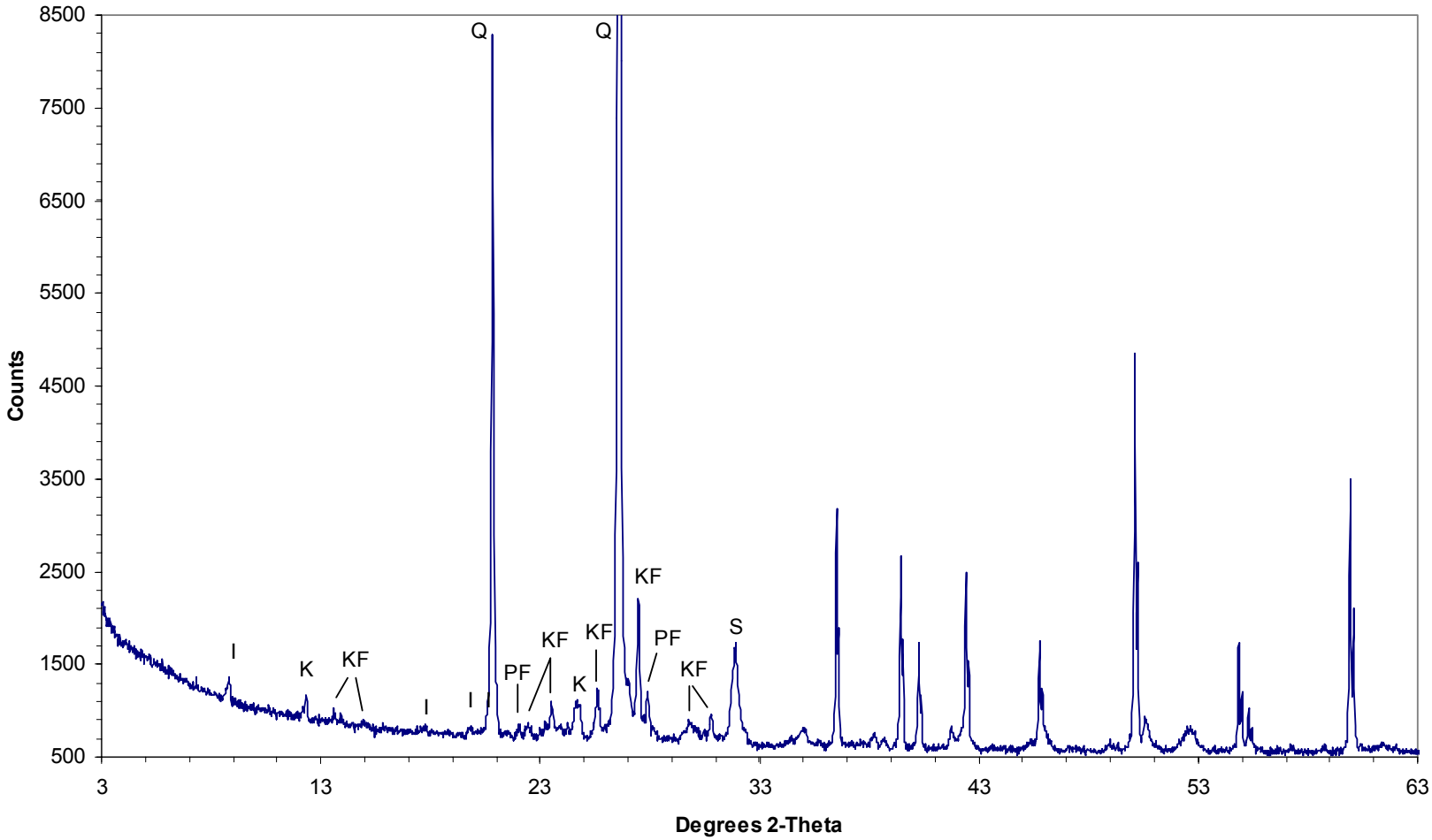
S = siderite

MSCT #2/17 2996.8m
Bulk rock

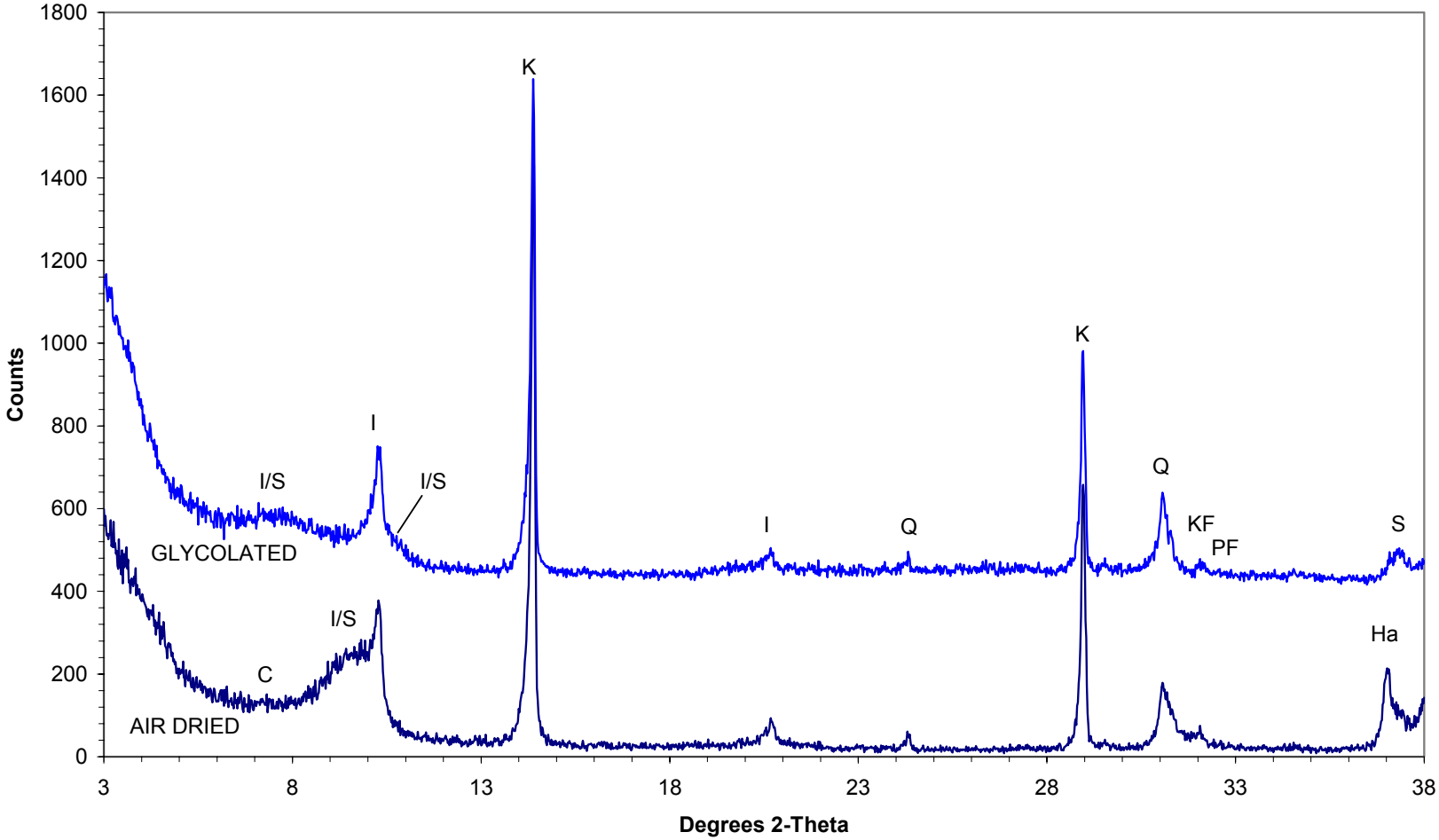



MSCT #2/17 2996.8m
Fine fraction
Counts
Degrees 2-Theta
GLYCOLATED
AIR DRIED
I/S
I
K
Q
KF
PF
Ha
0
200
400
600
800
1000
1200
3
8
13
18
23
28
33
38

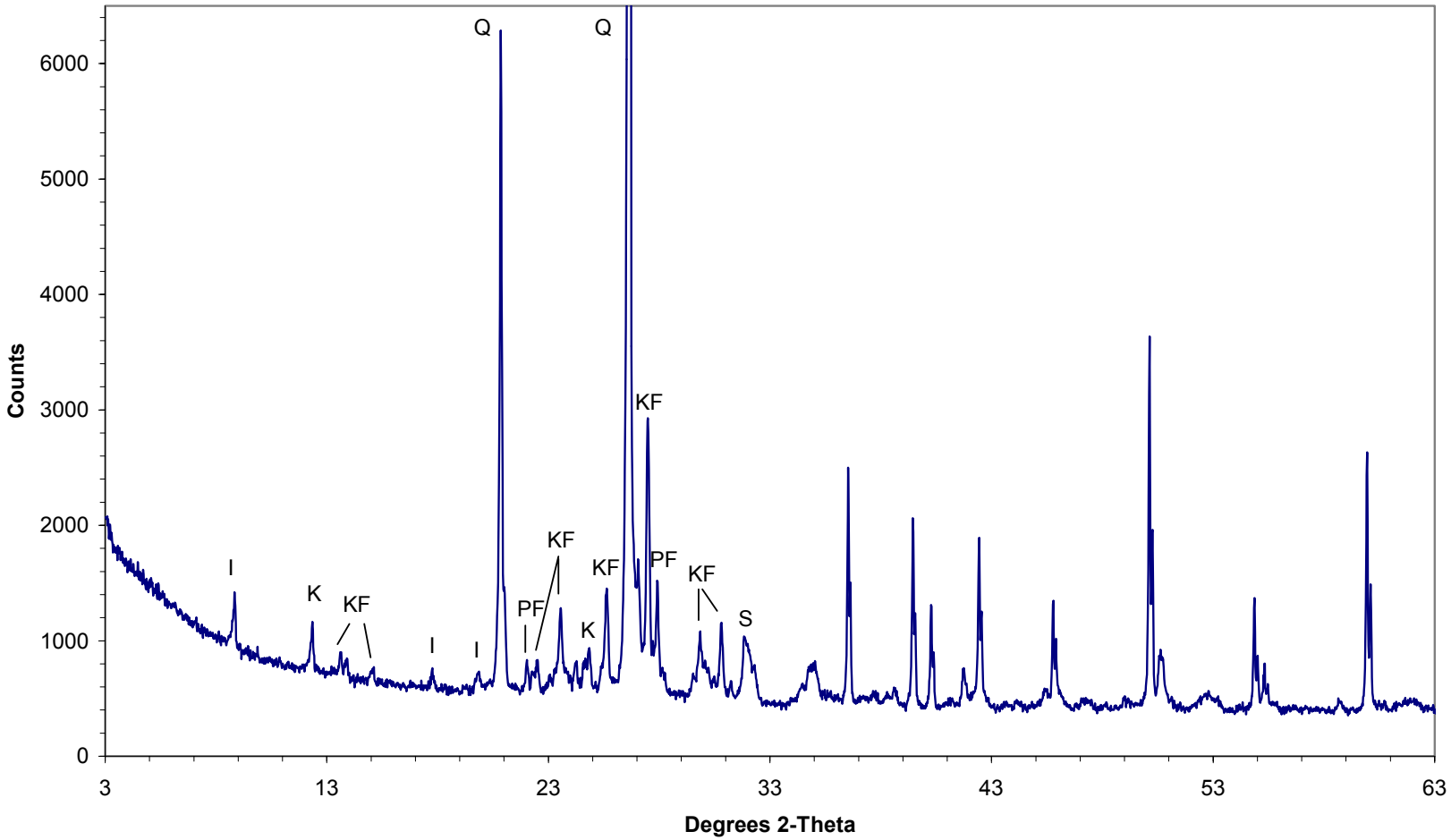
MSCT #2/21 3000.2m
Bulk rock



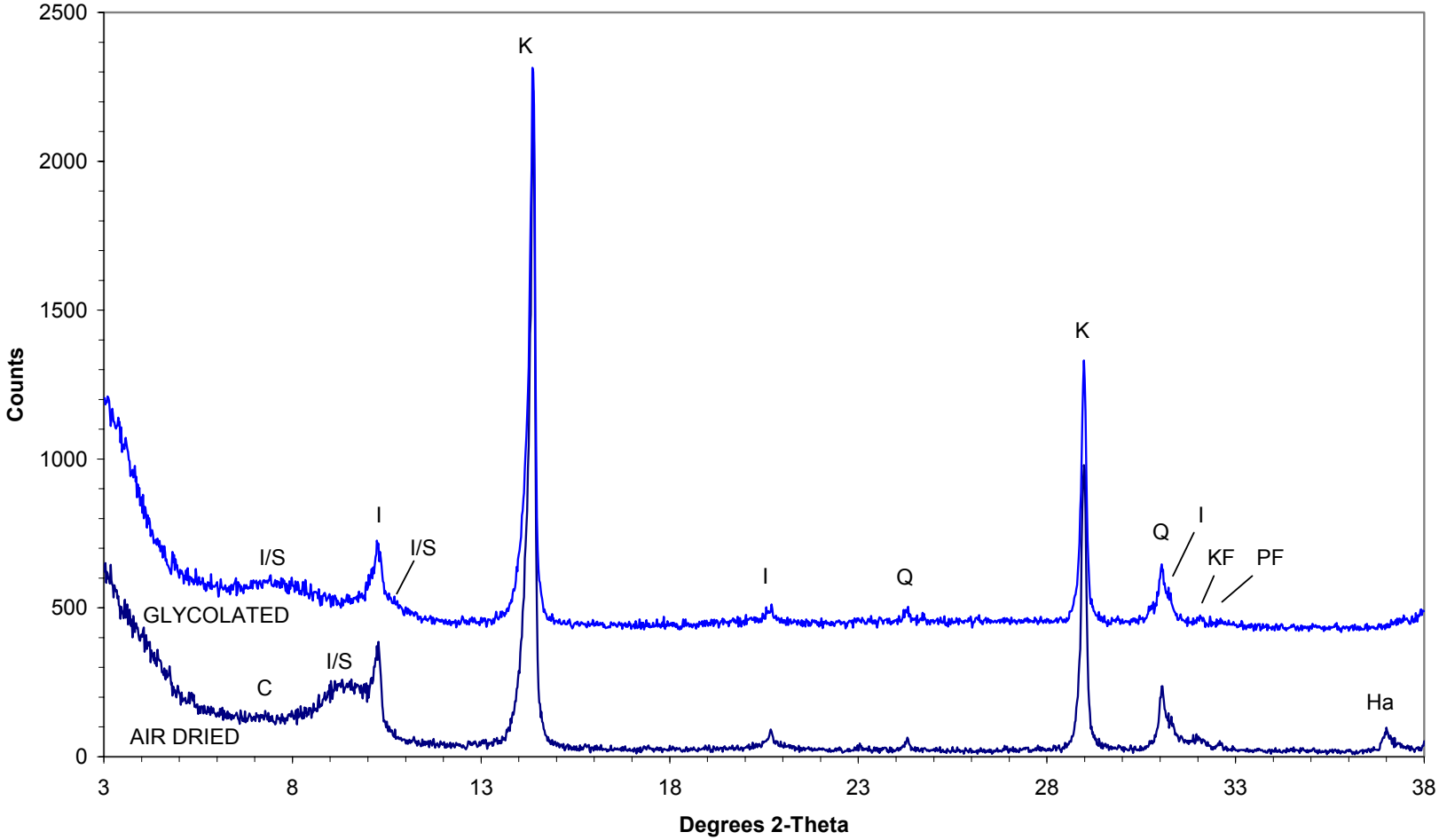
MSCT #2/21 3000.2m
Fine fraction



MSCT #3/2 3018.4m
Bulk rock



MSCT #3/2 3018.4m
Fine fraction



APPENDIX 2.

PHOTOMICROGRAPHS

Key to plates

Sample #	Depth (m)	Plate #
2/17	2996.8	1, 2, 3*
2/21	3000.2	4, 5, 6*, 7*
3/2	3018.4	8, 9, 10, 11*, 12*

* SEM micrograph

PLATE 1: MSCT #2/17 2996.8m

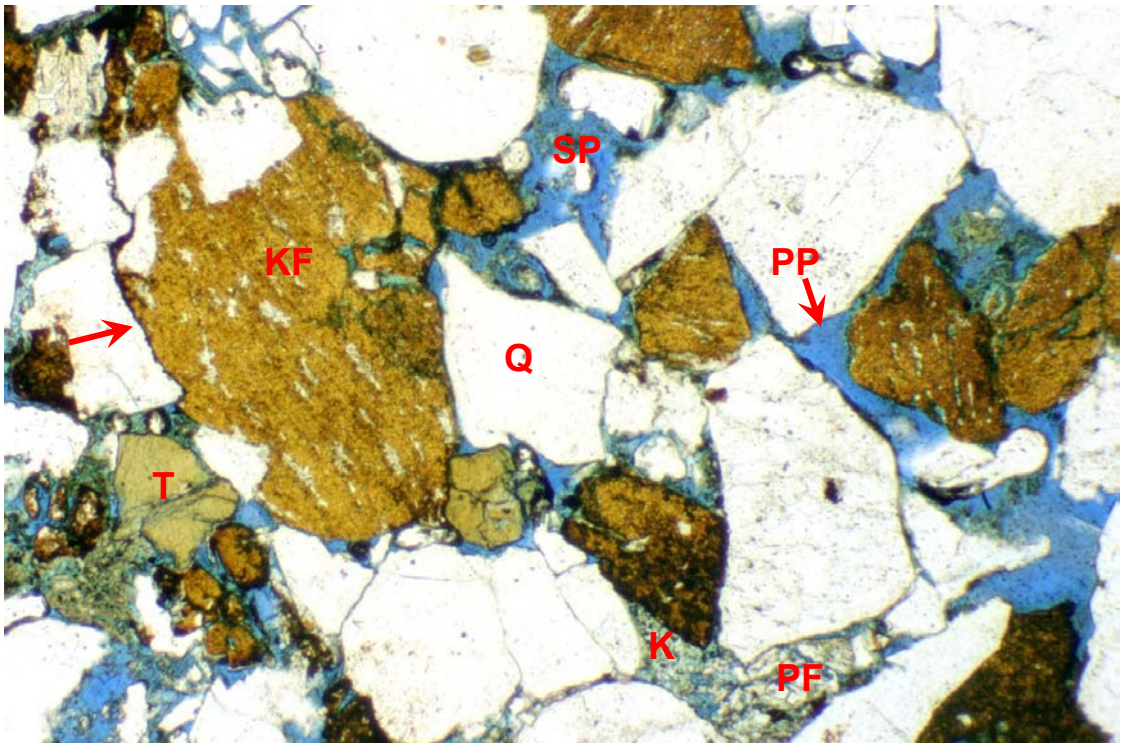
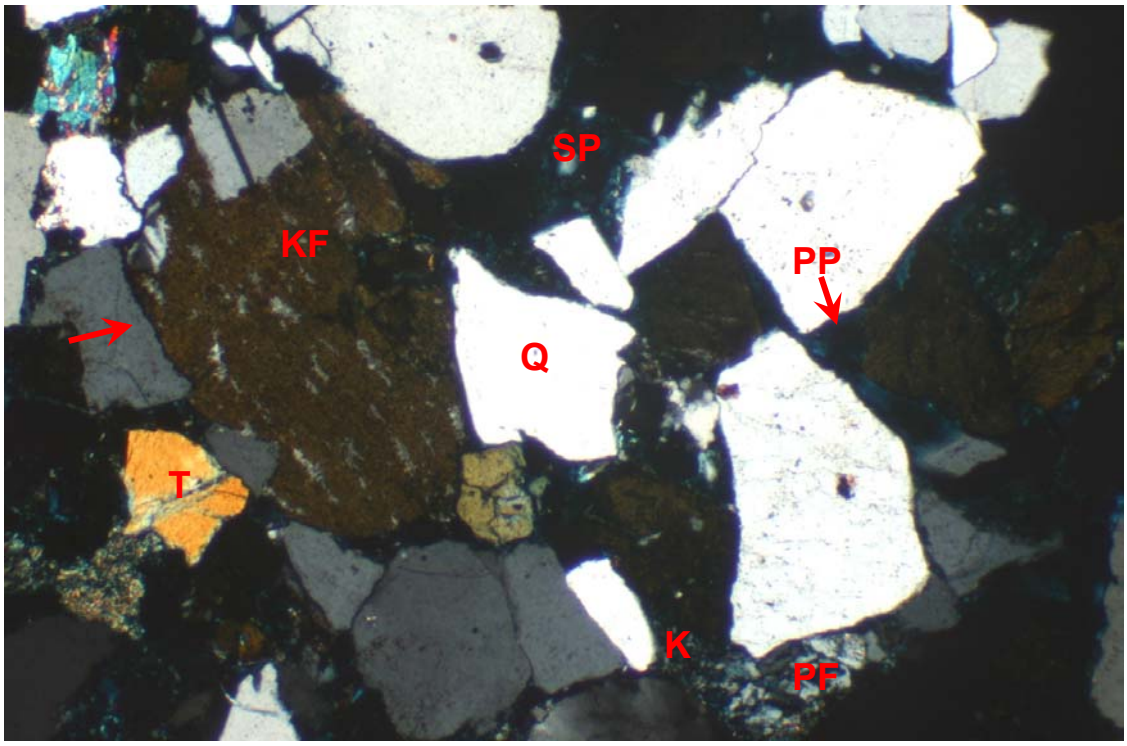


FIGURE 1 Plane polarised light
FIGURE 2 Crossed polarisers

0.4 mm



Porosity has been reduced in this very coarse grained arkose by grain contact dissolution (arrow) and localised pore filling by authigenic kaolinite (K), but the sandstone still contains sufficient primary intergranular porosity (PP) for high permeability (531mD). A large component of macroporosity is secondary intergranular porosity (SP) that results from labile grain dissolution. Framework grains are mainly granitic quartz (Q) and perthitic K-feldspar (KF) (stained brown) and also include compactionally-crushed plagioclase (PF) and accessory brown tourmaline (T). Porosity detail is shown in Plate 2.

PLATE 2: MSCT #2/17 2996.8m (cont.)

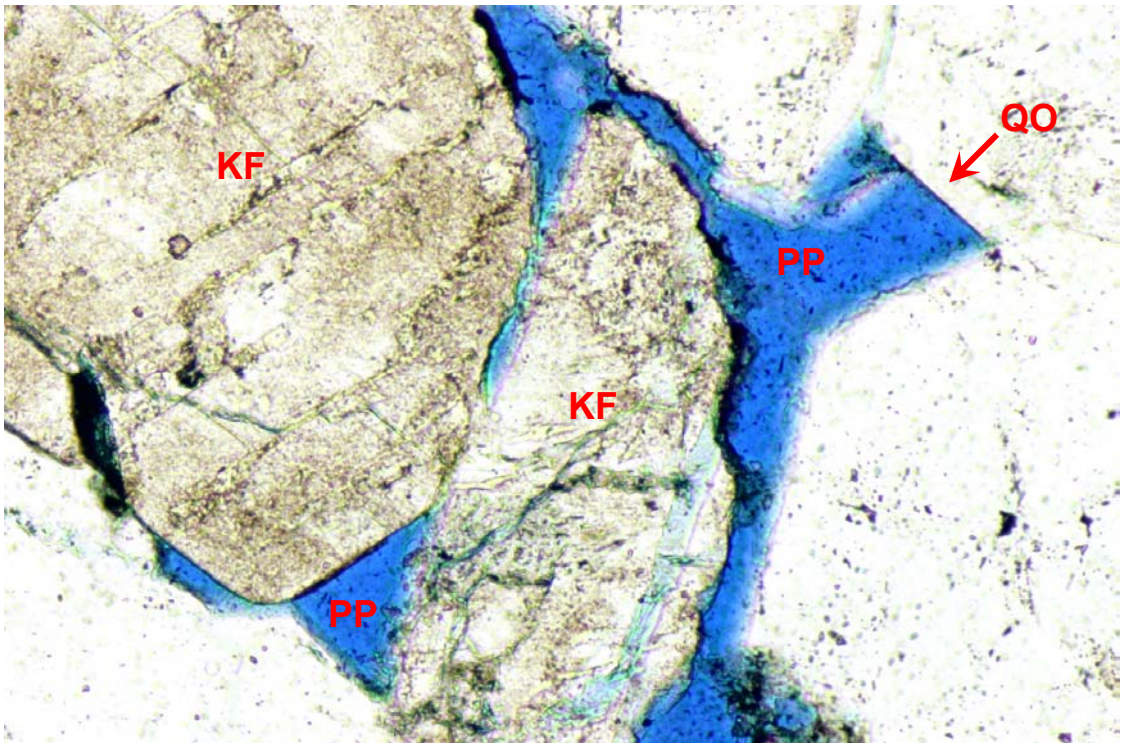
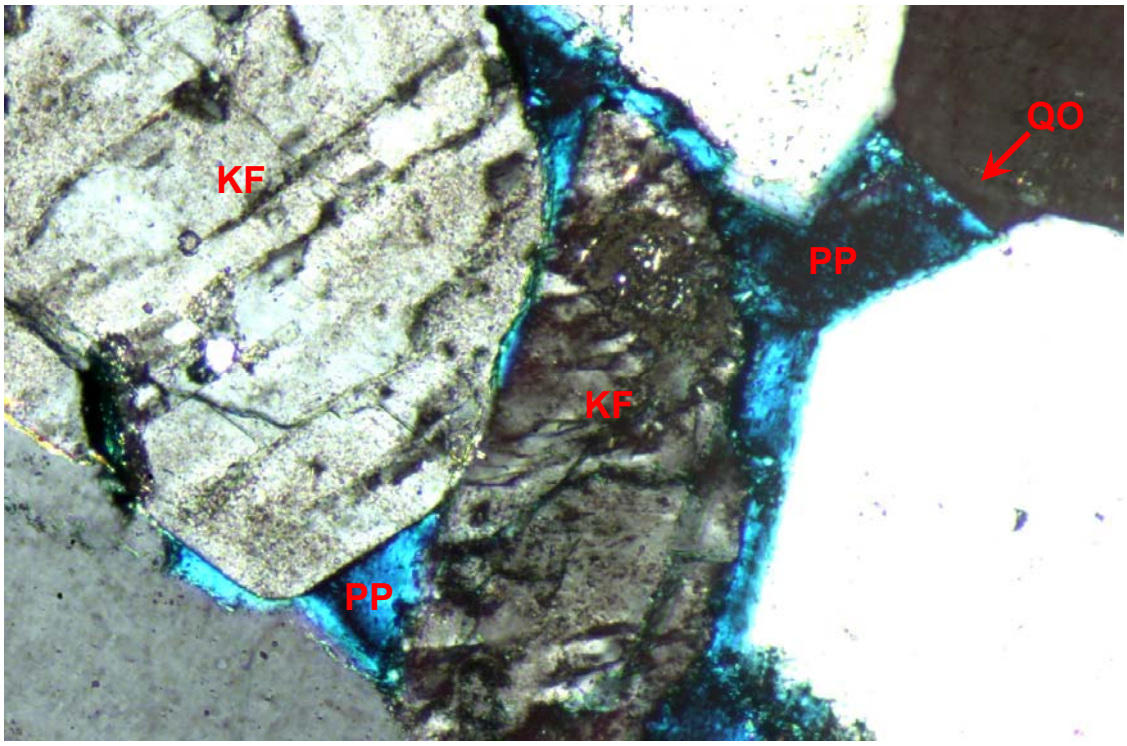


FIGURE 1 Plane polarised light
FIGURE 2 Crossed polarisers

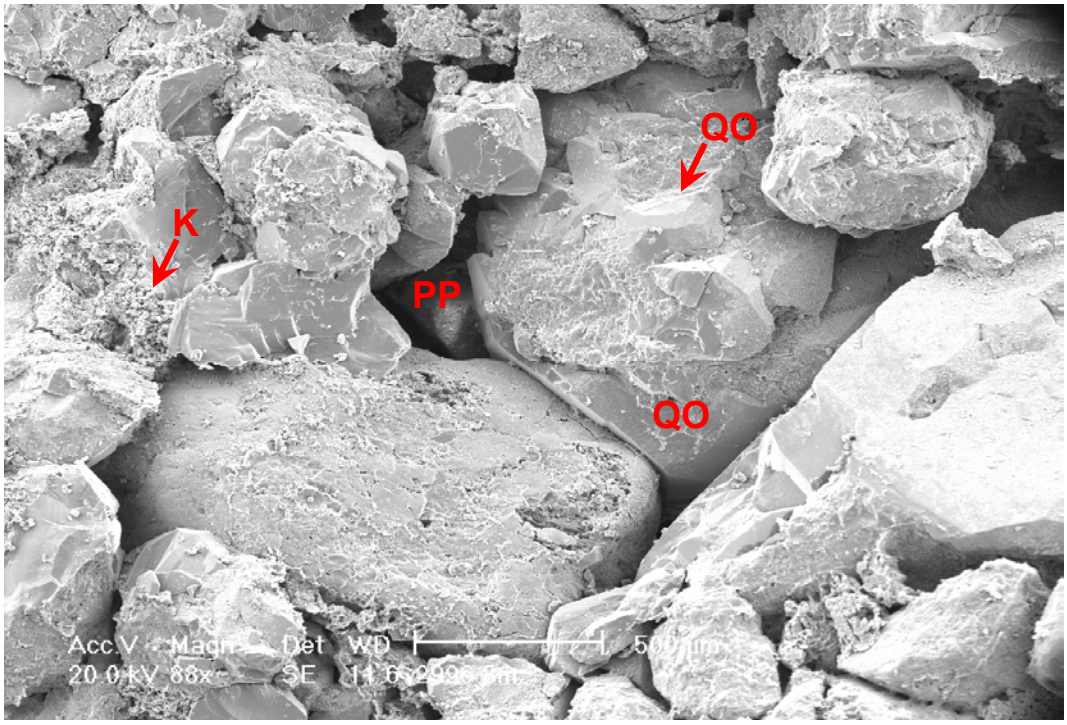
0.2mm



Unlike in the two deeper samples, intergranular spaces are commonly free of clay matrix and consequently the sandstone contains a well-interconnected system of primary intergranular pores (PP). Quartz overgrowths (QO) are well developed on some quartz grains, but only ever partly occlude intergranular pores. Quartz and K-feldspar (KF) grains are derived from a nearby granitic provenance. K = 531mD (Thin-section micrographs)

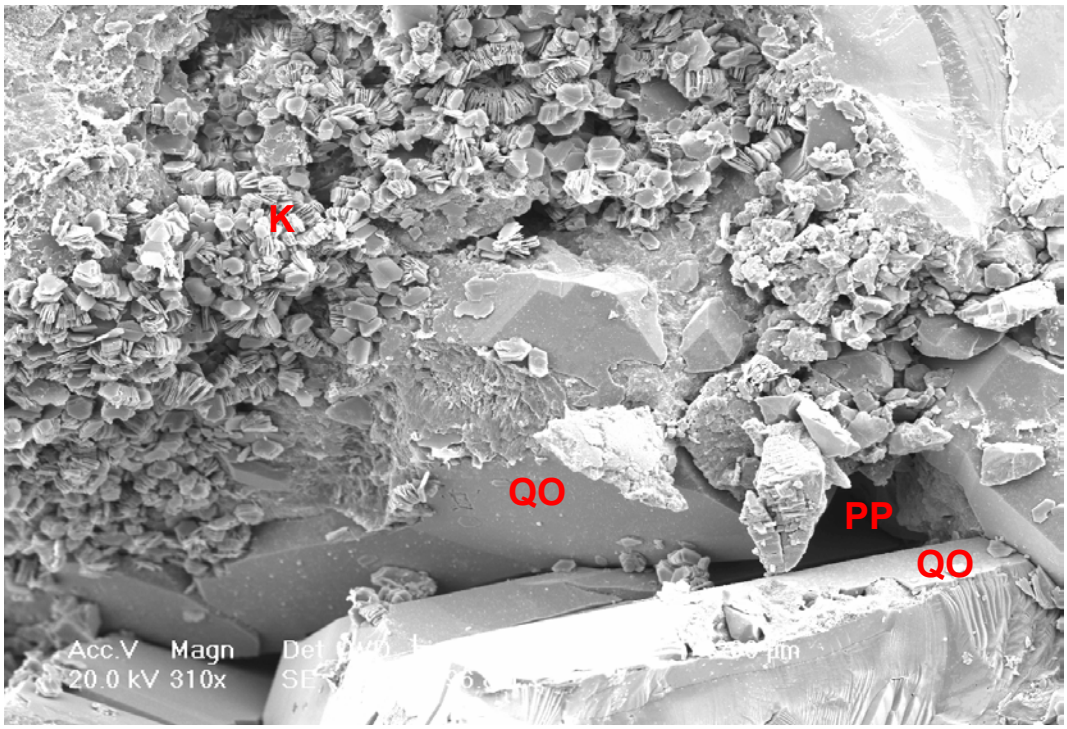
PLATE 3: MSCT #2/17 2996.8m (cont.)

FIGURE 1



Intergranular porosity has been reduced by quartz overgrowth (QO) cementation and localised authigenic kaolinite (K) formation, but the sandstone still contains large, clean primary intergranular pores (PP) that are conducive to high permeability (531mD). (SEM micrograph)

FIGURE 2



Primary pores (PP) are commonly preserved between juxtaposed quartz grains, despite cementation by quartz overgrowths (QO). Clay is mainly patchy authigenic kaolinite (K) that occurs where labile grains have altered. (SEM micrograph)

PLATE 4: MSCT #2/21 3000.2m

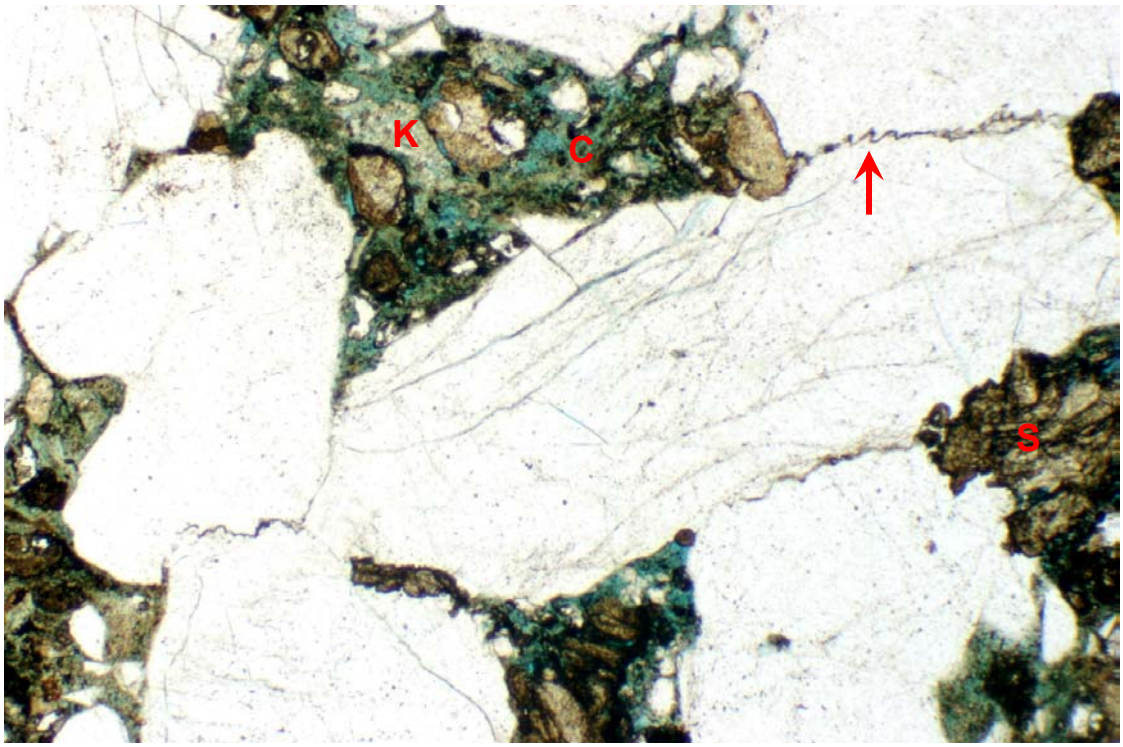
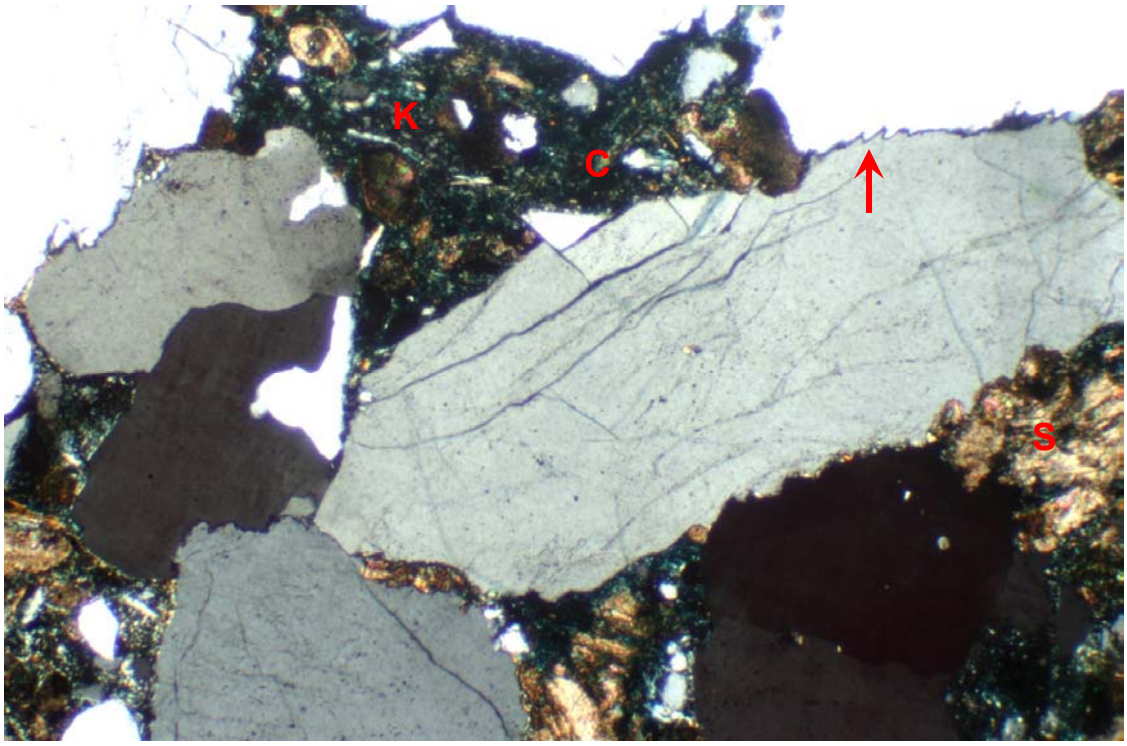


FIGURE 1 Plane polarised light
FIGURE 2 Crossed polarisers

0.4 mm



In this representative area, intergranular porosity is lacking due to complete pore filling by illitic detrital clay matrix (C), some of which has recrystallised to kaolinite (K) and is replaced by siderite (S). Further porosity reduction results from advanced grain contact dissolution between coarse quartz grains to form sutured/microstylolitic grain contacts (arrow). Matrix detail is shown in Plate 5. K = 10.8mD (Thin-section micrographs)

PLATE 5: MSCT #2/21 3000.2m (cont.)

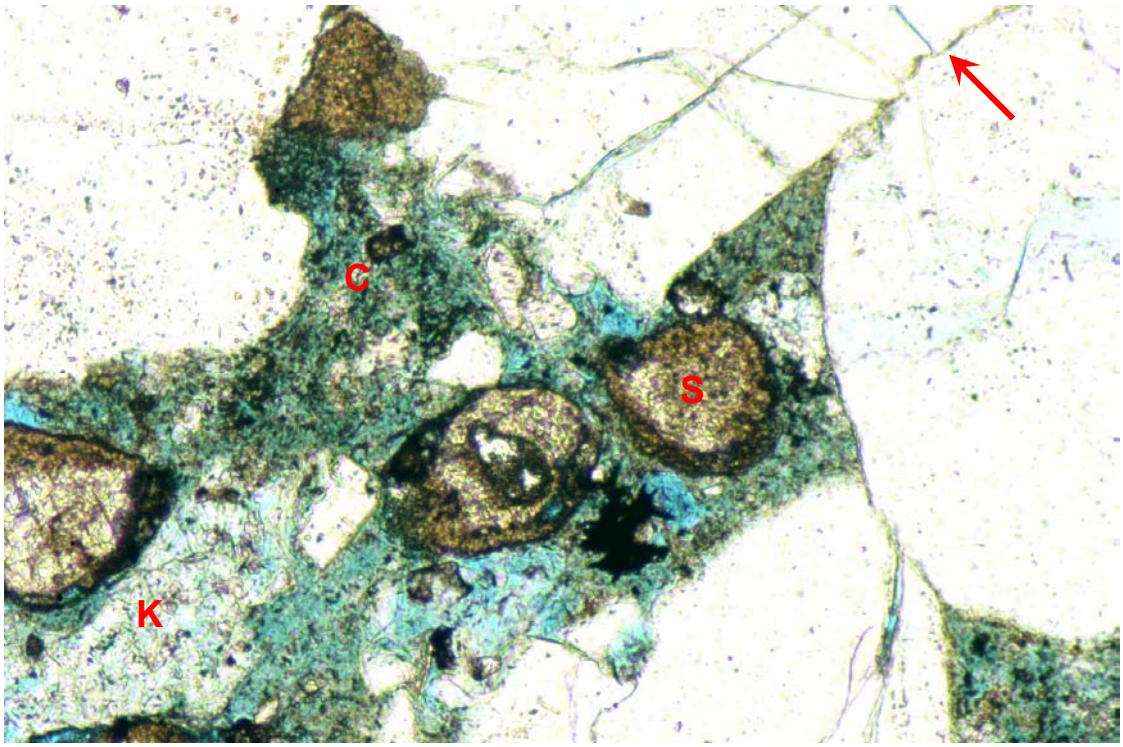
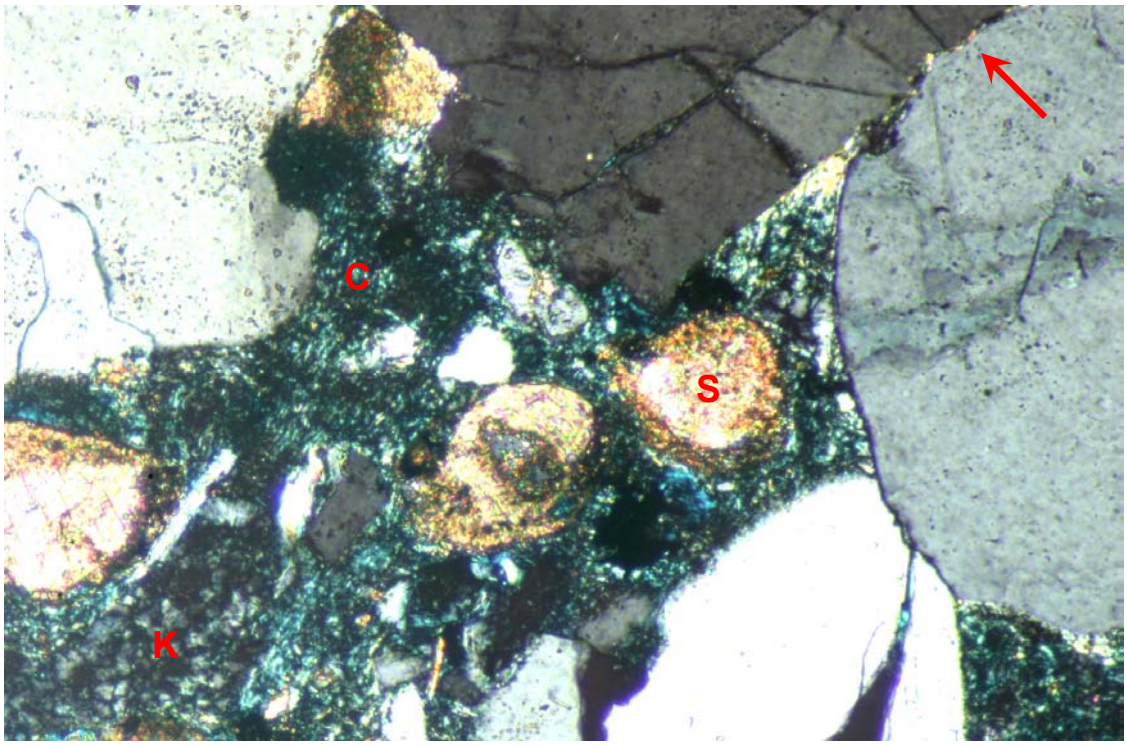


FIGURE 1 Plane polarised light
FIGURE 2 Crossed polarisers

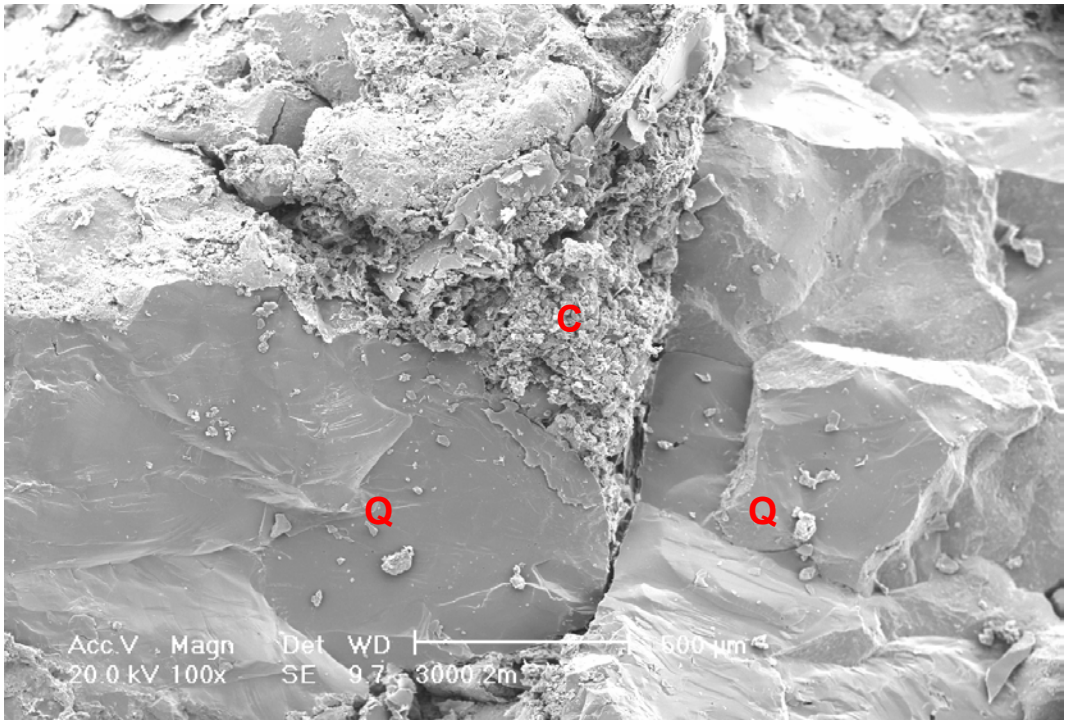
0.2mm



Relatively low permeability (10.8mD) reflects widespread pore filling by illitic detrital clay matrix (C) and associated authigenic kaolinite (K) and siderite replacement (S). Illitic clay films have promoted grain contact dissolution between coarse quartz grains (arrow). K = 10.8mD (Thin-section micrographs)

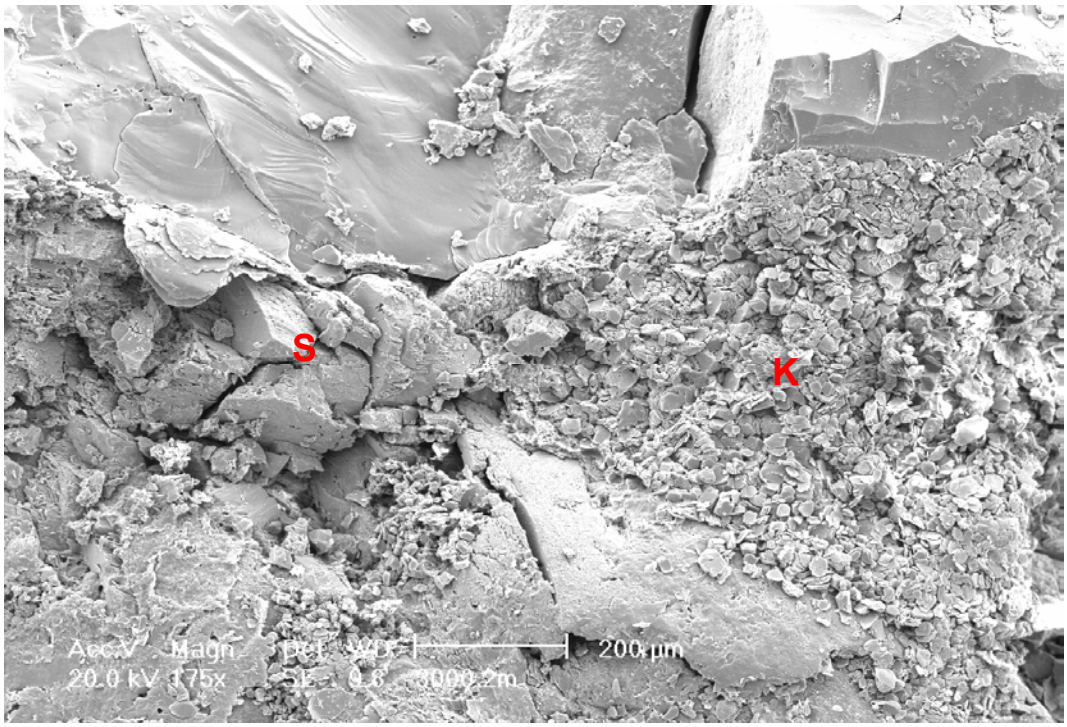
PLATE 6: MSCT #2/21 3000.2m (cont.)

FIGURE 1



Throughout the sandstone, intergranular spaces between welded quartz grains (Q) are filled by clay matrix (C). (SEM micrograph)

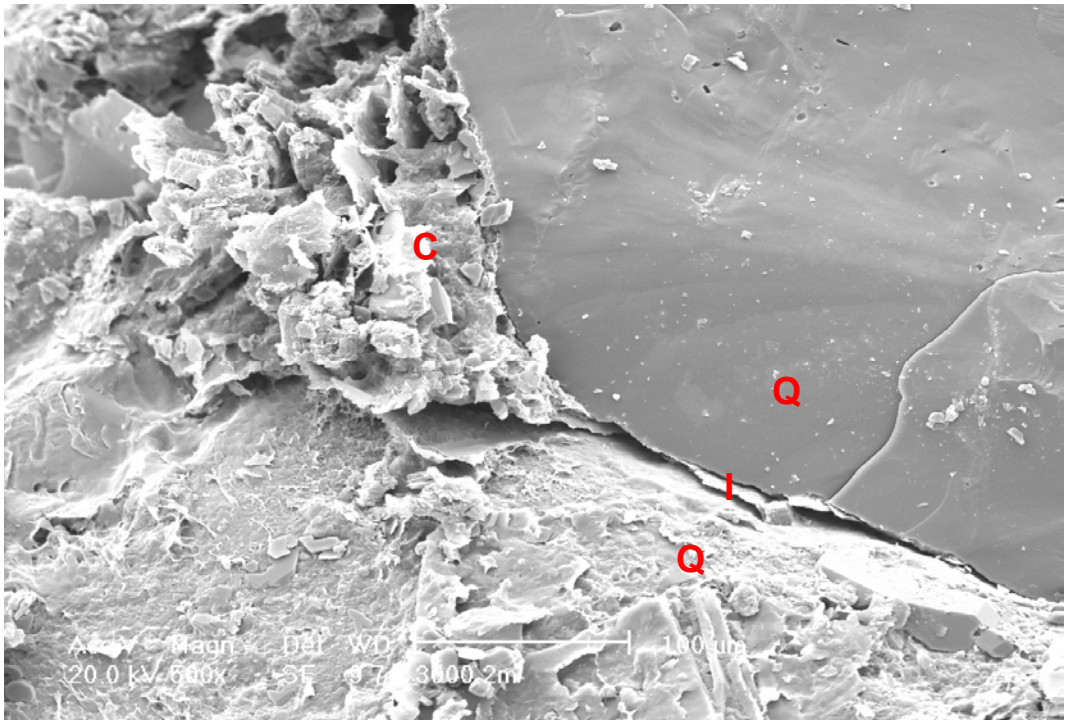
FIGURE 2



Much detrital clay matrix has recrystallised to kaolinite (K) and is replaced by siderite (S). Matrix detail is shown in Plate 7. (SEM micrograph)

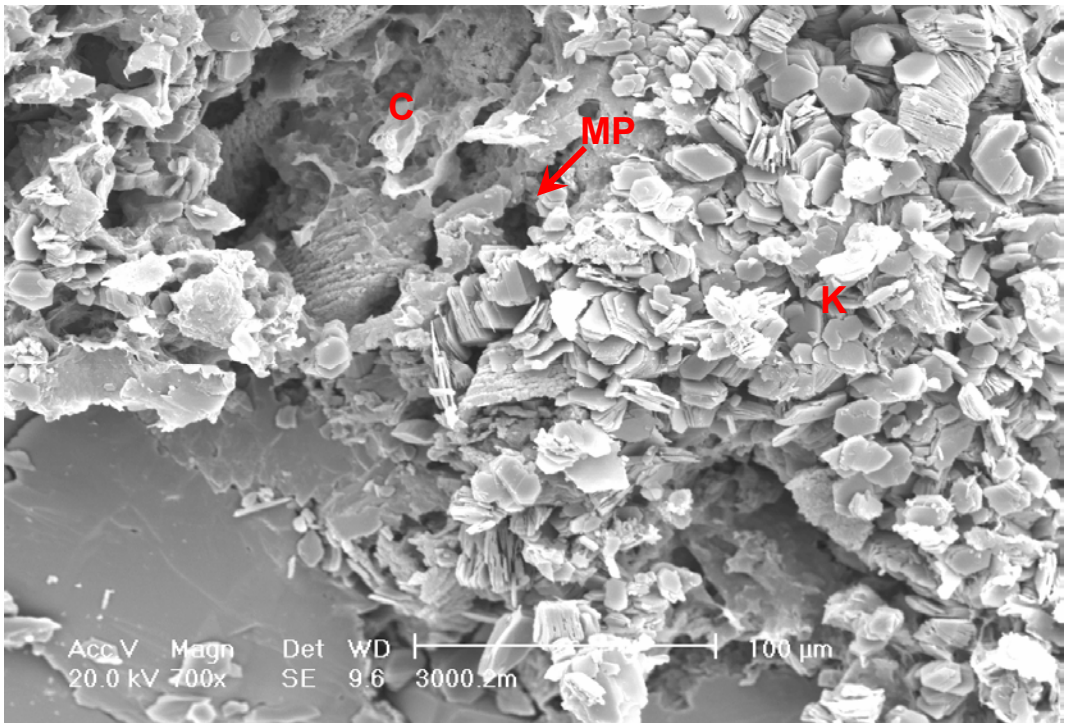
PLATE 7: MSCT #2/21 3000.2m (cont.)

FIGURE 1



Detail of illitic detrital clay matrix (C). Grain contact dissolution between two quartz grains (Q) was promoted by an illitic clay film (I) that is compactionally-dispersed detrital clay matrix. (SEM micrograph)

FIGURE 2



Authigenic kaolinite (K) is common as a recrystallisation product of illitic clay matrix (C). Clay matrix is highly microporous (MP). (SEM micrograph)

PLATE 8: MSCT #3/2 3018.4m

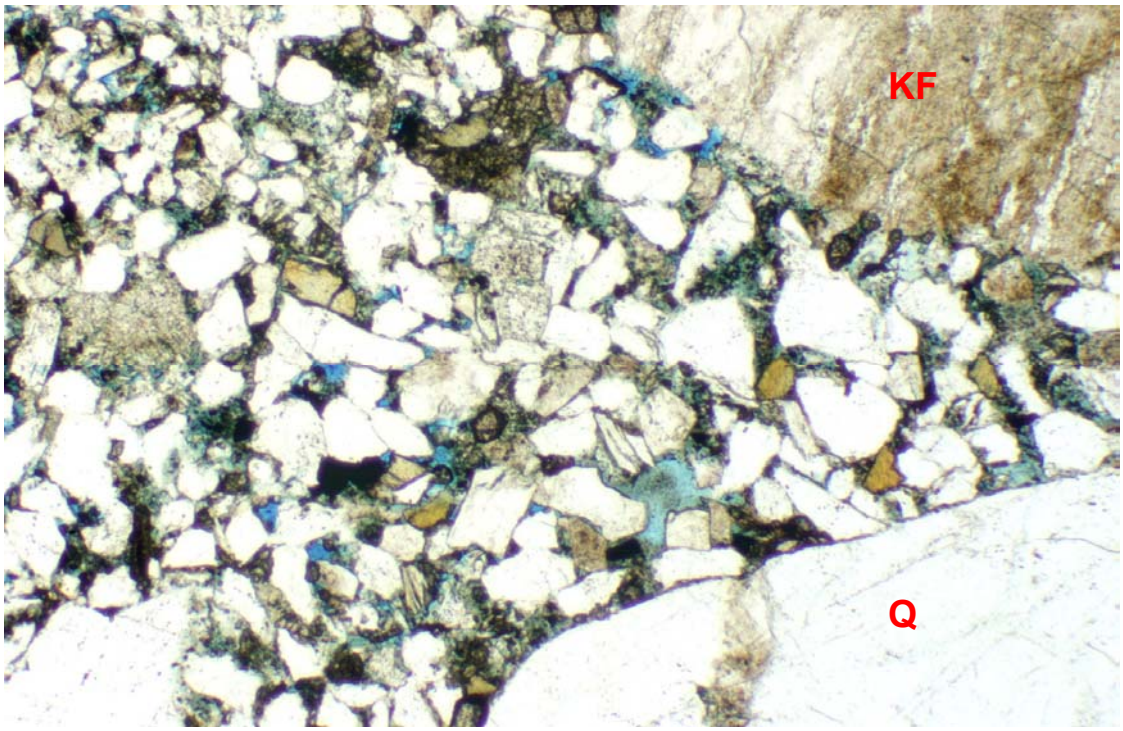
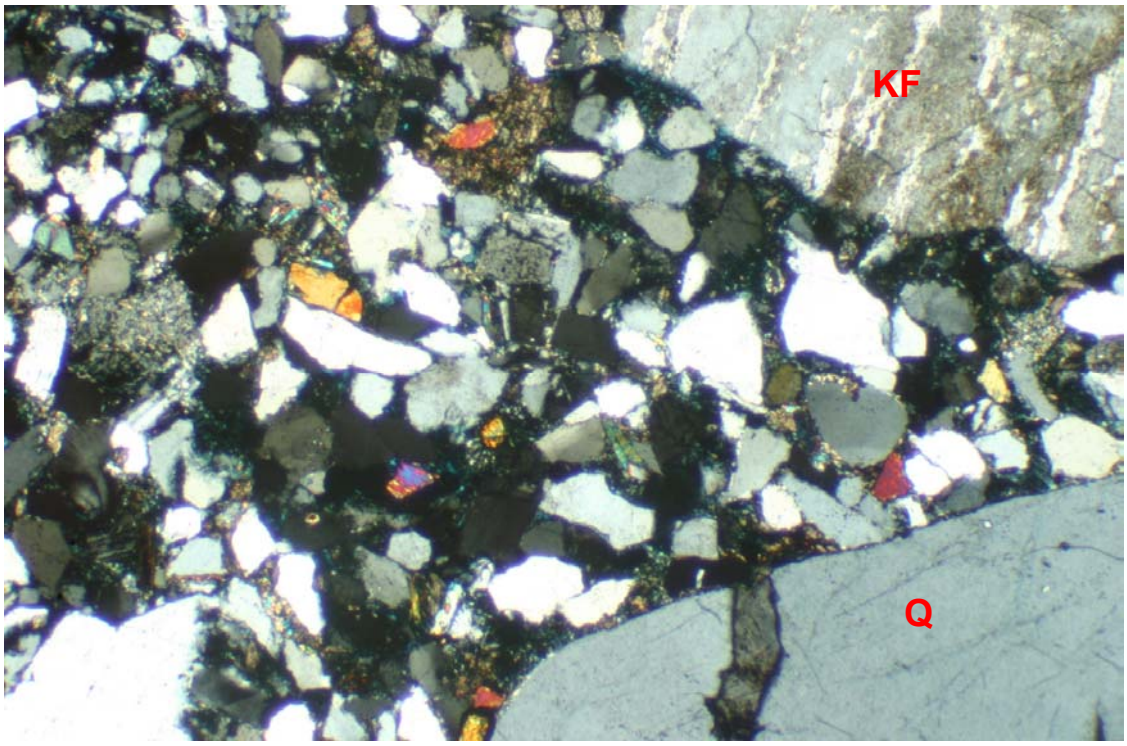


FIGURE 1 Plane polarised light
FIGURE 2 Crossed polarisers

0.4 mm



Low magnification micrographs showing general texture of a very poorly sorted sandstone. Very coarse sand- and granule-sized granitic quartz (Q) and K-feldspar (microperthite) (KF) grains are supported by fine sandy matrix in which there is localised intergranular porosity (blue). Matrix detail is shown in Plates 9 and 10. K = 1.10mD (Thin-section micrographs)

PLATE 9: MSCT #3/2 3018.4m (cont.)

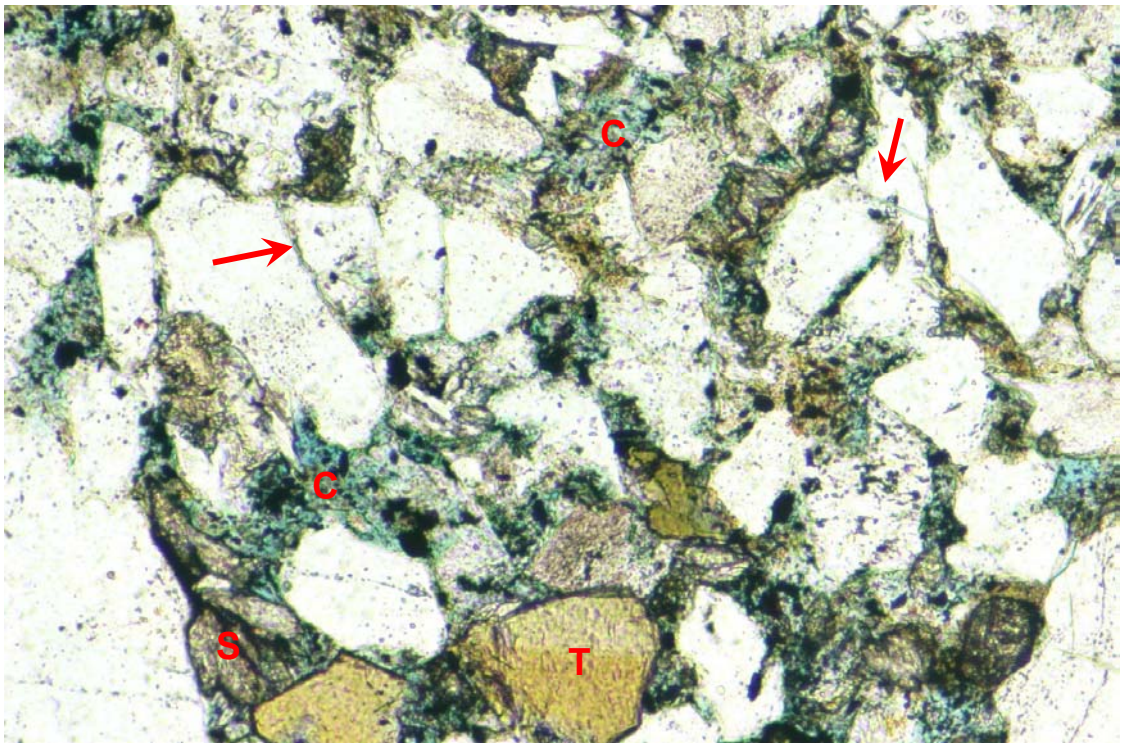
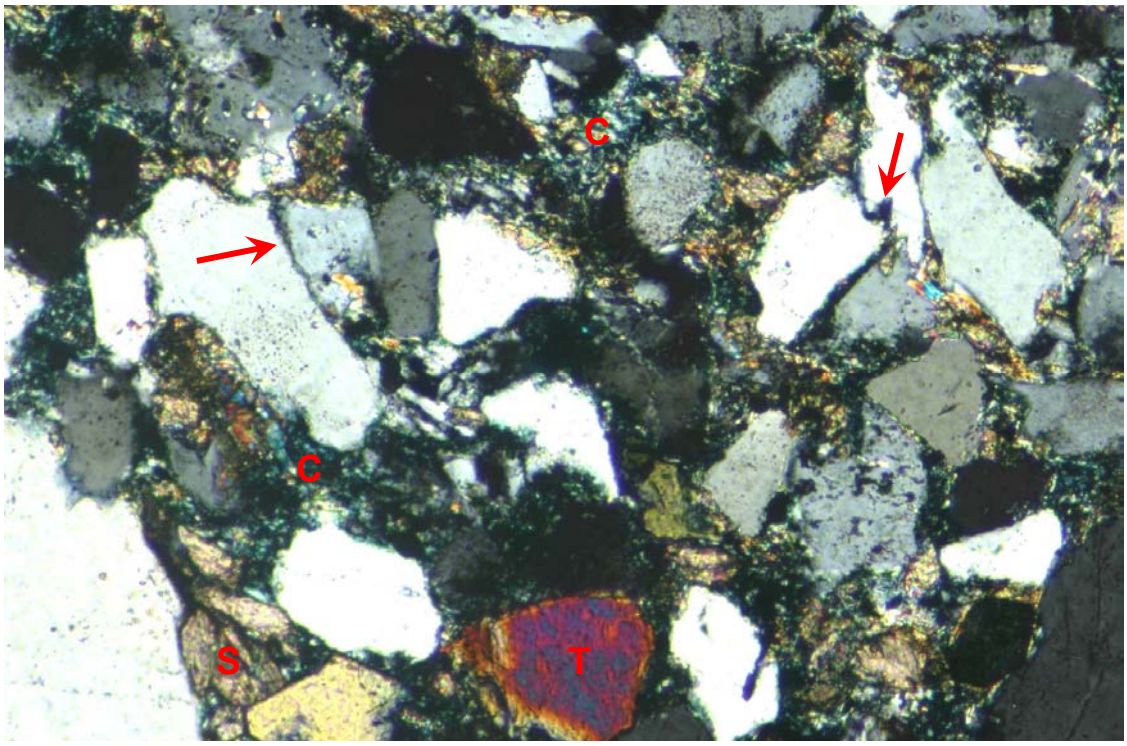


FIGURE 1 Plane polarised light
FIGURE 2 Crossed polarisers

0.2mm



Except in localised areas (see Plates 8 and 10), fine sandy matrix contains no intergranular porosity due to grain contact dissolution/microstylolitisation (arrows) and pore filling by dispersed illitic clay matrix (C) that is locally replaced by siderite (S). Brown tourmaline (T) is a common accessory heavy mineral. K = 1.10mD (Thin-section micrographs)

PLATE 10: MSCT #3/2 3018.4m (cont.)

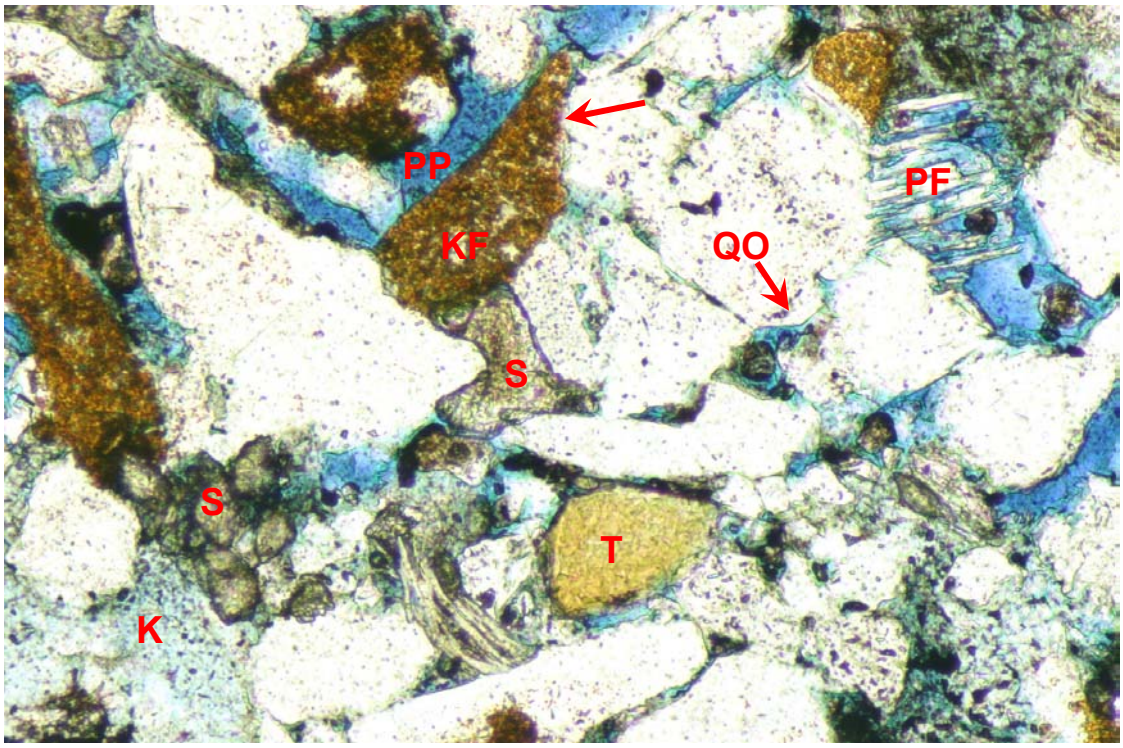
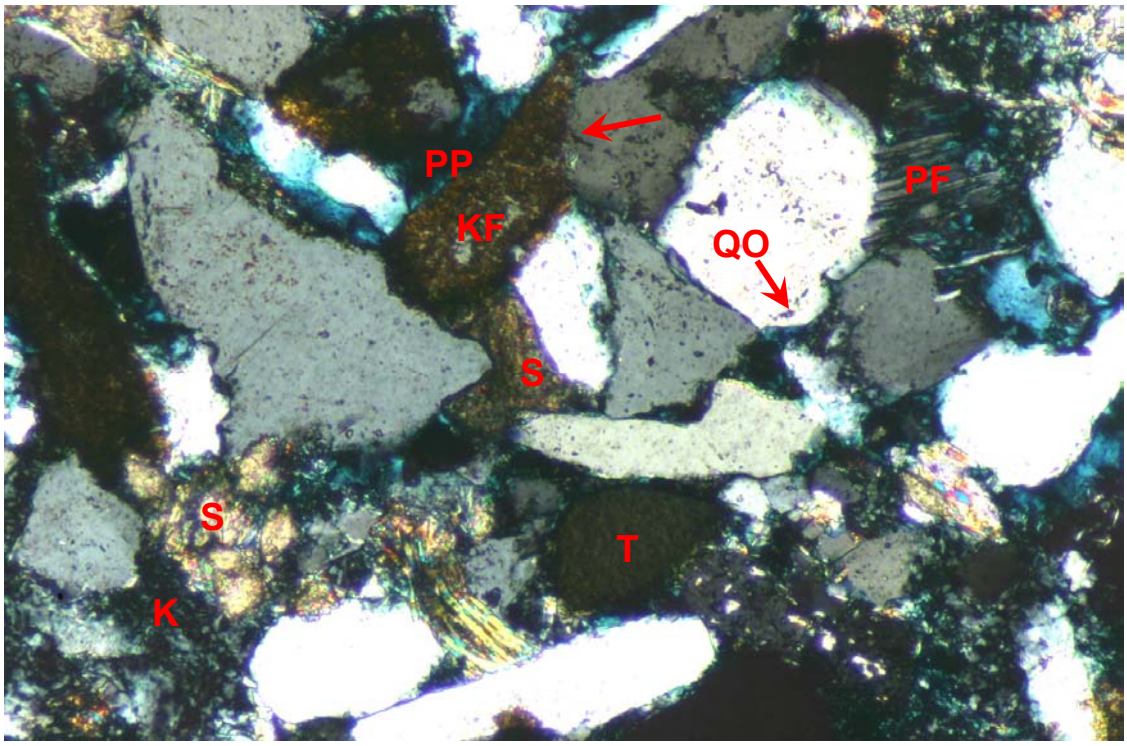


FIGURE 1 Plane polarised light
FIGURE 2 Crossed polarisers

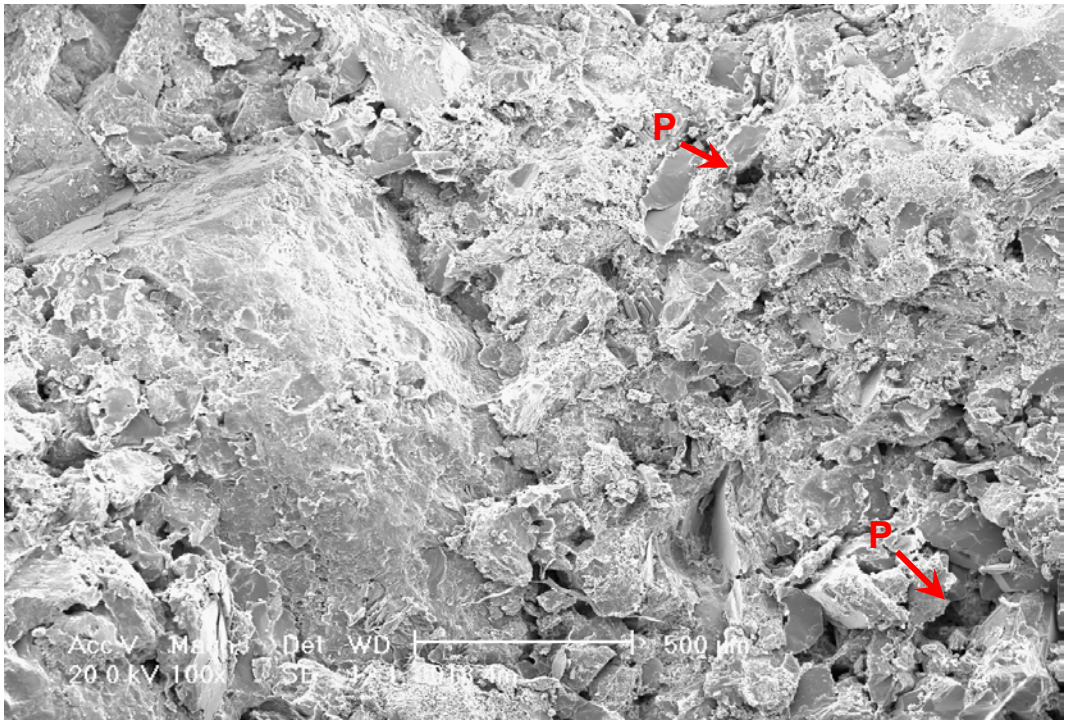
0.2mm



Primary intergranular porosity (PP) is preserved in localised areas where there is little or no dispersed illitic clay matrix, but even in these areas there has been severe intergranular porosity reduction by grain contact dissolution (arrow) and pore filling by authigenic kaolinite (K), siderite (S) and quartz overgrowths (QO). Secondary intragranular porosity is associated with the skeletal remnant of a largely dissolved plagioclase grain (PF). Framework grains include K-feldspar (KF) (stained brown) and accessory brown tourmaline (T). K = 1.10mD (Thin-section micrographs)

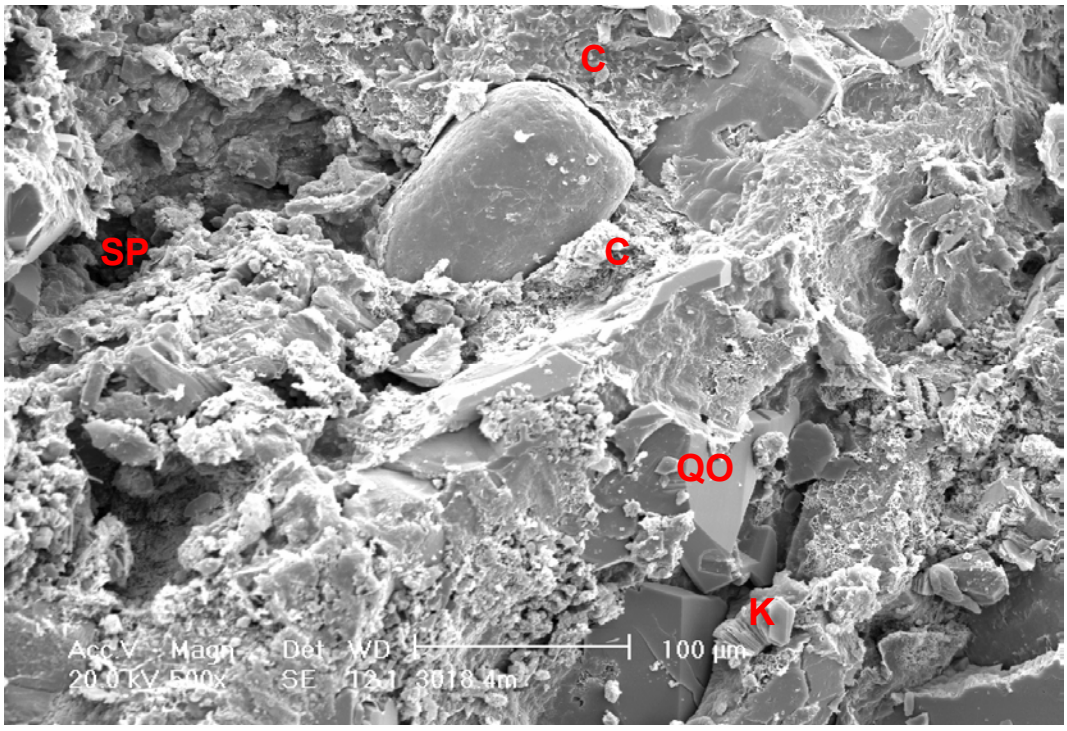
PLATE 11: MSCT #3/2 3018.4m (cont.)

FIGURE 1



Low magnification micrograph showing general texture. Coarse grains are supported by fine sandy matrix in which macropores (P) are small and isolated and thus are not conducive to permeability. (SEM micrograph)

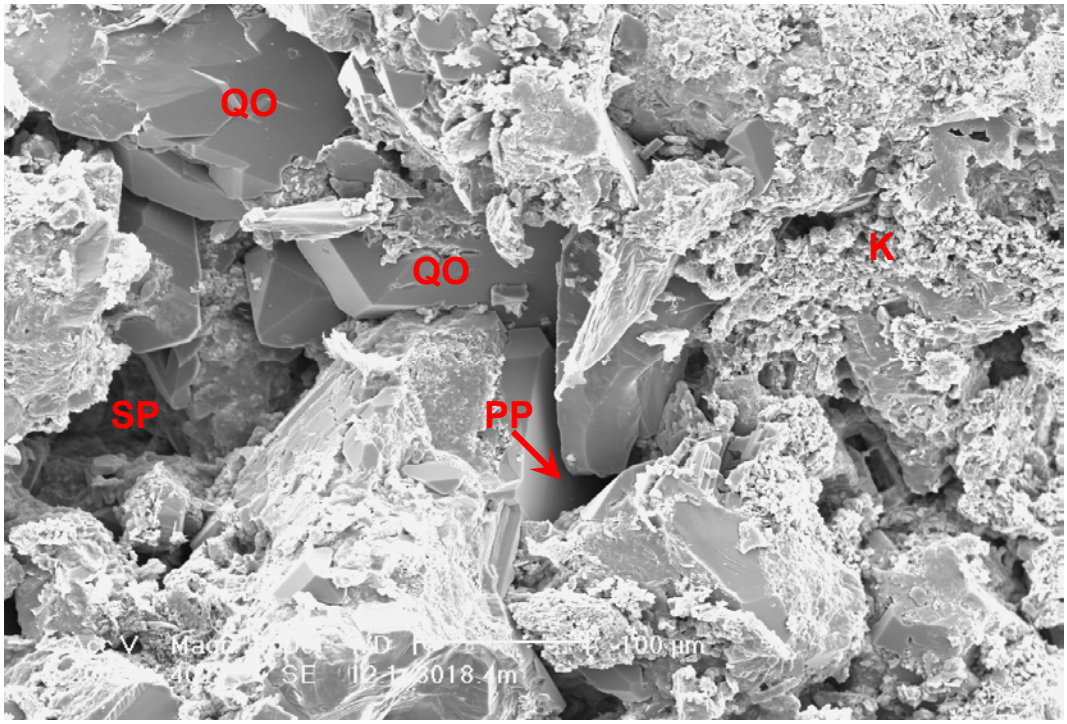
FIGURE 2



Throughout most of the sandstone, intergranular areas are filled by dispersed illitic clay matrix (C), authigenic kaolinite (K) and localised quartz overgrowths (QO). Being surrounded by microporous sandstone, secondary labile grain dissolution pores (SP) would have no connection with any macropores that occur in their vicinity. (SEM micrograph)

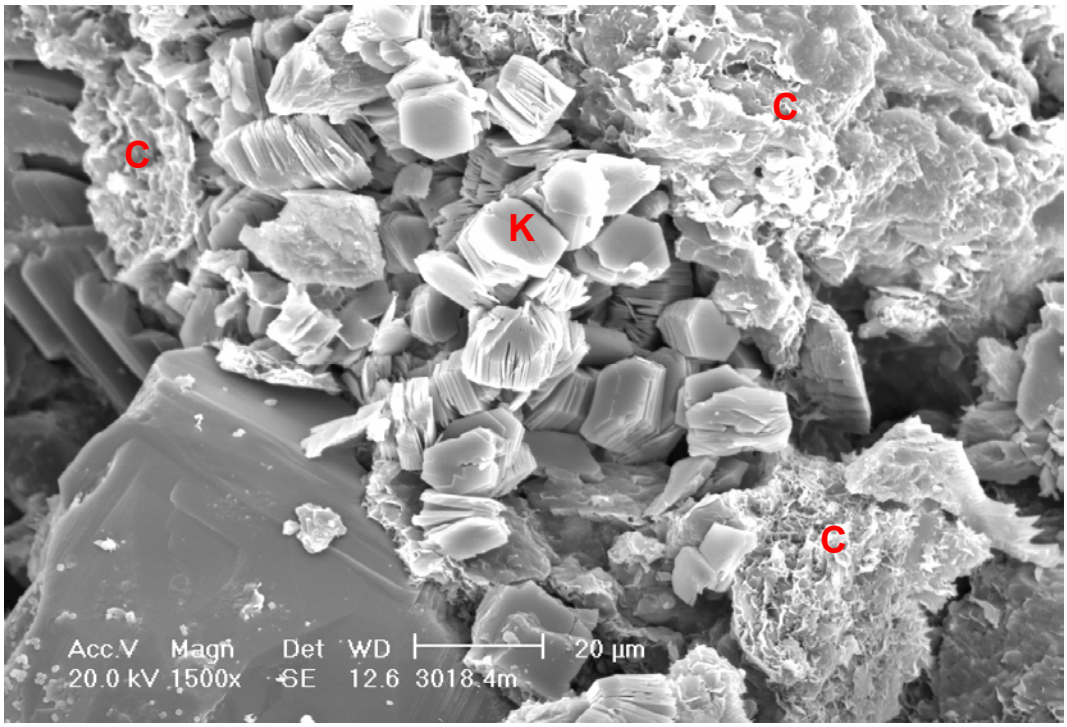
PLATE 12: MSCT #3/2 3018.4m (cont.)

FIGURE 1



In an area that lacks illitic clay matrix, minor primary porosity (PP) is preserved where intergranular spaces are incompletely filled by quartz overgrowths (QO) and authigenic kaolinite (K). A secondary pore (SP) occurs where a labile grain has dissolved. With macropores having an erratic distribution throughout the sandstone, pore interconnectivity on a thin-section scale is low. (SEM micrograph)

FIGURE 2



Authigenic kaolinite (K) occurs as an alteration product of illitic clay matrix (C). (SEM micrograph)

APPENDIX 8: CORE INTERPRETATION



delivering the goods

Trefoil 1

Core Description Report

T/18P
BASS BASIN

Brett Pidgeon
June 2005

EXECUTIVE SUMMARY

A sedimentological study of Core 1 from the Eastern View Coal Measures in Trefoil 1 indicates that this interval was deposited in a brackish water shoreface setting. Interpreted depositional environments include shelf, lower offshore, proximal lower shoreface, middle and upper shoreface. The degree and diversity of bioturbation in the core indicate that the interval was subject to environmental stress, possibly reduced salinity. This is confirmed by a biostratigraphic sample from the shelf facies containing limited dinoflagellates and predominantly fresh water algae.

The lower offshore and proximal lower shoreface are separated by an erosion surface demarcated by a *Glossifungites* ichnofacies; a characteristic ichnofacies assemblage of robust, sharp walled, passively filled, vertical to sub-vertical domichnia (dwelling burrows), that is excavated into semi-consolidated (firmground) substrates. This surface demarcates a discontinuity surface that reflects a pause in sedimentation, generally accompanied by erosion. High resolution sequence stratigraphy and ichnofacies analysis has been used to subdivide the cored interval into high-order systems tracts that form the components of a longer period, lower-order sequence.

The succession is dominated by intervals in which there was an over supply of sediment relative to the rate of base level change, producing progradational stacking. A sequence boundary (SB) separates the lower offshore from the proximal lower shoreface indicating a fall in relative base level. The lower offshore represents a highstand systems tract (HST) and the overlying proximal lower shoreface comprises a lowstand systems tract (LST) of a high-order, high frequency sequence. The HST and LST comprise components of a lower-order, low frequency HST.

Reservoir quality is strongly influenced by facies with the highest permeability occurring in the middle and upper shoreface facies. The degree of bioturbation does not control the reservoir quality in these facies as the majority of bioturbation comprises cryptobioturbation.

TABLE OF CONTENTS

Executive summary i

INTRODUCTION 2

Overview 2

Objectives 2

Methodology 2

SEDIMENTOLOGY 3

Facies A – Weakly laminated mudstone 3

Facies B – Interbedded mudstone and thin sandstone 5

Facies C – Sandstone with interbedded mudstone 7

Facies D – Amalgamated sandstone with carbonaceous debris 9

Facies E – Massive to faintly laminated sandstone 10

DEPOSITIONAL MODEL 11

Shelf 11

Lower offshore 11

Proximal lower shoreface 11

Middle shoreface 11

Upper shoreface 12

SEQUENCE STRATIGRAPHY 12

Stratal surfaces 12

Sequence stratigraphic model 12

RESERVOIR QUALITY 13

REFERENCES 14

APPENDIX 1 TREFOIL 1 INTERPRETED CORE PHOTOGRAPHS 20

APPENDIX 2 TRACE FOSSIL DESCRIPTIONS 23

INTRODUCTION

Overview

One core, 7.25 m in length, was described in detail from Trefoil 1. The core was cut in the Eastern View coal Measures (EVCM) and the core barrel jammed after cutting 8.2 m (2735 – 2743.2 m) with a recovery of 88%. All depths refer to drillers depth unless otherwise stated; note, there is approximately a 0.8 m depth shift between drillers depth and loggers depth.

Objectives

The main objectives of the core description were the following:

1 Provide a detailed description of the cored intervals
2 Determine lithofacies and ichnofacies
3 Interpret depositional environment
4 Describe sedimentary sequences and key stratal surfaces present within the core
5 Describe the reservoir potential

Methodology

The core was logged at 1:20 scale. Grainsize, colour, composition, physical sedimentary structures, macro palaeontology, ichnology (including Bioturbation index) were recorded. Bioturbation index (BI) records the intensity of bioturbation within a unit on a scale of 1 to 6. Where 1 indicates sparse bioturbation and disturbance of primary physical sedimentary structures and 6 indicates complete reworking of sediment and removal of all evidence of original sedimentary structures. Other ichnology characteristics including community succession resulting from environmental modification as the habitat becomes less suitable; and tiering in which bioturbation is vertically partitioned, resulting from vertical zoning of physical, chemical and biological parameters were also noted.

SEDIMENTOLOGY

The cored interval can be subdivided into five facies on the basis of preserved sedimentary structures and bioturbation that are characteristic of particular depositional environments. The facies, labelled A through E, range from very fine-grained sand to mud. A summary of the main features of the facies is in Table 1 and the ichnofossils assemblages are in Table 2. Interpreted core photographs are included in Appendix 1.

Table 1. Summary of the main features of the sedimentary facies in Trefoil 1 Core 1.

Facies	Main features	Inferred depositional process	Depositional environment
A	Weakly laminated mudstone, rare siltstone lam. Bioturbation not distinct.	Suspension settling, infrequent storm activity	Shelf
B	Mudstone with thin interbedded sandstone.	Combination of suspension settling (fair-weather) and storm activity.	Lower offshore
C	Sandstone with interbedded mudstone	Combination of fair-weather and storm wave activity.	Proximal lower shoreface
D	Amalgamated sandstone with carbonaceous debris	Combination of fair-weather and storm wave activity.	Middle shoreface
E	Massive to faintly laminated sandstone	Fair-weather wave activity	Upper shoreface

Facies A – Weakly laminated mudstone

Sedimentology

This facies occurs at the base of the core, comprises a relatively homogeneous interval of weakly laminated black or dark grey mudstone and rare admixed and interlaminated sandy siltstone that comprise less than 5% of the facies. The siltstone laminations increase toward the top of the facies and, where preserved, are generally discontinuous and structureless.

Ichnology

The traces identified occur toward the top of this facies where the proportion of interlaminated siltstone increases. The ichnogenera identified are *Chondrites, Helminthopsis* and *Planolites* and reflect deposit feeding and grazing structures attributable to a distal *Cruziana* assemblage (Raychaudhuri et al, 1992).

Table 2. Relative abundance of ichnofossils within the facies observed in the EVCM, Trefoil 1. The basal zone for Facies C represents the *Glossifungites* assemblage.

Ichnofossils	Facies A	Facies B	Basal Facies C	Facies C	Facies D	Facies E
Bergaueria	-	-	-	r	-	-
Cryptobioturbation	-	-	-	-	c	a
Chondrites	c	a	-	c	-	-
Helminthopsis/ Phycosiphon	c	a	-	c-a	c	c
Lockeia	-	-	-	r	-	-
Palaeophycus	-	-	-	r	-	r
Planolites	o-r	o-r	-	r	-	-
Skolithos	-	-	-	-	r	r
Teichichnus	-	r	-	a	-	-
Thalassinoides	-	-	c	r	-	-

Interpretation

The siltstone intervals are interpreted to represent distal equivalents of storm beds in the offshore and lower shoreface. Facies A is interpreted to have been deposited in relatively deep quiet waters corresponding to shelfal conditions (MacEachern et al, 1992a; Raychaudhuri et al, 1992).

The paucity of visible traces in this facies may be explained in two ways. The first is that relatively few organisms actually occupied that particular ecological niche, possibly due to reduced salinity and localised or periodic euxinic conditions. The trace fossils associated with the coarser-grained units may therefore correspond to episodic storm emplacement of more oxygenated and non-toxic waters transporting the event bed into shelfal areas that generally were stressful to organisms. Presumedly, most of the colonisers of the substrate would have been entrained in the flow, possibly from the offshore and lower shoreface, or reflect larval settling by opportunistic organisms. With time, the shelfal area would

progressively return to stagnant conditions, resulting in the demise of the colonisers (MacEachern et al, 1992a).

The second possibility is that relatively abundant burrows were present throughout but are essentially invisible due to a lack of lithological contrast, or they have been subsequently destroyed. Although grazers and foragers may have been abundant, upon compaction and dewatering these structures are unlikely to have been preserved. Much of the fill of these structures are faecal casts, rather than contrasting lithology, so that essentially no record of the biogenic activity of the organisms may be preserved, except in association with the sandy siltstone laminations, which are less susceptible to compaction (MacEachern et al, 1992a). Inhabitants of soup-grounds and watery soft-grounds tend to cause diffusive turbulence by their passage through the substrate and produce a structureless fabric (Bromley, 1996).

The low diversity of trace fossils suggests that the environment was restricted (Pemberton and Wightman, 1992) and the low numbers and diversity of saline dinoflagellates, coupled with the number of freshwater algae (Morgan, 2005), also indicates that the environment was stringent

Facies B – Interbedded mudstone and thin sandstone

Sedimentology

The base of this facies is gradational and overlies Facies A. The facies comprises mudstone with thin interbedded silty sandstone to very fine-grained sandstone (Figure 1). Bedding thickness of the mudstones is generally on the order of several centimetres, while the sandstones thicken from laminations in the lower part to several centimetres toward the top of the facies. The amount of mudstone decreases as the sandstones thicken upward. The sandstones are very fine-grained, contain carbonaceous laminae and flat to undulatory laminae. The sandstones are sharp based and are normally graded. Some beds contain symmetrical starved ripples.

Ichnology

This facies is characterised by diminutive, low density and low diversity ichnofossil assemblage of *Planolites, Chondrites* and ?*Helminthopsis* that predominantly occur in the mudstone beds and at the tops of the thin sandstone beds. The ichnogenera present are deposit feeding structures that are preferentially concentrated along discrete laminae.

Also present are discrete horizontal to sub-vertical *Thalassinoides* burrows that cross cut the other ichnogenera and are sand filled.

Interpretation

The sandstone beds with sharp bases, normal grading and starved ripples are interpreted as distal storm deposits in a lower offshore setting (Raychaudhuri and Pemberton, 1992). Storm units represent individual sandstone beds that were deposited rapidly (from a few hours to several days) from waning flow events that possessed a strong oscillatory flow component. The idealised successions generally show the following characteristics: 1) storm erosion; a basal erosion surface which may be undulatory, with sole marks, and intraclasts of pebbles, shells or mudstones, 2) main storm deposition; main hummocky or swaley cross stratification interval, locally with associated horizontal or parallel lamination; 3) waning storm deposition; combined flow and/or wave rippled sand layer, indicating a progressive return to lower regime oscillatory conditions; and 4) post-storm/ fair-weather mud deposition; reflecting either the final suspension fallout of storm derived sediment (i.e. post storm mud) or the return to normal background sedimentation (i.e. fair-weather mud) (Pemberton et al, 1992a).

Storm deposits may also be indicated by the thin zones of intense bioturbation that reflect increased levels of food availability in comparison to the background sedimentation rates. The increased organic material incorporated into these beds promoted increased bioturbation by deposit feeding organisms (Beynon and Pemberton, 1992).

The ichnogenera present (excluding *Thalassinoides*) are indicative of salinity fluctuations (combined with corresponding changes in temperature, exposure, turbulence, oxygen content, turbidity etc.) that result in a physiologically stressful environment for numerous organism groups. In general, the brackish water or stressed marine trace fossil suites are characterised by 1) low diversity, 2) forms typically found in marine environments, 3) simple structures constructed by tropic generalists, 4) suites that are commonly dominated by a single ichnogenus, 5) vertical and horizontal ichnofossils that are common to both the *Skolithos* and *Cruziana* ichnofacies; and 6) some forms may be found in prolific densities (Pemberton and Wightman, 1992).

Thalassinoides is not considered to be part of the lower offshore ichnofossil assemblage as this is typically a shallow tier structure and it cross cuts deeper tier structures such as *Chondrites*. Subaqueous sediments are vertically zoned with respect to physical, chemical

and biological parameters and differing species prefer different zones within the sediment (Bromley, 1996). The presence of un-lined sub-vertical burrows in the mudstone is also anomalous as vertical burrows cannot be constructed and maintained in soft muddy substrates (MacEachern et al, 1992b). *Thalassinoides* is considered to represent a *Glossifungites* assemblage, a substrate controlled assemblage of trace fossils characterised by a robust, sharp-walled, unlined, passively filled, vertical to sub-vertical domichnia (dwelling burrows), excavated into semi-consolidated (firmground) substrates and demarcates discontinuity surfaces that reflect pauses in sedimentation, generally accompanied by erosion (MacEachern et al, 1992b; Pemberton et al, 2002).

Facies C – Sandstone with interbedded mudstone

Sedimentology

Facies C is sharp based and overlies Facies B. This facies comprises very fine-grained sandstone and silty sandstone interbedded with mudstone. The sandstones are sharp based and, in places, contain horizontal to undulatory laminations; thinner beds also display normal grading. The majority of the sandstone has a churned fabric overprinting any laminations that were present (Figure 1). The mudstone contains normally graded lenticular bedded sandstone. Some sandstone beds have irregular bases that resemble load casts, however, these are not limited to beds where there is a large contrast in grainsize (sandstone overlying mudstone) but also occur in interbedded sandstones.

Ichnology

The base of this facies is delineated by a *Glossifungites* ichnofacies, comprising passively filled *Thalassinoides* that cross cut the background softground trace fossil assemblage of Facies B (Figure 1). The burrows extend up to 50 cm below the contact between Facies B and C. Immediately overlying the contact is a thoroughly bioturbated interval (bioturbation index of 6) comprising a monospecific assemblage of *Teichichnus* (Figure 1).

The bioturbation index throughout this facies is highly variable and ranges from 6 in some of the sandstones with the churned fabric to 3 for some of the mudstone beds and some of the less bioturbated sandstone beds. There is a low diversity of ichnogenera present with *Chondrites, Planolites, Helminthopsis/Phycosiphon,* rare *Thalassinoides, Bergaueria* and *Lockeia. Chondrites* and *Planolites* predominantly occur in the mudstone beds whereas *Helminthopsis/Phycosiphon* and *Thalassinoides* occur in the sandstone beds. *Bergaueria* and *Lockeia* occur at the base of some of the sandstone beds (Figure 1). This comprises a low diversity stressed mixed *Cruziana-Skolithos* ichnofacies.

Interpretation

Facies C is interpreted to record deposition in a proximal lower shoreface setting. There are intervals of wave produced structures (such as low angle and wavy laminated intervals representing hummocky cross stratification and amalgamated swaley cross stratification) that reflect storm deposition. The mudstone intervals with the lenticular bedded sandstone represent fair-weather generated oscillation ripples (MacEachern and Pemberton, 1992).

Biogenic features are dominated by the *Cruziana* ichnofacies with some representatives of the *Skolithos* ichnofacies, although the low diversity of trace fossils present implies stressed environmental conditions, similar to those that prevailed during the deposition of Facies B. The intensity of burrowing is interpreted to reflect a combination of storm intensity, storm frequency and sedimentation rate, rather than a change in water chemistry, distance from shore, or nature/abundance of infauna (MacEachern and Pemberton, 1992; Pemberton et al, 1992a). The well bioturbated sandstone intervals imply low intensity and infrequent storm events that lead to the homogenisation of the storm deposits (Pemberton et al, 2002). *Thalassinoides* reflect first stage opportunistic colonisation of sandy storm deposits, whereas *Helminthopsis/ Phycosiphon* represent a second stage re-burrowing of the original pioneer trace suite (Raychaudhuri and Pemberton, 1992).

The intensely bioturbated, monospecific *Teichichnus* assemblage overlying the *Glossifungites* surface records the establishment of the benthic community in response to more favourable physical and ecological conditions associated with a relative base level change (Beynon and Pemberton, 1992).

The irregularities on the bases of beds may not reflect load casts, instead, they may reflect hypichnia (a structure preserved at the lower surface of the main body of the casting medium (Pemberton et al, 2002)), preserved in hyporelief of surface features (MacEachern et al, 1992a). The occurrence of these features in interbedded sandstone implies that they are more likely to represent biogenically derived features as opposed to loading.

Facies D – Amalgamated sandstone with carbonaceous debris

Sedimentology

Facies D overlies Facies C and comprises amalgamated very fine-grained sandstone beds with rare mudstone laminations occurring between beds. The mudstones decrease upwards as the sandstones become more amalgamated. The sandstones are sharp-based, and in places contain low angle to parallel laminations (Figure 1), with rare beds passing upwards into small scale oscillations to combined flow ripples. Carbonaceous debris is common toward the tops of beds that are overlain by mudstone laminations. The sandstone beds that overlie the mudstone laminations have irregular bases whereas the amalgamated sandstone beds have erosional bases (Figure 1). The low angle truncation surfaces are ubiquitous in the thick sand beds; where they obliterate all trace of convex upward laminae, and represent swaley cross stratification. Where slightly convex upwards laminae are preserved, the sands represent hummocky cross stratification. These laminae are commonly accentuated by finely comminuted organic detritus (Raychaudhuri and Pemberton, 1992).

Ichnology

The dominant ichnogenera present within this facies is *Helminthopsis/Phycosiphon* that is restricted to the sandstone beds. Lined *Skolithos* are also present in the amalgamated sandstone intervals although these are very rare (Figure 1). The thoroughly bioturbated sandstone also contains cryptobioturbation. Rare diminutive *Planolites* occur in the mudstone laminae between sandstone beds. The bioturbation index is highly variable in this facies and ranges from 6 in some of sandstone beds to 0 in laminated sandstone intervals. The mudstone laminae typically have a BI of 2. This comprises a low diversity stressed mixed *Cruziana-Skolithos* ichnofacies.

Interpretation

Facies D is interpreted to have been deposited in a middle shoreface setting. The thickness of the sandstone beds is attributed to the amalgamation of storm beds and fair-weather deposits, with each successive storm eroding some of the interim fair-weather deposits (Raychaudhuri and Pemberton, 1992). These beds become more erosive with increased shallowing and associated enhancement of storm-induced scouring (Pemberton et al, 2002). The dominance of deposit feeding behaviours (constituting the *Cruziana* ichnofacies) over suspension feeding behaviours (*Skolithos* ichnofacies) indicates a low wave energy setting because as storm effects become more pronounced, the diversity of

deposit feeding structures declines markedly. This is attributable to the abundance of well winnowed sand and the paucity of deposited food for the *Cruziana* ichnofacies tracemakers to feed upon (Raychaudhuri et al, 1992; Pemberton et al, 2002).

The low diversity of the ichnogenera present implies a brackish water setting (Pemberton and Wightman, 1992; Beynon and Pemberton, 1992; Pemberton et al, 2002).

Facies E – Massive to faintly laminated sandstone

Sedimentology

This facies is almost entirely well-sorted, very fine-grained sandstone that is either massive or contains faint laminations that represent trough cross bedding and low angle laminations. The laminations are defined by finely comminuted organic detritus. Very rare discontinuous mudstone beds occur toward the base of this facies. The base of Facies E is erosive and overlies Facies D, and there are a number of internal scour surfaces, typically associated with the faintly laminated intervals.

Ichnology

This facies contains rare macrofauna trace fossils comprising lined *Skolithos* (Figure 1) and *Palaeophycus*. The majority of the bioturbation, however, comprises cryptobioturbation (Figure 1) that has resulted in widespread, very small scale disruption of grain fabrics through the sand's laminae, hence the blurred appearance.

Interpretation

The presence of low angle lamination and trough cross bedding indicates deposition in the upper shoreface. The diversity of trace fossils is low, as the continuously migrating bedforms present a major ecological problem to endobenthic organisms; consequently there is a general scarcity of animals that are capable of constructing permanent domiciles under such conditions. Those biogenic structures that are formed have a low preservation potential as, generally, only deeply penetrating structures are preserved (Raychaudhuri et al, 1992; Pemberton et al, 2002). The ichnological elements correspond to the *Skolithos* ichnofacies. The cryptobioturbation is similar to *Macaronichnus* except that instead of ingesting the sediment, the meiofauna jostle through the sediment. Cryptobioturbation has been found in brackish water and fully marine conditions (Pemberton et al,2002).

DEPOSITIONAL MODEL

The depositional setting for the succession in the core is a progradational marginal marine/brackish water shoreface. From the core it is possible to make some inferences about the overall setting as to whether the core was deposited in a restricted bay or was part of a larger brackish water, possibly basin-wide, setting. The well sorted, cross bedded and low angle laminated sandstone in the core indicates a moderate to high energy setting. The dominance of wave formed structures implies an open coast/strandplain setting (Figure 2) as restricted bays are low energy and are characterised by mixed mud and sand facies (Figure 3).

Shelf

There is only rare bioturbation in this setting, possibly resulting from anoxic conditions or the lack of preservation of grazing/deposit feeding structures. This facies was deposited in quiet water conditions, below storm wave base. The sandy siltstone intervals represent the distal equivalents of storm deposits in the offshore and shoreface.

Lower offshore

Mudstone is the dominant lithology in this facies but the silty sandstone/sandstone beds become more common and there is a notable increase in the preservation of bioturbation, mainly associated with lithological contrasts. The increased sandstone beds with undulatory laminae (HCS) and the dominance of mudstone implies a lower offshore setting. The low diversity of burrowing reflects environmental stresses e.g. reduced salinity.

Proximal lower shoreface

This facies overlies an erosion surface (*Glossifungites* surface) and comprise interbedded sandstone and mudstone. Wave energy is the dominant controlling process with sandstone beds reflecting storm deposition and mudstone intervals with lenticular bedded sandstones reflecting fair-weather deposition. The high intensity of burrowing reflects low intensity and infrequent storm events producing homogenisation of the tempestites and accumulation of thick fair-weather intervals.

Middle shoreface

Amalgamated sandstones with finely comminuted organic debris are typical of this facies. The amalgamation beds are typical of increased wave energy in which the beds are erosively based and the degree of erosion increases with progressive shallowing.

Upper shoreface

Amalgamated beds of massive to faintly laminated sandstone within the upper shoreface are thoroughly bioturbated by meiofauna producing a blurred appearance on the laminations. This facies is situated in the high energy build-up and surf zones where sediment transport results from multidirectional currents e.g. longshore currents, breaking waves etc.

SEQUENCE STRATIGRAPHY

The stratigraphic record can be subdivided into various scales or orders of cycles, resulting from cyclical variations in sediment supply and relative base level change, on the basis of the periodicities. These cycles occur at different time scales, forming a hierarchy of sequences at differing frequencies and, therefore, longer period sequences contain several shorter period, higher frequency sequences. In this nested periodicity, the longer period sequences influence the stratal patterns within the higher frequency sequences; this is a function of their position within the longer period sequence. The high resolution sequence stratigraphic approach to the analysis of sedimentary successions focuses attention on key stratal surfaces, facies dislocations and parasequence stacking patterns within the context of relative base level changes.

Stratal surfaces

There is only one key stratal surface identified in the core and it represents a sequence boundary (SB) of a high-order sequence. The diagnostic features of this surface are described below.

Sequence boundary (SB)

The sequence boundary occurs between Facies B and Facies C and is characterised by a *Glossifungites* ichnofacies, a marked increase in the bioturbation immediately overlying the SB and an increase in the proportion of sandstone. The SB separates the lower offshore from proximal lower shoreface deposits. The facies dislocations indicate a basinward shift in facies associated with a relative base level fall.

Sequence stratigraphic model

The facies within the cored interval represent a progradational shoreface, with a high-order relative base level fall resulting in the juxtaposition of proximal lower shoreface sediments and lower offshore sediments. In terms of lower-order sequences, this interval constitutes part of a highstand systems tract in which sediment supply was greater than the rate of creation of accommodation.

RESERVOIR QUALITY

Reservoir quality is strongly facies dependent with the upper and middle shoreface having the highest permeability (Figure 4). The degree of bioturbation, particularly cryptobioturbation, does not have an effect on, and may actually improve reservoir quality. The greatest control is exhibited by depositional energy with the shelf and lower offshore having the lowest porosity-permeability.

REFERENCES

Bann, K.L. and Fielding, C.R., 2004. Ichnology & Facies Analysis for Petroleum Exploration. Ichnofacies Pty and University of Nebraska Short Course, April 2004.

Beynon, B.M. and Pemberton, S.G., 1992. Ichnological signature of a brackish water deposit: an example from the Lower Cretaceous Grand Rapids Formation, Cold Lake Oil Sands area, Alberta. *In:* Pemberton, S.G., ed: *Applications of Ichnology to Petroleum Exploration: A Core Workshop.* Society for Sedimentary Geology, Tulsa, 199-221.

Bromley, R.G., 1996. Trace Fossils: Biology, taphonomy and applications. Chapman & Hall, London, 361 pp.

MacEachern, J.A. and Pemberton, S.G., 1992. Ichnological aspects of Cretaceous shoreface successions and shoreface variability in the Western Interior Seaway of North America. *In:* Pemberton, S.G., ed: *Applications of Ichnology to Petroleum Exploration: A Core Workshop.* Society for Sedimentary Geology, Tulsa, 57-84.

MacEachern, J.A., Bechtel, D.J. and Pemberton, S.G., 1992a. Ichnology and sedimentology of transgressive deposits, transgressive related deposits and transgressive systems tracts in the Viking Formation of Alberta. *In:* Pemberton, S.G., ed: *Applications of Ichnology to Petroleum Exploration: A Core Workshop.* Society for Sedimentary Geology, Tulsa, 251-290.

MacEachern, J.A., Raychaudhuri, I. and Pemberton, S.G., 1992b. Stratigraphic applications of the *Glossifungites* ichnofacies: delineating disconformities in the rock record. *In:* Pemberton, S.G., ed: *Applications of Ichnology to Petroleum Exploration: A Core Workshop.* Society for Sedimentary Geology, Tulsa, 169-198.

Morgan, R., 2005. Palynology of Trefoil 1, Bass Basin, Australia. Unpublished report for Origin Energy Resources Limited.

Pemberton, S.G. and Wightman, D.M., 1992. Ichnological characteristics of brackish water deposits. *In:* Pemberton, S.G. ed. *Applications of Ichnology to Petroleum*

Exploration: A Core Workshop. Society for Sedimentary Geology, Tulsa, pp141-167.

Pemberton S.G., MacEachern, J.A. and Ranger, M.J., 1992a. Ichnology and event stratigraphy: the use of trace fossils in recognising tempestites. *In:* Pemberton, S.G., ed: *Applications of Ichnology to Petroleum Exploration: A Core Workshop.* Society for Sedimentary Geology, Tulsa, 85-117.

Pemberton, S.G., Van Wagoner, J.C. and Wach, G.D., 1992b. Ichnofacies of a wave dominated shoreline. *In:* Pemberton, S.G., ed: *Applications of Ichnology to Petroleum Exploration: A Core Workshop.* Society for Sedimentary Geology, Tulsa, 339-382.

Pemberton, S.G., Spila, M., Pulham, A.J., Saunders, T., MacEachern, J.A., Robbins, D., and Sinclair, I.K., 2001. Ichnology & Sedimentology of Shallow to Marginal Marine Systems: Ben Nevis & Avalon Reservoirs, Jeanne d'Arc Basin. *Geological Association of Canada*, Newfoundland, 343.

Raychaudhuri, I., Brekke, H.G., Pemberton, S.G., and MacEachern, J.A., 1992. Depositional facies and trace fossils of a low wave energy shoreface succession, Albian Viking Formation, Chigwell Field, Alberta Canada. *In:* Pemberton, S.G., ed: *Applications of Ichnology to Petroleum Exploration: A Core Workshop.* Society for Sedimentary Geology, Tulsa, 319-337.

Raychaudhuri, I. and Pemberton, S.G., 1992. Ichnologic and sedimentologic characteristics of open marine to storm dominated restricted marine settings within the Viking/Bow Island Formations, south-central Alberta. *In:* Pemberton, S.G., ed: *Applications of Ichnology to Petroleum Exploration: A Core Workshop.* Society for Sedimentary Geology, Tulsa, 119-139.

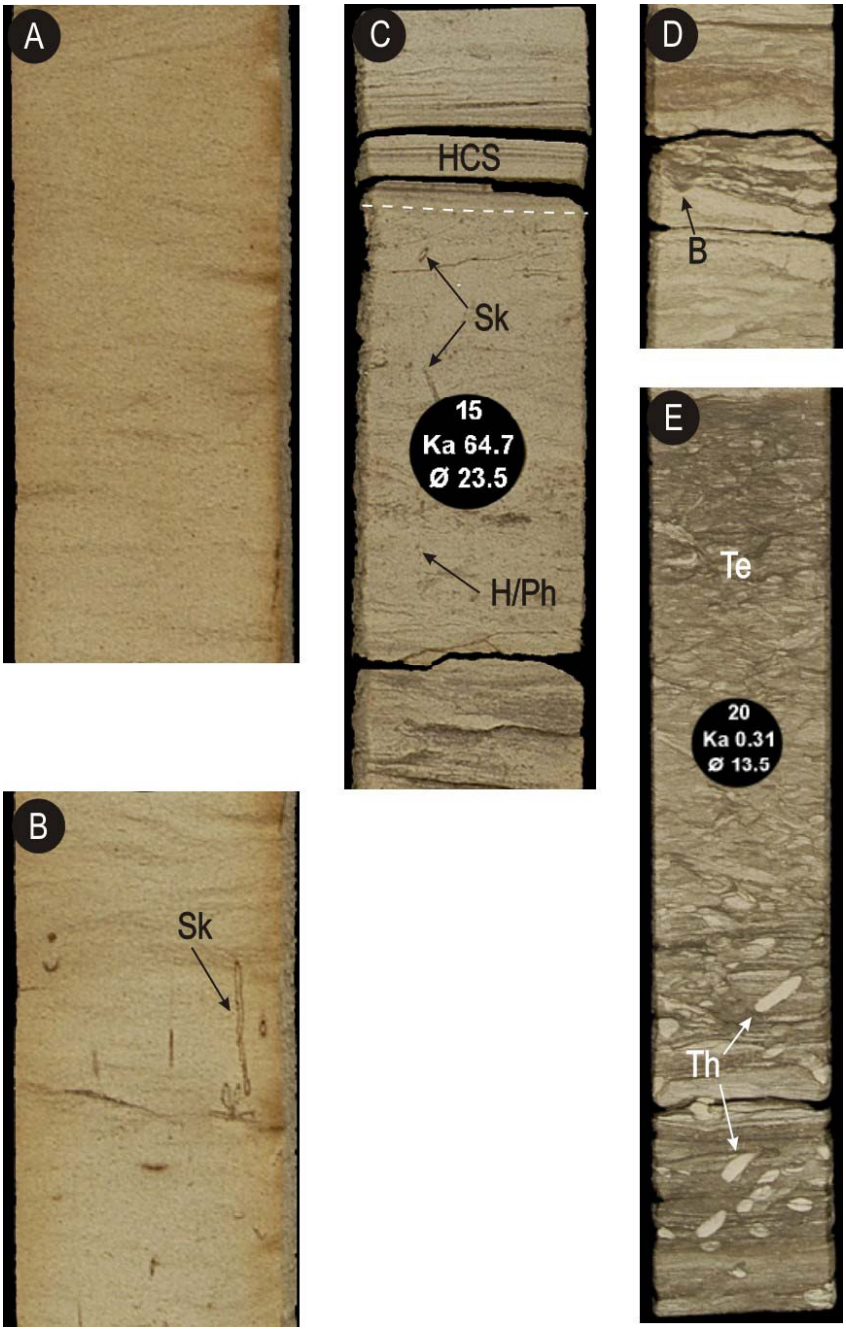


Figure 1. A) Cryptobioturbated massive to faintly laminated upper shoreface sandstone; 2735.15 – 2735.37 m. B) Lined *Skolithos* and cryptobioturbation within the upper shoreface; 2735.75 – 2735.92 m. C) Thoroughly bioturbated (*Helminthopsis* (H), *Phycosiphon* (Ph), *Skolithos* (Sk)) middle shoreface sandstone implying low frequency storm events, overlain by erosively based (dashed line) unbioturbated HCS/SCS. D) Interbedded mudstone and bioturbated sandstone of the proximal lower shoreface, *Bergaueria* (B); 2739.80 – 2739.98 m. E) Complete bioturbation of proximal lower shoreface overlying the lower offshore sediments by *Teichichnus* (Te). *Glossifungites* ichnofacies comprising *Thalassinoides* (Th) indicating erosion; 2740.52 – 2741.0 m.

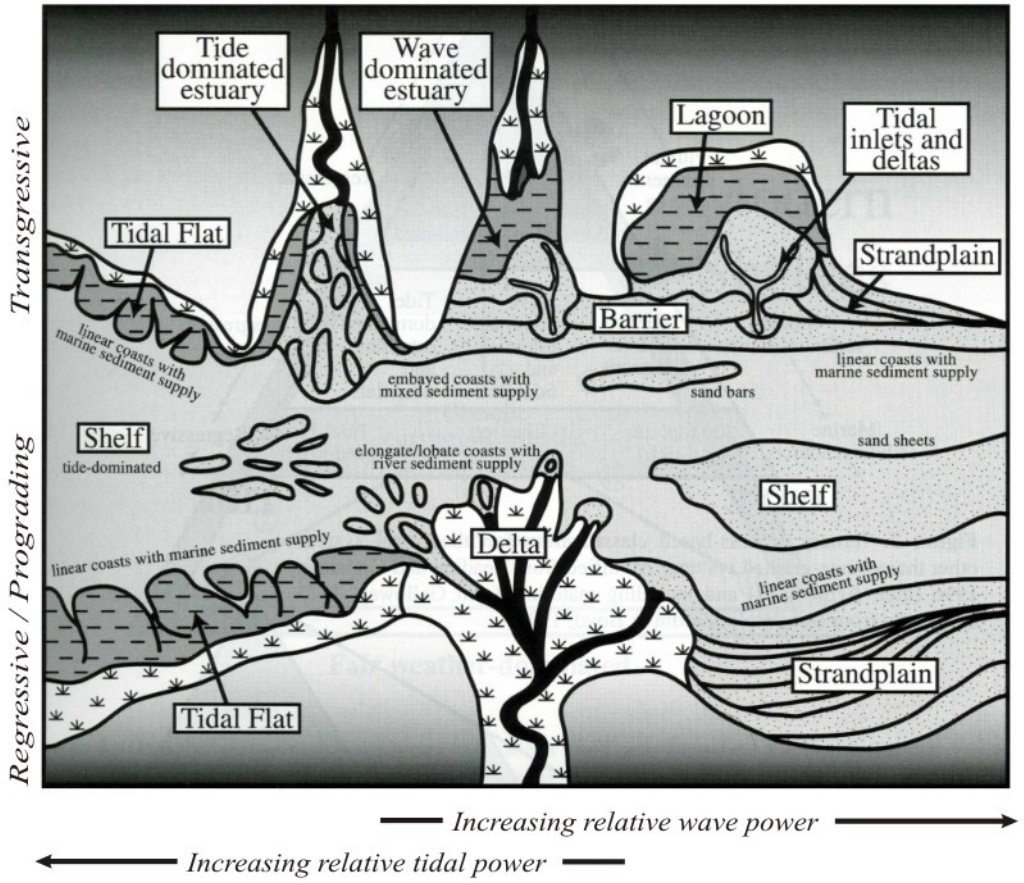


Figure 2. Siliciclastic marginal marine and shallow marine sub-environments of deposition under varying conditions of tidal power and wave power (Pemberton et al, 2002). Brackish water (lacustrine and restricted marine) settings are unlikely to have a strong tidal influence due to their limited size whereas wave dominated shorelines are more common. The Trefoil 1 Core 1 corresponds to a progradational strandplain environment in a brackish water (restricted marine?) setting.

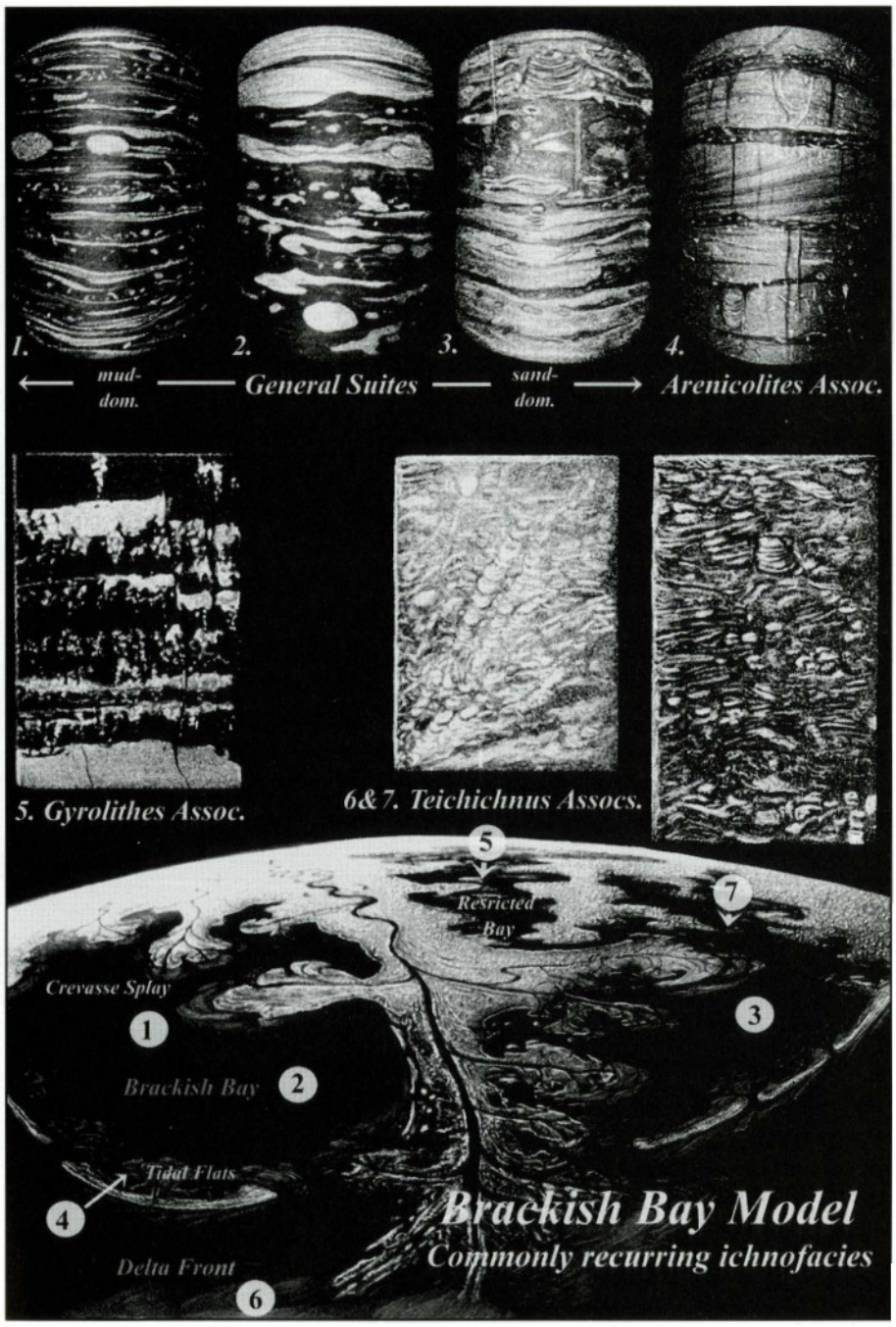


Figure 3. Schematic representations of typical recurring trace fossil associations in brackish water bay-like environments. 1,2 and 3 are general assemblages associated with either mud-dominated or sand-dominated facies; 4 is the *Arenicolites* assemblage that is commonly associated with tidal flats; 5 is the *Gyrolithes*-dominated from restricted, low-saline bays; and 6 and 7 are two variations on the *Teichichnus*-dominated assemblage, 6 is a monospecific assemblage of long *Teichichnus* that is common to delta front environments and 7 is a monospecific assemblage of short *Teichichnus* that is common to inter-distributary bays (Pemberton et al, 2002).

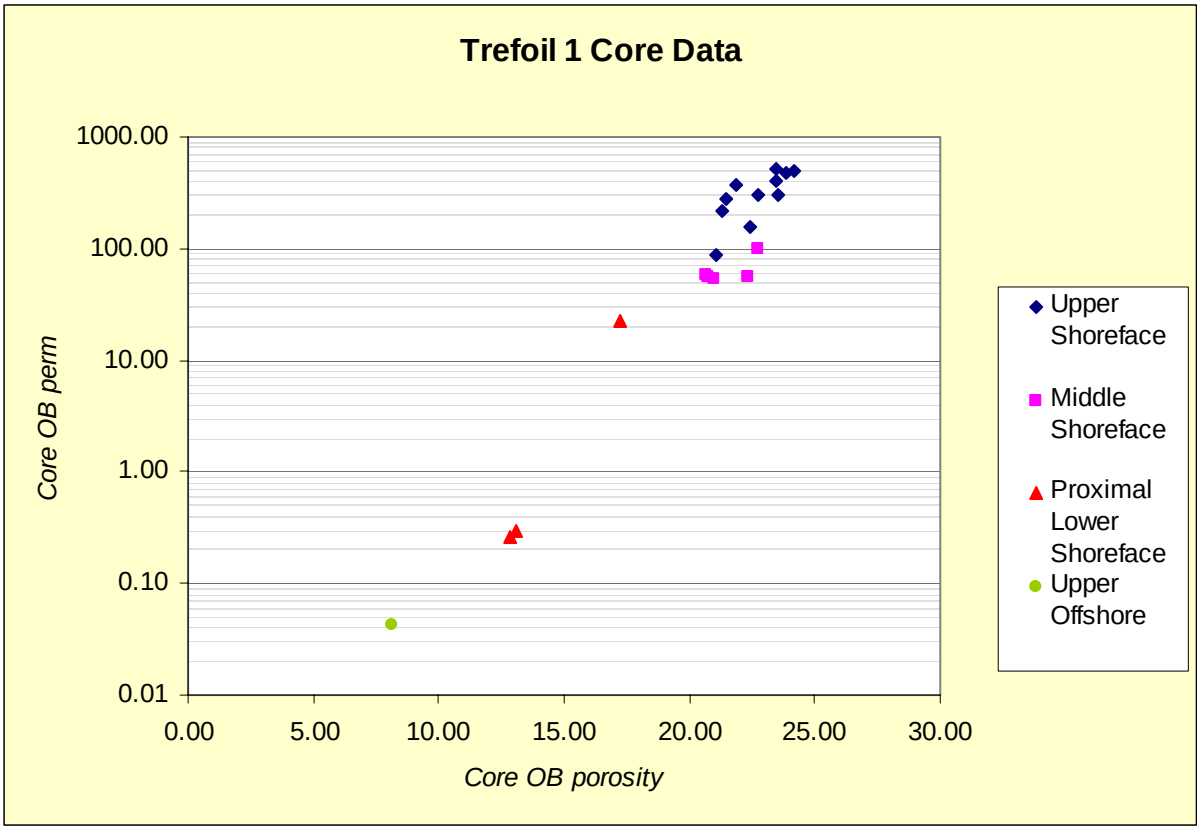
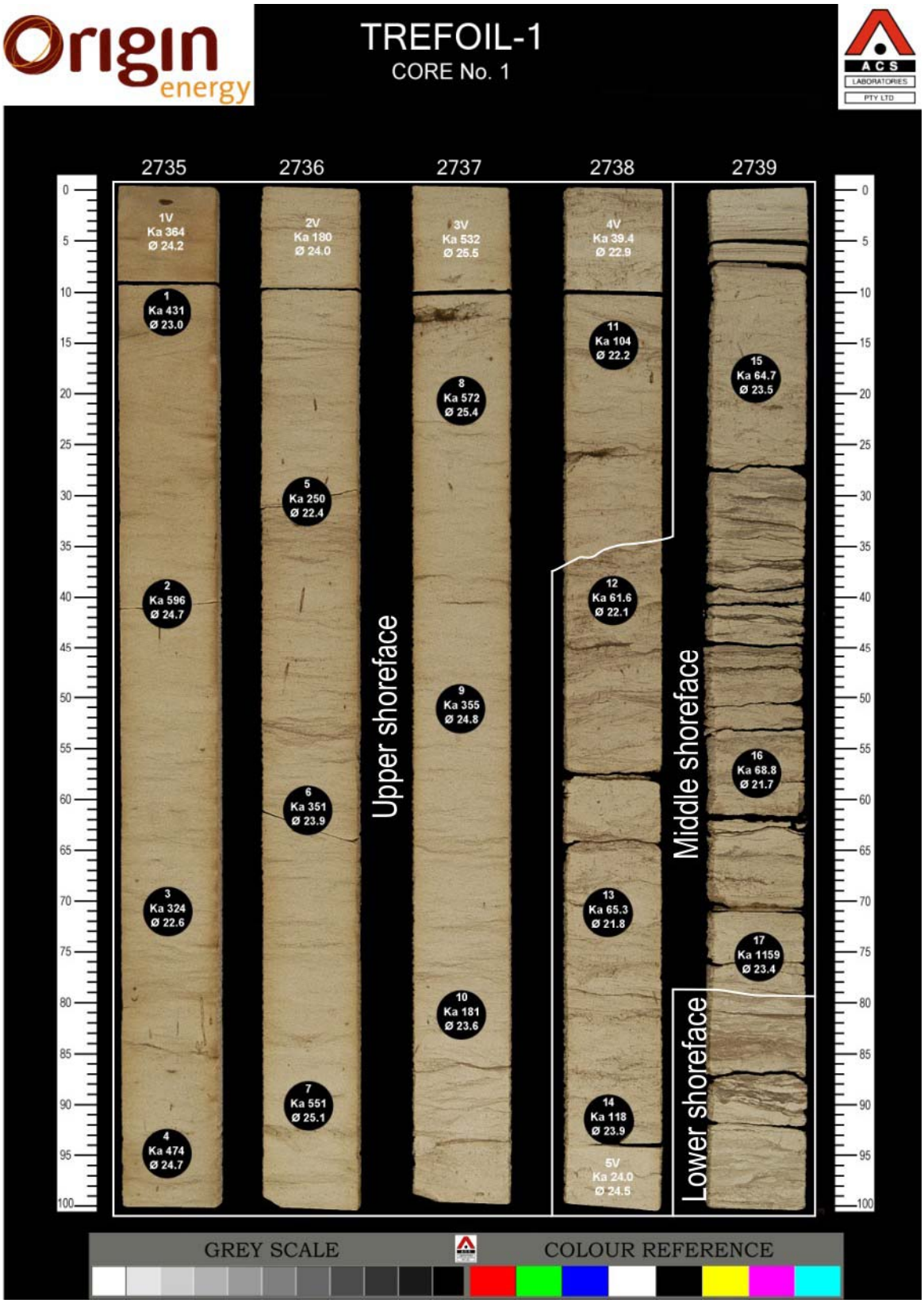
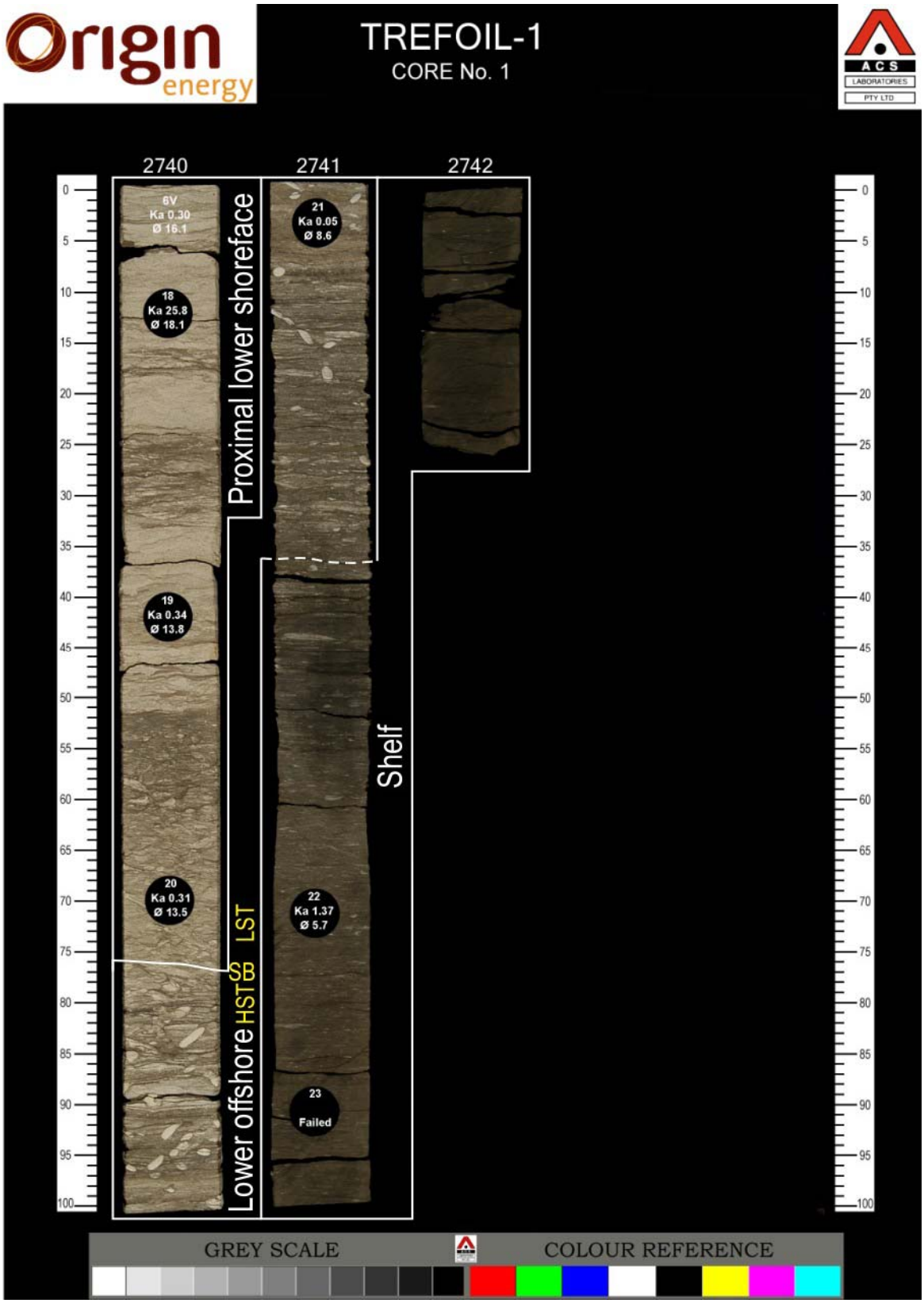


Figure 4. Core porosity and permeability plot. Note the relationship between facies and porosity/permeability.

APPENDIX 1

TREFOIL 1 INTERPRETED CORE PHOTOGRAPHS


TREFOIL-1
CORE No. 1
2735
2736
2737
2738
2739
1V Ka 364 Ø 24.2
2V Ka 180 Ø 24.0
3V Ka 532 Ø 25.5
4V Ka 39.4 Ø 22.9
1 Ka 431 Ø 23.0
2 Ka 596 Ø 24.7
3 Ka 324 Ø 22.6
4 Ka 474 Ø 24.7
5 Ka 250 Ø 22.4
6 Ka 351 Ø 23.9
7 Ka 551 Ø 25.1
8 Ka 572 Ø 25.4
9 Ka 355 Ø 24.8
10 Ka 181 Ø 23.6
11 Ka 104 Ø 22.2
12 Ka 61.6 Ø 22.1
13 Ka 65.3 Ø 21.8
14 Ka 118 Ø 23.9
5V Ka 24.0 Ø 24.5
15 Ka 64.7 Ø 23.5
16 Ka 68.8 Ø 21.7
17 Ka 1159 Ø 23.4
Upper shoreface
Middle shoreface
Lower shoreface
GREY SCALE
COLOUR REFERENCE


TREFOIL-1
CORE No. 1
2740
2741
2742
6V
Ka 0.30
Ø 16.1
18
Ka 25.8
Ø 18.1
19
Ka 0.34
Ø 13.8
20
Ka 0.31
Ø 13.5
21
Ka 0.05
Ø 8.6
22
Ka 1.37
Ø 5.7
23
Failed
Proximal lower shoreface
Shelf
Lower offshore
HST
SB
LST
GREY SCALE
COLOUR REFERENCE

APPENDIX 2

TRACE FOSSIL DESCRIPTIONS

The recognition of trace fossils in core is based primarily on their appearance in vertical cross section and due to preservational bias, full relief trace fossils (e.g. *Zoophycos, Teichichnus, Ophiomorpha, Palaeophycus* and *Chondrites*) are more easily recognised in core than epirelief or hyporelief traces (e.g. *Scolicia, Taenidium, Gyrochorte, Cochlichnus* and *Palaeodictyon*). Although it is important to recognise specific types of trace fossils, it is equally important to be able to differentiate between ethological groups, i.e. the behavioural groups traces represent. Such distinction has considerable ramifications for delineating typically depth related ichnofacies and reconstructing depositional histories. Behaviour is modified by prevailing ecological conditions that are dictated by the environment (Pemberton et al, 1992b). The following descriptions are taken from Pemberton et al, (1992b, 2002), Bromley (1996), and Bann and Fielding, (2004).

Bergaueria

Description: cylindrical to hemispherical, plug shaped vertical burrows with smooth, unornamented walls; circular to elliptical in cross section; infillings essentially structureless; rounded base with or without shallow central depression and radial ridges. The length-diameter ratio generally varies from 2.2 to 2.8.

Discussion: *Bergaueria* represents the activities of actinian anemones. Ethologically, two interpretations have been postulated, in which it represents a resting trace or dwelling burrow. Both are probably correct, with lined specimens representing dwelling traces and unlined specimens representing resting traces. Generally *Bergaueria* is indicative of normal marine conditions on a wave- or tide-dominated shoreface. It is a common element in the *Skolithos* ichnofacies. Found in brackish-water environments but greatly reduced in size.

Chondrites

Description: *Chondrites* is a complex burrow system consisting of regularly branching feeding tunnels of uniform diameter. These tunnels never inter-penetrate nor cross-cut one another. Branching typically is in one form of side branches (up to 5 or 6 orders) angling off a previous or main tunnel at 30 – 40°, rather than bifurcating at Y-shaped junctions. In core, *Chondrites* commonly appears as an array of thin elliptical dots where the vertical slice through the core truncates the numerous branching tunnels. In some instances, longitudinal sections through individual tunnels may show actual branches.

Discussion: it has been suggested that *Chondrites* represents tunnels produced by deposit feeding sipunculids, which worked from a fixed centre on the substrate surface and created the tunnels by extending its proboscis. However, some forms of *Chondrites*

penetrate so deeply into the substrate that they could only be produced by a vermiform animal dwelling within the structure, moving bodily through the sediment in a similar manner to some modern polychaetes. Although a well known facies crossing form, *Chondrites* is a common element of the *Cruziana* ichnofacies. It represents a complex feeding behaviour and is therefore more commonly associated with fully marine conditions. A monospecific association of *Chondrites* has been interpreted to be indicative of low oxygen zones.

Cryptobioturbation

Description: widespread, very small scale disruption of grain fabrics through the laminae; thus otherwise distinct laminae commonly appear blurred. In this way, sediments can be totally reworked without actual obliteration of pre-existing physical and biogenic sedimentary structures. This type of bioturbation is easily overlooked because of the minuteness of any given disruption, yet volumetrically it is one of the major biogenic processes observed.

Discussion: marine and estuarine sands teem with a diversity of tiny organisms called *meiofauna*, defined on the basis of size and include organisms ranging in size from 1 mm to 0.1 mm that live within the sediment. The meiofauna comprises two groups:

1. temporary meiofauna comprising the larval stages of benthic macroinvertebrates. These are only in the meiofauna size range for only a portion of their life history.
2. permanent meiofauna include representatives of the Rotifera, Gastrotricha, Kinorhyncha, Nematoda, Archiannelida, Tardigrada, Copepoda, Ostracoda, Mystacocarida, Halicarina, many groups of the Turbellaria and Oligochaeta, some Polychaeta and Amphipoda, and a few species of the Hydrozoa, Nemertina, Bryozoa, Gastropoda, Aplacophora, Holothuroidea, and Tunicata. These species pass their entire life cycle as members of the interstitial fauna living in the interstices between sediment grains.

With representatives of virtually every phylum, meiofauna fall intermediate in size between microfauna (<0.1 mm) and macrofauna (>1 mm). In upper-fine to medium-grained sands meiofauna are of little direct ichnological relevance; there, the interstitial spaces are such that virtually all organisms 'swim' and glide freely between the grains, without any sort of granular disruption. The potential for meiofaunally-induced bioturbation only occurs in sands that are finer than 200 micrometer where some of the dominant interstitial groups begin to approach the lower limits of metazoan body size and swimming gives way to jostling and burrowing.

Helminthopsis

Description: irregularly meandering, smooth walled burrows that never branch, interpenetrate or cut across one another. In cross section, the burrows are elliptical to sub-circular and are generally horizontal. General burrow fill is dissimilar from the surrounding matrix. In core, *Helminthopsis* commonly appears as tiny dark spots (transverse section) 1 to 3 mm in diameter, or dark lines (longitudinal section).

Discussion: *Helminthopsis* has been interpreted as a grazing structure produced by a systematic grazing polychaete (or worm-like organism). It is a common element of the distal *Cruziana* ichnofacies and proximal *Zoophycos* ichnofacies on a normal marine shallow shelf. In some instances, *Helminthopsis* can be associated with low energy, fine-grained bay environments.

Lockeia

Description: small almond-shaped oblong bodies typically preserved in convex hyporelief on the base of beds. The body has one sharp end and one obtuse end.

Discussion: *Lockeia* has been interpreted as the resting trace of suspension and deposit feeding bivalves.

Palaeophycus

Description: infrequently branched, distinctly lined, cylindrical, horizontal to inclined burrows in which the sediment typically is of the same lithology and texture as the host stratum. Wall linings range from very thin to relatively thick, and are either smooth, longitudinally striated, or with transverse annuli. Diameters are variable but commonly range from 3 to 8 mm.

Discussion: *Palaeophycus* is distinguished from morphologically similar ichnogenus *Planolites* primarily by the presence of wall linings and the character of the burrow fill. *Palaeophycus* fills represent passive, gravity induced sedimentation within open, lined burrows; the fillings, therefore, tend to be of the same composition as the surrounding matrix. Passively filled, lined burrows are typically interpreted as dwelling structures. The burrow of the predaceous glycerid polychaete, *Glyceria*, has been taken as an excellent modern analogue for the *Palaeophycus* organism. Associated with the *Skolithos* ichnofacies in both high energy and low energy shoreface environments. Commonly found with *Planolites* or *Macaronichnus;* can also be found in episodic storm sands and brackish-water assemblages.

Phycosiphon

Description: irregular meandering burrows with a black core and a pale halo of coarser silt particles. In cross section, the burrows are elliptical to sub-circular, U-shaped in the longitudinal profile with an erratic distribution. Extensive bioturbation creates a mottled texture that obscures most traces. In core, *Phycosiphon* commonly has the appearance of tiny dark pin-head size spots (transverse section) or dark U-shaped lines (longitudinal section), which may by discontinuous and surrounded by a pale silt halo.

Discussion: *Phycosiphon* represents the feeding/grazing burrows of polychaetes or other worm-like phyla. It is a common element of the *Cruziana* ichnofacies and is often found as an opportunistic coloniser of storm deposited sands.

Planolites

Description: unlined, rarely branched, straight to tortuous, smooth to irregular walled or annulated burrows in which the structureless fill is different from the host rock. *Planolites* is circular to elliptical in cross section and its dimensions are highly variable (typically 3 to 8 mm).

Discussion: *Planolites* is distinguished from *Palaeophycus* primarily by having unlined walls and burrow fills differing in texture from that of the adjacent rock; fills may also differ in fabric, composition and colour as well. Fills of *Planolites* represent sediment processed by the trace-maker especially through the deposit feeding activities of mobile endobients (bottom-feeders), probably infaunal polychaetes (or other worm-like organisms). Due to its simple morphology, *Planolites* has been found in virtually every environment, from fluvial overbank to deep sea.

Skolithos

Description: single entrance, vertical to inclined, straight to curved burrows that never branch, cross over or interpenetrate. In cross sections the shafts are cylindrical to sub-cylindrical and either lined or unlined. Linings, where present, seldom exceed 1 mm, and consist of either dark organic mud or clean agglutinated sand. The walls are generally smooth, but they may be annulated and the fill is typically massive.

Discussion: ethologically, *Skolithos* represents the dwelling burrow of a suspension feeder or passive carnivore. Probable originators could include a large number of organisms from polychaetes to phoronids, to insect larvae. Lined specimens generally associated with marine or brackish environments. It is an element of the *Skolithos* ichnofacies. But because *Skolithos* can be constructed by many different kinds of organisms it is found in virtually every type of environment from marine to non-marine.

Teichichnus

Description: *Teichichnus* appears in split core sections as a vertical series of tightly packed concave up or (more rarely) concave down, crescentic laminae. Longitudinal sections show wavy, long laminae that usually merge upward at the ends. A distinct horizontal, circular to sub-circular, burrow is always present as the upper or lower end of the laminae. It is formed by the upward migration of a horizontal to sub horizontal tunnel produced by an organism moving back and forth in the same vertical plane, probing the sediment for food.

Discussion: *Teichichnus* is generally interpreted as the dwelling/feeding burrow of a deposit feeding organism. Probable originators include annelids, or other worm-like phyla. The *Teichichnus* producing animal appears to be migrating either upward or downward in its burrow. The spreite probably represents an equilibrium response of the trace maker i.e. an attempt to maintain the bottom of its burrow at an optimal depth below the sediment water interface. Commonly found in lower shoreface to offshore environments associated with the *Cruziana* ichnofacies. Prevalent in lagoon/bay facies characterised by brackish-water. Never associated with freshwater.

Thalassinoides

Description: relatively large burrow system consisting of smooth walled, essentially cylindrical components. Branches are Y- to T-shaped and are enlarged at points of bifurcation. Burrow dimensions may vary within a given system and cross sections are half moon shaped to elliptical. Although most systems are essentially horizontal, others are irregularly inclined. Structureless to parallel laminated or graded burrow fills represent passive (gravity induced) sedimentation whereas meniscoid or chevron laminated fill represents active backfilling by the trace maker.

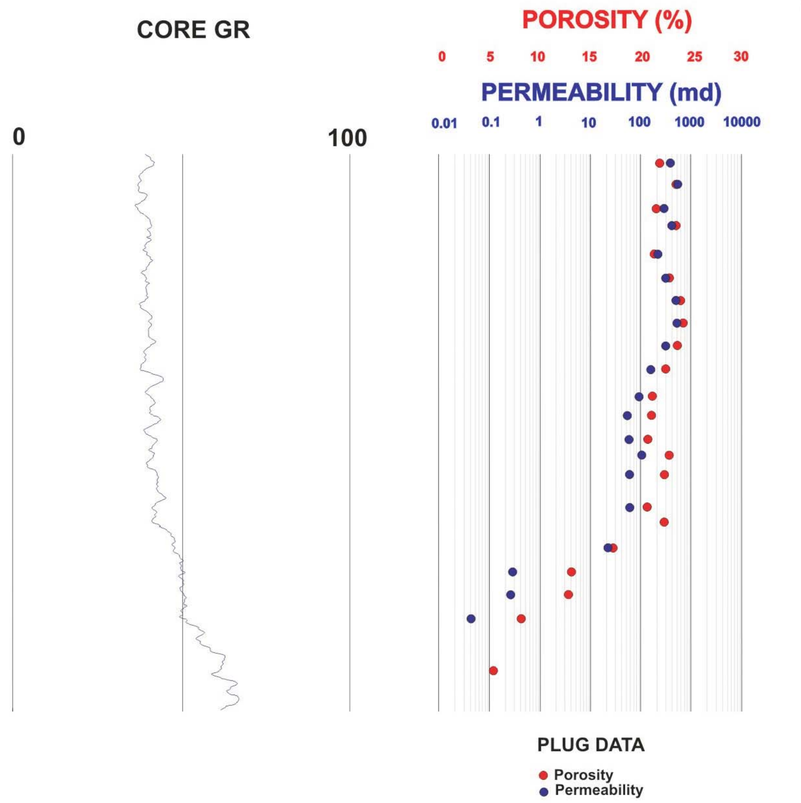
Discussion: very thinly lined to essentially unlined burrow systems are characteristic of fine grained coherent substrates that do not require reinforcement. *Thalassinoides* is generally regarded as a dwelling and/or feeding burrow of a decapod crustacean (thalassinid shrimp). Enlarged junction points are often used as turning points for the organism, or as breeding chambers. It is associated with the *Cruziana* ichnofacies in the lower shoreface to offshore environments and is also found in low diversity, brackish water assemblages.

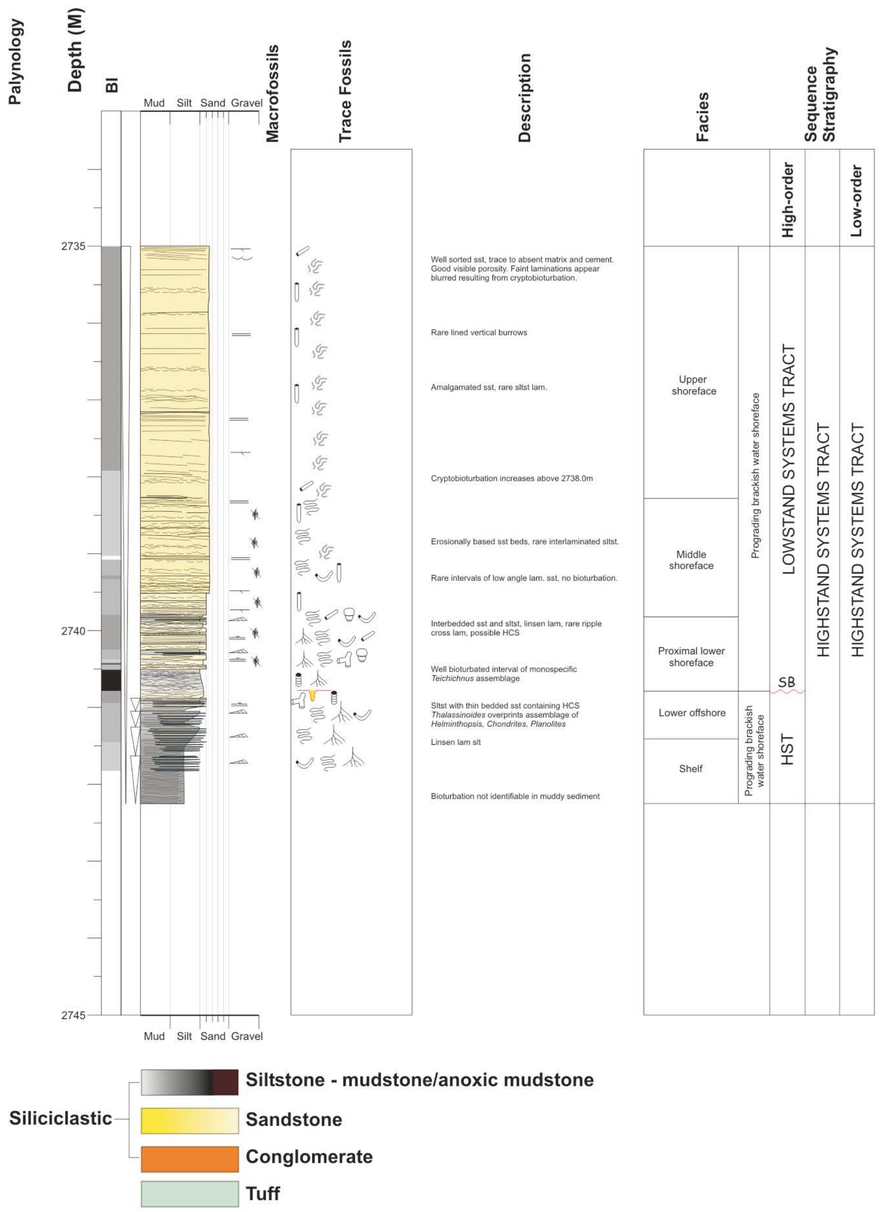
TREFOIL 1

CORE 1

Origin energy

delivering the goods





PHYSICAL SEDIMENTARY STRUCTURES

- Trough cross-bedding
- Planar cross-bedding
- Flat lamination
- Plane bedding
- Low-angle lamination
- Current Ripple Cross-lamination
- Wave Ripple Cross-lamination
- Flaser bedding
- Lenticular lamination
- Wavy lamination
- Hummocky cross-stratification
- Bioturbation
- Plant debris
- Wood
- Rip-up clasts
- Extraformational pebbles
- Soft sediment deformation
- Convoluted bedding
- Synaeresis cracks
- Stylolites
- Coaly trace
- Root trace
- Carbonaceous laminae
- Fault
- Erosional base
- Slumped sediment
- Fining upwards
- Coarsening upwards
- Herring bone cross stratification
- Calcite cementation
- Glauconite
- Pyrite
- Siderite/Fe-concretion
- Silica cementation
- Calcite-healed fracture
- Silica-healed fracture
- Fracture/fault with slickensides

ICHNOLOGY

- *Ophiomorpha*
- *Skolithos*
- *Diplocraterion*
- *Macaronichnus*
- *Thalassinoides*
- *Planolites*
- *Palaeophycus*
- *Rhizocorallium*
- *Teichichnus*
- *Phycosiphon*
- *Taedium*
- *Cylindrichnus*
- *Zoophycus*
- *Rosselia*
- *Conichnus*
- *Chondrites*
- *Undifferentiated*
- *Asterosoma*
- *Helminthopsis*
- *Schaubcylindrichnus*
- *Terebellina*
- *Glossifungites surface*
- *Escape burrow*
- *Cryptobioturbation*
- *Bergaueria*

Bioturbation Index

0 1 2 3 4 5 6

MACROFOSSILS

- *Brachiopods*
- *Molluscs*
- *Bryozoans*
- *Crinoids*
- *Forams*
- *Algae*
- *Stromatolites/stromatoporoids*
- *Unidentified shell fragments*
- *Ammonite*
- *Gastropods*

APPENDIX 9: SPECIAL CORE ANALYSIS

SPECIAL CORE ANALYSIS FINAL REPORT

of

TREFOIL-1

for

ORIGIN ENERGY RESOURCES LIMITED

by

ACS LABORATORIES PTY LTD

28 July, 2005

Origin Energy Resources Limited
Level 6
1 King William Street
ADELAIDE SA 5000

Attention: Joe Parver

Origin Energy Resources Limited
1st Floor, John Oxley Centre
339 Coronation Drive
MILTON QLD 4064

Attention: Andy Hall

FINAL REPORT: 0485-08

CLIENT REFERENCE: O4831

MATERIAL: Core Plugs & MSCT Samples

LOCALITY: Trefoil-1

WORK REQUIRED: Special Core Analysis

Please direct technical enquiries regarding this work to the signatories below under whose supervision the work was carried out.

KEVIN H FLYNN
General Manager

ACS Laboratories Pty Ltd shall not be liable or responsible for any loss, cost, damages or expenses incurred by the client, or any other person or company, resulting from any information or interpretation given in this report. In no case shall ACS Laboratories Pty Ltd be responsible for consequential damages including, but not limited to, lost profits, damages for failure to meet deadlines and lost production arising from this report.

CONTENTS

CHAPTERS PAGE

1. INTRODUCTION 1

2. SUMMARY OF TEST PROGRAM 3

3. SAMPLE PREPARATION AND BASE PARAMETER DETERMINATIONS

3.1 Test and Calculation Procedures

3.1.1 CT Scanning 7
3.1.2 Base Parameters 7
3.1.3 Sample Saturation 9

3.2 Test Results 10

4. ELECTRICAL PROPERTIES AND CAPILLARY PRESSURE

4.1 Test and Calculation Procedures

4.1.1 Formation Resistivity Factor 13
4.1.2 Formation Resistivity Index and Capillary Pressure 14
4.1.3 Capillary Pressure 15
4.1.4 Cation Exchange Capacity 15

4.2 Test Results4

4.2.1 Formation Factor 17
4.2.2 Resistivity Index 19
4.2.3 Capillary Pressure (Air–Brine) 27
4.2.4 Cation Exchange Capacity 44
4.2.5 Summary 46

5. RESIDUAL GAS

5.1 Test and Calculation Procedures

5.1.1 Permeability to Air at Residual Water Saturation 50
5.1.2 Waterflood 50

5.2 Test Results 51

APPENDICES

***I*. FLUID PROPERTIES**
***II*. EQUIPMENT SCHEMATICS**
***III*. CT SCAN IMAGES**
***IV*. ABBREVIATIONS**

CHAPTER 1

INTRODUCTION

1. INTRODUCTION

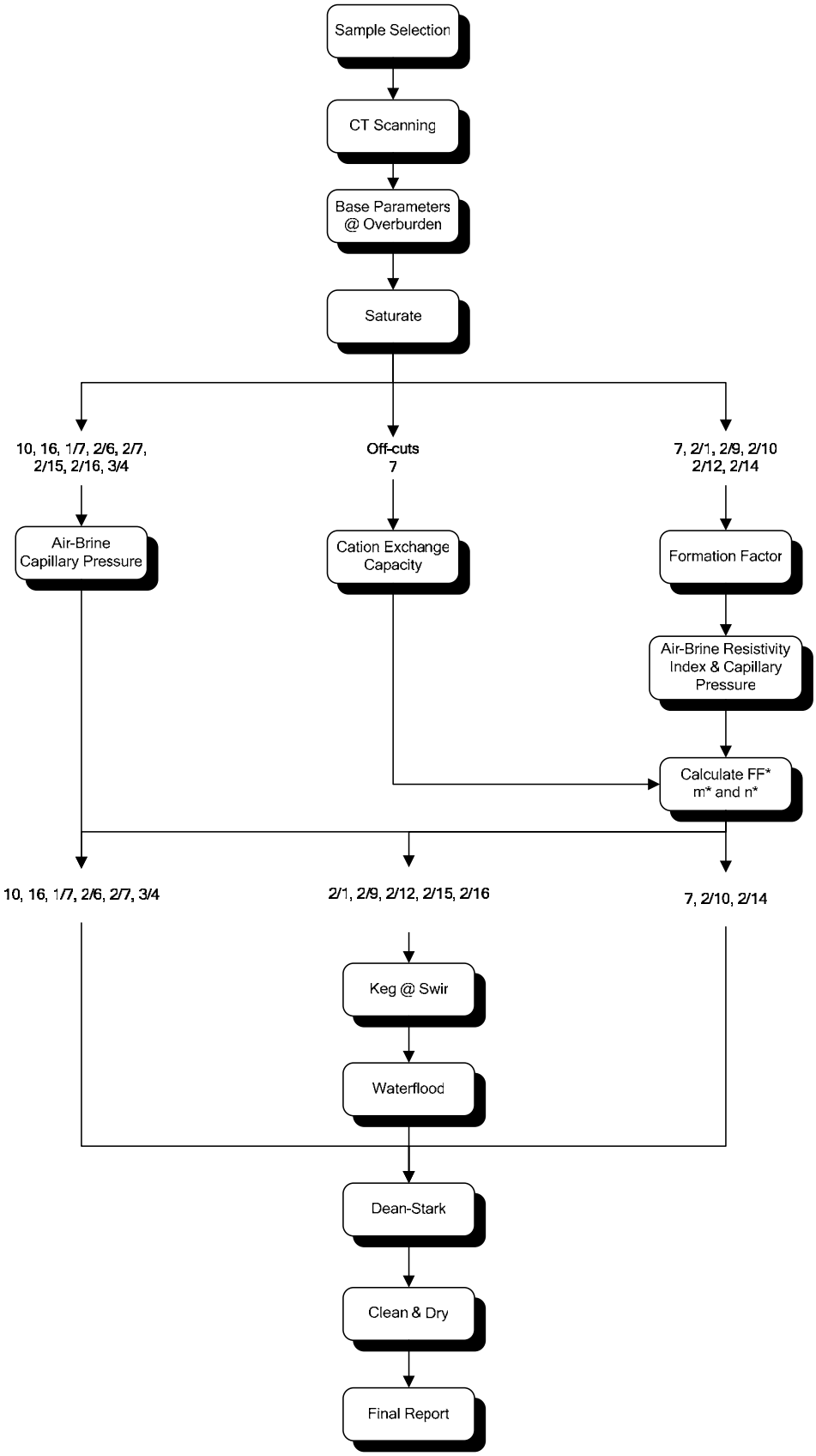
This final report presents the results from a special core analysis study of the Trefoil-1 well. The samples utilized were 1½ inch diameter core plugs originally drilled for a routine core analysis study (performed by ACS Laboratories) on the same well and MSCT samples provided.

Following discussions between Origin Energy Resources Limited and ACS Laboratories representatives, the test program was refined to that presented in summary format in Chapter 2 of this report. The subsequent chapters encompass descriptions of procedures and test results. The Appendices include ancillary information pertinent to the study.

CHAPTER 2

SUMMARY OF TEST PROGRAM

FLOW CHART


Sample Selection
CT Scanning
Base Parameters @ Overburden
Saturate
10, 16, 1/7, 2/6, 2/7, 2/15, 2/16, 3/4
Off-cuts 7
7, 2/1, 2/9, 2/10 2/12, 2/14
Air-Brine Capillary Pressure
Cation Exchange Capacity
Formation Factor
Air-Brine Resistivity Index & Capillary Pressure
Calculate FF* m* and n*
10, 16, 1/7, 2/6, 2/7, 3/4
2/1, 2/9, 2/12, 2/15, 2/16
7, 2/10, 2/14
Keg @ Swir
Waterflood
Dean-Stark
Clean & Dry
Final Report

TEST SCHEDULE

Client: Origin Energy Resources Limited
Well/Project: Trefoil-1
ACS File No: 0485-08

F = failed
C = cancelled

Sample	*Depth*	*Sample Type*	*Test Sequence*											
			Sample Inspection	*CT Scan*	*Base Parameters @ Overburden*	*Saturate*	*Formation Factor*	*Air-Brine Capillary Pressure*	*Resistivity Index*	*Keg @ Swir*	*Waterflood*	*Dean-Stark*	*Clean & Dry*	*Cation Exchange Capacity*
7	2736.90	1½"	X	X		X	X	X	X			X	X	X
10	2737.80	1½"	X	X		X		X				X	X	
16	2739.59	1½"	X	X		X		X				X	X	
1/7	2993.80	MSCT	X	X	X	X		X				X	X	
2/1	2968.30	MSCT	X	X	X	X	X	X	X	X	X	X	X	C
2/6	2981.00	MSCT	X	X	X	X		X				X	X	
2/7	2982.00	MSCT	X	X	X	X		X				X	X	
2/9	2987.80	MSCT	X	X	X	X	X	X	X	X	X	X	X	C
2/10	2988.80	MSCT	X	X	X	X	X	X	X			X	X	C
2/12	2991.80	MSCT	X	X	X	X	X	X	X	X	X	X	X	C
2/14	2993.80	MSCT	X	X	X	X	X	X	X			X	X	C
2/15	2994.80	MSCT	X	X	X	X		X		X	X	X	X	
2/16	2995.80	MSCT	X	X	X	X		X		X	X	X	X	
2/17	2996.80	MSCT	X	C	C	C	C	C	C			C	C	C
2/24	3006.70	MSCT	C	C	C	C	C	C	C	C	C	C	C	C
3/4	3021.20	MSCT	X	X	X	X		X				X	X	
	Total		15	14	11	14	6	14	6	5	5	14	14	1

CHAPTER 3

SAMPLE PREPARATION AND BASE PARAMETER DETERMINATIONS

3.1 Test and Calculation Procedures

3. SAMPLE PREPARATION AND BASE PARAMETER DETERMINATIONS

3.1 Test and Calculation Procedures

3.1.1 CT Scanning

CT Scanning was undertaken in order that internal inhomogeneities and/or drilling fluid invasion zones may be noted. Typical inhomogeneities may be clasts, bedding, sedimentary structures, cementation, fractures and any other discontinuities that may not be readily visible to the naked eye.

The principle of CT Scanning and its applications is presented by Hove et al, 1987 and Wellington and Vinegar, 1987.

CT Scanners generate cross-sectional image slices through the sample by revolving an X-ray tube around the sample and obtaining projections at many different angles (Appendix I). From these image slices, a cross-sectional image was reconstructed by a back projection algorithm in the scanner's computer.

Prior to analysis, an arbitrary orientation line was inscribed onto the sample using a marker to facilitate subsequent re-orientation. The sample was placed vertically within the scanner, with the orientation arrow left to right, and a longitudinal section image obtained. The sample was then rotated through exactly 90^o to the initial orientation, and another section image recorded. These two images are labelled '0' and '90' on the prints.

All images are presented here in a standard ACS format and are stored digitally.

3.1.2 Base Parameters

All ambient base parameters were performed during the routine core analysis study.

Porosity

Porosity was determined in two stages. Initially each sample was placed in a sealed matrix cup. Helium held at 100 psi reference pressure was then introduced to the cup. From the resultant pressure drop the unknown grain volume was determined using Boyle's Law.

$$P_1 V_1 = P_2 V_2$$

$$\Rightarrow P_1 Vr = P_2 (Vr + Vc + Vl - Vg)$$

where

P_1	=	*initial pressure (psig)*
Vr	=	*reference cell volume (cm^3)*
Vc	=	*matrix cup volume (cm^3)*
Vl	=	*line volume (cm^3)*
Vg	=	*grain volume (cm^3)*
P_2	=	*final pressure (psig)*

$$\text{and} \quad \rho = \frac{Wt}{Vg}$$

where ρ = grain density (g/cm^3)
Wt = weight of sample (g)
Vg = grain volume (cm^3)

The samples were then placed into individual thick walled rubber sleeves and the assembly loaded into a hydrostatic cell. With an ambient pressure (400 psi) applied to the sample, helium held at 100 psi reference pressure was released into the samples pore volume. The resultant pressure drop was used to determine pore volume at ambient. The confining pressure was then increased to overburden pressure (5000 psi for plug samples and 5400 psi for MSCT samples) and the resultant change in internal pore pressure was monitored and used to determine pore volume at overburden conditions.

$$Vb = Vp + Vg$$

$$\text{Ambient Porosity \%} = \frac{Vp}{Vb} x\,100$$

$$\text{Overburden Porosity \%} = \frac{Vp - \Delta Vp}{Vb - \Delta Vp} x\,100$$

where Vp = ambient pore volume (cm^3)
Vb = ambient bulk volume (cm^3)
Vg = grain volume (cm^3)
ΔVp = change in pore volume (cm^3)

Permeability to Air

The samples were placed into a hydrostatic cell (Appendix II) with an ambient confining pressure of 400 psi applied. The confining pressure was used to prevent bypassing of air around the sample when the measurement was made. In order to determine permeability a known air pressure was applied to the upstream face of each sample, creating a flow of air through the core plug. Air permeability for each core sample was calculated using Darcy's Law through knowledge of the upstream pressure, flow rate, viscosity of air and sample dimensions.

$$Ka = \frac{2000.BP.\mu.q.L}{(P_1^2 - P_2^2).A}$$

where	*Ka*	=	*air permeability (milliDarcy's)*
	BP	=	*barometric pressure (atmospheres)*
	μ	=	*gas viscosity (cP)*
	q	=	*flow rate (cm^3/s)*
	L	=	*sample length (cm)*
	P_1	=	*upstream pressure (atmospheres)*
	P_2	=	*downstream pressure (atmospheres)*
	A	=	*sample cross sectional area (cm^2)*

The confining pressure was then increased to overburden pressure and the above procedure repeated to give permeability at overburden conditions.

3.1.3 Sample Saturation

The selected samples were initially vacuum saturated with 20000 ppm NaCl equivalent brine (Appendix I) followed by pressure saturation at 2000 psi for a minimum of 12 hours. To determine complete saturation, the saturations were determined by mass balance and compared with that of porosimetry. In all cases the samples were deemed suitable to proceed with the test program.

CHAPTER 3

SAMPLE PREPARATION AND BASE PARAMETER DETERMINATIONS

3.2 Test Results

BASE PARAMETERS

Client : Origin Energy Resources Limited
Well : Trefoil-1

Overburden Pressure 1: 5000 psi
Overburden Pressure 2: 5400 psi

Sample Number	Depth (metres)	Sample Type	Ambient Porosity (percent)	OB1 Porosity (percent)	OB2 Porosity (percent)	Grain Density (g/cm^3)	Ambient Permeability (milliDarcy's)	OB1 Permeability (milliDarcy's)	OB2 Permeability (milliDarcy's)
7	2736.90	1½"	25.1	24.0		2.66	551	461	
10	2737.80	1½"	23.6	22.6		2.66	181	153	
16	2739.59	1½"	21.7	20.3		2.66	68.8	52.5	
1/7	2993.80	MSCT	14.5		12.4	2.64	151		125
2/1	2968.30	MSCT	16.9		14.8	2.64	336		259
2/6	2981.00	MSCT	16.8		14.9	2.71	116		95.6
2/7	2982.00	MSCT	15.4		14.0	2.62	356		330
2/9	2987.80	MSCT	11.7		10.0	2.64	8.0		4.86
2/10	2988.80	MSCT	16.2		14.1	2.64	145		123
2/12	2991.80	MSCT	13.1		11.0	2.63	32.4		21.3
2/14	2993.80	MSCT	13.0		10.8	2.64	87.3		64.1
2/15	2994.80	MSCT	14.1		12.9	2.64	51.0		40.0
2/16	2995.80	MSCT	15.9		14.1	2.63	180		152
3/4	3021.20	MSCT	14.4		13.0	2.64	36.7		29.4

CHAPTER 4

ELECTRICAL PROPERTIES AND CAPILLARY PRESSURE

4.1 Test and Calculation Procedures

4. ELECTRICAL PROPERTIES AND CAPILLARY PRESSURE

4.1 Test and Calculation Procedures

4.1.1 Formation Resistivity Factor

On completion of base parameter and pressure saturation with 20000 ppm brine, the six selected samples continued on for formation resistivity factor analyses.

Each fully brine saturated sample was sandwiched between a pair of stainless steel core holder platens. These platens also act as the current carrying and potential electrodes. A thin silver leaf was also placed between the plug endfaces and electrodes, to ensure electrical contact. A strongly hydrophilic membrane was placed at the bottom end of the sample. This assembly was placed into a snugly fitting rubber overburden sleeve and then loaded into a Hydrostatic type core holder. A confining pressure was gradually applied as an effective overburden pressure (see Appendix II for schematic).

Synthetic brine (Appendix I) was slowly flowed through each sample at a rate of $0.5 cm^3$/min. During this process sample resistivity was monitored on a digi-bridge capable of measuring sample resistance to 0.001 (ohms) accuracy. In each case the current frequency was selected to yield minimum phase angles, thus ensuring maximum electrical contact (between each sample and the current carrying and potential electrodes). Values of sample resistance (Rc) and effluent brine resistivity (Rw) were recorded daily. Each sample was deemed to be at ionic equilibrium when three consecutive daily readings were recorded within 1%.

From these stable data, the following results were recorded:

$$Ro = \frac{A \,.\, Rc}{100 L}$$

where Ro = *sample resistivity (ohm.m)*
Rc = *sample resistance (ohms)*
L = *electrode gap (sample length - cm)*
A = *cross sectional area (cm^2)*
100 = *units conversion*

Formation resistivity factor was calculated using the following equations:

$$FF = \frac{a}{\Phi^m}$$

and

$$FF = \frac{Ro}{Rw}$$

where Rw = *brine resistivity (ohm.m)*
a = *intercept (assumed = 1)*
m = *cementation exponent*

and Φ = *porosity (fraction)*

The brine resistivity (Rw) was accurately determined by a NATA certified fluids laboratory.

4.1.2 Formation Resistivity Index and Capillary Pressure

Upon completion of the preceding formation resistivity factor analyses, the selected samples continued immediately for formation resistivity index analyses in conjunction with drainage capillary pressure curves. The top endface port was connected to a supply of humidified air and the bottom port connected to a graduated receiving tube (Appendix II). The samples were desaturated by gradually increasing the displacing fluid pressure to the samples. The actual pressures utilised were inversely proportional to the individual sample permeability data. A small amount of oil was placed into the collection tubes to prevent any potential brine loss by evaporation. Sample resistances were measured at successive decreasing brine saturations, which were calculated from the following equation:

$$\textit{Water Saturation (\%)} = \frac{\textit{Pore Volume @ OB}\left(cm^3\right) - \textit{Brine Expelled}\left(cm^3\right)}{\textit{Pore Volume @ OB}\left(cm^3\right)} \times 100$$

Capillary pressure curves plot water saturation (x-axis) against applied displacing fluid pressure. A hyperbolic curve is used to define this relationship. The ratio of the sample resistance (Rc) values to the previously determined FF values (at 100% saturation) were used to calculate the formation resistivity indices.

$$Rt = \frac{A \,.\, Rc}{100 L}$$

where Rt = *resistivity of partially brine saturated sample (ohm.m)*
Rc = *sample resistance (ohms)*

and $$RI = \frac{Rt}{Rw \,.\, FF}$$

where RI = *resistivity index*
Rw = *resistivity of brine (ohm.m)*

(modified from standard Archie equation to include Rw).

These RI values (for each sample) were plotted against brine saturation (Sw) on graphs with logarithmic axes and the gradient of the best-fit line through the co-ordinate (1.0, 1.0) was calculated. Each gradient is quoted as the saturation exponent (n) for that sample, in accordance with Archie's formula.

$$RI = \frac{1}{Sw^n}$$

4.1.3 Capillary Pressure

Each fully brine saturated sample was sandwiched between a pair of stainless steel core holder platens with a strongly hydrophilic membrane at the bottom end of the sample. This assembly was placed into a snugly fitting rubber overburden sleeve and loaded into a hydrostatic type core holder and an overburden pressure was applied.

The top endface port was connected to a supply of humidified air and the bottom port connected to a graduated receiving tube (Appendix II). The samples were desaturated by gradually increasing the displacing fluid pressure to the samples. The actual pressures utilised were inversely proportional to the individual sample permeability data. A small amount of oil was placed into the collection tubes to prevent any potential brine loss by evaporation. Brine saturations, which were calculated from the following equation:

$$Water\ Saturation(\%) = \frac{Pore\ Volume\ @\ OB\ (cm^3) - Brine\ Expelled\ (cm^3)}{Pore\ Volume\ @\ OB\ (cm^3)}\ x\ 100$$

Capillary pressure curves plot water saturation (x-axis) against applied displacing fluid pressure. A hyperbolic curve is used to define this relationship.

4.1.4 Cation Exchange Capacity

Cation exchange capacity was determined on approximately 5 grams of sample (off-cuts) using the wet chemistry method. Only sample 7 had sufficient off-cut to perform the analysis. The sample was first washed with an ammonium chloride solution to exchange ions with the available clay cations. An exchange reagent was then washed through the sample and the resultant solution titrated.

Values of exchangeable cations (theoretical minimum of zero) present in the sample is reported as milliequivalents per 100 grams of dry sample (meq/100 g). Values of Q_v have been calculated using the following equation:

$$Q_v = \frac{CEC\ (1 - \Phi)\rho}{100\ \Phi}$$

where ρ = *grain density (g/cm^3)*
Φ = *porosity (fraction)*
Q_v = *volume concentration of clay exchange cations (meq/cm^3 pore space)*
CEC = *cation exchange capacity (meq/100 g dry sample)*

Based on these CEC/Qv data, values of shaly sand equivalent formation factor (FF*), cementation factor (m*) and saturation exponent (n*) were calculated using the following equations:

$$FF^* = FF \,.\, (1 + B.Qv.Rw)$$

$$m^* = \frac{\log FF^*}{-\log \Phi}$$

$$n^* = \frac{\log\left[\dfrac{1 + Rw.B.Qv}{1 + Rw.B.Qv / Sw}\right] - \log FRI}{\log Sw}$$

where[1]

$$B = \frac{-1.28 + 0.225.T - 0.0004059.T^2}{1 + Rw^{1.23} \,.\, (0.045.T. - 0.27)}$$

FF	=	*formation resistivity factor*
*FF**	=	*shaly sand equivalent formation resistivity factor*
*m**	=	*shaly sand equivalent cementation factor*
Φ	=	*porosity (fraction)*
*n**	=	*shaly sand equivalent saturation exponent*
Rw	=	*brine resistivity (ohm.m @ 25°C)*
T	=	*temperature of 25°C*
B	=	*equivalent conductance of clay exchange cations*
Qv	=	*volume concentration of clay exchange cations*
Sw	=	*final saturation (fraction)*
FRI	=	*resistivity index @ saturation Sw*

[1] Juhasz, I., 1981, Normalized Q, - the key to shaly sand evaluation using the Waxman-Smits equation in the absence of core data, paper Z, in 22nd Annual Logging Symposium Transactions: Society of Professional Well Log Analysts, 36p.

CHAPTER 4

ELECTRICAL PROPERTIES AND CAPILLARY PRESSURE

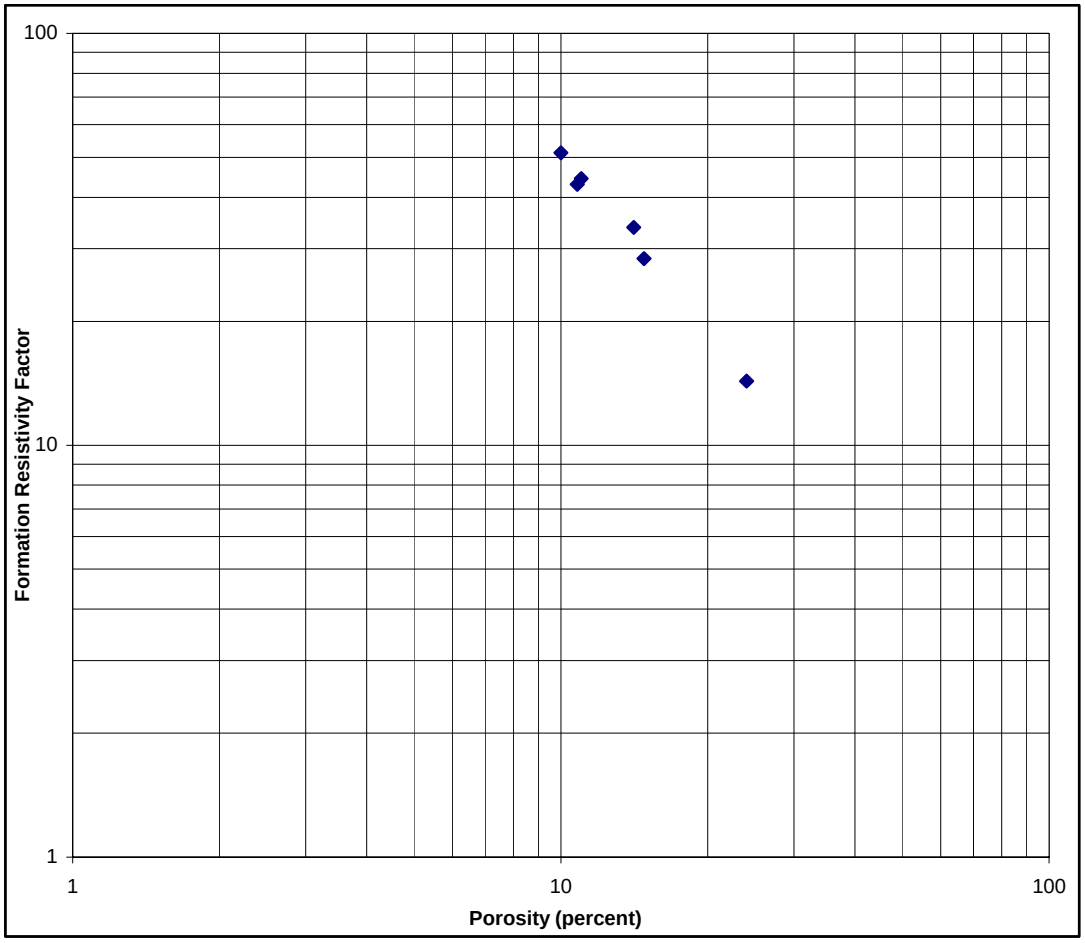
4.2 Test Results

4.2.1 Formation Factor

FORMATION RESISTIVITY FACTOR

Client	Origin Energy Resources Limited	**Saturant**	20000 ppm
Well	Trefoil-1	**Rw of Saturant**	0.28 at 25ºC
		Overburden	
		Average m	1.76

Sample Number	Depth (metres)	Permeability to Air (milliDarcy's)	Porosity (percent)	Formation Factor FF	Cementation Exponent m
7	2736.90	461	24.0	14.3	1.86
2/1	2968.30	259	14.8	28.4	1.75
2/9	2987.80	4.86	10.0	51.3	1.71
2/10	2988.80	123	14.1	33.8	1.80
2/12	2991.80	21.3	11.0	44.4	1.72
2/14	2993.80	64.1	10.8	43.0	1.69



CHAPTER 4

ELECTRICAL PROPERTIES AND CAPILLARY PRESSURE

4.2 Test Results

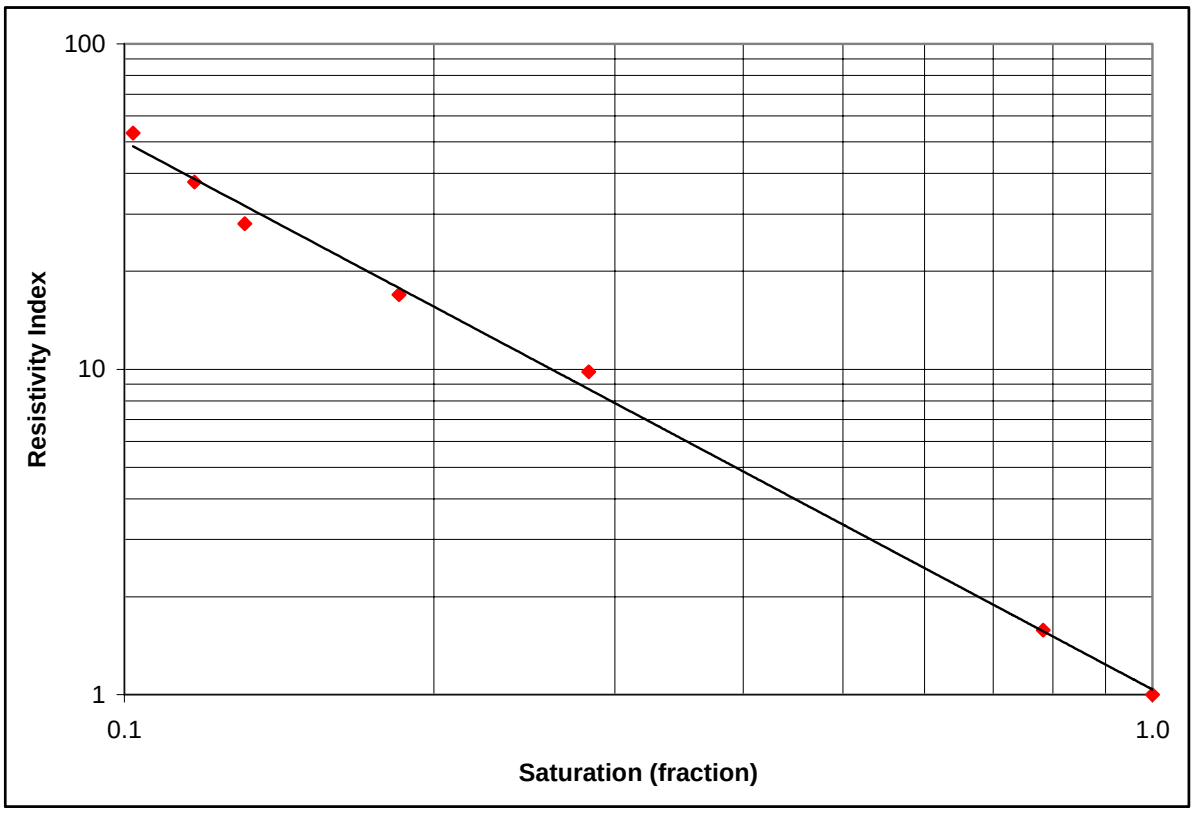
4.2.2 Resistivity Index

RESISTIVITY INDEX

Client Origin Energy Resources Limited
Well Trefoil-1

Rw of Saturant 0.28 at 25ºC
Method Air/Brine Porous Plate @ Overburden

Sample Number	Depth (metres)	Permeability to Air (milliDarcy's)	Porosity (percent)	Formation Factor FF	Brine Saturation (fraction)	Resistivity Index RI	Saturation Exponent n
7	2736.90	461	24.0	14.3	1.000	1.00	
					0.783	1.58	
					0.283	9.83	
					0.185	17.0	
					0.131	28.0	
					0.117	37.6	
					0.102	53.2	1.74

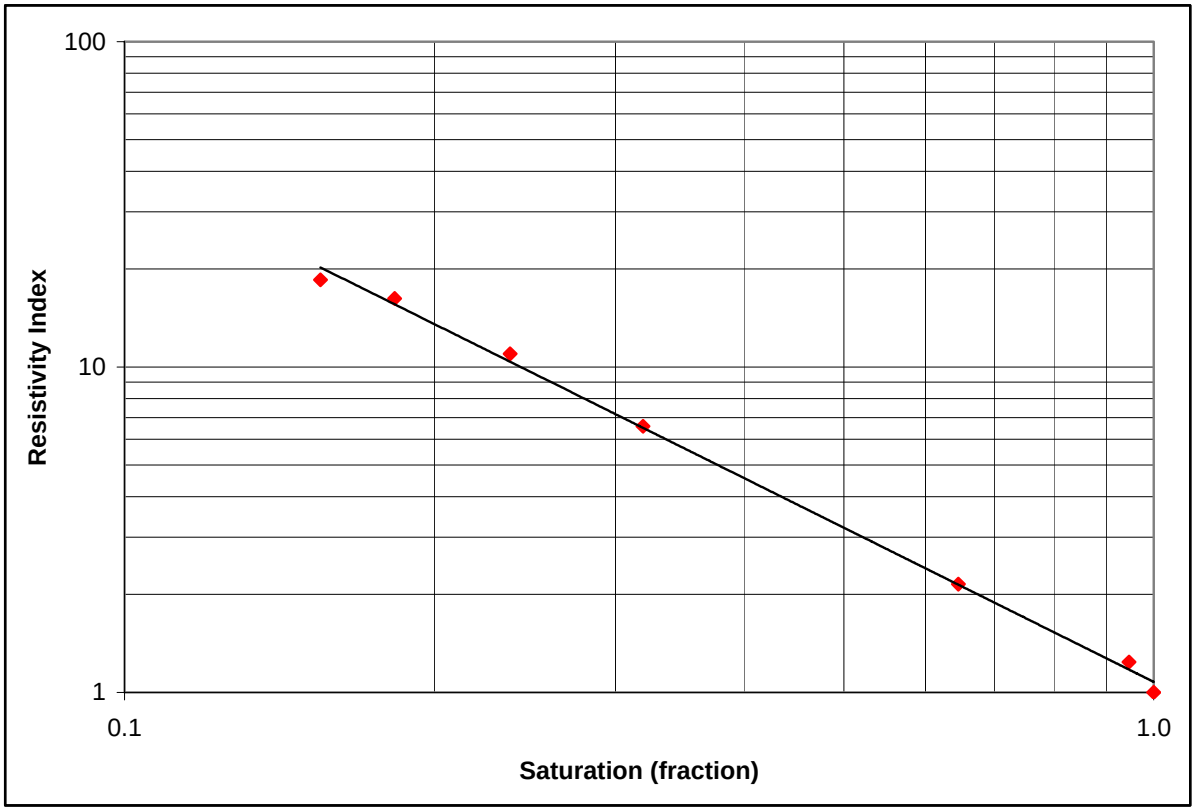


RESISTIVITY INDEX

Client Origin Energy Resources Limited
Well Trefoil-1

Rw of Saturant 0.28 at 25ºC
Method Air/Brine Porous Plate @ Overburden

Sample Number	Depth (metres)	Permeability to Air (milliDarcy's)	Porosity (percent)	Formation Factor FF	Brine Saturation (fraction)	Resistivity Index RI	Saturation Exponent n
2/1	2968.30	259	14.8	28.4	1.000	1.00	
					0.946	1.24	
					0.646	2.15	
					0.319	6.57	
					0.237	11.0	
					0.183	16.2	
					0.155	18.5	2.02

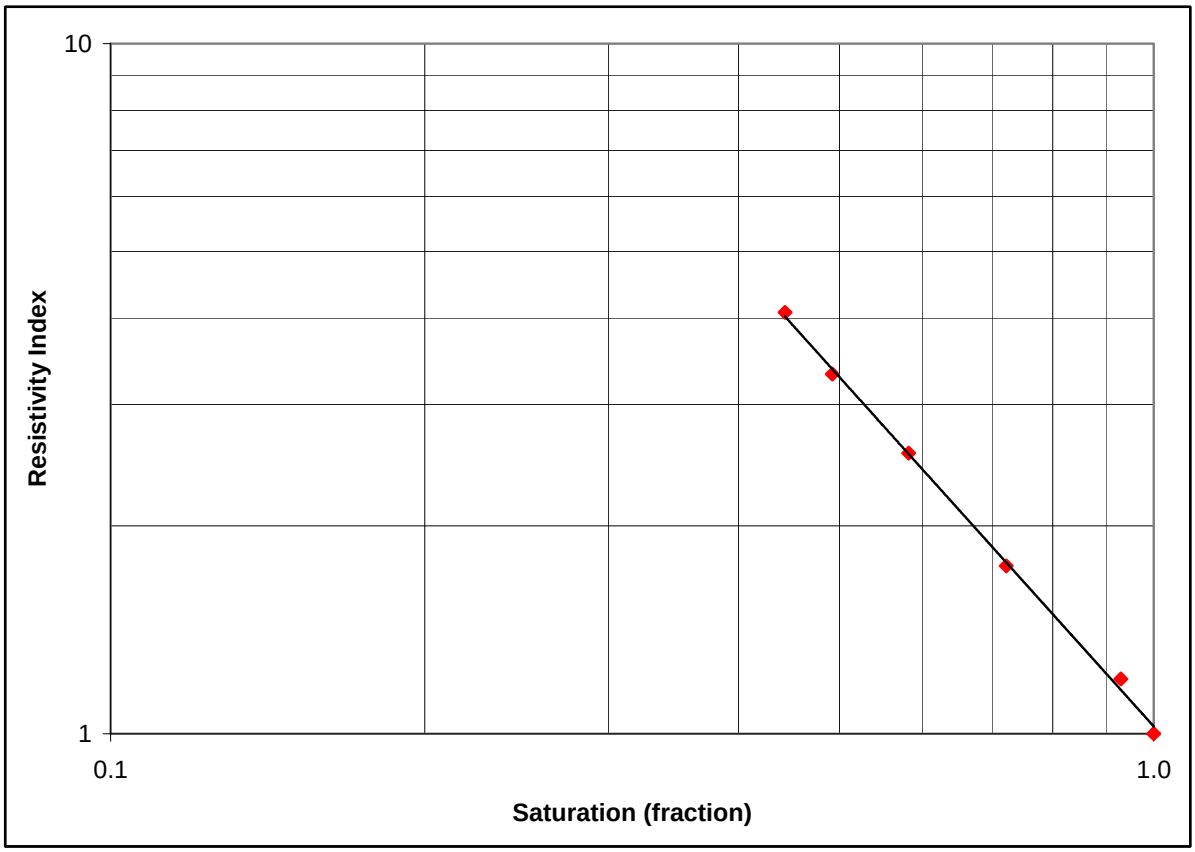


RESISTIVITY INDEX

Client Origin Energy Resources Limited
Well Trefoil-1

Rw of Saturant 0.28 at 25ºC
Method Air/Brine Porous Plate @ Overburden

Sample Number	Depth (metres)	Permeability to Air (milliDarcy's)	Porosity (percent)	Formation Factor FF	Brine Saturation (fraction)	Resistivity Index RI	Saturation Exponent n
2/9	2987.80	4.86	10.0	51.3	1.000	1.00	
					0.930	1.20	
					0.722	1.75	
					0.582	2.55	
					0.492	3.32	
					0.443	4.08	1.72

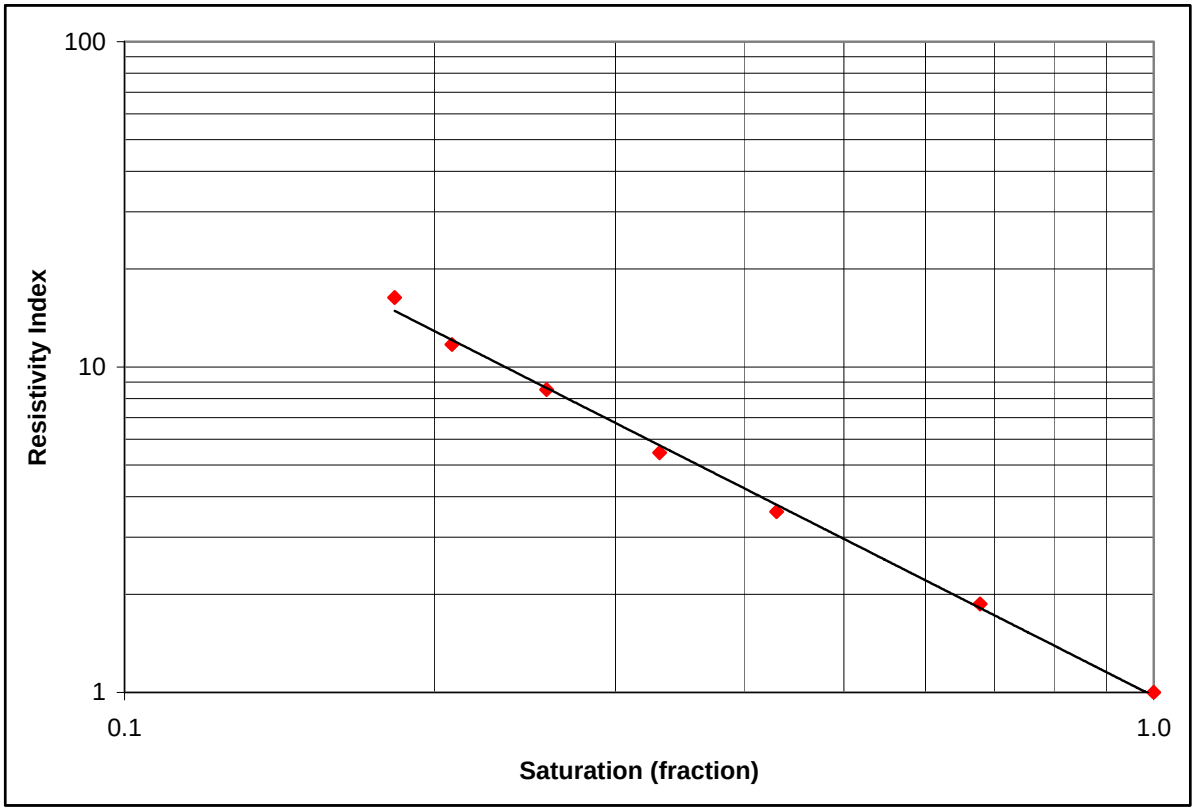


RESISTIVITY INDEX

Client Origin Energy Resources Limited
Well Trefoil-1

Rw of Saturant 0.28 at 25ºC
Method Air/Brine Porous Plate @ Overburden

Sample Number	Depth (metres)	Permeability to Air (milliDarcy's)	Porosity (percent)	Formation Factor FF	Brine Saturation (fraction)	Resistivity Index RI	Saturation Exponent n
2/10	2988.80	123	14.1	33.8	1.000	1.00	
					0.678	1.87	
					0.430	3.59	
					0.331	5.45	
					0.257	8.52	
					0.208	11.7	
					0.183	16.3	1.60

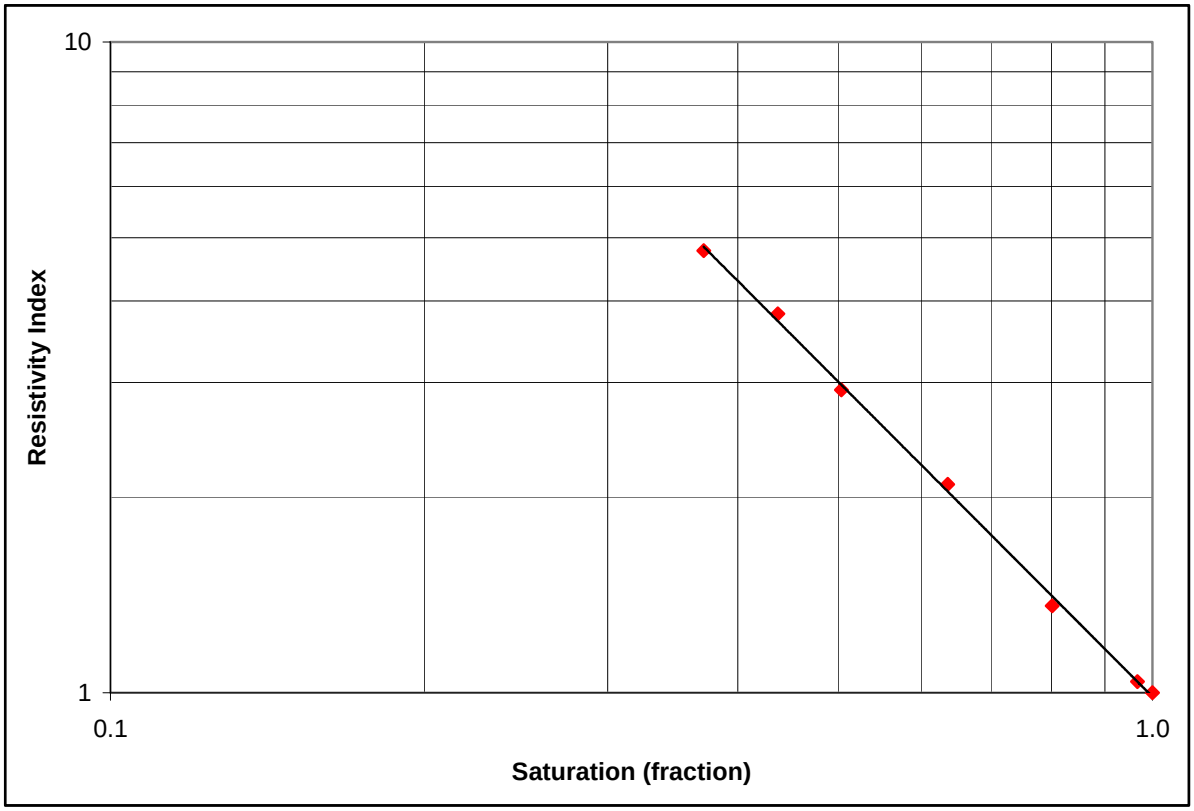


RESISTIVITY INDEX

Client Origin Energy Resources Limited
Well Trefoil-1

Rw of Saturant 0.28 at 25ºC
Method Air/Brine Porous Plate @ Overburden

Sample Number	Depth (metres)	Permeability to Air (milliDarcy's)	Porosity (percent)	Formation Factor FF	Brine Saturation (fraction)	Resistivity Index RI	Saturation Exponent n
2/12	2991.80	21.3	11.0	44.4	1.000	1.00	
					0.967	1.04	
					0.801	1.36	
					0.636	2.09	
					0.503	2.92	
					0.437	3.82	
					0.371	4.78	1.62

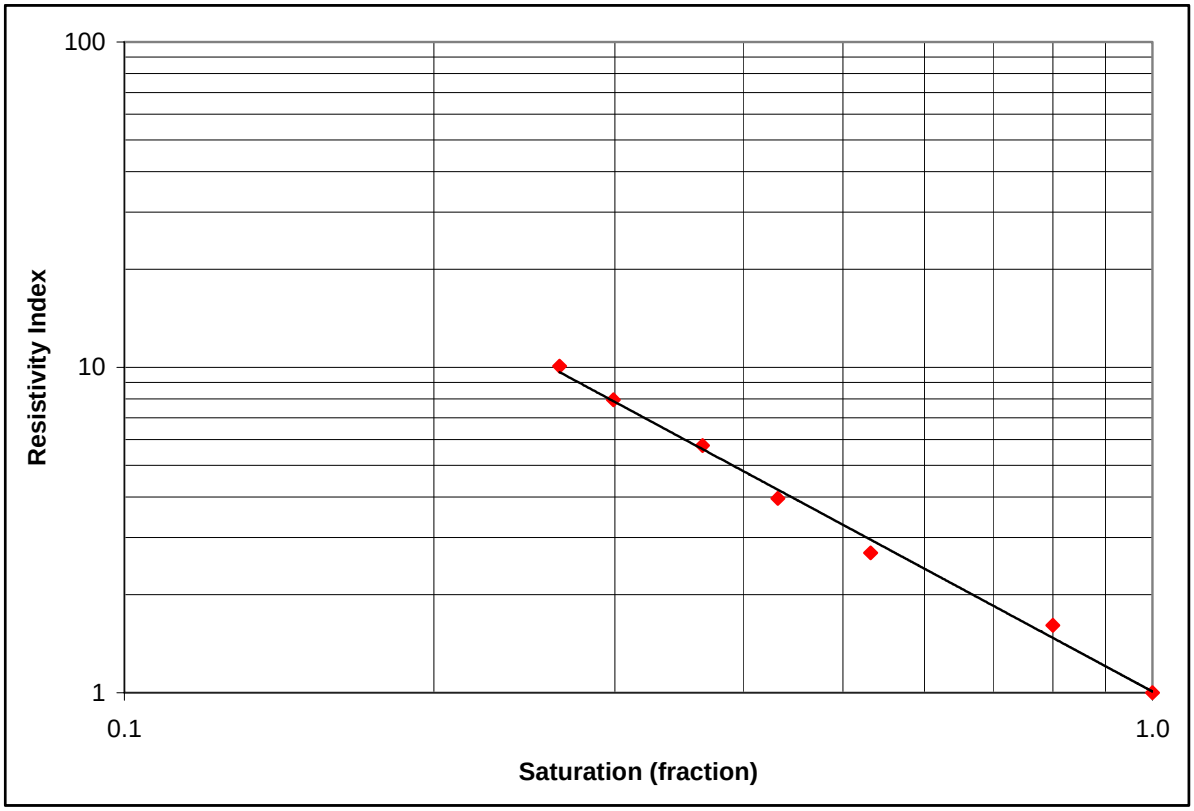


RESISTIVITY INDEX

Client Origin Energy Resources Limited
Well Trefoil-1

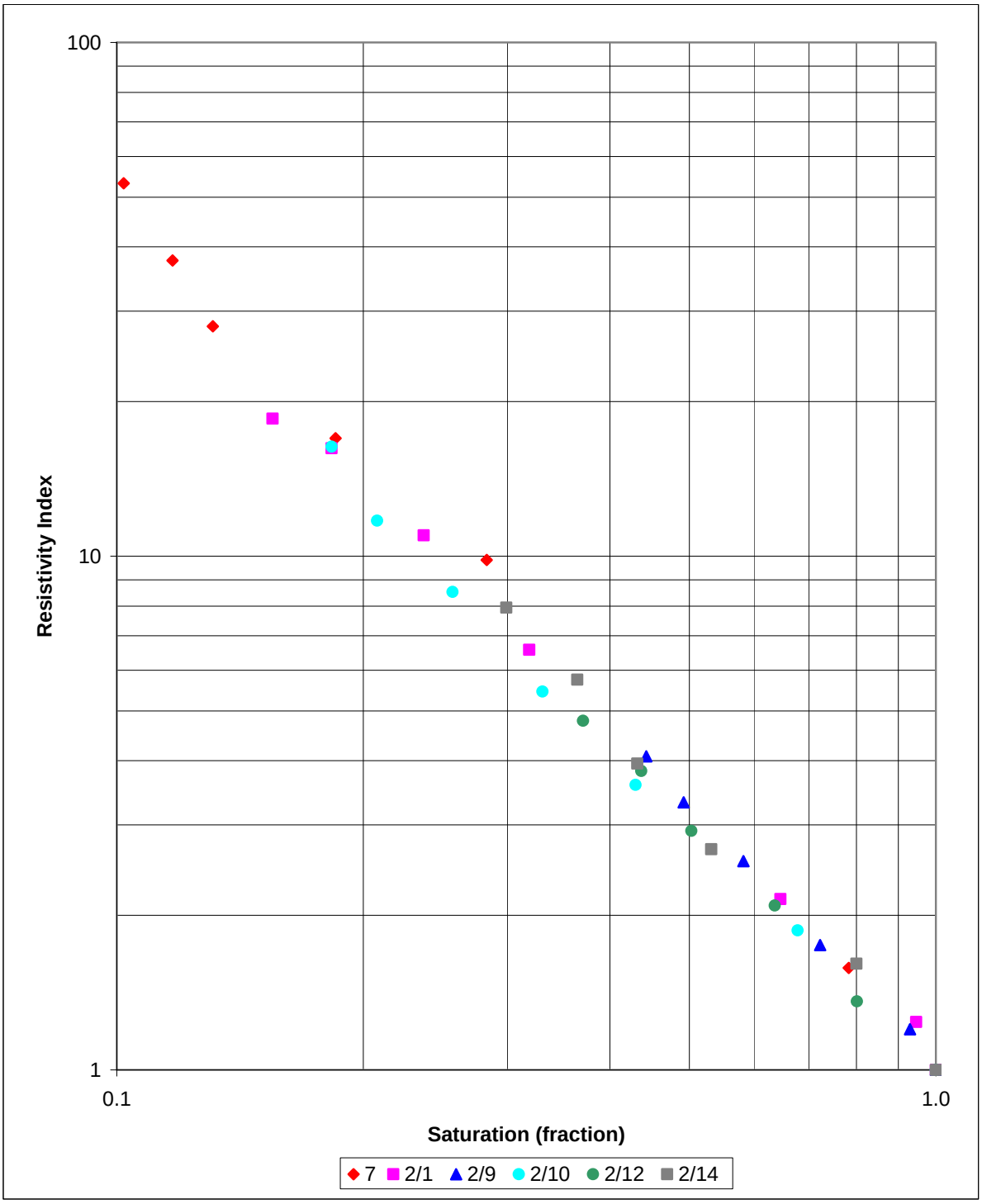
Rw of Saturant 0.28 at 25ºC
Method Air/Brine Porous Plate @ Overburden

Sample Number	Depth (metres)	Permeability to Air (milliDarcy's)	Porosity (percent)	Formation Factor FF	Brine Saturation (fraction)	Resistivity Index RI	Saturation Exponent n
2/14	2993.80	64.1	10.8	43.0	1.000	1.00	
					0.800	1.61	
					0.532	2.69	
					0.432	3.95	
					0.365	5.75	
					0.299	7.94	
					0.265	10.1	1.70



RESISTIVITY INDEX

Client Origin Energy Resources Limited
Well Trefoil-1



CHAPTER 4

ELECTRICAL PROPERTIES AND CAPILLARY PRESSURE

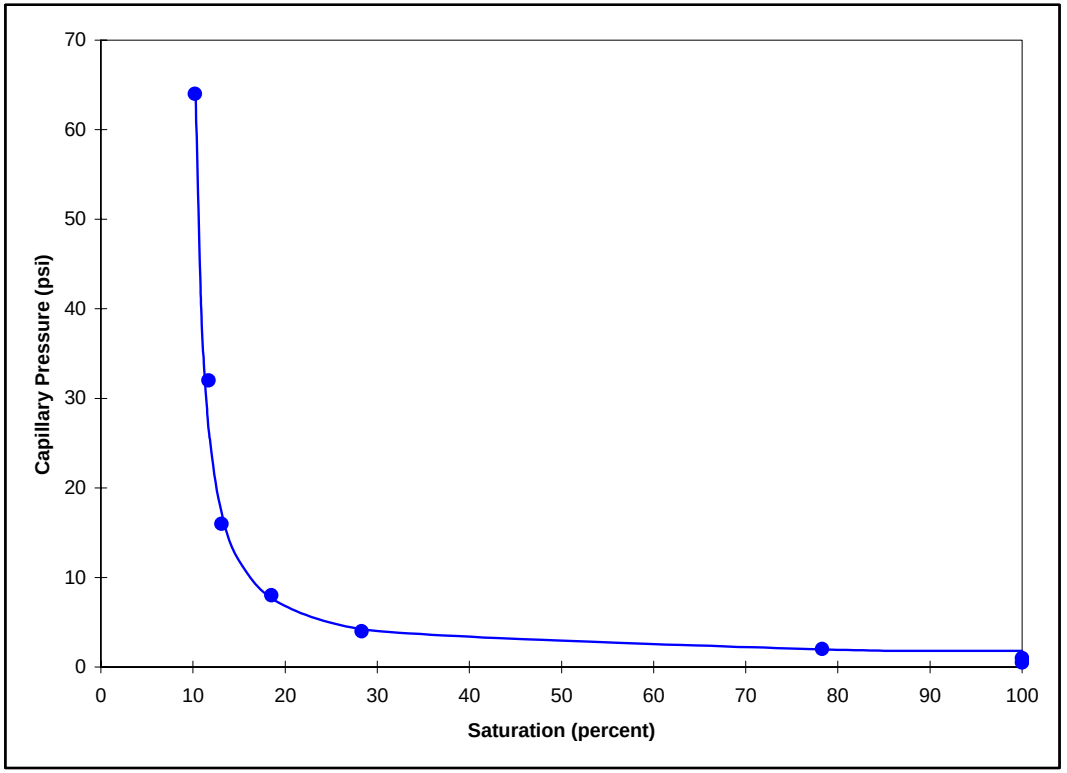
4.2 Test Results

4.2.3 Capillary Pressure (Air-Brine)

CAPILLARY PRESSURE
Overburden

Client	Origin Energy Resources Limited	**Air Permeability**	461 milliDarcy's
Well	Trefoil-1	**Porosity**	24.0 percent
Sample	7		
Depth	2736.90 metres		
Test Method	Air/Brine Porous Plate @ Overburden		
Overburden	5000 psi		

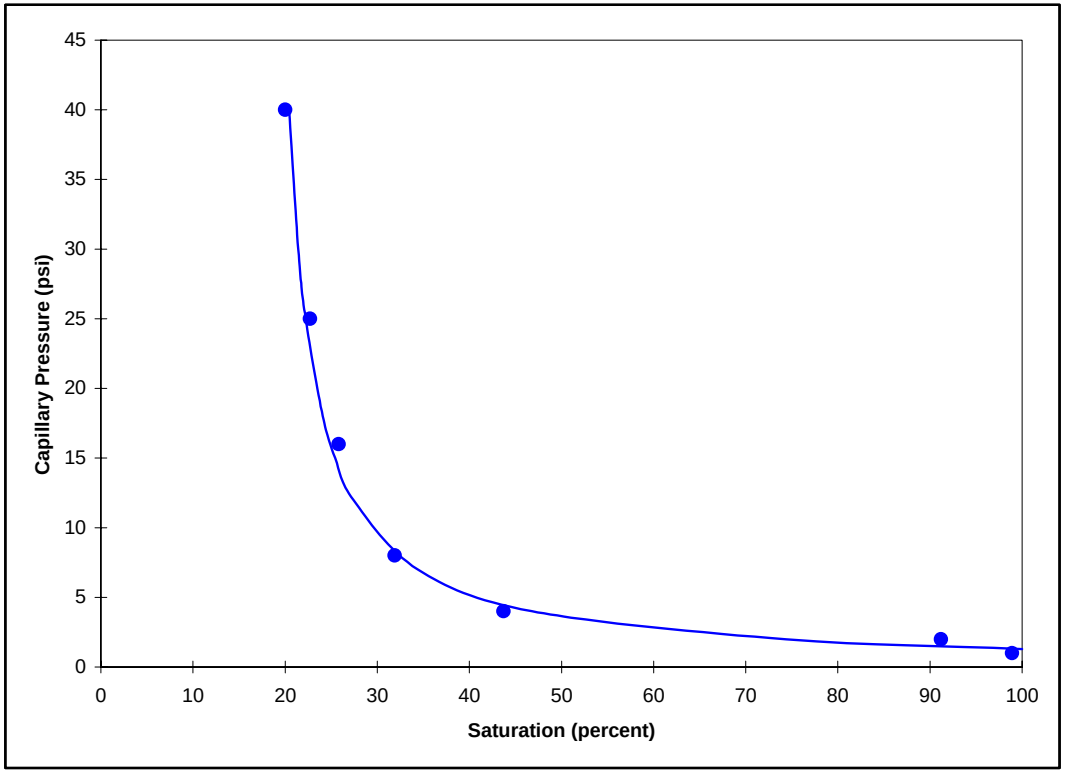
Capillary Pressure (psi)	Brine Saturation (percent)
0.50	100.0
1.0	100.0
2.0	78.3
4.0	28.3
8.0	18.5
16	13.1
32	11.7
64	10.2



CAPILLARY PRESSURE
Overburden

Client	Origin Energy Resources Limited	**Air Permeability**	153 milliDarcy's
Well	Trefoil-1	**Porosity**	22.6 percent
Sample	10		
Depth	2737.80 metres		
Test Method	Air/Brine Porous Plate @ Overburden		
Overburden	5000 psi		

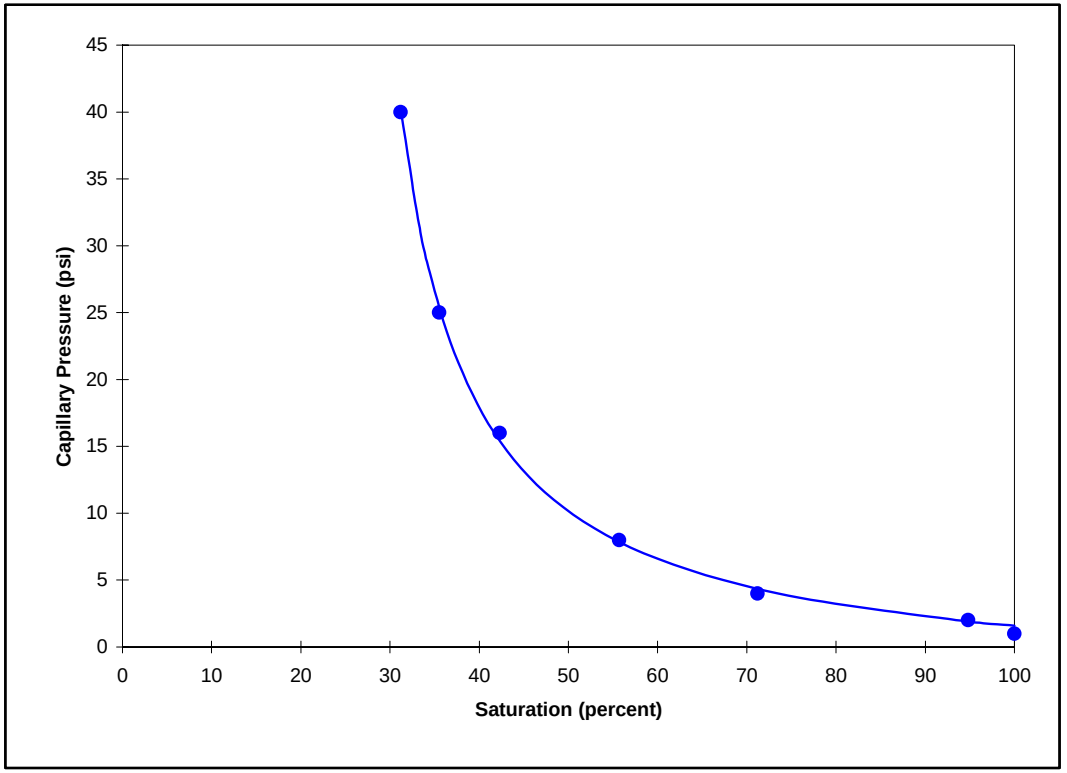
Capillary Pressure (psi)	Brine Saturation (percent)
1.0	98.9
2.0	91.2
4.0	43.7
8.0	31.9
16	25.8
25	22.7
40	20.0



CAPILLARY PRESSURE
Overburden

Client	Origin Energy Resources Limited	**Air Permeability**	52.5 milliDarcy's
Well	Trefoil-1	**Porosity**	20.3 percent
Sample	16		
Depth	2739.59 metres		
Test Method	Air/Brine Porous Plate @ Overburden		
Overburden	5000 psi		

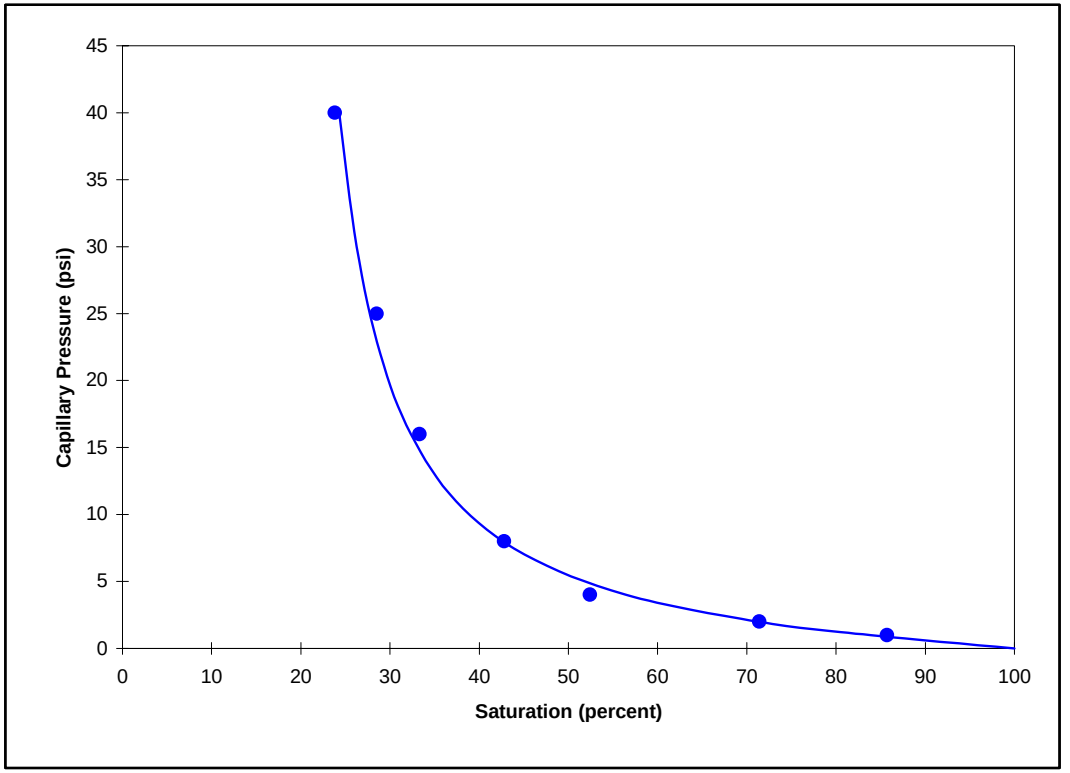
Capillary Pressure (psi)	Brine Saturation (percent)
1.0	100.0
2.0	94.8
4.0	71.2
8.0	55.7
16	42.3
25	35.5
40	31.2



CAPILLARY PRESSURE
Overburden

Client	Origin Energy Resources Limited	**Air Permeability**	125 milliDarcy's
Well	Trefoil-1	**Porosity**	12.4 percent
Sample	1/7		
Depth	2993.80 metres		
Test Method	Air/Brine Porous Plate @ Overburden		
Overburden	5400 psi		

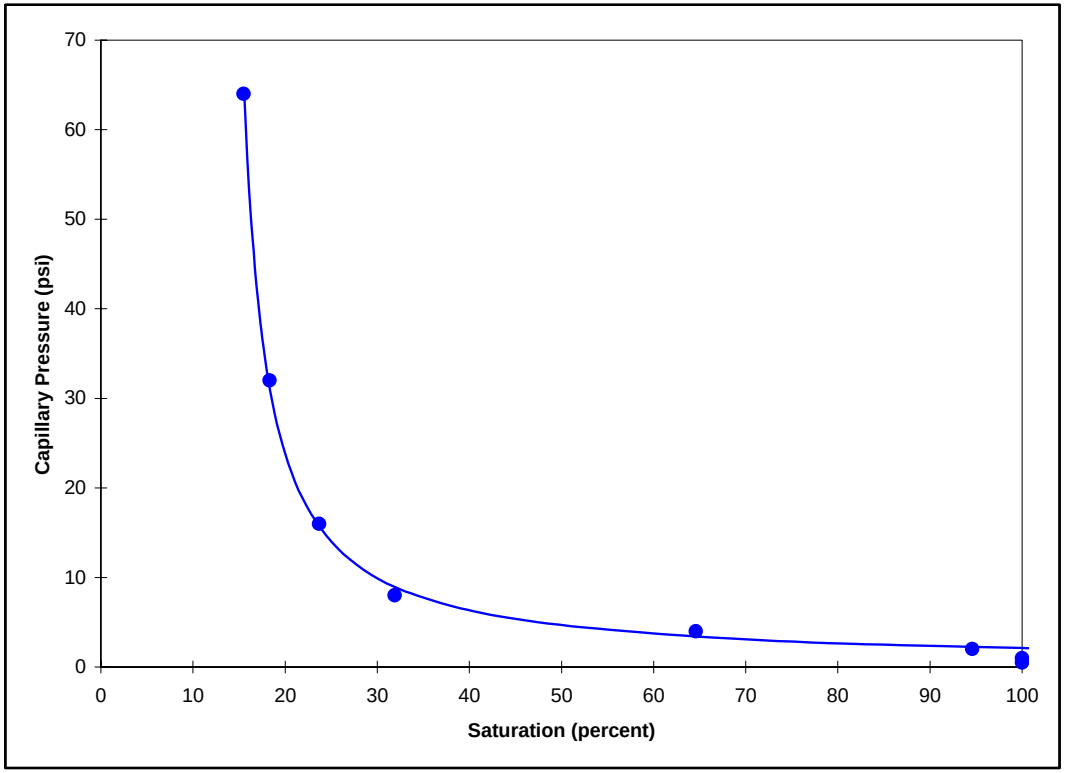
Capillary Pressure (psi)	Brine Saturation (percent)
1.0	85.7
2.0	71.4
4.0	52.4
8.0	42.8
16	33.3
25	28.5
40	23.8



CAPILLARY PRESSURE
Overburden

Client	Origin Energy Resources Limited	**Air Permeability**	259 milliDarcy's
Well	Trefoil-1	**Porosity**	14.8 percent
Sample	2/1		
Depth	2968.30 metres		
Test Method	Air/Brine Porous Plate @ Overburden		
Overburden	5400 psi		

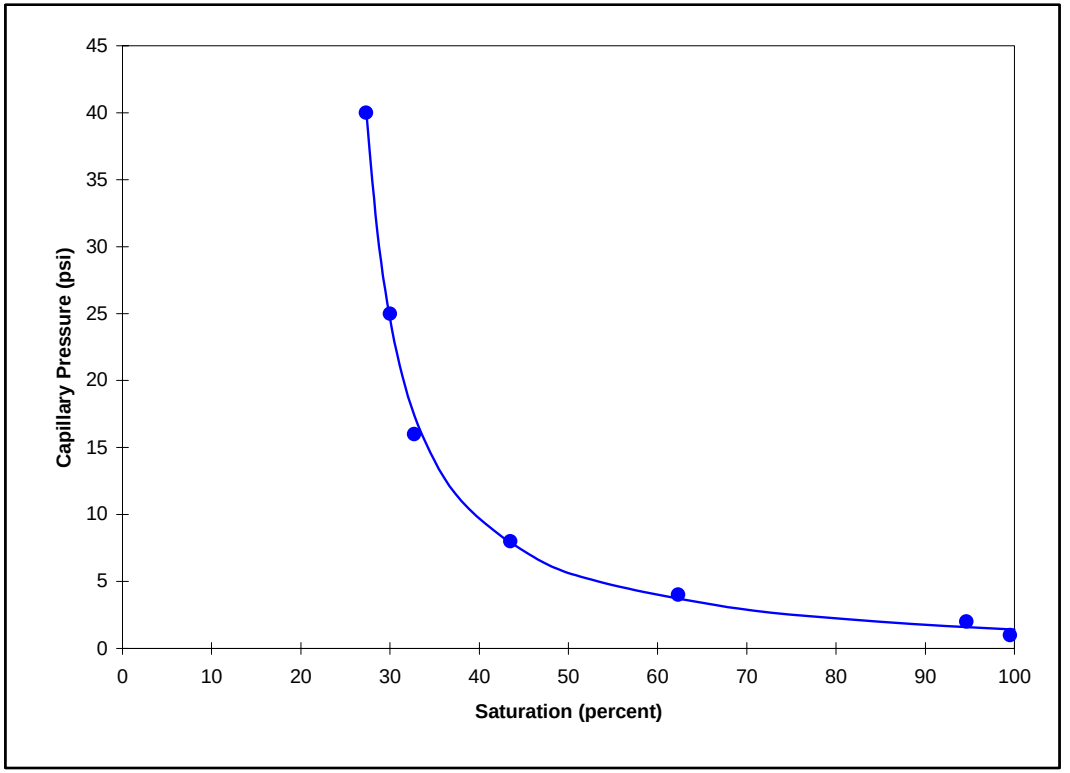
Capillary Pressure (psi)	Brine Saturation (percent)
0.50	100.0
1.0	100.0
2.0	94.6
4.0	64.6
8.0	31.9
16	23.7
32	18.3
64	15.5



CAPILLARY PRESSURE
Overburden

Client	Origin Energy Resources Limited	**Air Permeability**	95.6 milliDarcy's
Well	Trefoil-1	**Porosity**	14.9 percent
Sample	2/6		
Depth	2981.00 metres		
Test Method	Air/Brine Porous Plate @ Overburden		
Overburden	5400 psi		

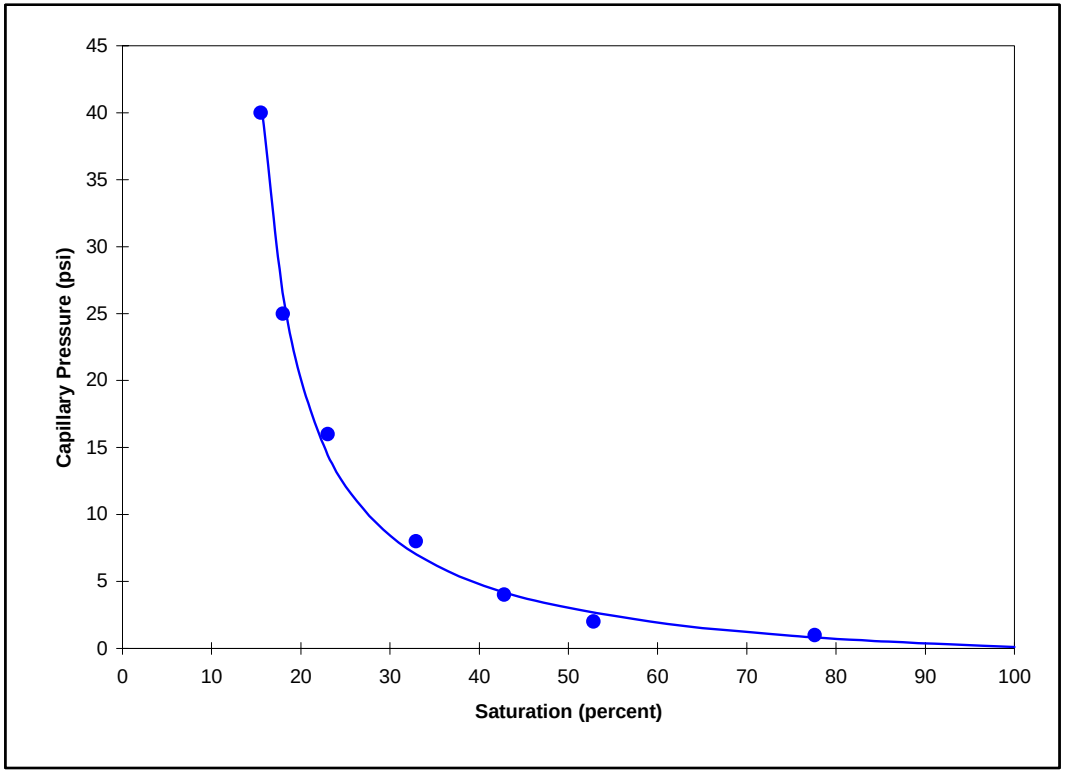
Capillary Pressure (psi)	Brine Saturation (percent)
1.0	99.5
2.0	94.6
4.0	62.3
8.0	43.5
16	32.7
25	30.0
40	27.3



CAPILLARY PRESSURE
Overburden

Client	Origin Energy Resources Limited	**Air Permeability**	330 milliDarcy's
Well	Trefoil-1	**Porosity**	14.0 percent
Sample	2/7		
Depth	2982.00 metres		
Test Method	Air/Brine Porous Plate @ Overburden		
Overburden	5400 psi		

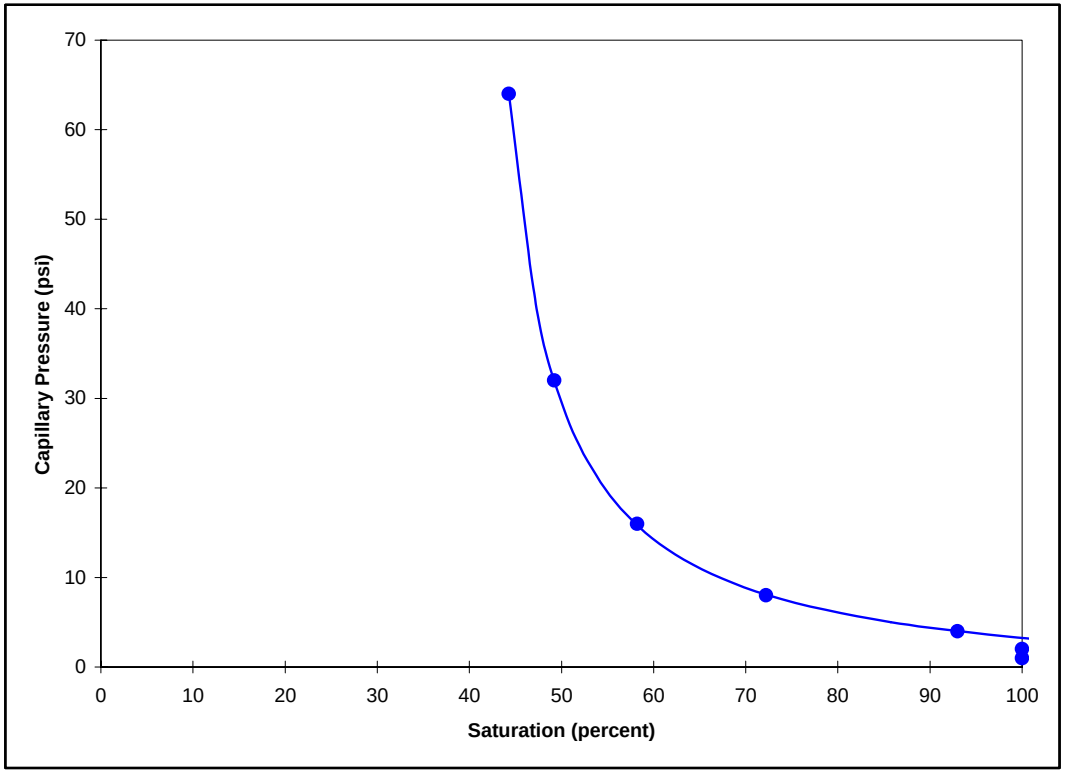
Capillary Pressure (psi)	Brine Saturation (percent)
1.0	77.6
2.0	52.8
4.0	42.8
8.0	32.9
16	23.0
25	18.0
40	15.5



CAPILLARY PRESSURE
Overburden

Client	Origin Energy Resources Limited	**Air Permeability**	4.86 milliDarcy's
Well	Trefoil-1	**Porosity**	10.0 percent
Sample	2/9		
Depth	2987.80 metres		
Test Method	Air/Brine Porous Plate @ Overburden		
Overburden	5400 psi		

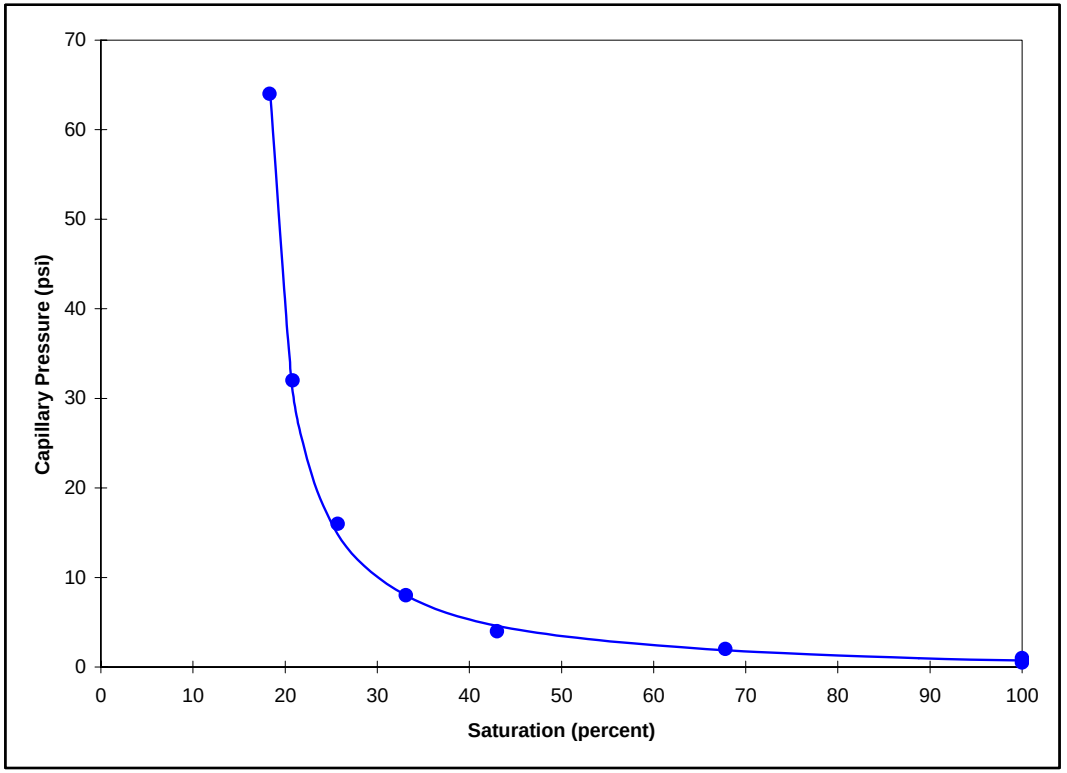
Capillary Pressure (psi)	Brine Saturation (percent)
1.0	100.0
2.0	100.0
4.0	93.0
8.0	72.2
16	58.2
32	49.2
64	44.3



CAPILLARY PRESSURE
Overburden

Client	Origin Energy Resources Limited	**Air Permeability**	123 milliDarcy's
Well	Trefoil-1	**Porosity**	14.1 percent
Sample	2/10		
Depth	2988.80 metres		
Test Method	Air/Brine Porous Plate @ Overburden		
Overburden	5400 psi		

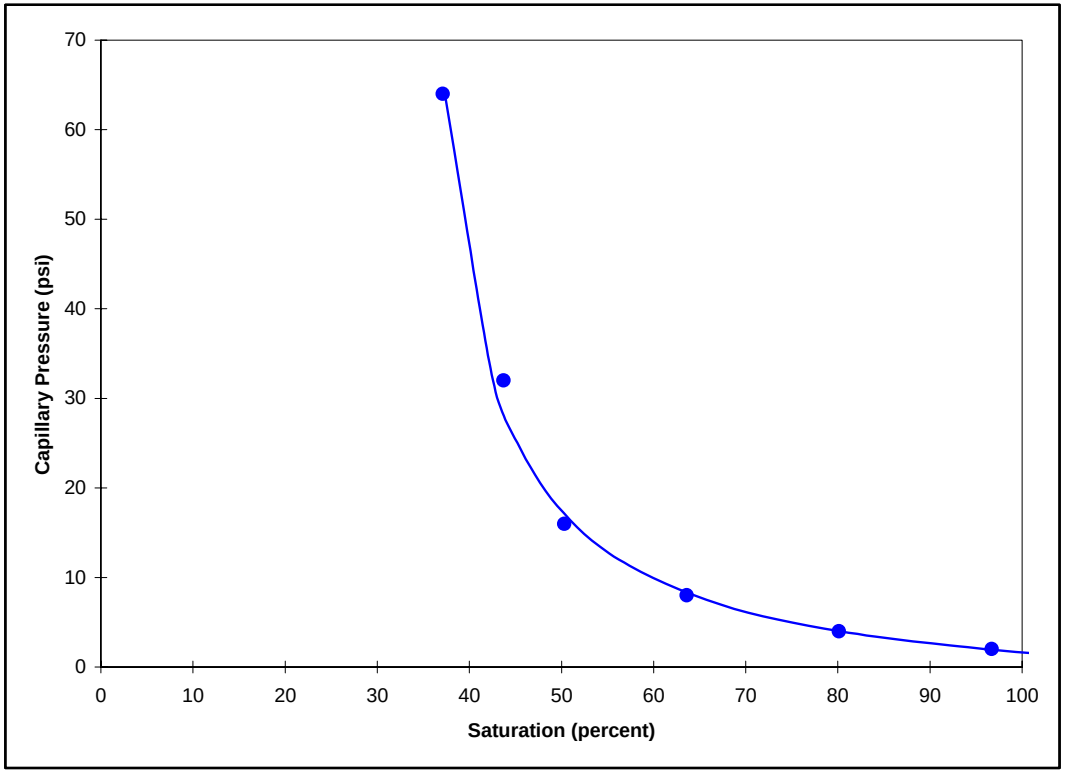
Capillary Pressure (psi)	Brine Saturation (percent)
0.50	100.0
1.0	100.0
2.0	67.8
4.0	43.0
8.0	33.1
16	25.7
32	20.8
64	18.3



CAPILLARY PRESSURE
Overburden

Client	Origin Energy Resources Limited	**Air Permeability**	21.3 milliDarcy's
Well	Trefoil-1	**Porosity**	11.0 percent
Sample	2/12		
Depth	2991.80 metres		
Test Method	Air/Brine Porous Plate @ Overburden		
Overburden	5400 psi		

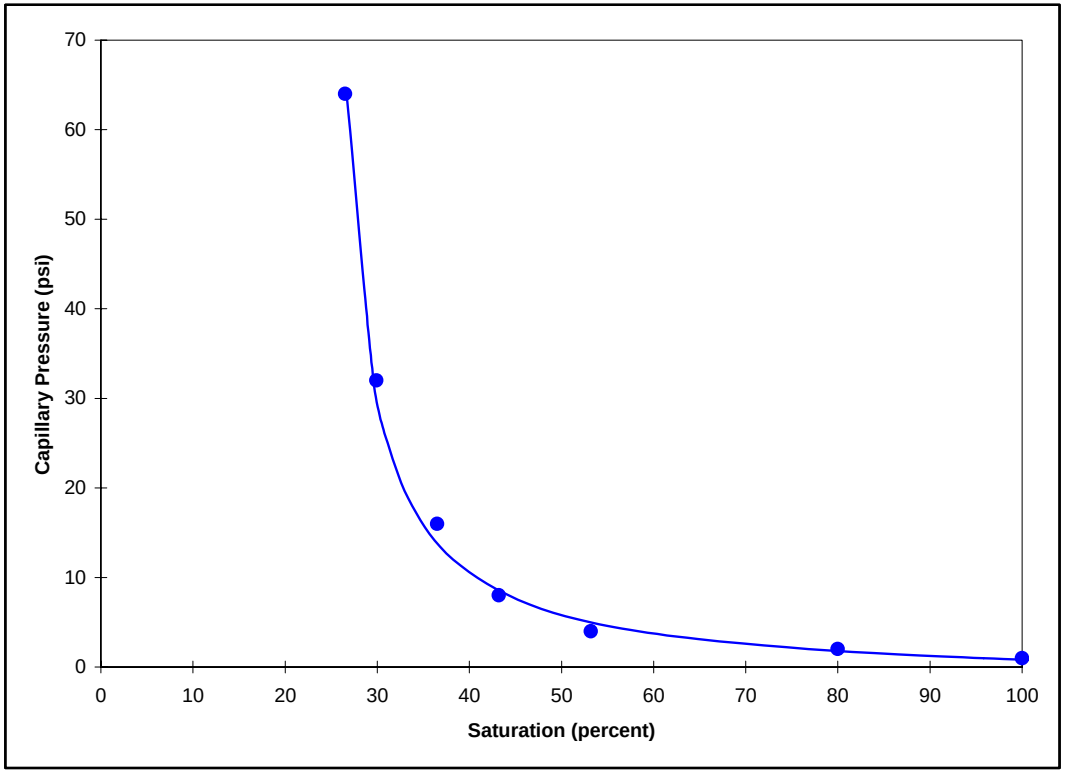
Capillary Pressure (psi)	Brine Saturation (percent)
2.0	96.7
4.0	80.1
8.0	63.6
16	50.3
32	43.7
64	37.1



CAPILLARY PRESSURE
Overburden

Client	Origin Energy Resources Limited	**Air Permeability**	64.1 milliDarcy's
Well	Trefoil-1	**Porosity**	10.8 percent
Sample	2/14		
Depth	2993.80 metres		
Test Method	Air/Brine Porous Plate @ Overburden		
Overburden	5400 psi		

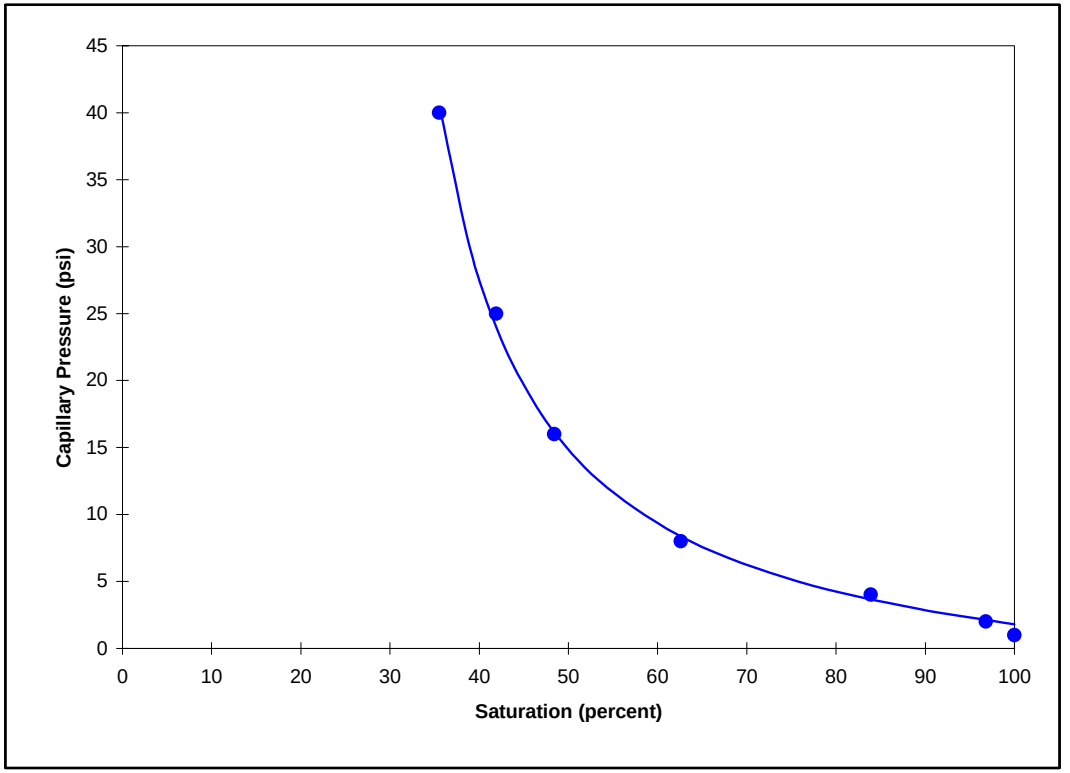
Capillary Pressure (psi)	Brine Saturation (percent)
1.0	100.0
2.0	80.0
4.0	53.2
8.0	43.2
16	36.5
32	29.9
64	26.5



CAPILLARY PRESSURE
Overburden

Client	Origin Energy Resources Limited	**Air Permeability**	40.0 milliDarcy's
Well	Trefoil-1	**Porosity**	12.9 percent
Sample	2/15		
Depth	2994.80 metres		
Test Method	Air/Brine Porous Plate @ Overburden		
Overburden	5400 psi		

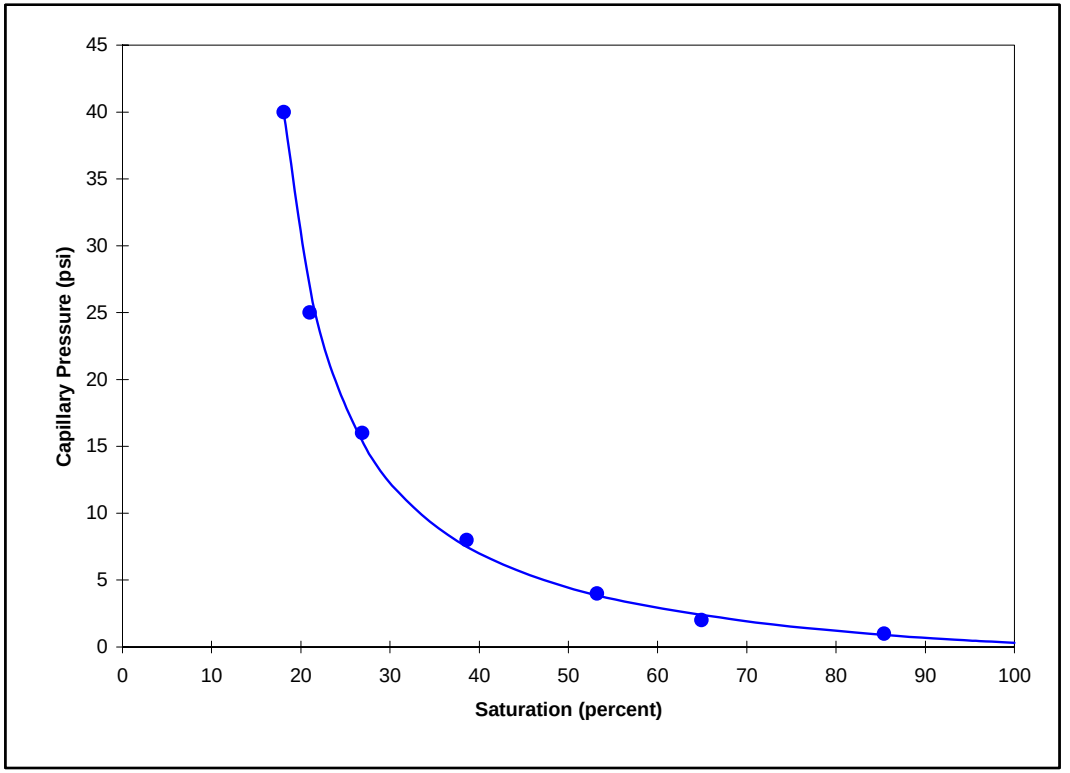
Capillary Pressure (psi)	Brine Saturation (percent)
1.0	100.0
2.0	96.8
4.0	83.9
8.0	62.6
16	48.4
25	41.9
40	35.5



CAPILLARY PRESSURE
Overburden

Client	Origin Energy Resources Limited	**Air Permeability**	152 milliDarcy's
Well	Trefoil-1	**Porosity**	14.1 percent
Sample	2/16		
Depth	2995.80 metres		
Test Method	Air/Brine Porous Plate @ Overburden		
Overburden	5400 psi		

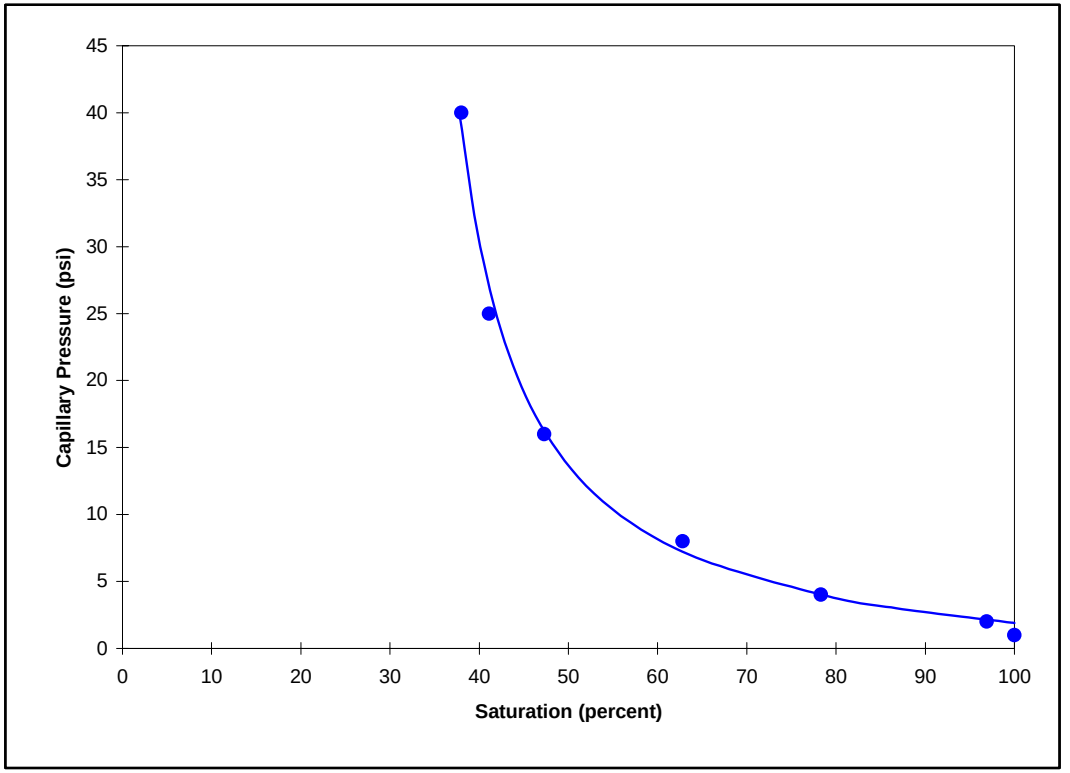
Capillary Pressure (psi)	Brine Saturation (percent)
1.0	85.4
2.0	64.9
4.0	53.2
8.0	38.6
16	26.9
25	21.0
40	18.1



CAPILLARY PRESSURE
Overburden

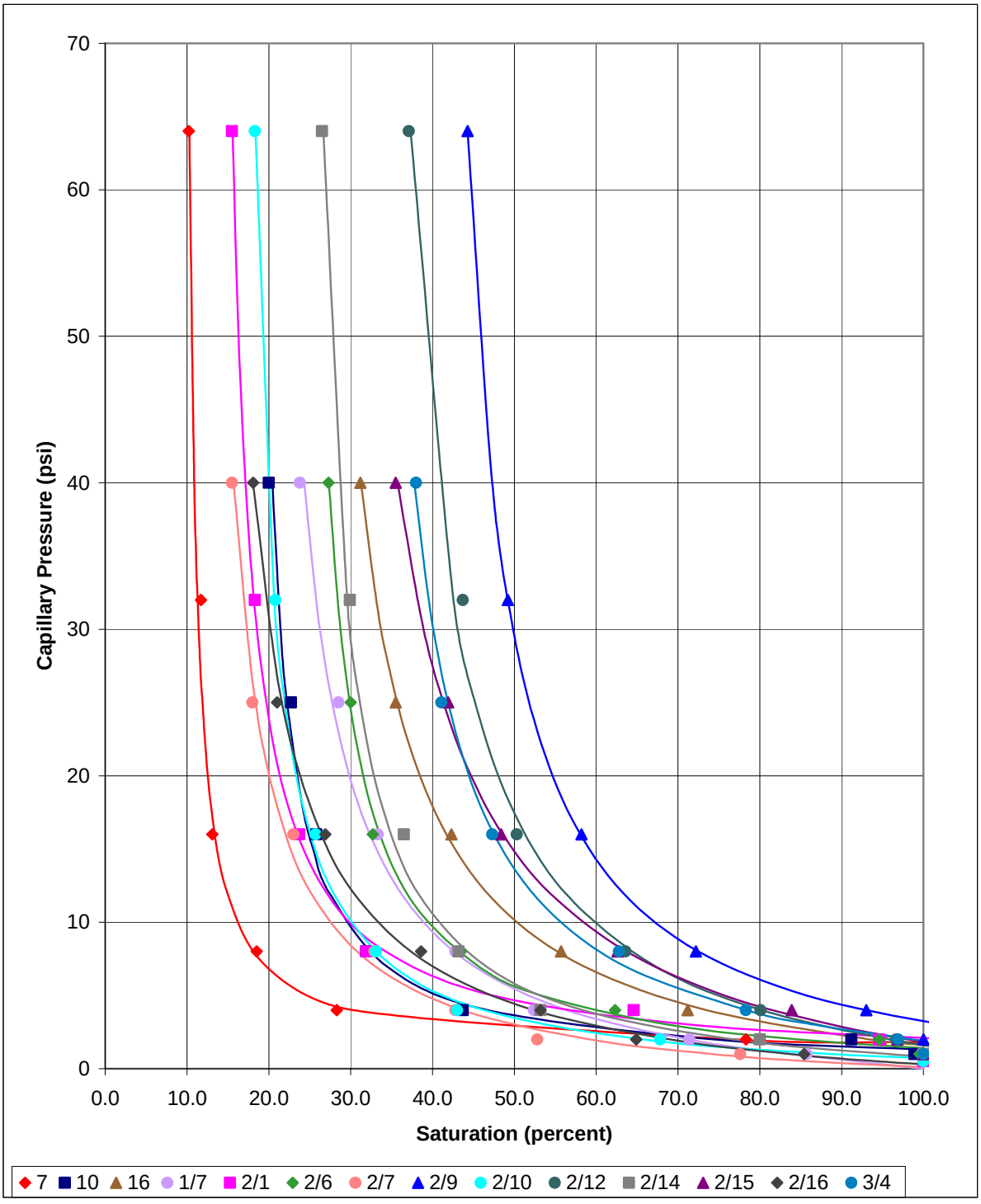
Client	Origin Energy Resources Limited	**Air Permeability**	29.4 milliDarcy's
Well	Trefoil-1	**Porosity**	13.0 percent
Sample	3/4		
Depth	3021.20 metres		
Test Method	Air/Brine Porous Plate @ Overburden		
Overburden	5400 psi		

Capillary Pressure (psi)	Brine Saturation (percent)
1.0	100.0
2.0	96.9
4.0	78.3
8.0	62.8
16	47.3
25	41.1
40	38.0



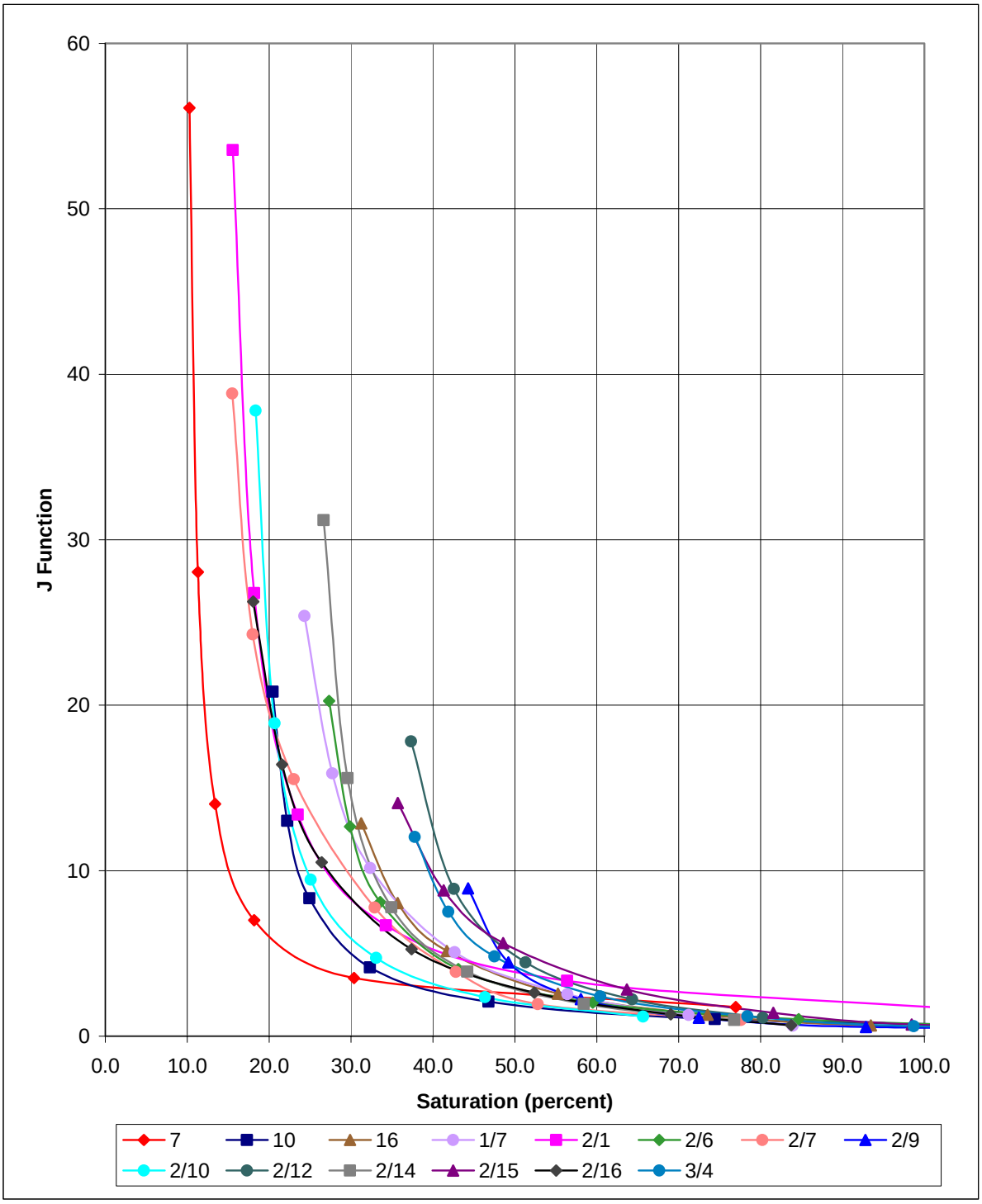
CAPILLARY PRESSURE

Client Origin Energy Resources Limited
Well Trefoil-1



J FUNCTION

Client Origin Energy Resources Limited
Well Trefoil-1



CHAPTER 4

ELECTRICAL PROPERTIES AND CAPILLARY PRESSURE

4.2 Test Results

4.2.4 Cation Exchange Capacity

CATION EXCHANGE CAPACITY

Client Origin Energy Resources Limited
Well Trefoil-1

Sample Number	Depth (metres)	Porosity (percent)	Grain Density (g/cm^3)	Cation Exchange Capacity (meq/100g)		Quantity of Cation Exchangeable Clay Qv (meq/cm^3)	
				Uncrushed	Crushed	Uncrushed	Crushed
7	2736.90	25.1	2.66	0.28	0.29	0.02	0.02

CHAPTER 4

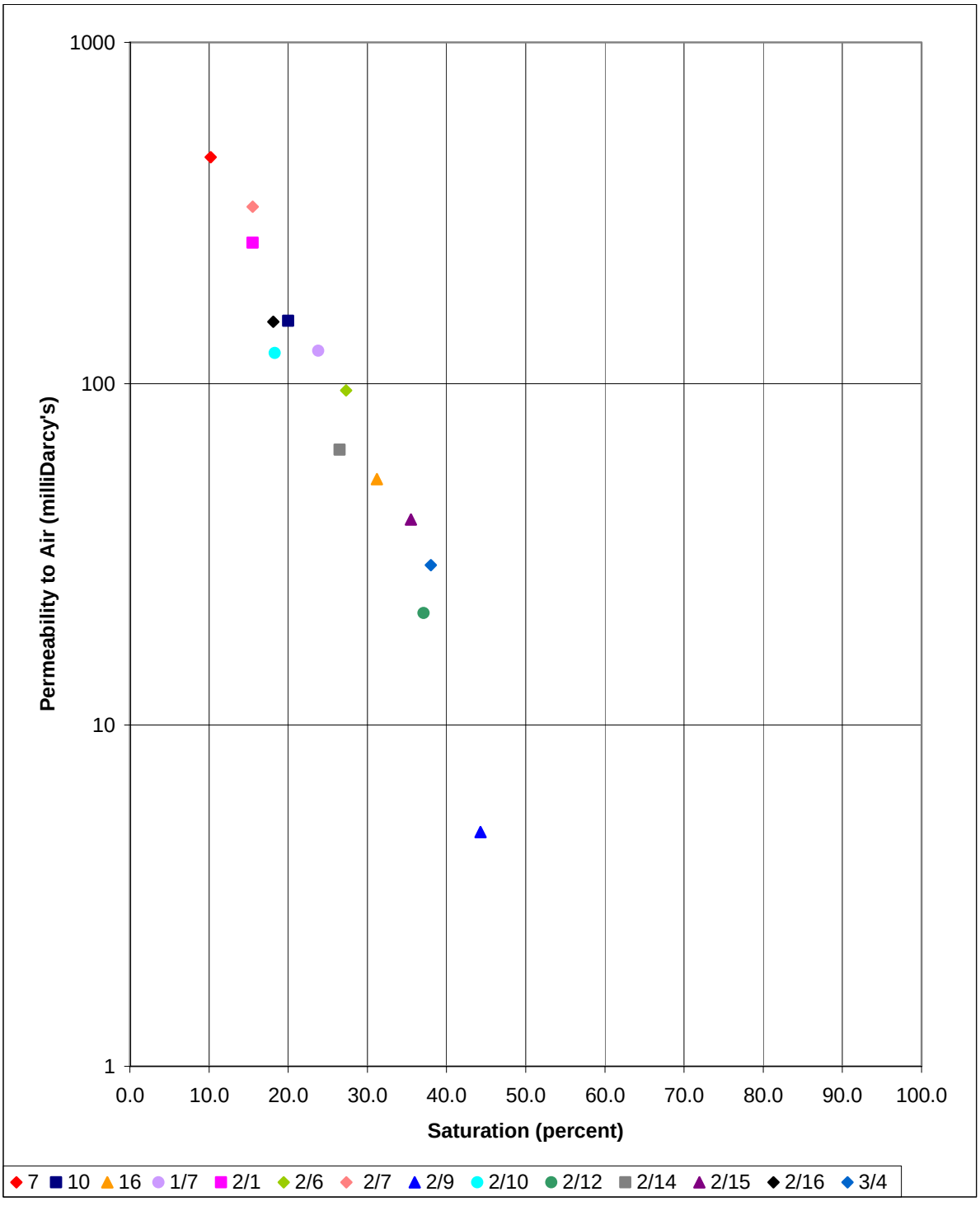
ELECTRICAL PROPERTIES AND CAPILLARY PRESSURE

4.2 Test Results

4.2.5 Summary

RESIDUAL SATURATION

Client Origin Energy Resources Limited
Well Trefoil-1



SUMMARY

Client	Origin Energy Resources Limited	**Rw of Saturant**	0.28 at 25ºC
Well	Trefoil-1	**Overburden**	

Sample Number	Depth (metres)	Permeability to Air (milliDarcy's)	Porosity (percent)	Formation Factor FF	Cementation Exponent m	Saturation Exponent n	Shaley Sand Equivalent † Formation Factor FF*	Shaley Sand Equivalent † Cementation Exponent m*	Shaley Sand Equivalent † Saturation Exponent n*
7	2736.90	461	24.0	14.3	1.86	1.74	14.6	1.88	1.81
2/1	2968.30	259	14.8	28.4	1.75	2.02			
2/9	2987.80	4.86	10.0	51.3	1.71	1.72			
2/10	2988.80	123	14.1	33.8	1.80	1.60			
2/12	2991.80	21.3	11.0	44.4	1.72	1.62			
2/14	2993.80	64.1	10.8	43.0	1.69	1.70			

† Calculated from Cation Exchange Capacity
CEC was not determined on the MSCT samples due to insufficient off-cuts

CHAPTER 5

RESIDUAL GAS

5.1 Test and Calculation Procedures

5. RESIDUAL GAS

5.1 Test and Calculation Procedures

5.1.1 Permeability to Air at Residual Water Saturation

On completion of air-brine capillary pressure desaturation the selected samples at residual water saturation (Swr) underwent effective permeability to air. Each sample was individually placed into a hydrostatic cell with an overburden pressure applied. A known pressure of humidified air was applied to the upstream face of each sample, creating a flow of air through the core plug. Effective permeability to air was calculated using Darcy's Law through knowledge of the upstream pressure, flow rate, viscosity of air and sample dimensions.

$$Keg = \frac{2000.BP.\mu.q.L}{(P_1^2 - P_2^2).A}$$

where	Keg	=	*effective permeability to air @ Swr (milliDarcy's)*
	BP	=	*barometric pressure (atmospheres)*
	μ	=	*gas viscosity (cP)*
	q	=	*flow rate (cm^3/s)*
	L	=	*sample length (cm)*
	P_1	=	*upstream pressure (atmospheres)*
	P_2	=	*downstream pressure (atmospheres)*
	A	=	*sample cross sectional area (cm^2)*

5.1.2 Waterflood

Brine was pumped through the samples at a low rate (4 cc/hour). Flow continued until gas production ceased and a brine permeability at residual gas saturation was determined through knowledge of the differential flooding pressure, flow rate, viscosity of brine and the sample dimensions.

$$Kw = \frac{14696.q.L.\mu T}{\Delta P.A}$$

where	*14696*	=	*units conversion*
	Kw	=	*effective permeability to brine*
	q	=	*flow rate (cm^3/s)*
	ΔP	=	*differential flooding pressure (psig)*
	L	=	*sample length (cm)*
	A	=	*sample cross sectional area (cm^2)*
	μT	=	*brine viscosity (cP) at T (° C)*

The flow rate was then increased (to 4cc/min) and further production measured. Once stable gas saturation was reached permeability was measured as per above.

CHAPTER 5

RESIDUAL GAS

5.2 Test Results

WATERFLOOD
Air-Brine

Client Origin Energy Resources Limited
Well Trefoil-1

Saturant 20000 ppm
Overburden 5400 psi

Sample Number	Permeability to Air (milliDarcy's)	Porosity (percent)	Initial Brine Saturation (percent)	Permeability to Air @ Swir (milliDarcy's)	Low Rate		Bump Flood		Gas Recovery	
					Residual Gas Saturation (percent)	Effective Brine Permeability (milliDarcy's)	Residual Gas Saturation (percent)	Effective Brine Permeability (milliDarcy's)	Percent of Pore Volume (percent)	Percent of Gas in Place (percent)
2/1	259	14.8	15.5	220	41.1	17.3	29.4	62.8	55.1	65.2
2/9	4.86	10.0	44.3	3.45	24.0	0.54	9.4	1.38	46.3	83.1
2/12	21.3	11.0	37.1	16.0	30.8	1.53	22.6	5.7	40.3	64.1
2/15	40.0	12.9	35.5	28.5	27.9	1.51	20.4	7.7	44.1	68.4
2/16	152	14.1	18.1	144	36.6	3.27	26.6	28.4	55.3	67.5

APPENDIX I

FLUID PROPERTIES

FLUID PROPERTIES

Brine

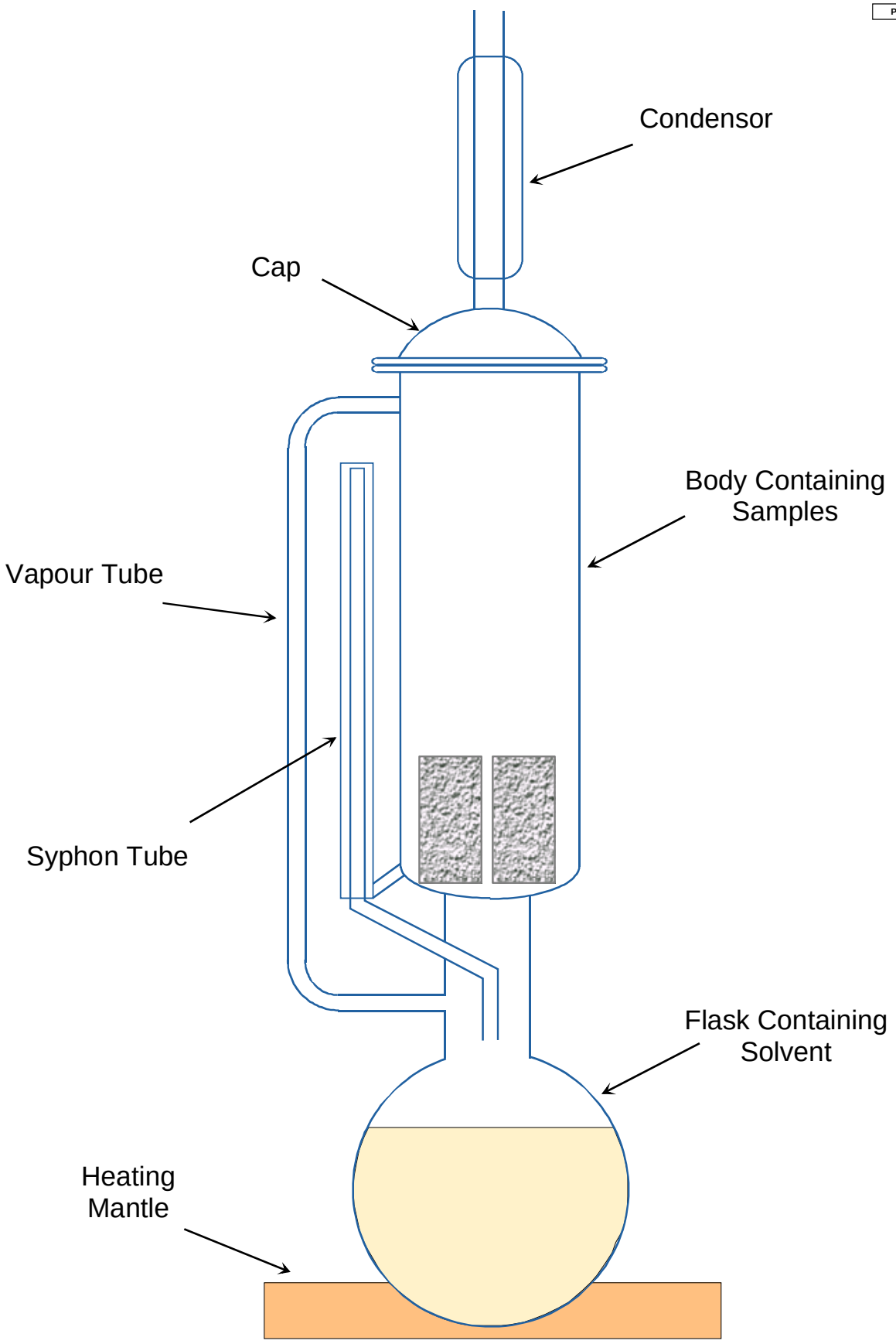
20000 ppm NaCl equivalent

Density	=	1.018	g/cm^3 @ 25°C
Resistivity	=	0.28	ohm.m @ 25°C
Viscosity	=	1.008	cP @ 25°C

APPENDIX II

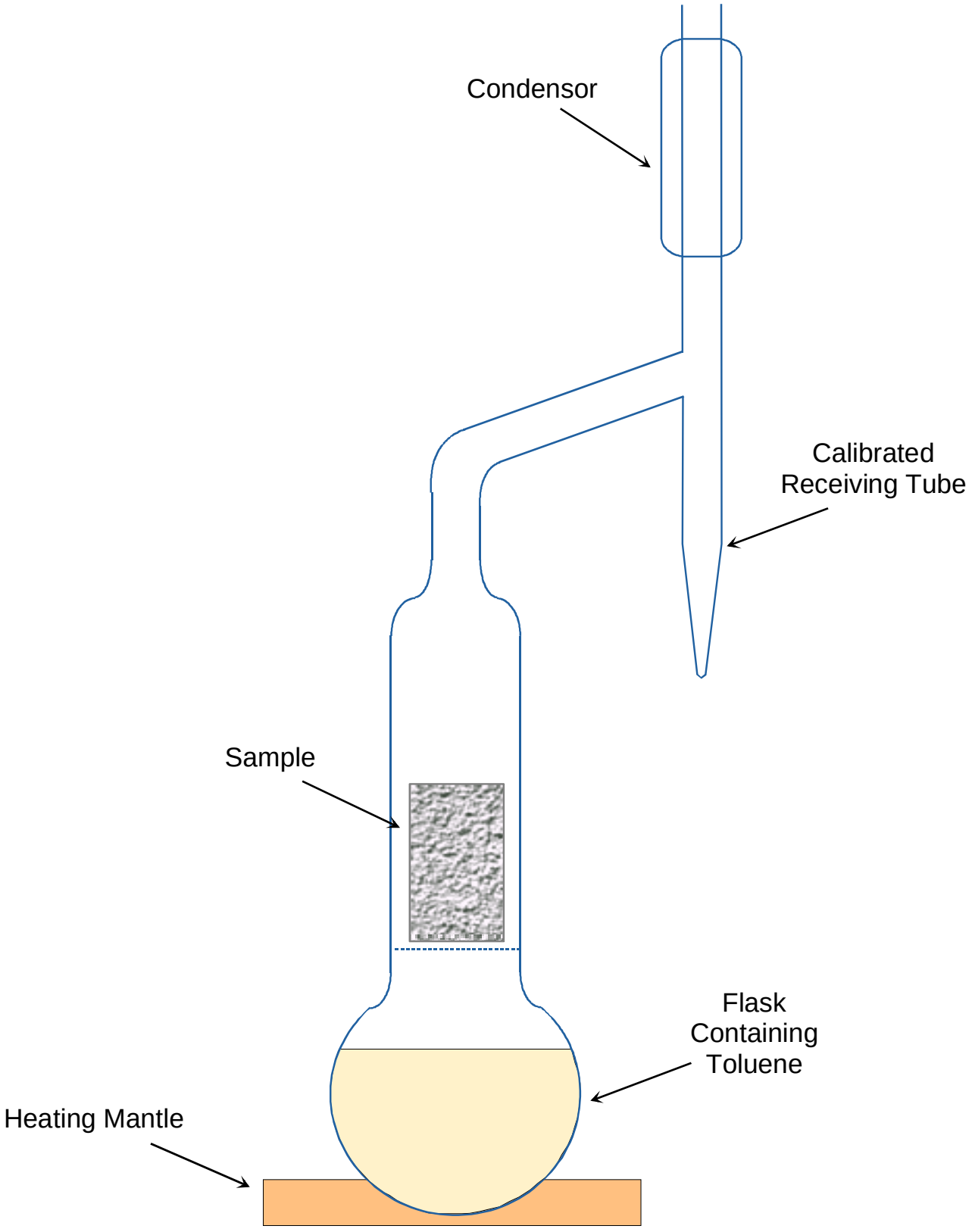
EQUIPMENT SCHEMATICS

SOXHLET CLEANING APPARATUS



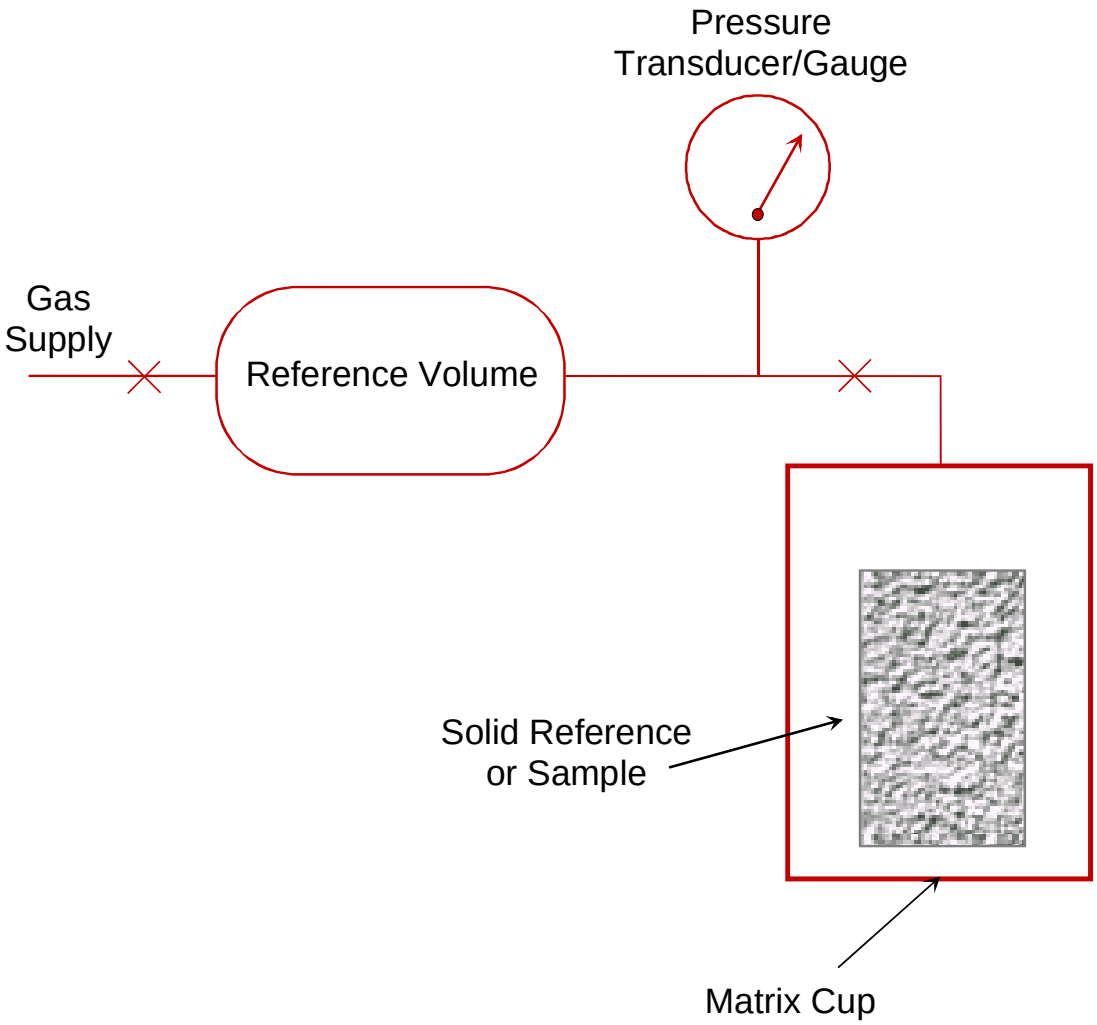
ACS Laboratories Pty Ltd
ABN: 81 008 273 005

DEAN-STARK APPARATUS



ACS Laboratories Pty Ltd
ABN: 81 008 273 005

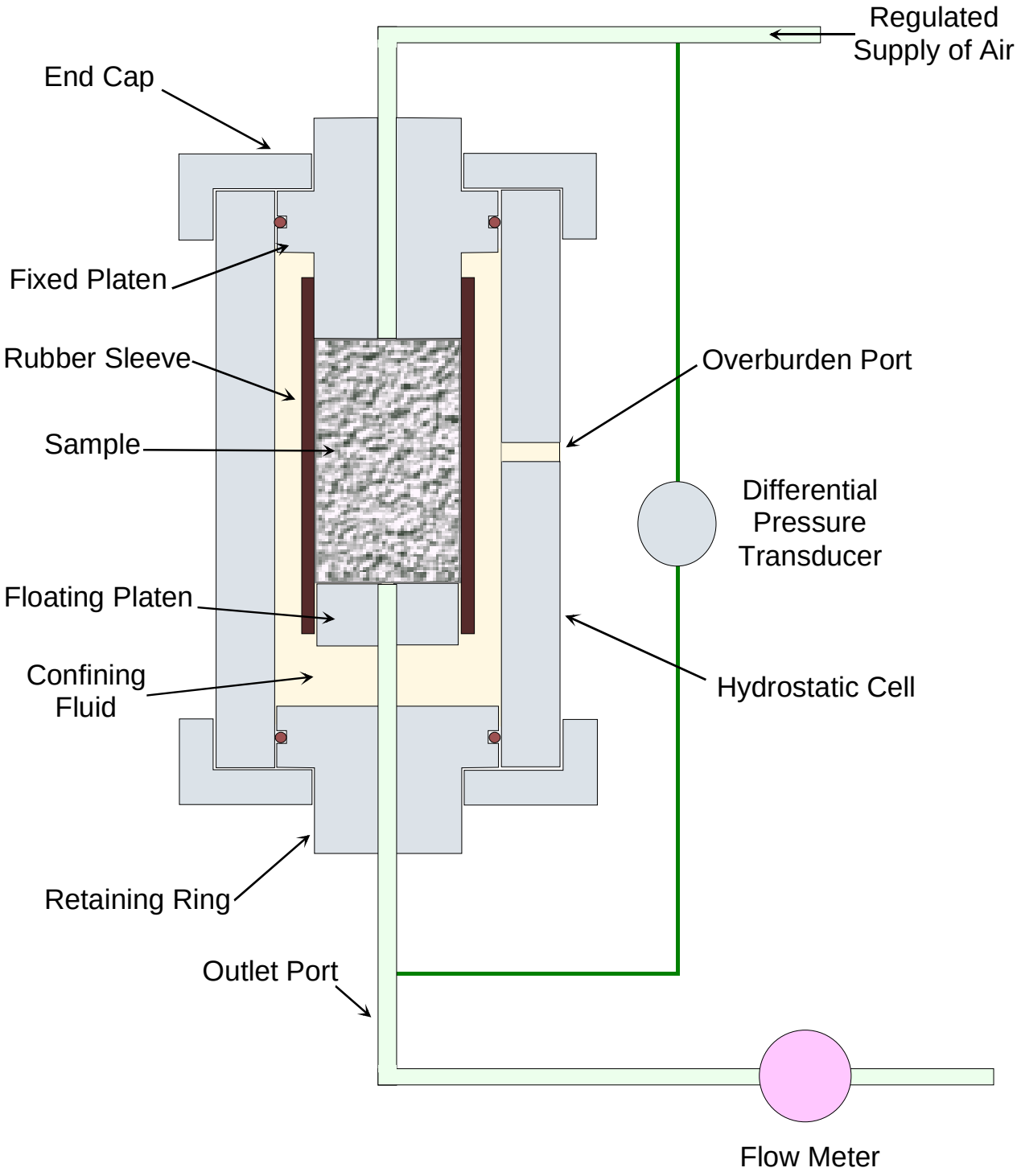
POROSIMETER SCHEMATIC



P1.V1 (reference) = P2.V2 (sample)

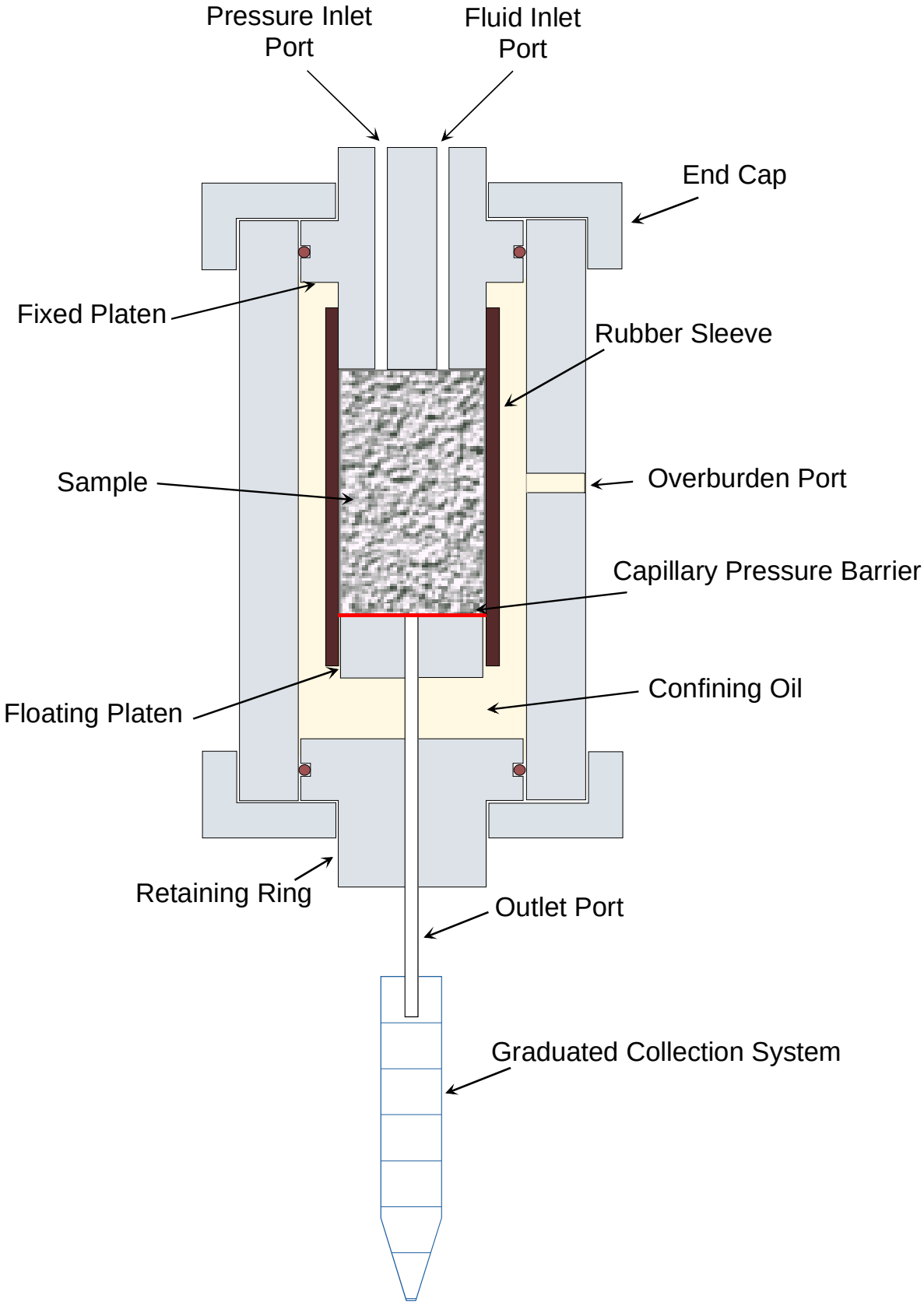
ACS Laboratories Pty Ltd
ABN: 81 008 273 005

GAS PERMEAMETER SCHEMATIC (Hydrostatic)



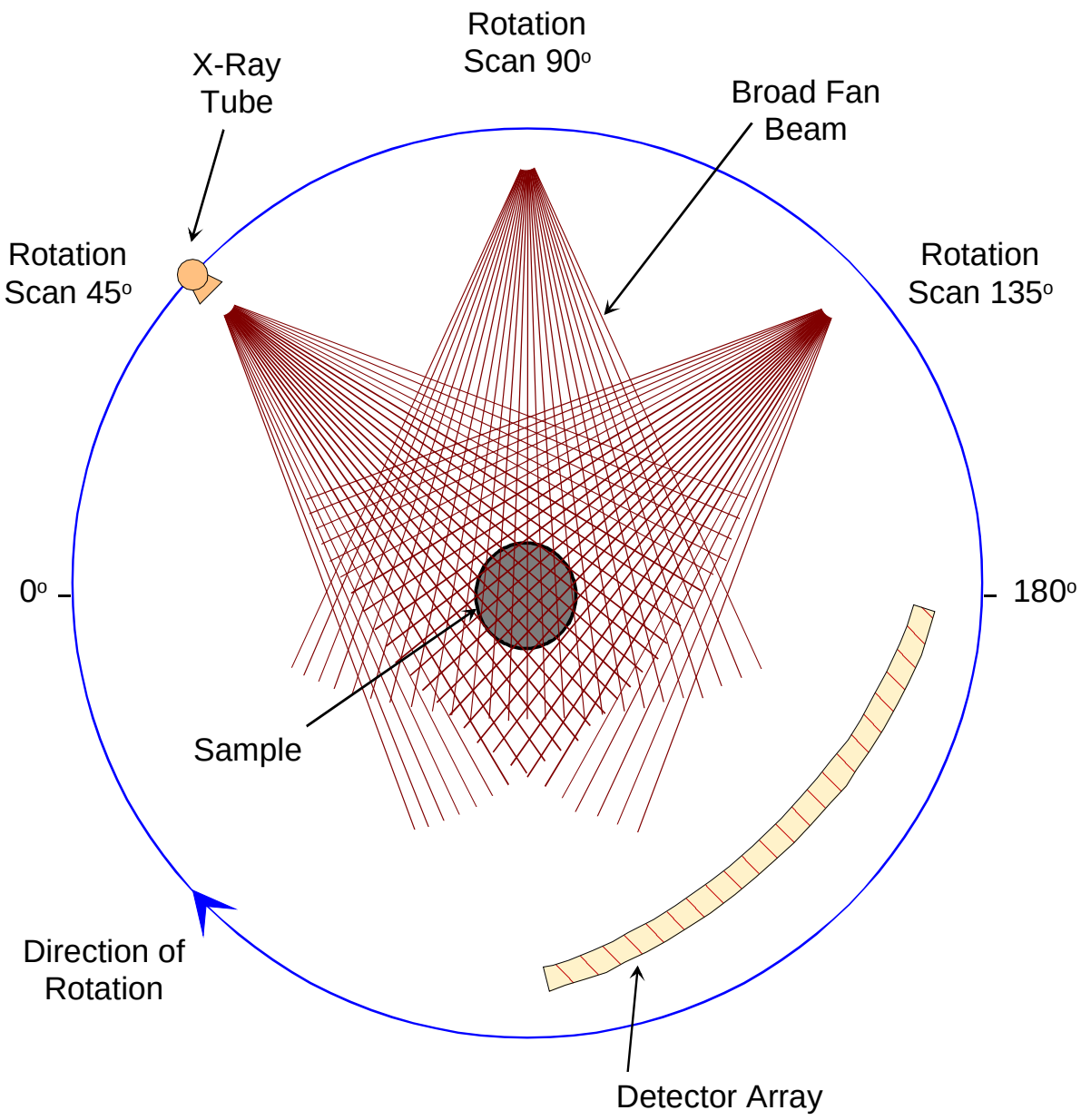
ACS Laboratories Pty Ltd
ABN: 81 008 273 005

HYDROSTATIC CAPILLARY PRESSURE CELL

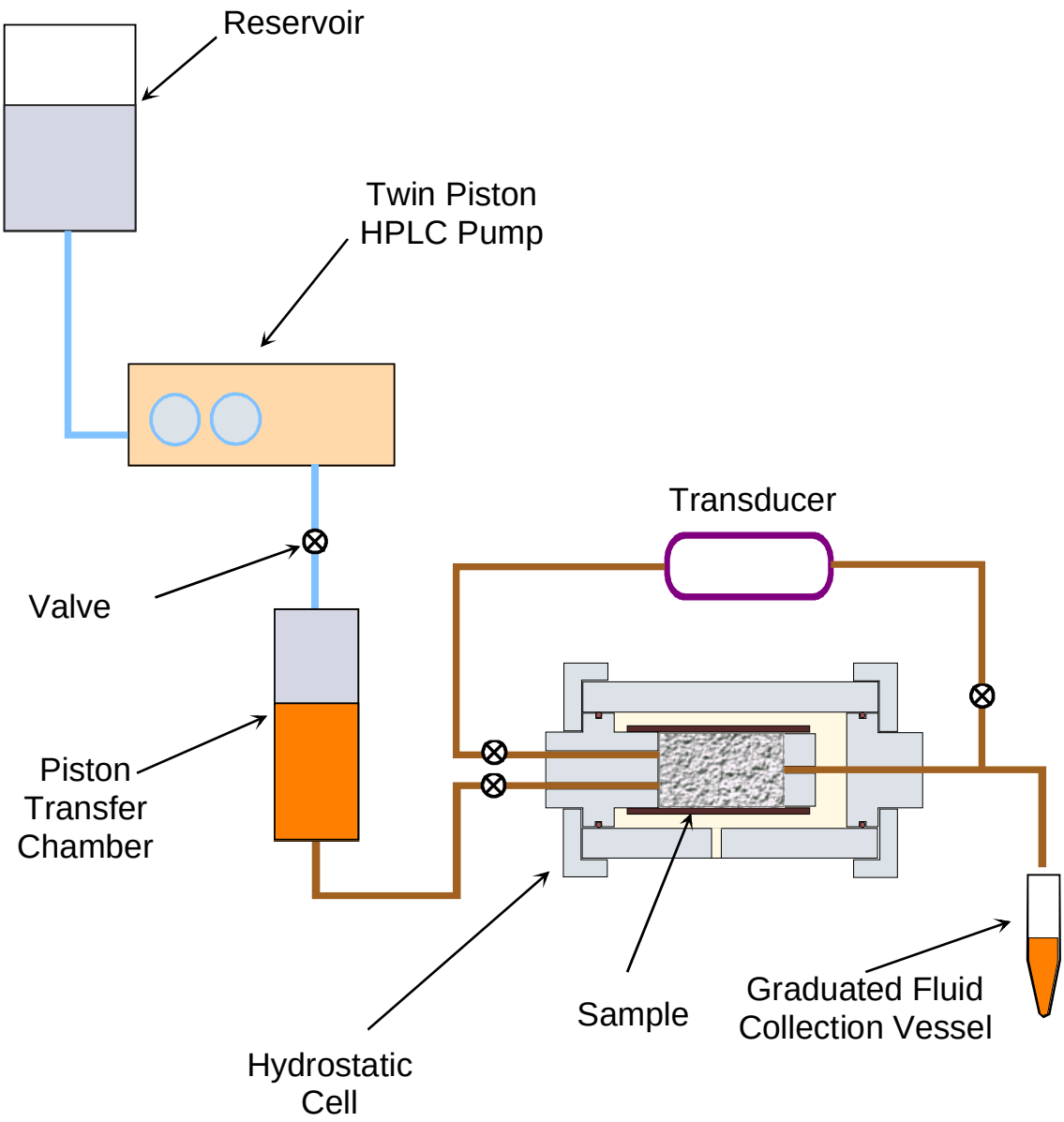


ACS Laboratories Pty Ltd
ABN: 81 008 273 005

CT SCANNER SCHEMATIC



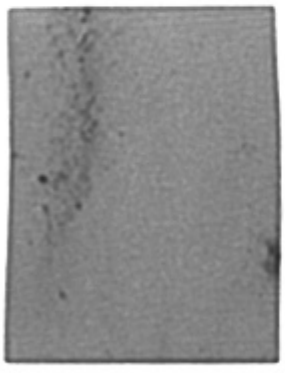
LIQUID PERMEABILITY SCHEMATIC



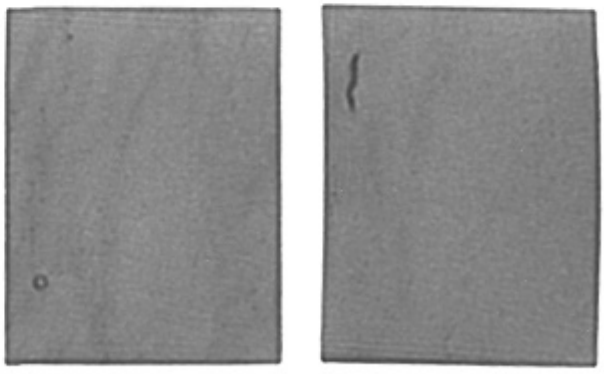
APPENDIX III

CT SCAN IMAGES

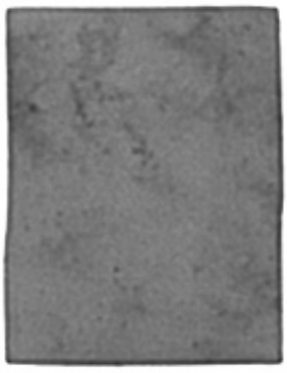
Trefoil-1
C.T. Scans



Sample No:	7
Depth:	2736.90 m
Permeability:	551 mD
Porosity:	25.1 %

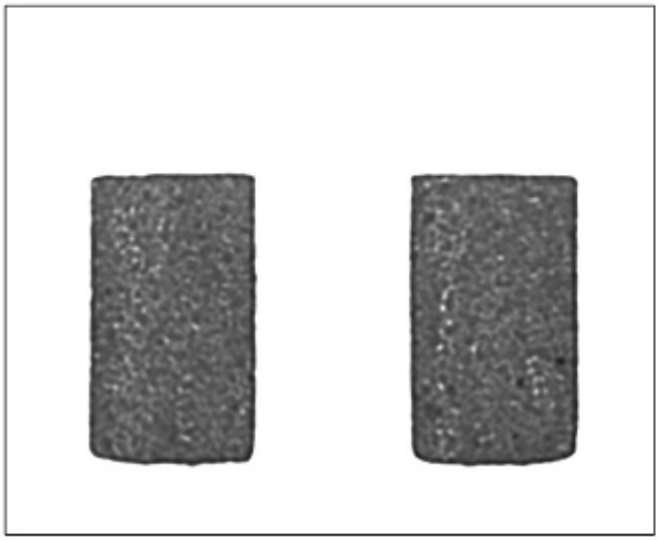


Sample No:	10
Depth:	2737.80 m
Permeability:	181 mD
Porosity:	23.6 %

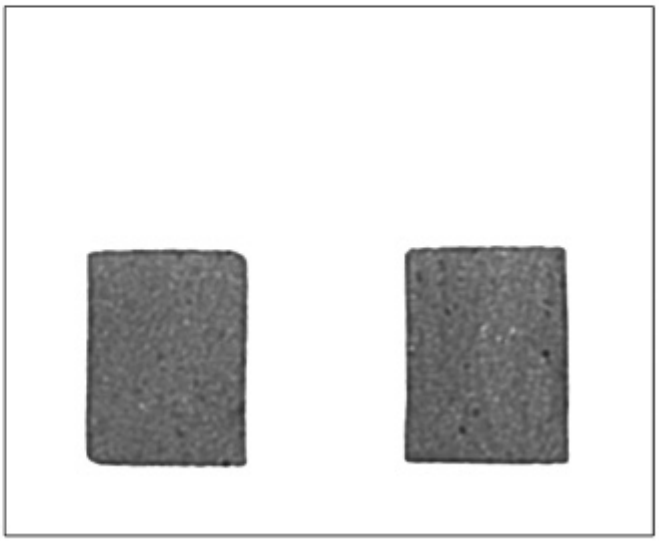


Sample No:	16
Depth:	2739.59 m
Permeability:	68.8 mD
Porosity:	21.7 %

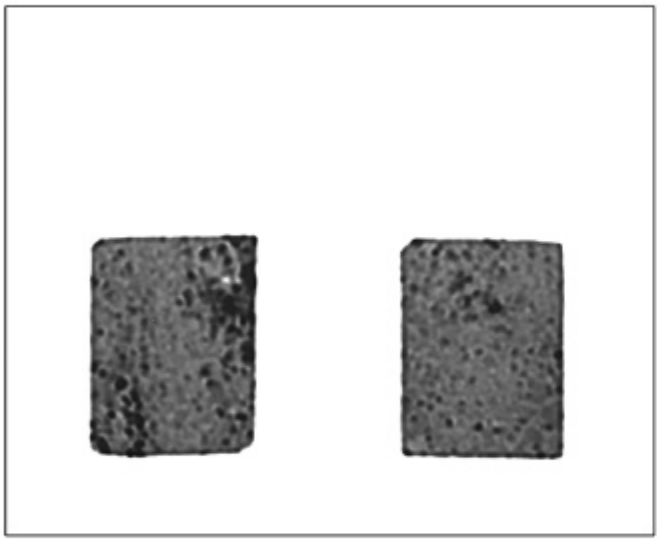
Trefoil-1
C.T. Scans



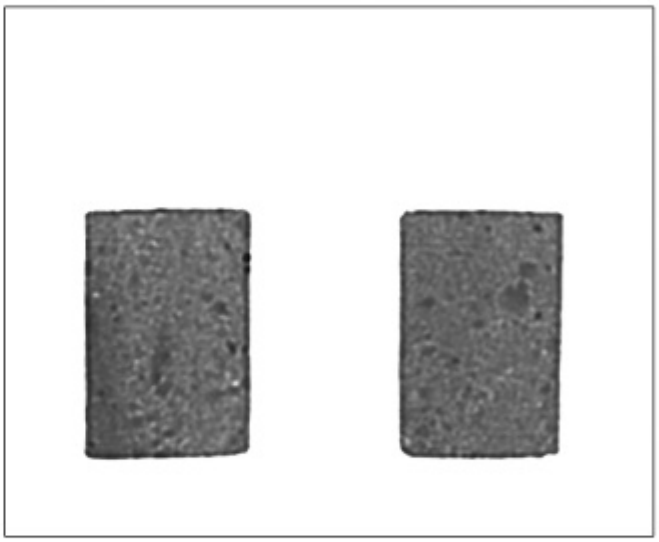
Sample No:	1/7
Depth:	2993.80 m
Permeability:	151 mD
Porosity:	14.5 %



Sample No:	2/1
Depth:	2968.30 m
Permeability:	336 mD
Porosity:	16.9 %

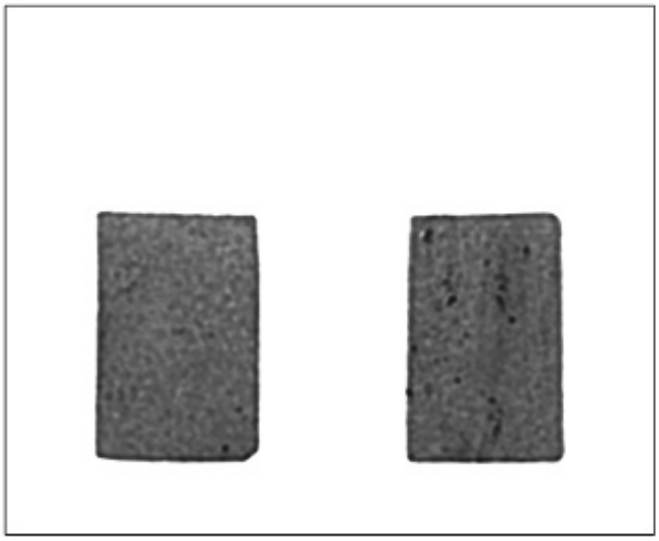


Sample No:	2/6
Depth:	2981.00 m
Permeability:	116 mD
Porosity:	16.8 %

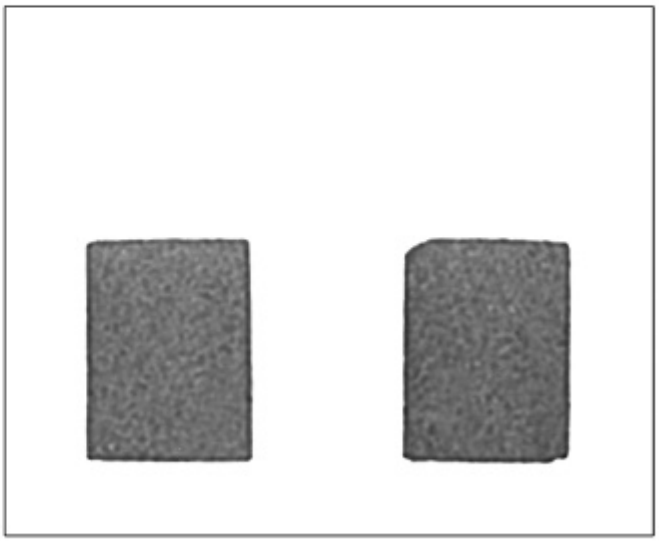


Sample No.:	2/7
Depth:	2982.00 m
Permeability:	356 mD
Porosity:	15.4 %

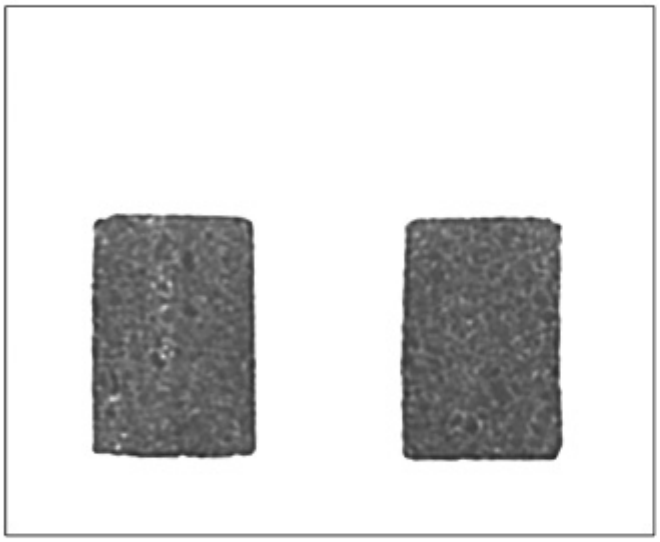
Trefoil-1
C.T. Scans



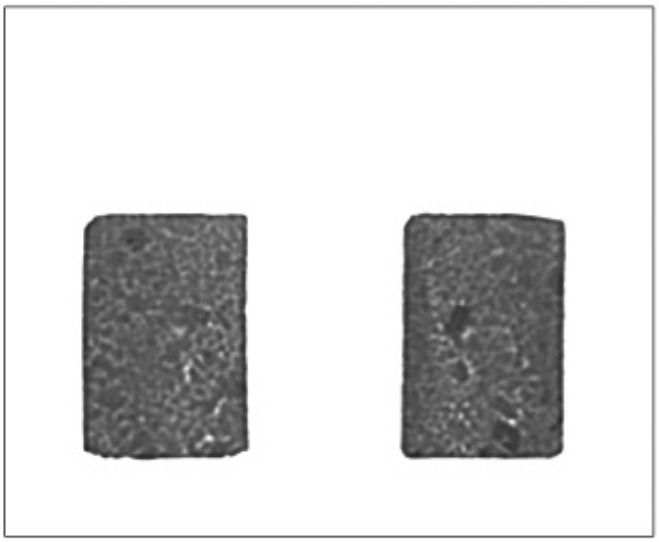
Sample No:	2/9
Depth:	2987.80 m
Permeability:	8.0 mD
Porosity:	11.7 %



Sample No:	2/10
Depth:	2988.80 m
Permeability:	145 mD
Porosity:	16.2 %

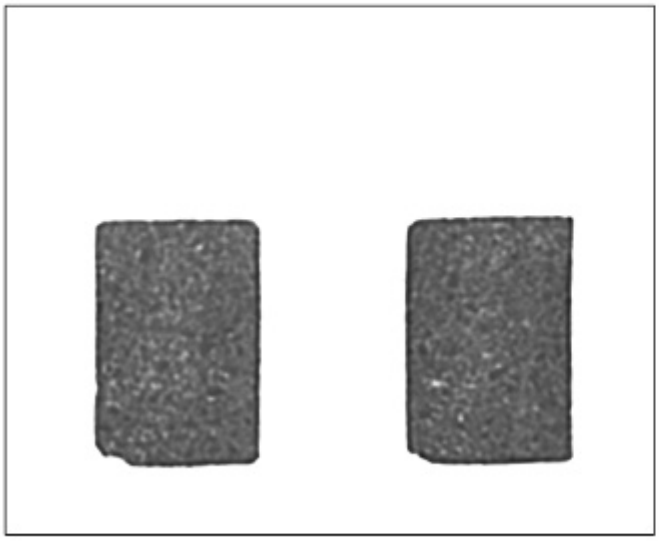


Sample No:	2/12
Depth:	2991.80 m
Permeability:	32.4 mD
Porosity:	13.1 %

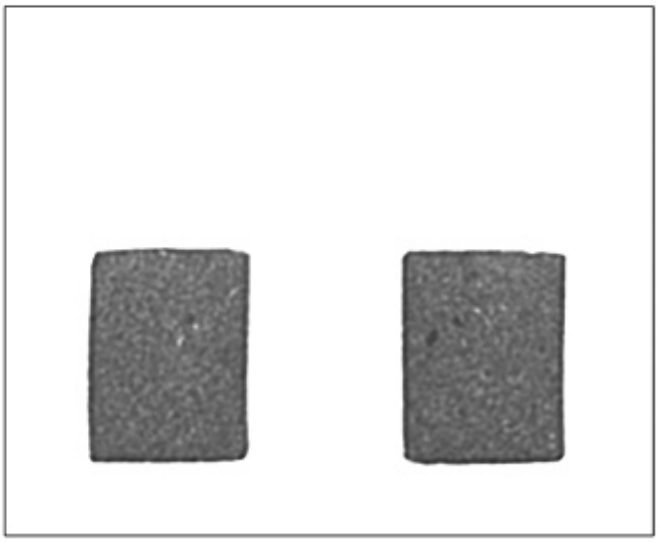


Sample No.:	2/14
Depth:	2993.80 m
Permeability:	87.3 mD
Porosity:	13.0 %

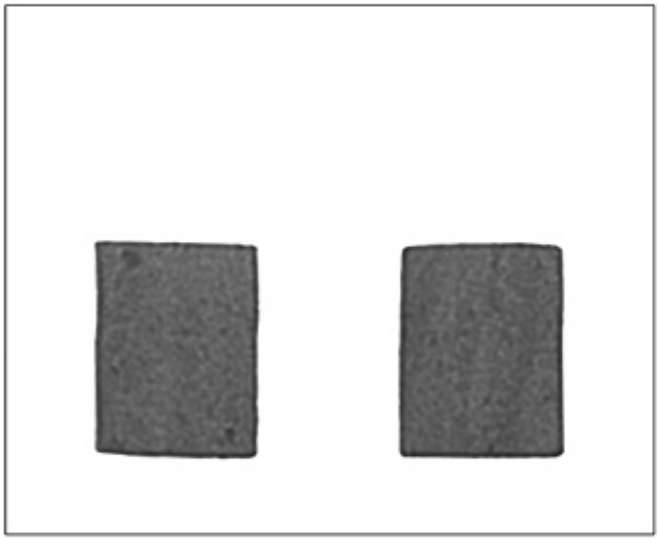
Trefoil-1
C.T. Scans



Sample No:	2/15
Depth:	2994.80 m
Permeability:	51.0 mD
Porosity:	14.1 %



Sample No:	2/16
Depth:	2995.80 m
Permeability:	180 mD
Porosity:	15.9 %



Sample No:	3/4
Depth:	3021.20 m
Permeability:	36.7 mD
Porosity:	14.4 %

APPENDIX IV

ABBREVIATIONS

ABBREVIATIONS for CORE PROPERTIES

a	Intercept (assumed = 1)
A	Sample Cross Sectional Area (cm^2)
ABPc	Air-Brine Capillary Pressure
Amb	Ambient Conditions (No Overburden Pressure)
B	Equivalent Conductance of Clay Exchange Cations ($mho/m.cm^2.meq^{-1}$)
β	Beta Factor (ft^{-1})
BF	Basic Flood
BHN	Brinell Hardness Number (kg/mm^2)
BP	Barometric Pressure (atm)
CEC	Cation Exchange Capacity (meq/100g dry sample)
Cent	Centrifuge
Co	Conductivity of Fully Brine Saturated Sample (mho/m)
cP	Centipoise
Cw	Conductivity of Brine (mho/m)
Dr	Drainage (i.e. draining of the wetting fluid - usually brine)
Φ	Porosity
FF	Formation Factor
*FF**	Shaly Sand Equivalent Formation Factor
g	grams
HeInj	Helium Injection
HgInj	Mercury Injection Capillary Pressure
Imb	Imbibition (i.e. imbibition of the wetting fluid - usually brine)
K	Permeability (mD)
Ka	Air Permeability (mD)
Keg	Effective Permeability to Gas (mD)
Keo	Effective Permeability to Oil (mD)
Kew	Effective Permeability to Water (mD)
Kg	Gas Permeability (mD)
KgKo	Gas-Oil Relative Permeability

ABBREVIATIONS for CORE PROPERTIES

KgKw	Gas-Water Relative Permeability
Klink or Kl	Klinkenberg Permeability (mD)
Ko	Oil Permeability (mD)
Krg	Relative Gas Permeability
Kro	Relative Oil Permeability
Krw	Relative Water Permeability
Kw	Brine Permeability (mD)
KwKo	Oil-Water Relative Permeability
L	Sample Length (cm)
m	Cementation Factor
*m**	Shaly Sand Equivalent Cementation Factor
mD	milliDarcy's
n	Saturation Exponent
*n**	Shaly Sand Equivalent Saturation Exponent
OB	Overburden Pressure (psig)
OBPc	Oil-Brine Capillary Pressure
P	Pressure (psi)
Pc	Capillary Pressure (psig)
PP	Porous Plate
PvComp	Pore Volume Compressibility
PVR	Pore Volume Reduction (cm^3)
ρ	Density (g/cm^3)
q	Flow Rate (cm^3/s)
θ	Contact Angle (degrees)
Qv	Volume Concentration of Clay Exchange Cations (meq/cm^3)
r	Radius (cm)
Rc	Sample Resistance (ohm)
RCA	Routine Core Analysis

ABBREVIATIONS for CORE PROPERTIES

ResCon	Reservoir Conditions
RI	Resistivity Index
RICP	Resistivity Index & Capillary Pressure
Ro	Resistivity of Fully Brine Saturated Sample (ohm.m)
Rt	Resistivity of Partially Saturated Sample (ohm.m)
Rw	Resistivity of Brine (ohm.m)
S	Saturation
s	Seconds
SCA	Special Core Analysis
Sg	Gas Saturation
Sgr	Residual Gas Saturation
SngPt	Single Point
So	Oil Saturation
Sor	Irreducible Oil Saturation (or Residual Oil Saturation)
SS	Steady State
Sw	Brine Saturation
Swi	Initial Water Saturation
Swir	Irreducible Water Saturation
Swr	Residual Water Saturation
T	Temperature (^{o}C)
USS	Unsteady State
μ	Viscosity (cP)
Vb	Bulk Volume (cm^3)
Vg	Grain Volume (cm^3)
Vp	Pore Volume (cm^3)
ω	Angular Velocity (rad/s)
Wett	Wettability
Wt	Weight (g)

APPENDIX 10: FMI INTERPRETATION REPORT

Origin energy

delivering the goods

Trefoil 1

Formation Micro-Imager (FMI) Interpretation Report

T/18P
BASS BASIN

Brett Pidgeon
July 2005

SUMMARY

This report presents processed and interpreted FMI images from the interval 2700 – 3400 m within Trefoil 1. The studied succession within Trefoil 1 is of Cretaceous – Palaeocene age, and is characterised by variable structural dips, typically in the range 1-4º, as is listed below.

Structural Zone	Depth Interval	Tectonic Tilt	Comments
2700 – 3400 m			
Zone I	2700 – 2734	1.4°/225°	Bounded by sandstone at base
Zone II	2734 – 2770	2.0°/113°	Bounded by maximum flooding surface
Zone III	2770 – 2826	1.2°/196°	Bounded by sandstone at base
Zone IV	2826 – 2918	2.8°/079°	Interbedded sandstone & mudstone, bounded by unconformity at 2918 m
Zone V	2918 - 3080	1.5°/252°	Bounded by maximum flooding surface
Zone VI	3080 – 3237	4.0°/286°	Bounded by flooding surface
Zone VII	3237 – 3374	4.2°/249°	Bounded by maximum flooding surface
Zone VIII	3374 – 3400	3.1°/032°	Bounded by volcanics

Lithofacies identified from FMI images have been calibrated with cuttings descriptions. Cuttings descriptions match well with lithofacies interpretations derived using wireline log response and FMI image fabrics, and indicate a succession comprising sandstone and mudstone with minor coal. Six lithofacies associations have been identified within the studied section. These are interpreted as having been deposited in fluvial, marginal lacustrine (shelf-shoreface?) and shelf settings. The lithofacies associations identified are summarised as follows:

I. Mudstones that either occur at the base of upward coarsening facies successions (interpreted as either prodeltaic muds, or shelf-shoreface deposits), or interbedded with sandstones that have sharp bases and tops (interpreted as suspension settling in a shelf environment) or interbedded with sandstones and rare coal (interpreted as floodplain deposits).
II. Heterolithic intercalations of sandstone and mudstone, typically occurring within the lower-mid parts of upward coarsening facies successions (interpreted as shelf-shoreface deposits). When it is interbedded with Lithofacies Association IV, this implies a sub-aerial setting in a floodplain environment. This lithofacies association also occurs with Lithofacies Association V as possible thin bedded turbidite deposits.
III. Stratified sandstones with mottled image fabric and low angle (typically <5º) internal bedding surfaces, typically occurring towards the top of upward coarsening facies successions (shoreface deposits).
IV. Successions of thick bedded stratified sandstones and rare pebbly sandstones with dominant internal bedding fabrics inclined at angles <10°, rare intervals of up to 25°. These deposits represent fluvial channels.
V. Stratified sandstones with sharp bases and tops, interbedded with Lithofacies Association I, and characterised by low angle (typically <5º) internal bedding surfaces represent massive to parallel stratified sandstones deposited from turbidite flows.
VI. Coals (deposits of swampy coastal plain environments).

Palaeotransport analyses of sandstones from Lithofacies Association III reveals them to be characterised by internal stratification fabrics with very wide ranging sedimentary dip azimuth, suggesting they were originally deposited as “flat lying” strata. Few palaeotransport interpretations can be made for these sandstones. However, in some examples, a dominant sedimentary dip is present, and may represent the original palaeoslope, implying an E - W shoreline orientation.

Palaeotransport analyses of sandstones from Lithofacies Association IV reveals them to be characterised by low angle internal stratification fabrics with variable azimuth and cross bedding with a 240º azimuthal spread. The relationship between intra-set lamination and coset boundaries suggest that sediment transport occurred normal to, i.e. bedforms migrated downcurrent, and at a high angle to, i.e. lateral migration, the depositional dip. Interpreted channel drainage directions are variable but have an overall northerly direction.

Palaeotransport analysis of sandstones from Lithofacies Association V reveals them to be almost exclusively dominated by low angle internal stratification fabrics that have a variable orientation, but have an overall easterly trend that may reflect the original palaeoslope.

TABLE OF CONTENTS

SUMMARY **1**

TABLE OF CONTENTS **3**

LIST OF TABLES **5**

LIST OF FIGURES **6**

LIST OF ENCLOSURES **7**

INTRODUCTION **8**

Objectives **8**

Depth and directional references **8**

Processing and quality control **9**

Borehole conditions **9**

Data processing **10**

Speed correction *10*

Image processing *10*

Block depth shifts *10*

Dip processing *10*

Sedimentological analysis **12**

Tectonic tilt determination **12**

Classification of sedimentary features **12**

Lithofacies characterisation **15**

Lithofacies identified from FMI logs. *15*

Calibration of image log fabrics using cuttings descriptions *16*

Image log calibration using cuttings *16*

FMI derived lithological fabric index *17*

Lithofacies associations **17**

Lithofacies Association I *18*

Lithofacies Association II *18*

Lithofacies Association III *19*

Lithofacies Association IV *19*

Lithofacies Association V *20*

Lithofacies Association VI *20*

Summary *21*

Summary of environmental interpretations **21**

Interval 3375 – 3390 m *21*

Interval 3090 – 3160 m *22*

Interval 2960 – 3065 m *23*

Interval 2820 – 2920 m *24*

Interval 2730 – 2745 m *25*

Bedform orientation and sediment dispersal **26**

Lithofacies Associations I, II & III **26**

Lithofacies Association IV **26**

Lithofacies Association V **28**

Lithofacies Association VI **29**

CONCLUSIONS **30**

REFERENCES **32**

LIST OF TABLES

Table 1 Summary of well details, study objectives and the data set used for this analysis.

Table 2 Summary of hole conditions through the study interval in Trefoil 1

Table 3 Tectonic tilt summary of Trefoil 1

Table 4 Classification of surfaces identified from FMI images

Table 5 Lithofacies identified from FMI images within the study interval

Table 6 Simple fabric index (applied to sandstone lithofacies) based upon mnemonics scheme used for FMI interpretation of lithofacies. Note the fabric index may approximate to a bioturbation index within sandstone lithologies free of granular-pebbly detritus

Table 7 Summary of deposits in the interval 3375 – 3400 m

Table 8 Summary of deposits in the interval 3090 – 3160 m

Table 9 Summary of deposits in the interval 2960 – 3165 m

Table 10 Summary of deposits in the interval 2820 – 2920 m

Table 11 Summary of deposits in the interval 2730 – 2745 m

Table 12. Bedding orientations of Lithofacies Association IV within the interval 3375 – 3400 m

Table 13. Bedding orientations of Lithofacies Association IV within the interval 2820 – 2920 m

Table 14. Bedding orientation of Lithofacies Association V within the interval 3090 – 3160 m

Table 15. Bedding orientation of Lithofacies Association V within the interval 2060 – 3065 m

LIST OF FIGURES

Figure 1. Cumulative automatic (A), muds and hets (B), and manual (C) dip azimuth plots for the studied section (2700 – 3400 m).

Figure 2 Dip categories used in this study

Figure 3 FMI Image through well laminated to massive mudstone (lithofacies Ml & Mm)

Figure 4 FMI image through dm-scale heterolithic sandstone-mudstone lithofacies with well developed lamination fabric (Hl) becoming less well developed, fabric (Hm), toward the base. Sandstone with well developed lamination fabric (Sl) is also present (2837.75 – 2838.3 m).

Figure 5 FMI image illustrating well laminated sandstone Sl (3102.25 – 3104 m) with thin mottled sandstone with vague lamination Sm(Sl) (3105.5 – 3106 m) and laminated sandstone with vague mottling Sl(Sm) (3104 – 3105.5 m).

Figure 6 FMI image illustrating sandstone with coarse scale mottled fabric, Scm and mottled sandstone with weak lamination Sm(Sl) overlying laminated mudstone (Ml).

Figure 7 Cumulative dip azimuth plot for the interval 3375 – 3400 m. ISSf and ISS surfaces are shown with structural dip removed. ISSf surfaces are dominant and large changes in azimuth are associated with these nearly flat lying structures.

Figure 8 Cumulative dip azimuth plot for the interval 3090 – 3160 m. ISSf and ISS surfaces are shown with structural dip removed. ISSf surfaces are dominant and large changes in azimuth are associated with these nearly flat lying structures.

Figure 9 Cumulative dip azimuth plot for the interval 2960 – 3065 m. ISSf and ISS surfaces are shown with structural dip removed. ISSf surfaces are dominant and large changes in azimuth are associated with these nearly flat lying structures.

Figure 10. Cumulative dip azimuth plot for the interval 2820 – 2920 m. ISSf and ISS surfaces are shown with structural dip removed. ISSf surfaces are dominant and large changes in azimuth are associated with these nearly flat lying structures

LIST OF ENCLOSURES

		Scale
Enclosure 1	Quality control plot of FMI log, 2700 - 3400 m	1:500
Enclosure 2	Overview structural summary log, 2700 – 3400 m	1:500
Enclosure 3	Data overview plot, 2820 – 2920 m	1:200
Enclosure 4	Data overview plot, 2918 – 3075 m	1:200
Enclosure 5	Data overview plot, 3090 – 3170 m	1:200
Enclosure 6	Data overview plot, 3320 – 3400 m	1:200
Enclosure 7	Sedimentological summary plot, 2820 – 2920 m	1:100
Enclosure 8	Sedimentological summary plot, 2960 – 3065 m	1:100
Enclosure 9	Sedimentological summary plot, 3090 – 3160 m	1:100
Enclosure 10	Sedimentological summary plot, 3375 – 3390 m	1:100
Enclosure 11	Core composite plot, 2730 – 2745 m	1:20

INTRODUCTION

The processing and interpretation of the Formation Micro-Imager (FMI) images from Trefoil 1 are documented in this report. The detailed sedimentological report is based on FMI images for the interval 2700 – 3400 m.

Objectives

The well details and project objectives for Trefoil 1 are summarised in Table 1 with the data that was incorporated into this study.

Table 1. Summary of well details, study objectives and the data set used for this analysis.

Well Details	
Well: Surface Latitude: Surface Longitude: Intervals of interest:	Trefoil 1 39° 51' 41.58" S 145° 22' 30.87" E Cretaceous – Palaeocene succession interpreted as shelf, marginal lacustrine – alluvial environments.
Summary of study objectives	
Log Depth Intervals	Objectives
2700 – 3400 m	Processing of FMI images to provide speed corrected false colour images. QC of images to determine the quantity of information that is interpretable.
2700 – 3400 m	Summary structural overview using automatic dip calculations, supplemented by manual dip-picking.
2700 – 3400 m	Overview sedimentological interpretation of features evident within FMI images with the aim of focusing upon variations in palaeocurrent transport directions. This required the manual characterisation of dip features and their interpretation over these intervals.
2730 – 2745 m 2820 – 2920 m 2960 – 3065 m 3090 – 3160 m 3375 – 3390 m	Detailed sedimentological interpretation and lithofacies characterisation.
Data incorporated in study	
2700 – 3400 m	Open hole logs from Platform Express suite. Raw FMI data in DLIS format.
2700 – 3400 m	Cuttings description
2735 – 2743 m	Core 1 (2735.0 – 2742.25 m Driller's depth)

Depth and directional references

Unless otherwise mentioned, all depths in this report reference log depths. Orientation data is referenced using the standard convention of dip/dip azimuth. For example, 3°/313° indicates a dip of 3° (measured from the horizontal) towards 313° (referenced clockwise from north). Borehole orientation data follows a convention of deviation/azimuth of deviation. For example, 2°/300° indicates a 2° deviation from the vertical towards 300° (SW).

PROCESSING AND QUALITY CONTROL

The Formation Micro-Imager (FMI) tool was run by Schlumberger on 22nd November 2004 in the 8½ inch section of Trefoil 1 over the interval 2387 – 3530 m.

The Schlumberger Formation Micro-Imager tool is a pad based micro-resistivity imaging device, with an array of 24 measuring electrodes (buttons) on each of pad and flap, with 192 buttons in total. Flaps are offset vertically from the pads by approximately 6 inches. The electrodes are 0.2 inch in diameter and data is sampled at 0.1 inch vertically and horizontally with a bedding resolution of approximately 1 cm. The data is processed to provide 75% coverage of the borehole wall in an 8.5 inch hole. This data also provides 12 Stratigraphical High Resolution Dipmeter (SHDT) tool curves for standard dipmeter processing.

Processing was carried out over the logged interval using Terrasciences TerraStation Formation Viewer module.

The mud system was sea water/Drispac/Soltex with a resistivity of 0.206 Ωm, a viscosity of 49 S and a density of 9.40 lbm/gal. The fluid losses encountered during drilling were minimal (3.8 cm^3). The borehole reached a maximum temperature of 133°C.

An FMI log quality control plot is shown in Enclosure 1. These plots provide detailed information concerning hole orientation, tool orientation, hole condition and FMI operating parameters.

Borehole conditions

FMI image quality is related to borehole condition, which is good throughout the section in Trefoil 1 with clear geological detail visible and only very minor image artefacts. Borehole deviation is minimal with 0.56°/071° at 2725 m and 0.34°/080° at 3015 m, 0.31°/090° at 3103 m, and 0.39°/069° at 3302 m.

A summary of hole conditions is included in Table 2.

Within the study interval (2700 – 3400 m) the callipers show that the hole is consistently in gauge. There is little difference in the C1 and C2 callipers (typically only 0.25 inch) and the callipers usually overlie. Intervals of ovalisation (up to 1 inch) are not limited to one direction, but present in both calliper directions.

Table 2. Summary of hole conditions through the study interval in Trefoil 1

Normal Hole Size	Interval Depth	Comments
2700 – 3400 m		
8.5	2700 - 2706	Up to 1.5” overgauge
	2706 – 3400*	In gauge

* interval contains up to 0.5” filtercake build-up on permeable sections

Data processing

Speed correction

The accelerometer speed correction utility corrects FMI micro-resistivity data for minor variations in recording velocity induced by tool or cable friction. Extremes in velocity variation may occur when the tool is either stationary or rapidly accelerating as a result of being stuck or the logging being stopped for pipe removal. The most important parameter for the speed correction procedure is the zero-sum window, which prevents cumulative build-up of erroneous shifts within a window. Thus all shifts applied by the speed correction should add up to zero within a certain window length. The length of this window is decided by experimenting and the general roughness of the logging run. In the case of Trefoil 1, a window of 4 ft was chosen. The speed correction shift curve is calculated by double integration of the Z-accelerometer curve with the cable speed representing the window constant. The resulting shift curve is then applied synchronously to all curves in the log.

Image processing

Before generating the false-colour images from the speed corrected data, the individual curves are transferred back to their physical depth referenced positions. The images are produced with two types of resistivity scaling:

- *Static normalised* images have the same relative resistivity scaling over larger intervals and therefore illustrate large-scale resistivity variations related to lithology and phase changes. Dependent on Emex current variability.

- *Dynamic normalised* images were scaled within a 0.5 m sliding window, thereby maximising the expression of more detailed rock fabrics (and noise).

In this study, the dynamic normalised images were used primarily for bedding, lithofacies and structure identification. Image polarity was correctly matched to openhole resistivity logs.

Block depth shifts

No block depth shifts were applied to the Trefoil 1 data.

Dip processing

Two types of dip computation were conducted on the Trefoil 1 dataset.

Computed dip correlations were carried out on the SHDT curve sub-set from the loaded interval (Enclosures 1). These correlations use refined least-squares algorithms with regression coefficients cut-offs for each correlation pair. The interval computation parameters were aimed at correlating bedding features using pad-to-pad (PTP) algorithms with the following parameters:

- 60 cm correlation interval, 50 cm step distance and a 70° search angle (referenced to borehole axis) and the cut-off set at 0.4 for individual curve pairs.

These parameters are referenced as “4X2X70” in Enclosure 1. This computation was repeated using a stacking of three consecutive correlation surfaces. The stacking of dips in this way tends to smooth dip patterns and trends and is a viable method of “quick-look”

identification of structural dip. These parameters are referenced as “4X2X70ST3” in Enclosure 1. Detailed interpretation of dip patterns should not be carried out on results from this processing.

Manual dips were computed directly from the images using the TerraStation Formation Viewer (e.g. Enclosure 2). The major advantage of the manual dip technique is that each feature may then be classified into a geological category and that only the results in which the interpreter has confidence are used for further interpretation. A further advantage of manual dip picking is the ability to measure and orientate discordant surfaces such as fractures and faults, which are unlikely to be correlated by standard interval correlation techniques

SEDIMENTOLOGICAL ANALYSIS

Tectonic tilt determination

Prior to detailed sedimentary analyses, it is first required to evaluate structural dip, so that the sedimentary surfaces identified in FMI images can be restored to their original orientation or "sedimentary dip". Structural dip (or tectonic tilt) is the attitude of formations resulting solely from tectonic movements. Structural dip is best determined from beds that were originally deposited as horizontally stratified deposits. These beds can include mudstones, or parallel stratified laminations within heterolithic successions comprising interbedded sandstone-mudstone laminae. The structural dip interpretation within well Trefoil 1 was an iterative process involving:

- Initial evaluation of automatic computed dips to identify general data trends.
- Manual picking of mudstone bed dips to confirm tectonic tilt throughout the studied succession.

Tectonic tilt evaluated on the basis of dip data through shale intervals is summarised in Table 3. Before undertaking a sedimentological interpretation structural dip was removed from the “manual” data set. The structural dip was removed following identification of intervals of strata (structural zones) of consistent structural dip. The structural dips are summarised in Enclosure 2.

Table 3. Tectonic tilt summary of Trefoil 1.

Structural Zone	Depth Interval	Tectonic Tilt	Comments
2700 – 3400 m			
Zone I	2700 – 2734	1.4°/225°	Bounded by sandstone at base
Zone II	2734 – 2770	2.0°/113°	Bounded by maximum flooding surface
Zone III	2770 – 2826	1.2°/196°	Bounded by sandstone at base
Zone IV	2826 – 2918	2.8°/079°	Interbedded sandstone & mudstone, bounded by unconformity at 2918 m
Zone V	2918 - 3080	1.5°/252°	Bounded by maximum flooding surface
Zone VI	3080 – 3237	4.0°/286°	Bounded by flooding surface
Zone VII	3237 – 3374	4.2°/249°	Bounded by maximum flooding surface
Zone VIII	3374 – 3400	3.1°/032°	Bounded by volcanics

Cumulative dip azimuth plots for mudstone bedding surfaces within the studied interval (2700 – 3400 m) from Trefoil 1 are presented in Figure 1. These plots clearly illustrate the structural subdivisions proposed for this well.

Classification of sedimentary features

Classification of sedimentary surfaces recognised from borehole image logs is a three stage iterative process involving:

- First pass dip picking. This phase of feature identification is carried out in conjunction with examination of wireline logs, and results in a simple 2-fold sub-division of dip features into mudstone and "others".

- Structural dip is removed from the data set using a workstation based stereographic technique to provide sedimentary dips.
- Sedimentary dips are re-classified in the workstation environment. Wireline logs are used to drive lithofacies interpretation. Sedimentary dips within sandstone lithologies are characterised using a hierarchical scheme depending upon their dip and orientation.

The hierarchical scheme applied to Trefoil 1 is illustrated in Figure 2 and Table 4 below, and sedimentary dips for the studied intervals 2730 - 2745 m, 2820 – 2920 m, 2960 – 3065 m, 3090 – 3160 m and 3375 - 3390 m are indicated in Enclosures 7 - 10.

Table 4. Classification of surfaces identified from FMI images.

Dip type	Interpreted dip category	Colour	Description
LB	Lithological boundary	Blue green	Low true dip angle surfaces which define a marked resistivity between overlying and underlying beds. Wireline logs indicate a lithological contrast.
LBe	Erosional lithological boundary	Dark green	Erosive surfaces which define a marked resistivity between overlying and underlying beds. Truncation of bedding fabrics beneath the surface may be evident. Wireline logs indicate a lithological contrast.
LBc	Cemented lithological boundary	Pale blue green	Sharply defined highly resistive or conductive bed. Bounding surfaces may define planar or "nodular" features. Normally associated with change in wireline log response.
ISS	Intra set surface	Yellow	Inclined surfaces typically dipping at a true dip angle greater than 5°. Surfaces may be inclined at angles up to 25°-30° (i.e. close to angle of repose), and occur within distinct groups of similar orientation. Surfaces typically show cm-dm scale spacing in borehole image logs. They are discordant to set (or bed) and coset boundaries.
SB	Set (bed) boundary	Brown	Surfaces within sandstone lithologies which are typically (though not exclusively) inclined at sedimentary dip of < 15°. Set boundaries define a group or "set" of intraset surfaces of similar orientation. The set boundary is distinguished from the intraset surfaces by its different orientation. Set boundaries typically occur at dm - m scale spacing in borehole image logs.
CSB	Coset boundary	Cyan	A surface separating a group of sets of similar orientation. Note: Coset boundaries may also define a single bed or set displaying a significantly different internal fabric to those sets surrounding it. Set boundaries are typically identified at m scale spacing in borehole image logs. Note: Coset boundaries may also define a single bed or set at dm scale which displays a significantly different internal fabric to those sets surrounding it.
ISSf	Flat/horizontal	Purple	Near horizontal intraset surfaces with true dip angle (<5°), characterised by resistivity contrast several cm thick. Sedimentary dip azimuth may be variable due to flat lying nature of these beds, and errors associated with fitting dips to such surfaces. Surfaces typically show cm scale spacing in borehole image logs.
PDf	Poorly defined feature	Dark purple	These surfaces may be any of the above but are very poorly defined in terms of continuity around the borehole.
XSB	Small scale cross beds	Red	Cm-dm scale cross stratification fabric, too small to be characterised in detail.
MUDS	Shale bedding	Green	Confident bedding features with consistent magnitudes.
HETS	Heterolithic bedding	Orange	Confident bedding features with approximately consistent magnitudes.

Lithofacies characterisation

Lithofacies identification was first carried out using FMI images in conjunction with openhole log suites. The FMI interpretations were then calibrated against cuttings.

Lithofacies identified from FMI logs.

The sedimentological interpretation of FMI images and dipmeter data were carried out with the aid of gamma ray, density, neutron porosity and sonic logs. Lithofacies were interpreted on the basis of variations in wireline log response in conjunction with fabrics observed in FMI images (Table 5). During interpretation, cuttings descriptions were also used to help provide a guide to lithology, but were found to have only moderate depth resolution (i.e. matching of cuttings description to log response) due to dispersion of cuttings during circulation of drilling muds. Four broad lithofacies were interpreted as being present, i.e. sandstones, mudstones, finely inter-bedded heterolithic successions and coals. Heterolithic successions comprise centimetre-decimetre scale interbedded sandstone and mudstone beds. Coals formed a minor lithofacies within the study intervals, and are clearly recognisable by their low density, high porosity and high resistivity log response.

Lithofacies types were classified according to a simple scheme using mnemonics based upon interpreted lithology and contained fabric, the latter being determined from borehole image log and associated dip data. Examples of identified lithofacies are summarised below in Table 5.

Table 5. Lithofacies identified from FMI images within the study interval.

Inferred Lithology/Grain Size	Typical Log Response	Image Log Fabrics	Lithofacies Mnemonic
Sandstone	GR <70 API RHOB 2.2 – 2.5 g/cc HTNP 0.12 – 0.20	Laminated	Sl
		Fine scale mottled or "speckled" texture with poorly defined or disrupted lamination fabric	Sm
		Coarse scale mottled texture with poorly defined or disrupted lamination fabric. Mottling comprises resistivity elements several cm in diameter	Scm
Heterolithics	GR 70 – 110 API RHOB 2.5 – 2.65 g/cc HTNP 0.20 – 0.25	Laminated	Hl
		Mottled with disrupted lamination fabric	Hm
Mudstone	GR 110 – 180 API RHOB >2.65 g/cc HTNP 0.25 – 0.35	Laminated	Ml
		Mottled with disrupted lamination fabric	Mm
Coal	GR variable typically <60 API RHOB <2.2 g/cc HNTP >0.35	Mottled	Cm

The hierarchical combinations of different lithofacies mnemonics were used to provide detailed descriptions of lithofacies types. In these descriptions, the enclosure of lithofacies mnemonics in parenthesis was used to denote the minor presence of a lithofacies type, or poor development or preservation of a sedimentary structure, e.g.

- Mm (Ml) mottled mudstones with relict lamination or minor laminated intervals.
- Sm (Sl) mottled sandstone with poorly defined relict lamination.
- Sl (Sm) laminated sandstone with minor fabric loss due to mottling/ disruption of lamination etc.

Figures 3 - 6 illustrate examples of different lithofacies types for the lithologies identified, together with their fabric index.

There is uncertainty in the interpretation of the mottled fabrics lithofacies as this fabric in borehole image logs may arise from a number of different mechanisms. These could include:

- Differential cementation or the presence of nodular cements.
- Artefacts such as scattered drilling debris on the borehole wall.
- Textural variations due to biogenic disruption of sediments (bioturbation or rootlets).
- Textural variations associated with dewatering fabrics in sediments.
- The presence of coarse detritus such as pebbles or clay flakes.

Close examination of FMI images reveals that the rare mottled textures are present at 2 distinct scales:

Speckled image texture, in which scattered mottles and speckles occur at *circa* 1 cm scale, and are associated with diffuse bedding fabric. This "fine" scale mottling occurs within sandstone displaying poorly defined lamination, and vague mottled texture. These intervals are characterised by the presence of coarse detritus (pebble clasts etc.).

Mottled/disrupted lamination fabrics observed within image logs through mudstone and heterolithic lithologies may reflect bioturbation within sediments. However, in the absence of sufficient core calibration, this interpretation should be treated with caution. Similar fabrics could be generated by a variety of phenomena including nodular cementation patchy sand distribution etc.

Calibration of image log fabrics using cuttings descriptions

Calibration of image log fabrics was carried out using:

- Cuttings descriptions through the logged intervals. Cuttings descriptions are summarised on Enclosures 3 - 6.

Image log calibration using cuttings

Generally, cuttings descriptions match well with lithofacies interpretations derived using wireline log response and FMI image fabrics. Cuttings descriptions reveal a succession comprising sandstone and mudstone with rare intervals of coal.

Characterisation of heterolithic successions comprising individual beds beneath the resolution of wireline logs is difficult. However, image logs revealing extreme resistivity

variation within strata containing cm-dm scale bedding fabrics provide some insight as to the presence of these heterogeneous lithologies. Cuttings descriptions through successions interpreted from wireline log and FMI as comprising heterolithic deposits, invariably yield documentation of cuttings of mudstone and sandstone in varying proportions.

FMI derived lithological fabric index

The hierarchical lithofacies nomenclature scheme applied to description of lithofacies from borehole image logs was also used to provide a simple four-fold fabric index as illustrated for sandstones in Table 6 below. This type of fabric index may be useful for comparison of reservoir properties with image log derived lithological properties. Note, if mottled fabrics identified within sandstones are due to bioturbation, this fabric index may also approximate to a four-fold bioturbation index, which may be useful in construction of sedimentary models using data derived from image logs.

Table 6. Simple fabric index (applied to sandstone lithofacies) based upon mnemonics scheme used for FMI interpretation of lithofacies. Note the fabric index may approximate to a bioturbation index within sandstone lithologies free of granular-pebbly detritus.

Lithofacies	Approximate degree of fabric development within sediments.	Fabric Index
Sl	Minimal <10%	1
Sl (Sm)	approximately 25 %	2
Sm (Sl)	approximately 75 %	3
Sm	near total 100 %	4

The implication of the fabric index is that low indices will result in strongly anisotropic reservoir properties (e.g. Kv > Kh). If due to phenomenon, such as bioturbation, creating mottled image fabric and loss of stratification, higher fabric indices may reflect more homogeneous reservoir properties (e.g. decrease in Kv:Kh ratio due to loss of stratification).

Lithofacies associations

The sedimentary deposits in the interval 2700 – 3400 m within Trefoil 1 comprise a heterolithic succession of sandstones and mudstones with minor intervals of coal. The successions can be sub-divided into a number of discrete sub-units based upon log trends and stacking patterns of interpreted lithofacies.

Some sub-units are characterised by alternation between low and high gamma ray intervals and NPHI and RHOB log response that similarly alternate between sandstone and mudstone. Sedimentary dips within these successions are typically very low (< 5°).

Other sub-units are characterised by upward increasing gamma ray log trends, and NPHI and RHOB log response that trends toward mudstone indicate fining upward deposits. Sedimentary dips within these upward fining successions decrease upwards. These deposits possibly represent deposition within channels.

There are rare intervals of upward decreasing gamma ray log trends, and NPHI and RHOB log response which trends towards sandstones indicate stacked successions of upward

coarsening/upward cleaning deposits that represent parasequences. Sedimentary dips within these upward cleaning successions are typically low (< 12°).

The intervals that alternate between sandstone and mudstone are consistent with a model of deposition in a sub-aqueous setting with periodic turbidity current deposition and suspension settling. The fining upward successions, with associated laminated mudstones and coal, are consistent with deposition in a fluvial setting. The upward coarsening parasequences described are consistent with a model of deposition in a marginal lacustrine environment, with upward coarsening profiles forming as a result of shoreface or delta front progradation.

The lithofacies identified are described in detail in the following sections. In the absence of core calibration the following discussions are should be considered speculative.

Observed vertical transitions in lithofacies types identified in borehole images have enabled lithofacies to be grouped into genetically related successions of strata or *lithofacies associations*, which have some environmental significance (Walker 1992a). Six lithofacies associations were identified within the studied data set, and their distribution within the studied intervals is illustrated in Enclosures 7 - 10. The lithofacies associations identified are summarised below.

Lithofacies Association I

Lithofacies Association I is argillaceous, mainly comprising mudstone lithologies (Ml and Mm), with minor interbedded heterolithic lithologies. The mudstones occur either as thick deposits associated with the overall upward cleaning (and coarsening) gamma ray log trend (e.g. Enclosure 11) and commonly display a laminated to slightly mottled fabric, which decreases in intensity upward through the succession, or as thin intervals, displaying a laminated fabric, associated with laminated sandstones or upward fining intervals.

Generally, Lithofacies Association I forms relatively thick deposits up to several tens of metres thick, and is characterised by blocky to serrate, overall high gamma-ray log response (>110 API), reflecting the presence of a predominantly argillaceous succession of lithofacies types. Gamma ray log response within mudstones typically decreases slightly upward, forming part of an overall upward decreasing trend. Lithofacies Association I typically pass upward into heterolithic lithofacies of Lithofacies Association II or abruptly into laminated sandstone lithofacies of Lithofacies Association V.

The mudstones of Lithofacies Association I display low sedimentary dip (typically <10°), except where associated with compaction features, with wide ranging dip azimuths (covering 360° spread) indicative of their original deposition as parallel stratified sediments upon a flat lying substrate.

Sedimentation within Lithofacies Association I was probably dominated by suspension fallout of argillaceous material, resulting in the accumulation of laminated mudstone lithofacies (Ml, etc.).

Lithofacies Association II

Lithofacies Association II comprises heterolithic lithologies. Heterolithic sediments consist of centimetre to decimetre scale interbedded sandstones and mudstones, and often display a mottled image fabric. Within the studied intervals, heterolithic deposits may form successions in excess of 2-4 m thick. Heterolithic deposits occur towards the base of

these facies successions which display overall upward cleaning (and coarsening) gamma ray log trends within the grossly fining upward successions.

Sedimentary dips within heterolithic deposits are typically characterised by low angle fabrics (inclined typically <10° sedimentary dip). Removal of structural dip reveals these bedding fabrics to be characterised wide ranging (up to 360° spread) dip azimuths, indicative of their original deposition as approximately horizontally stratified sediments.

The heterolithic nature of these deposits suggests deposition via both tractional and suspension processes. In a shallow lacustrine setting, this style of deposition may have occurred at or around fair weather wave base in lower-shoreface setting. When it is interbedded with Lithofacies Association IV, this implies a fluvial setting.

Lithofacies Association III

Lithofacies Association III mainly comprises sandstone lithologies, with predominantly a well laminated fabric. Lithofacies Association III is characterised by low angle sedimentary dips (typically approximately 10°), and forms successions up to 5 m thick within the studied sections. The sandstones typically rest gradationally upon heterolithic deposits of Lithofacies Association II, in the upper parts of upward coarsening successions. The sandstones of Lithofacies Association III are distinguished from those of Lithofacies Association IV and V, discussed below, by lower sedimentary dips and stacking patterns. The low angle sedimentary dips (typically <10° rarely up to 15°) that are characteristic of this lithofacies association, often display dm to m scale cosets, which may display a relatively tight cluster of unimodal dip azimuths. Flat lying intraset surfaces are also common within this lithofacies association.

The low angle stratification within these sediments is indicative of deposition by traction processes. The occurrence of these sediments within the upper parts of interpreted upward coarsening lithofacies successions, and the often variable orientations of cosets comprising low angle internal stratification that is common within successions, may be consistent with deposition in a shallow lacustrine environment. In these settings, both unidirectional and oscillatory currents (together forming combined flows) during storms produce a variety of 2- and 3-dimensional bedforms. Sedimentary fabrics characterised by sets of low angle stratification of variable orientation may indicate deposition as low amplitude, perhaps strongly 3-dimensional mounded bedforms. In a shallow lacustrine setting, this style of deposition may have occurred above fair weather wave base in shoreface setting. Successions where low angle surfaces display a more unimodal distribution of azimuths may indicate the presence of a more significant palaeoslope or sediment transport and deposition under the influence of more unidirectional current systems.

Lithofacies Association IV

This FMI derived lithofacies is sand dominated, mainly comprising, Sl, Sm, Scm, Sm(Sl) and Sl(Sm), with minor heterolithic and mudstone lithofacies. Lithofacies Association IV occurs in successions up to 10 m thick within the studied intervals. Few conclusions can be drawn concerning the spatial distribution of different lithologies within these deposits.

The coset boundaries occur at dm to m scale and dip data sets, in places, for Lithofacies Association IV indicate an azimuthal spread of up to 240°, however there is a low azimuthal dispersion within cosets. Some of the coset boundaries within this lithofacies association have similar orientations to the XBS indicating downcurrent progradation,

whereas other intervals have a high angle between the coset boundaries and the XBS implying lateral accretion. Other intervals, comprising ISSf only, have variable orientations implying deposition as flat lying sediments.

The cross stratified sediments of Lithofacies Association IV may represent the deposits of channels (fluvial or distributary) within a floodplain setting, whereas intervals dominated by Sl and the thin cross stratified sets indicates unconfined flows, possibly crevasse splays. Evidence of primary stratification within these deposits testifies to the development and migration of bedforms, with the cross-bedding indicating dunes and sand waves. Mottled FMI lithofacies Scm reflects the presence of coarse grained pebbly sandstones and mudstone rip up clasts. Finer scale mottling and disrupted lamination/relict internal stratification fabrics within lithofacies Sm may indicate de-stratification a result of sediment de-watering. De-watering may have arisen as a result of pore-pressure adjustments during rapid deposition and burial of sediments, or as a result of a rapid rise/ fall in fluvial stage. Alternatively, the mottling could result from biogenic activity (rootlets).

Palaeotransport implications for this lithofacies association are discussed in detail in the following sections.

Lithofacies Association V

Lithofacies Association V comprises Sl, Sl(Sm), minor Sm(Sl) and rare intervals of heterolithic and mudstone lithofacies. Lithofacies Association V is characterised by low angle sedimentary dips (typically <10°), and the thickness of the successions increases upwards from 2 – 3 m at the base of the studied interval (3160 m), to up to 10 m at the top (2960 m). The sandstones typically have sharp bases and tops and are interbedded with deposits of Lithofacies Association I, and rarely Lithofacies Association II.

The low angle stratification within these sediments is indicative of deposition by traction processes. The occurrence of these sediments interbedded with Lithofacies Association I and II, and the often variable orientations of cosets comprising low angle internal stratification, may be consistent with deposition from turbidity currents that lack a basal lag. In this setting, unidirectional currents are dominant and the lack of identifiable cross bedding may indicate Bouma sequence A (structureless) and B (parallel laminated) or massive, channelised deposits (Walker, 1992b). Successions where low angle surfaces display a preferred unimodal distribution of azimuths may indicate the presence of a more significant palaeoslope or sediment transport and deposition.

Lithofacies Association VI

Coals form a very minor lithology within the studied section, and are only present in the interval between 2878 – 2896 m. The coal is characterised by high resistivity, low density and high porosity. In images they either display little internal structure, other than rare flat lying internal “bedding” surfaces or have a mottled texture reflecting a lack of internal structure.

Coals occur within mudstone-heterolithic successions in association with thick sandstone intervals.

Summary

The integrated analyses of wireline log signature and FMI fabric allows identification of a variety of different lithofacies types. Calibration with cuttings descriptions has permitted limited lithofacies interpretation from FMI logs. However, in absence of core calibration the environmental interpretations outlined in the following section should be treated with caution as it is only speculative.

Summary of environmental interpretations

A brief summary of the sedimentary successions analysed in detail and their environmental interpretation is provided in the following sections. Detailed discussions of palaeotransport observations are included in the Bedform Orientation and Sediment Dispersal section of this report.

Interval 3375 – 3390 m

Wireline logs and FMI interpretations through this interval indicate that it can be subdivided into two intervals; a lower fining upward interval and an upper aggradational interval. The succession is sandstone at the base that passes upwards into mudstone. Details are summarised below in Table 7.

Table 7. Summary of deposits in the interval 3375 – 3390 m

Interval 3375 – 3390 m			
Depth (m)	**Lithofacies Association**	**Brief Description**	**Interpretation**
3375 - 3384	I	Laminated and massive mudstone	Overbank
3384 – 3390	IV	Sharp based sandstone with Sm, Sl(Sm) and Sl. Laminations increase toward top	Fining upward succession represents channel deposits

Interval 3090 – 3160 m

This interval comprises interbedded sandstones, with sharp bases and tops, and mudstones. Heterolithic intervals are associated with the sandstones but only comprise a minor proportion of the lithofacies present. Details are summarised in Table 8.

Table 8. Summary of deposits in the interval 3090 – 3160 m

Interval 3090 – 3160 m			
Depth (m)	**Lithofacies Association**	**Brief Description**	**Interpretation**
3090 - 3098	I, V	Interval of interbedded mudstone and sandstone	Suspension settling with turbidity current deposits
3098 - 3107	V, II	Laminated sandstone with heterolithic interval at top	Stacked turbidity current deposits with thin heterolithic intervals
3107 - 3121	I, II, V	Interbedded sandstone, mudstone and heterolithics	Suspension settling with thin turbidity current deposits
3121 - 3123	V	Laminated sandstone	Turbidity current deposits
3123 - 3126	I	Laminated mudstone	Suspension settling
3126 – 3131	V, I	Sandstone with thin mudstone interbeds	Stacked turbidity current deposits with thin intervals of suspension settling
3131 - 3141	I, V	Mudstone with sandstone interbeds	Suspension settling with thin turbidity current deposits
3141 – 3151	V, rare II	Sandstone with thin heterolithic intervals	Stacked turbidity current deposits with limited suspension settling
3151 - 3160	I, II, V	Interbedded sandstone, heterolithics and mudstone	Suspension settling with turbidity current deposits

Interval 2960 – 3065 m

This interval is similar to the previous interval however; the beds are not as finely interbedded. Details are summarised in Table 9.

Table 9. Summary of deposits in the interval 2960 – 3065 m

Interval 2960 – 3065 m			
Depth (m)	**Lithofacies Association**	**Brief Description**	**Interpretation**
2960 – 2967	I, V	Mudstone with sandstone interbeds	Suspension settling with thin turbidity current deposits
2967 – 2972	V, rare I	Sandstone with thin interbedded mudstone	Stacked turbidity current deposits with rare interbedded suspension settling intervals
2972 – 2977	I, V	Mudstone with thin interbedded sandstone	Suspension settling with rare turbidity current deposits
2977 – 3002	V, rare I	Sandstone with thin interbedded mudstone	Stacked turbidity current deposits with thin suspension settling dominated intervals
3002 – 3047	I, V, rare II	Interbedded mudstone and sandstone with thin heterolithic intervals	Thick bedded suspension settling deposits and turbidity current deposits
3047 - 3065	I, II, V	Mudstone with thin intervals of sandstone and heterolithics	Suspension settling with thin turbidity current deposits

Interval 2820 – 2920 m

Wireline logs and FMI interpretations through this interval suggest that it comprises a succession of interbedded mudstone and sandstone with heterolithic intervals are rare coal. Details are summarised in Table 10.

Table 10. Summary of deposits in the interval 2820 – 2920 m

Interval 2820 – 2920 m			
Depth (m)	**Lithofacies Association**	**Brief Description**	**Interpretation**
2820 - 2844	I, II, III	Interbedded heterolithic, mudstone and sandstone intervals	Overbank or low energy marginal lacustrine
2844 - 2856	IV, rare II	Sandstone with rare interbedded heterolithic intervals	Stacked channels or turbidity current deposits, cleaning upward trend may reflect reworking at top
2856 - 2859	I	Laminated mudstone	Overbank or low energy lacustrine
2859 - 2875	IV, II, I	Sandstone with interbedded heterolithic and mudstone intervals	Overbank with crevasse splay deposits, or turbidity current deposits with suspension settling.
2875 - 2895	I, II, rare IV	Interbedded laminated and massive mudstone with sandstone, heterolithic and coal intervals	Overbank/floodplain with splay deposits
2895 – 2903	IV, I	Sandstone with interbedded mudstone	Stacked proximal splay deposits with overbank
2903 – 2909	I, II	Laminated and massive mudstone at base overlain by heterolithic interval	Overbank
2909 - 2918	IV	Laminated to slightly mottled sandstone	Stacked fluvial channels overlying unconformity
2918 - 2920	I	Massive to weakly laminated mudstone	Predominantly suspension settling deposits

Interval 2730 – 2745 m

Wireline logs, core, and FMI interpretations through this interval indicates that it comprises a heterolithic succession of strata, with lithologies comprising mudstones, heterolithics and sandstones within a upward cleaning (coarsening) trend. The succession is dominated by sandstone. Details of interpretations are summarised in Table 11.

Table 11. Summary of deposits in the interval 2730 – 2745 m

Interval 2730 –2745 m			
Depth (m)	**Lithofacies Associations**	**Brief Description**	**Interpretation**
2730 - 2733	I	Laminated mudstone	Offshore lacustrine
2733 - 2743	I -> II -> III	Upward cleaning (coarsening) succession comprising massive to laminated mudstones, heterolithics and laminated sandstones	Upward coarsening profile and core indicates a progradational shoreface environment.
2743 - 2745	I	Laminated to massive mudstone	Offshore lacustrine

BEDFORM ORIENTATION AND SEDIMENT DISPERSAL

Following sub-division of the succession into the six lithofacies associations described above, detailed analysis of the orientation of different bedforms within these successions was undertaken in order to evaluate sediment dispersal, and orientation of the depositional system. Sedimentary dips for the different bedding categories identified are summarised in Enclosures 7 - 10. Cumulative dip azimuth plots for the interval 2700 – 3400 m are shown in Figures 7 – 10.

Lithofacies Associations I, II & III

Sedimentary dips within mudstone and heterolithic lithologies (interpreted as comprising cm-dm scale interbedded sandstone and mudstone laminae) from Lithofacies Associations I and II typically display 360º azimuthal spread, indicative of the original deposition of these lithologies as "flat lying" effectively parallel stratified sediments. However, in some intervals, e.g. where they occur as part of a well developed overall upward cleaning succession comprising Lithofacies Associations I to III, heterolithic lithologies display a preferred orientation, possibly reflecting palaeoslope. These sediments are mainly interpreted to have been deposited in fluvial to lacustrine settings, in shelf-shoreface environments, or overbank environments.

Sedimentary dips within sandstones of Lithofacies Association III are also typically highly variable, and indicative of original deposition as "flat lying" sediments. This may have occurred within shallow shoreface settings. However, intraset surfaces (XBS) and flat lying intraset surfaces (ISSf) do show a weak bimodal orientation with a dominance of surfaces in a northerly direction with only a minor component oriented at 180° to the main direction. This lithofacies association is interpreted to represent a shoreface environment. The main flow direction may represent the original palaeoslope with only minor onshore migration of fair weather wave formed structures.

Lithofacies Association IV

The low gamma ray log response typical of Lithofacies Association IV indicates that these successions contain a significant proportion of clean, potentially high reservoir quality sandstones. This lithofacies association within Trefoil 1 is interpreted as fluvial channels and associated splay deposits on the basis of the dominance of low angle lamination and the spread of palaeocurrent data (240°).

The presence of low angle laminations and thin sets of cross bedding indicates that the channels were shallow, as the thickness of the bedforms is proportional to the channel depth (Bridge and Tye, 2000). Intraset surfaces (XBS) show a 240° azimuthal spread with a predominant northwest direction whereas the flat lying intraset surfaces (ISSf) show a 360° azimuthal spread, indicative of deposition as original "flat lying" sediments.

The orientation of bedding surfaces within these intervals are summarised in Tables 12 – 13 below.

Table 12. Bedding orientations of Lithofacies Association IV within the interval 3375 – 3400 m

Interval 3375 – 3400 m (Log depth)				
Depth (m)	Orientation of ISSf's	Orientation of XBS's	Orientation of CSB's	Comments
3384 – 3390	Variable	E - SE	ENE	Variable orientation may reflect original flat lying deposition. CSB (ENE) and XSB (E - SE) orientations imply lateral migration of bar forms.

Table 13. Bedding orientations of Lithofacies Association IV within the interval 2820 – 2920 m

Interval 2820 – 2920 m (Log depth)				
Depth (m)	Orientation of ISSf's	Orientation of XBS's	Orientation of CSB's	Comments
2820 – 2844	Variable	NW		Variable orientation of low angle bedforms indicates original flat bedding. The presence of thin intervals containing XBS indicates possible offshore flow.
2844 - 2856	Variable	N	NE - SW	XBS oriented at high angle to CSB possibly indicating lateral migration within channel
2856 - 2908	Variable	SW, NW, E	NE	Variable orientation may reflect original flat lying deposition in overbank environment. XBS within sandstone intervals have similar orientations reflecting possible crevasse splay deposition within floodplain environment.
2908 - 2918	Variable	NE, NW, WSW	Variable	XSB at high and low angle to CSB and SB may reflect downstream and lateral migration of barforms within (braided?) channels.

Lithofacies Association V

Sedimentary dips within sandstones of Lithofacies Association V display 360º azimuthal spread, indicative of the original deposition of these lithologies as "flat lying" effectively parallel stratified sediments. There is an overall easterly orientation that may reflect the original palaeoslope. These sediments are mainly interpreted to have been deposited in a shelf environment from turbidity currents, possibly originating from failures on delta fronts.

The orientation of bedding surfaces within these intervals are summarised in Tables 14 – 15 below.

Table 14. Bedding orientation of Lithofacies Association V within the interval 3090 – 3160 m

Interval 3090 – 3160 m (Log depth)				
Depth (m)	Orientation of ISSf's	Orientation of XBS's	Orientation of CSB's	Comments
3090 - 3098	Variable			Variable orientation may reflect original flat lying deposition in distal fan environment. Lithofacies Associations I & II dominate.
3098 - 3112	Variable	ENE	E - ENE	XBS at low angle to CSB indicates downcurrent progradation (palaeoslope?)
3112 - 3138	Variable E			Thin intervals of Lithofacies Association V interbedded with Lithofacies Associations I & II. Predominant easterly direction in ISSf may reflect original palaeoslope.
3138 – 3151	E Variable			Amalgamated Lithofacies Association V with thin intervals of Lithofacies Associations I & II occurring toward the top of the interval. Predominant easterly direction may reflect palaeoslope.
3151 – 3160	E – N			Interbedded Lithofacies Associations I, II & V. Palaeoslope possibly reflected in predominant easterly direction of ISSf.

Table 15. Bedding orientation of Lithofacies Association V within the interval 2060 – 3065 m.

Interval 2060 – 3065 m (Log depth)				
Depth (m)	Orientation of ISSf's	Orientation of XBS's	Orientation of CSB's	Comments
2060 - 2084	Variable E			Interbedded Lithofacies Associations I, II & V. Palaeoslope possibly reflected in predominant easterly direction of ISSf.
2084 - 3002	Variable E			Stacked Lithofacies Association V interbedded with thin intervals of Lithofacies Associations I & II. Predominant easterly direction may reflect palaeoslope.
3002 - 3065	Variable E			Interbedded Lithofacies Associations I, II & V. Palaeoslope possibly reflected in predominant easterly direction of ISSf.

Lithofacies Association VI

These data sets are too small and biased for orientation analyses.

CONCLUSIONS

1. The studied successions dip at low angles in variable orientations. A number of structural zones have been defined, these are summarised as follows:

Interval 2700 – 3400 m

Zone I	2700 – 2734	1.4°/225°	Bounded by sandstone at base
Zone II	2734 – 2770	2.0°/113°	Bounded by maximum flooding surface
Zone III	2770 – 2826	1.2°/196°	Bounded by sandstone at base
Zone IV	2826 – 2918	2.8°/079°	Interbedded sandstone & mudstone, bounded by unconformity at 2918 m
Zone V	2918 - 3080	1.5°/252°	Bounded by maximum flooding surface
Zone VI	3080 – 3237	4.0°/286°	Bounded by flooding surface
Zone VII	3237 – 3374	4.2°/249°	Bounded by maximum flooding surface
Zone VIII	3374 – 3400	3.1°/032°	Bounded by volcanics

2. The sedimentary succession is highly heterolithic, comprising sandstones, mudstones and heterolithic intervals, composed of dm scissile intercalations of sandstone mudstone, and very rare coal.

3. Six lithofacies associations have been identified, these comprise:

   I. Mudstones that either occur at the base of upward coarsening facies successions (interpreted as either prodeltaic muds, or shelf-shoreface deposits), or interbedded with sandstones that have sharp bases and tops (interpreted as suspension settling in a shelf environment) or interbedded with sandstones and rare coal (interpreted as floodplain deposits).
   II. Heterolithic intercalations of sandstone and mudstone, typically occurring within the lower-mid parts of upward coarsening facies successions (interpreted as shelf-shoreface deposits). When it is interbedded with Lithofacies Association IV, this implies a sub-aerial setting in a floodplain environment. This lithofacies association also occurs with Lithofacies Association V as possible thin bedded turbidite deposits.
   III. Stratified sandstones with mottled image fabric and low angle (typically <5°) internal bedding surfaces, typically occurring towards the top of upward coarsening facies successions (shoreface deposits).
   IV. Successions of thick bedded stratified sandstones and rare pebbly sandstones with dominant internal bedding fabrics inclined at angles <10°, rare intervals of up to 25°. These deposits represent fluvial channels.
   V. Stratified sandstones with sharp bases and tops, interbedded with Lithofacies Association I, and characterised by low angle (typically <5°) internal bedding surfaces represent massive to parallel stratified sandstones deposited from turbidite flows.
   VI. Coals (deposits of swampy coastal plain environments).

4. Palaeotransport analyses of sandstones from Lithofacies Association III reveals them to be characterised by internal stratification fabrics with very wide ranging sedimentary dip azimuth, suggesting they were originally deposited as “flat lying” strata. Few

palaeotransport interpretations can be made for these sandstones. However, in some examples, a dominant sedimentary dip is present, and may represent the original palaeoslope, implying an E - W shoreline orientation.

5. Palaeotransport analyses of sandstones from Lithofacies Association IV reveals them to be characterised by low angle internal stratification fabrics with variable azimuth and cross bedding with a 240° azimuthal spread. The relationship between intra-set lamination and coset boundaries suggest that sediment transport occurred normal to, i.e. bedforms migrated downcurrent, and at a high angle to, i.e. lateral migration, the depositional dip. Interpreted channel drainage directions are variable but have an overall northerly direction.

6. Palaeotransport analysis of sandstones from Lithofacies Association V reveals them to be almost exclusively dominated by low angle internal stratification fabrics that have a variable orientation, but have an overall easterly trend that may reflect the original palaeoslope.

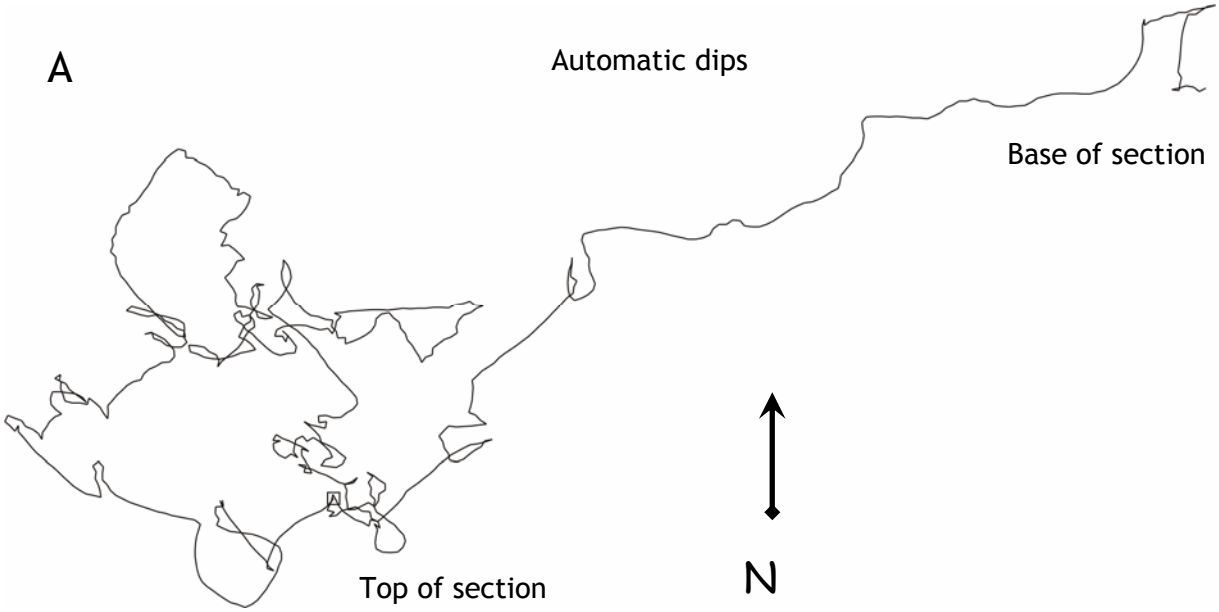
7. In the absence of a detailed core calibration environmental interpretations are highly subjective. However, observed lithofacies stacking patterns do appear to be consistent with an interpretation of deposition of strata within fluvial, marginal lacustrine and shelf settings.

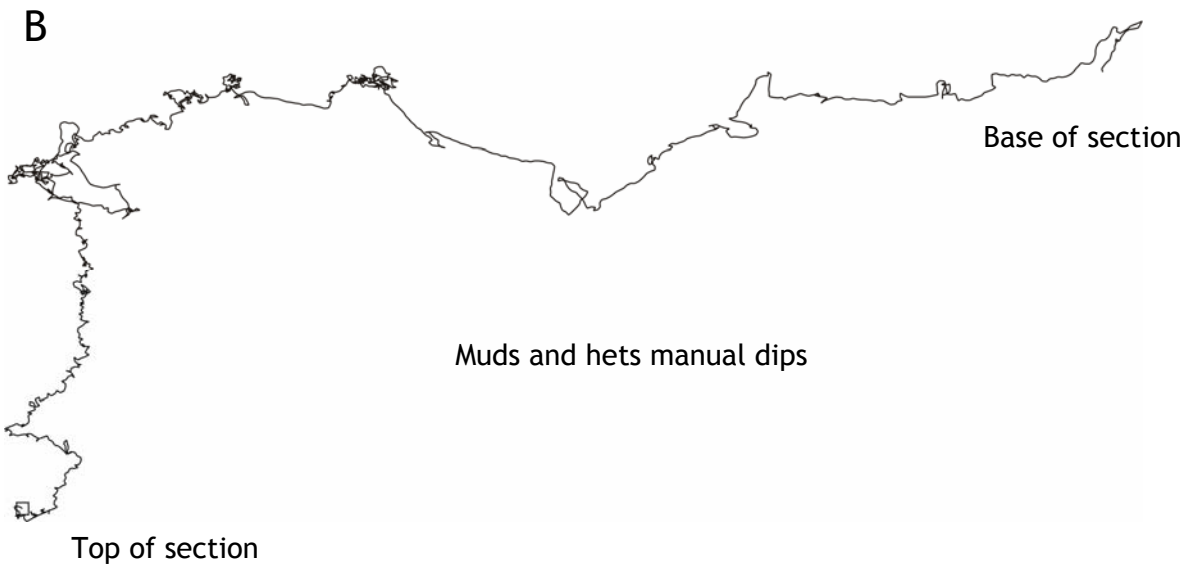
REFERENCES

Bridge, J.S., and Tye, R.S., 2000. Interpreting the dimensions of ancient fluvial bars, channels and channel belts from wireline logs and cores. *American Association of Petroleum Geologists Bulletin*, 84, 1205-1228.

Walker, R.G. 1992a. Facies models. *In:* Walker, R.G. and James, N.P. eds. *Facies Models: Response to Sea Level Change*, Geological Association of Canada, Newfoundland, 1-14.

Walker, R.G., 1992b. Turbidites and submarine fans. *In:* Walker, R.G. and James, N.P. eds. *Facies Models: Response to Sea Level Change*, Geological Association of Canada, Newfoundland, 239-263.


A
Automatic dips
Base of section
Top of section
N


B
Base of section
Muds and hets manual dips
Top of section

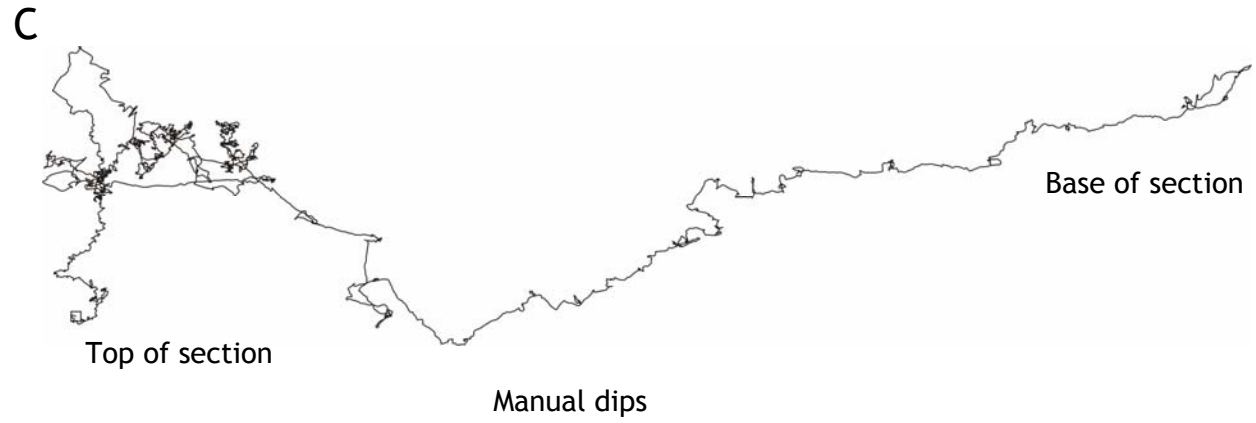


Figure 1. Cumulative automatic (A), muds and hets (B), and manual (C) dip azimuth plots for the studied section (2700 – 3400 m).

Code	Description	Interpreted category
MUD	Confident bedding features, with consistent magnitudes.	Shale Bedding
HETS	Confident bedding surfaces characterised by high resistivity contrasts.	Inter-bedded dm-scale sand and mud. (Heterolithics)
LB	Low true dip angle (typically less than 5°), marked resistivity contrast with overlying/underlying beds	Lithological boundary
LBe	Low true dip angle (typically less than 5°), marked resistivity contrast with overlying/underlying beds and truncation of underlying beds.	Erosional lithological boundary
LBc	Separates a highly resistive zone from overlying and underlying beds. May be a planar layer or non-planar nodular feature.	Cemented lithological boundary
SB	Surface (typically less than 15°) enclosing a bed that may have internal stratification with consistent dip and azimuth.	Set (bed) boundary
CSB	Surface separating groups of beds or a single bed displaying a significantly different character.	Coset boundary
ISS	Steeply dipping true dip angle (15-40°), highly discordant to set (bed) boundaries, and are characterised by resistivity contrast of cm scale with constant dip azimuth trends.	Intra set, cross-bedding surface
ISSF	Near horizontal surfaces with true dip angle (<5°), characterised by resistivity contrast several cm thick. Azimuth trends may be variable due to the low precision associated with determining the azimuth of flat lying beds.	Flat/horizontal intra set surface
FRAC	Generally discordant plane with moderate to steep dip (resistive or conductive).	Fracture
FAULTR	Generally discordant plane with moderate to steep dip, with identifiable displacement (resistive or conductive).	Fault

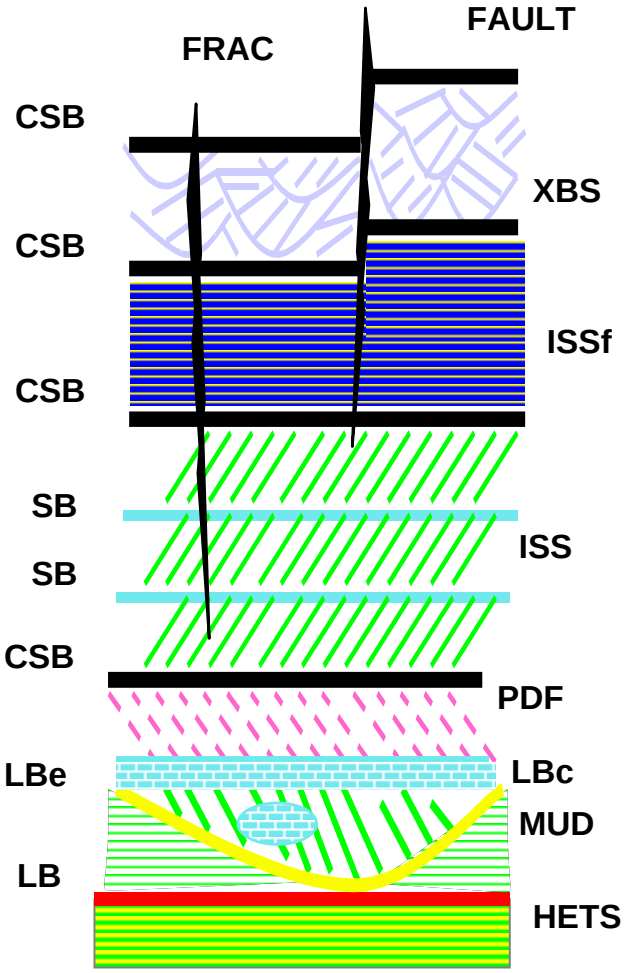


Figure 2. Dip categories used in this study.

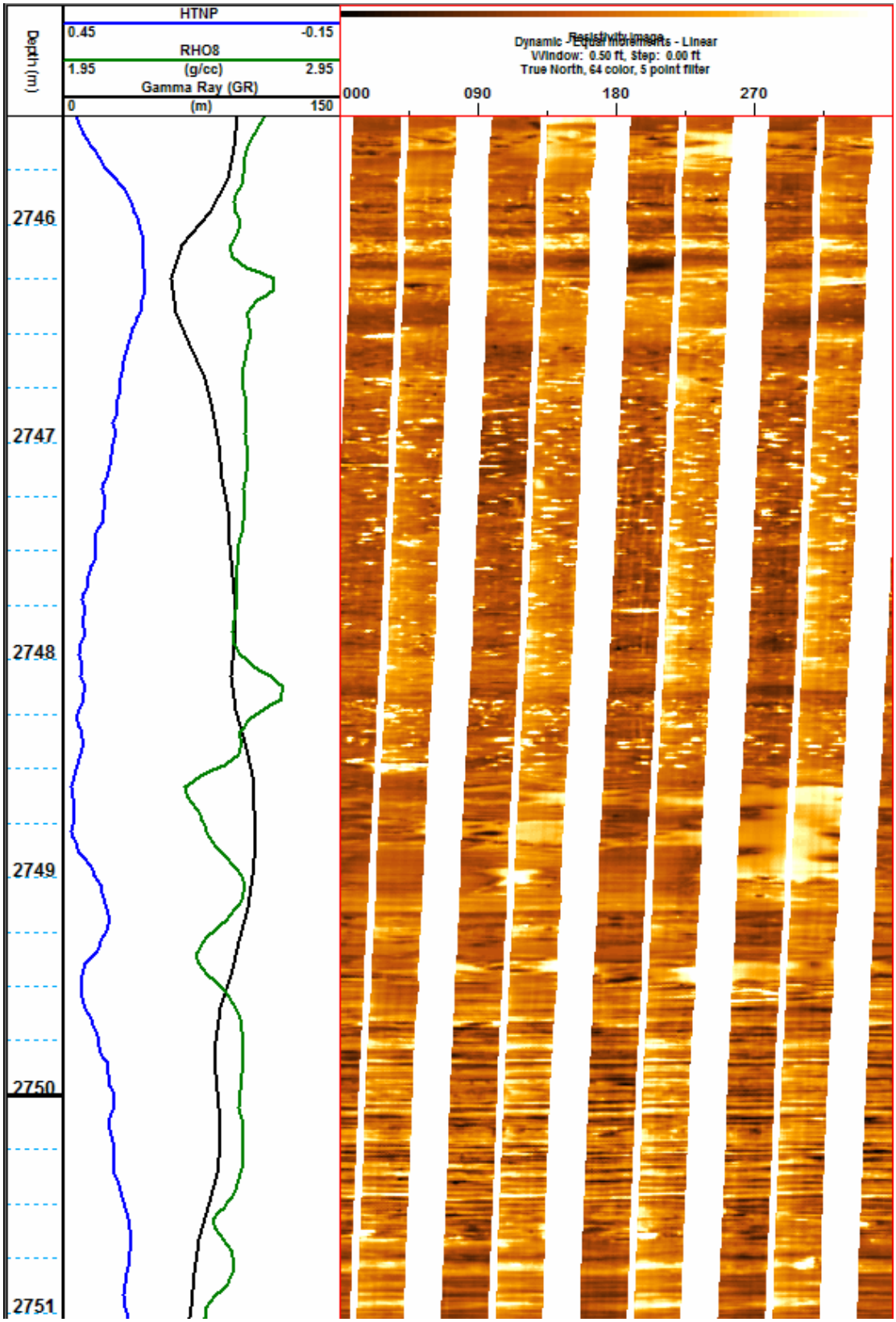


Figure 3. FMI Image through well laminated to massive mudstone (lithofacies Ml & Mm)

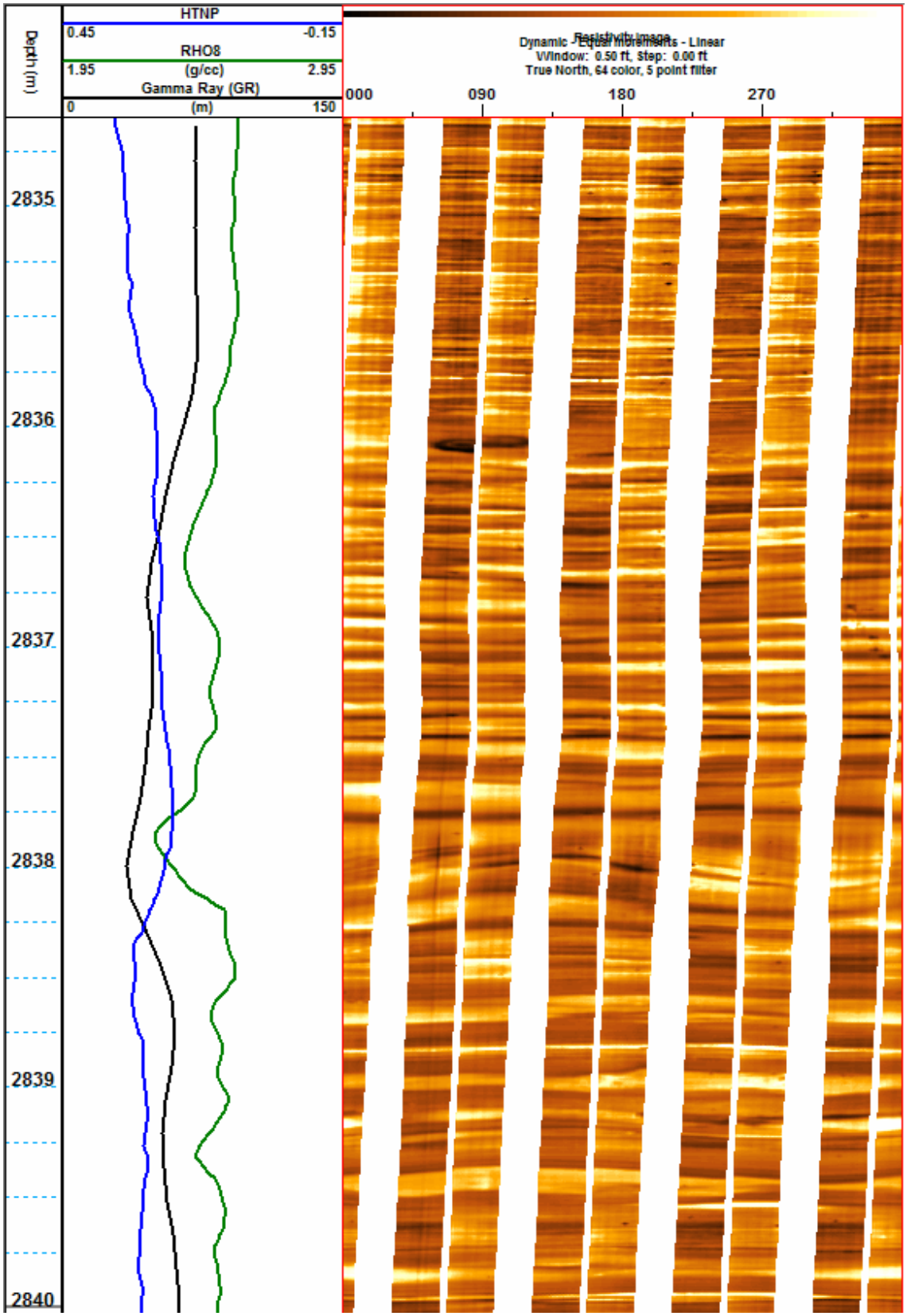


Figure 4. FMI image through dm-scale heterolithic sandstone-mudstone lithofacies with well developed lamination fabric (Hl) becoming less well developed, fabric (Hm), toward the base. Sandstone with well developed lamination fabric (Sl) is also present (2837.75 – 2838.3 m).

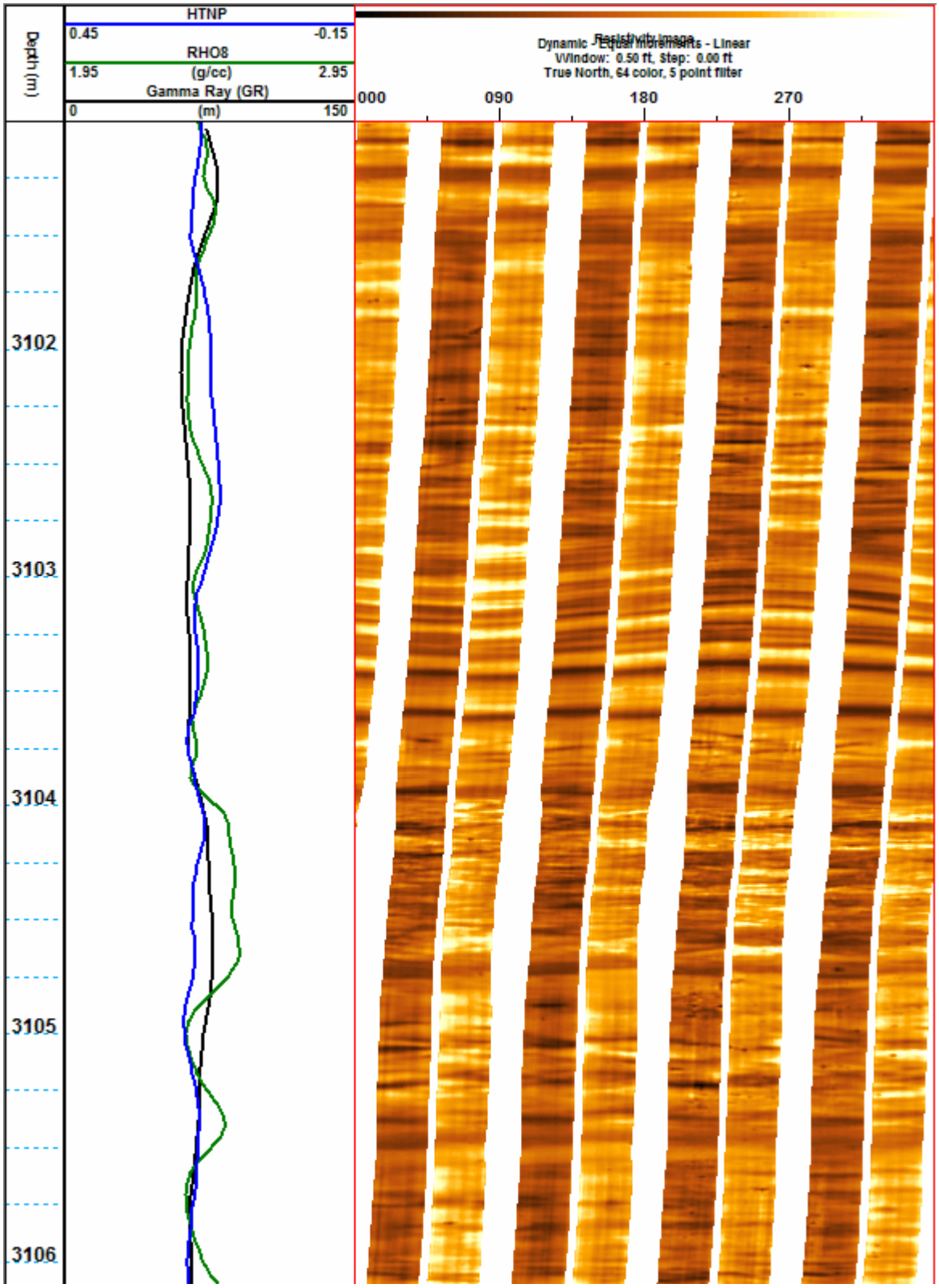


Figure 5. FMI image illustrating well laminated sandstone Sl (3102.25 – 3104 m) with thin mottled sandstone with vague lamination Sm(Sl) (3105.5 – 3106 m) and laminated sandstone with vague mottling Sl(Sm) (3104 – 3105.5 m).

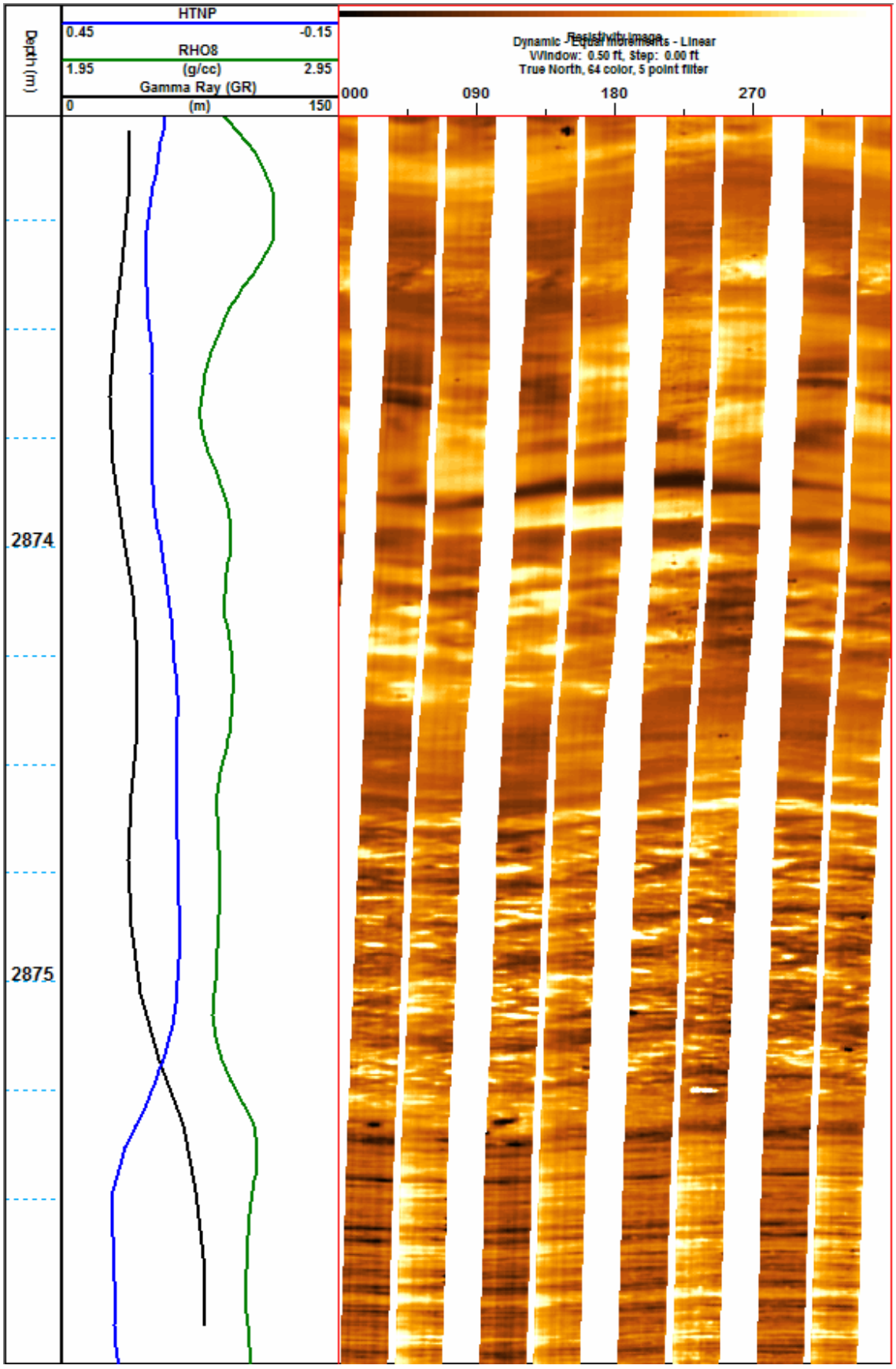


Figure 6. FMI image illustrating sandstone with coarse scale mottled fabric, Scm and mottled sandstone with weak lamination Sm(Sl) overlying laminated mudstone (Ml).

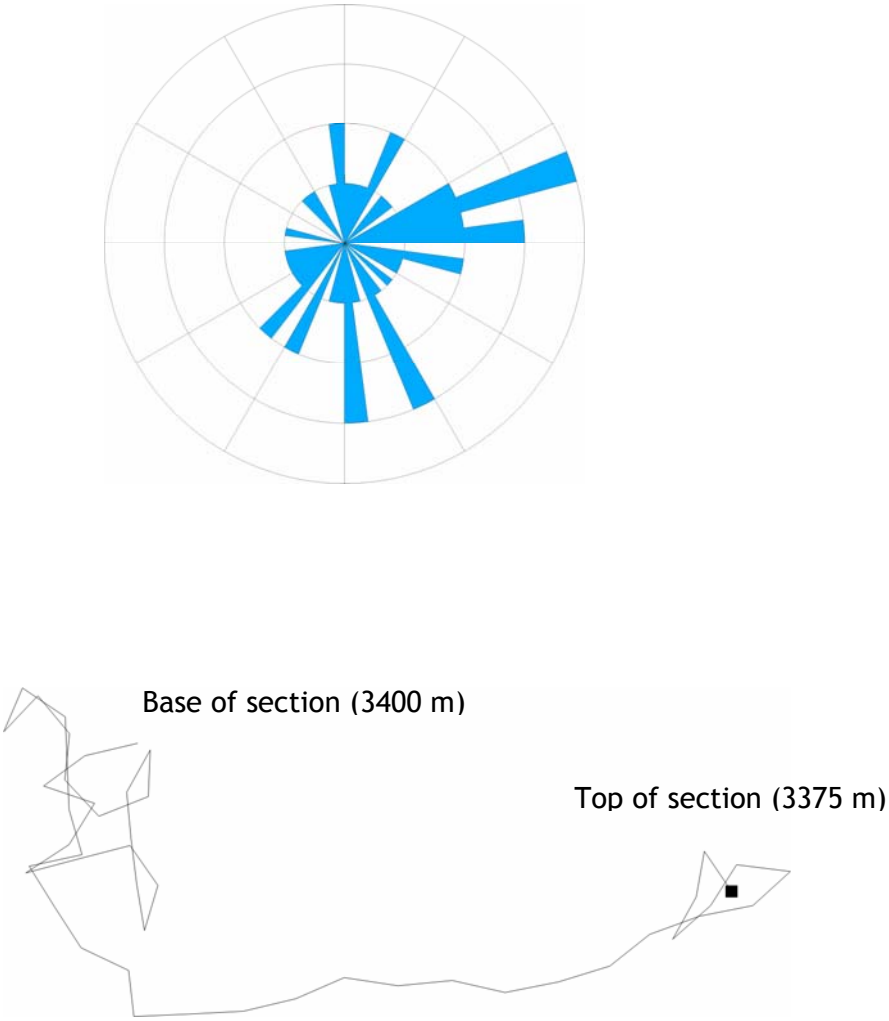


Figure 7. Cumulative dip azimuth plot for the interval 3375 – 3400 m. ISSf and ISS surfaces are shown with structural dip removed. ISSf surfaces are dominant and large changes in azimuth are associated with these nearly flat lying structures.

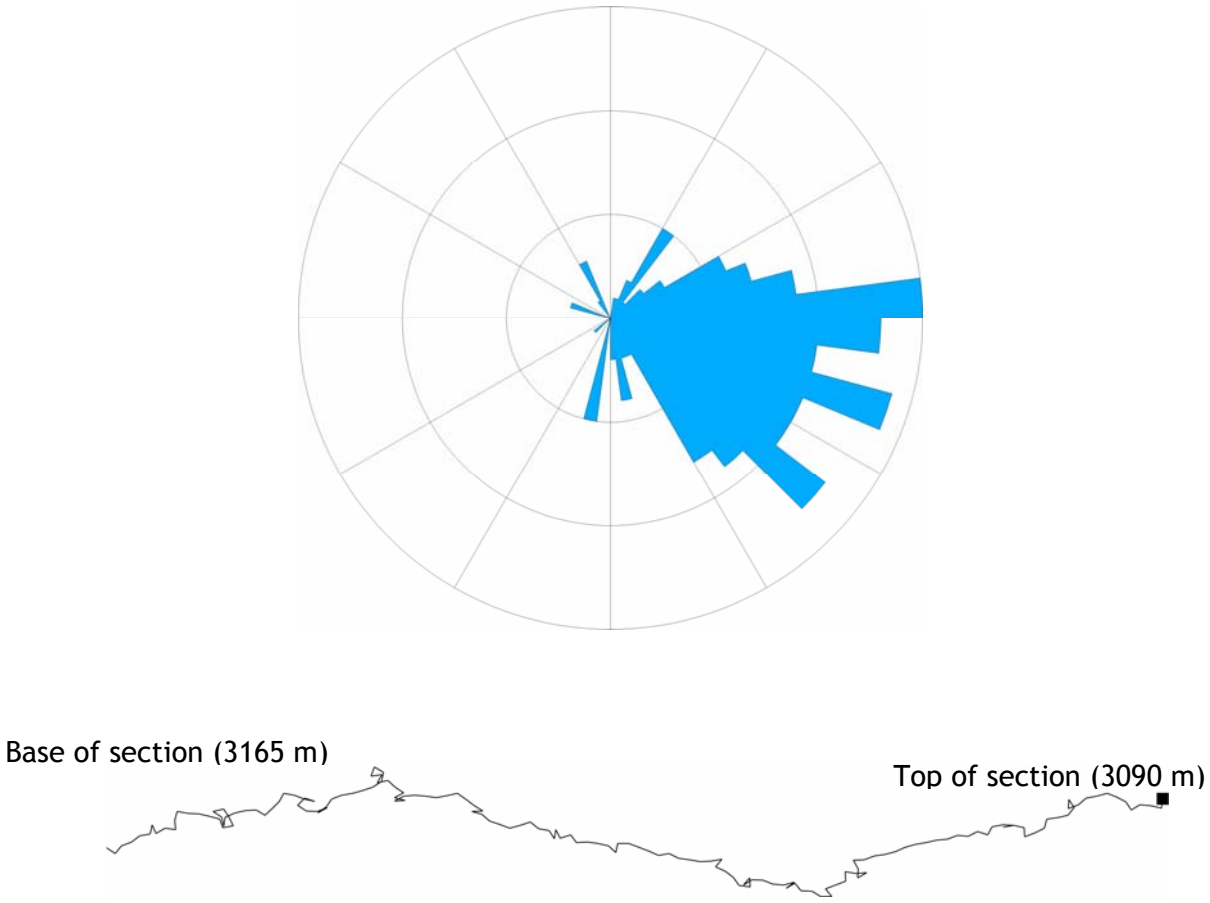


Figure 8. Cumulative dip azimuth plot for the interval 3090 – 3160 m. ISSf and ISS surfaces are shown with structural dip removed. ISSf surfaces are dominant and large changes in azimuth are associated with these nearly flat lying structures.

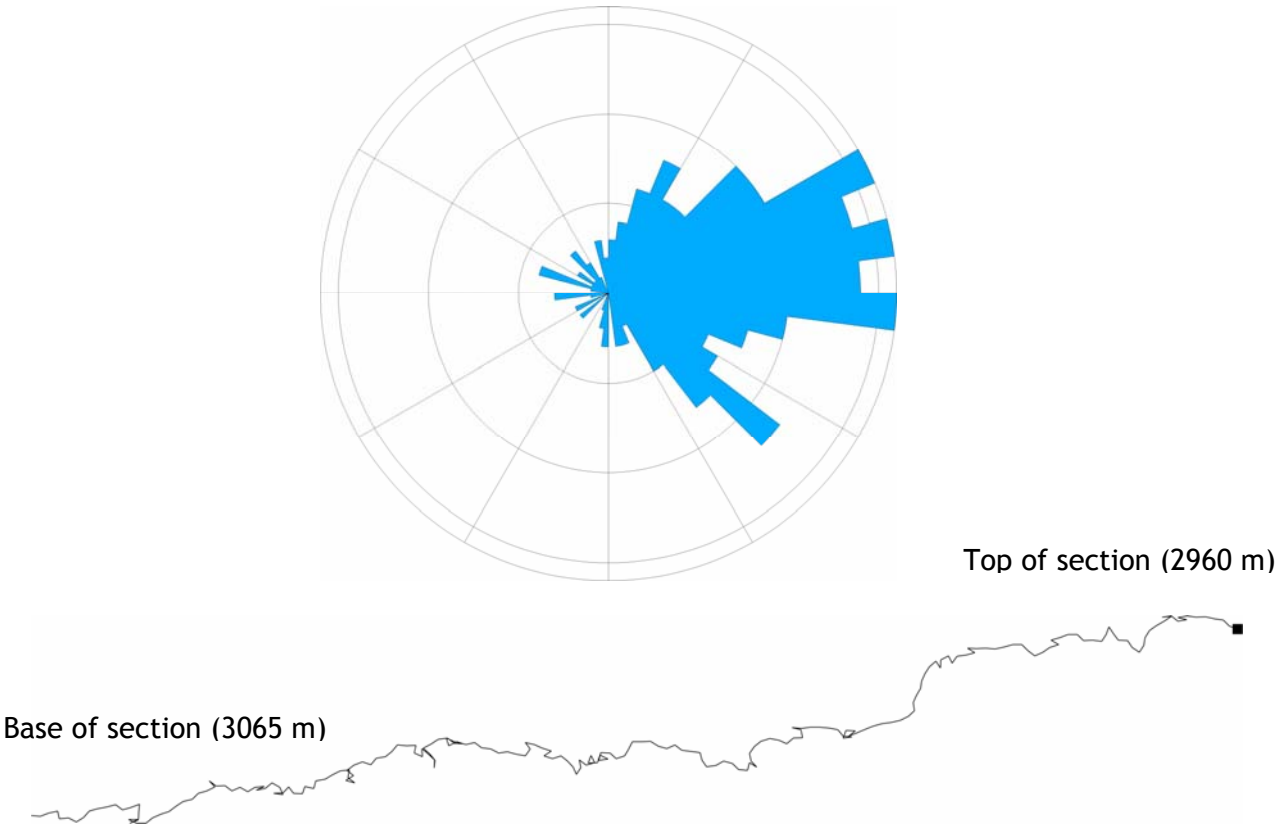


Figure 9. Cumulative dip azimuth plot for the interval 2960 – 3065 m. ISSf and ISS surfaces are shown with structural dip removed. ISSf surfaces are dominant and large changes in azimuth are associated with these nearly flat lying structures.

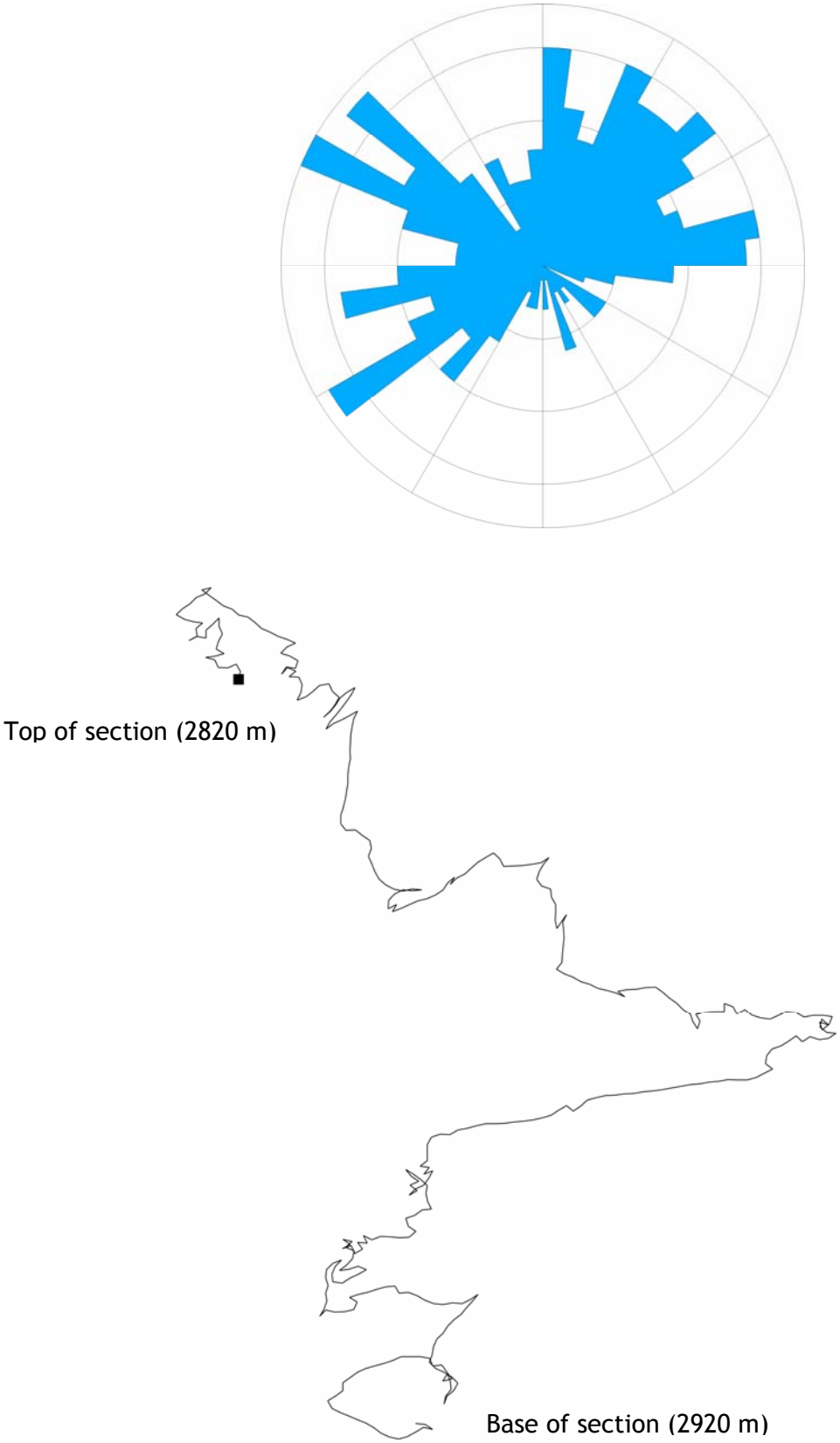


Figure 10. Cumulative dip azimuth plot for the interval 2820 – 2920 m. ISSf and ISS surfaces are shown with structural dip removed. ISSf surfaces are dominant and large changes in azimuth are associated with these nearly flat lying structures.

APPENDIX 11: CASED HOLE DSI (SONIC) PROCESSING REPORT

Schlumberger

Cased Hole
DSI* Sonic Processing
Report

Products:	• MPS: Compressional Slowness • UDP: Shear Slowness
Company:	• Origin Energy Resources Ltd
Well(s):	• Trefoil-1
Interval:	• 2420 to 650m MD (1770m)
Analysis Date:	• September 6th, 2005
Logging Date:	• Nov 24th, 2004
Location:	• Schlumberger Data Services Centre • Perth, Western Australia
Analyst(s):	• Sylvia Tokic
Logging Engineer:	• Josie Robertson

Prepared by:
Sylvia Tokic
Schlumberger Oilfield Australia Pty Ltd
Data & Consulting Services
Level 5, 256 St Georges Terrace
Perth WA 6000
Telephone: +61-8-9420-4800/812
Facsimile: +61-8-9322-3080
mailto:dcs@perth.oilfield.slb.com
stokic@perth.oilfield.slb.com

*Mark of Schlumberger

1 Executive Summary

The DSI* (Dipole Shear Sonic Imager tool with Upper Dipole (UDP), Lower Dipole (LDP) and Monopole (MPS) mode) logs were acquired in vertical exploration well Trefoil-1 (Longitude 145°22'30.87" East and Latitude 39°51' 41.58" South) logged on the 24th of November 2004. Open hole data was processed on the 17th of January, 2005 and cased hole data was processed on the 6th September, 2005 after a request from Origin Energy Resources Ltd. This report discusses the cased hole results.

The data was acquired in both 8.5in open hole section and 9.25in cased hole section, with water-based mud (Seawater/Drispac/Soltex). Measurements were made both in MPS and Dipole modes from TD to 1697m MD and a further MPS downlog was acquired from 280 to 2390m MD. Subsequently, the entire cased hole interval was processed and analysed to obtain compressional and shear slowness within the cased hole section.

Overall, cased hole data was of mostly good coherency which enabled extraction of a non-continuous compressional slowness from the MPS downlog from 2402 to 650m MD. A non-continuous shear slowness was extracted from the UDP uplog from 2401 to 1692m MD.

Schlumberger

TABLE OF CONTENTS

1 Executive Summary 2

2 Processing Result and Evaluation 4

TABLE OF FIGURES

Figure 1: Cased Hole Best DT-3* Results for part of the log 5
Figure 2: Cased Hole MPS Quality Control for part log 6
Figure 3: Move-out determination on a set of monopole array waveforms 10
Figure 4: Slowness time coherence computation principle 11
Figure 5: Slowness-Time Plane monopole example. Figure 6: Coherence peak labelling and slowness dot-logs generation 12
Figure 7: Flexural wave propagation to measure shear velocity 14
Figure 8: Shear wave splitting Figure 9: DSI tool showing X-Dipole (BCR) Mode 16

APPENDICES

Appendix A:
Mnemonics……8

Appendix B:
Processing
Parameters……..……..8

Appendix C:
Theory……11

2 Processing Result and Evaluation

2.1 Cased Hole Upper Dipole (UDP) and Monopole P & S (MPS) Results

Compressional slowness was obtained from the MPS mode processing using both the *Receiver* and *Transmitter Arrays* and used to produce Depth Derived Borehole Compensated (DDBHC) final output. Processing used the latest BestDT-3* technique that is based on STC (Slowness Time Coherence) computation, on GeoQuest's GeoFrame 4.0.3 platform. The final DT compressional (DTCO) is therefore an average of DT output from receiver and transmitter array processing, and used in the computation of the Poisson's ratio and VpVs ratio on the final DSI presentation. **Figure 1** shows a section of the results for cased hole. Using the DDBHC method corrects for any slight eccentralising and unfavourable borehole conditions, such as tool tilt and changes in borehole size.

Figure 2 shows the STC versus depth for the MPS. Note the strong and consistent coherence.

Shear curves were obtained from UDP Processing. Unlike MPS, dipole shear is usually derived using receiver array only. BestDT-3* processing uses sophisticated dispersion correction to give a more accurate true formation shear slowness. This is based on using the entire waveform as opposed to part of a waveform and look up chart, which is used in the field. Refer to **Appendix C** for theory and **Appendix A** for mnemonics description.

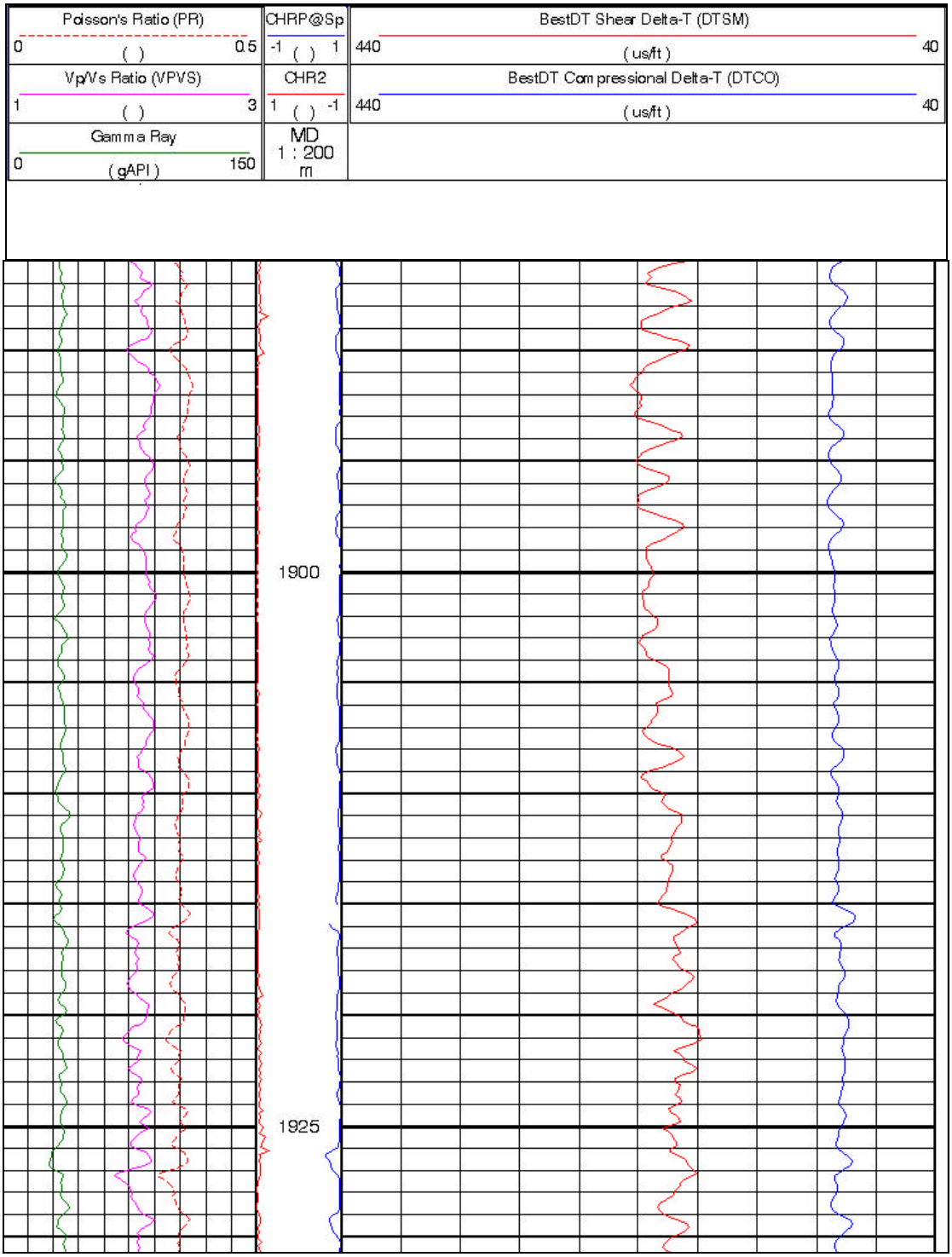


Figure 1: Cased Hole Best DT-3* Results for part of the log

Track 1 shows GR, Poisson's Ratio and VpVS Ratio. See attached print for entire depth section. Depth track contains Label Peak Coherence curves for MPS (blue) and UDP (red), which tend to increase (high uncertainty) across low coherency zones. The last track displays the BestDT-3* results.

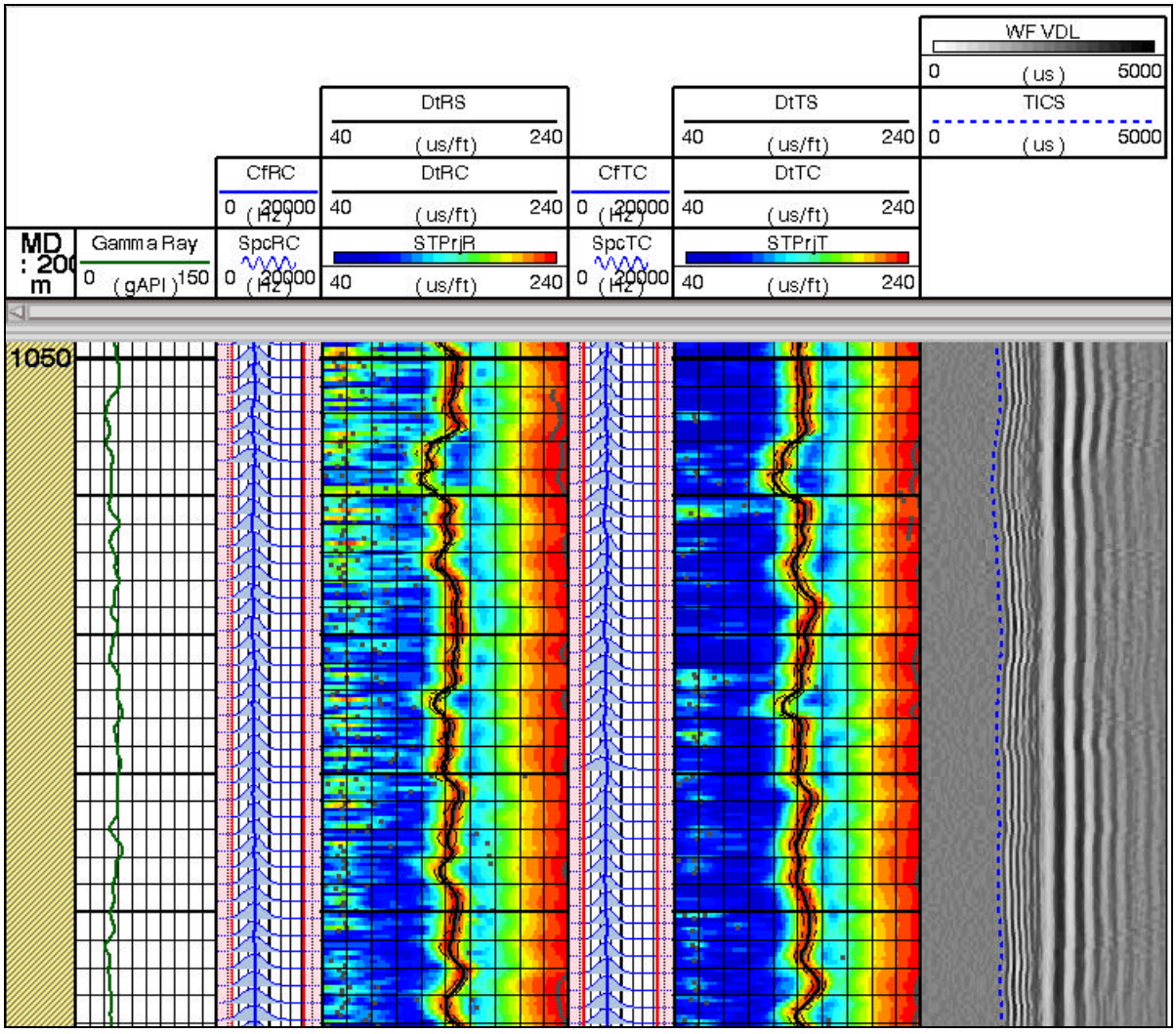


Figure 2: Cased Hole MPS Quality Control for part log

Figure 2, representing the STC quality for cased hole**,** shows that overall, output quality is good, compressional arrivals were shown by strong coherency on both receiver and transmitter array.

Track 1 shows the GR, tracks 2 and 4 show the compressional curve and the frequency window, which the data was processed. Tracks 3 and 5 shows the STC plane in relation to depth. In this example the slowness is very coherent, represented here by a red band. Where the band is not red, the coherency is not as good. This occurs mostly in the shallower sections of the log. The software then selects the most coherent path by using a similar method to 'Tracking and Classification' as discussed in **Appendix C**. Track 6 represents the waveform in variable density log format (VDL). The TICS curve is the compressional transit time. Note that the compressional transit curve matches very well with the first formation arrivals, indicating good quality data whereby the STC semblance processing has detected the correct slowness.

Appendix A: Mnemonics

CfRC	Coherency (Stacked Signal Center Frequency – Receiver Array)
CfTC	Coherency (Stacked Signal Center Frequency – Transmitter Array)
CHRP	Label peak coherence, receiver array – monopole.
CHR2	Label peak coherence, receiver array – upper dipole
CHTP	Label peak coherence, transmitter array – monopole
DDBHC	Depth derived borehole compensated
DT1	Delta-T Shear – Lower Dipole
DT2	Delta-T Shear – Upper Dipole
DT4P	Delta-T Compressional – Monopole P&S
DtRC	Delta-T Compressional – Receiver Array
DtRS	Delta-T Shear – Receiver Array
DtTC	Delta-T Compressional – Transmitter Array
DtTS	Delta-T Shear – Transmitter Array
DTCO	Final BestDT-3* Delta-T Compressional Curve
DTSM	Final BestDT-3* Delta-T Shear Curve
LDP	Lower Dipole Mode
MPS	Monopole P&S Mode
PR	Poisson's Ratio
REC	Receiver
SPcRC	Frequency Spectrum – Receiver Array
SPcTC	Frequency Spectrum – Transmitter Array
STPrjR	STC Slowness Projection – Receiver Array
STPrjT	STC Slowness Projection – Transmitter Array
TICS	Compressional Integrated Transit Time
TISS	Shear Integrated Transit Time
TENS	Tension
UDP	Upper Dipole Mode
VPVS	Ratio of Compressional Velocity to Shear Velocity

Appendix B: Parameters

Table 1: Cased Hole MPS

Parameter	Value	Description
Dtmud	194 us/ft	Mud Slowness
SFTY	Intermediate	Formation Type
HD	8.5 in	Hole diameter
CSIZ	9.625 in	Casing Size
BHS	Cased	Borehole Status
TWI	504 ms	Integrated Time Window
SLL	40	Slowness Lower Limit
SUL	240	Slowness Upper Limit
SST	2	Slowness Step
TLL	504	Time Lower Limit
TUL	4368	Time Upper Limit
TST	168	Time Step
SBW	2730	Search Band Width
SBO	520	Search Band Offset
SWD	20	Slowness Width
TWD	2046	Time Width
SEM	0.35	Semblance Threshold
FLENG	49	Filter Length
FLOW	3000	Filter Band Low
FHIGH	10486	Filter Band High

Table 2: Cased Hole Dipole

Parameter	Value	Description
Dtmud	194 us/ft	Mud Slowness
SFTY	Intermediate	Formation Type
HD	8.5 in	Hole diameter
CSIZ	9.625 in	Casing Size
BHS	Cased	Borehole Status
TWI	1500 ms	Integration Time Window
SLL	80	Slowness Lower Limit
SUL	540	Slowness Upper Limit
SST	4	Slowness Step
TLL	1200	Time Lower Limit
TUL	12800	Time Upper Limit
TST	400	Time Step
SBW	8000	Search Band Width
SBO	1480	Search Band Offset
SWD	60	Slowness Width
TWD	6000	Time Width
SEM	0.35	Semblance Threshold
FLENG	47	Filter Length
FLOW	1000	Filter Band Low
FHIGH	3000	Filter Band High

Appendix C: Theory

Monopole P and S Mode (MPS)

A set of eight monopole sonic waveforms is shown in **Figure 4**. As expected the arrival time of the various arrivals in the waveforms increases with the transmitter-receiver spacing. The slope of a line drawn through the arrival of the same component at each waveform is called the move-out. It represents how much the arrival time is moving out as the distance from the transmitter increases. The moveout can be expressed in μsec/ft and actually represents the slowness of the wave component over the interval covered by the array.

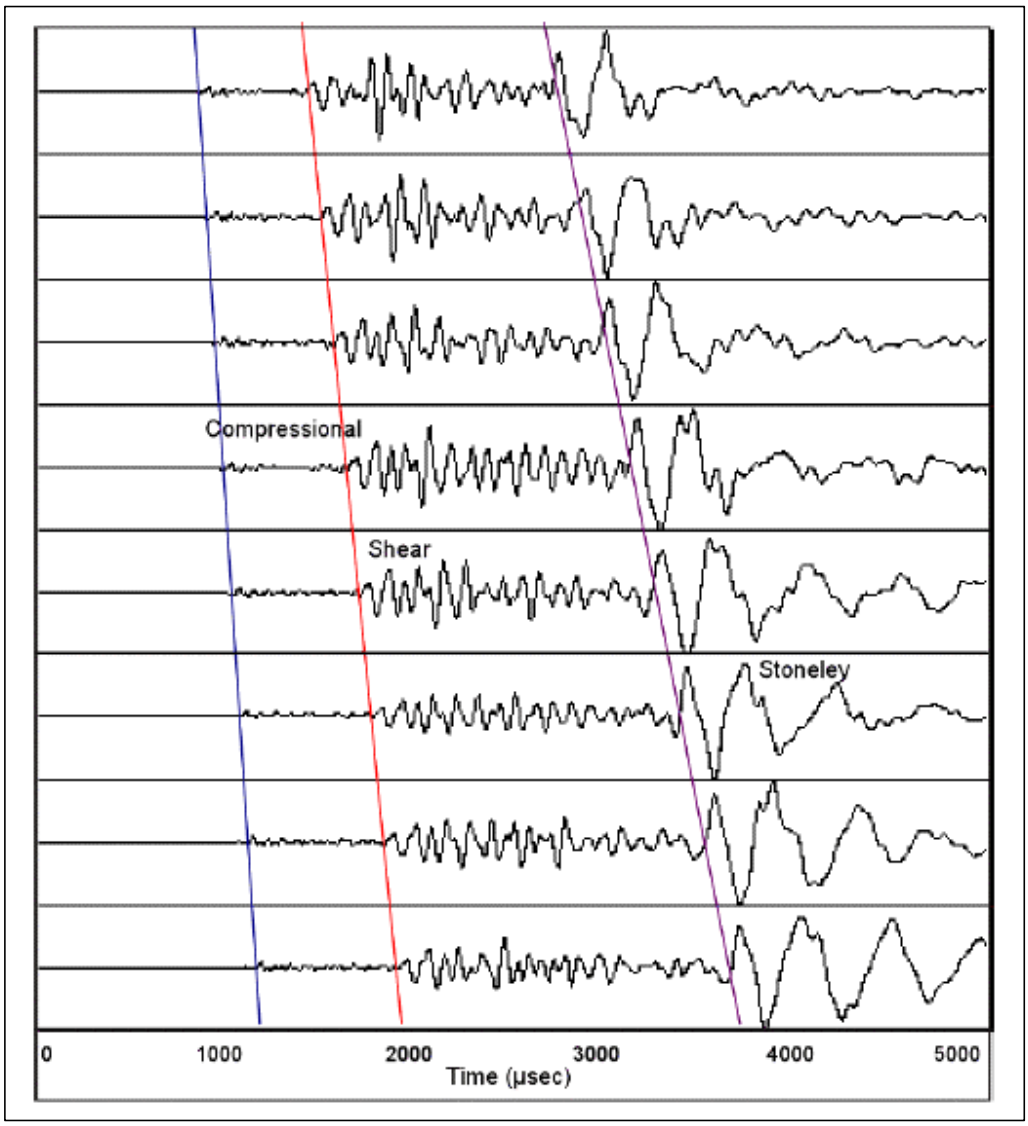


Figure 3: Move-out determination on a set of monopole array waveforms

Slowness time coherence processing, STC, is a processing technique based on semblance that performs this operation automatically. It searches for coherent components along all moveouts in a waveform array. We start by positioning a time window on the reference waveform at time *T* and then defining a corridor through the array with a move-out *S* (**Figure 5**). The total or incoherent energy, *Ei*, is calculated as the sum of the squares of the samples within the corridor (**Eq. 2-1**). The coherent energy, *Ec*, is then calculated as the arithmetic sum of the samples along the moveout squared (**Eq. 2-2**). When the signal on all waveforms within the window are perfectly correlated, the coherent energy is equal to the total energy times the number of waveforms.

$$E_i(T,S) = \sum_{i=1}^{n} \int_0^{Tw} \left[x_i\left(t - \left[T + S(z_i - z_1)\right]\right)\right]^2 dt \qquad (2\text{-}1)$$

$$E_c(T,S) = \int_0^{Tw} \left[\sum_{i=1}^{n} x_i\left(t - \left[T + S(z_i - z_1)\right]\right)\right]^2 dt \qquad (2\text{-}2)$$

Where *i* is the waveform number, *xi* is the value of the waveform sample at time *t* ,*Tw* the length of the integration time window and *zi* the waveform depth.
The coherence is defined as:

$$Coh(T,S) = \frac{1}{n}\frac{E_c(T,S)}{E_i(T,S)} \qquad (2\text{-}3)$$

The coherence varies between 0 and 1. A value of 0 means that there is no correlated arrival in the window. On the opposite, a value of 1 means that the waveform components in the window correlate perfectly.

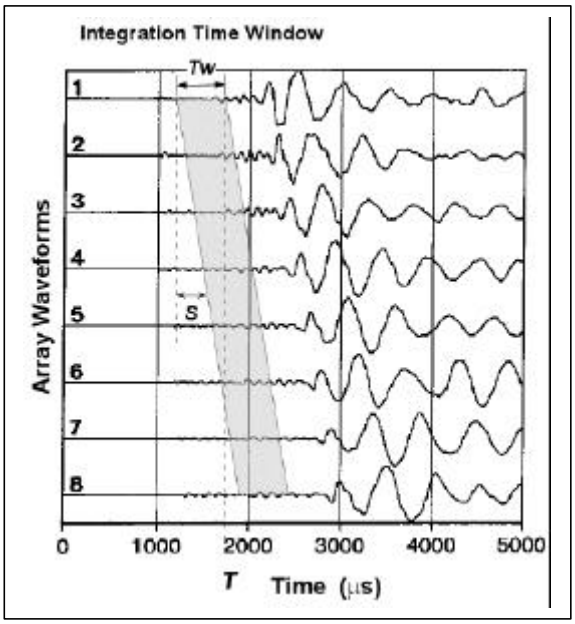
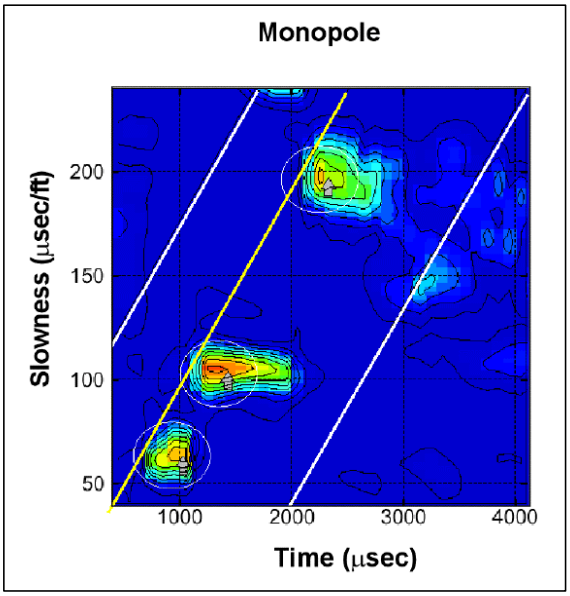


Figure 4: Slowness time coherence computation principle

The computation is done for a range of moveout *S*, for every possible position of the window in time *T*. A convenient representation of the coherence results is to display

them on a contour plot versus time and slowness, the ST-Plane (**Figure. 6**). On such a plot each point represents the value of the coherence for a specific time and move out (slowness).

Coherence has a low value unless the integration corridor is positioned over a wave propagating at the considered moveout. Therefore, most of the ST plane is filled with coherence values close to 0 (blue). However, when a coherent arrival is present in the waveforms it shows as a peak of coherence with values that can go up to 1. The process locates the position of the maximum coherence at each peak and outputs the value of slowness, time and coherence in a list. For a given tool configuration, we expect that the time of arrival of a wave will be approximately the product of the slowness by the spacing between the transmitter and the reference receiver. This relation is represented on the plot by the TR line. The ST-plane shown on the example is from a set of monopole waveforms. The three main peaks observed, starting from bottom left, probably represent the compressional, the shear and the Stoneley arrivals. However, at this stage the peaks only represent coherent arrivals in the waveforms and are not identified. The process is repeated for each set of waveforms acquired by the tool at each depth sample.



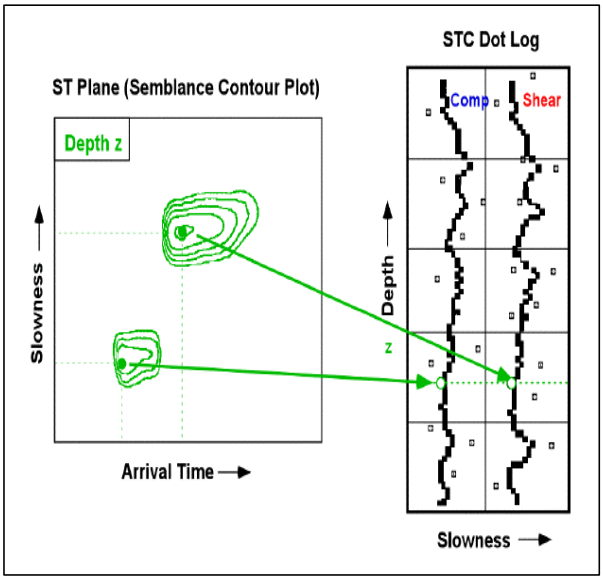


Figure 5: Slowness-Time Plane monopole example. Figure 6: Coherence peak labelling and slowness dot-logs generation

STC processing outputs a list of coherence peaks at every measurement depth. We can represent these peaks as dots on a slowness versus depth plot (**Figure 7**). On such a plot, coherent arrivals display as continuous series of dots. There may also be scattered coherence peaks caused by noise, bed boundaries or other spurious effects that do not match with continuous trends. 'Tracking and classification' identifies the peaks that belong to consistent arrivals versus depth, assigns them to a specific wave type, for example compressional or shear, and output the values in the form of a continuous slowness log. Tracking and classification uses rules to identify the different waves. Typical rules used by tracking and classification are that the peaks have sufficient continuity in depth, sufficient coherence, that the compressional is faster than

the shear arrival and that the ratio of their respective slownesses is larger than 1.45.

Sometimes, dots are missing and there are gaps in the trends. These may originate among other causes from unfavourable borehole conditions, layering or noise. As long as the gap is small, tracking and classification interpolates in between existing peaks to obtain a continuous log, but if the gap is larger than a couple of feet, the log is set to absent.

Upper and Lower Dipole Mode (UDP & LDP)

A flexural wave is propagated through the borehole by inducing a pressure wave perpendicular to the borehole wall and propagates throughout the borehole wall. The borehole wall then experiences a transverse displacement as indicated in **Figure 8,** which is similar to the shear velocity of the formation.

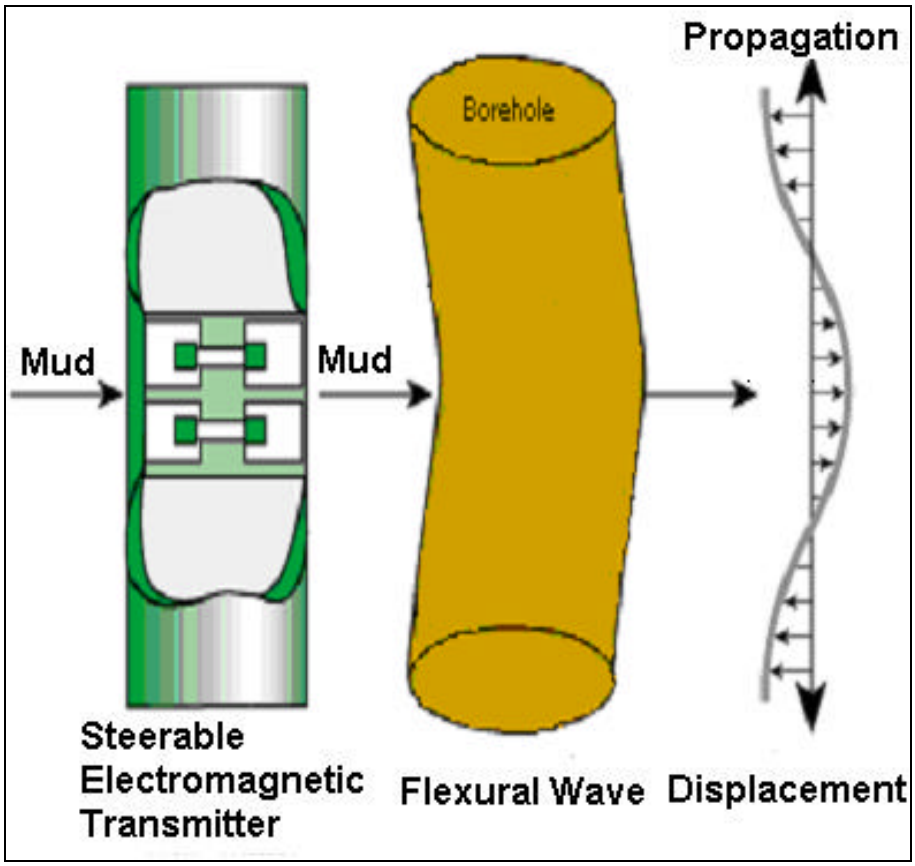


Figure 7: Flexural wave propagation to measure shear velocity

A problem of dispersion effects occurs with shear velocity measurements. Dispersion is the effect of variation of velocity with frequency and makes it difficult to determine a true formation shear. The higher the frequency, the more dispersion occurs. A method known as Bias Correction is applied real time in the field, which basically uses a correction based on numerical modelling. It is also based on a narrow frequency band at low frequencies where dispersion effect is less and so does not take into account the entire waveform. Although this is a fast and simple technique, it is not the best. Best-DT 3* uses a more advanced technique known as Dispersive STC Processing and is based on the entire waveform and uses model dispersion curves to correct for dispersion rather than a look up table, as with Bias correction. Correction is therefore more refined and accurate.

Dispersion depends on frequency, borehole size, formation shear slowness, mud slowness and formation to mud density ratio. In hard formations, mud slowness has less of an effect on dispersion.

Shear Anisotropy Measurement

For sonic measurements, it is well recognized that sedimentary rocks generally exhibit some degree of anisotropy. Anisotropy may arise from intrinsic structural effects, such as aligned fractures and layering of thin zones, or from unequal stresses within the formation. These effects lead to differences in formation elastic properties, and if they are on a smaller scale than the sonic wavelengths, then sonic wave propagation can be used to detect and quantify the anisotropy.

Sonic waves travel fastest when the direction of particle motion (polarization) is aligned with the material's stiffest direction. Shear-wave particle motion is in a plane perpendicular to the wave propagation direction. If the formation is anisotropic in this plane, meaning that there is one direction that is stiffer than another, then the shear-wave polarization aligned in the stiff direction will travel faster than one aligned in the other, more compliant direction. As a result, the shear wave splits into two components, one polarized along the formation's stiff (or fast) direction, and the other polarized along the formation's compliant (or slow) direction.

For example, in the case of vertically aligned dense micro-cracks or fractures, a shear wave that is polarized parallel to the fracture strike will propagate faster than a shear wave polarized perpendicular to it (**Figure 9**). In general, a shear (or flexural) wave, generated by a dipole source, will split into two orthogonal components polarized along the X- and Y-directions in the formation. As they propagate along the borehole, the fast wave will be polarized along the direction parallel to the fracture strike and a slow wave in the direction perpendicular to it.

With two orthogonal dipole transmitters and multiple receiver pairs aligned in orthogonal directions, the DSI Dipole Shear Sonic Imager tool can measure the components of shear slowness in any direction in a plane perpendicular to the borehole axis (**Figure 10**). The measurement involves recording the waveforms on receivers pointing in directions parallel and normal to each transmitter along the tool x- and y-axes.

Four sets of waveforms are recorded at each depth and receiver level. These measurements are labelled xx, xy, yx and yy. The first direction refers to the transmitter and the second direction to the receiver. The direction and speed of the fast and slow split shear waveforms travelling in the formation can be easily determined by mathematically rotating the measured waveforms through an azimuthal angle so that they line up with the two orthogonal formation X- and Y-directions. This is done by minimizing the cross-receiver energies, xy and yx.

The rotated direction of the fastest shear wave becomes the fast-shear tool azimuth; and the tool orientation, measured by a magnetometer, is used to determine the fast

shear azimuth relative to true north. This rotation, called the Alford method, uses the fact that the anisotropy model expects the amplitude of the cross-receiver measurements to vanish when the measured axes x and y align with the anisotropy axes X and Y.

In addition to the fast and slow shear-wave velocities, determined by a slowness time coherence (STC) processing on the rotated waveforms, three measurements of anisotropy are computed. These are **energy anisotropy, slowness anisotropy** and **time anisotropy.**

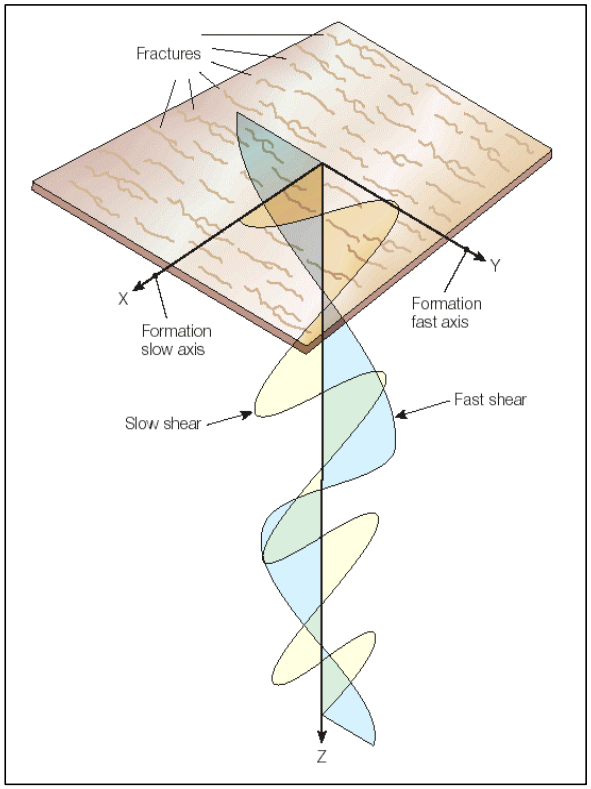


Figure 8: Shear wave splitting

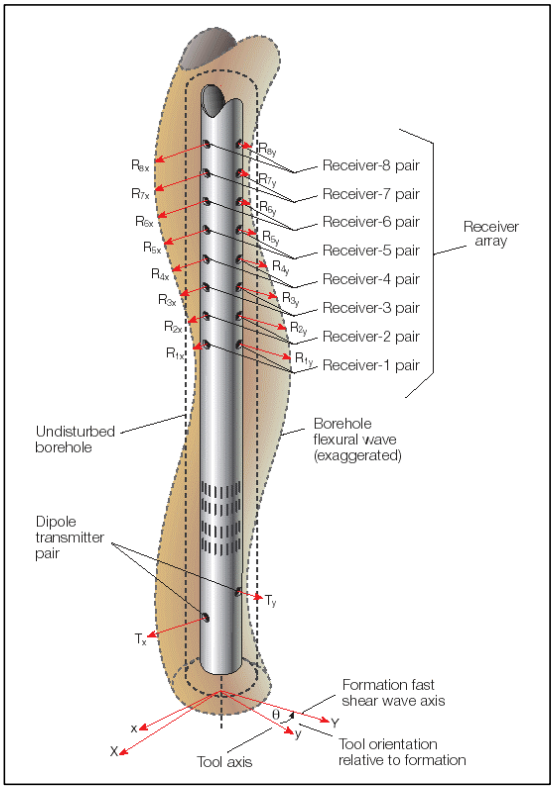


Figure 9: DSI tool showing X-Dipole (BCR) Mode

Figure 9. Shear-wave splitting. Shear waves travel in an anisotropic formation with different speeds along the directions of the formation anisotropy. In this example, anisotropy is caused by the vertical fractures (or micro-cracks) with a strike direction along the formation Y-axis, and the fastest shear wave, with the longer wavelength component, will be polarized along the fracture strike direction as it propagates along the borehole (Z-axis). When shear wave splitting is the result of stress anisotropy, the Y-axis corresponds to the direction of maximum stress, and the X-axis corresponds to the direction of minimum stress.

Figure 10. During logging, flexural waves are induced by dipole transmitters fired sequentially in two perpendicular directions, first along the tool x and then the tool y-

axes. In this example, the fastest component of the induced shear wave is polarized along the formation Y-axis direction, which is aligned along the fracture strike or maximum stress direction. The sloTrefoil-1 component of the shear wave is polarized along the formation X-axis. Projections of these two shear-wave components are received by each of the dipole sonic tool x- and y-receiver pairs. The inline signals xx and yy are the x-receiver and y-receiver waveforms received when the x and y-transmitters are fired. Cross-signal components xy and yx are the y- and x-receiver waveforms received as the x- and y-transmitters are fired. The Alford rotation angle, q, is determined by minimizing the cross signal components. This would happen automatically if the tool axes were rotated through an angle, q, and aligned with the two orthogonal directions in the anisotropic formation.

Slowness anisotropy is the difference between the fast and slow slownesses calculated by STC on the rotated waveforms. It yields a quantitative measure of slowness anisotropy, and has the best vertical resolution at about 3 ft [1 m]; the size of the receiver array. It can be compared directly with seismic or core measurements of slowness anisotropy.

Travel time anisotropy is the arrival-time difference between the fast- and slow-shear waves at the receivers. It is obtained from a cross-correlation between fast and slow shear-wave arrivals at each receiver spacing. Time lags computed at each receiver are referenced to the largest offset receiver and averaged across the receiver array. This is divided by the average of the fast and slow arrival times to compute a percentage difference. The travel time anisotropy indicator is robust and quantitative, and has the vertical resolution of the average transmitter-receiver spacing, 13 ft [4 m]. Slowness and travel time anisotropy indicators are identical in formations with homogeneous beds thicker than 13 ft.

Energy anisotropy is the energy in the cross component waveforms as a percentage of energy in all four components. In an isotropic formation, energy anisotropy reads zero. In an anisotropic formation, the reading depends on the degree of anisotropy. Two curves are computed from the waveforms: minimum and maximum cross-energy.

The minimum cross-energy is the energy in the cross-components when the tool measurement axis lines up with the formation anisotropy axis. Minimum cross-energy reads zero in an ideal formation whether anisotropic or not. This curve is a good relative measure of whether the assumed model for anisotropy inversion fits the real formation.

The maximum cross-energy is a measure of the amount or strength of anisotropy. Unlike the two previous anisotropy measurements (slowness and time), energy anisotropy is a measure of both slowness and amplitude differences of the fast and slow shear waves. Large differences between the maximum and minimum values, especially when the minimum energy is low, indicate zones of significant anisotropy. Energy anisotropy, though qualitative, is little affected by processing, and is the principal measure of anisotropy.

ENCLOSURE 1: COMPOSITE LOG

Trefoil 1
Composite Well Log

Origin Energy

Well Location



Well Data Card

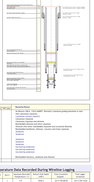
Operator: Origin Energy
Well Name: Trefoil 1
Well Type: Development
Location: 10S 121 E 27 Sub
Latitude: 10° 31' 30.21" South
Longitude: 121° 49' 27.69" East
Grid Zone: GDA 94 / MGA zone 51
Grid North: 9836 234.76 m
Easting: 695 000.00 m

Seismic Location: 20.3km on bearing of 90.4 degrees from CRA2007-07 SEISAT Site No.

Elevation: 25.00 m AHD
Water Depth: 84.00 m AHD
Total Depth: 3700.00 m AHD
Rig: Ocean Patriot
Rig Type: Semi-Submersible
Spud Date: 07-Dec-11 0300
Rig Release Date: 24-Dec-11 0600
Total Days: 17.00 days
Rental Amounts: Drilling Contract Rate: AUD
Drilling Fluid Rate: AUD
Logging Rate: AUD
Coring Rate: AUD
Total Rental Amount: AUD

Rig Name: Ocean Patriot
Operator: Woodside Energy Ltd.
Agents: Bell Lake

Casing Schematic



Time vs Depth

Formation Tops

Formation / Seismic Marker	Age	Top MD (mRT)	Top TVD (mRT)	Thickness (m)
Sea Level (Datum)		0.00	0.00	
Sea Bed		109.00	109.00	
Top Mesozoic Extrusive		1,000.00	1,000.00	
Base Mesozoic Extrusive		1,074.00	1,074.00	74.00
Lower Mesozoic Seismic Marker		1,884.00	1,884.00	810.00
Top Anglesea Fm		2,149.00	2,149.00	265.00
Top Anglesea Volcanics		2,340.00	2,340.00	191.00
Top Lower Anglesea		2,579.00	2,579.00	239.00
Top Sahul Shale		2,818.00	2,818.00	239.00
Top Sahul Sst		2,868.00	2,868.00	50.00
Top Plover Fm		2,888.00	2,888.00	20.00
Top Elang Fm		3,000.00	3,000.00	112.00
Top Jamieson Fm		3,000.00	3,000.00	0.00
Top Echuca Shoals Fm		3,000.00	3,000.00	0.00
Top Vulcan Fm		3,000.00	3,000.00	0.00
Top Puffin Fm		3,000.00	3,000.00	0.00
Top Oxfordian		3,000.00	3,000.00	0.00
Top Callovian		3,000.00	3,000.00	0.00
Top Bathonian		3,000.00	3,000.00	0.00
Top Bajocian		3,000.00	3,000.00	0.00
Top Aalenian		3,000.00	3,000.00	0.00
Top Toarcian		3,000.00	3,000.00	0.00
Top Pliensbachian		3,000.00	3,000.00	0.00
Top Sinemurian		3,000.00	3,000.00	0.00
Top Hettangian		3,000.00	3,000.00	0.00
Top Triassic		3,000.00	3,000.00	0.00
Top Permian		3,000.00	3,000.00	0.00
Top Basement		3,000.00	3,000.00	0.00

Drilling Problems

Problems Noted: STUCK PIPE, Washout intervals,grading,fractures in hole
Stuck Pipe Incidents:
Lost Circulation Incidents:
Abnormal Pressure Incidents:
Hydrocarbon Shows and Gas Kicks:
Hydrocarbon Shows and Gas Kicks:
Hydrocarbon Shows and Gas Kicks:

Geological Hazards: Shallow gas, Overpressure zones

Wireline Log Runs

Run	Service	Logs	Interval (mRT)
1	Schlumberger	DSI-HNGS-ECS-HLDS-APS-HRLA-PEX-MSIP	2,000 - 3,000
2	Schlumberger	VSI-GR	2,000 - 3,000
3	Schlumberger	CMR-GR	2,000 - 3,000
4	Schlumberger	MDT-GR	2,000 - 3,000
5	Schlumberger	CST-GR	2,000 - 3,000
6	Schlumberger	VSI-GR	2,000 - 3,000
7	Schlumberger	CMR-GR	2,000 - 3,000
8	Schlumberger	MDT-GR	2,000 - 3,000
9	Schlumberger	CST-GR	2,000 - 3,000

Logging Parameters

Run	Hole Size (mm)	Casing Size (mm)	Mud Type	Mud Density (kg/m³)	Viscosity (cP)	Fluid Loss (mL/30min)	pH	Rm (ohm.m)	Rmf (ohm.m)	Rmc (ohm.m)
1	914.40	762.00	Seawater	1,030	5	0	8.5	0.5	0.4	0.6
2	660.40	508.00	Seawater	1,030	5	0	8.5	0.5	0.4	0.6
3	508.00	339.73	Seawater	1,030	5	0	8.5	0.5	0.4	0.6
4	339.73	244.48	Seawater	1,030	5	0	8.5	0.5	0.4	0.6
5	244.48	177.80	Seawater	1,030	5	0	8.5	0.5	0.4	0.6
6	177.80	Open Hole	Seawater	1,030	5	0	8.5	0.5	0.4	0.6
7	177.80	Open Hole	Seawater	1,030	5	0	8.5	0.5	0.4	0.6
8	177.80	Open Hole	Seawater	1,030	5	0	8.5	0.5	0.4	0.6
9	177.80	Open Hole	Seawater	1,030	5	0	8.5	0.5	0.4	0.6

Temperature Data Recorded During Wireline Logging

Run	Depth (mRT)	Temperature (°C)	Time Since Circulation
1	2,000	45.2	24-12-11 06:30
1	2,500	52.1	24-12-11 06:30
1	3,000	58.4	24-12-11 06:30
2	2,000	45.2	24-12-11 08:45
2	2,500	52.1	24-12-11 08:45
2	3,000	58.4	24-12-11 08:45
3	Mid-Interval	48.6	24-12-11 11:15
4	Mid-Interval	49.3	24-12-11 14:00
5	Mid-Interval	50.1	24-12-11 16:30

Lithologies

Shale | Limestone | Sandstone | Coal | Dolomite | Calcareous Sediment
Basement

Legend

Gamma Ray | Caving Zone | Core Recovered

Well Log | Lithology | Core Photo

Gamma Ray (GR) (API) 0 – 150 | Resistivity (ohm.m) 0.2 – 2000 | Porosity (v/v) 0.45 – -0.15 | Density (g/cm³) 1.95 – 2.95

CORE 1 | CORE 2 | CORE 3 | CORE 4 | CORE 5

Core Photo

Sea Level (25 ft)

Sea Bed (109 ft)

Top Mesozoic Extrusive (1000 ft)

Base Mesozoic Extrusive (1074 ft)

Lower Mesozoic Seismic Marker (1884 ft)

Top Anglesea Fm (2149 ft)

Top Anglesea Volcanics (2340 ft)

Top Lower Anglesea (2579 ft)

Top Sahul Shale (2818 ft)

Top Sahul Sst (2868 ft)

Top Plover Fm (2888 ft)

Top Elang Fm (3000 ft)

Top Jamieson Fm (3000 ft)

Top Echuca Shoals Fm (3000 ft)

Top Vulcan Fm (3000 ft)

Top Puffin Fm (3000 ft)

Top Oxfordian (3000 ft)

Top Callovian (3000 ft)

Top Bathonian (3000 ft)

Top Bajocian (3000 ft)

Top Aalenian (3000 ft)

Top Toarcian (3000 ft)

Top Pliensbachian (3000 ft)

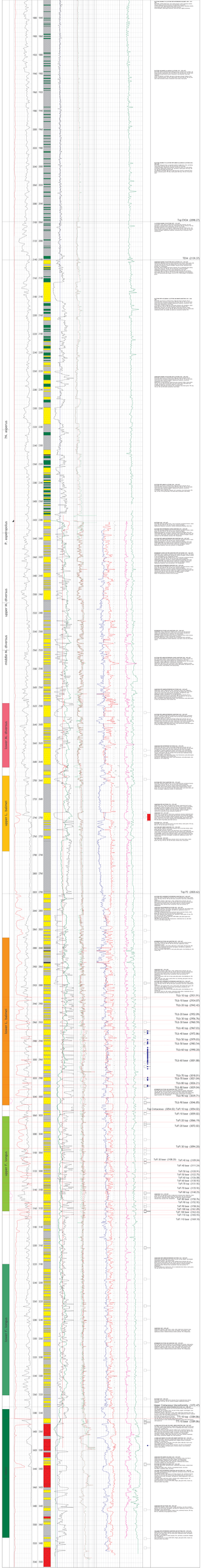
Top Sinemurian (3000 ft)

Top Hettangian (3000 ft)

Top Triassic (3000 ft)

Top Permian (3000 ft)

Top Basement (3000 ft)


Top EVCH. (2098.17)
TEH (2129.17)
Top P3 (2820.42)
T3.10 top (2933.91)
T3.10 base (2934.07)
T3.20 top (2940.42)
T3.20 base (2952.29)
T3.30 top (2956.79)
T3.30 base (2966.79)
T3.40 top (2967.05)
T3.40 base (2972.86)
T3.50 top (2979.05)
T3.50 base (2983.54)
T3.60 top (2990.29)
T3.60 base (3001.88)
T3.70 top (3018.01)
T3.70 base (3020.71)
T3.80 top (3026.27)
T3.80 base (3029.04)
Top Cretaceous (3054.02)
T3.90 top (3054.02)
T3.90 base (3064.71)
T4P1.10 top (3065.02)
T4P1.10 base (3066.19)
T4P1.20 top (3072.02)
T4P1.20 base (3094.20)
T4P1.30 top (3099.20)
T4P1.30 base (3109.39)
T4P1.40 top (3109.04)
T4P1.40 base (3111.04)
T4P1.50 top (3120.91)
T4P1.50 base (3122.79)
T4P1.60 top (3126.08)
T4P1.60 base (3127.58)
T4P1.70 top (3131.92)
T4P1.70 base (3135.92)
T4P1.80 top (3140.29)
T4P1.80 base (3142.29)
T4P1.90 top (3158.76)
T4P1.90 base (3172.42)
T4P1.100 top (3176.29)
T4P1.100 base (3181.29)
T4P1.100 base (3182.42)
T4P1.110 top (3183.42)
T4P1.110 base (3184.10)
Upper Cretaceous Unconformity (3191.47)
T5.10 top (3194.86)
T5.10 base (3194.86)
N. diversus
P. alaskensis
T. alpinus
upper T. alpinus
lower P. alaskensis
middle N. diversus
upper N. diversus
lower T. alpinus
upper P. stargeri
lower P. stargeri